

**Synthetic studies on oxidative dearomatization reactions and applications in synthesis of  
the KB343 core structure, and investigation of bioactive thiazolidines**

**By**

**Marian N Aziz (Awadalla)**

**DISSERTATION**

**Submitted in partial fulfillment of the requirements**

**For the degree of**

**DOCTOR OF PHILOSOPHY**

**Organic Chemistry**

**The University of Texas at Arlington**

**Arlington, Texas**

**August 2022**

Copyright © by Marian N. Aziz 2022

All Rights Reserved



## ACKNOWLEDGMENTS

Firstly, I would like to express my deep appreciation and gratitude to my advisor Dr. Carl J. Lovely, Professor, Chemistry and Biochemistry Department at the University of Texas at Arlington (UTA) for his kind supervision, encouragement, and critical comments during the preparation of this dissertation. Deep thanks are also extended to Dr. Jeon Junha, Dr. Frank Foss and Dr. Subhrangsu Mandal for being on my committee and being so encouraging and cordial.

Deep thanks to our collaborators, Dr. Marco Brotto, Dr. Subhrangsu Mandal, Dr. Zui Pan, Dr. Venu Varanasi, Dr. Kwangho Nam, and Dr. Leticia Brotto for their help and support to my research by collaborating with me and performing some of the presented biological studies. Special thanks and appreciation to Dr. Adel Girgis (my previous advisor) at the National Research Center at Egypt for his support, encouragement, helpful and critical discussion, and collaboration during the entire journey of my PhD program.

I am also thankful to my colleagues of the Lovely lab at the chemistry and Biochemistry department; Dr. Andy Seal, Dr. Ravi Singh, Dr. Ojo Olatunji, Dr. Moumita Roy, Brandon Fulton, Key Tse, Nazmee Parveen, Nilakshi Dey, Anasuya Ghorai, and the undergraduate researchers, Arzoo Patel, Amany Iskander, Ibrahim El-Kasseh, Amber Waldron, Gabrielle Cevallos. My sincere acknowledgment to the entire Chemistry and biochemistry department family, Dr. Delphine Gout, Dr. Brian Edward, Dr. Roy McDougald, Deborah cook, Jill Howard, Beth Klimek and Stephanie Henry, Dr. Bian Liangqiao, Dr. James Mao, Avisankar Chini.

Also, sincere acknowledgment to the National Research Centre in Egypt, especially Dr. Adel Girgis, Dr. Azza Kamel, Dr. Neven Ganoub, Dr. Walid Fayad, and Dr. May A. El-Manawaty.

Also, I would like to thank my colleagues from the Bone-Muscle Research Center, Dr. Kamal Awad, Dr. Jian Huang, Dr. Zhiying Wang, Dr. Yan Chang, Linh Nguyen.

Finally, my deep gratitude is due to my parents, my husband and my wonderful daughter and son for being very supportive and encouraging throughout my endeavor in the USA over the last five years.

**DEDICATION**

**THIS DISSERTATION IS DEDICATED WITH LOVE AND AFFECTION**

**TO**

**MY PARENTS**

**AND**

**MY HUSBAND**

**Dr. KAMAL AWAD**

**AND**

**MY LOVELY KIDS**

**PARTHENIA AND PETER AWAD**

## **ABSTRACT**

### **Synthetic studies on oxidative dearomatization reactions and applications in synthesis the core structure of KB343, and investigation of bioactive thiazolidines**

**Marian N. Aziz, Ph.D.**

**The University of Texas at Arlington, 2022**

**Supervising Professor: Carl J. Lovely**

Natural products have inspired researchers over the years due to their complexity and biological activity. Organic chemists have made great efforts to investigate new unambiguous methodologies toward the synthesis of these complex structures. Moreover, the synergy between total chemical synthesis and medicinal applications to evaluate the biological activity of the isolated compounds significantly raised the desire for discovery of novel synthetic approaches. The research described in this dissertation focuses on oxidative dearomatization reactions as a key reaction to construct natural products. The three specific aims are as follows: Aim 1: investigation of the applications of oxidative dearomatization reactions for different classes of molecules using environmentally benign hypervalent iodine reagents and electrochemical oxidation conditions. Aim 2: investigating an oxidative dearomatization reaction to construct the core scaffold of the tris guanidine natural product, KB343. Aim 3: studying the validation of our developed synthetic method towards thiazolidine and benzothiazole structures and investigating their biological activity as antiproliferative and GABA regulator agents, respectively.

The dissertation contains two parts. The first part discusses the oxidative dearomatization reactions of urea, thiourea and guanidine derivatives, while the second part focuses on developing novel stable thiazolidines and their antiproliferative activity. Chapter one describes and summarizes the oxidative dearomatization literature. Chapter two focuses on the development of oxidative

spirocyclizations of *N*-aryl urea, *N*-aryl thiourea and guanidine derivatives, and includes a DFT investigation of the putative cyclization mechanisms. Oxidative dearomatization reactions of nonphenolic thiourea derivatives produce benzothiazole derivatives, which serve as a novel synthetic methodology for this intriguing ring system. Chapter three discusses how electrochemical oxidations are considered a realistic solution to solve issues observed by the conventional hypervalent iodine oxidations. In addition, it discusses an investigation of the stabilizing effect of *N*-alkoxy group on the nitrenium ion formation, which resulted in improving the isolated yields and the chemoselectivity of C-X bond transformations. In chapter four, we evaluate “oxidative dearomatization methods” to construct the KB343 core structure on vinyl guanidine candidates. The key Grignard reaction towards synthesis the targeted guanidine is still ongoing. Also, new synthetic methodology towards *N*-methoxy hydantoin construction is uncovered via three-component reaction. Chapter five discusses the biological activity of the synthesized benzothiazoles as a potential antiepileptic agent.

The second part of the dissertation reports the development of novel thiazolidine derivatives and investigating their antiproliferative activity as presented in chapters six, seven, and eight. We further validated our previously reported solid support methodology with substituted propargyl amines and a series of aryl isothiocyanate derivatives to isolate chemically stable anticancer candidates. The progress of this portion discusses the synthesis of three thiazolidine libraries and the third group was the most chemically stable which is discussed in chapter eight. Three different carcinomic cells were utilized for testing the anti-proliferative activity including breast, colon, and esophageal cell lines. Investigation of the apoptotic mechanism revealed that the thiazolidines probably block the phosphorylation of extracellular signal-regulated kinases (ERK).

## TABLE OF CONTENTS

ACKNOWLEDGMENTS.....	III
DEDICATION.....	V
ABSTRACT.....	VI
TABLE OF CONTENTS.....	VIII
LIST OF ILLUSTRATIONS.....	XI
LIST OF TABLES.....	I
CHAPTER ONE: OXIDATIVE DEAROMATIZATION REACTION IS A VERSATILE TOOL IN NATURAL PRODUCT SYNTHESIS.....	1
1.1 Oxidative dearomatization reaction is a versatile tool in natural product synthesis.....	2
1.2 SUMMARY.....	13
1.3 REFERENCES.....	14
CHAPTER TWO: DEAROMATIZING SPIROCYCLIZATION OF THIOUREAS, UREAS AND GUANIDINES.....	17
ABSTRACT.....	18
2.1 INTRODUCTION.....	18
2.2 RESULTS AND DISCUSSION.....	20
2.2.1 Putative mechanism for benzothiazole and acetated benzothiazole isolation.....	20
2.2.2 Phenolic derivatives subjected to oxidative dearomatization (OD) reactions.....	23
2.2.3 Spiro-oxazolidines/imidazolidines derived from OD of phenolic urea derivatives.....	28
2.2.4 Attempts towards synthesis related phenolic carbamate derivatives.....	30
2.2.5 Attempts to synthesis N,N'-disubstituted urea and thiourea derivatives derived from 4- isopropylphenol.....	31
2.2.6 Developing OD for guanidine derivatives:.....	32
2.2.7 A putative mechanism for the dearomatization reactions.....	35
2.2.8 DFT Study: Oxygen spirocyclization for electro-deficient urea derivative (36e).....	37
2.3 SUMMARY:.....	42
2.4 REFERENCES:.....	43
CHAPTER THREE: ANODIC OXIDATION IS A REALISTIC SOLUTION FOR ISSUES ASSOCIATED WITH CONVENTIONAL DEAROMATIZATION OF ARENES MEDIATED BY NITRENIUM FORMATION.....	45
ABSTRACT.....	46
3.1 INTRODUCTION.....	46
3.2 RESULT AND DISCUSSION:.....	48
3.2.1 IBDA mediated OD reactions.....	48



3.2.2 Developing an anodic oxidative dearomatization reactions: .....	60
3.2.3 Nitrenium ion formation via electrochemical oxidation reactions:.....	65
3.3 SUMMARY:.....	72
3.4 REFERENCES:.....	74
CHAPTER FOUR: OXIDATIVE DEAROMATIZATION (OD) ATTEMPTS TOWARD THE CORE SCAFFOLD OF KB343 .....	77
ABSTRACT.....	78
4.1 INTRODUCTION:.....	78
4.1.1 CHEMISTRY AND BIOACTIVITY OF KB343 NATURAL PRODUCT .....	78
4.1.2 RETROSYNTHETIC SCHEME TOWARDS SYNTHESIS KB343 VIA TOADS AS A KEY STEP REACTION .....	79
4.2 RESULTS AND DISCUSSION.....	80
4.2.1 Attempts towards synthesis urea derivatives.....	80
4.2.2 Isolation of novel hydantoin derivatives instead of targeted urea derivatives .....	85
4.2.3 Novel three component reactions for one-pot cascade hydantoin synthesis.....	88
4.2.4 Attempts towards synthesis the core structure of KB343.....	90
4.3 SUMMARY:.....	98
4.4 REFERENCES:.....	99
CHAPTER FIVE: BENZOTHIAZOLES FISSURE A NEW GATE FOR A DISCOVERY OF NOVEL DERIVATIVES REGULATING GABA RECEPTORS .....	101
ABSTRACT.....	102
5.1 INTRODUCTION.....	102
5.2 RESULT AND DISCUSSION .....	105
5.2.1 Chemistry .....	105
5.2.2 Biological studies of benzothiazoles .....	107
5.3 SUMMARY.....	118
5.4 REFERENCES.....	119
PART-II: NOVEL THIAZOLIDINES AS ANTI-APOPTOTIC AGENTS FOR CANCER DRUG DISCOVERY .....	123
CHAPTER SIX: NOVEL THIAZOLIDINES: SYNTHESIS, ANTI-PROLIFERATIVE PROPERTIES AND 2D-QSAR STUDIES.....	124
ABSTRACT:.....	125
6.1 INTRODUCTION.....	125
6.2 RESULTS AND DISCUSSION.....	128
6.2.1 Chemistry .....	128

6.2.2 Single crystal X-ray studies.....	131
6.2.3 Anti-proliferative properties.....	133
6.2.4 2D-QSAR study.....	136
6.3 SUMMARY.....	139
6.4 REFERENCES.....	140
CHAPTER SEVEN: ONE-POT SYNTHESIS OF NOVEL 2-IMINO-5-ARYLIDINE-THIAZOLIDINE ANALOGUES AND EVALUATION OF THEIR ANTI-PROLIFERATIVE ACTIVITY AGAINST MCF7 BREAST CANCER CELL LINE.....	143
ABSTRACT:.....	144
7.1 INTRODUCTION:.....	144
7.2 RESULTS AND DISCUSSION:.....	146
7.2.1 Chemistry:.....	146
7.2.2 Anti-proliferative activity:.....	151
7.3 SUMMARY:.....	154
7.4 REFERENCES:.....	156
CHAPTER EIGHT: NOVEL THIAZOLIDINES OF POTENTIAL ANTI-PROLIFERATION PROPERTIES AGAINST ESOPHAGEAL SQUAMOUS CELL CARCINOMA VIA ERK PATHWAY.....	160
ABSTRACT:.....	161
8.1 INTRODUCTION.....	161
8.2 RESULT AND DISCUSSION:.....	165
8.2.1 Chemistry.....	165
8.2.2 Anti-tumor activity:.....	169
Apoptosis analysis of 9g in KYSE-30 and KYSE-150 cells.....	174
Compound 9g induced apoptosis through the ERK pathway.....	174
8.2.3 Molecular Modeling Studies.....	176
8.2.4 Molecular Docking Study.....	176
8.2.5 3D-Pharmacophore study.....	179
8.2.6 QSAR study.....	179
8.3 SUMMARY.....	181
8.4 REFERENCES:.....	183
CHAPTER NINE: DISSERTATION CONCLUSION.....	192
CHAPTER TEN: EXPERIMENTAL SECTION.....	194
10.1. GENERAL PROCEDURE:.....	194
10.2 SYNTHESIS.....	195

## LIST OF ILLUSTRATIONS

## Chapter 1

- Scheme 1.1:** A promising pathway towards total synthesis of tetrodotoxin. Reagent and conditions: (a) RuCl<sub>3</sub>·2H<sub>2</sub>O, CeCl<sub>3</sub>·7H<sub>2</sub>O, NaIO<sub>4</sub>, MeCN/EtOAc/H<sub>2</sub>O, 0 °C; (b) I<sub>2</sub> (10 mol %), acetone/2,2-dimethoxypropane, 30 °C; (c) tBuNH<sub>2</sub>·BH<sub>3</sub> (1.1 equiv), AcOH (1.1 equiv), DCM, rt; (d) Pd/C, H<sub>2</sub>, EtOH, rt; (e) KO<sup>t</sup>Bu, *t*-amyOH, 45 °C. 4
- Scheme 1.2:** Asymmetric total synthesis of callilongisin B (**12**) via OD reaction. 5
- Scheme 1.3:** Total synthesis of (-)-daphenylline (**21**). 6
- Scheme 1.4:** OD approach towards synthesis core structure of ent-kauranoid natural product (**29**). 7
- Scheme 1.5:** Total synthesis (-)-crinipellin F via OD-[5+2] cycloaddition cascade reaction. 8
- Scheme 1.6:** Oxidative-dearomatization Wanger-Meerwein rearrangement. 9
- Scheme 1.7:** Retrosynthetic pathway toward synthesis the core structure of calyciphylline N (**41**). 10
- Scheme 1.8:** Synthesis calyciphylline core structure via OD/Diels-Alder reactions as key steps. 11
- Scheme 1.9:** Synthesis of suberitine C and D from 3,3'-diaaptamine hydrochloride (**59**) via OD reactions. Reagent and conditions: (a) IBDA (3.0 equiv.), MeCN/MeOH (2:1), 0 °C, 3 h, (68%); (b) IBDA (1.5 equiv.), MeCN/H<sub>2</sub>O (2:1), 0 °C, 3 h; then IBDA (1.5 equiv.), HFIP/MeOH (2:1), 0 °C, 3 h, (73%); (c) IBDA (3.0 equiv.), HFIP/H<sub>2</sub>O (2:1), 0 °C, 3 h, (73%). 12
- Scheme 1.10:** Synthesis of Suberitine A and B from 3,6'-Diaaptamine hydrochloride (**60**) via OD reactions. Reagent and conditions: (a) IBDA (3.0 equiv.), MeCN/MeOH (2:1), 0 °C, 3 h (58%); (b) IBDA (3.0 equiv.), HFIP/H<sub>2</sub>O (2:1), 0 °C, 3 h, (60%); (c) IBDA (1.5 equiv.), MeCN/MeOH (2:1), 0 °C, 3 h; then IBDA (1.0 equiv.), HFIP/H<sub>2</sub>O (2:1), 0 °C, 3 h, suberitine B (30%) and suberitine A (23%); (d) IBDA (1.5 equiv.), MeCN/H<sub>2</sub>O (2:1), 0 °C, 3 h; then IBDA (1.5 equiv.), HFIP/MeOH (2:1), 0 °C, 3 h, (52%). 13

## Chapter 2

- Figure 2.1:** Dearomatization reactions. 19
- Figure 2.2:** Unsuccessful oxidative dearomatization reactions toward guanidine substrates. 35
- Figure 2.3:** C-O and C-N spirocyclization of the electron-deficient urea derivative **35e**. 38
- Figure 2.4:** The proposed Gibbs free energy profile (kcal/mol) for the oxidative dearomatization reaction of urea **35e**. 41
- Figure 2.5:** LUMO molecular orbitals for intermediate **1** and **2**. 42

<b>Scheme 2.1:</b> Synthesis of the desired thiourea derivatives <b>6a-f</b> using <i>N</i> -methyl <i>p</i> -methoxybenzylamine ( <b>4</b> ).	20
<b>Scheme 2.2:</b> Preliminary dearomatization experiments (conditions (a) = IBDA (1 equiv), Cs <sub>2</sub> CO <sub>3</sub> (1.2 equiv), HFIP; (b) = IBDA (2 equiv), Cs <sub>2</sub> CO <sub>3</sub> (1.2 equiv), HFIP).	21
<b>Scheme 2.3:</b> Dearomatization of deactivated thiourea (conditions (a) = IBDA (1 equiv), Cs <sub>2</sub> CO <sub>3</sub> (1.2 equiv), HFIP; (b) = IBDA (2 equiv), Cs <sub>2</sub> CO <sub>3</sub> (1.2 equiv), HFIP). a)- Oxidative dearomatization reaction on deactivated thiourea <b>6f</b> . b)- Putative mechanism for the formation of isothiourea <b>12</b> .	22
<b>Scheme 2.4:</b> The isolated benzothiazoles using hypervalent iodine chemistry.	22
<b>Scheme 2.5:</b> Synthesis the targeted phenolic thioureas ( <b>22a-e</b> ).	23
<b>Scheme 2.6:</b> OD reactions of phenolic thiourea ( <b>22a</b> ) providing S and N spiro-cyclization.	24
<b>Scheme 2.7:</b> Acetylated <i>S</i> -spirocyclization reaction of phenolic thiourea ( <b>22a</b> ).	26
<b>Scheme 2.8:</b> Spirothiazolidines derived from OD of phenolic-thiourea derivatives ( <b>22b-e</b> ).	27
<b>Scheme 2.9:</b> Additional products from dearomatizing spirocyclization of phenolic thioureas.	27
<b>Scheme 2.10:</b> Synthesis of the targeted masked ureas ( <b>34a-d</b> ).	28
<b>Scheme 2.11:</b> The deprotection of masked urea derivatives ( <b>34a-d</b> ).	28
<b>Scheme 2.12:</b> Oxidative dearomatization of urea derivatives.	29
<b>Scheme 2.13:</b> Trials toward synthesis of phenolic carbamate derivative.	30
<b>Scheme 2.14:</b> Synthesis of carbamate ( <b>40</b> ) from secondary alcohol ( <b>39</b> ).	31
<b>Scheme 2.15:</b> Synthesis tertiary amine ( <b>43</b> ) via reduction of azido compound ( <b>42</b> ).	31
<b>Scheme 2.16:</b> Synthesis di-BOC guanidines ( <b>45a-c</b> ) and their oxidative dearomatization.	33
<b>Scheme 2.17:</b> Attempt towards synthesis of the CBZ-protected guanidine ( <b>49</b> ).	33
<b>Scheme 2.18:</b> Synthesis di-TEOC guanidine and its OD reaction.	34
<b>Scheme 2.19:</b> Putative mechanism for the dearomatization reactions.	36
<b>Chapter 3</b>	
<b>Figure 3.1:</b> Nitrenium ion stabilized by resonance of alkoxy group (a) and aryl group (b).	47
<b>Figure 3.2:</b> Nitrenium ion formation as a key step in natural products' syntheses.	47
<b>Figure 3.3:</b> New guanidine derivatives <b>39</b> derived from thermal Boc deprotection of guanidine <b>35</b> .	57
<b>Figure 3.4:</b> Synthesis of <i>O</i> -methylthalibrine, verbenachalcone and isodityrosine via electrochemical reactions.	62
<b>Scheme 3.1:</b> Carbonylation reactions toward synthesis urea <b>12</b> .	48
<b>Scheme 3.2:</b> Synthesis targeted 1-(alkyloxy)-3-(4-methoxybenzyl) urea <b>12</b> and <b>13</b> .	49
<b>Scheme 3.3:</b> Nucleophilic attack of HFIP with <i>N</i> -alkyloxy urea derivatives.	49
<b>Scheme 3.4:</b> Synthesis targeted secondary amines <b>16</b> , <b>18</b> and <b>21</b> .	51
<b>Scheme 3.5:</b> Synthesis of trisubstituted urea derivatives <b>22-24</b> .	51
<b>Scheme 3.6:</b> OD reactions of trisubstituted ureas mediated by <i>N</i> -methoxy nitrenium ion generation.	52
<b>Scheme 3.7:</b> Attempts toward synthesis trisubstituted thioureas using TCD.	54
<b>Scheme 3.8:</b> Synthesis of targeted guanidine derivatives ( <b>85</b> ) and ( <b>86</b> ) using Mitsunobu reaction.	55

<b>Scheme 3.9:</b> OD reactions of the synthesized guanidine <b>35</b> .	56
<b>Scheme 3.10:</b> Electrochemical phenol-aryl cross coupling by the Waldvogel group.	60
<b>Scheme 3.11:</b> C-C biaryl coupling via electrochemical oxidation of mono-halogenated phenols.	61
<b>Scheme 3.12:</b> Electrooxidative dimerization of ortho-dihalo phenols.	62
<b>Scheme 3.13:</b> Electrochemical synthesis of Heliannuol E ( <b>62</b> ).	63
<b>Scheme 3.14:</b> [3+2] cycloaddition reactions mediated by electrooxidations of phenols and naphthols.	63
<b>Scheme 3.15:</b> PIFA electrochemical formation mediated the synthesis of tetrahydropyrroloiminoquinone alkaloids ( <b>73</b> and <b>74</b> ) and glycozoline ( <b>77</b> ).	65
<b>Scheme 3.16:</b> Oxidative cyclization reactions of methoxy amides <b>2</b> using different oxidative conditions.	66
<b>Scheme 3.17:</b> Oxidative dearomatization reactions for nonphenolic carboxylic derivatives.	66
<b>Scheme 3.18:</b> Chlorinated guanidine <b>83</b> .	68
<b>Scheme 3.19:</b> Electrochemical oxidation attempts for <i>N</i> -methoxy urea <b>12</b> .	70
<b>Scheme 3.20:</b> Under optimization anodic oxidation conditions for the previously synthesized derivatives.	71

#### Chapter 4

<b>Figure 4.1:</b> KB343 chemical structure.	78
<b>Figure 4.2:</b> Important naturally and synthetic hydantoin derivatives ( <b>26-31</b> ).	85
<b>Figure 4.3:</b> Cram-chelate model explaining the transition state of nucleophilic addition of Grignard reagent.	93
<b>Figure 4.4:</b> Felkin-Anh model transition state for Grignard reaction corresponding to the major 1,2-anti product.	94
<b>Figure 4.5:</b> Hyperconjugation and negative hyperconjugation patterns.	96
<b>Scheme 4.1:</b> Retrosynthetic approach towards synthesis KB343 ( <b>1</b> ).	79
<b>Scheme 4.2:</b> Synthesis of the protected amino alcohol ( <b>11</b> ).	80
<b>Scheme 4.4:</b> Unsuccessful <i>N</i> -alkylation attempts using benzyl protected alcohol ( <b>17</b> ).	81
<b>Scheme 4.5:</b> Unselective deprotection of TBDMS group while removing Boc group.	83
<b>Scheme 4.6:</b> OD conditions for the di-substituted urea ( <b>24</b> ) resulted in isolating the corresponding urethane product ( <b>25</b> ).	84
<b>Scheme 4.6:</b> Short total synthesis of (±)-oxoaplysinopsin B ( <b>28</b> ) via cascade approach of hydantoin construction.	86
<b>Scheme 4.7:</b> Recent approaches toward constructions of hydantoin structures.	87
<b>Scheme 4.8:</b> Discovery of the three components cascade formation of hydantoin ( <b>42</b> ).	88
<b>Scheme 4.9:</b> Application of three components cascade formation of hydantoin ( <b>47</b> ) using different amino ester ( <b>46</b> ).	89
<b>Scheme 4.10:</b> Unsuccessful attempts for Mitsunobu reaction with secondary alcohol ( <b>52</b> ).	90
<b>Scheme 4.11:</b> Grignard reaction attempts with aldehyde ( <b>54</b> ) and proposed next steps towards the core structure KB343.	91
<b>Scheme 4.12:</b> Attempts toward synthesis the core structure of KB343 related structure ( <b>62</b> ).	92
<b>Scheme 4.13:</b> Cerium chloride mediated the addition of Grignard reagent to aldehyde <b>54</b> .	95

<b>Scheme 4.14:</b> New approach towards synthesis the KB343 core structure.	96
<b>Chapter 5</b>	
<b>Figure 5.1:</b> Marketed benzothiazole drugs (1-4).	103
<b>Figure 5.2:</b> Cytotoxicity of benzothiazoles. Six different compounds of benzothiazoles derivatives were screened at different concentrations to test their cytotoxicity effect on C2C12 cells. Low concentrations of 5 $\mu$ M to 10 $\mu$ M showed no cytotoxicity while higher doses indicated significant decrease in cell's viability as shown * $p$ <0.05, ** $p$ <0.01, *** $p$ <0.001. Compounds <b>7b</b> , <b>7c</b> , <b>7e</b> , and <b>7g</b> indicated significant increase in cells viability at low dose of 5 $\mu$ M as shown # $p$ <0.05, ## $p$ <0.01, ### $p$ <0.001.	108
<b>Figure 5.3:</b> Myogenic effects of benzothiazoles. Six different compounds of benzothiazoles derivatives were studied at two concentrations to test their myogenic effect on C2C12 cells. A) Differentiated C2C12 cells (Myotubes) stained with Myosin Heavy Chain and DAPI. B) Calculated fusion index of tested benzothiazoles compared to positive control and DMSO, statistical analysis based on One-Way ANOVA with Tukey Post Hoc test; # $p$ <0.05, ## $p$ <0.01, ### $p$ <0.001.	109
<b>Figure 5.4:</b> Concentrations of aminobutyric acids in conditioned media (CM) and C2C12 cells at the 5 <sup>th</sup> day post-treatment with 10 $\mu$ M benzothiazole agents <b>7b</b> and <b>7g</b> . (A) GABA in cells, (B) <i>L</i> -BAIBA in cells, (C) GABA in CM, (D) <i>L</i> -BAIBA in CM, and (E) <i>D</i> -BAIBA in CM. Mean $\pm$ SD (n=3). One-way ANOVA with Tukey's post-hoc test ( $\alpha$ =0.05) was performed for multiple comparisons between groups.	111
<b>Figure 5.5:</b> Detection of GABA receptors by Mouse GABA & Glutamate RT <sup>2</sup> Profiler PCR Array. A) GABA array for benzothiazole agent <b>7b</b> indicated more than 2-folds downregulation of <i>Gabrg2</i> , <i>Grm7</i> , <i>Gria1</i> , <i>Grin2a</i> , and <i>Slc17a7</i> . B) GABA array for benzothiazole agent <b>7g</b> indicated more than 2-folds upregulation of <i>Gabrg1</i> , <i>Gabrg3</i> , <i>Slc7a11</i> , <i>Slc1a6</i> , and downregulation of <i>Slc7a7</i> .	115
<b>Scheme 5.1:</b> Synthesis of the benzothiazoles <b>7a-g</b> via oxidation of thioureas <b>6a-e</b> .	105
<b>Chapter 6</b>	
<b>Figure 6.1:</b> Structures of some anti-tumor thiazolidinones.	127
<b>Figure 2.</b> ORTEP views of compounds <b>15a</b> (top) and <b>31</b> (bottom) showing the atom-numbering scheme. Displacement ellipsoids are drawn at the 50% probability level and H atoms are shown as small spheres of arbitrary radii. Blue, red, yellow, purple and brown spheres refer to carbon, oxygen, sulfur, nitrogen and bromide atoms, respectively.	132
<b>Scheme 6.1:</b> Synthesis of 3-(substituted)-prop-2-yn-1-amines <b>10a-b</b> .	128
<b>Scheme 6.2:</b> Synthesis of (Z)-2-imino-5-(Z)ylidene-N-substituted thiazolidines <b>11a-18a</b> , <b>19b</b> , <b>20c-21c</b> , and <b>20d</b> .	129
<b>Scheme 6.3:</b> Synthesis of (Z)-2-substituted imino -5-((Z)-ylidene)-thiazolidin-4-ones <b>28-38</b> .	131
<b>Chapter 7</b>	
<b>Figure 7.1:</b> Recently published thiazolidinones targeting breast cancer.	146
<b>Figure 7.2:</b> Approved drugs containing the thiazolidine core structure.	147
<b>Figure 7.3:</b> Anti-proliferative activity of thiazolidines <b>5a-f</b> and <b>5h-l</b> ; A-C show the cell viability of MCF7 cell incubated with thiazolidine and tested by MTT assay after 96 h. Figure 3-D shows the calculated IC <sub>50</sub> based on non-linear data obtained from the cell viability study.	155

<b>Scheme 7.1:</b> Previously synthesized and screened thiazolidines against breast and colon cancers.	147
<b>Scheme 7.2:</b> Synthesis of the targeted 4-(4-methoxyphenyl)-N-methylbut-3-yn-2-amine (ON = overnight).	148
<b>Scheme 7.3:</b> Synthesis of the fully substituted thiazolidines <b>5a-l</b> .	149
<b>Chapter 8</b>	
<b>Figure 8.1:</b> ERK1/2 inhibitors in the clinical stages.	165
<b>Figure 8.2:</b> IC <sub>50</sub> values of thiazolidines 9a-i tested with KYSE-30 cell line.	171
<b>Figure 8.3:</b> Inhibitory effects on cell proliferation by thiazolidine compounds variations. Cell viability with thiazolidine compounds at 10 μM treatments for 72 h were calculated by MTT assay and normalized inhibitory effects were compared in KYSE-30, KYSE-150, HET-1A cells. Data were from 4 independent experiments with biological triplicates for each experiment.	173
<b>Figure 8.4:</b> Compound <b>9g</b> selectively inhibited cell proliferation in ESCC cells: (A) Cell viability of KYSE-30 and KYSE-150 with <b>9e</b> and <b>9g</b> compounds at eight different concentrations using MTT assay; (B) Cell viability with <b>9g</b> treatment after 72 h were calculated by MTT assay in KYSE-30, KYSE-150, HET-1A, and NES-G4T.	173
<b>Figure 8.5:</b> DAPI staining of KYSE-30 and KYSE-150 cells treated with <b>9g</b> for 48 h, and 72 h.	174
<b>Figure 8.6:</b> Induced apoptosis through the ERK pathway in KYSE-150 cells. (A) Western blots of proteins ERK, pERK, Akt, and pAkt in KYSE-150 and NES-G4T treated with <b>9g</b> (10 μL) for 4 h, 8 h, and 12 h. Beta actin was used as the loading control. (B) Statistical data analysis of western blot results. Data is showed as mean ± SEM. **p ≤ 0.05.	175
<b>Figure 8.7:</b> Important ERK inhibitors.	176
<b>Figure 8.8:</b> The docking study of 6gdq ERK protein with ulixertinib (A) and an example of thiazolidines (9g) (B).	177
<b>Scheme 8.1:</b> Previous developed/published anti-proliferative thiazolidines <b>2</b> , <b>3</b> , and <b>5</b> .	167
<b>Scheme 8.2:</b> Novel synthesized thiazolidines <b>9a-i</b> using on-surface methodology.	168

## LIST OF TABLES

### Chapter 2

<b>Table 2.1:</b> Benzothiazoles derived from oxidation of thiourea mediated by hypervalent iodine.	<b>24</b>
<b>Table 2.2:</b> Initial screening experiments	<b>25</b>
<b>Table 3:</b> Frontier molecular orbital calculations for cyclization reaction of urea <b>36e</b> .	<b>39</b>

### Chapter 3

<b>Table 3.1:</b> Optimization dearomatization spirocyclization reaction of guanidine <b>37</b> .	<b>57</b>
<b>Table 3.2:</b> Photochemical Oxidative Conditions.	<b>58</b>
<b>Table 3.3:</b> Anodic iodine-free oxidation reactions for guanidine cyclization	<b>68</b>

### Chapter 4

<b>Table 4.1:</b> Attempts for reduction and hydrolysis of benzamide ( <b>11</b> ).	<b>82</b>
---	-----------

### Chapter 5

<b>Table 5.1:</b> Benzothiazoles derived from oxidation of thiourea mediated by hypervalent iodine.	<b>105</b>
<b>Table 5.2:</b> Lipidomic analysis of the synthesized benzothiazoles <b>7b</b> and <b>7g</b> .	<b>116</b>

### Chapter 6

<b>Table 6.1:</b> Synthesis of ( <i>Z</i> )-2-imino-(5 <i>Z</i> )-ylidene- <i>N</i> -substituted thiazolidines <b>11a-18a</b> , <b>19b</b> , <b>20c-21c</b> , and <b>20d</b> . <sup>a</sup>	<b>130</b>
<b>Table 6.2:</b> Synthesis of ( <i>Z</i> )-2-substituted imino-5-(( <i>Z</i> )-ylidene)-thiazolidin-4-ones <b>28-38</b> <sup>a</sup> via air oxidation.	<b>133</b>
<b>Table 6.3:</b> Anti-proliferative properties of the synthesized thiazoline-containing compounds and 5-fluorouracil (standard reference).	<b>136</b>

### Chapter 7

<b>Table 7.1:</b> The synthesized thiazolidines <b>5a-1</b> and their IC <sub>50</sub> against an MCF7 cell line.	<b>150</b>
---	------------

### Chapter 8

<b>Table 8.1:</b> Synthesis of ( <i>Z</i> )-5-(( <i>Z</i> )-substituted benzylidene)- <i>N</i> -(4-bromophenyl)-4,4-dimethylthiazolidin-2-imine.	<b>170</b>
--	------------



**CHAPTER ONE: OXIDATIVE DEAROMATIZATION REACTION IS A VERSATILE  
TOOL IN NATURAL PRODUCT SYNTHESIS**

Marian N. Aziz <sup>1,2</sup> and Carl J. Lovely <sup>1</sup>

1. Department of Chemistry and Biochemistry, 700 Planetarium Place, University of Texas at  
Arlington, TX 76019, USA

2. Department of Pesticide Chemistry, National Research Centre, Dokki, Giza 12622, Egypt

Corresponding author

Prof. Carl J. Lovely

Professor, Chemistry and Biochemistry Department

University of Texas at Arlington

Address: 700 Planetarium Place, Box 19065, UT Arlington, TX 76019-0065

Email: lovely@uta.edu

Phone: +1 817 272 5446

(Not published)

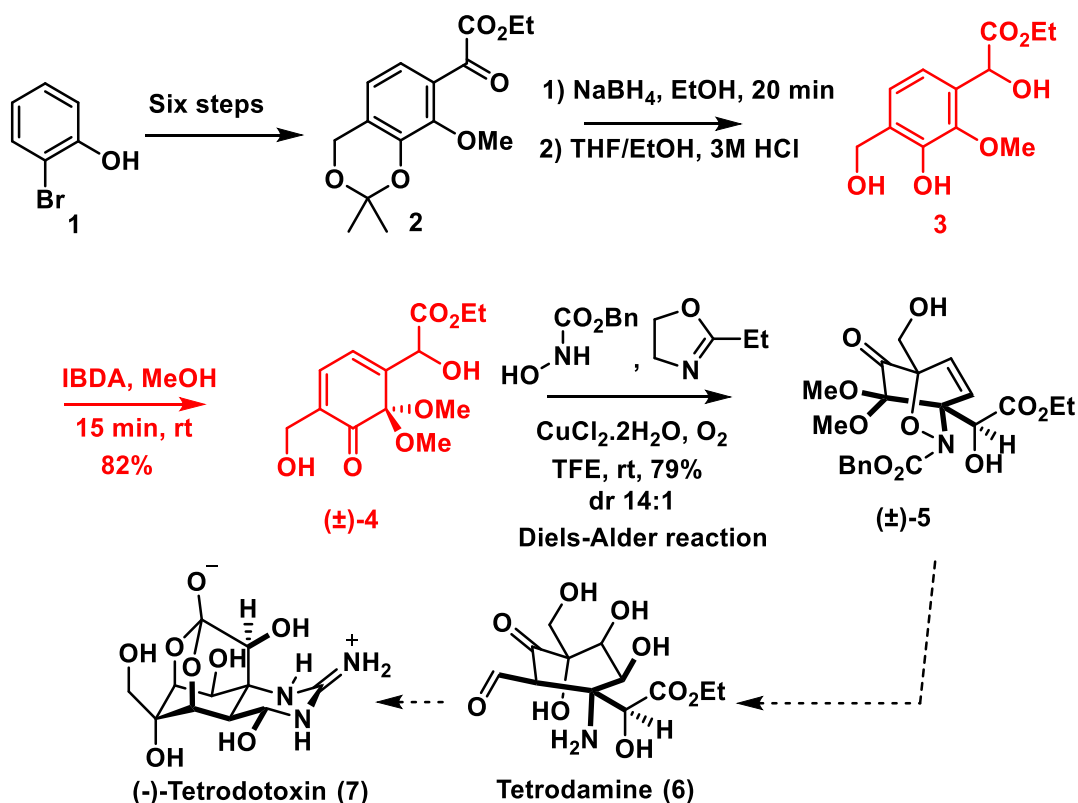
## 1.1 Oxidative dearomatization reaction is a versatile tool in natural product synthesis

The oxidative dearomatization (OD) reactions are considered one of the most interesting of the classical biosynthetic transformations, which has now been translated into a chemical tool for biomimetic/bioinspired synthesis.<sup>1</sup> As much as the concept of aromaticity has received a significant interest due to the corresponding stability of the aromatic compounds, disrupting this aromaticity has inspired chemists to discover their broad applications in synthetic chemistry. Thus, the dearomatization of phenols has received much attention mainly due to the synthetic value of the de-aromatized product, usually a cyclic ketone. Such frameworks are useful for further reaction(s) to provide a number of different and interesting chemical scaffolds that might be biological active molecules and/or useful in route to natural products. Interestingly, in biological systems the oxidative transformation of flavonoids to isoflavonoids occurs through the oxidation of a phenolic ring which is catalyzed by a cytochrome P-450 enzyme via the formation of a cyclohexadienone.<sup>2</sup>

The oxidative dearomatization reaction turns electron rich phenols into an electron deficient system that can act as a dienophile or can be attacked readily by nucleophiles. The utility of this aromatic ring umpolung in the construction of complex and functionalized heterocycles comes from the resulting reactivity of the electrophilic unsaturation and carbonyl subunits, which permit further elaboration into a diverse array of derivatives.<sup>3</sup> About 100 articles have been published in 2021 targeting and developing the OD reactions, and over 800 studies have been reported during the last decade.<sup>4</sup> In the present review, we have filtered out these publications to discuss chronologically reported natural product total syntheses via oxidative dearomatization reactions during the last decade.

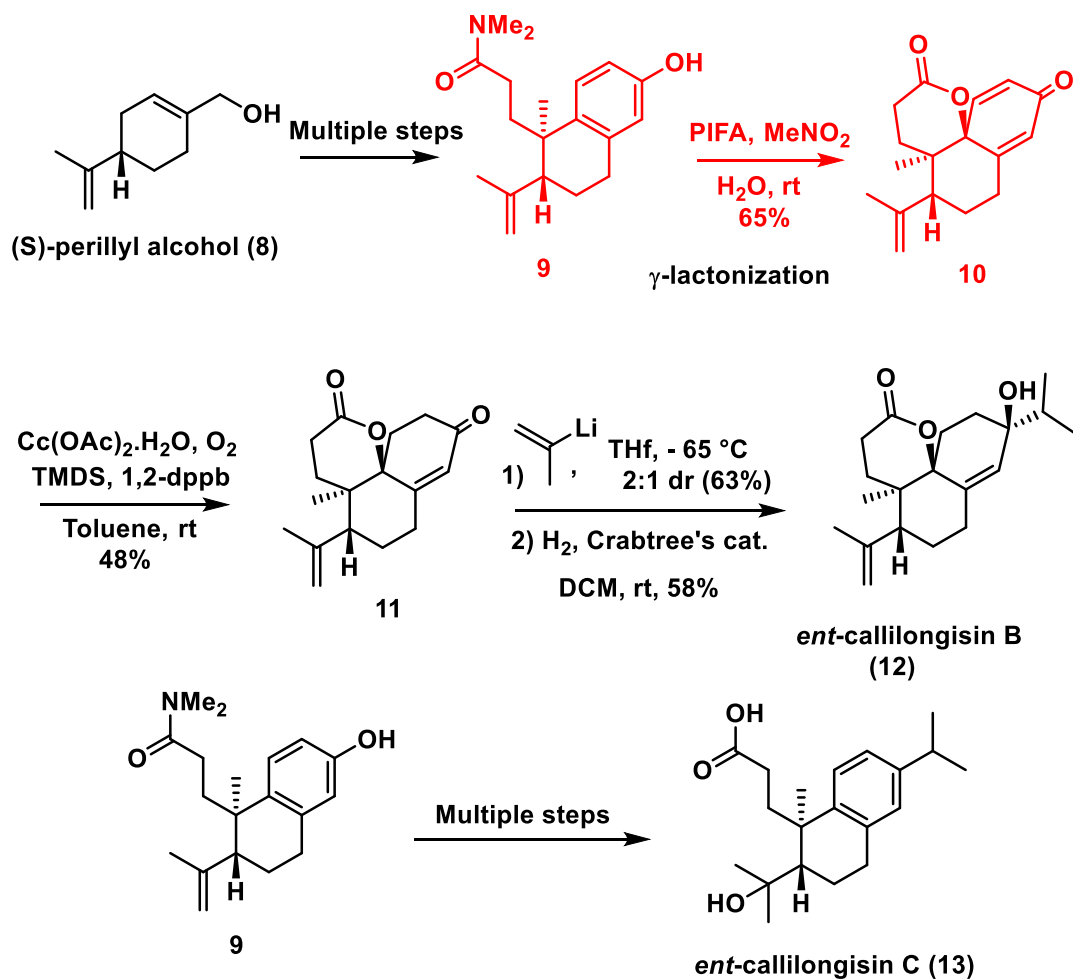
Recently, Robins and Johnson have targeted the oxidative dearomatization reaction to synthesize a complex lactone **6** from a simple phenol derivative **1** in 16 steps (Scheme 1.1).<sup>5</sup>

However, they could not finalize the total synthesis of tetrodotoxin (**8**) through this targeted pathway due to issues associated to the final guanidinylation of the sterically hindered primary amine **6** and homologation of the neopentyl ketone steps. They presented an interesting route towards the total synthesis of tetrodotoxin including the OD reaction of a tetrasubstituted guaiacol **3** using iodosobenzene diacetate (IBDA) as a hypervalent iodine reagent, delivering a dearomatized electron poor diene product **4** (Scheme 1.1). The latter was subjected to a Diels-Alder reaction with an acyl nitroso species which generated in situ by the aerobic oxidation of acyl hydroxylamines mediated by a copper catalyst. Through this route, they were able to establish six of the seven contiguous stereocenters in tetrodamin intermediate to tetrodotoxin (**7**). Ito and co-workers reported the first asymmetric total synthesis of two natural products from callilongisins family, callilongisin B (**12**) and C (**13**).<sup>6</sup> Interestingly, callilongisin B has been achieved by converting non-aromatic alcohol **8** into a phenolic derivative **9**, which was further subjected to the OD to deliver a dearomatized product **10**. Synthesis of the tricyclic dearomatized intermediate **10** is the key stage of the synthetic pathway towards *ent*-callilongisins. However, IBDA mediated oxidation did not work with the phenolic substrate **9**, treatment with phenyliodine bis(trifluoroacetate) (PIFA) in nitromethane yielded the desired adduct **10** as single diastereomer which co-occurred with  $\gamma$ -lactonization. The cyclohexandienone product **10** was parlayed via 1,2-addition reaction with isopropenyl lithium and a 1,4-reduction reaction which produced chemoselectivity the tri-cyclic product **11**. Reduction of the isopropenyl group with Crabtree's reduction produced callilongisin B (**12**).



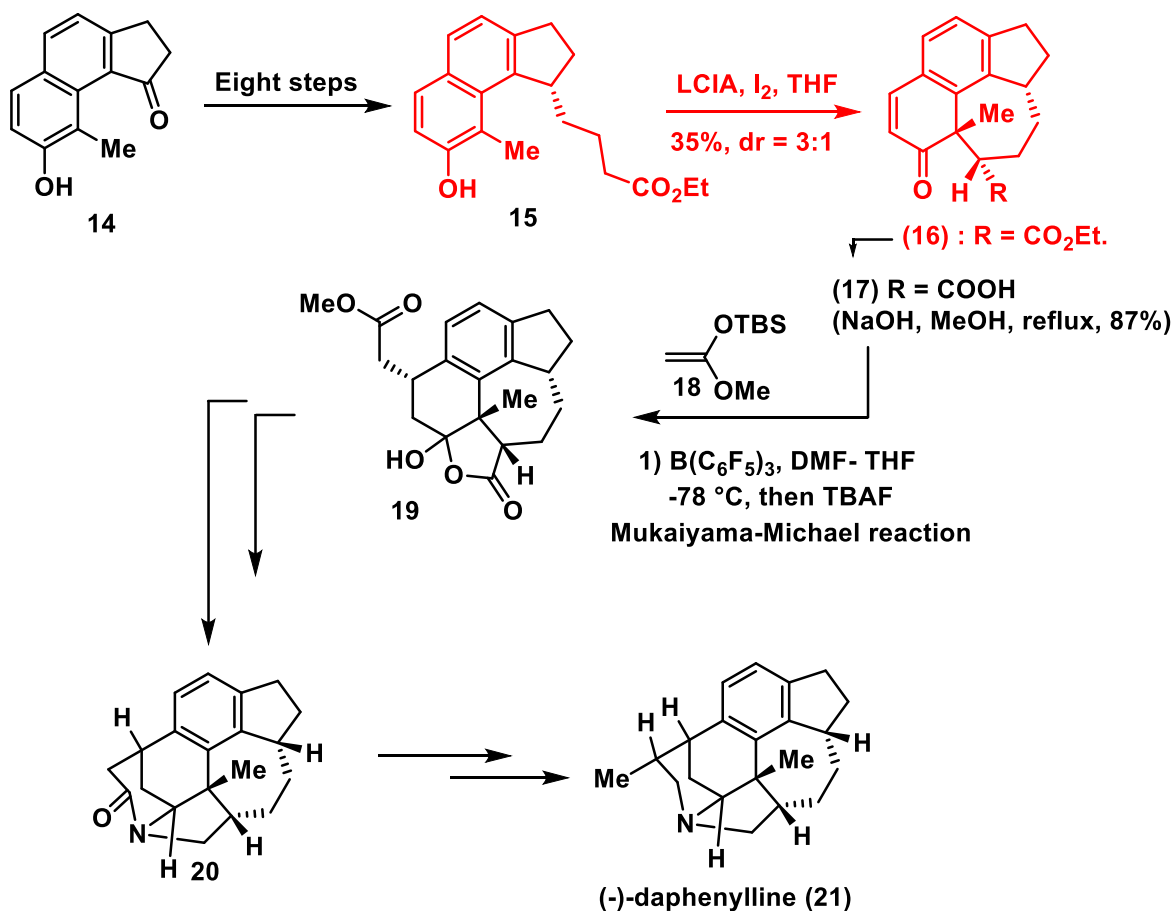
**Scheme 1.1.** A promising pathway towards total synthesis of tetrodotoxin. Reagent and conditions: (a)  $\text{RuCl}_3 \cdot 2\text{H}_2\text{O}$ ,  $\text{CeCl}_3 \cdot 7\text{H}_2\text{O}$ ,  $\text{NaIO}_4$ , MeCN/EtOAc/ $\text{H}_2\text{O}$ , 0 °C; (b)  $\text{I}_2$  (10 mol %), acetone/2,2-dimethoxypropane, 30 °C; (c)  $t\text{BuNH}_2 \cdot \text{BH}_3$  (1.1 equiv), AcOH (1.1 equiv), DCM, rt; (d) Pd/C,  $\text{H}_2$ , EtOH, rt; (e)  $\text{KO}^t\text{Bu}$ ,  $t$ -amylOH, 45 °C.

Seven total syntheses towards the triterpenoid daphenylline natural alkaloid (**21**) (Scheme 1.3) have been reported in the literature, of which six targeted phenolic dearomatization to construct a key intermediate in their routes.<sup>7–13</sup> The possible methodologies for intramolecular oxidative enolization are single electron transfer mechanism, Cu(I) mediated cyclization, and oxidative dearomatization approaches.<sup>14–18</sup> The latter pathway is extensively utilized for total synthesis of indoline alkaloids,<sup>16,19–22</sup> Lu and co-workers applied the same approach with ester-tethered  $\beta$ -naphthol **15** using iodine as an oxidant and lithium cyclohexyl isopropyl amide as a strong base (Scheme 1.3).<sup>7</sup> The dearomatized benzofused cyclohexanone **16** was then subjected to Mukaiyama–Michael reaction mediated by tris(pentafluorophenyl)borane and directed by the free



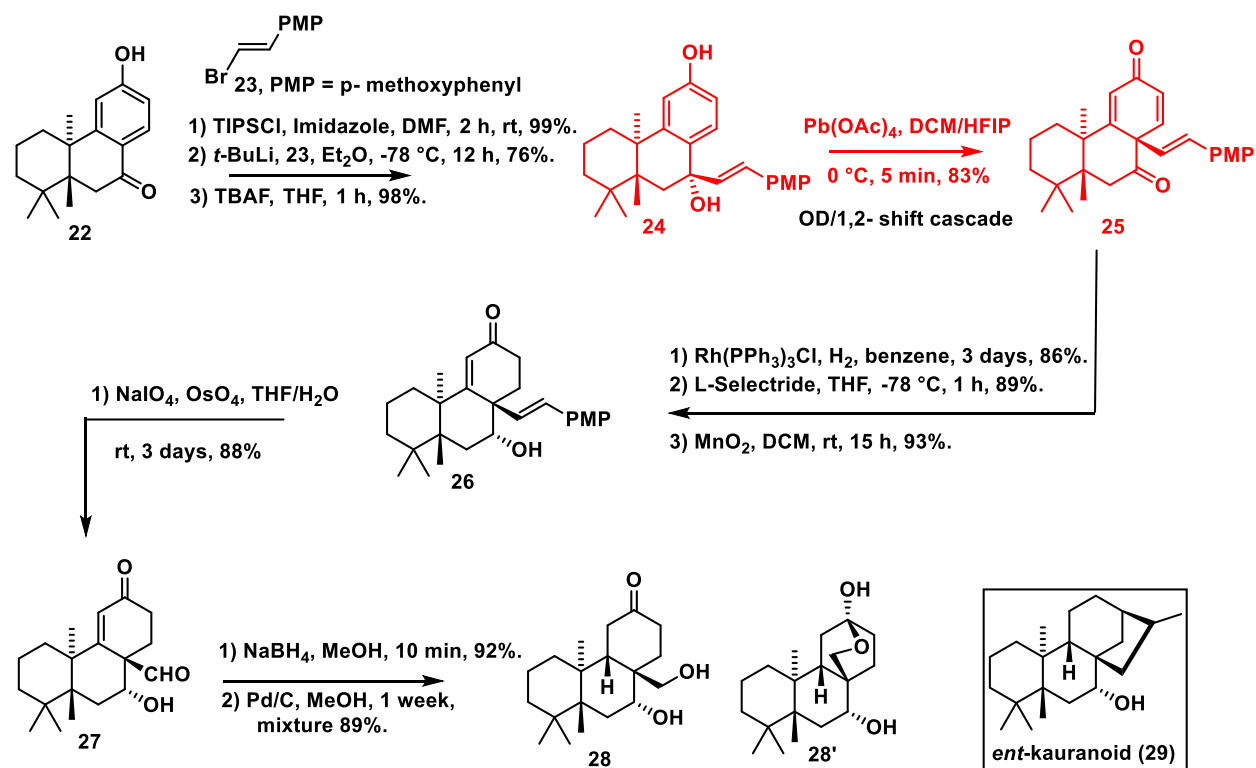
**Scheme 1.2:** Asymmetric total synthesis of callilongisin B (**12**) via OD reaction.

acid of **17**. The daphenylline natural product was isolated after few steps including thioesterification, Fukuyama reduction and a reductive amination/amidation that provides double cyclization, constructing the common motif of *Daphniphyllum* family, azapolycyclic cage-like structure **20**.



**Scheme 1.3:** Total synthesis of (-)-daphenylline (21).

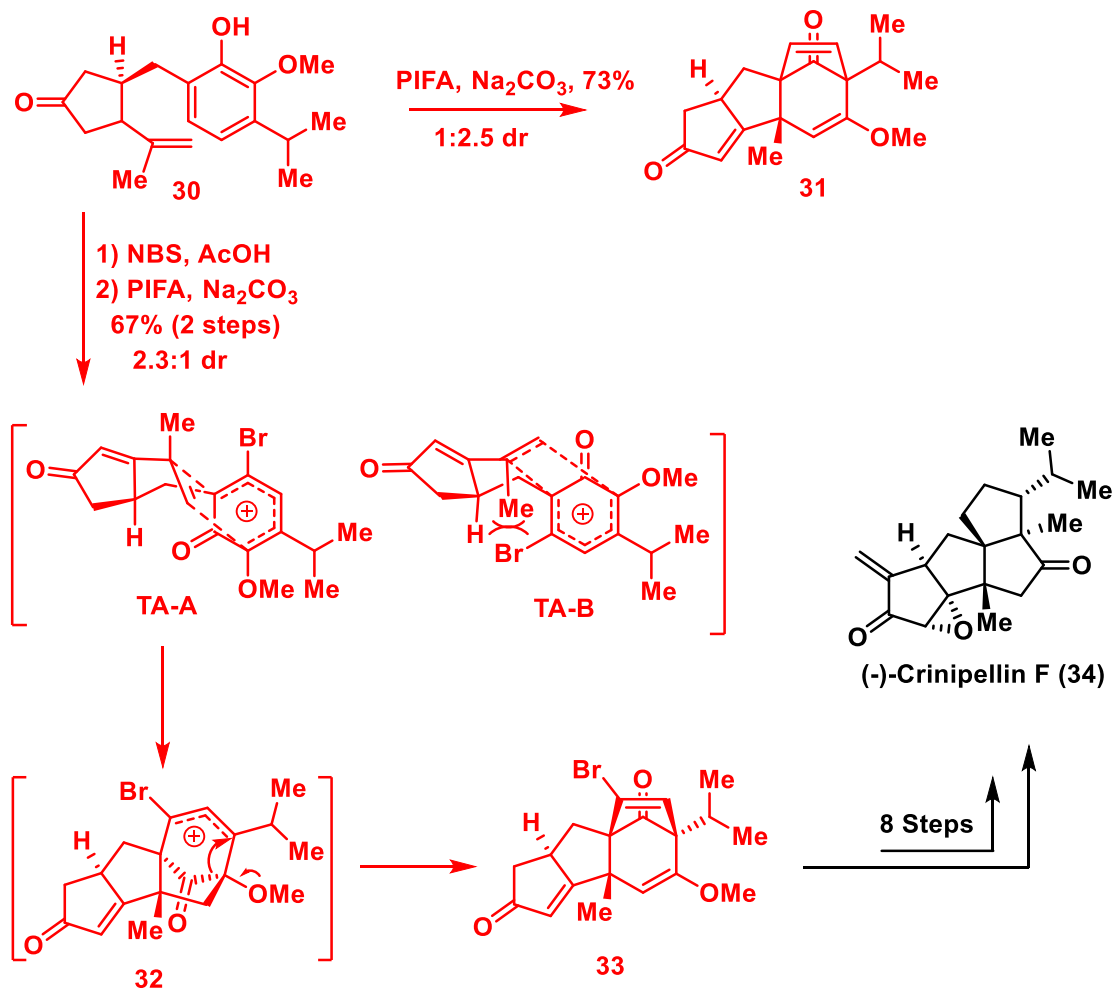
*ent*-Kauranoids are a unique class of diterpenoid natural products, behaving oppositely to the kaurene diterpenoids because of their stereochemistry and negative optical rotation properties.<sup>23</sup> A recent study has developed the OD reactions to construct the core motif of *ent*-kauranoid (29), which is also a precursor for core structures for many other diterpenoids (Scheme 1.4).<sup>24</sup> The OD/1,2- shift cascade has been recognized under phenolic OD condition using lead acetate to effect oxidation to isolate dearomatized product 25. The driving force behind the observed 1,2- chemical shift is the stereoelectronic effect of the tertiary alcohol and a good choice for a designed migrated group. The dearomatized product was subjected to a few more steps to isolate an intermediate bearing same stereochemical relationship as *ent*-kauranoid 28.<sup>24</sup>



**Scheme 1.4:** OD approach towards synthesis core structure of *ent*-kauranoid natural product (29).

Total syntheses of (–)-crinipellins A–F and (–)-dihydrocrinipellins A and B have been achieved with the help of an OD-[5+2] cycloaddition cascade to deliver a key intermediate in the reported approaches by the Ding group (Scheme 1.5).<sup>25</sup> The OD approach promotes intramolecular [5+2] cycloaddition and pinacol rearrangement cascade. Subjecting a vinyl phenol **30** to the OD conditions using PIFA yielded the desired product **31** with an undesired dr ratio (1:2.5), meanwhile introducing a bromine group to the phenyl ring directed the cycloaddition step under the OD conditions in the desired pathway.<sup>25</sup> (–)-Crinipellin F is isolated after eight steps from the polycyclic dearomatized product **33** which is an intermediate and a key step in synthesis the other six natural products within few steps toward each product.

Oxidative dearomatization reactions offer a divergent approach among tetracyclic terpenoid families by inducing the oxidative Wanger-Meerwein rearrangement. Micalizio and co-workers subjected terpenoid **35** to OD conditions facilitating methyl group migration from

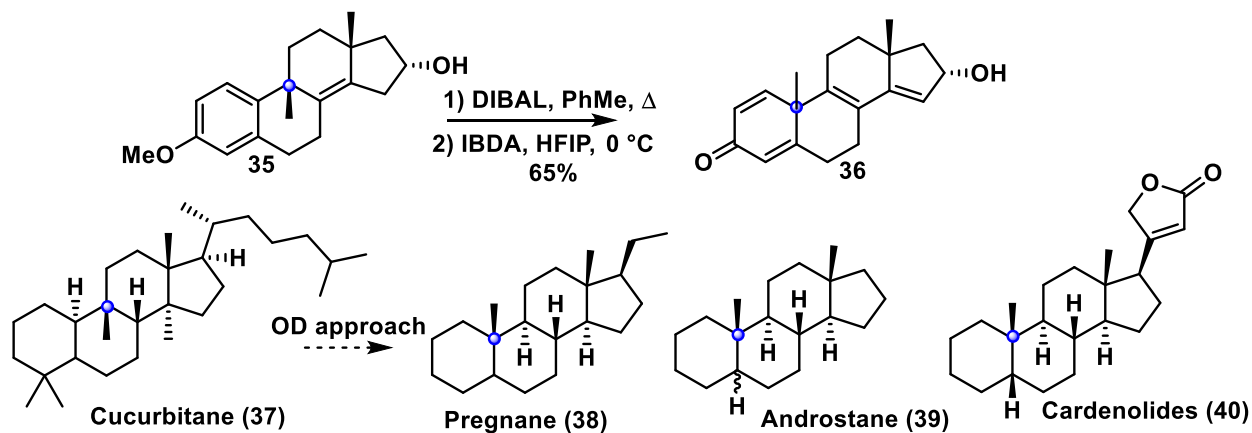


**Scheme 1.5:** Total synthesis (-)-crinipellin F via OD-[5+2] cycloaddition cascade reaction.

C9 to C10, which is less likely to be achieved by semi-pinacol rearrangement.<sup>26–29</sup> They have performed demethylation reaction with DIBAL hydride based on the previously developed methodology for dealkylation of complex sugar and cyclodextrin.<sup>30–32</sup> The authors performed OD reactions for the free phenolic derivatives without mentioning any failures for direct oxidation of anisolic structure **35**. The typical phenolic OD mechanisms generate a phenoxenium cation which is then attacked by a source of nucleophile or alkyl migration as shown in this example. The competition between alkyl group migrations is based on stability of the formed allylic cation, thus methyl group migration provides the more favorable and electronic stable cation. This kind of

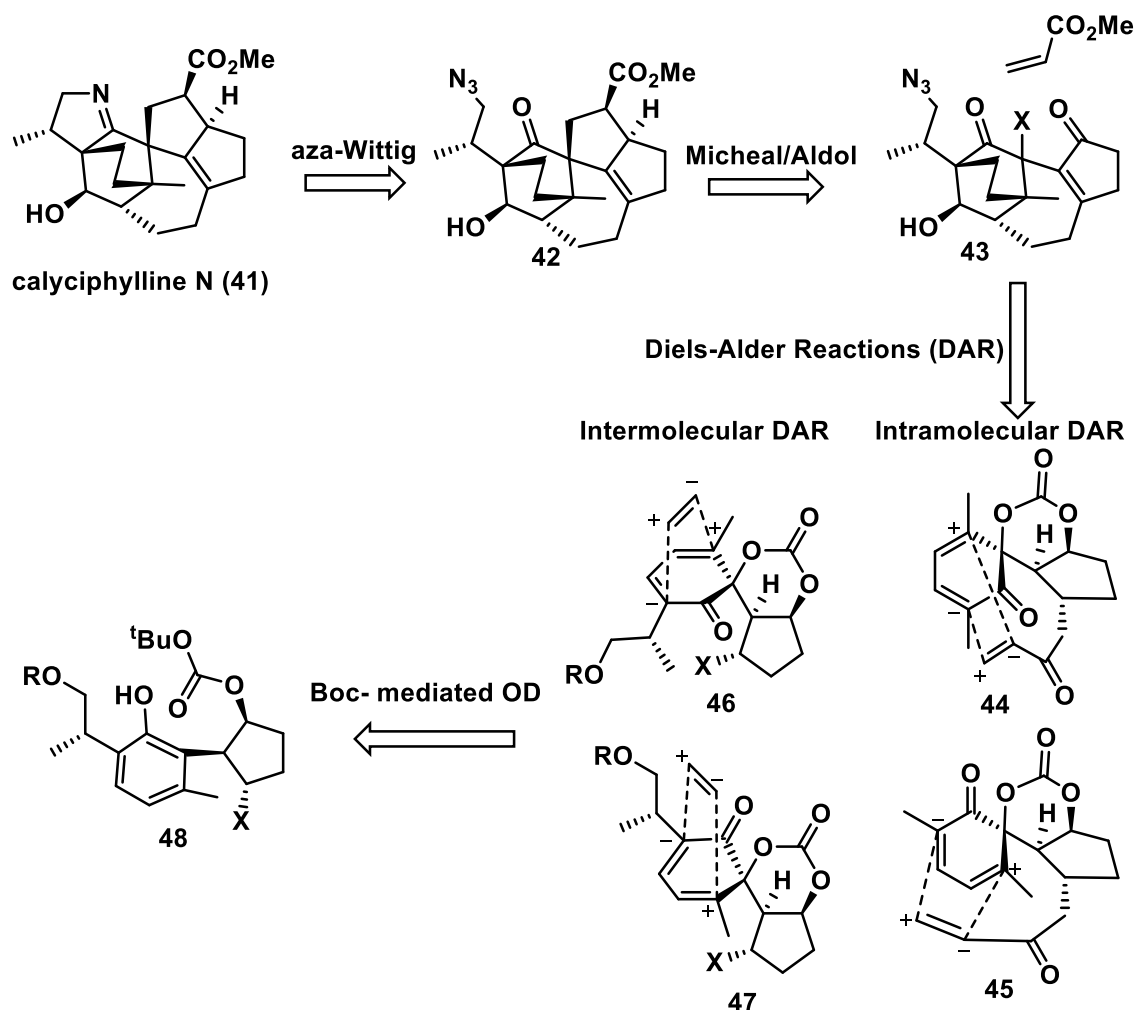


transformation using OD approach will easy access variety of terpenoids as example converting cucurbitanes structures (**37**) into analogues belonging to pregnanes (**38**), androstanes (**39**), and cardenolides (**40**) frameworks (Scheme 1.6).<sup>28</sup>



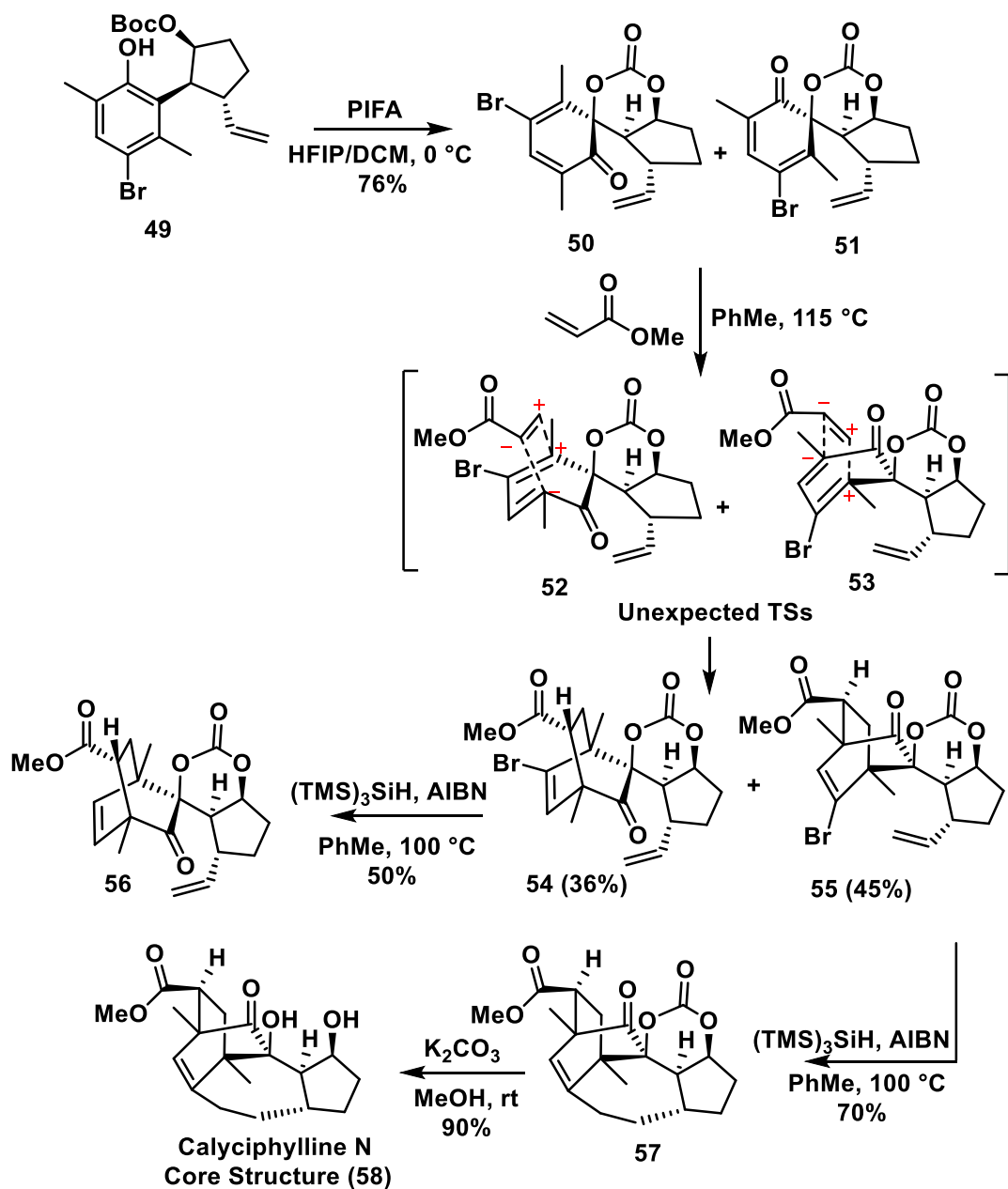
**Scheme 1.6:** Oxidative-dearomatization Wanger-Meerwein rearrangement.

As Robins and Johnson targeted the OD reactions to perform Diels-Alder cyclization, here is another example presented by Zhang group, employing a similar concept of generating an electronic poor diene from a phenolic compound to construct the core structure of calyciphylline N (**41**).<sup>33</sup> The initial proposed retrosynthetic scheme depended on intra- or intermolecular Diels-Alder reaction after formation of dienone from the OD reactions (Scheme 1.7). Unexpectedly, Diels-Alder reactions are highly stereospecific to the unexpected abnormal electronic demand products (Scheme 1.8). Therefore, the initial phenolic substrate was manipulated by introducing a bromine group which was subjected to the late-stage radical cyclization to construct a seven-member ring **57** (Scheme 1.8).<sup>33</sup>

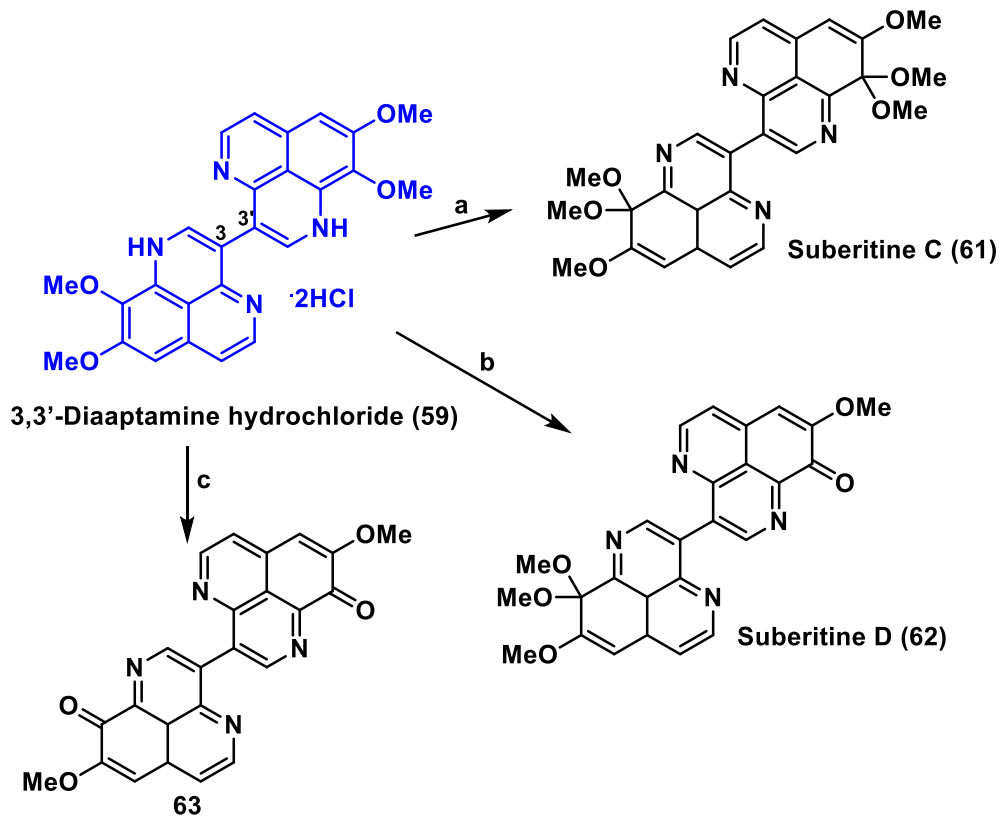


**Scheme 1.7:** Retrosynthetic pathway toward synthesis the core structure of calyciphylline N (**41**).

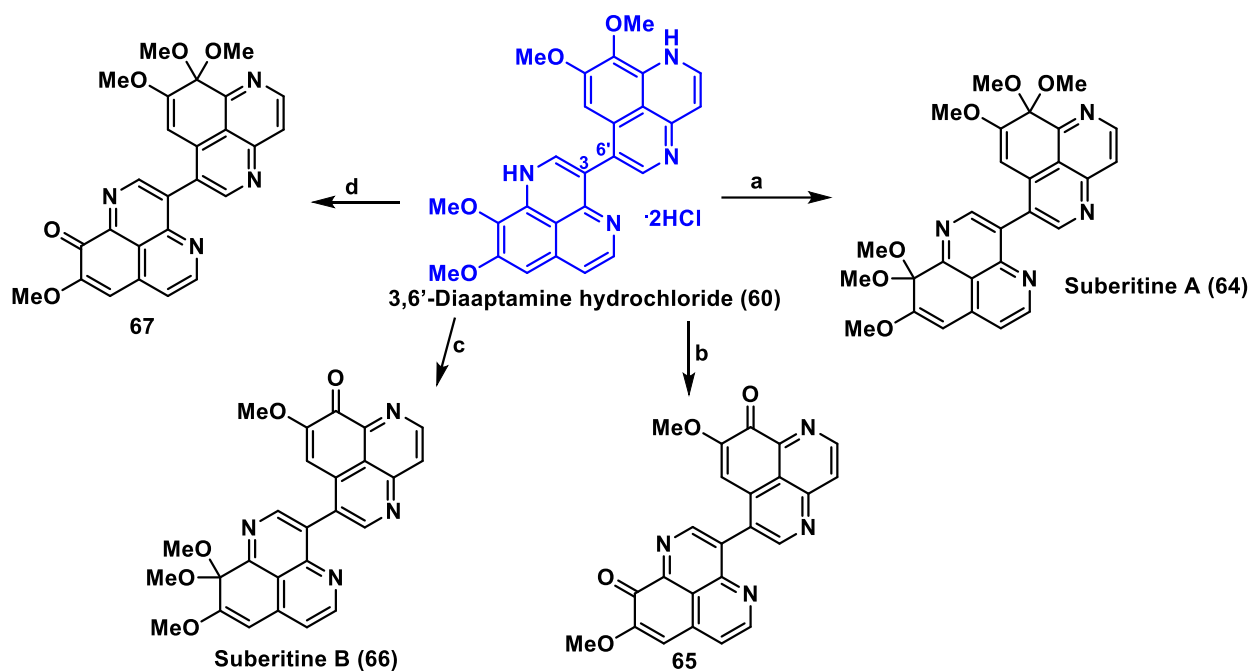
A biomimetic oxidative dearomatization reaction has been utilized in late-stage transformation of 3,3'-diaaptamine hydrochloride (**59**) and 3,6'-diaaptamine hydrochloride (**60**) into number of marine natural products belong to aptaminoid alkaloids. Treating the benzo[de][1,6]-naphthyridines **59** and **60** with IBDA, resulting in partial and full oxidative dearomatization accompanied by mono- and diketalization to provide number of suberitine alkaloids (Scheme 1.9 and 1.10).<sup>34</sup>



**Scheme 1.8:** Synthesis calyciphylline core structure via OD/Diels-Alder reactions as key steps.



**Scheme 1.9:** Synthesis of suberitine C and D from 3,3'-diaaptamine hydrochloride (**59**) via OD reactions. Reagent and conditions: (a) IBDA (3.0 equiv.), MeCN/MeOH (2:1), 0 °C, 3 h, (68%); (b) IBDA (1.5 equiv.), MeCN/H<sub>2</sub>O (2:1), 0 °C, 3 h; then IBDA (1.5 equiv.), HFIP/MeOH (2:1), 0 °C, 3 h, (73%); (c) IBDA (3.0 equiv.), HFIP/H<sub>2</sub>O (2:1), 0 °C, 3 h, (73%).



**Scheme 1.10:** Synthesis of Suberitine A and B from 3,6'-Diaaptamine hydrochloride (**60**) via OD reactions. Reagent and conditions: (a) IBDA (3.0 equiv.), MeCN/MeOH (2:1), 0 °C, 3 h (58%); (b) IBDA (3.0 equiv.), HFIP/H<sub>2</sub>O (2:1), 0 °C, 3 h, (60%); (c) IBDA (1.5 equiv.), MeCN/MeOH (2:1), 0 °C, 3 h; then IBDA (1.0 equiv.), HFIP/H<sub>2</sub>O (2:1), 0 °C, 3 h, suberitine B (30%) and suberitine A (23%); (d) IBDA (1.5 equiv.), MeCN/H<sub>2</sub>O (2:1), 0 °C, 3 h; then IBDA (1.5 equiv.), HFIP/MeOH (2:1), 0 °C, 3 h, (52%).

## 1.2 SUMMARY

Oxidative dearomatization has a potential value as a synthetic methodology towards synthesis complex structures and natural products via formation of a reactive unsaturated ketones or dienes. Through this powerful synthetic method, several natural products have been synthesized annually. In this chapter, we have discussed the reported OD approaches and highlighted the important role of their dearomatized products in the total synthesis of natural products which were published in 2022. Analyzing the rest of these OD synthetic methods during the last decade is ongoing.

### 1.3 REFERENCES

- (1) Mullapudi, V.; Bhogade, R. B.; Deshpande, M. V.; Ramana, C. V. Phenol Oxidative Dearomatization of Modified Nucleoside Templates: A Simple Access to the C7-Spiroannulated Octosyl Acid Framework. *Synthesis (Stuttg)*. **2017**, *49*, 4221–4228.
- (2) Ibrahim, R. K.; Anzellotti, D. Chapter One The Enzymatic Basis of Flavonoid Biodiversity. In *Integrative Phytochemistry: from Ethnobotany to Molecular Ecology*; Romeo, J. T., Ed.; Recent Advances in Phytochemistry; Elsevier, 2003; Vol. 37, pp 1–36. [https://doi.org/https://doi.org/10.1016/S0079-9920\(03\)80016-3](https://doi.org/https://doi.org/10.1016/S0079-9920(03)80016-3).
- (3) Krische, M. J. Hypervalent Iodine Chemistry: Modern Developments in Organic Synthesis. Topics in Current Chemistry, 224 Edited by T. Wirth (Cardiff University). Springer-Verlag: Berlin, Heidelberg, New York. 2003. x + 264 Pp. \$189.00. ISBN 3-540-44107-7. *J. Am. Chem. Soc.* **2003**, *125* (36), 11136. <https://doi.org/10.1021/ja033530e>.
- (4) The Statistical Is Based on Sci Finder Search Engine Using “Oxidative Dearomatization” Keywords in the First Week of July 2022.
- (5) Robins, J. G.; Johnson, J. S. An Oxidative Dearomatization Approach to Tetrodotoxin via a Masked Ortho-Benzoquinone. *Org. Lett.* **2022**, *24* (2), 559–563. <https://doi.org/10.1021/acs.orglett.1c03998>.
- (6) Kamiya, A.; Kawamoto, Y.; Kobayashi, T.; Ito, H. Asymmetric Syntheses of Ent-Callilongisins B and C. *Tetrahedron* **2022**, *111*, 132712. <https://doi.org/https://doi.org/10.1016/j.tet.2022.132712>.
- (7) Cao, M.-Y.; Ma, B.-J.; Gu, Q.-X.; Fu, B.; Lu, H.-H. Concise Enantioselective Total Synthesis of Daphenylline Enabled by an Intramolecular Oxidative Dearomatization. *J. Am. Chem. Soc.* **2022**, *144* (13), 5750–5755. <https://doi.org/10.1021/jacs.2c01674>.
- (8) Zhang, W.; Ding, M.; Li, J.; Guo, Z.; Lu, M.; Chen, Y.; Liu, L.; Shen, Y.-H.; Li, A. Total Synthesis of Hybridaphniphylline B. *J. Am. Chem. Soc.* **2018**, *140* (12), 4227–4231. <https://doi.org/10.1021/jacs.8b01681>.
- (9) Lu, Z.; Li, Y.; Deng, J.; Li, A. Total Synthesis of the Daphniphyllum Alkaloid Daphenylline. *Nat. Chem.* **2013**, *5* (8), 679–684. <https://doi.org/10.1038/nchem.1694>.
- (10) Yamada, R.; Adachi, Y.; Yokoshima, S.; Fukuyama, T. Total Synthesis of (–)-Daphenylline. *Angew. Chemie Int. Ed.* **2016**, *55* (20), 6067–6070. <https://doi.org/https://doi.org/10.1002/anie.201601958>.
- (11) Chen, X.; Zhang, H.-J.; Yang, X.; Lv, H.; Shao, X.; Tao, C.; Wang, H.; Cheng, B.; Li, Y.; Guo, J.; Zhang, J.; Zhai, H. Divergent Total Syntheses of (–)-Daphnilongeranin B and (–)-Daphenylline. *Angew. Chemie Int. Ed.* **2018**, *57* (4), 947–951. <https://doi.org/https://doi.org/10.1002/anie.201709762>.
- (12) Xu, B.; Wang, B.; Xun, W.; Qiu, F. G. Total Synthesis of (–)-Daphenylline. *Angew. Chemie Int. Ed.* **2019**, *58* (17), 5754–5757. <https://doi.org/https://doi.org/10.1002/anie.201902268>.
- (13) Wang, B.; Xu, B.; Xun, W.; Guo, Y.; Zhang, J.; Qiu, F. G. A General Strategy for the Construction of Calyciphylline A-Type Alkaloids: Divergent Total Syntheses of (–)-

- Daphenylline and (-)-Himalensine A. *Angew. Chemie Int. Ed.* **2021**, *60* (17), 9439–9443. <https://doi.org/https://doi.org/10.1002/anie.202016212>.
- (14) Richter, J. M.; Whitefield, B. W.; Maimone, T. J.; Lin, D. W.; Castroviejo, M. P.; Baran, P. S. Scope and Mechanism of Direct Indole and Pyrrole Couplings Adjacent to Carbonyl Compounds: Total Synthesis of Acremoauxin A and Oxazinin 3. *J. Am. Chem. Soc.* **2007**, *129* 42, 12857–12869.
- (15) DeMartino, M. P.; Chen, K.; Baran, P. S. Intermolecular Enolate Heterocoupling: Scope, Mechanism, and Application. *J. Am. Chem. Soc.* **2008**, *130* (34), 11546–11560. <https://doi.org/10.1021/ja804159y>.
- (16) Opatz, T. J. Christoffers, A. Baro: Quaternary Stereocenters – Challenges and Solutions for Organic Synthesis. *Adv. Synth. & Catal.* **2006**, *348*, 593.
- (17) Zi, W.; Zuo, Z.; Ma, D. Intramolecular Dearomative Oxidative Coupling of Indoles: A Unified Strategy for the Total Synthesis of Indoline Alkaloids. *Acc. Chem. Res.* **2015**, *48* (3), 702–711. <https://doi.org/10.1021/ar5004303>.
- (18) Rudolph, A.; Bos, P. H.; Meetsma, A.; Minnaard, A. J.; Feringa, B. L. Catalytic Asymmetric Conjugate Addition/Oxidative Dearomatization Towards Multifunctional Spirocyclic Compounds. *Angew. Chemie Int. Ed.* **2011**, *50* (26), 5834–5838. <https://doi.org/https://doi.org/10.1002/anie.201102069>.
- (19) Zhang, D.; Song, H.; Qin, Y. Total Synthesis of Indoline Alkaloids: A Cyclopropanation Strategy. *Acc. Chem. Res.* **2011**, *44* (6), 447–457. <https://doi.org/10.1021/ar200004w>.
- (20) Zhu, M.; Xu, H.; Zhang, X.; Zheng, C.; You, S.-L. Visible-Light-Induced Intramolecular Double Dearomative Cycloaddition of Arenes. *Angew. Chemie Int. Ed.* **2021**, *60* (13), 7036–7040. <https://doi.org/https://doi.org/10.1002/anie.202016899>.
- (21) Lin, Z.; Xue, Y.; Liang, X.-W.; Wang, J.; Lin, S.; Tao, J.; You, S.-L.; Liu, W. Oxidative Indole Dearomatization for Asymmetric Furoindoline Synthesis by a Flavin-Dependent Monooxygenase Involved in the Biosynthesis of Bicyclic Thiopeptide Thiostrepton. *Angew. Chemie Int. Ed.* **2021**, *60* (15), 8401–8405. <https://doi.org/https://doi.org/10.1002/anie.202013174>.
- (22) Liu, X.; Yan, X.; Tang, Y.; Jiang, C.-S.; Yu, J.-H.; Wang, K.; Zhang, H. Direct Oxidative Dearomatization of Indoles: Access to Structurally Diverse 2-,3-Disubstituted Indolin-3-Ones. *Chem. Commun.* **2019**, *55* (46), 6535–6538. <https://doi.org/10.1039/C9CC02956G>.
- (23) Wu, Y.-C. New Research and Development on the Formosan Annonaceous Plants. In *Studies in Natural Products Chemistry*; Atta-ur-Rahman, Ed.; Studies in Natural Products Chemistry; Elsevier, 2006; Vol. 33, pp 957–1023. [https://doi.org/https://doi.org/10.1016/S1572-5995\(06\)80044-X](https://doi.org/https://doi.org/10.1016/S1572-5995(06)80044-X).
- (24) Imamura, Y.; Mizutani, H.; Nakada, M. Construction of Successive Stereogenic Centers of Ent-Kauranoid through an Oxidative Dearomatization/1,2-Shift Cascade. *Synlett* **2022**, No. EFirst.
- (25) Zhao, Y.; Hu, J.; Chen, R.; Xiong, F.; Xie, H.; Ding, H. Divergent Total Syntheses of (-)-Crinipellins Facilitated by a HAT-Initiated Dowd–Beckwith Rearrangement. *J. Am. Chem.*

- Soc.* **2022**, *144* (6), 2495–2500. <https://doi.org/10.1021/jacs.1c13370>.
- (26) Guérard, K. C.; Guérinot, A.; Bouchard-Aubin, C.; Menard, M.; Lepage, M. L.; Beaulieu, M. A.; Canesi, S. Oxidative 1,2- and 1,3-Alkyl Shift Processes: Developments and Applications in Synthesis. *J. Org. Chem.* **2012**, *77* (5), 2121–2133.
- (27) Epstein, O. L.; Cha, J. K. Rapid Access to the “in,out”-Tetracyclic Core of Ingenol. *Angew. Chemie* **2004**, *44* (1), 121–123.
- (28) Jørgensen, L.; McKerrall, S. J.; Kuttruff, C. A.; Ungeheuer, F.; Felding, J.; Baran, P. S. 14-Step Synthesis of (+)-Ingenol from (+)-3-Carene. *Science* (80-. ). **2013**, *341* (6148), 878–882. <https://doi.org/10.1126/science.1241606>.
- (29) Nicholson, J. M.; Millham, A. B.; Bucknam, A. R.; Markham, L. E.; Sailors, X. I.; Micalizio, G. C. General Enantioselective and Stereochemically Divergent Four-Stage Approach to Fused Tetracyclic Terpenoid Systems. *J. Org. Chem.* **2022**, *87* (5), 3352–3362. <https://doi.org/10.1021/acs.joc.1c02979>.
- (30) Xiao, S.; Yang, M.; Sinaÿ, P.; Blériot, Y.; Sollogoub, M.; Zhang, Y. Diisobutylaluminium Hydride (DIBAL-H) Promoted Secondary Rim Regioselective Demethylations of Permethylated  $\beta$ -Cyclodextrin: A Mechanistic Proposal. *European J. Org. Chem.* **2010**, *2010* (8), 1510–1516. <https://doi.org/https://doi.org/10.1002/ejoc.200901230>.
- (31) Guieu, S.; Sollogoub, M. Multiple Homo- and Hetero-Functionalizations of  $\alpha$ -Cyclodextrin through Oriented Deprotections. *J. Org. Chem.* **2008**, *73* (7), 2819–2828. <https://doi.org/10.1021/jo7027085>.
- (32) Lecourt, T.; Herault, A.; Pearce, A. J.; Sollogoub, M.; Sinaÿ, P. Triisobutylaluminium and Diisobutylaluminium Hydride as Molecular Scalpels: The Regioselective Stripping of Perbenzylated Sugars and Cyclodextrins. *Chem. – A Eur. J.* **2004**, *10* (12), 2960–2971. <https://doi.org/https://doi.org/10.1002/chem.200305683>.
- (33) Lv, Y.; Feng, Y.; Dai, J.; Zhang, Y.; Zhang, H.; Liu, Z.; Zheng, H. Synthesis of the [6.6.7.5] Tetracyclic Core of Calyciphylline N via a Boc-Mediated Oxidative Dearomatization/Diels–Alder Approach. *Org. Lett.* **2022**, *24* (14), 2694–2698. <https://doi.org/10.1021/acs.orglett.2c00797>.
- (34) Tang, S.; Wu, Z.; Gao, M.; Li, G.; Yao, Z.-J. Total Synthesis of Suberitines A–D Featuring Tunable Biomimetic Late-Stage Oxidative Dearomatization and Acetalization. *Chem. – A Eur. J.* **2022**, *28* (24), e202200644. <https://doi.org/https://doi.org/10.1002/chem.202200644>.



**CHAPTER TWO: DEAROMATIZING SPIROCYCLIZATION OF THIOUREAS,  
UREAS AND GUANIDINES**

Marian N. Aziz <sup>a,b</sup>, Ravi P. Singh <sup>a</sup>, Delphine Gout <sup>a</sup>, Carl J. Lovely <sup>a</sup>

a. Department of Chemistry and Biochemistry, 700 Planetarium Place, University of Texas at  
Arlington, TX 76019, USA

b. Department of Pesticide Chemistry, National Research Centre, Dokki, Giza 12622, Egypt

Corresponding author

Prof. Carl J. Lovely

Professor, Chemistry and Biochemistry Department

University of Texas at Arlington

Address: 700 Planetarium Place, Box 19065, UT Arlington, TX 76019-0065

Email: lovely@uta.edu

Phone: +1 817 272 5446

(Partially Published)

## ABSTRACT

An investigation of the dearomatization reactions of benzylic thioureas, ureas and guanidines using hypervalent iodine reagents is described. Initial attempts to perform this reaction with methyl aryl ethers was compromised by electrophilic addition leading to the formation of benzo[*d*]thiazoles. However, inverting the direction of the process and oxidizing the corresponding phenol delivered the desired spiro fused heterocycles in moderate to good yield.

## 2.1 INTRODUCTION

Dearomatization has emerged as a powerful strategy for the construction of highly functionalized frameworks which are primed for further elaboration.<sup>1-4</sup> In particular, oxidative methods to effect dearomatization have attracted significant attention; typically this involves the reaction of a phenol with a hypervalent iodine reagent followed by nucleophilic trapping thus generating a 4,4-disubstituted cyclohexadienone.<sup>1-3</sup> Most frequently, amides, carboxylic acids, and alcohols have served as the trap, although alkynes<sup>5</sup> and alkenes<sup>6</sup> can also be used (Figure 2.1a). When this reaction is conducted intramolecularly, it gives rise to spiro fused derivatives. In connection with an approach to the *Leucetta* derived alkaloids,<sup>7</sup> spirocalcaridines A (**1**) and B (**2**),<sup>8</sup> the Lovely group has reported a tandem oxidative amination dearomatizing spirocyclization (TOADS) reaction of propargyl guanidines that leads directly to the complete framework of the natural products.<sup>9-11</sup> The use of alkynes had been reported previously in dearomatization reactions, but we were unaware of guanidines (or (thio)ureas)<sup>12</sup> participating in simple dearomatization reactions when we commenced this investigation.<sup>13</sup> Further, cyclic guanidines are prevalent structural motifs in marine derived natural products<sup>14</sup> and there are numerous examples of spiro fused systems.<sup>15-17</sup> One particularly attractive target, KB343 (**3**), contains two spiro fused guanidines that may be accessible by such a dearomatizing spirocyclization.<sup>18</sup>

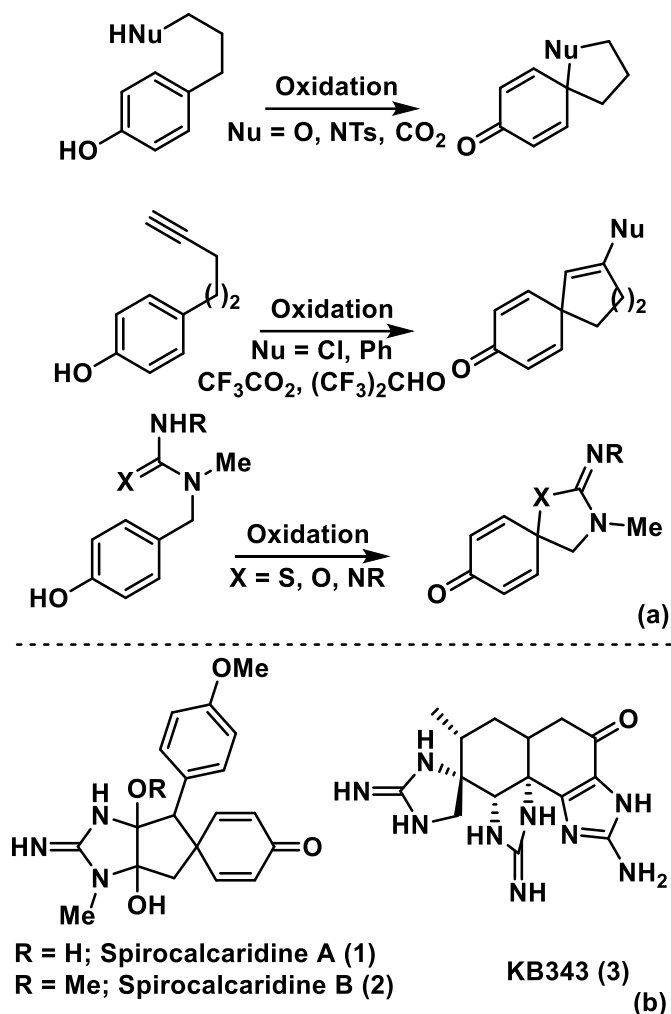
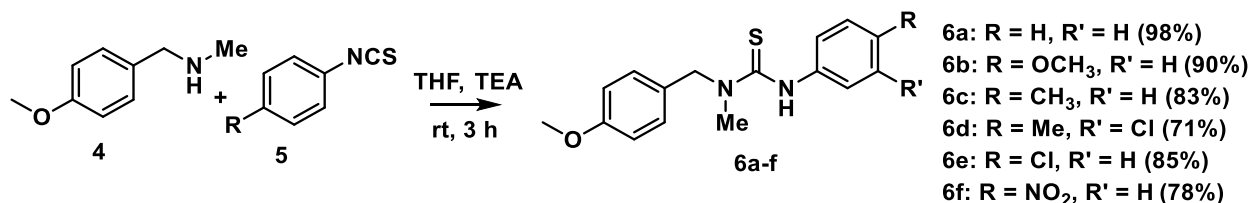


**Figure 2.1:** Dearomatization reactions.

The group previously employed propargyl guanidine and urea derivatives containing a *p*-methoxybenzene moiety and proposed that a nitrenium equivalent triggered the cascade process.<sup>11</sup> In addition, it was found in this earlier investigation that propargyl thioureas were prone to hydrothiolation<sup>19-20</sup> and did not participate in the TOADS chemistry<sup>11</sup> and thus our proposed study would also permit us to establish the utility of thioureas in dearomatization processes.

## 2.2 RESULTS AND DISCUSSION

The investigation was initiated by examining *p*-methoxybenzyl derivatives. Accordingly, *N*-methyl *p*-methoxybenzylamine (**4**) was treated with phenylisothiocyanates (**5**) to afford the corresponding thioureas **6a-f** (Scheme 2.1).



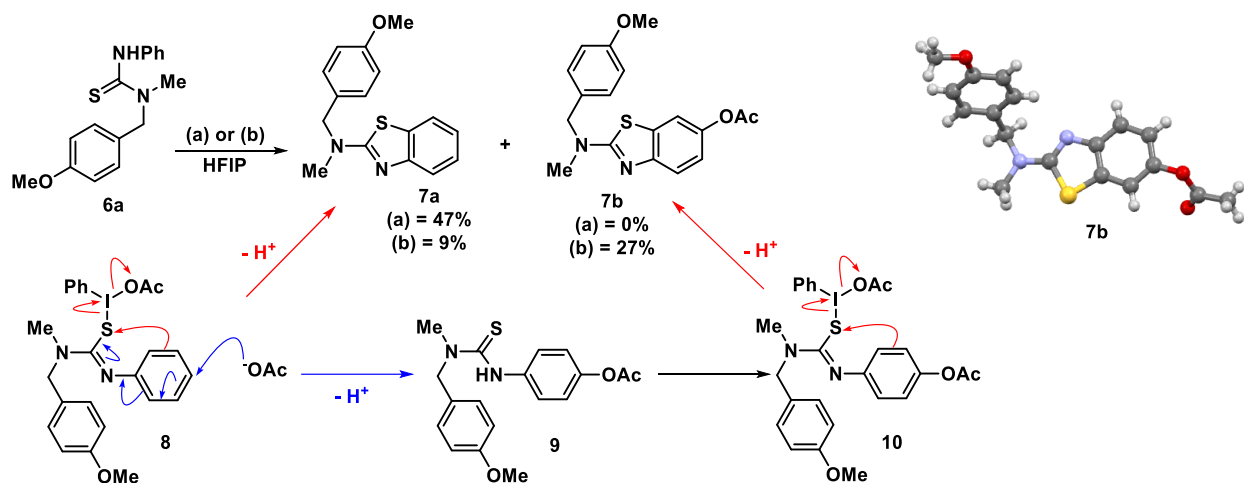
**Scheme 2.1:** Synthesis of the desired thiourea derivatives **6a-f** using *N*-methyl *p*-methoxybenzylamine (**4**).

The substrate was then treated with iodosobenzene diacetate (IBDA) under specific conditions (Cs<sub>2</sub>CO<sub>3</sub>, hexafluoroisopropanol, HFIP) previously utilized in TOADS chemistry. However, the desired dearomatized product was not obtained but rather benzothiazole **7a** was formed via electrophilic aromatic substitution in 47% yield (Scheme 2.2).<sup>21-22</sup> Increasing the oxidant equivalents did not increase the yield but resulted in the formation of acetylated product **7b** (X-ray) in addition to benzothiazole **7a** (Scheme 2.2).

### 2.2.1 Putative mechanism for benzothiazole and acetated benzothiazole isolation

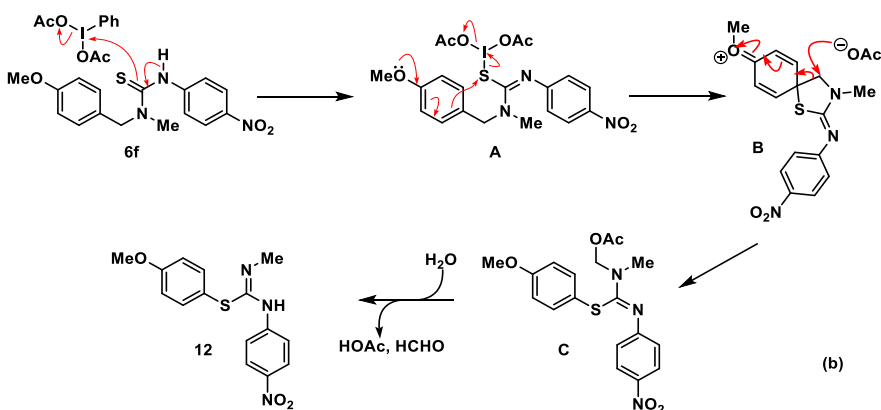
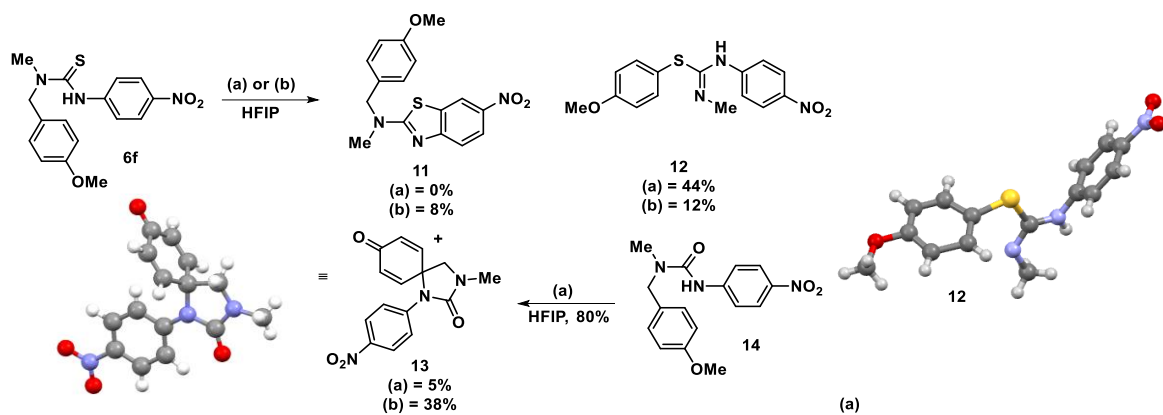
Presumably, this outcome is the result of activation of the sulfur of the thiourea via **8** which can then undergo electrophilic aromatic substitution to afford **7a** or alternatively addition of acetate followed by rearomatization to afford **9** (Scheme 2.2a).<sup>23</sup> The acetylated derivative undergoes a second oxidation at sulfur to trigger the formation of the thiazole. To circumvent this possibility, a thiourea derivative was prepared in which electrophilic substitution was less likely or not possible (Scheme 2.2b). In the case where a deactivated aromatic was employed, a spiro fused product was obtained, but interestingly it was the cyclic urea **13** (X-ray) rather than the expected thiourea or thiazole (Scheme 2.3a). Presumably, oxidation of the thiourea **6e** to the urea **14**

proceeds oxidative dearomatization. A control reaction with the corresponding urea derivative **14** confirms that it is at least a competent substrate. In addition to the urea, two further products were obtained including the benzothiazole **11** and the isothio urea **12** (X-ray).

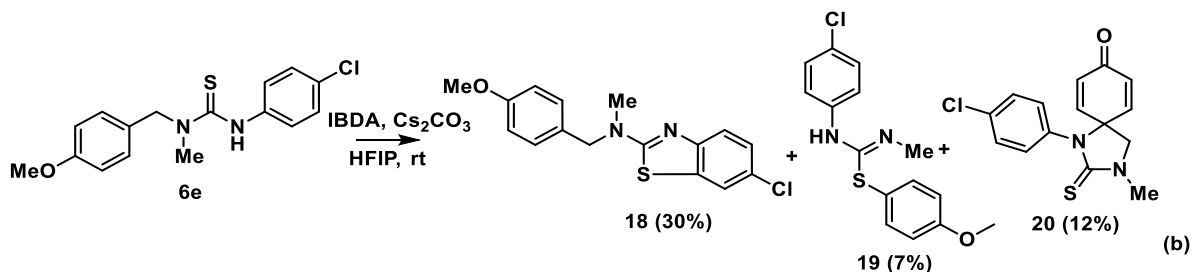
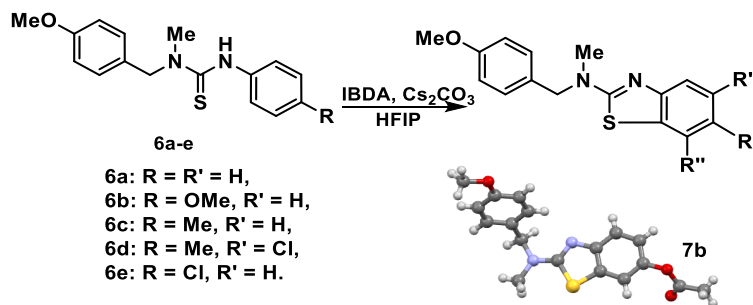


**Scheme 2.2:** Preliminary dearomatization experiments (conditions (a) = IBDA (1 equiv), Cs<sub>2</sub>CO<sub>3</sub> (1.2 equiv), HFIP; (b) = IBDA (2 equiv), Cs<sub>2</sub>CO<sub>3</sub> (1.2 equiv), HFIP).

Moreover, we have isolated a benzothiazole ring system as a major product using electron-rich isothiocyanate derivatives or less deactivated derivatives as shown in Scheme 4a and Table 1, affording new methodology towards this biologically active scaffold. Interestingly, the reaction of 3-(4-chlorophenyl)-1-(4-methoxybenzyl)-1-methylthiourea (**6e**) yielded three different products. Inversely to the reaction of thiourea **6f**, the corresponding benzothiazole **18** as a major product, isothiourea derivative **19**, and spiro cyclic thiourea spiro system **20** were isolated (assignment based on <sup>13</sup>C NMR study compared to **13**) (Scheme 2.4b). The biological activity of the isolated benzothiazoles has been discussed in chapter five.



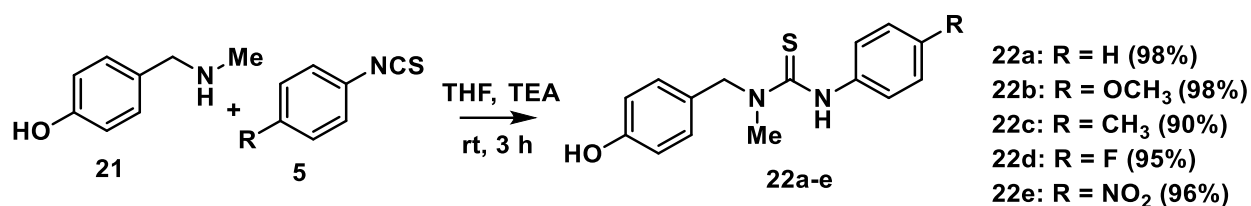
**Scheme 2.3:** Dearomatization of deactivated thiourea (conditions (a) = IBDA (1 equiv),  $\text{Cs}_2\text{CO}_3$  (1.2 equiv), HFIP; (b) = IBDA (2 equiv),  $\text{Cs}_2\text{CO}_3$  (1.2 equiv), HFIP). a)- Oxidative dearomatization reaction on deactivated thiourea **6f**. b)- Putative mechanism for the formation of isothiurea **12**.



**Scheme 2.4:** The isolated benzothiazoles using hypervalent iodine chemistry.

### 2.2.2 Phenolic derivatives subjected to oxidative dearomatization (OD) reactions

Given that oxidation to form nitrenium-like intermediates was compromised by addition to the *N*-aryl substituent we considered changing the role of the thiourea to serving as a nucleophilic trap and oxidizing the phenol, essentially employing an umpolung tactic. Accordingly, the corresponding phenol derivative **22a** was constructed using 4-((methylamino)methyl) phenol (**21**) and phenyl isothiocyanate (**5**) in the presence of triethylamine as a base and tetrahydrofuran or methylene chloride as a solvent at room temperature. Scheme 2.5 shows all the targeted thioureas derived from phenolic amines. 1-(4-Hydroxybenzyl)-1-methyl-3-phenylthiourea (**22a**) was subjected to oxidation with IBDA and Cs<sub>2</sub>CO<sub>3</sub> in HFIP (hexafluoro isopropanol) conditions used in our previous studies. It is important to indicate that the dearomatization occurred in moderate yield (entry 1, Table 2.2). The influence of reaction solvents was observed in TOADS chemistry, and reactions conducted in HFIP provided better yields than dichloromethane or acetonitrile (entries 2-3, Table 2.2). The identity of the solvent used is very important in this chemistry because the formation of a reactive phenoxonium cation is followed by nucleophilic attack. Therefore, the selected solvent must be non-nucleophilic.<sup>8b</sup>



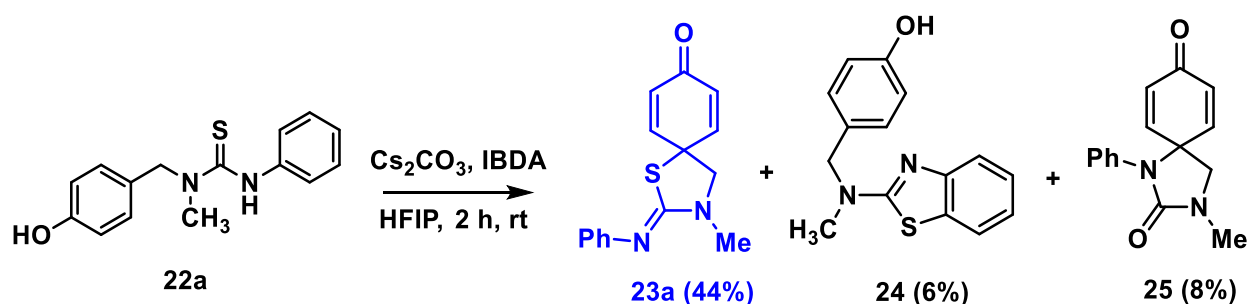
**Scheme 2.5:** Synthesis the targeted phenolic thioureas (**22a-e**).

**Table 2.1:** Benzothiazoles derived from oxidation of thiourea mediated by hypervalent iodine.

	Thiourea derivative	IBDA molar equivalents	Benzothiazoles				Yield (%) <sup>*</sup>
			Compound	R	R'	R''	
1	6a	2.0	7a	H	H	H	11
2	6a	1.0	7a	H	H	H	47
3	6a	2.0	7b	OAc	H	H	27
4	6b	2.0	15a	OMe	H	H	23
5	6b	2.0	15b	OMe	H	OAc	14
6	6b	1.0	15a	OMe	H	H	65
7	6c	2.0	16	Me	H	H	20
8	6c	1.0	16	Me	H	H	19
9	6d	1.0	17	Me	Cl	H	22
10	6e	1.0	18	Cl	H	H	30

\*) Isolated yields by column chromatography.

With the success of this preliminary reaction a screen of other reaction conditions was conducted using both inorganic bases ( $\text{Cs}_2\text{CO}_3$ ,  $\text{NaHCO}_3$ ) or an organic base (N-methylmorpholine = NMM) and different solvents (entries 1-9, Table 2.2). Out of the three bases evaluated,  $\text{Cs}_2\text{CO}_3$  delivered the best yields, but ultimately it was determined that base was not required (Table 2.2, entry 10). On isolating the product from this final set of conditions the desired spiro thiazoline **23a** (X-ray) was obtained in 44% yield (Scheme 2.6 and 2.7) along with small amounts of the benzothiazole **24** (X-ray) and spiro imidazolidinone **25**.

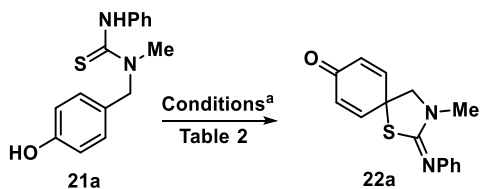
**Scheme 2.6:** OD reactions of phenolic thiourea (**22a**) providing S and N spiro-cyclization.

On increasing the equivalents of the oxidant to 1.5, **23a** was now obtained in 55% yield (Scheme 2.7), along with small amounts of the 4-acetoxy adduct **26** (X-ray). When the reaction



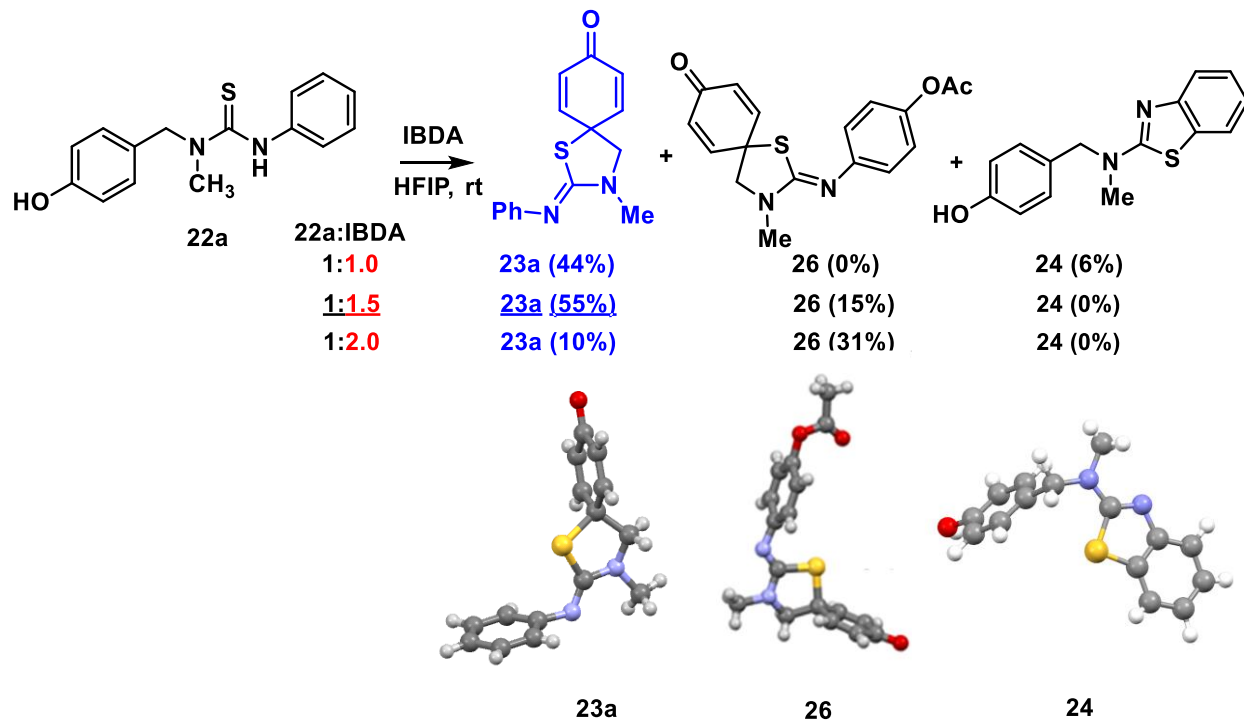
was conducted with 2.0 molar equivalents of IBDA, the spiro 4-acetoxyated product **26** was now isolated as the major product (31%).

**Table 2.2:** Initial screening experiments



Entry	Oxidant	Base	Solvent	Yield%
<b>1</b>	IBDA	Cs <sub>2</sub> CO <sub>3</sub>	HFIP	43 <sup>b,c</sup>
<b>2</b>	IBDA	Cs <sub>2</sub> CO <sub>3</sub>	DCM	8 <sup>b</sup>
<b>3</b>	IBDA	Cs <sub>2</sub> CO <sub>3</sub>	ACN	36 <sup>b</sup>
<b>4</b>	IBDA	NMM	HFIP	34 <sup>b</sup>
<b>5</b>	IBDA	NMM	DCM	ND
<b>6</b>	IBDA	NMM	ACN	6 <sup>b</sup>
<b>7</b>	IBDA	NaHCO <sub>3</sub>	HFIP	34 <sup>b</sup>
<b>8</b>	IBDA	NaHCO <sub>3</sub>	DCM	10 <sup>b</sup>
<b>9</b>	IBDA	NaHCO <sub>3</sub>	ACN	11 <sup>b</sup>
<b>10</b>	IBDA	No base	HFIP	44 <sup>c</sup>
<b>11</b>	PIFA	No base	HFIP	10 <sup>c</sup>
<b>12</b>	PhI(OTs)OH	No base	HFIP	ND

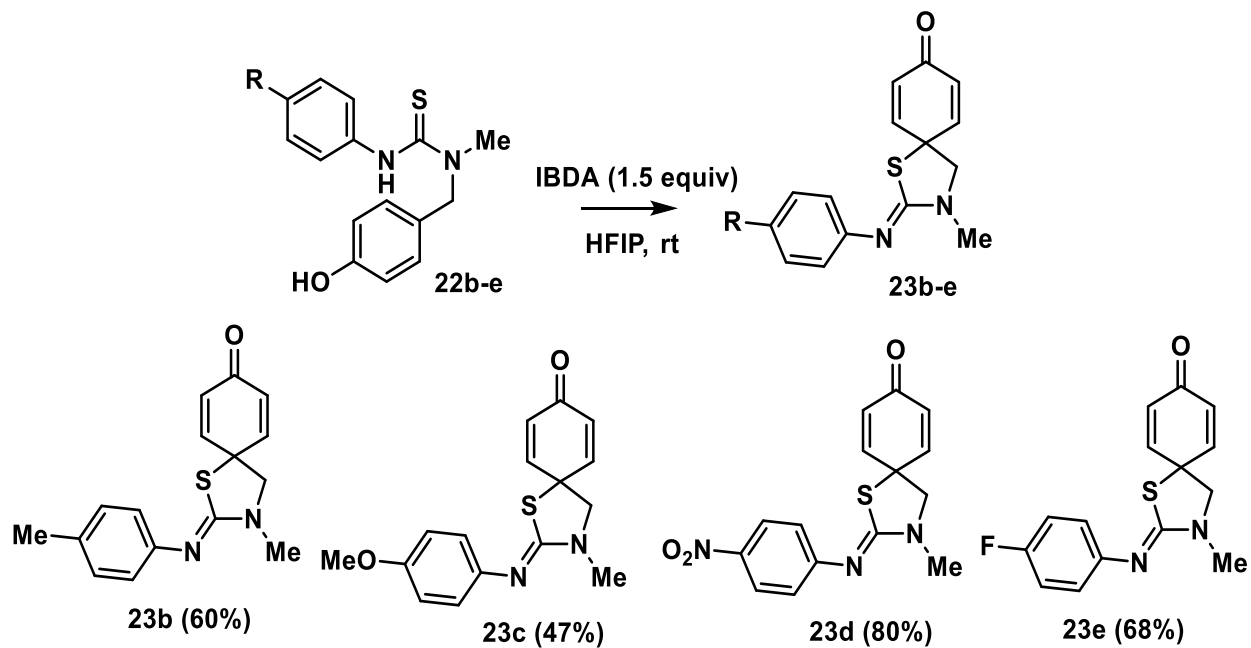
- 21a** (0.1 mmol), IBDA for entries 1-10 (0.1 mmol), for entries 11-12 (0.15 mmol), HFIP (7 mL), rt, 2 h.
- The yield of **22a** compound was determined by <sup>1</sup>H NMR spectroscopy using one equiv of dibromomethane as internal reference.
- Isolated yield after chromatography



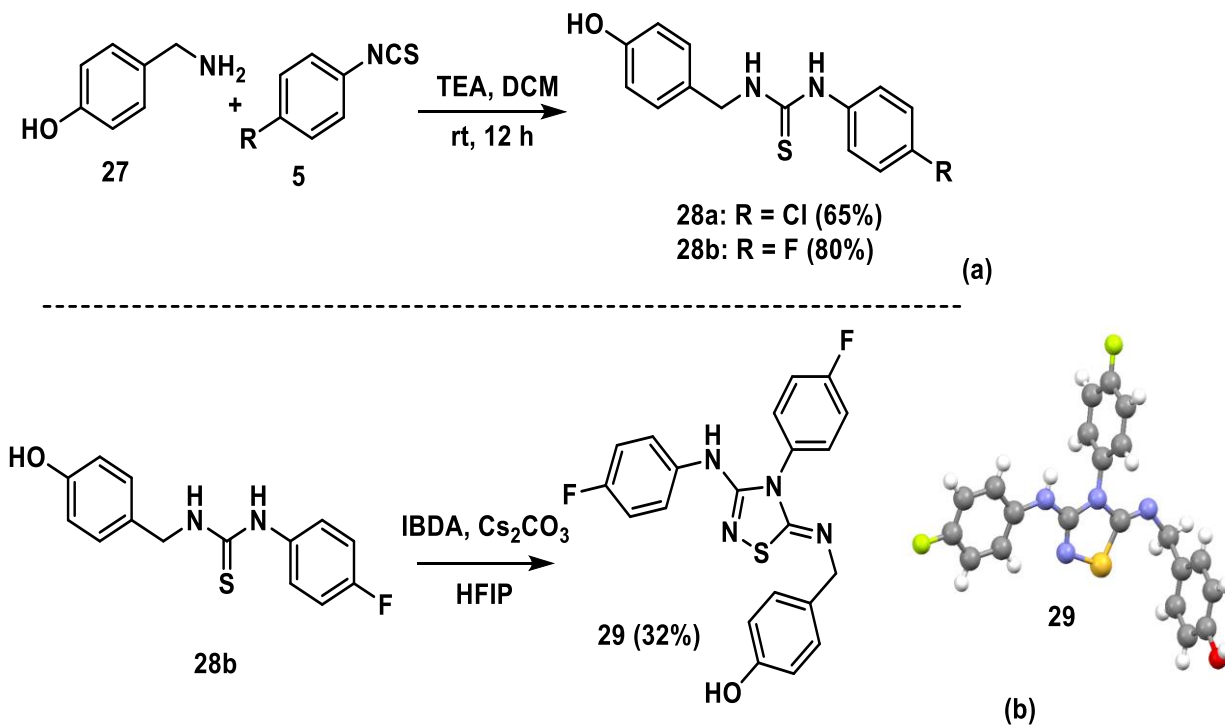
**Scheme 2.7:** Acetylated *S*-spirocyclization reaction of phenolic thiourea (**22a**).

As shown in Scheme 2.8, intramolecular oxidative cyclizations of *N*'-methyl- *N*'-(4-hydroxybenzyl)-*N*-arylthioureas (**22b-e**) via C-S bond formation was examined with four additional thiourea derivatives using these optimized conditions (1.5 equivalents of IBDA) forming (*Z*)-2-((aryl)imino)-3-methyl-1-thia-3-azaspiro[4.5]deca-6,9-dien-8-ones (**23b-e**) in moderate to good yields.

An attempt to extend the spirocyclization was made to a thiourea lacking the *N*-methyl substituent (NH free) **28a-b** which prepared by hydroxybenzyl amine with electron-deficient isothiocyanates **5** (Scheme 2.9a). The synthesized di-substituted thioureas **28a-b** were subjected to oxidation conditions, resulting in multiple unidentified products. Therefore, we were unable to identify any specific product from the reaction with chlorinated thiourea **28**. But we were able to isolate a new thiadiazole ring system (X-ray, Scheme 2.9b) from the reaction with the fluorinated thiourea **28b** rather than the desired spiro derivative.



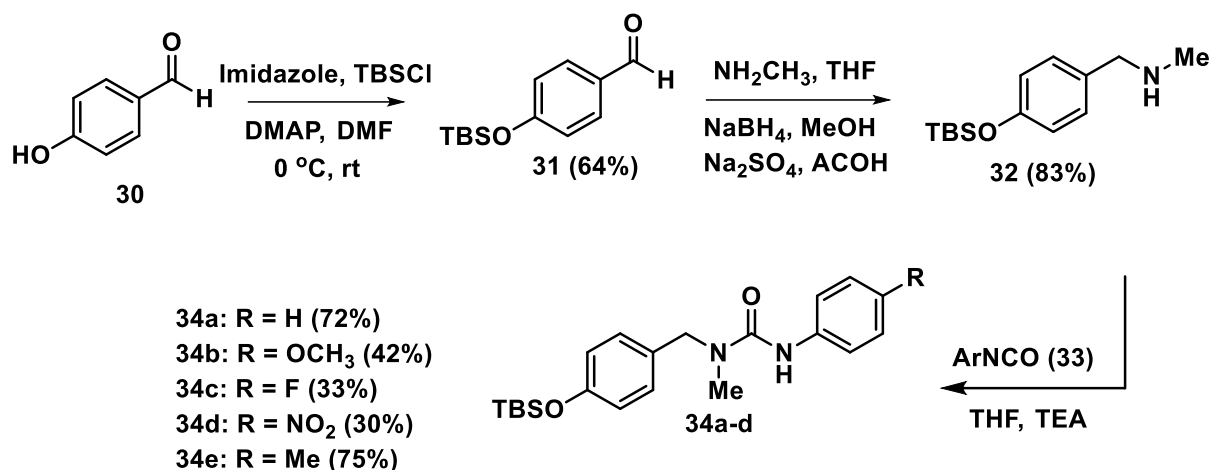
**Scheme 2.8:** Spirothiazolidines derived from OD of phenolic-thiourea derivatives (**22b-e**).



**Scheme 2.9:** Additional products from dearomatizing spirocyclization of phenolic thioureas.

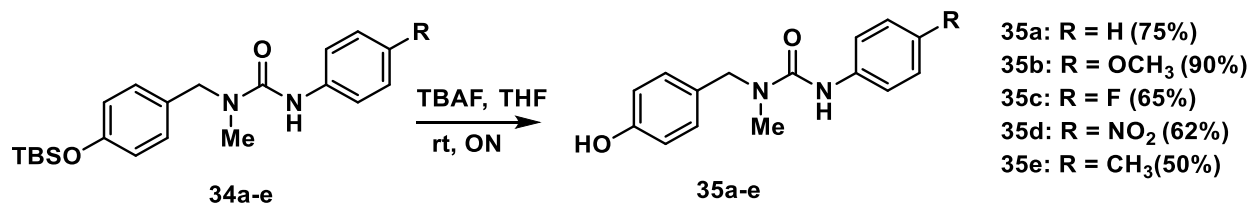
### 2.2.3 Spiro-oxazolidines/imidazolidines derived from OD of phenolic urea derivatives

With this generally positive outcome, cyclohexadienone-spiro-oxazolidine derivatives were obtained using the same optimized conditions. The required substrates could not be assessed directly from the phenolic benzylamine rather through use of a protection and deprotection pathway which provided the targeted ureas **34a-d** (Scheme 2.10). The initial attempts using *p*-hydroxybenzyl amine resulted in formation of multiple and inseparable spots.



**Scheme 2.10:** Synthesis of the targeted masked ureas (**34a-d**).

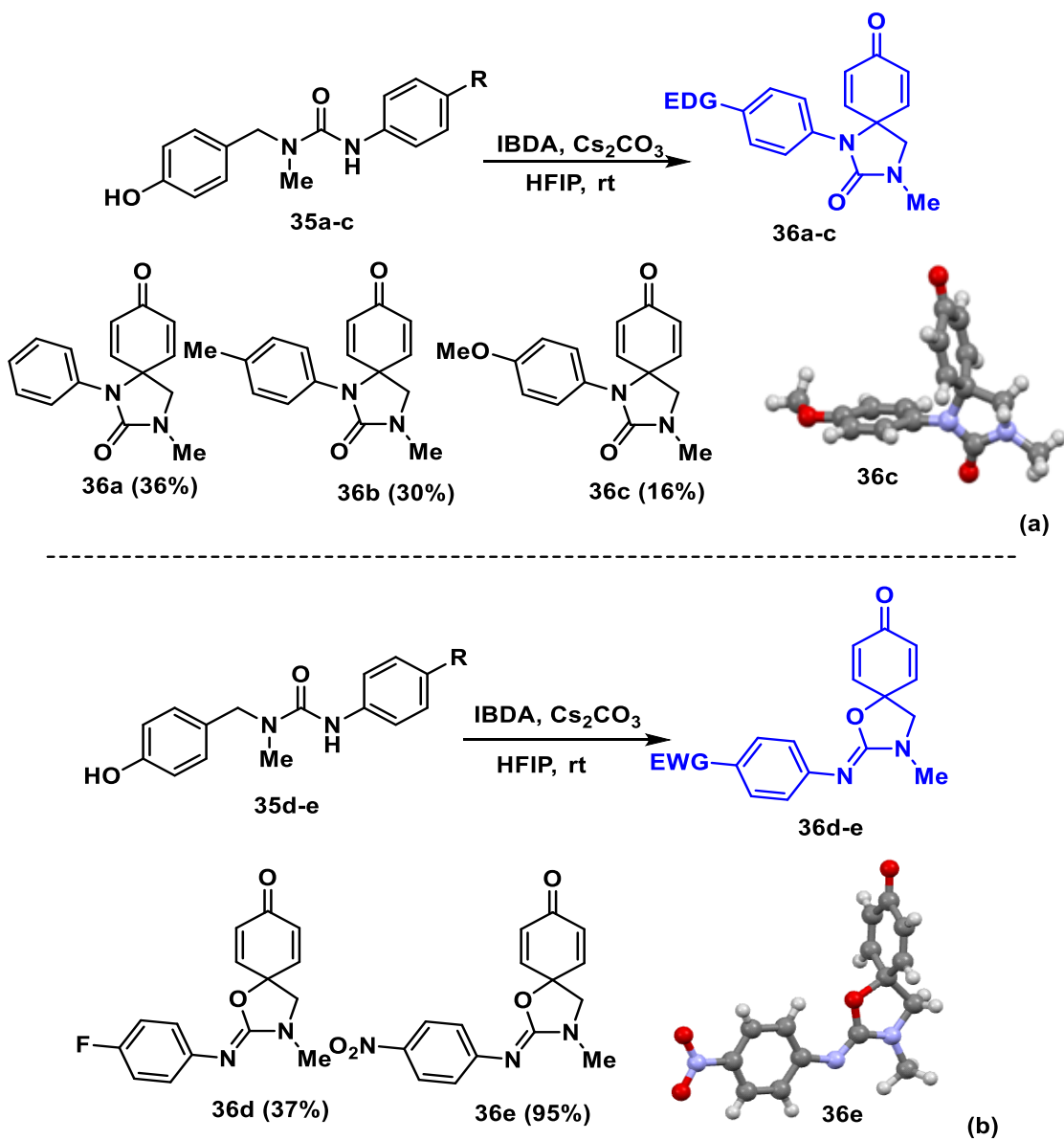
The corresponding urea derivatives **21a-e** were prepared by treating the protected phenolic urea derivatives **13a-d** with TBAF in tetrahydrofuran overnight at rt (Scheme 2.11).



**Scheme 2.11:** The deprotection of masked urea derivatives (**34a-d**).

The oxidative dearomatization conditions were applied to the synthesized urea derivatives. In this case, however, the reactions proceeded better in the presence of Cs<sub>2</sub>CO<sub>3</sub>. All five derivatives produced spiro fused cyclohexadienones (**36a-c**), (**36d-e**) but interestingly, they did

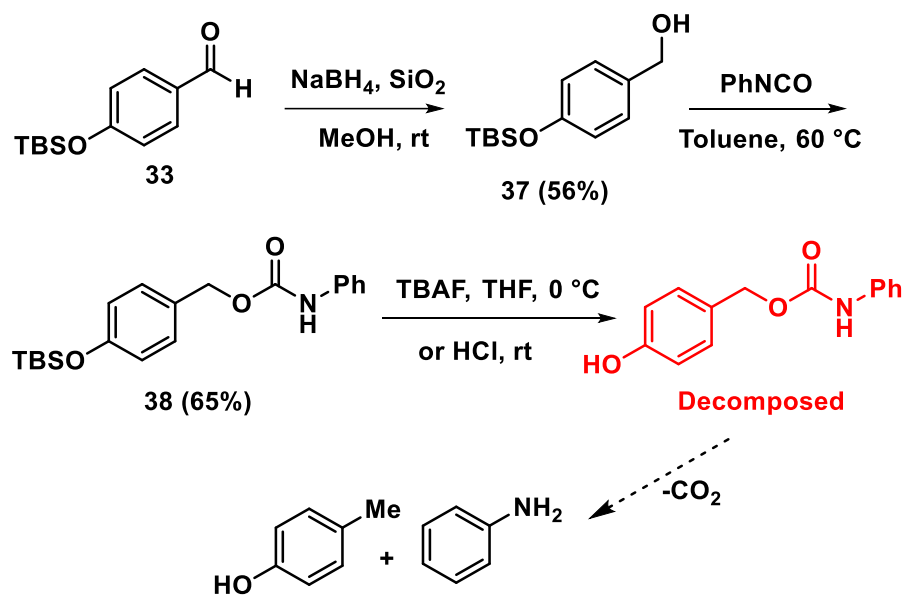
not all cyclize to form the same heterocycle. Ureas **35a-c** with electron-rich aryl groups provided the corresponding imidazolones **36a-c** (Scheme 2.12a) via C-N bond formation whereas those with electron-poor aryl groups **35d-e** cyclized via oxygen affording the oxazolines **36d-e** via O-cyclization (Scheme 2.12b). Connectivities were established either through X-ray crystallography **36c** and **36e** or by comparison of the  $^{13}\text{C}$  NMR chemical shifts of the spiro carbon ( $\delta\text{c} = 59$  (imidazolone) vs  $\delta\text{c} = 75$  (oxazole)).



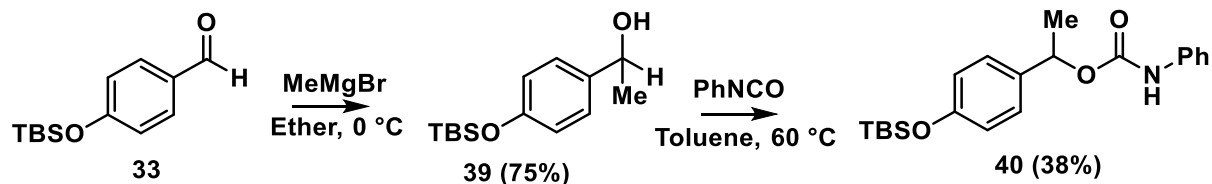
**Scheme 2.12:** Oxidative dearomatization of urea derivatives.

### 2.2.4 Attempts towards synthesis related phenolic carbamate derivatives

Various unsuccessful experiments towards synthesis phenolic carbamate derivatives were carried out to subject it to oxidative dearomatization. Starting with protection of 4-hydroxy benzaldehyde using TBS group, then reduction of aldehydic group using  $\text{NaBH}_4$  to provide benzyl alcohol, which is further subjected to reaction with phenyl isocyanate, yielding the corresponding masked phenolic carbamate **38** (Scheme 2.13). Unfortunately, the carbamate decomposed during the deprotection of silyl group, and it could not be isolated. Therefore, a methyl group was inserted to the benzylic methylene position using  $\text{MeMgBr}$ , producing the corresponding secondary alcohol **39** which was treated with phenyl isocyanate to produce carbamate **40** (Scheme 2.14). The same observation of decomposition of free phenolic carbamate was gained, losing the hope of dearomatizing these targeted carbamate derivatives.



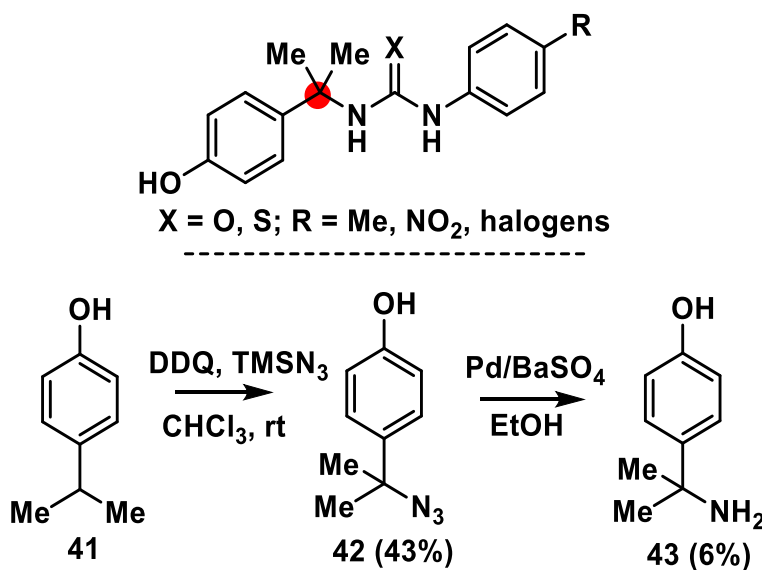
**Scheme 2.13:** Trials toward synthesis of phenolic carbamate derivative.



**Scheme 2.14:** Synthesis of carbamate (40) from secondary alcohol (39).

### 2.2.5 Attempts to synthesis *N,N'*-disubstituted urea and thiourea derivatives derived from 4-isopropylphenol

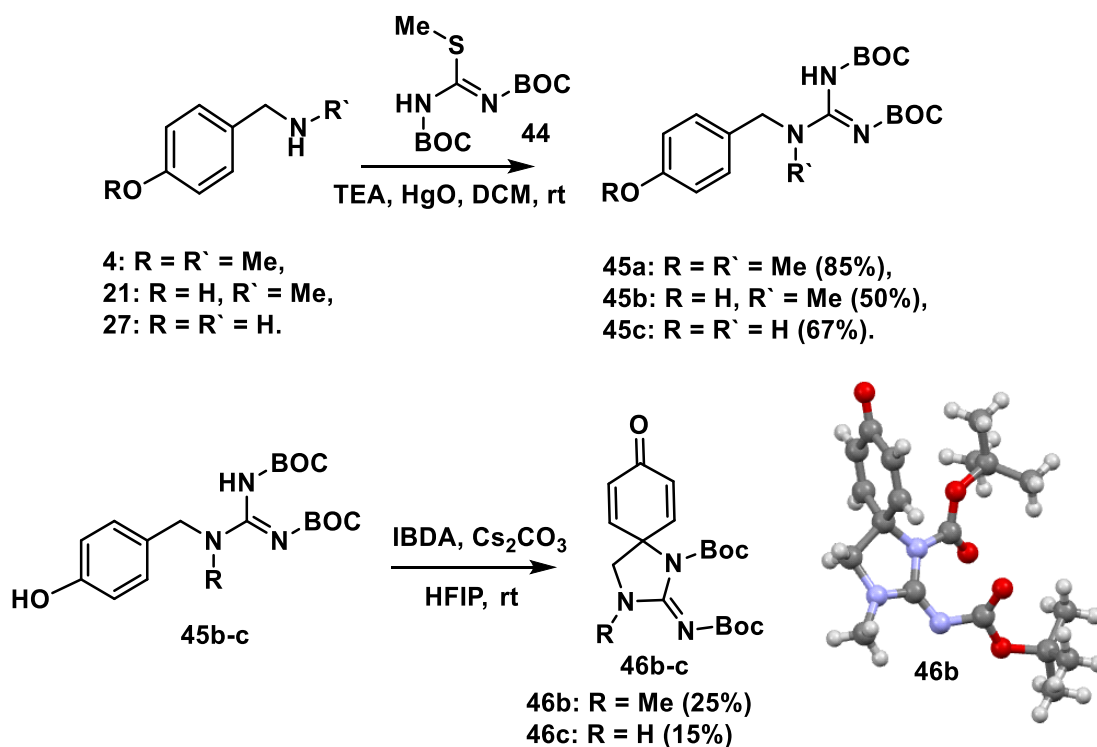
Introducing two methyl groups at the benzylic methylene group was designed for synthesis tertiary amines and alcohols. Starting with urea and thiourea derivatives derived from tertiary phenolic amine which had been targeted to be synthesized a tertiary amine. Scheme 2.15 presents this approach through azidation of 4-isopropylphenol (41) using DDQ and TMSN<sub>3</sub>, then followed by reduction reaction of the corresponding azide 42 using Pd/BaSO<sub>4</sub>. Various unsuccessful reduction trails had been performed to improve the very low isolated yield of the targeted tertiary amine 43 using small- and large-scale reactions. Therefore, we have directed to apply the developed chemistry with guanidine derivatives.



**Scheme 2.15:** Synthesis tertiary amine (43) via reduction of azido compound (42).

### 2.2.6 Developing OD for guanidine derivatives:

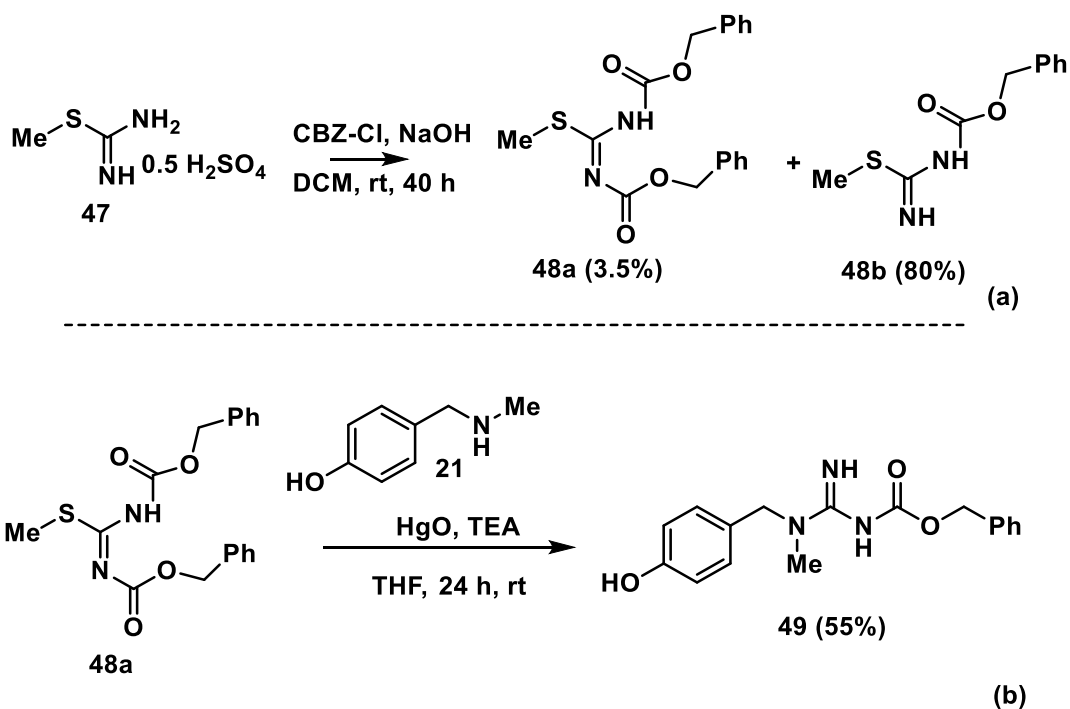
The primary motivation for this study was to apply the chemistry towards the total synthesis of spiroguanidines such KB343 (**3**) and initially the core structure, thus we examined the possibility of using guanidines in this chemistry. Oxidative cyclization of guanidines has been achieved by preparing guanidine-containing phenol derivatives **45a-c** using 1,3-diBOC-2-methylisothiourea (**44**) with 4-[(methylamino)methyl]phenol (**4**), (1-methoxybenzyl) methyl amine (**21**) or hydroxybenzyl amine (**27**). The expected cyclized spiro product was not obtained using the synthesized guanidine derivative **45a**. That might be due to decomposition to unidentifiable product mixtures. However, it was found that the N-methyl bis BOC guanidine **45b** underwent dearomatization to afford the spirocyclic derivative **46b** (Scheme 2.16) in modest yield (confirmed by X-ray crystallography).



**Scheme 2.16:** Synthesis di-BOC guanidines (**45a-c**) and their oxidative dearomatization.

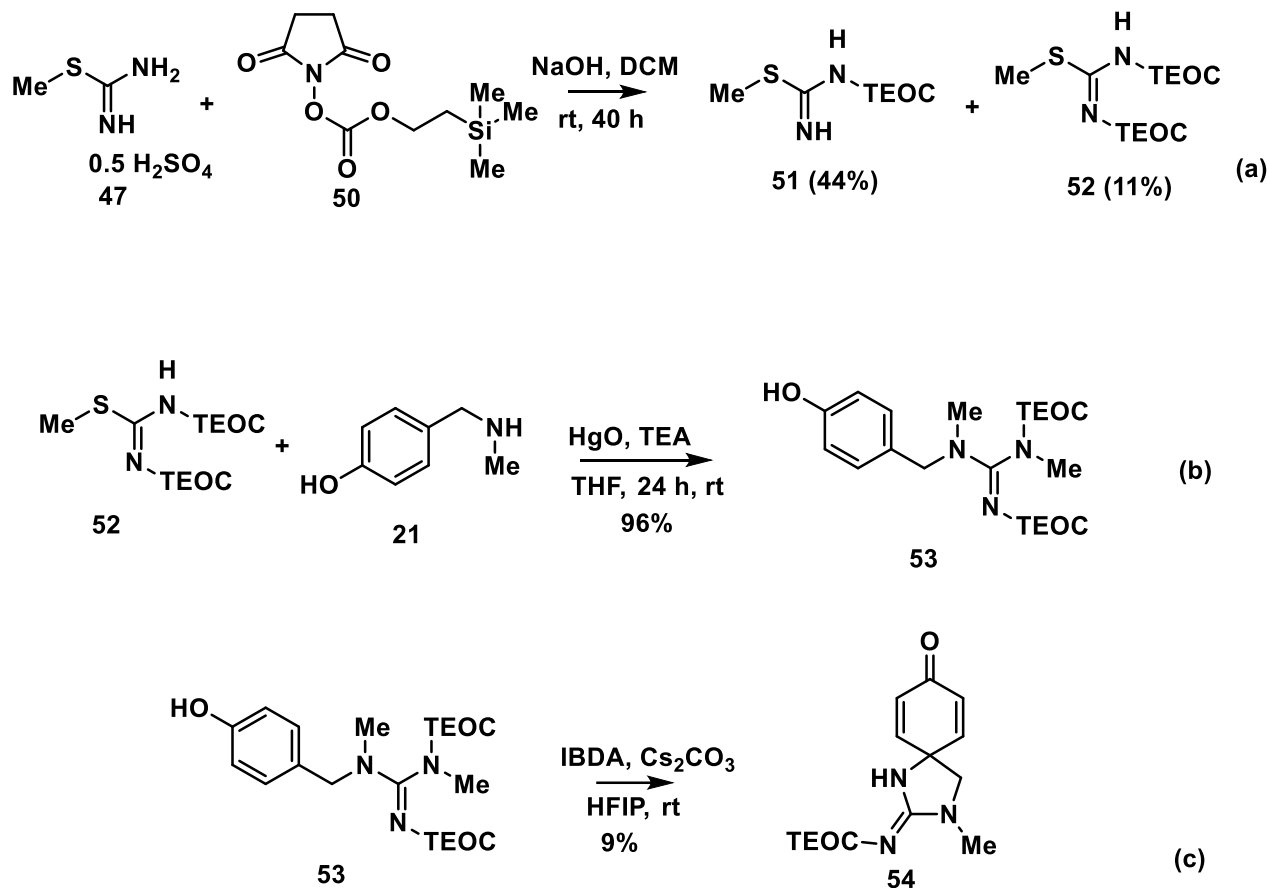


Interestingly, the corresponding NH derivative **45c** also provided the desired spirocyclic derivative **46c** in low yield. The low isolated yields of the dearomatized spiro guanidines **46b-c** drove us to synthesize new masked guanidine derivatives. Therefore, methylisothiourea hemi sulfate **47** was treated with 2.5 equivalent of benzyl chloroformate (CBZ-Cl) in presence of NaOH in dichloromethane with stirring for 40 hours at rt. The monoprotected isothiourea **48b** was isolated as a major product (Scheme 2.17a). However, the targeted di-cbz protected isothiourea **48a** was isolated with very low yield, its amount was enough to be subjected to guanidination reaction with (1-methoxybenzyl) methyl amine (**21**), surprisingly yielding the mono protected guanidine derivative **49** (Scheme 2.17b), which is not further dearomatized under the developed oxidation conditions.



**Scheme 2.17:** Attempt towards synthesis of the CBZ-protected guanidine (**49**).

Three other derivatives were evaluated, the TEOC-protected congener **52** was isolated by similar previously applied chemistry using 1-[2-(trimethylsilyl)ethoxycarbonyloxy]pyrrolidin-2,5-dione (**50**) (Scheme 2.18b). The TEOC guanidine **53** afforded a spirocyclic product **54** under the oxidative dearomatization conditions, but it underwent mono deprotection (Scheme 2.18c) with very low isolated yield (9%), which direct our attention to a different type of protecting groups. The mono CBZ adduct **55** and the anisole precursor **56** (Figure 2.2) were subjected to dearomatization but these attempts were unsuccessful.



**Scheme 2.18:** Synthesis di-TEOC guanidine and its OD reaction.

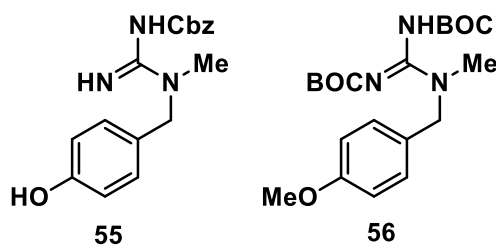
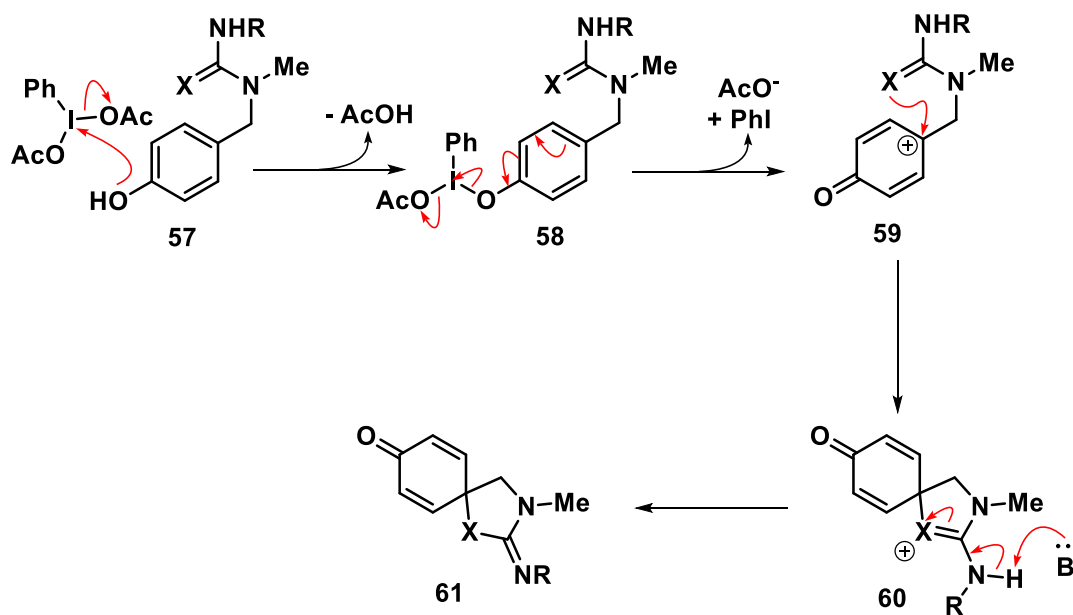


**Figure 2.2:** Unsuccessful oxidative dearomatization reactions toward guanidine substrates.

### 2.2.7 A putative mechanism for the dearomatization reactions

It is assumed mechanistically that these dearomatization reactions proceed via the accepted pathway involving reaction of the phenolic oxygen via substitution of one of the acetates **57**→**58** on the I(III) center (Scheme 2.19). There is some debate whether ionization to the phenoxonium ion followed by nucleophilic attack (shown **58**→**59**) or a concerted process ensues.<sup>24-27</sup> Whichever

sequence is followed, the spirocyclic derivative is formed by intramolecular nucleophilic attack and proton transfer.<sup>28</sup> One observation that requires further comment is the divergent activity of ureas, which deliver different heterocycles depending on the electronic character of the urea nitrogen substituent. Presumably, the nitrogen atom of the urea is rendered more electron rich with electron donating substituents on the aromatic moiety, whereas with the electron withdrawing groups deprotonation of the aniline nitrogen may occur prior to cyclization. It is also conceivable that there is a mechanistic changeover such that with electron withdrawing substituents activation of the urea occurs, which is likely the pathway in this TOADS chemistry from our group, rather than the phenol.

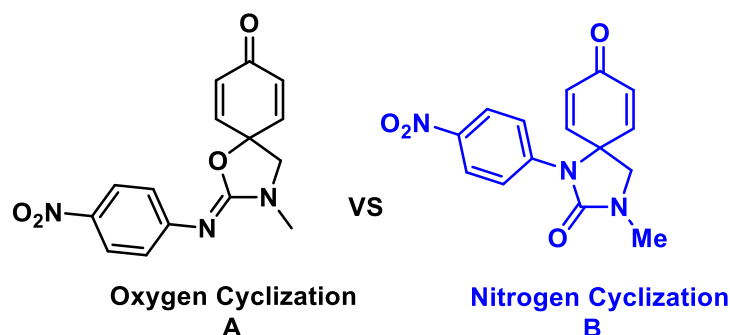


**Scheme 2.19:** Putative mechanism for the dearomatization reactions.

### 2.2.8 DFT Study: Oxygen spirocyclization for electro-deficient urea derivative (36e)

DFT study of spirocyclization reaction mediated by hypervalent iodine reagents have been attempted. In 2018, Tang and Harned reported a study to understand the mechanistic steps underpinning this reaction by performing a Hammett analysis and DFT calculations.<sup>29</sup> Their data suggest that the initial step involved activation of the phenol which occurs via ligand exchange on the hypervalent iodine reagent, substituting an acetate group with the phenol moiety. Then based on Harned's study, the mechanism involves a unimolecular redox decomposition pathway. Therefore, an SN1-like mechanism in which the initially formed phenoxonium ion is rapidly trapped by a nucleophile to obtain the corresponding dienone. Based on these reported studies, we were interested in applying DFT calculations to investigate the possible mechanisms behind urea cyclization that we have developed in our lab and published last year. As shown in scheme 12, *N*-aryl urea derivatives cyclized under oxidative dearomatization conditions differently based on substituents attached to *N*-aryl group. Electron-deficient urea derivatives cyclized via oxygen, while the electron-rich ureas cyclized by nitrogen. Thus, we have started computing the transition state of phenoxenium cation for each transformation (O and N cyclization). The initial attempts were unsuccessful due to formation of the corresponding spiro cyclized products and producing the wrong imaginary frequency (the values are corresponding to bond rotations and not bond formations). One of the promising approaches was performing the optimization calculations by fixing bond distances between the involved atoms in the reaction, resulting in reasonable imaginary frequencies. Thus, considering the optimized structure as an input for TS calculations using DFT theory resulted in the same previously obtained results by producing wrong imaginary frequencies with forming the direct cyclized product. Thus, we concluded that these two steps might occur spontaneously. Interestingly, in 2019, Ganjia and Ariaferd have reported DFT studies

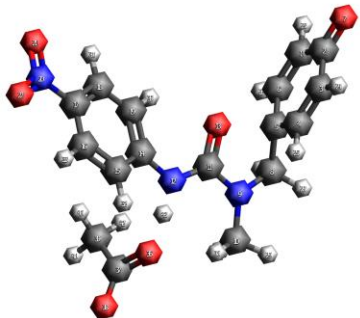
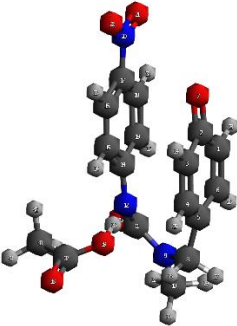
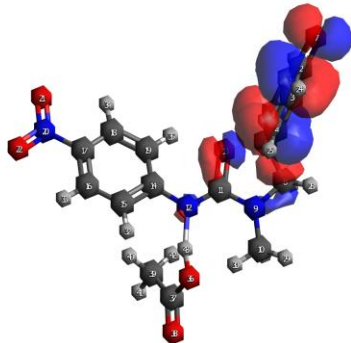
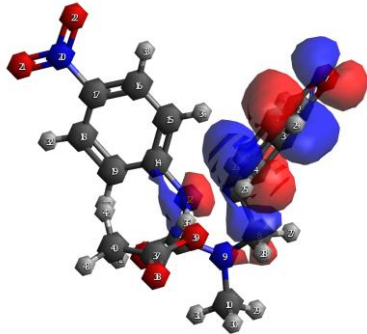
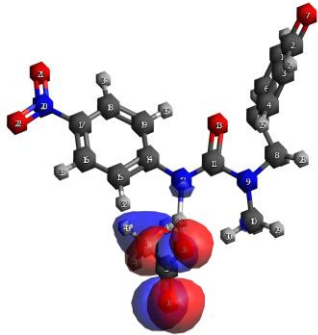
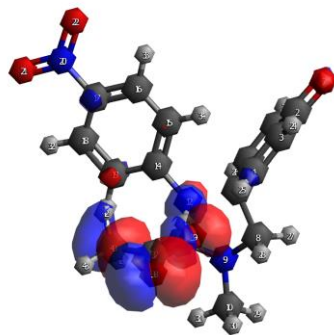
for oxidative dearomatization reaction of simple phenol compound and they considered this structure (phenoxenium cation) as an intermediate and not a transition state.<sup>30</sup>



**Figure 2.3:** C-O and C-N spirocyclization of the electron-deficient urea derivative **35e**.

Therefore, we have considered the phenoxenium cation as an intermediate, and computed their optimized energy. As a result, the energy of the optimized cation intermediate structure corresponding to oxygen cyclization (**A**) for the urea substituted with *p*-nitro phenyl was less than the nitrogen cyclization (**B**) with 2.63 kcal/mol which referring to favorable reaction path. It was interesting to check the frontier molecular orbitals of each intermediate, specifically the lowest occupied molecular orbital (LUMO) and the highest occupied molecular orbital (HOMO). LUMO energy of *O*-cyclization intermediate is much lower than LUMO energy for N-cyclization intermediate (Table 2.3, entry 3). Moreover, the energy gap between the HOMO and LUMO molecular orbitals of the oxygen cyclization is less than the energy required for nitrogen cyclization by 0.208 eV. In addition, other parameters have been computed and supported the oxygen cyclization for the electron deficient urea derivative including the electronegativity index of the structure of (**A**) intermediate shows higher electronegativity index compared to the nitrogen cyclization (Table 2.3).

**Table 2.3:** Frontier molecular orbital calculations for cyclization reaction of urea **36e**.

		Oxygen Cyclization	Nitrogen Cyclization
1	Optimized Structure (Int. 3)		
2	LUMO MO		
3	LUMO Energy	0.938 eV	1.261 eV
4	HOMO MO		
5	HOMO Energy	-5.135 eV	-5.666 eV
6	Optimized Energy	-1272.053998 Hartree -798226.10567873 Kcal/mol	-1272.049806 Hartree -798223.47515845 Kcal/mol
7	HOMO-LUMO gap	4.197 eV	4.405 eV
8	Hardness	3.0365	3.4635
9	Softness	0.329327	0.288725
10	Electronegativity	2.0985	2.2025
11	Electronegativity Index	0.725128	0.700304

Energy gap = -HOMO – LUMO

Softness = 1/Hardness

Electronegativity Index = (Electronegativity\* Electronegativity)/(2\*Hardness))

Functional and basis set: m062x/gen, 6-311G(d), LANL2DZ.

Hardness = 0.5 \* (LUMO – HOMO)

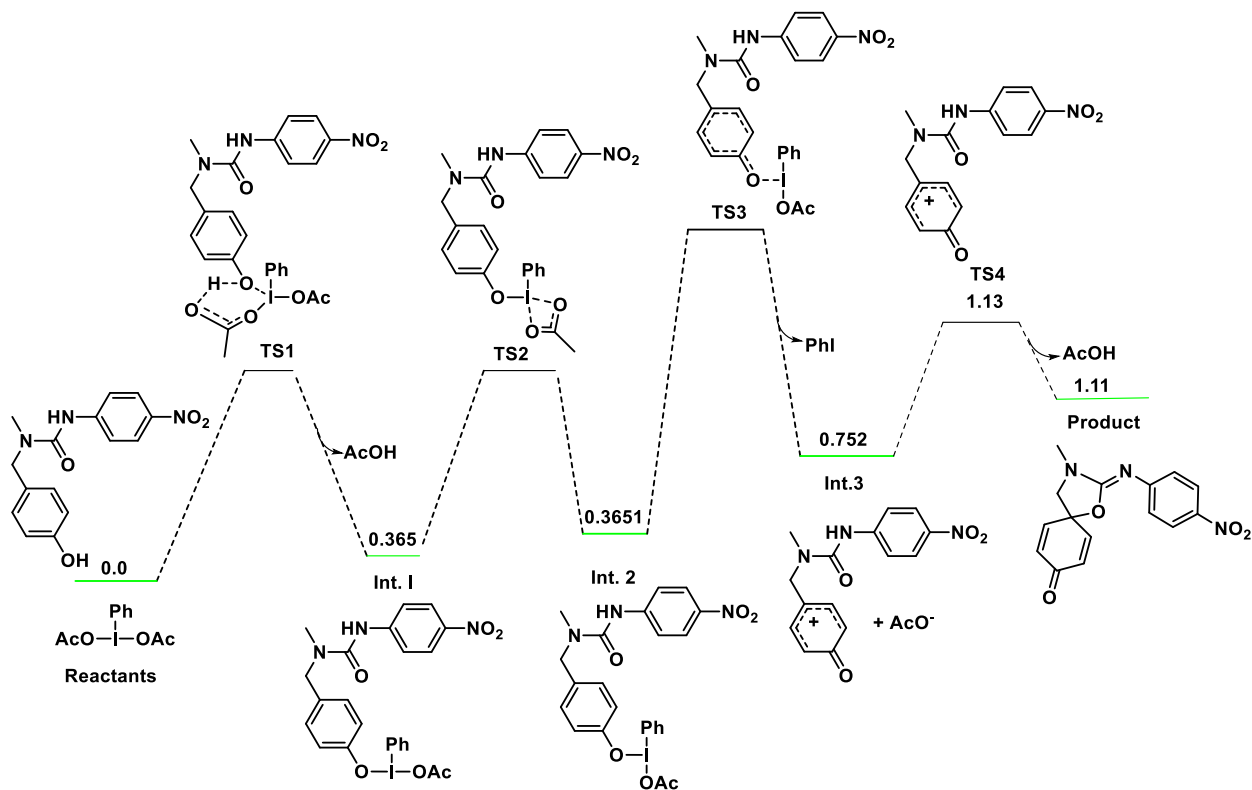
Electronegativity = (-0.5\* (LUMO + HOMO))

Figure 2.4. describes the proposed Gibbs free energy profile for oxidative dearomatization of urea **36e** by IBDA. The mechanistic pathway is divided into three stages. The first is ligand – ligand exchange between the phenolic moiety and acetate group of hypervalent iodine reagent. The second stage is the isomerization of hypervalent iodine reagent from cis isomer to the trans adduct which is facilitated by the existence of the bidentate acetate ligand. This type of isomerization generates a vacant coordination site in the trans adduct which is subsequently occupied by a phenol  $\pi$ -bond stabilizing the following transition state and promoting the next transformation.<sup>30</sup> Therefore, frontier molecular orbitals have been investigated for both intermediates **1** and **2**. It was found that LUMO energy of intermediate **2** is – 3.277 eV which is much lower relative to the LUMO energy of intermediate **1** (-1.612 eV) (Figure 2.5), providing evidence for the importance of this isomerization in the mechanistic pathway. The third stage is the final C-X cyclization which depends on the geometry of intermediate **3** (Table 2.3, Entry 1).

Since the first and the second stages are the same in the mechanistic pathway for both C-N and C-O cyclization, it is appropriate to focus initially on the third stage by optimizing their corresponding structures. As mentioned previously, the LUMO energy of intermediate **3** corresponding to *O*-cyclization is much lower than LUMO energy of *N*-cyclization (Table 2.3, entry 3). Computing energy of the final products resulted in remarkably close values for both C-N and C-O cyclization, thus an intensive study of the associative and dissociative mechanisms will be performed to distinguish between these two different pathways. Interestingly, the optimized energy for the final products is higher than the energy for intermediate **3** which reflects the importance of computing the energy of the transition state (phenoxenium cation) and that was not mentioned in the Gibbs free energy profile developed by Ganjia and Ariaifard.<sup>30</sup> However, computing the transition states of our substrates is not an easy task due to failure of convergency



of the large, complicated structures compared to the reported ones. Thus, screening different basis sets and functions is currently ongoing.



**Figure 2.4:** The proposed Gibbs free energy profile (kcal/mol) for the oxidative dearomatization reaction of urea **35e**.

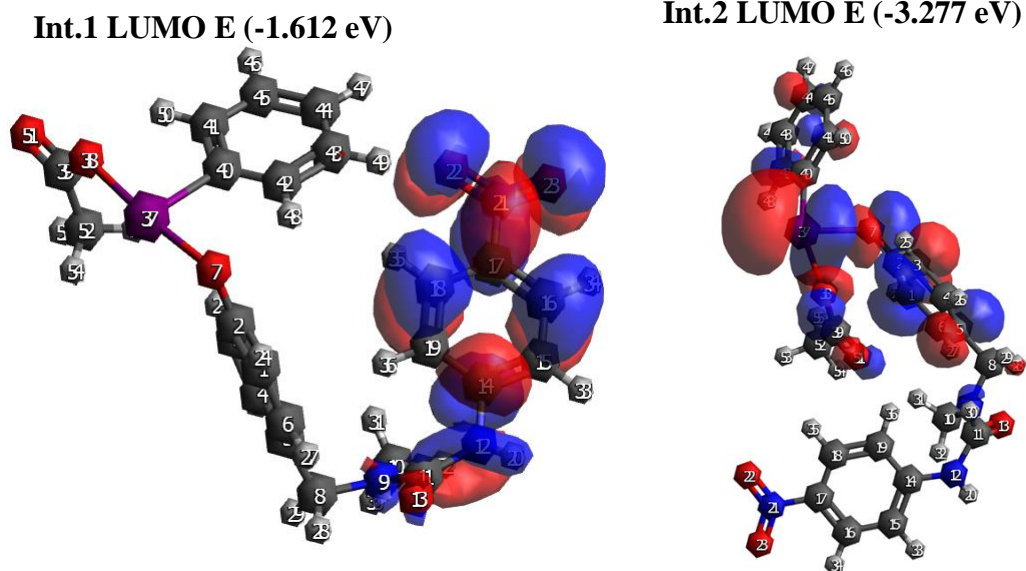


**Figure 2.5:** LUMO molecular orbitals for intermediate **1** and **2**.

### 2.3 SUMMARY:

Oxidative dearomatization reactions with environmentally benign conditions have been targeted for carbon-nitrogen/oxygen/sulfur spiro-cyclization using hypervalent iodine reagent. Various types of phenolic and non-phenolic derivatives have been examined under oxidative dearomatizing reactions. The tandem oxidative amination dearomatizing spirocyclization of guanidine derivatives was successfully carried out via C-N bond formation for the corresponding spiro products. Oxidative dearomatization reactions of nonphenolic thiourea derivatives produces benzothiazole derivatives which serve as a novel synthetic methodology for this intriguing ring system.

## 2.4 REFERENCES:

1. Roche, S. P.; Porco Jr., J. A., Dearomatization Strategies in the Synthesis of Complex Natural Products. *Angew. Chem. Int. Ed.* **2011**, 50, 4068–4093.
2. Quideau, S.; Pouysegu, L.; Deffieux, D., Oxidative dearomatization of phenols: Why, how and what for? *Synlett* **2008**, 467-495.
3. Ding, Q.; Ye, Y.; Fan, R., Recent Advances in Phenol Dearomatization and Its Application in Complex Syntheses. *Synthesis* **2013**, 1-16.
4. Wertjes, W. C.; Southgate, E. H.; Sarlah, D., Recent advances in chemical dearomatization of nonactivated arenes. *Chem. Soc. Rev.* **2018**, 47, 7996-8018.
5. Andrez, J.-C.; Giroux, M.-A.; Lucien, J.; Canesi, S., Rapid Formation of Hindered Cores Using an Oxidative Prins Process. *Org. Lett.* **2010**, 12, 4368-4371.
6. Desjardins, S.; Andrez, J.-C.; Canesi, S., A Stereoselective Oxidative Polycyclization Process Mediated by a Hypervalent Iodine Reagent. *Org. Lett.* **2011**, 13, 3406-3409.
7. Koswatta, P. B.; Lovely, C. J., Structure and synthesis of 2-aminoimidazole alkaloids from *Leucetta* and *Clathrina* sponges. *Nat. Prod. Rep.* **2011**, 28, 511-528.
8. Edrada, R. A.; Stessman, C. C.; Crews, P., Uniquely Modified Imidazole Alkaloids from a calcereous *Leucetta* Sponge. *J. Nat. Prod.* **2003**, 66, 939-942.
9. Koswatta, P. B.; Das, J.; Yousufuddin, M.; Lovely, C. J., Studies towards the *Leucetta*-derived Alkaloids Spirocalcaridine A and B – Possible Biosynthetic Implications. *Eur. J. Org. Chem.* **2015**, 2603-2013.
10. Singh, R. P.; Spears, J. A.; Dalipe, A.; Yousufuddin, M.; Lovely, C. J., Dearomatizing spirocyclization reactions of alkynyl cyanamides. *Tetrahedron Lett.* **2016**, 57, 3096-3099.
11. Singh, R. P.; Das, J.; Yousufuddin, M.; Gout, D.; Lovely, C. J., Tandem Oxidative Dearomatizing Spirocyclizations of Propargyl Guanidines and Ureas. *Org. Lett.* **2017**, 19, 4110-4113.
12. Guo, W.-S.; Gong, H.; Zhang, Y. A.; Wen, L.-R.; Li, M., Fast Construction of 1,3-Benzothiazepines by Direct Intramolecular Dehydrogenative C–S Bond Formation of Thioamides under Metal-Free Conditions. *Org. Lett.* **2018**, 20, 6394-6397.
13. Odagi, M.; Okuda, K.; Ishizuka, H.; Adachi, K.; Nagasawa, K., Synthesis of Spiroguanidine Derivatives by Dearomative Oxidative Cyclization using Hypervalent Iodine Reagent. *Asian J. Org. Chem.* **2020**, 9, 218-221.
14. Carroll, A. R.; Copp, B. R.; Davis, R. A.; Keyzers, R. A.; Prinsep, M. R., Marine Natural Products. *Nat. Prod. Rep.* **2020**, 37, 175-223
15. Lindel, T., Chemistry and Biology of the Pyrrole-Imidazole Alkaloids. *Alkaloids* **2017**, 77, 117-219.
16. Weinreb, S. M., Some recent advances in the synthesis of polycyclic imidazole-containing marine natural products. *Nat. Prod. Rep.* **2007**, 24, 931-948.
17. Ma, Y.; De, S.; Chen, C., Syntheses of Cyclic Guanidine-Containing Natural Products. *Tetrahedron* **2015**, 71, 1145-1173.

18. Matsumura, K.; Taniguchi, T.; Reimer, J. D.; Noguchi, S.; Fujita, M. J.; Sakai, R., KB343, a Cyclic Tris-guanidine Alkaloid from Palauan Zoantharian Epizoanthus illoricatus. *Org. Lett.* **2018**, *20*, 3039-3043.
19. Singh, R.; Gout, D.; Lovely, C. J., Tandem thioacylation-intramolecular hydrosulfenylation of propargyl amines – rapid access to 2-aminothiazolines. *Eur. J. Org. Chem.* **2019**, 1726-1740.
20. Singh, R. P.; Aziz, M. N.; Gout, D.; Fayad, W.; El-Manawaty, M. A.; Lovely, C. J., Novel thiazolidine derivatives: Synthesis, anti-proliferative properties and 2D-QSAR studies. *Bioorg. Med. Chem.* **2019**, *27*, 115047.
21. Mariappan, A.; Rajaguru, K.; Roja, S. S.; Muthusubramanian, S.; Bhuvanesh, N., Hypervalent Iodine Promoted Regioselective Oxidative C–H Functionalization: Synthesis of N-(Pyridin-2-yl)benzo[d]thiazol-2-amines. *Eur. J. Org. Chem.* **2016**, 302-307.
22. Kumar, R. K.; Manna, S.; Mahesh, D.; Sar, D.; Punniyamurthy, T., Oxidative Aromatic C-H Functionalization Promoted by Phenyliodine(III) Diacetate to form C-N, C-S, and C-Se Bonds. *Asian J. Org. Chem.* **2013**, *2*, 843-847.
23. Ghosh, H.; Yella, R.; Nath, J.; Patel, B. K., Desulfurization Mediated by Hypervalent Iodine(III): A Novel Strategy for the Construction of Heterocycles. *Eur. J. Org. Chem.* **2008**, 6189-6196.
24. Tang, T.; Harned, A. M., Experimental evidence for the formation of cationic intermediates during iodine(III)-mediated oxidative dearomatization of phenols. *Org. Biomol. Chem.* **2018**, *16*, 6871-6874.
25. Harned, A. M., Concerning the mechanism of iodine(III)-mediated oxidative dearomatization of phenols. *Org. Biomol. Chem.* **2018**, *16*, 2324-2329.
26. Ganji, B.; Ariaifard, A., DFT mechanistic investigation into phenol dearomatization mediated by an iodine(III) reagent. *Org. Biomol. Chem.* **2019**, *17*, 3521-3528.
27. Kaur, A.; Ariaifard, A., Mechanistic Investigation into phenol oxidation by IBX elucidated by DFT calculations. *Org. Biomol. Chem.* **2020**, *18*, 1117-1129.
28. Kraszewski, K.; Tomczyk, I.; Drabinska, A.; Bienkowski, K.; Solarska, R.; Kalek, M., Mechanism of Iodine(III)-Promoted Oxidative Dearomatizing Hydroxylation of Phenols: Evidence for a Radical-Chain Pathway. *Chem. Eur. J.* **2020**, *26*, 11584-11592.
29. Tang, T.; Harned, A. M., Experimental evidence for the formation of cationic intermediates during iodine(III)-mediated oxidative dearomatization of phenols. *Org. Biomol. Chem.* **2018**, *16*, 8249-8252.
30. Ganji, B.; Ariaifard, A., DFT mechanistic investigation into phenol dearomatization mediated by an iodine(III) reagent. *Org. Biomol. Chem.* **2019**, *17*, 3521-3528.

**CHAPTER THREE: ANODIC OXIDATION IS A REALISTIC SOLUTION FOR ISSUES  
ASSOCIATED WITH CONVENTIONAL DEAROMATIZATION OF ARENES  
MEDIATED BY NITRENIUM FORMATION**

Marian N. Aziz <sup>a,b</sup>, Delphine Gout <sup>a</sup>, Carl J. Lovely <sup>a</sup>

a. Department of Chemistry and Biochemistry, 700 Planetarium Place, University of Texas at  
Arlington, TX 76019, USA

b. Department of Pesticide Chemistry, National Research Centre, Dokki, Giza 12622, Egypt

Corresponding author

Prof. Carl J. Lovely

Professor, Chemistry and Biochemistry Department

University of Texas at Arlington

Address: 700 Planetarium Place, Box 19065, UT Arlington, TX 76019-0065

Email: lovely@uta.edu

Phone: +1 817 272 5446

(Not Published)

## ABSTRACT

Oxidative dearomatization (OD) reactions using stabilized nitrenium ions have been studied extensively for urea and guanidine containing anisole moieties. Interestingly, di-substituted urea derivatives do not follow the oxidative dearomatization pathways but undergo nucleophilic attack by the fluorinated alcohol solvent. Meanwhile, tri-substituted urea derivatives follow the expected spiro-cyclization pathway, resulting in formation of spiro imidazolinones in good to excellent yield. Subjecting a di-Boc guanidine derivative to OD reaction resulted in Boc deprotection of the starting material and formation of the dearomatized spiro product as a minor product. Simple electrochemical oxidation conditions have been found to largely circumvent all the encountered issues that we observed using regular oxidative dearomatization conditions via hypervalent iodine oxidations.

## 3.1 INTRODUCTION

Nitrenium ions are considered an important synthetic intermediate due to their diverse and unique reactivity that provide an entry to array of heterocyclic compounds. The first generation of nitrenium ion was detected by Haque's group in 1965 using a silver salt with *N*-chloroamines or *N*-chloroamides.<sup>1</sup> Currently, hypervalent iodine reagents are extensively used for generation of these very reactive species as they avoid the intermediacy of *N*-chloro derivatives.<sup>2</sup> The secret behind utilizing these types of ions in several synthetic transformation is extending the stability of the positive charge on nitrogen atom due to the existence of a vacant p-orbital.<sup>3,4</sup> Thus, most of the reported derivatives are aryl amines in which the aromatic ring will participate by localization of electron density via resonance structure to form carbenium ions or *N*-alkoxyamines/*N*-alkoxy acetamides leading to alkoxy nitrenium ions stabilized by the neighboring electron donating heteroatom (oxygen) (Figure 3.1).<sup>5-14</sup> Thus these formed nitrenium ions can undergo two different processes, either electrophilic attack or radical reactions based on the corresponding electronic

structures. There are two possible electronic structures formed from the nitrogen atom with six valence electrons which are the singlet and triplet electronic forms.<sup>3,4</sup>

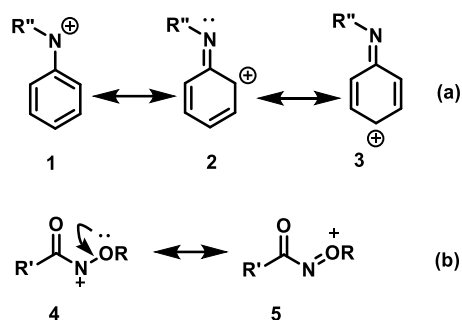


**Figure 3.1:** Nitrenium ion stabilized by resonance of aryl group (a) and alkoxy group (b).

The formation of these reactive acyl nitrenium intermediates has been utilized in total synthesis of complex structure including (+)-kishi lactam, (-)-dysibetaine, and (-)-swainsonine (Figure 3.2).<sup>14-</sup>

19

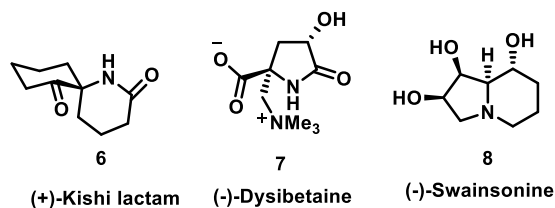


**Figure 3.2:** Nitrenium ion formation as a key step in natural products' syntheses.

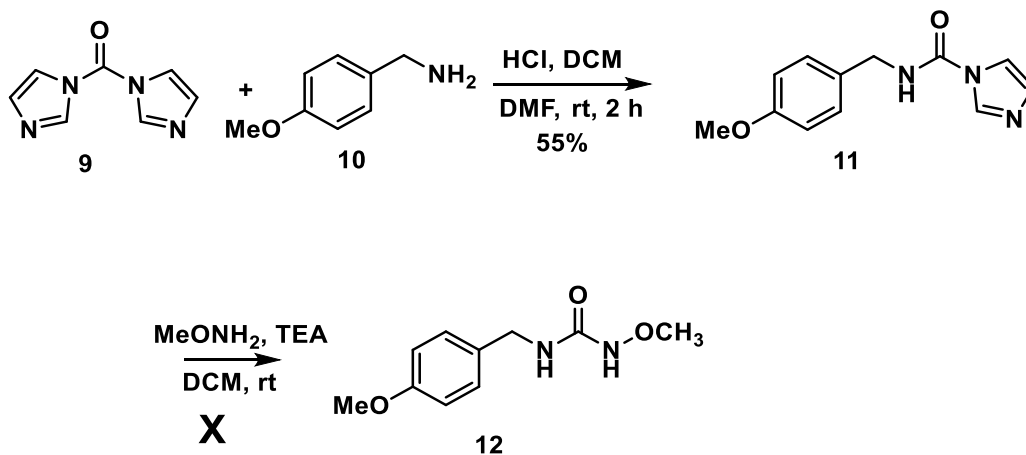
In this chapter, *N*-alkoxy-*N*-acetamido nitrenium ion formation is targeted for spiro azacyclization of specific urea and guanidine derivatives. The reactive iodine(III) reagents have been extensively used and the application of the electrochemical oxidation conditions for nitrenium ion formation has been tested to provide an alternative approach when conventional hypervalent iodine induced dearomatization fails.

## 3.2 RESULT AND DISCUSSION:

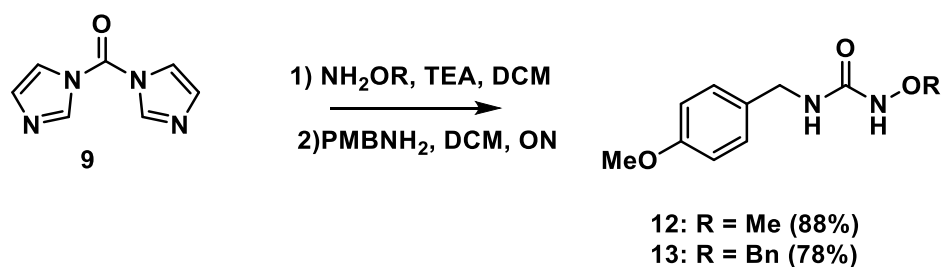
### 3.2.1 IBDA mediated OD reactions

One of the factors that has driven the idea of targeting nitrenium ion formation is improving the yield of the synthesized spiro products. The motivation behind this research is to evaluate guanidine derivatives in which the NHR group is substituted with an alkoxy group. Therefore, the nitrenium ion formed will be stabilized by a lone pair of the neighboring oxygen. Thus, initially we have started investigating this chemistry with urea derivatives due to ease of accessibility to such urea derivatives compared to thiourea and guanidine analogues. Formation of the targeted urea derivatives has been achieved by a carbonylation reaction of phenolic/anisolic amines and alkoxy hydroxy amines with 1, 1'-carbonyldiimidazole (**9**) (CDI) as a source of the carbonyl group. The initial trials were carried out by formation of carbamate of (4-methoxyphenyl) methanamine (**10**) with CDI, then followed by addition of alkoxy hydroxy amine in one-pot reaction. Surprisingly, this pathway did not work out and carbamate **11** was isolated as a major product instead of targeted urea **12** (Scheme 3.1). Therefore, switching the order of reagent addition was performed by treating CDI first with methyl hydroxy amine in presence of TEA in DCM then followed by addition of **10** (PMBNH<sub>2</sub>), providing targeted urea derivative **12** in an excellent yield (Scheme 3.2).



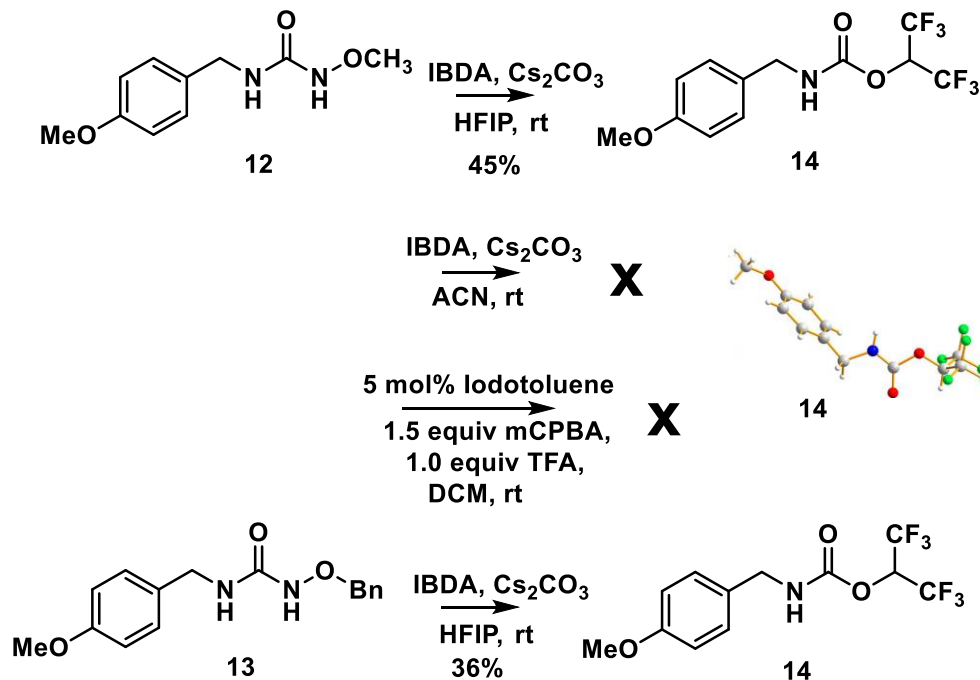


**Scheme 3.1:** Carbonylation reactions toward synthesis urea **12**.



**Scheme 3.2:** Synthesis targeted 1-(alkyloxy)-3-(4-methoxybenzyl) urea **12** and **13**.

Subjecting the urea to oxidative dearomatizing reaction afforded the product from nucleophilic substitution reaction, urethane derivative **14** (supported by X-ray, Scheme 3.3) instead of the dearomatized spiro product.

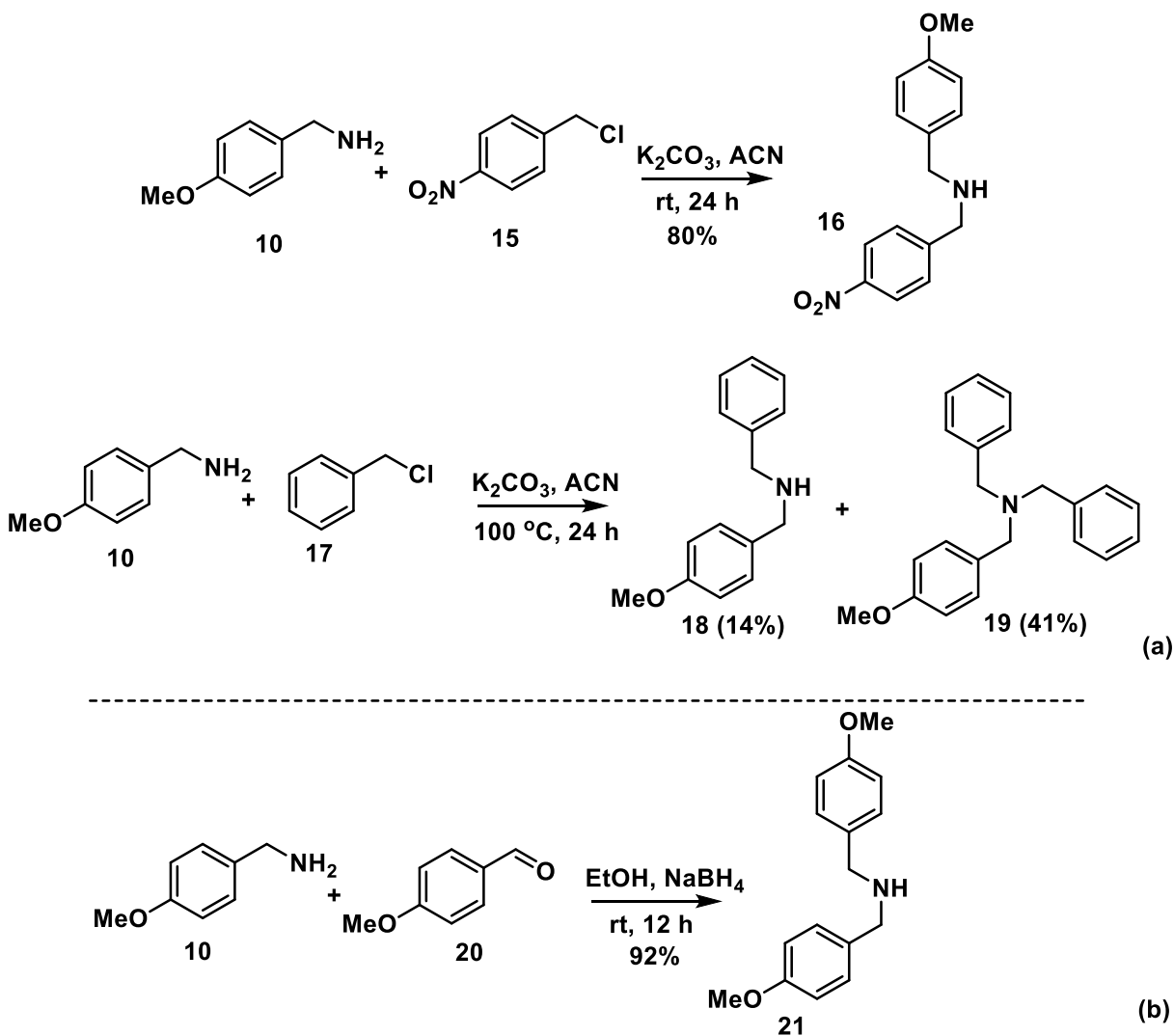


**Scheme 3.3:** Nucleophilic attack of HFIP with *N*-alkoxy urea derivatives.

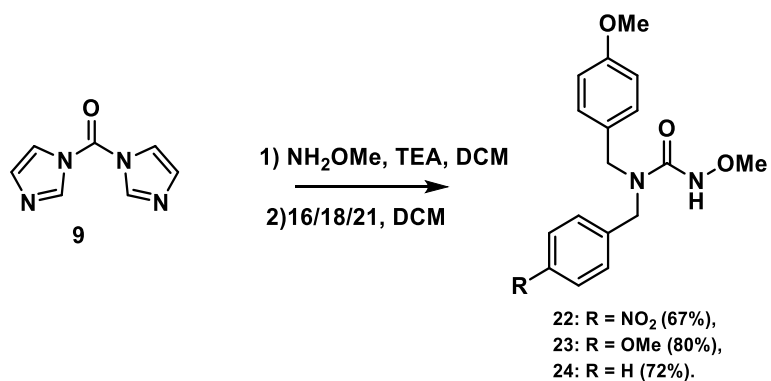
Application of the same conditions with urea **13** produced a similar urethane derivative **14**. Therefore, screening different conditions were carried out using acetonitrile as a solvent instead of hexafluoroisopropanol (HFIP). Hypervalent iodine reagent was synthesized in-situ using 1.5 equivalent of *m*-chloroperoxybenzoic acid (mCPBA), 5 mol% iodotoluene and in presence of TFA in DCM at rt. Unfortunately, all these experiments were unsuccessful (Scheme 3.3). Blocking that side of urea scaffold by substituting the nitrogen with another group might be a successful approach as this would increase the reactive rotamer population. Thus, we prepared trisubstituted urea from secondary amines instead of using primary amines.

Synthesis of secondary amines was performed by protecting (4-methoxyphenyl) methylamine (**10**) with benzyl chloride derivatives. The protection with deactivated benzyl chloride **15** was performed with isolating desired secondary amine **16** in an excellent yield. The use of benzyl chloride **17** afforded tertiary amine **19** as a major product and the desired secondary amine **18** was isolated with low yield (14%) but sufficient to establish the viability of the

cyclization (Scheme 3.4a). Protection with activated benzyl chloride did not work under the same conditions, so reductive amination conditions were performed using 4-methoxy benzaldehyde (**20**) followed by NaBH<sub>4</sub> addition to yield secondary amine **21** in an excellent yield. The targeted tri-substituted ureas **22-24** were synthesized using the previously described carbonylation chemistry using CDI (Scheme 3.5).

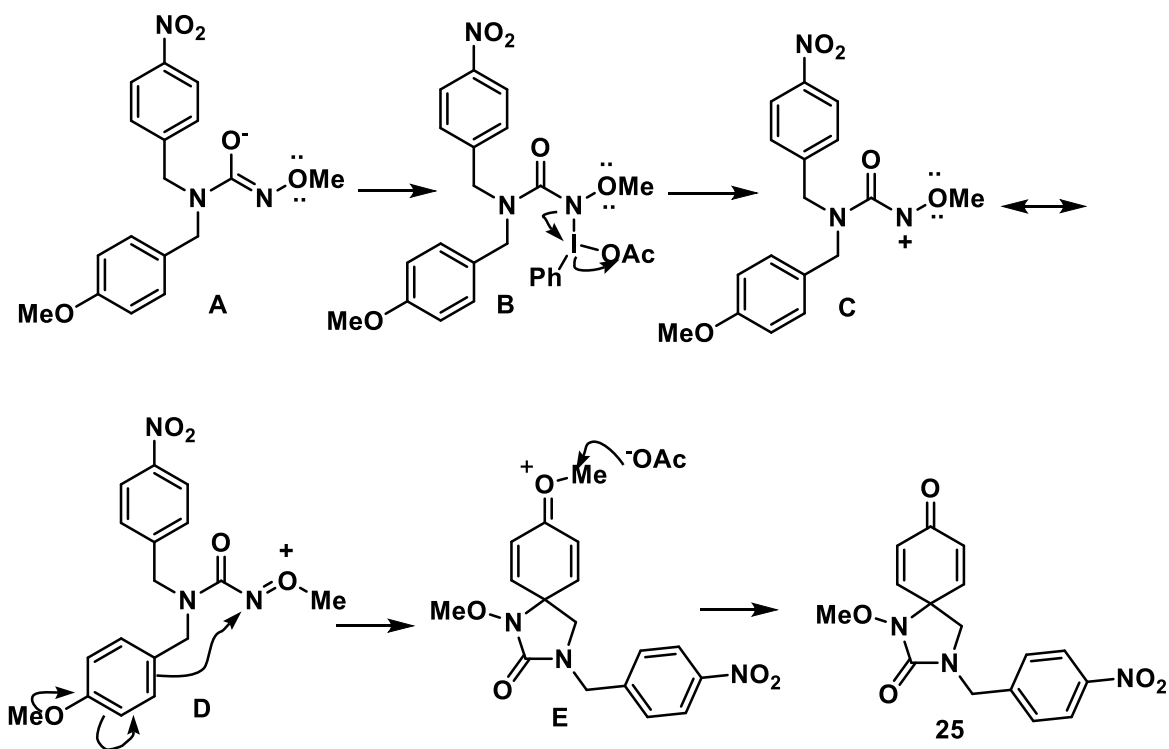
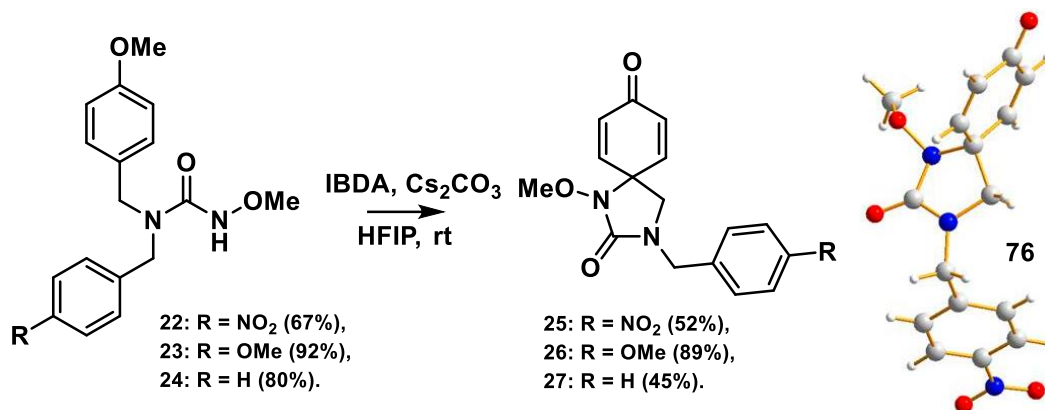


**Scheme 3.4:** Synthesis targeted secondary amines **16**, **18** and **21**.



**Scheme 3.5:** Synthesis of trisubstituted urea derivatives **22-24**.

Ureas **22-24** underwent dearomatization reaction producing the desired spiro imidazolines in good to excellent yields. The structure was confirmed with X-ray for nitro derivative as an example (Scheme 3.6). The yield of the anisole analogue **26** improved by increasing the number of equivalents of IBDA from 1.5 to 2.0 molar equivalent.



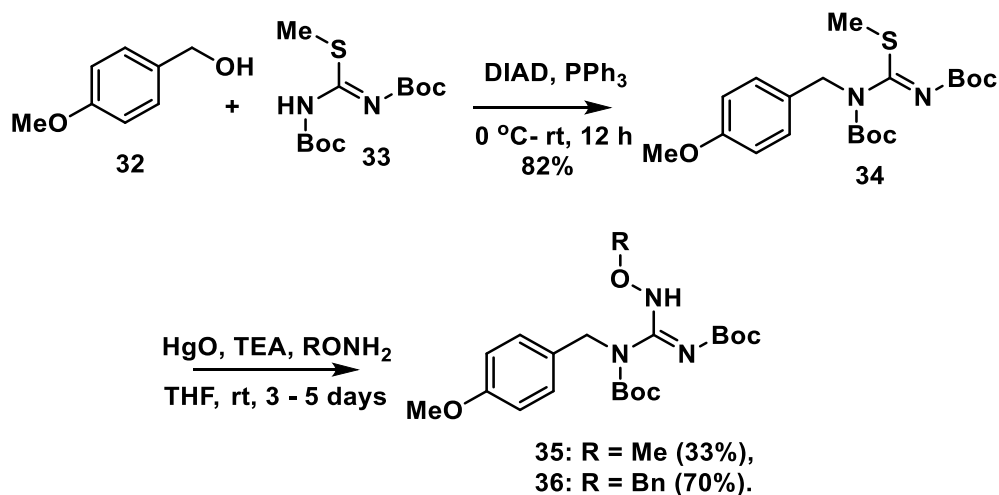
**Scheme 3.6:** OD reactions of trisubstituted ureas mediated by *N*-methoxy nitrenium ion generation.

Moving forward we wished to establish the viability of *N*-methoxy thioureas, however the synthesis of these analogues using the same chemistry with thiocarbodiimidazole **28** was not straightforward. Multiple attempts toward the synthesis of thiourea derivatives were unsuccessful. This lack of success might be attributed to the instability of the intermediates derived from di(1H-imidazol-1-yl) methanethione (TCDI) (**28**) (Scheme 3.7). Treating TCDI (**28**) with methoxy amine

in presence of TEA in DCM at 50 °C following the developed methodology for urea derivatives resulted in isolating an insoluble TEA salt. Switching to benzyloxy amine in diethyl ether at rt did not yield the desired corresponding thiocarbamate, while changing the solvent to DCM for 3 hours at rt resulted in isolating desired thiocarbamate **29**. The reaction of the latter with the previously synthesized secondary amine **21** produced multiple unidentified products. The reaction of primary amines with TCDI (**28**), which is the reverse addition of thiocarbonylation reaction, was performed to isolate the corresponding isothiocyanate **30** using chloroform as a solvent at 0 °C. This reaction delivered a low yield of the desired product **30**. Reaction optimization conditions were not successful in improving the isolated yield. Therefore, the reaction was repeated using ethyl acetate as a solvent and heating the reaction mixture at 50 °C for 30 minutes, producing the isothiocyanate **30** in an excellent yield. The reaction of **30** with alkoxy hydroxy amines was performed using different conditions but failed to produce the desired substrates.



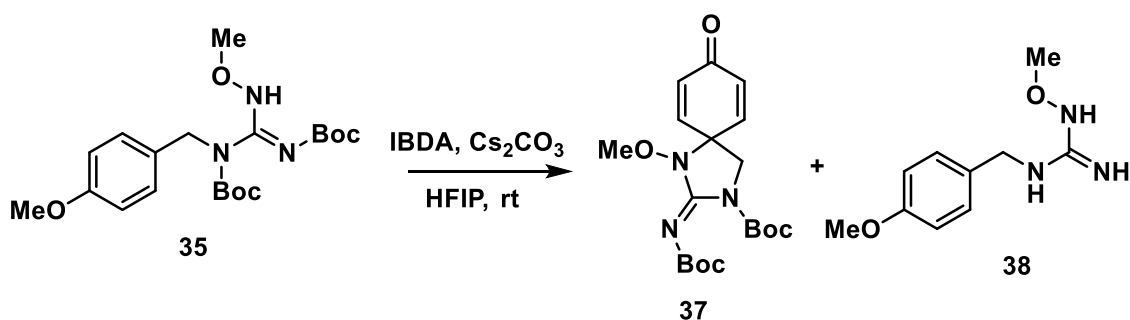
Reaction of TCDI with secondary amine was performed and successfully afforded the desired thiocarbamate **31** which was not stable at rt nor at  $-10^{\circ}\text{C}$ . The freshly prepared thiocarbamate **31** was treated with an alkoxy amine and/or primary amine but no reaction took place using different reaction conditions as shown in Scheme 3.7. The initial plan behind the synthesis of the urea and thiourea derivatives was to convert them into the corresponding guanidine derivatives due to easy synthesis of these derivatives, evaluation of nitrenium ion formation for OD reactions, and the corresponding yields. Since thiourea synthesis was not successful, a different synthetic pathway for guanidines bearing an *N*-alkoxy protected group was designed. Mitsunobu reaction of (4-methoxyphenyl)methanol (**32**) with 1,3-diBoc-2-methylisothiurea (**33**) was performed in presence of triphenylphosphine and diisopropyl azodicarboxylate (DIAD) to afford the corresponding isothiurea **34**. The guanidine precursor **34** was treated with methoxy amine and benzyloxy amine in the presence of mercury(II) for desulfurization, producing the desired guanidine derivative **35** and **36** respectively (Scheme 3.8).



**Scheme 3.8:** Synthesis of targeted guanidine derivatives (**85**) and (**86**) using Mitsunobu reaction.



Developing conditions for oxidative dearomatizing spirocyclization reaction of the synthesized guanidine **35** is an important step to test the applicability of such reaction conditions with our planned approach to the core structure of the natural product KB343. The initial result of OD produced the spiro targeted product **37** and the unprotected guanidine starting material **38** (Scheme 3.9). Table 1 shows the corresponding yields for different conditions that changed including the solvent, temperature, and oxidizing agent to avoid the deprotection and enhance the yield. Interestingly, using acetonitrile (entry 8) as a solvent, 3.0 equiv of IBDA and heating the reaction mixture in a sealed tube at 100 °C afforded a different product **39** (35%, same Rf as **37**) and the X-ray confirmed the structure as shown in Figure 3.



**Scheme 3.9:** OD reactions of the synthesized guanidine **35**.

The bond length of C-N double bond is shorter than C-N single bond, therefore studying the C-N bond length has been confirmed the hydrogen attached to acetamide group not to alkoxy amine group (Figure 3.3). Presumably, the acetylated guanidine **39** formed due to a pathway involving the thermal BOC deprotection and IBDA serving as an acylating agent.

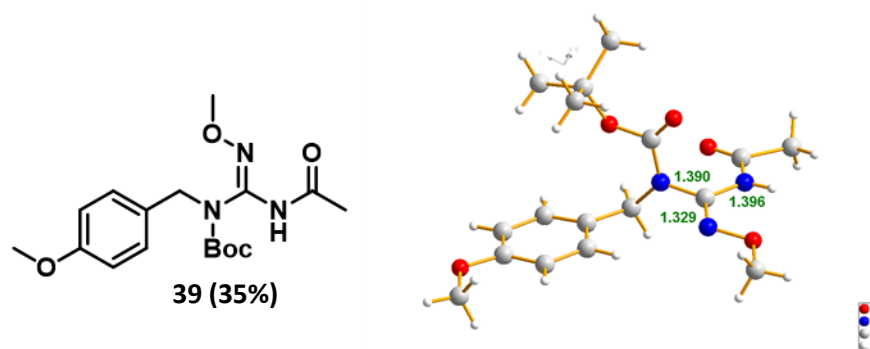


**Figure 3.3:** New guanidine derivatives **39** derived from thermal Boc deprotection of guanidine **35**.

**Table 3.1:** Optimization dearomatization spirocyclization reaction of guanidine **37**.

Entry	Solvent (0.1 M)	No. of equiv (Oxidant)	Additives	Temp.	Time	37(%) <sup>a</sup>	38 (%) <sup>a</sup>
1	HFIP	1.5 (IBDA)	Cs <sub>2</sub> CO <sub>3</sub>	rt	ON	30	60
2	HFIP	2.0 (IBDA)	Cs <sub>2</sub> CO <sub>3</sub>	rt	4 h	31	65
3	HFIP	0.0 (IBDA)	Cs <sub>2</sub> CO <sub>3</sub>	rt	5 days	0.0 <sup>b</sup>	0.0 <sup>b</sup>
4	TFE	1.5 (IBDA)	Cs <sub>2</sub> CO <sub>3</sub>	rt	4 h	20	52
5	ACN	1.5 (IBDA)	Cs <sub>2</sub> CO <sub>3</sub>	rt	2 days	0.0 <sup>b</sup>	0.0 <sup>b</sup>
6	ACN	1.5 (IBDA)	Cs <sub>2</sub> CO <sub>3</sub>	80 °C	3 days	Traces <sup>b</sup>	0.0 <sup>b</sup>
7	ACN	2.5 (IBDA)	Cs <sub>2</sub> CO <sub>3</sub>	80 °C	3 days	Traces <sup>b</sup>	0.0 <sup>b</sup>
8	ACN	3.0 (IBDA)	Cs <sub>2</sub> CO <sub>3</sub>	100 °C	2 days	0.0	0.0
9	HFIP/ACN	1.5 (IBDA)	Cs <sub>2</sub> CO <sub>3</sub>	rt	2 days	14	44
10	THF	1.5 (IBDA)	Cs <sub>2</sub> CO <sub>3</sub>	rt – 60 °C	3 days	0.0 <sup>b</sup>	0.0 <sup>b</sup>
11	HFIP	0.0 (IBDA)	Cs <sub>2</sub> CO <sub>3</sub>	Rt	ON	0.0 <sup>b</sup>	0.0 <sup>b</sup>
12	HFIP	10% (IBDA)	Cs <sub>2</sub> CO <sub>3</sub>	rt	2 days	Traces <sup>b</sup>	Traces <sup>b</sup>
13	HFIP	1.5 (HTIP)	Cs <sub>2</sub> CO <sub>3</sub>	rt	ON	36	49
14	HFIP	2.0 (IBDA)	No Base	rt	ON	14	52
17	HFIP	2.0 (IBDA)	Cs <sub>2</sub> CO <sub>3</sub>	0 °C	5 h	32	69
18	HFIP (0.05 M)	2.0 (IBDA)	Cs <sub>2</sub> CO <sub>3</sub>	rt	ON	25	51

<sup>a</sup>Isolated yields after flash column chromatography, <sup>b</sup>reactions were monitored by TLC.

A study has recently shown that photochemical conditions induce dearomatization of phenolic derivatives by irradiation of the reaction mixture with a 5 W blue LED and using acetoxybenziodoxole (BI-OAc) as an oxidant and in the presence of 2.0 mol% of

Ru(bpy)<sub>3</sub>Cl<sub>2</sub>·6H<sub>2</sub>O as a photocatalyst. Therefore, we had tried the same conditions with the guanidine substrate **35**. Unfortunately, using the 5 W blue LED and laboratory photoreactor as a source for irradiation did not help to initiate the reaction (Table 3.2, Entry 2-4). In addition to that, using ruthenium catalyst as an additive with IBDA lowered the yield of the two isolated products (Table 3.2, Entry 5). Subjecting the reaction mixture without a photocatalyst to the blue light lowered the isolated yields (Table 3.2, Entry 6) compared to the standard conditions using HFIP as a solvent, BIDA as an oxidant, and Cs<sub>2</sub>CO<sub>3</sub> as a base (Table 3.2, Entry 1).

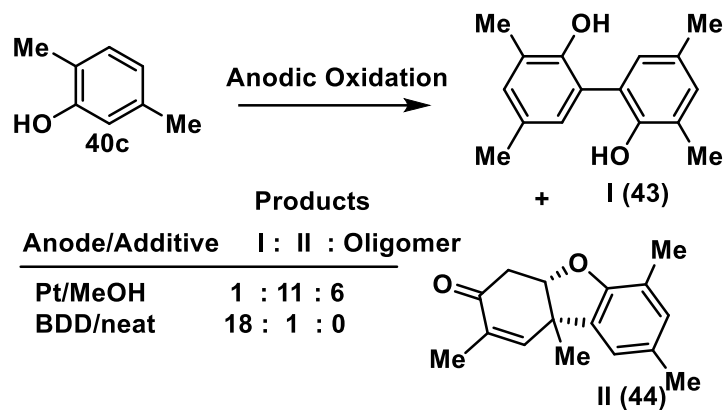
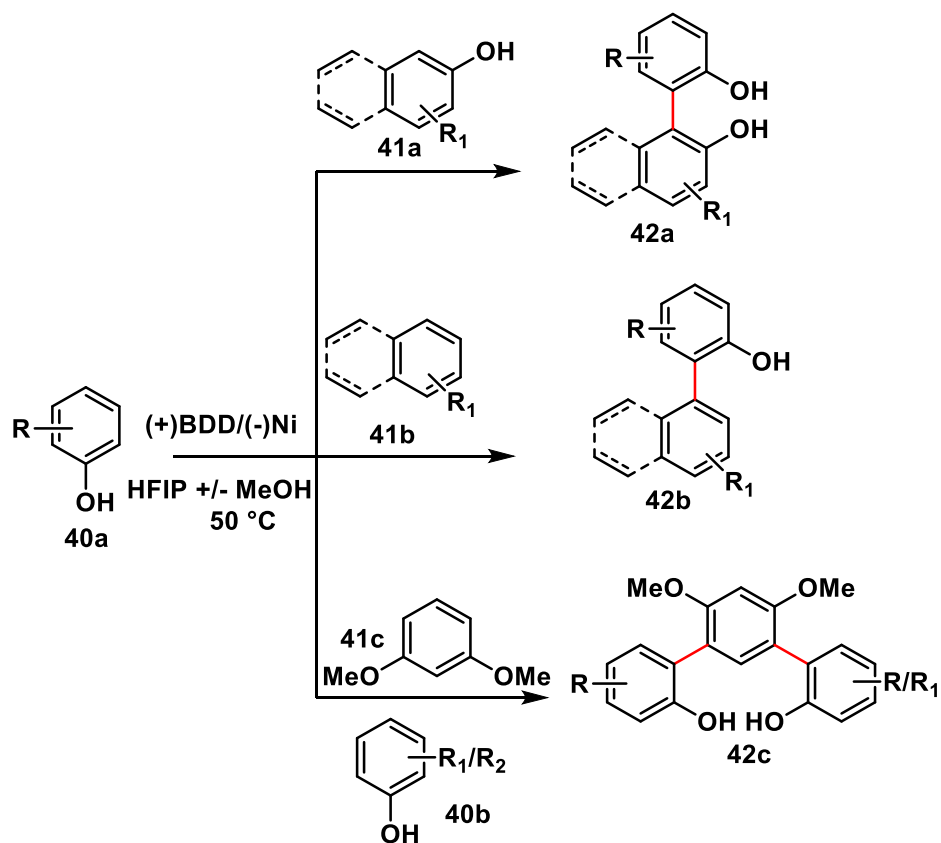
**Table 3.2:** Photochemical Oxidative Conditions.

Entry	Solvent	No. of equiv (Oxidant)	Additives	Temp.	Time	87 (%) <sup>a</sup>	88 (%) <sup>a</sup>
1	HFIP (0.1 M)	1.5 (IBDA)	Cs <sub>2</sub> CO <sub>3</sub>	rt	ON	30	60
2	ACN (0.06M)	1.1 (BI-OAc)	Ru-bpy/ Blue light	rt	2 days	0.0 <sup>b</sup>	0.0 <sup>b</sup>
3	ACN (0.06M)	1.1 (BI-OAc)	Ru-bpy/ Blue light	rt	ON	0.0 <sup>b</sup>	0.0 <sup>b</sup>
4	ACN (0.06M)	1.1 (BI-OAc)	Ru-bpy/ photoreactor	rt	ON	0.0 <sup>b</sup>	0.0 <sup>b</sup>
5	HFIP (0.1 M)	1.5 (IBDA)	1% Rubpyl	rt	ON	14	42
6	HFIP (0.1 M)	2.0 (IBDA)	1.2 Cs <sub>2</sub> CO <sub>3</sub> , Blue light	rt	2 days	23	48

<sup>a</sup> Isolated yields by flash column chromatography, <sup>b</sup> Based on TLC analysis.

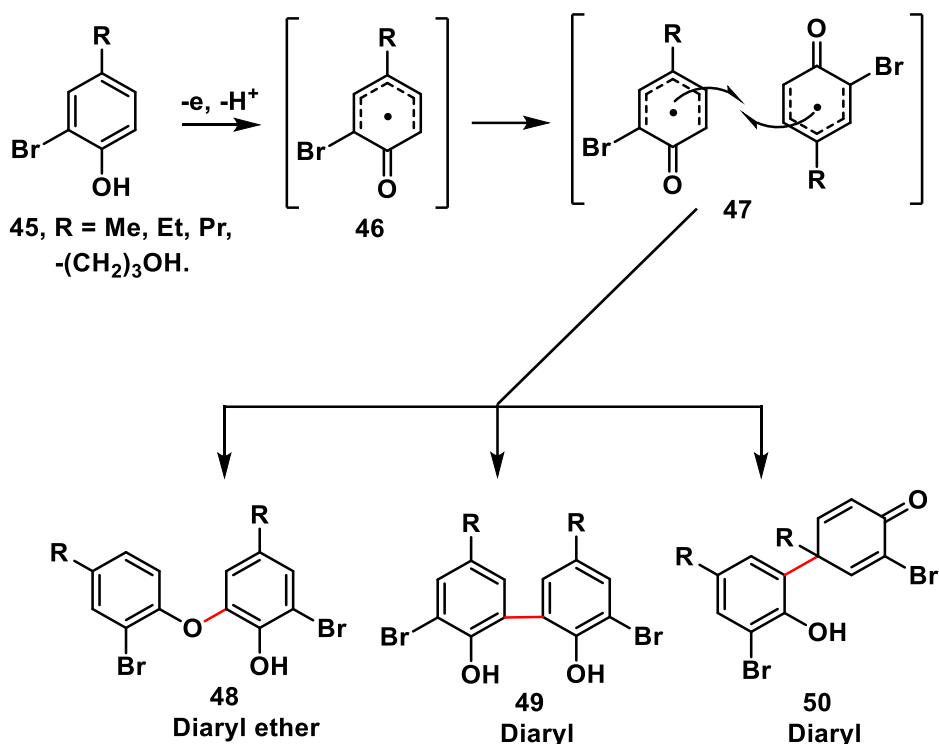
### ***3.2.2 Developing an anodic oxidative dearomatization reactions:***

Electroorganic synthesis offers a powerful approach for green synthetic methodologies, tackling many challenges associated with traditional synthetic chemistry. Various organic-electrochemical reactions have been discovered to provide number of synthetic transformations including carbon-carbon and carbon-heteroatom bond formations.<sup>20</sup> Especially after the great discovery of Kolbe electrolysis and reductive dimerization acrylonitrile, researchers have initiated electro-synthetic studies extensively to discover novel methods in synthetic chemistry.<sup>21</sup> Phenolic electrooxidation reactions furnish various types of carbon-carbon/heteroatom transformations which are widely utilized to obtain functionalized molecules and complex natural products. Most anodic phenolic oxidation reactions are performed in an environmentally friendly and atom economical condition. Phenols undergo two different electron transfer processes including single electron transfer reactions, producing phenolic dimerization. The Waldvogel group has studied anodic oxidative phenolic coupling reactions extensively and developed an electrochemical method for phenolic derivative **40** coupling with electron rich arenes **41a-c** (Scheme 3.10).<sup>22-24</sup>

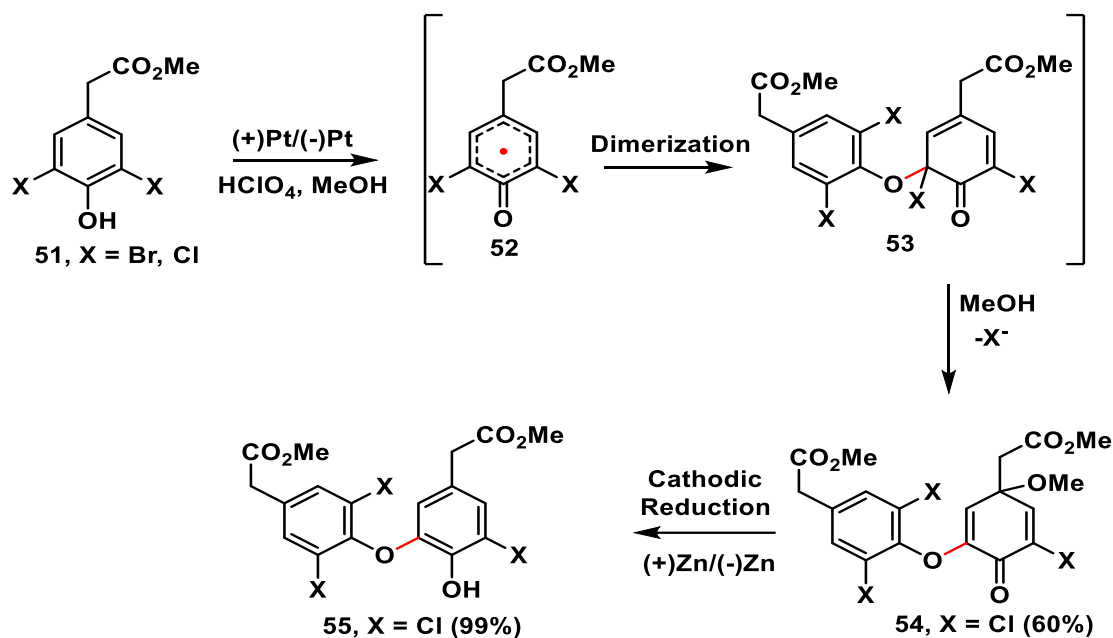


**Scheme 3.10:** Electrochemical phenol-aryl cross coupling by the Waldvogel group.

The solvent and electrodes choices were crucial in this process and a combination of the mixed solvent was important. Addition of methanol to HFIP was considered as a base to form hydrogen bonding with phenol derivatives and thus lowering the corresponding oxidative potential.<sup>23</sup> However, anodic oxidation of mono-halogenated phenols leads mainly to C-C coupled products (Scheme 3.11).<sup>25</sup> The Nishiyama group has successfully isolated the C-O coupling biaryl products by subjecting 2,5-dihalo phenol derivatives to anodic oxidation followed by cathodic reduction by C-X cleavage bond as shown in scheme 3.12.



**Scheme 3.11:** C-C biaryl coupling via electrochemical oxidation of mono-halogenated phenols.



**Scheme 3.12:** Electrooxidative dimerization of otho-dihalo phenols.

The Nishiyama group utilized this electrochemical methodology to successfully synthesize *O*-methylthalibrine **56**, verbenachalcone **57** and isodityrosine **58** (Figure 3.4).<sup>26–28</sup>

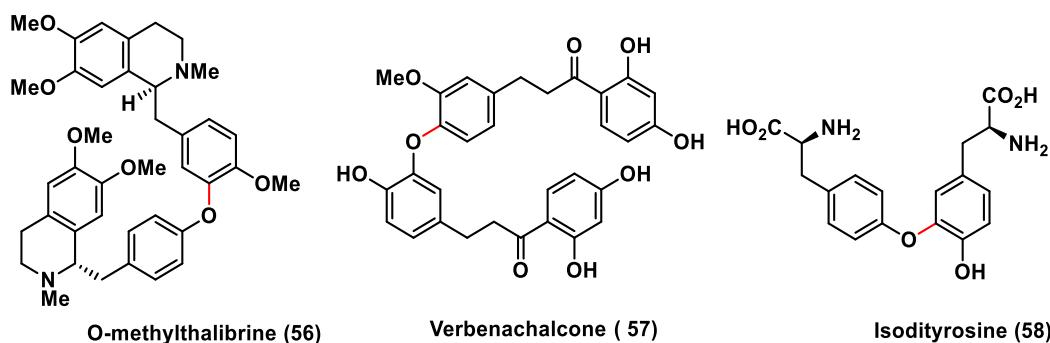
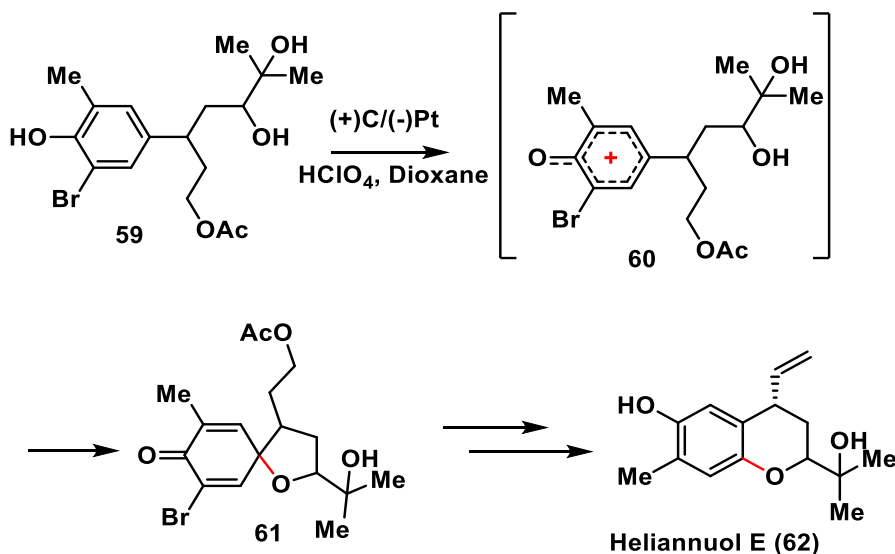


**Figure 3.4:** Synthesis of *O*-methylthalibrine, verbenachalcone and isodityrosine via electrochemical reactions.

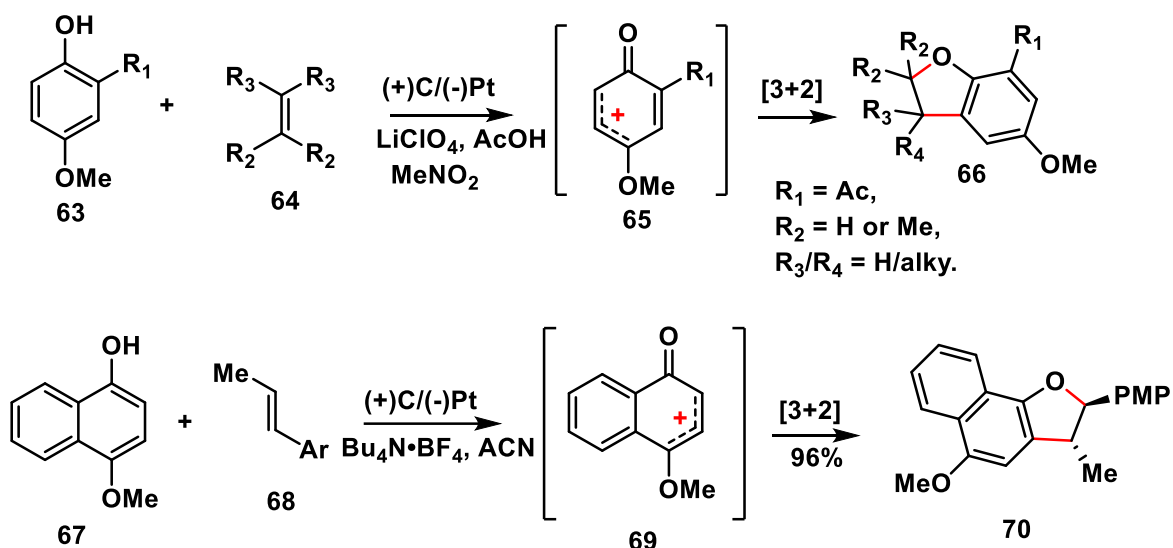
In addition to phenolic cross-coupling mediated by single electron transfer mechanism, phenols undergo double electron transfer reactions, forming a phenonium cation which is attacked by surrounding nucleophiles for intra and/or intermolecular C-X bond formations. The two-electron phenolic oxidation yields a highly reactive spirodienone product which has been used in

syntheses targeting several natural products as a key step reaction via intramolecular nucleophilic attack. For example, after electrochemical phenonium cation formation, the spirodienone intermediate **61** underwent ring expansion which ultimately furnishes heliannuol E natural product (Scheme 3.13).<sup>28,29</sup> Moreover, electrochemically generated cyclohexanedienone cation species are strong electrophiles for intermolecular [3+2] cycloaddition reactions in presence of electron rich alkene derivatives (Scheme 3.14).<sup>30-32</sup>



**Scheme 3.13:** Electrochemical synthesis of heliannuol E (**62**).



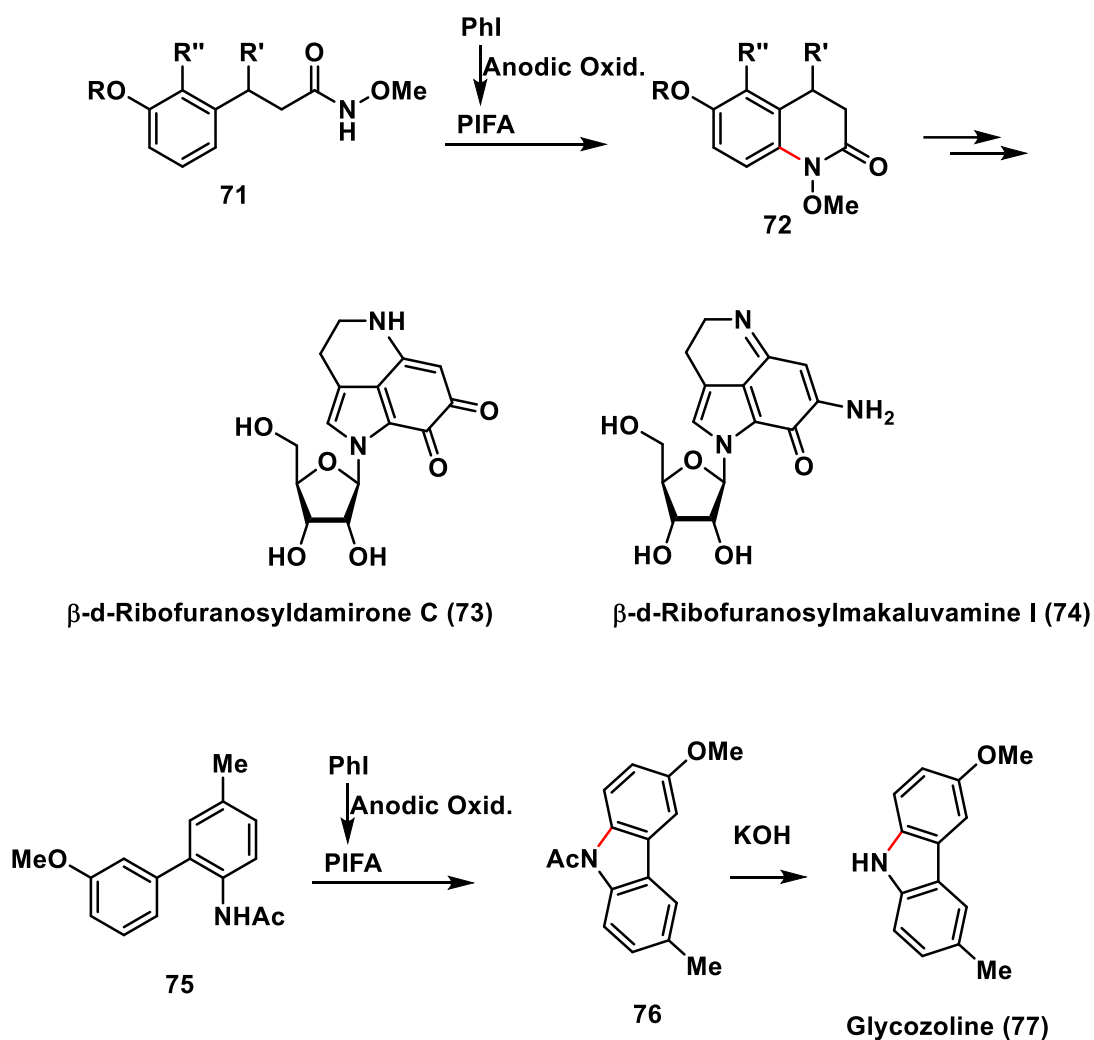


**Scheme 3.14:** [3+2] cycloaddition reactions mediated by electrooxidations of phenols and naphthols.

### 3.2.3 Nitrenium ion formation via electrochemical oxidation reactions:

Electrochemical nitrenium ion formation is an interesting area of research due to applications resulting in the easy construction of the corresponding cyclic scaffold found in number of natural products. Electrochemical oxidation has been utilized for the in-situ generation of hypervalent iodine reagents which are necessary for the nitrenium ion formation.<sup>22,33–36</sup> Thus, the combination of electrochemical conditions and hypervalent iodine reagents facilitates the nitrenium ions formation with minimizing the formation of unfavorable and unidentified byproducts.<sup>37,38</sup> Direct oxidation presumably yields number of different radical and radical cation intermediates which undergo (self) coupling reactions or reaction with the solvent, yielding multiple components.<sup>39,40</sup> Reported studies showed that the incorporation of NH(alkyl), NH(alkoxy) or NH(COR) substituents to amino derivatives would increase the stability of the formed positive charge and decrease the electrical potential required for oxidative cyclization/coupling reactions.<sup>38–40</sup> For example, the synthesis of

tetrahydropyrroloimidinoquinone alkaloids (**73** and **74**) and glycozoline (**77**) had been achieved by electrochemical C-N transformation of anisolic compounds containing *N*-methoxy amine and *N*-acetyl aryl derivatives mediated by electrochemical generation of hypervalent iodine (PIFA) reagent (scheme 3.15).<sup>34,36</sup>

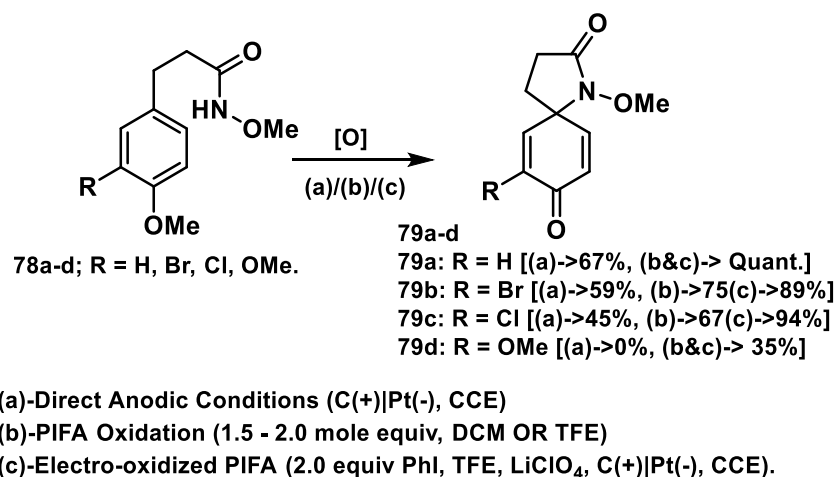


**Scheme 3.15:** PIFA electrochemical formation mediated the synthesis of tetrahydropyrroloiminoquinone alkaloids (**73** and **74**) and glycozoline (**77**).

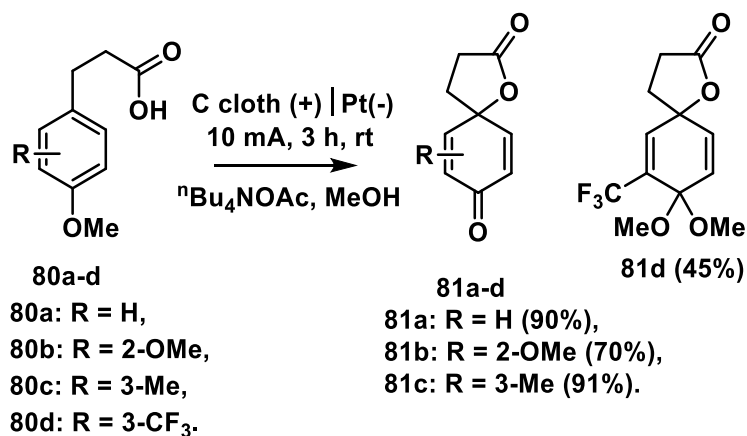
Nishiyama's group has studied oxidative cyclization reactions of *N*-methoxy amide derivatives utilizing different oxidation conditions including direct anodic oxidation using carbon as an anode and platinum as a cathode under constant current electrolysis conditions (CCE),

traditional oxidation conditions with PIFA, and (in-situ) electrochemical pre-oxidation of PIFA conditions.<sup>35</sup> It was found that using electrochemical pre-oxidized PIFA improves the yields dramatically compared to direct anodic oxidation and regular PIFA oxidations (Scheme 3.16).

On the other hand, Zhang and Lei groups have developed iodine-free direct electrochemical oxidation conditions inducing spirocyclization of non-phenolic amines and carboxylic acid (Scheme 3.17).<sup>39</sup>



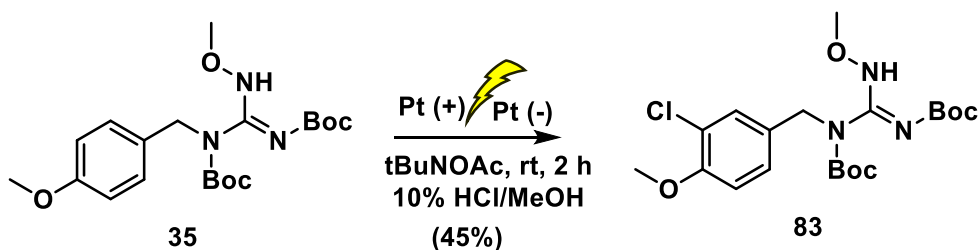
**Scheme 3.16:** Oxidative cyclization reactions of methoxy amides 2 using different oxidative conditions.



**Scheme 3.17:** Oxidative dearomatization reactions for nonphenolic carboxylic derivatives.

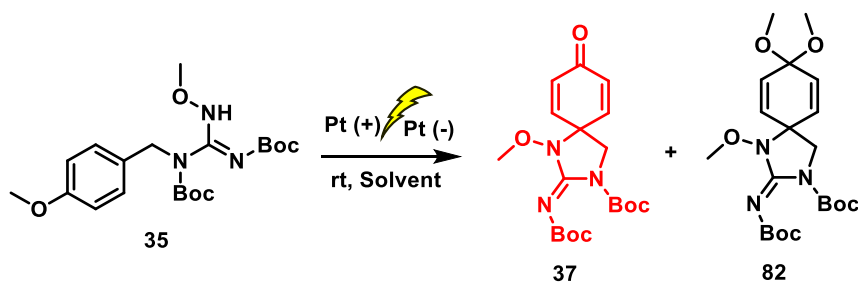
## RESULT AND DISCUSSION:

Failure to isolate good yield of the targeted spiro derivatives derived from the synthesized guanidine **35** has encouraged us to test the anodic oxidative conditions. However, all the reported anodic methods for arene oxidations containing amines or amides utilized electrochemically pre-oxidized PIFA. Iodine free anodic conditions were of interest to be tested with the nitrogen rich compound **35**. Therefore, an undivided electrochemical cell was used with Pt rods as cathode and anode. Tetrabutyl ammonium acetate was utilized as an electrolyte to facilitate electron motion in methanol as a solvent. Constant current and voltage were utilized to optimize the best conditions for iodine-free anodic oxidation reactions (Table 3.3). Interestingly, rather than the desired spiro cyclohexadienone **36**, the dimethyl ketal **82** was detected as the major product in good yield. Different conditions were evaluated to isolate the targeted spiro guanidine product as a major product. Meanwhile, the ketal product could be converted into the corresponding spiro cyclohexadienone product in the deuterated chloroform. As shown in table 3.3, most attempts were not successful compared to entries 1 and 2. Surprisingly, using a mixture of methanol and hydrochloric (10%) aqueous solution as a solvent resulted in isolation of a new product. This new product was identified as the chlorinated guanidine starting material **83** (Scheme 3.18) which was confirmed by mass spectrometry and 2D <sup>1</sup>HNMR spectroscopy techniques. A mixture of methanol and water resulted in formation of the desired cyclohexadienone product (10%) which might be isolated by further treating the ketal with acidic solutions. Interestingly, addition of IBDA to electrochemical conditions (entry 9) resulted in isolation of the desired spiro cyclohexadienone **36** in a moderate yield. Optimization of the number of molar equivalents of IBDA, electrolyte, and the solvent is planned to be studied to improve the yield of the targeted dearomatized products.



**Scheme 3.18:** Chlorinated guanidine **83**.

**Table 3.3:** Anodic iodine-free oxidation reactions for guanidine cyclization



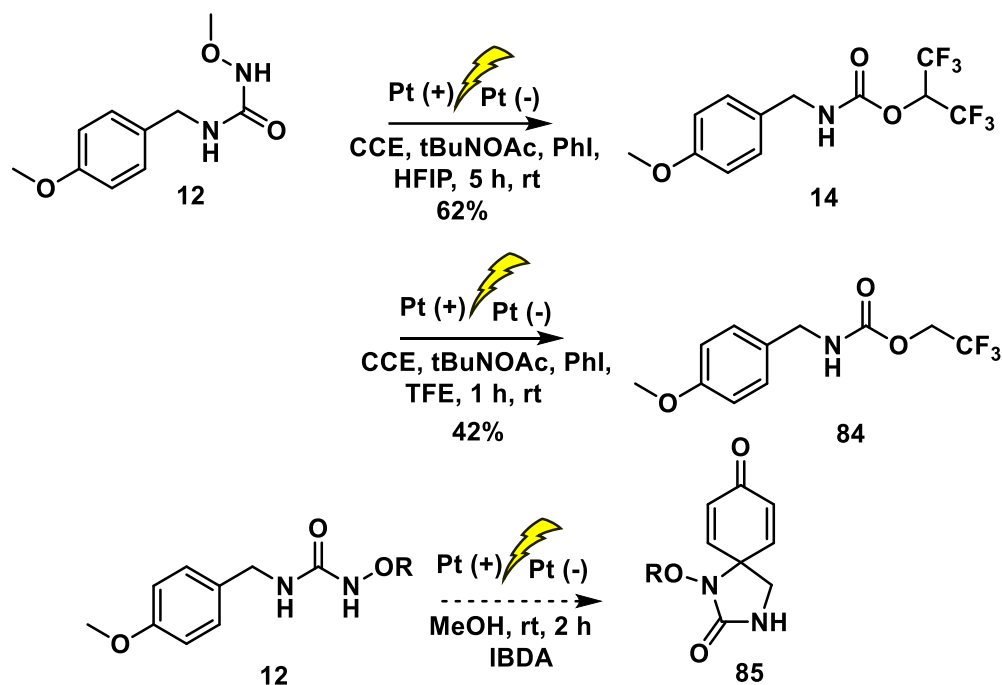
Entry	Solvent (0.1 M)	Current (I (mA)) <sup>a</sup>	Additives (1.0 equiv)	Time	37 (%) <sup>c</sup>	82 (%) <sup>c</sup>
1	MeOH (Dry)	20.0 (CC)	tBuNOAc	3h	0.0	60
2	MeOH (Dry)	20.0 (CC)	tBuNOAc	3h	0.0	60
3	MeOH	20.0 (CC)	tBuNOAc	3h	0.0	67
4	MeOH/H <sub>2</sub> O (1.5:1)	15-19 (CV ~28.3v)	tBuNOAc	8h	10	0.0
5	MeOH	10 (CC), then 20 (CC)	LiO <sub>4</sub> Cl	3h	Traces	Traces
6	MeOH	10 (CC), then 20 (CC)	tBuNOAc <sup>b</sup> & LiO <sub>4</sub> Cl	1h	Traces	Traces
7	5% NaOH/MeOH	10 (CC), then 20 (CC)	tBuNOAc	5h	Traces	Traces
8	MeOH/(10% aq.) HCl (4:1)	20.0 (CC) & 4.5 V	tBuNOAc	2h	0.0	0.0
9	MeOH	10 (cc)	tBuNOAc & 1.0 equiv IBDA	1h	30	0.0

a) CC is abbreviated for constant current and CV for constant voltage. For entry 6 and 7, 10 mA current was used first then after 1 h the current increased to 20 mA.

b) 0.2 equiv of tBuNOAc was used and 1.0 equiv of LiO<sub>4</sub>Cl.

c) The traces detected yields are based on TLC observations while the 60%, 67% and 0.0% are based on chromatographical purification.

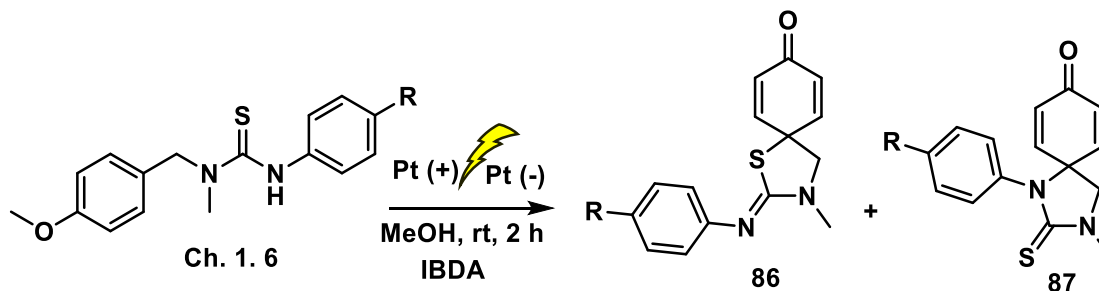
With success of anodic guanidine cyclization, it was worthwhile to evaluate these developed conditions with the urea and thiourea derivatives which are previously subjected to IBDA direct oxidation conditions and resulted in isolating off-target products. Subjecting *N*-methoxy urea derivative **12** to IBDA oxidations did not produce the desired dearomatized product but rather yielded the carbamate product **14**. In addition to *N*-methoxy urea **12**, anisolic thiourea derivatives (Chapter 2.6a-e) yielded benzo fused systems instead of dearomatized spiro cyclohexadieneones under IBDA direct oxidation reactions. Therefore, it was of interest to subject these derivatives to electrochemical conditions. The reaction of *N*-methoxy urea derivative **12** under electrochemical conditions using tetrabutylammonium acetate as an electrolyte in methanol at room temperature resulted in a complex mixture of products. Therefore, the electrochemical generation of hypervalent iodine reagents was attempted using iodobenzene with fluorinated solvent and the application of a constant current. The first attempt involved adding the reaction components altogether at the same time resulting in long reaction time (5 h) and isolating the previously obtained carbamate **14** (62%) (Scheme 3.19). Based on literature data, electrochemical conditions are targeted for iodine pre-oxidation, thus iodobenzene was added in trifluoroethanol in presence of an electrolyte and subjected to a constant current electrolysis for 1h. Then *N*-methoxy urea derivative **12** was added and after 15 minutes it was completely consumed and converted into a new product based on TLC analysis.



Addition of IBDA directly is under optimization

**Scheme 3.19:** Electrochemical oxidation attempts for *N*-methoxy urea **12**.

However, the product of this stepwise addition of the reaction components was not the desired product but rather the corresponding carbamate product **84** (Scheme 3.19). The idea of readymade hypervalent iodine addition has been applied to this substrate, resulting in a new product with same functional groups indicating no dearomatization of the anisolic ring and no loss of the NOME. Similar observation was made with addition of NaI as a source for iodine. Moreover, anisolic thiourea derivatives were subjected to electrochemical conditions, resulting in the detection of a mixture of the two possible spiro systems (Scheme 3.20). The outcomes of these conditions are still under investigation, giving hope for tackling the issue associated to the conventional IBDA condition.



**Scheme 3.20:** Under optimization anodic oxidation conditions for the previously synthesized derivatives.

### 3.3 SUMMARY:

In conclusion, research described in the current chapter investigated the possibility of oxidative dearomatization reactions on non-phenolic urea and guanidine derivatives, targeting stabilized nitrenium ion formation. We found that alkoxy group stabilizes the formation of nitrenium ions more than the aryl stabilization based on our previous work (Chapter two). The scope and limitations of OD reactions of urea derivatives have been defined due to unsuccessful OD reactions on *N,N'*-disubstituted urea derivatives in fluorinated solvents. As a result, this is limiting OD reactions for this specific class of ureas (trisubstituted urea derivatives). The presence of BnNH free group stabilizes the carbonyl group and facilitates the removal of ammonium cation formed with NHOMe group. The rationale behind targeting nitrenium ion formation mediated the dearomatization spirocyclization mechanism is the low yield and weak selectivity of the previously studied *N*-aryl thio/urea derivatives and guanidines protected with carbonyl groups. Therefore, *N*-alkoxy anisolic guanidine derivatives have been subjected to OD reactions and resulted in isolation of the targeted spiro cyclohexandienone products and the deprotected starting guanidine. Thus, anodic oxidation conditions have been developed to solve most of these issues associated to the conventional hypervalent iodine reagent including the limitation for trisubstituted urea derivatives and deprotection of Boc protected guanidines. The electrochemical oxidation of guanidines yielded the dearomatized product as a main target for developing this simple electrochemical



reaction. Moreover, we found that fresh electrochemical oxidation of iodine reagent to the corresponding hypervalent iodine derivatives did not afford the desired outcomes as it is reported in the literature. While the addition of readymade hypervalent iodine reagent has shown a different impact on the dearomatization of urea and thiourea derivatives which is required further investigations.

### 3.4 REFERENCES:

- (1) Edwards, O. E.; Vocelle, D.; ApSimon, J. W.; Haque, F. Transannular Reactions of Nitrenium Ions. *J. Am. Chem. Soc.* **1965**, *87* (3), 678–679. <https://doi.org/10.1021/ja01081a067>.
- (2) Kaiho, T.; Zhdankin, V. V. Industrial Applications. In *PATAI'S Chemistry of Functional Groups*; John Wiley & Sons, Ltd, 2018; pp 1–13. <https://doi.org/https://doi.org/10.1002/9780470682531.pat0954>.
- (3) Borodkin, G. I.; Shubin, V. G. Nitrenium Ions and Problem of Direct Electrophilic Amination of Aromatic Compounds. *Russ. J. Org. Chem.* **2005**, *41* (4), 473–504. <https://doi.org/10.1007/s11178-005-0193-z>.
- (4) Maiti, S.; Alam, M. T.; Bal, A.; Mal, P. Nitrenium Ions from Amine-Iodine(III) Combinations. *Adv. Synth. Catal.* **2019**, *361* (19), 4401–4425. <https://doi.org/https://doi.org/10.1002/adsc.201900441>.
- (5) Miyazawa, E.; Sakamoto, T.; Kikugawa, Y. Synthesis of Spirodienones by Intramolecular Ipso-Cyclization of N-Methoxy-(4-Halogenophenyl)Amides Using [Hydroxy(Tosyloxy)Iodo]Benzene in Trifluoroethanol. *J. Org. Chem.* **2003**, *68* (13), 5429–5432. <https://doi.org/10.1021/jo034318w>.
- (6) Itoh, N.; Sakamoto, T.; Miyazawa, E.; Kikugawa, Y. Introduction of a Hydroxy Group at the Para Position and N-Iodophenylation of N-Arylamides Using Phenyl iodine(III) Bis(Trifluoroacetate). *J. Org. Chem.* **2002**, *67* (21), 7424–7428. <https://doi.org/10.1021/jo0260847>.
- (7) Kikugawa, Y.; Nagashima, A.; Sakamoto, T.; Miyazawa, E.; Shiiya, M. Intramolecular Cyclization with Nitrenium Ions Generated by Treatment of N-Acylaminophthalimides with Hypervalent Iodine Compounds: Formation of Lactams and Spiro-Fused Lactams. *J. Org. Chem.* **2003**, *68* (17), 6739–6744. <https://doi.org/10.1021/jo0347009>.
- (8) Malamidou-Xenikaki, E.; Spyroudis, S.; Tsanakopoulou, M.; Hadjipavlou-Litina, D. A Convenient Approach to Fused Indeno-1,4-Diazepinones through Hypervalent Iodine Chemistry. *J. Org. Chem.* **2009**, *74* (19), 7315–7321. <https://doi.org/10.1021/jo9013063>.
- (9) Couto, I.; Pardo, L. M.; Tellitu, I.; Domínguez, E. A Diastereocontrolled Route to 10-Arylpyrrolo[1,2-b]Isoquinolines. *J. Org. Chem.* **2012**, *77* (24), 11192–11199. <https://doi.org/10.1021/jo302287v>.
- (10) Lucchetti, N.; Scalone, M.; Fantasia, S.; Muñiz, K. An Improved Catalyst for Iodine(I/III)-Catalysed Intermolecular C–H Amination. *Adv. Synth. & Catal.* **2016**, *358* (13), 2093–2099. <https://doi.org/https://doi.org/10.1002/adsc.201600191>.
- (11) Ousmer, M.; Braun, N. A.; Bavoux, C.; Perrin, M.; Ciufolini, M. A. Total Synthesis of Tricyclic Azaspirane Derivatives of Tyrosine: FR901483 and TAN1251C. *J. Am. Chem. Soc.* **2001**, *123* (31), 7534–7538. <https://doi.org/10.1021/ja016030z>.
- (12) Canesi, S.; Belmont, P.; Bouchu, D.; Rousset, L.; Ciufolini, M. A. Efficient Oxidative Spirocyclization of Phenolic Sulfonamides. *Tetrahedron Lett.* **2002**, *43* (29), 5193–5195. [https://doi.org/https://doi.org/10.1016/S0040-4039\(02\)00949-8](https://doi.org/https://doi.org/10.1016/S0040-4039(02)00949-8).
- (13) Wardrop, D. J.; Zhang, W.; Landrie, C. L. Stereoselective Nitrenium Ion Cyclizations: Asymmetric Synthesis of the (+)-Kishi Lactam and an Intermediate for the Preparation of Fascicularin. *Tetrahedron Lett.* **2004**, *45* (22), 4229–4231. <https://doi.org/https://doi.org/10.1016/j.tetlet.2004.04.028>.
- (14) Wardrop, D. J.; Bowen, E. G. Nitrenium Ion-Mediated Alkene Bis-Cyclofunctionalization: Total Synthesis of (–)-Swainsonine. *Org. Lett.* **2011**, *13* (9), 2376–2379.

- <https://doi.org/10.1021/ol2006117>.
- (15) Wardrop, D. J.; Burge, M. S. Total Synthesis of (–)-Dysibetaine via a Nitrenium Ion Cyclization–Dienone Cleavage Strategy. *Chem. Commun.* **2004**, No. 10, 1230–1231. <https://doi.org/10.1039/B403081H>.
  - (16) Wardrop, D. J.; Burge, M. S. Nitrenium Ion Azaspirocyclization–Spirodienone Cleavage: A New Synthetic Strategy for the Stereocontrolled Preparation of Highly Substituted Lactams and N-Hydroxy Lactams. *J. Org. Chem.* **2005**, *70* (25), 10271–10284. <https://doi.org/10.1021/jo051252r>.
  - (17) Wardrop, D. J.; Yermolina, M. V; Bowen, E. G. Iodine(III)-Mediated Cyclization of Unsaturated O-Alkyl Hydroxamates: Silyl-Assisted Access to  $\alpha$ -Vinyl and  $\alpha$ -(2-Silylvinyl) Lactams. *Synthesis (Stuttg)*. **2012**, *44* (08), 1199–1207.
  - (18) Wardrop, D. J.; Burge, M. S.; Zhang, W.; Ortíz, J. A.  $\pi$ -Face Selective Azaspirocyclization of  $\omega$ -(Methoxyphenyl)-N-Methoxyalkylamides. *Tetrahedron Lett.* **2003**, *44* (12), 2587–2591. [https://doi.org/https://doi.org/10.1016/S0040-4039\(03\)00227-2](https://doi.org/https://doi.org/10.1016/S0040-4039(03)00227-2).
  - (19) Wardrop, D. J.; Bowen, E. G.; Forslund, R. E.; Sussman, A. D.; Weerasekera, S. L. Intramolecular Oxamidation of Unsaturated O-Alkyl Hydroxamates: A Remarkably Versatile Entry to Hydroxy Lactams. *J. Am. Chem. Soc.* **2010**, *132* (4), 1188–1189. <https://doi.org/10.1021/ja9069997>.
  - (20) Yoshida, J.; Kataoka, K.; Horcajada, R.; Nagaki, A. Modern Strategies in Electroorganic Synthesis. *Chem. Rev.* **2008**, *108* (7), 2265–2299. <https://doi.org/10.1021/cr0680843>.
  - (21) T. Shono. *Electroorganic Chemistry as a New Tool in Organic Synthesis*; Springer:Berlin, 1984.
  - (22) Kirste, A.; Schnakenburg, G.; Stecker, F.; Fischer, A.; Waldvogel, S. R. Anodic Phenol–Arene Cross-Coupling Reaction on Boron-Doped Diamond Electrodes. *Angew. Chemie Int. Ed.* **2010**, *49* (5), 971–975. <https://doi.org/https://doi.org/10.1002/anie.200904763>.
  - (23) Kirste, A.; Elsler, B.; Schnakenburg, G.; Waldvogel, S. R. Efficient Anodic and Direct Phenol–Arene C,C Cross-Coupling: The Benign Role of Water or Methanol. *J. Am. Chem. Soc.* **2012**, *134* (7), 3571–3576. <https://doi.org/10.1021/ja211005g>.
  - (24) Elsler, B.; Wiebe, A.; Schollmeyer, D.; Dyballa, K. M.; Franke, R.; Waldvogel, S. R. Source of Selectivity in Oxidative Cross-Coupling of Aryls by Solvent Effect of 1,1,1,3,3,3-Hexafluoropropan-2-ol. *Chem. – A Eur. J.* **2015**, *21* (35), 12321–12325. <https://doi.org/https://doi.org/10.1002/chem.201501604>.
  - (25) Mori, K.; Takahashi, M.; Yamamura, S.; Nishiyama, S. Anodic Oxidation of Monohalogenated Phenols. *Tetrahedron* **2001**, *57* (26), 5527–5532. [https://doi.org/https://doi.org/10.1016/S0040-4020\(01\)00478-1](https://doi.org/https://doi.org/10.1016/S0040-4020(01)00478-1).
  - (26) Kawabata, Y.; Naito, Y.; Saitoh, T.; Kawa, K.; Fuchigami, T.; Nishiyama, S. Synthesis of (+)-O-Methylthalibrine by Employing a Stereocontrolled Bischler–Napieralski Reaction and an Electrochemically Generated Diaryl Ether. *European J. Org. Chem.* **2014**, *2014* (1), 99–104. <https://doi.org/https://doi.org/10.1002/ejoc.201301128>.
  - (27) Naito, Y.; Tanabe, T.; Kawabata, Y.; Ishikawa, Y.; Nishiyama, S. Electrochemical Construction of the Diaryl Ethers: A Synthetic Approach to o-Methylthalibrine. *Tetrahedron Lett.* **2010**, *51* (36), 4776–4778. <https://doi.org/https://doi.org/10.1016/j.tetlet.2010.07.037>.
  - (28) Tanabe, T.; Doi, F.; Ogamino, T.; Nishiyama, S. A Total Synthesis of Verbenachalcone, a Bioactive Diaryl Ether from Verbena Littoralis. *Tetrahedron Lett.* **2004**, *45* (17), 3477–3480. <https://doi.org/https://doi.org/10.1016/j.tetlet.2004.02.154>.

- (29) Doi, F.; Ogamino, T.; Sugai, T.; Nishiyama, S. Enantioselective Synthesis of Heliannuol E; Structural Consideration of Natural Molecule. *Tetrahedron Lett.* **2003**, *44* (26), 4877–4880. [https://doi.org/https://doi.org/10.1016/S0040-4039\(03\)01094-3](https://doi.org/https://doi.org/10.1016/S0040-4039(03)01094-3).
- (30) El-Seedi, H. R.; Yamamura, S.; Nishiyama, S. Reactivity of Naphthol towards Nucleophiles in Anodic Oxidation. *Tetrahedron* **2002**, *58* (37), 7485–7489. [https://doi.org/https://doi.org/10.1016/S0040-4020\(02\)00829-3](https://doi.org/https://doi.org/10.1016/S0040-4020(02)00829-3).
- (31) Kim, S.; Hirose, K.; Uematsu, J.; Mikami, Y.; Chiba, K. Electrochemically Active Cross-Linking Reaction for Fluorescent Labeling of Aliphatic Alkenes. *Chem. – A Eur. J.* **2012**, *18* (20), 6284–6288. <https://doi.org/https://doi.org/10.1002/chem.201103630>.
- (32) Kim, S.; Noda, S.; Hayashi, K.; Chiba, K. An Oxidative Carbon–Carbon Bond Formation System in Cycloalkane-Based Thermomorphic Multiphase Solution. *Org. Lett.* **2008**, *10* (9), 1827–1829. <https://doi.org/10.1021/ol8004408>.
- (33) Elsherbini, M.; Winterson, B.; Alharbi, H.; Folgueiras-Amador, A. A.; Génot, C.; Wirth, T. Continuous-Flow Electrochemical Generator of Hypervalent Iodine Reagents: Synthetic Applications. *Angew. Chemie* **2019**.
- (34) Inoue, K.; Ishikawa, Y.; Nishiyama, S. Synthesis of Tetrahydropyrroloiminoquinone Alkaloids Based on Electrochemically Generated Hypervalent Iodine Oxidative Cyclization. *Org. Lett.* **2010**, *12* (3), 436–439. <https://doi.org/10.1021/ol902566p>.
- (35) Amano, Y.; Nishiyama, S. Oxidative Synthesis of Azacyclic Derivatives through the Nitrenium Ion: Application of a Hypervalent Iodine Species Electrochemically Generated from Iodobenzene. *Tetrahedron Lett.* **2006**, *47* (37), 6505–6507. <https://doi.org/https://doi.org/10.1016/j.tetlet.2006.07.050>.
- (36) Kajiyama, D.; Inoue, K.; Ishikawa, Y.; Nishiyama, S. A Synthetic Approach to Carbazoles Using Electrochemically Generated Hypervalent Iodine Oxidant. *Tetrahedron* **2010**, *66* (52), 9779–9784. <https://doi.org/https://doi.org/10.1016/j.tet.2010.11.015>.
- (37) Roth, H. G.; Romero, N. A.; Nicewicz, D. A. Experimental and Calculated Electrochemical Potentials of Common Organic Molecules for Applications to Single-Electron Redox Chemistry. *Synlett* **2015**, *27*, 714–723.
- (38) Yan, M.; Kawamata, Y.; Baran, P. S. Synthetic Organic Electrochemical Methods Since 2000: On the Verge of a Renaissance. *Chem. Rev.* **2017**, *117* (21), 13230–13319. <https://doi.org/10.1021/acs.chemrev.7b00397>.
- (39) Zhang, C.; Bu, F.; Zeng, C.; Wang, D.; Lu, L.; Zhang, H.; Lei, A. Electrochemical Oxidation Dearomatization of Anisol Derivatives toward Spiropyrrolidines and Spirolactones. *CCS Chem.* **2022**, *4* (4), 1199–1207. <https://doi.org/10.31635/ccschem.021.202100860>.
- (40) Falck, J. R.; Miller, L. L.; Stermitz, F. R. Electrooxidative Synthesis of Morphinandienones from 1-Benzyltetrahydroisoquinolines. *Tetrahedron* **1974**, *30* (8), 931–934. [https://doi.org/https://doi.org/10.1016/S0040-4020\(01\)97477-0](https://doi.org/https://doi.org/10.1016/S0040-4020(01)97477-0).
-

**CHAPTER FOUR: OXIDATIVE DEAROMATIZATION (OD) ATTEMPTS TOWARD  
THE CORE SCAFFOLD OF KB343**

Marian N. Aziz <sup>a,b</sup>, Delphine Gout <sup>a</sup>, Carl J. Lovely <sup>a</sup>

a. Department of Chemistry and Biochemistry, 700 Planetarium Place, University of Texas at  
Arlington, TX 76019, USA

b. Department of Pesticide Chemistry, NatPional Research Centre, Dokki, Giza 12622, Egypt

Corresponding author

Prof. Carl J. Lovely

Professor, Chemistry and Biochemistry Department

University of Texas at Arlington

Address: 700 Planetarium Place, Box 19065, UT Arlington, TX 76019-0065

Email: lovely@uta.edu

Phone: +1 817 272 5446

(Not Published)

## ABSTRACT

An investigation of oxidative dearomatization approaches to construct frameworks related to KB343 has been performed. Applications of OD conditions for the synthesized tri-substituted ureas yielded hydantoin structures instead of the desired dearomatized product. Thus, a novel methodology of hydantoin ring system has been explored through one-pot three component reactions. Similar observations have been made for di-substituted ureas subjected to OD conditions by isolating the corresponding urethane products. Attempts towards synthesizing the core structure of KB343 have been performed using the commercially available *p*-phenyl glycine amino acid. The basicity effect of Grignard reagent derived from (2-bromoallyl)trimethylsilane results in reduction of the aldehyde rather than the desired alkylation reactions. An alternative pathway towards synthesis of the core structure of KB343 is ongoing.

## 4.1 INTRODUCTION:

### 4.1.1 CHEMISTRY AND BIOACTIVITY OF KB343 NATURAL PRODUCT

Marine alkaloids have been isolated from various marine organisms such as zoantharians, which are considered a rich source for a variety of cyclized guanidine natural products.<sup>1,2</sup> KB343, a tris guanidine has been added to the count of cyclic guanidine natural products in 2018, after its isolation from *Epizoanthus illoricatus* by Sakai's group.<sup>3</sup> The intriguing chemical structure of the cyclic guanidine alkaloids and their broad range biological activities attract a plethora of organic chemists. KB343 structure is tris cyclic guanidine attached to a decalin ring system containing five contiguous chiral carbons (Figure 4.1). The Sakai lab had tested the aqueous extract of a Palauan zoantharian by direct injection into the cerebrospinal fluid of mice which resulted in convulsions and the death of the animals a few days after. Thus, the observed biological activity directed the group to the isolation of KB343. Attempts to convert the isolated material into different derivatives were performed by treating KB343 with 2,4-pentanedione to isolate the mono, bis, and tris

pyrimidine derivatives. The group tested their anti-proliferative activity against neuronal (SH-SY5Y), cervical (HeLa), and murine leukemia (L1210) cell lines. Interestingly, the tested compound showed moderate cytotoxicity against the cell lines. The mono-pyrimidine derivative (**2**) ( $IC_{50} = 0.38 \mu M$ ) was more active than KB343 ( $IC_{50} = 1.96 \mu M$ ) against L1210 cell line. Therefore, in addition to the unique chemical structure, the synthesis of KB343 natural product is highly considered as a medicinal target to discover new anti-proliferative compounds related to its interesting chemical structure.

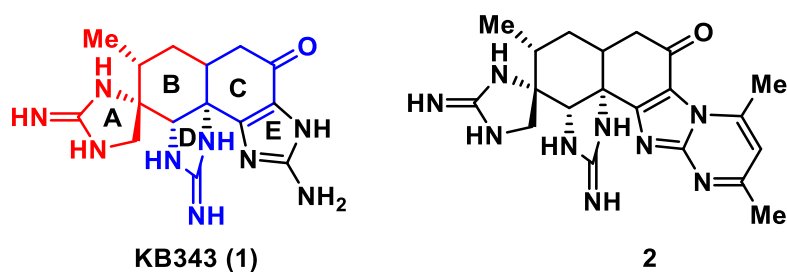
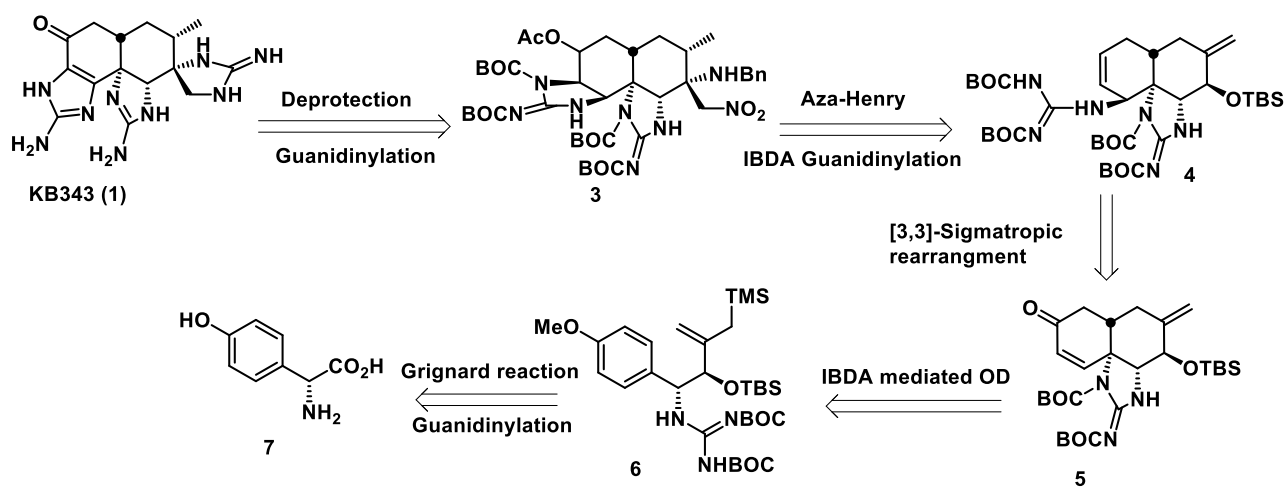


**Figure 4.1:** KB343 chemical structure.

#### ***4.1.2 RETROSYNTHETIC SCHEME TOWARDS SYNTHESIS KB343 VIA TOADS AS A KEY STEP REACTION***

The motivation behind elaborating the oxidative dearomatization reactions is to construct a complicated natural product via carbon-heteroatom bond formation in which two or three ring systems will fuse together to form the targeted structure. The KB343 decalin core structure (**5**) is targeted to be synthesized via establishing rings B, C, and D (Figure 3.1) via oxidative dearomatization as a key step reaction. As shown in scheme 3.1, the designed retrosynthetic scheme towards KB343 (**1**) starts with commercially available chiral *p*-hydroxyphenyl glycine (**7**). Different methodologies toward the construction of the three cyclic guanidine (Figure 3.1 (rings A, D, and E)) will be employed. Therefore, we envisioned that the KB343 skeleton would be synthesized from bis-cyclic guanidine **3** by a guanidinylation of 1,2-diamine to construct guanidine ring A and global BOC deprotection. The guanidine **3** could be prepared by oxidative

guanidinylation of decline **4** to construct ring E. The di-guanidine decline **4** could be prepared by [3,3]-sigmatropic rearrangement of allylic cyanate derived from decline **5** after reduction of carbonyl group and reaction with cyanogen bromide. The decalin fused guanidine **5** might be synthesized via OD key reaction from guanidine intermediate **6** which may be isolated from the commercially available amino acid (**7**) after eight steps including Grignard and guanylation reactions. Attempts toward synthesis the KB343 core scaffold (**5**) and related analogues are discussed in the present chapter.



**Scheme 4.1:** Retrosynthetic approach towards synthesis KB343 (**1**).

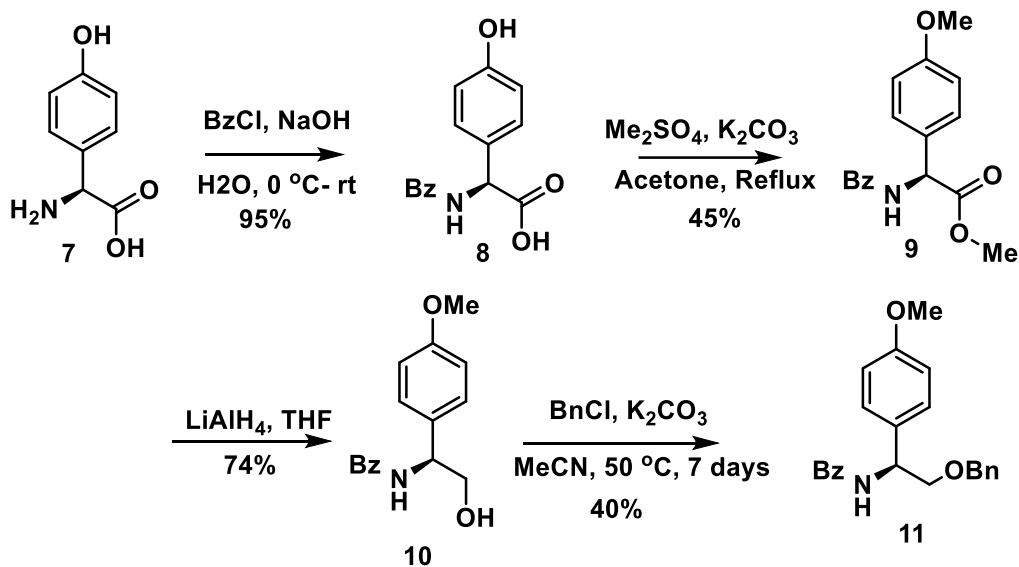
## 4.2 RESULTS AND DISCUSSION

### 4.2.1 Attempts towards synthesis urea derivatives

Initially, we have started to synthesize urea and thiourea derivatives related to the KB343 core structure before working on the designed guanidine **6**. Therefore, 4-hydroxyphenyl glycine was subjected to benzoyl protection, methylation using dimethyl sulfate, then reduction with  $\text{LiAlH}_4$ , and followed by protection of the resulting alcohol with benzyl group (Scheme 4.2).<sup>4</sup> Unfortunately, the protected benzoyl group was not successfully removed from benzamide **11**

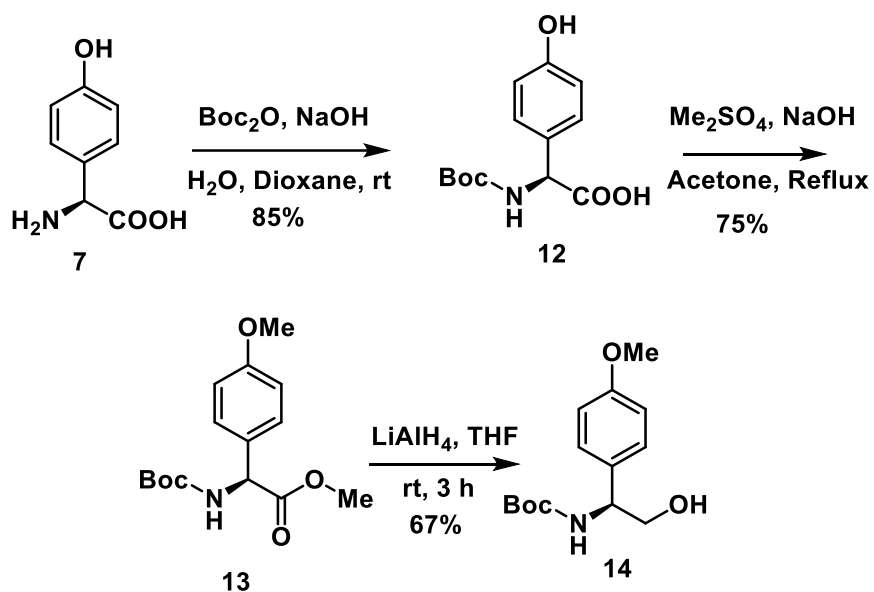


using different hydrolysis conditions (Table 4.1) and attempts to reduce the benzyl group did not work out with this substrate.

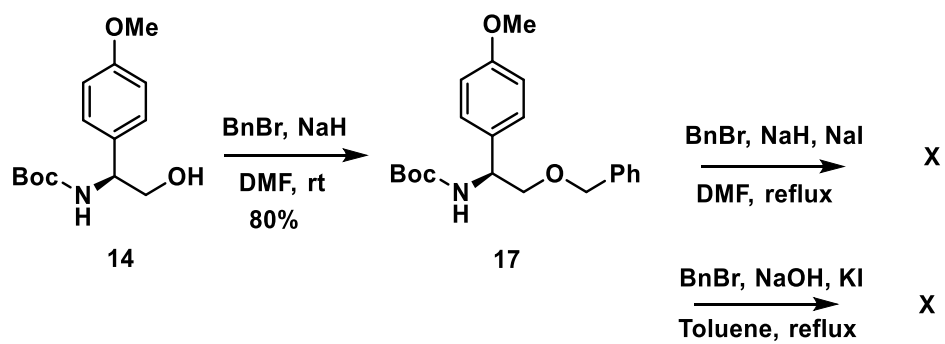


**Scheme 4.2:** Synthesis of the protected amino alcohol (**11**).

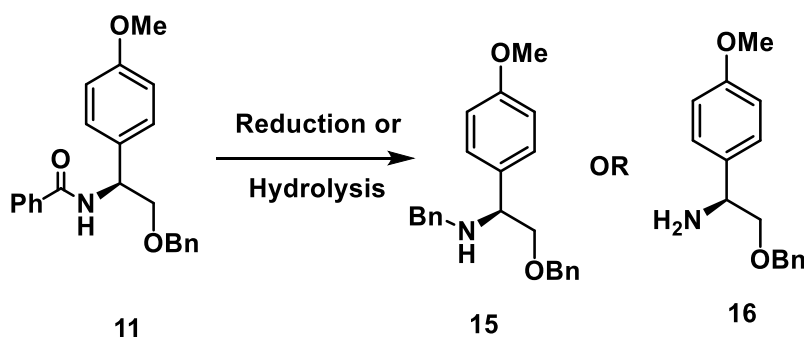
Therefore, we switched to the Boc protection approach and followed the same synthetic pathway as shown in Scheme 2 to isolate the protected amino alcohol **14** in good yield (Scheme 4.3). The protection of alcohol **14** with benzyl group did not help in alkylation of *N*-Boc secondary amine using different conditions (Scheme 4.4).

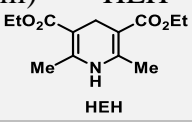


**Scheme 4.3.** Synthesis *N*-Boc amino alcohol (**14**).



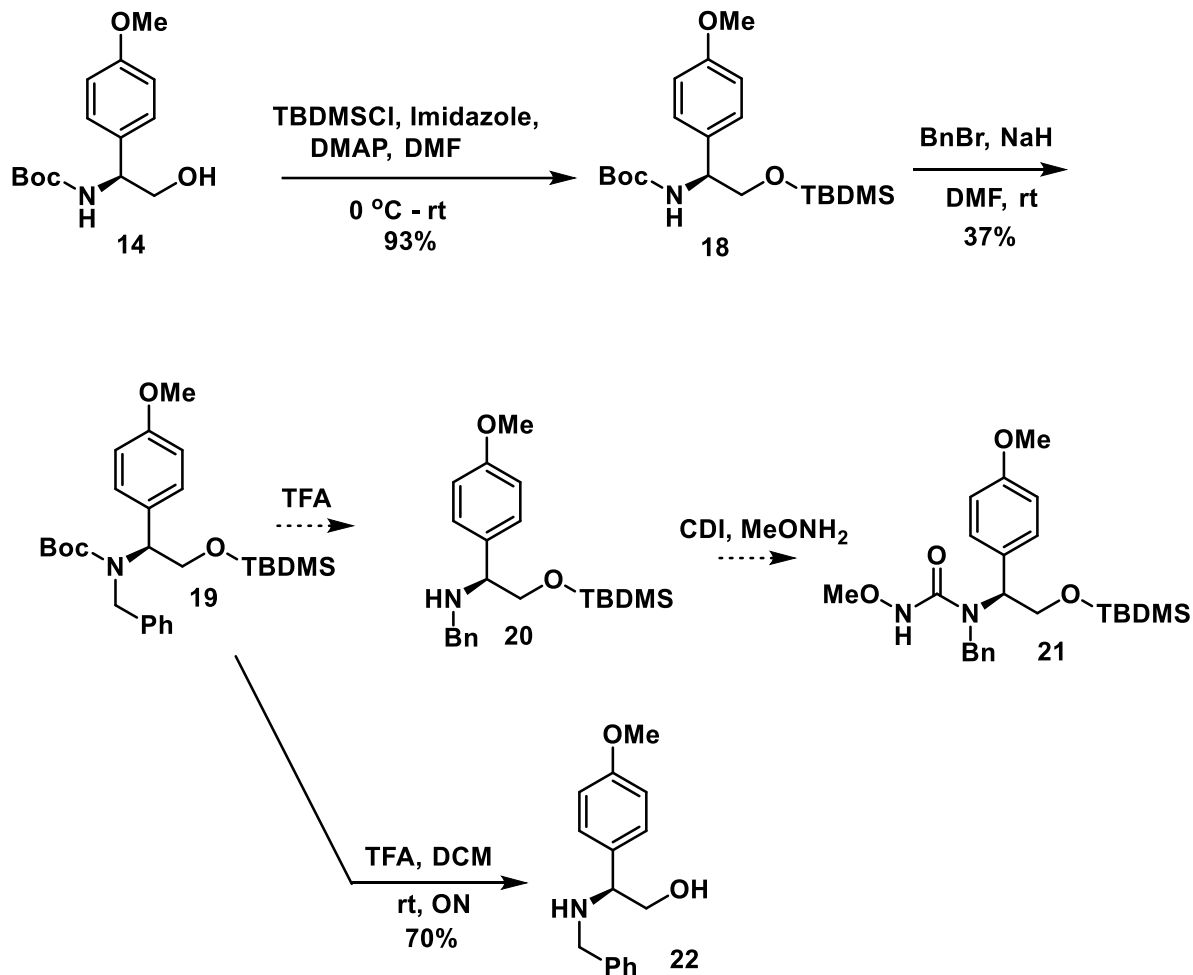
**Scheme 4.4:** Unsuccessful *N*-alkylation attempts using benzyl protected alcohol (**17**).

**Table 1:** Attempts for reduction and hydrolysis of benzamide (**11**).

	Reduction and hydrolysis Conditions for Benzamide ( <b>11</b> )	Result
<b>1</b>	LiAlH <sub>4</sub> , THF	NR*
<b>2</b>	LiAlH <sub>4</sub> , TMSCl, THF, 0 °C - rt	NR*
<b>3</b>	i) Tf <sub>2</sub> O (1.05 equiv.), DCM, 2-FPyr (1.1 equiv.), -78 °C, 0 °C ii) Et <sub>3</sub> SiH (1.1 equiv.), 0 °C, rt, 5 h iii) HEH (1.4 equiv.), rt, 12h 	No SM remained but product was not identified by NMR spectroscopy
<b>4</b>	20% KOH, reflux	NR*
<b>5</b>	HCl, reflux	NR*

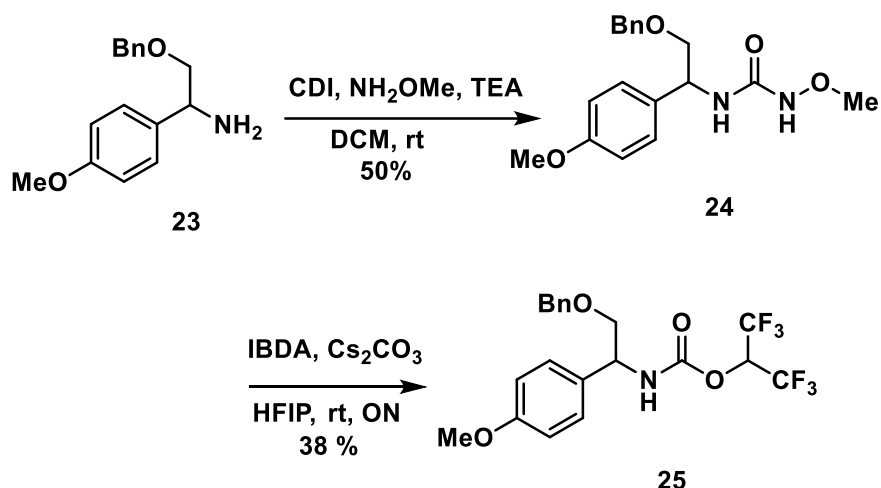
\*. No Reaction (NR) occurred based on the TLC analysis.

Thus, silyl protection of the alcohol was successfully achieved to facilitate the alkylation of the secondary amine using benzylation conditions (Scheme 4.5). Removal of the Boc group under acidic conditions was targeted to synthesize the designed tri-substituted urea **21** via isolation of secondary amine **20**. Since the *t*-butyl dimethyl silyl chloride (TBDMS) is a sensitive group to acidic conditions, it was removed also while subjecting the *N*-Boc protected amine **19** to Boc removal using TFA in dichloromethane. Based on the reactivity of the protecting silyl groups, the *t*-butyl diphenyl silyl group (TBDPS) is less reactive/sensitive under acidic conditions compared to TBDMS. Therefore, *t*-butyl diphenyl silyl chloride (TBDPSCl) was used instead of TBDMSCl for the protection step, but unfortunately it was resulting in a very low yield of silyl protected alcohol and thus was not pursued further.



**Scheme 4.5:** Unselective deprotection of TBDMS group while removing Boc group.

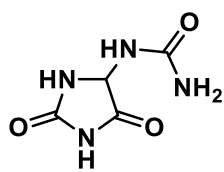
Attempts toward synthesizing targeted tri-substituted urea derivatives from the protected amino alcohol were unsuccessful, thus *N,N'*-disubstituted urea derivatives were proposed to be synthesized from free amine **23**. 1-(2-(Benzyloxy)-1-(4-methoxyphenyl)ethyl)-3-methoxyurea (**24**) was synthesized from carbonylation reaction of 1,1'-Carbonyldiimidazole (CDI) and methyl hydroxy amine hydrochloride, then it was subjected to oxidative dearomatization (OD) condition reaction using IBDA and in the presence of  $\text{Ce}_2\text{CO}_3$ . Similar observations were made by isolating the corresponding urethane product **25** resulting from nucleophilic attack of hexafluoroisopropanol (Scheme 4.6).



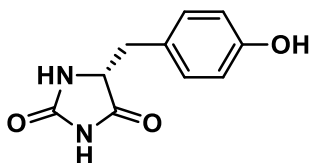
**Scheme 4.6:** OD conditions for the di-substituted urea (**24**) resulted in isolating the corresponding urethane product (**25**).

#### 4.2.2 Isolation of novel hydantoin derivatives instead of targeted urea derivatives

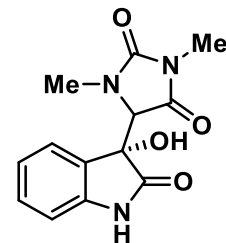
Hydantoin is a cyclized ureide of  $\alpha$ -amino acids which is an important family of heterocyclic compounds. A five-membered ring containing two nitrogen atoms and two carbonyl groups. The first discovery and synthesis of hydantoin derivatives was allantoin (**26**) by Adolf Bayer in 1861 (Figure 4.2), since that time researchers have investigated synthetic approaches to various derivatives of hydantoin.<sup>5-9</sup> Therefore, these cyclic ureides have been found in a number of natural products (Figure 4.2, (**27**)) with interesting synthetic pathways. For instance, the total synthesis of ( $\pm$ )-oxoaplysinopsin B (**28**) has been achieved recently via a cascade approach for the synthesis of 5-(indol-3-yl)hydantoin (Scheme 4.7).<sup>10</sup> Moreover, various privileged hydantoin structures exhibit different industrial applications. As an example, chiral 5-substituted hydantoins are broadly used as chiral auxiliaries, such as hydantoin (**29**) for enolate functionalization.<sup>11-14</sup> Also, a number of organic transformations are catalyzed by a hydantoin derivative, 1,3-dibromo-5,5'-dimethylhydantoin (DBDMH) (**30**) (Figure 4.2), which is also utilized as a di-brominating reagent for  $\alpha,\beta$ -unsaturated ketones or electron deficient alkenes.<sup>15,16</sup>



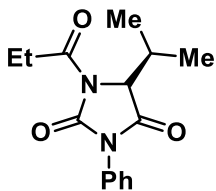
Allantoin (26)



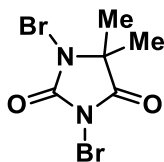
Hydantoin Natural Product (27)  
(Isolated from *Hemimycala arabica*)



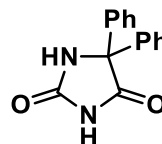
(±)-Oxoaplysinopsin B (28)



Chiral auxiliary (29)



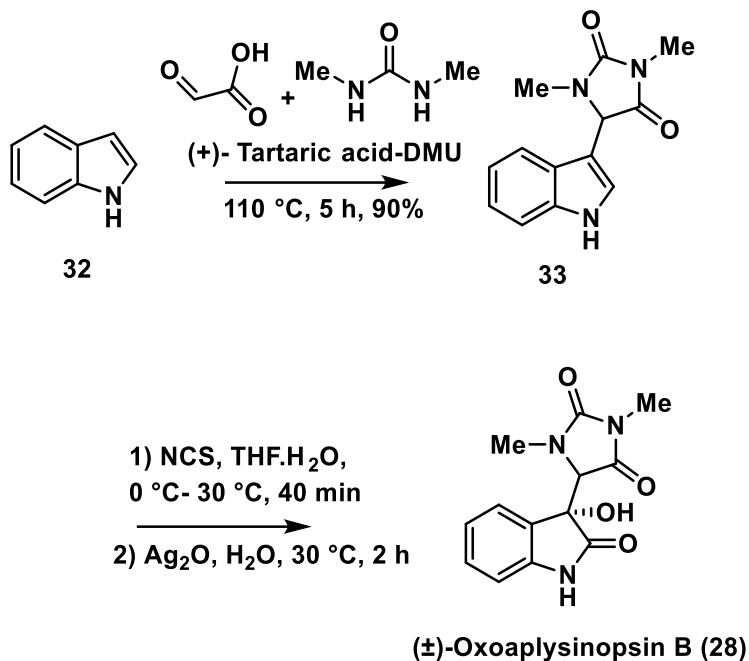
DBDMH (30)



Phenytoin (31)  
Anti-convulsant Drug

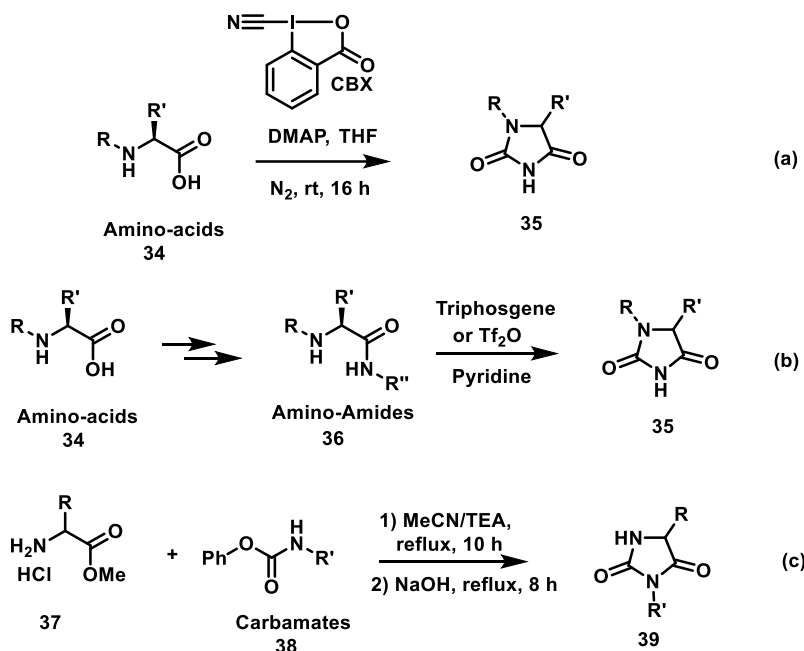
**Figure 4.2:** Important naturally and synthetic hydantoin derivatives (26-31).

Aside from the chemical application of hydantoin, this class of molecules possesses interesting pharmaceutical potentials, treating various type of diseases due to their bioactivity. Phenytoin is an antiepileptic drug used for treating different types of seizures. The easy and short synthetic pathways to hydantoin makes the discovery of novel active derivatives still in high demanded by medicinal chemists.



**Scheme 4.6:** Short total synthesis of (±)-oxoaplysinopsin B (**28**) via cascade approach of hydantoin construction.

Classical hydantoin synthetic methods have been developed by Bucherer-Bergs, Biltz, Urech and Read research groups, involving carbonyl condensations followed by basic or acidic cyclization.<sup>17-20</sup> All these classical conditions require harsh reaction conditions such as elevated high temperature or microwave conditions and toxic reagents such as commercially unavailable isocyanates, toxic cyanides and ammonium reagents.<sup>9</sup> Thus, the demand for alternative approaches remains high. A recent study showed that hypervalent iodine reagents serve as nitrile group donor for functionalization of chiral amino acids in one step in the presence of dimethyl amino pyridine (DMAP) (Scheme 4.7a).<sup>5</sup> In addition, amino amides and  $\alpha$ -amino methyl ester derivatives, which are synthesized in several steps from amino acids, are utilized for hydantoin cyclization reactions (Scheme 4.7b and 4.7c).<sup>21-24</sup>



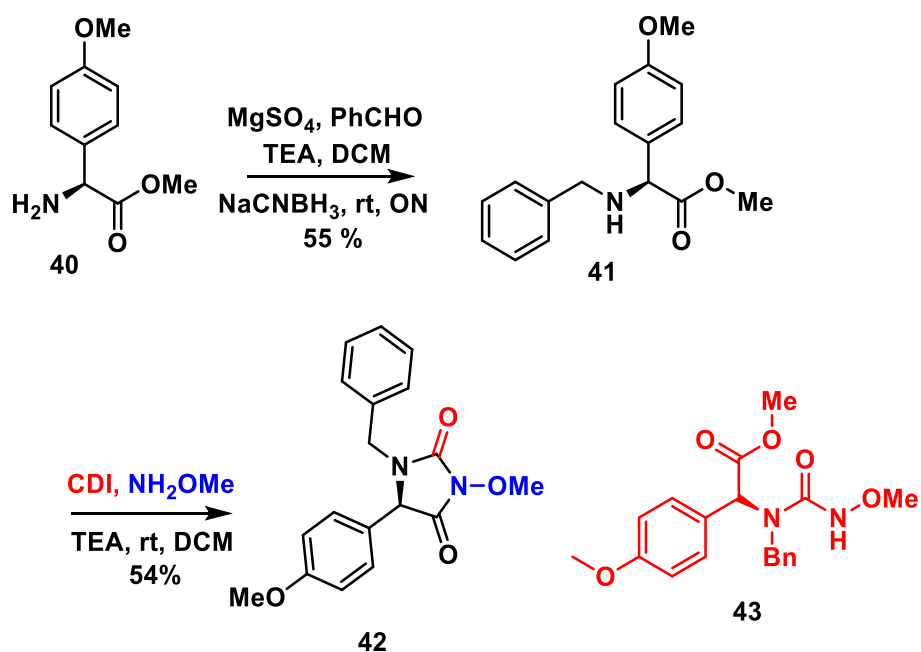
**Scheme 4.7:** Recent approaches toward constructions of hydantoin structures.

#### 4.2.3 Novel three component reactions for one-pot cascade hydantoin synthesis

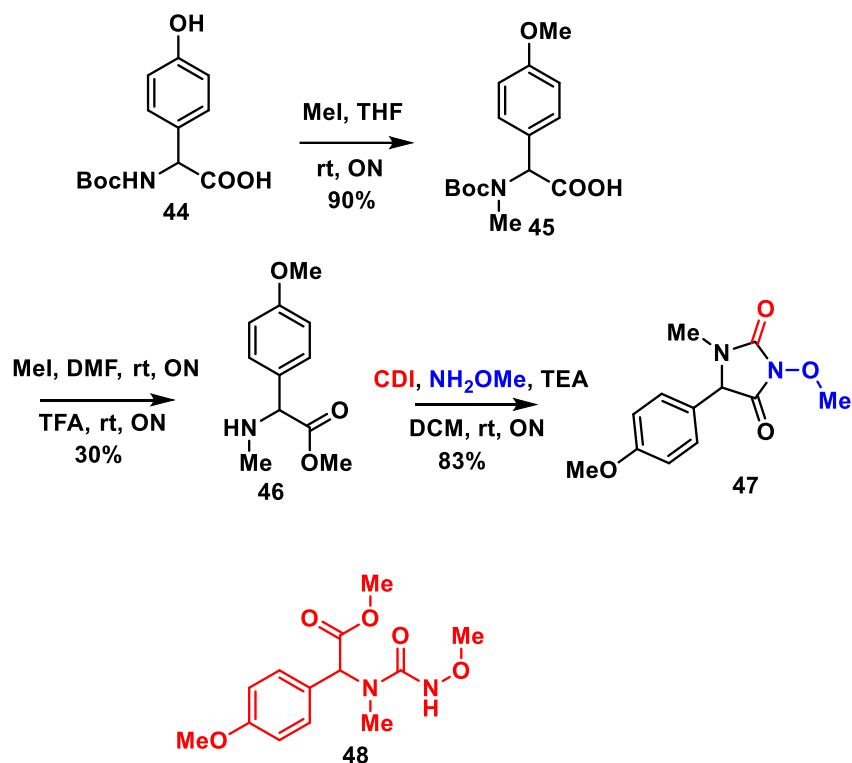
After unsuccessful attempts towards the synthesis of the targeted secondary amines using protected alcohols, our focus shifted to investigate the possibility of synthesizing secondary amines from amino ester derivatives. Thus, removal of Boc group from amino ester was followed by the protection of the primary amine using different conditions, but only one trial of many attempts of reductive amination reaction was successful. Then, the application of the carbonylation method using CDI and methyl hydroxy amine was performed with amino ester **41** in the presence of triethyl amine, but there is no success to isolate the desired urea derivative **43**. Interestingly, discovery of novel three component reaction of hydantoin synthesis was achieved from the amino ester, resulting in isolation of hydantoin **42** (Scheme 4.8). To confirm the observed pathway, another amino ester was obtained by treating Boc amino acid **44** with iodomethane to switch benzyl protection with a simple methyl protection and to isolate less steric hindered amino ester. However, similar observations were made by isolating the corresponding hydantoin derivatives **47** (Scheme



4.9). This novel three component methodology might be a new route towards synthesis and discovery of novel hydantoin derivatives in which one of the two nitrogen atoms is substituted by alkoxy or hydroxy group. This developed method does not require harsh reaction conditions and various derivatives may be designed from this technique using two different amines with CDI in presence of triethyl amine at room temperature overnight.



**Scheme 4.8:** Discovery of the three components cascade formation of hydantoin (**42**).



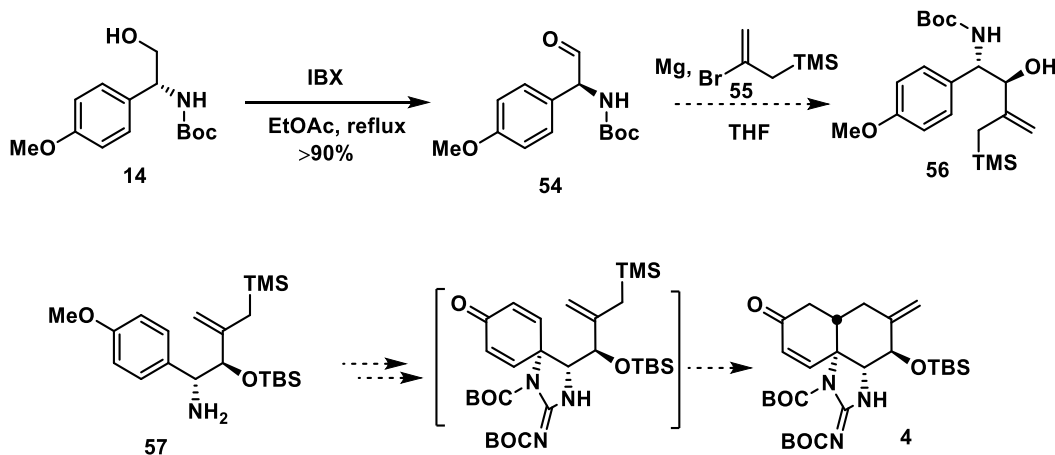
**Scheme 4.9:** Application of three components cascade formation of hydantoin (**47**) using different amino ester (**46**).

#### 4.2.4 Attempts towards synthesis the core structure of KB343

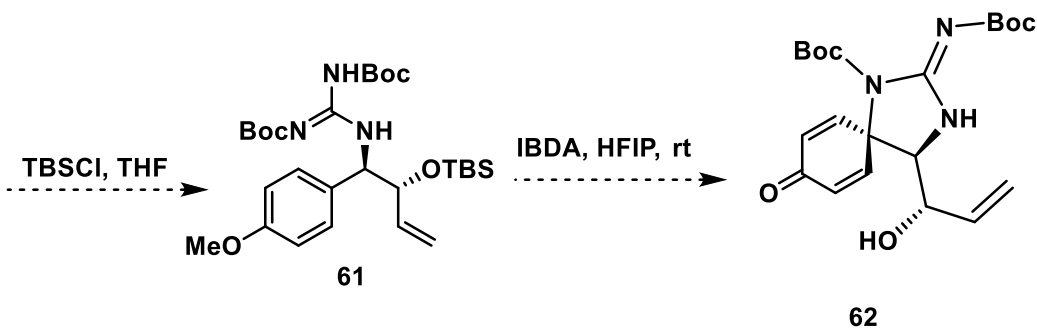
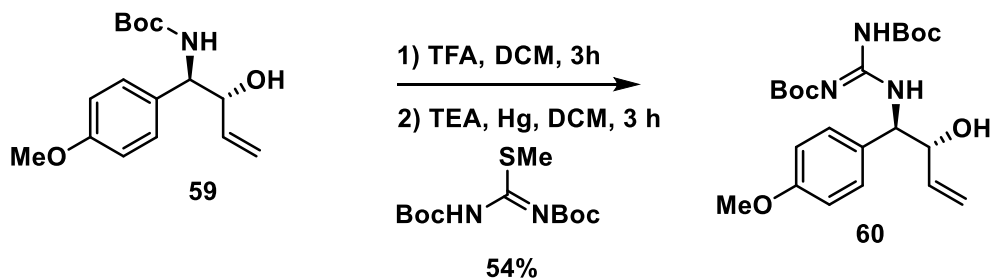
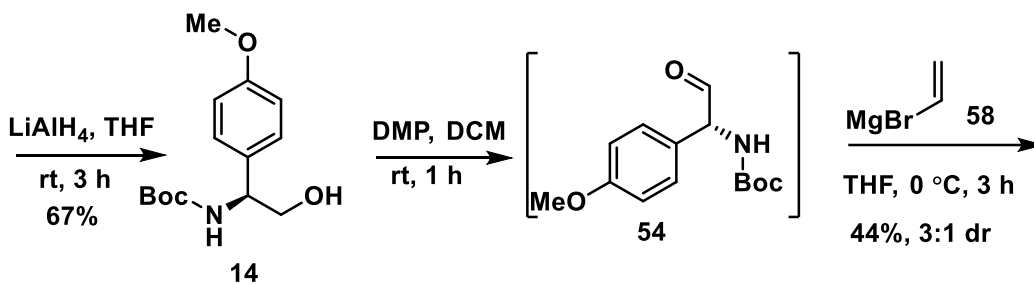
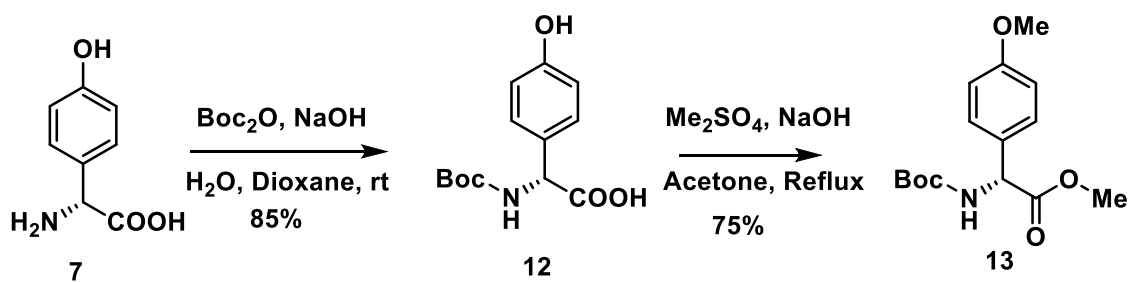
On the basis of previous success of Mitsunobu pathway for the previously synthesized guanidine (Chapter 2, Scheme 2.8), we have tried synthesizing a guanidine derivative related to the targeted KB343 guanidine precursor. Thus, synthesis of the styrene **50** was followed by a Sharpless asymmetric dihydroxylation to obtain the desired diol **51**, then the protection of the primary alcohol with TBS group to generate the free secondary alcohol **53**. Unfortunately, Mitsunobu reaction with the sterically hindered secondary alcohol did not work out under different conditions of using different solvent systems and different temperatures (Scheme 4.10).



and aldehyde. Treating the generated Grignard reagent with benzaldehyde was performed as a control reaction and worked efficiently, confirming that the generation of the Grignard reagent was performed successfully. The synthesized aldehyde was treated with the commercially available vinyl magnesium bromide (**58**) which resulted in isolating the desired corresponding alcohol in 3:1 dr (Figures 4.3 and 4.4 explain the stereoselectivity behind the observed dr ratio based on Felkin-Anh and Cram chelate models). The resulting alcohol **59** was treated with TFA then with guanidine precursor (Chapter 2.33) to generate the targeted guanidine derivative **60** in a good yield. Then the plan is to protect the resulting alcohol with TBS group and subject the guanidine **61** to OD reaction.



**Scheme 4.11:** Grignard reaction attempts with aldehyde (**54**) and proposed next steps towards the core structure KB343.



**Scheme 4.12:** Attempts toward synthesis the core structure of KB343 related structure (**62**).

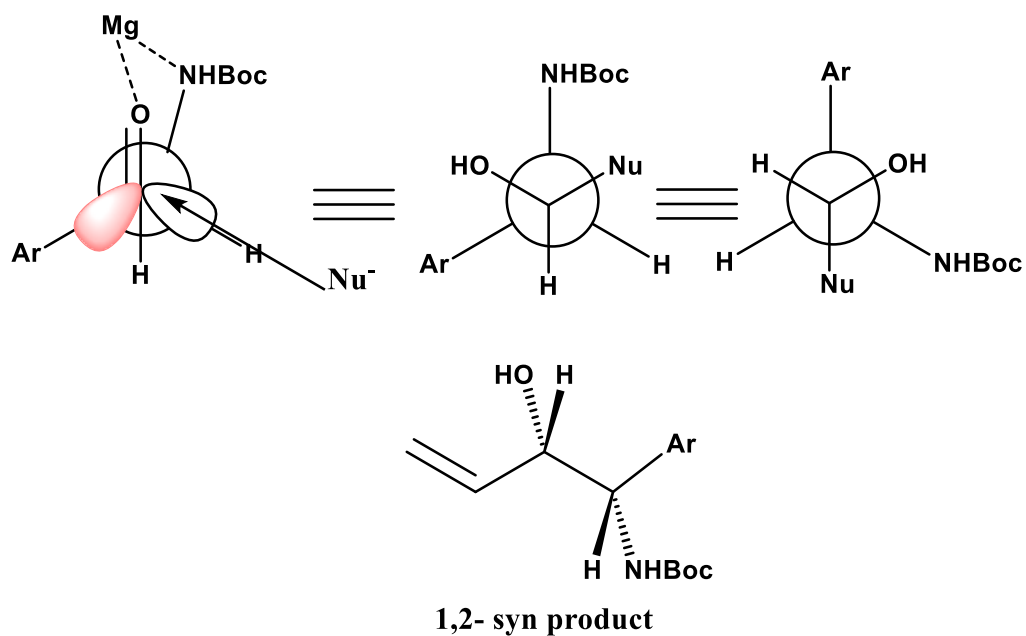


**Figure 4.3:** Cram-chelate model explaining the transition state of nucleophilic addition of Grignard reagent.

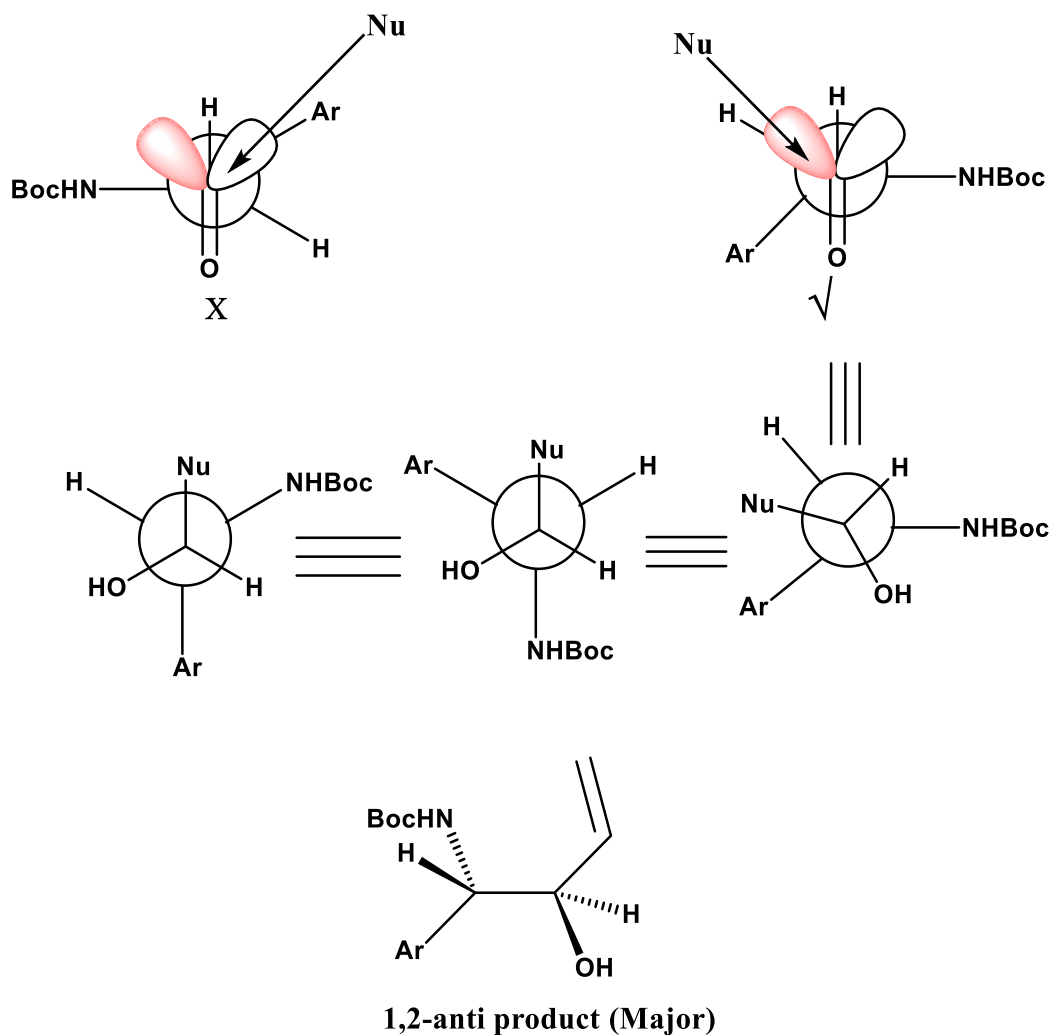
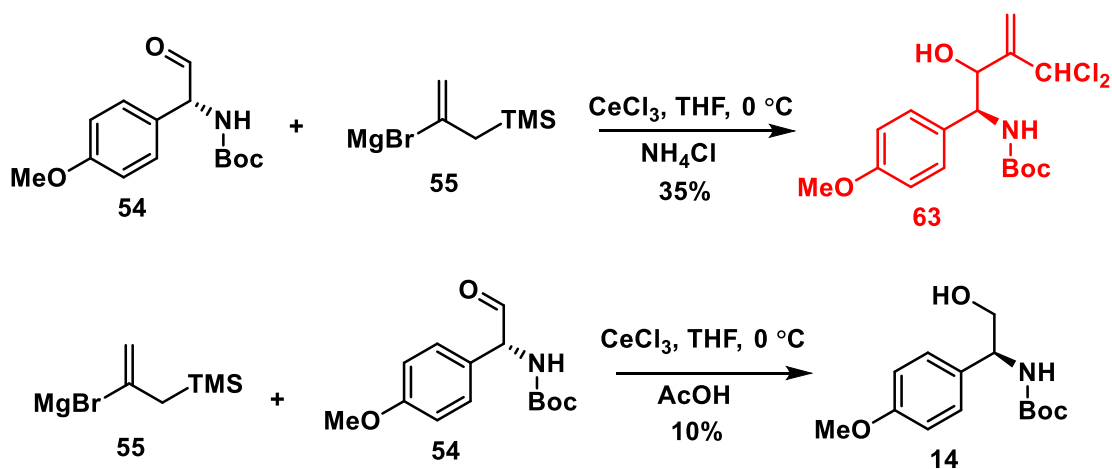


**Figure 4.4:** Felkin-Anh model transition state for Grignard reaction corresponding to the major 1,2-anti product.

Based on the previous results, we have investigated the addition of cerium(III) to Grignard reagent to improve the addition of the (2-bromoallyl)trimethylsilane (**55**) to aldehyde **54**. Interestingly, the addition of dry  $\text{CeCl}_3$  to the aldehyde **54** followed by Grignard reagent, derived from (2-bromoallyl)trimethylsilane **55**, results in isolation of an undesired product. Based on the  $^1\text{H}$  NMR spectroscopy, the loss of TMS and methylene groups was obvious, and the mass spectrometry showed a negative ion peak corresponding to  $\text{M}:\text{M}+2:\text{M}+4$  with intensity 9:6:1 which suggests two chlorine atoms in the product. Thus, the product may be similar to alcohol **63**

and further investigations will be performed to confirm the exact structure. The reaction was repeated with adding  $\text{CeCl}_3$  to the Grignard reagent, and this mixture was introduced to the aldehyde, surprisingly resulting in reduction of the aldehyde to the corresponding alcohol (Scheme 13). That confirms the strong basicity of the Grignard reagent derived from (2-bromoallyl)trimethylsilane **55** which related to our previous unsuccessful attempts to synthesize the desired alcohol **56**. That is presumably derived from the negative hyperconjugation effect of silyl group which stabilizes the corresponding six-membered transition state of hydrogen transfer reaction (Figure 5). Scheme 14 shows an alternative pathway to synthesize different aldehyde **66**. In the current ongoing approach, we will utilize organolithium chemistry instead of Grignard chemistry for alkylating aldehyde **54** or **64**. Also, we have an alternative plan to perform the OD reaction on guanidine **64** first then following the proposed scheme towards synthesis the core structure.



**Scheme 4.13:** Cerium chloride mediated the addition of Grignard reagent to aldehyde **54**.



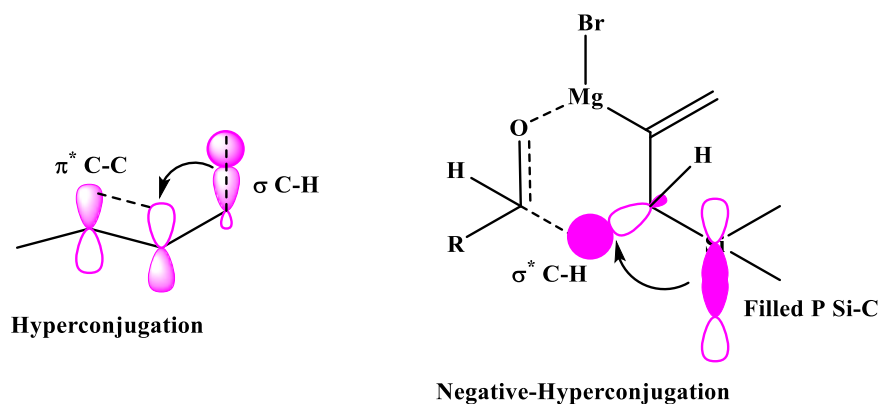
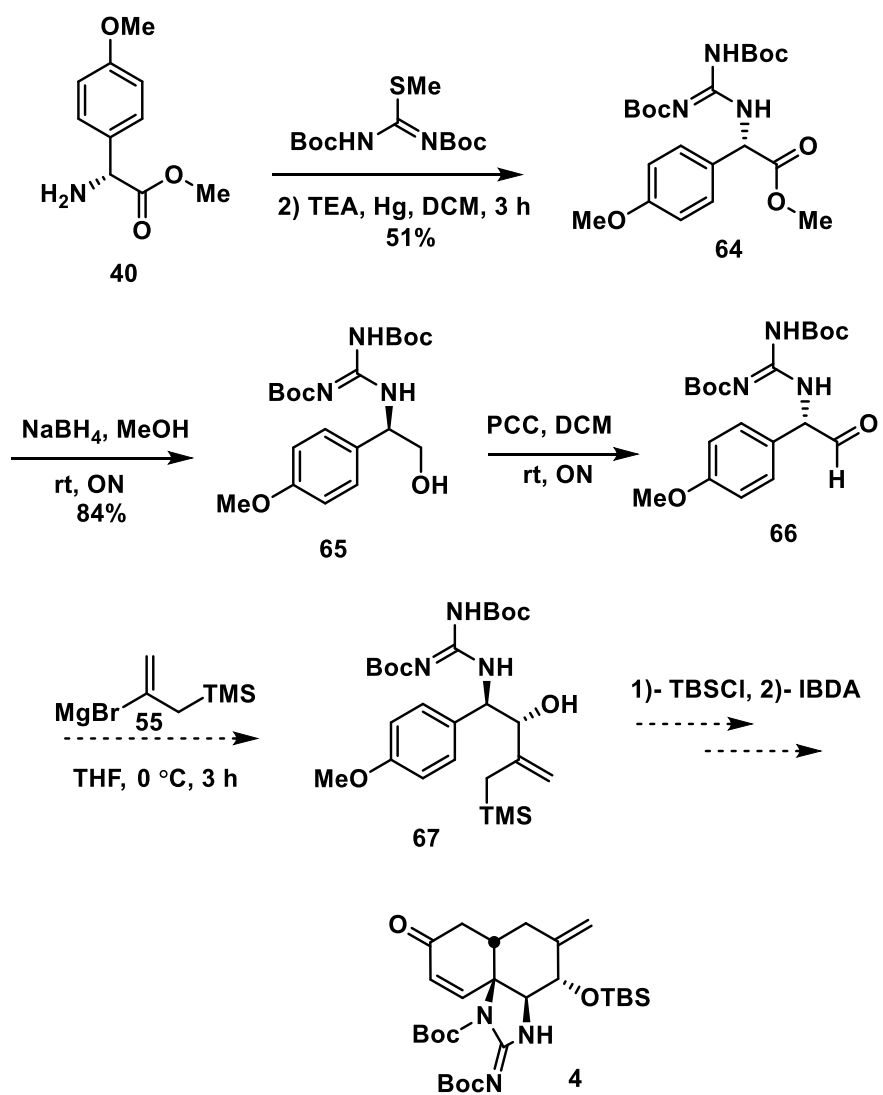


**Figure 4.5:** Hyperconjugation and negative hyperconjugation patterns.



**Scheme 4.14:** New approach towards synthesis the KB343 core structure.

### 4.3 SUMMARY:

Attempts towards synthesizing the core framework of the KB343 natural product are described. The high basicity of the Grignard reagent leads to a negative hyperconjugation effect which stabilizes the transition state of reduction of aldehyde rather the alkylation process. New approaches are ongoing by constructing rings C and D of KB343 structure firstly via oxidative dearomatization reaction then it will be followed by Grignard reaction and Michael-type cyclization. Novel synthetic methodology for *N*-methoxy hydantoin construction is discovered using  $\alpha$ -amino ester and 1,1'-carbonyldiimidazole. Application of oxidative dearomatization reaction for *N,N'*-disubstituted urea related to KB343 structure was performed and resulted in isolation of urethane products.

#### 4.4 REFERENCES:

- (1) Cariello, L.; Crescenzi, S.; Prota, G.; Giordano, F.; Mazzarella, L. Zoanthoxanthin, a Heteroaromatic Base from Parazoanthus Cfr. Axinellae (Zoantharia): Structure Confirmation by X-Ray Crystallography. *J. Chem. Soc., Chem. Commun.* **1973**, No. 3, 99–100. <https://doi.org/10.1039/C39730000099>.
- (2) Cariello, L.; Crescenzi, S.; Prota, G.; Capasso, S.; Giordano, F.; Mazzarella, L. Zoanthoxanthin, a Natural 1,3,5,7-Tetrazacyclopent-Azulene from Parazoanthus Axinellae. *Tetrahedron* **1974**, *30* (18), 3281–3287. [https://doi.org/https://doi.org/10.1016/S0040-4020\(01\)97501-5](https://doi.org/https://doi.org/10.1016/S0040-4020(01)97501-5).
- (3) Matsumura, K.; Taniguchi, T.; Reimer, J. D.; Noguchi, S.; Fujita, M. J.; Sakai, R. KB343, a Cyclic Tris-Guanidine Alkaloid from Palauan Zoantharian Epizoanthus Illoricatus. *Org. Lett.* **2018**, *20* (10), 3039–3043. <https://doi.org/10.1021/acs.orglett.8b01069>.
- (4) Kim, J.-S.; Kim, G.-W.; Kang, J.-C.; Myeong, I.-S.; Jung, C.; Lee, Y.-T.; Choo, G.-H.; Park, S.-H.; Lee, G.-J.; Ham, W.-H. Stereoselective Total Synthesis of (+)-Radicamine B via Anti,Syn,Syn-Oxazine. *Tetrahedron: Asymmetry* **2016**, *27* (4), 171–176. <https://doi.org/https://doi.org/10.1016/j.tetasy.2016.01.009>.
- (5) Declas, N.; Le Vaillant, F.; Waser, J. Revisiting the Urech Synthesis of Hydantoins: Direct Access to Enantiopure 1,5-Substituted Hydantoins Using Cyanobenziodoxolone. *Org. Lett.* **2019**, *21* (2), 524–528. <https://doi.org/10.1021/acs.orglett.8b03843>.
- (6) Baeyer, A. Vorläufige Notiz Über Das Hydantoin. *Justus Liebigs Ann. Chem.* **1861**, *117* (2), 178–180. <https://doi.org/https://doi.org/10.1002/jlac.18611170204>.
- (7) Ware, E. The Chemistry of the Hydantoins. *Chem. Rev.* **1950**, *46* (3), 403–470. <https://doi.org/10.1021/cr60145a001>.
- (8) Meusel, M.; Gütschow, M. RECENT DEVELOPMENTS IN HYDANTOIN CHEMISTRY. A REVIEW. *Org. Prep. Proced. Int.* **2004**, *36* (5), 391–443. <https://doi.org/10.1080/00304940409356627>.
- (9) Konnert, L.; Reneaud, B.; de Figueiredo, R. M.; Campagne, J.-M.; Lamaty, F.; Martinez, J.; Colacino, E. Mechanochemical Preparation of Hydantoins from Amino Esters: Application to the Synthesis of the Antiepileptic Drug Phenytoin. *J. Org. Chem.* **2014**, *79* (21), 10132–10142. <https://doi.org/10.1021/jo5017629>.
- (10) Konnert, L.; Lamaty, F.; Martinez, J.; Colacino, E. Recent Advances in the Synthesis of Hydantoins: The State of the Art of a Valuable Scaffold. *Chem. Rev.* **2017**, *117* (23), 13757–13809. <https://doi.org/10.1021/acs.chemrev.7b00067>.
- (11) Metallinos, C.; John, J.; Zaifman, J.; Emberson, K. Diastereoselective Synthesis of N-Substituted Planar Chiral Ferrocenes Using a Proline Hydantoin-Derived Auxiliary. *Adv. Synth. & Catal.* **2012**, *354*, 602–606.
- (12) Yamaguchi, J.; Harada, M.; Narushima, T.; Saitoh, A.; Nozaki, K.; Suyama, T. Diastereoselective Conjugate Addition of 1-( $\alpha,\beta$ -Unsaturated Acyl)Hydantoin with Nucleophiles. *Tetrahedron Lett.* **2005**, *46* (38), 6411–6415. <https://doi.org/https://doi.org/10.1016/j.tetlet.2005.07.116>.
- (13) Zhang, J.-S.; Lu, C.-F.; Chen, Z.-X.; Li, Y.; Yang, G.-C. Boron Enolates of a Hydantoin Chiral Auxiliary Derived from L-Phenylalanine: A Versatile Tool for Asymmetric Aldol Reactions. *Tetrahedron: Asymmetry* **2012**, *23* (1), 72–75. <https://doi.org/https://doi.org/10.1016/j.tetasy.2011.12.013>.
- (14) Lu, G.-J.; Nie, J.-Q.; Chen, Z.-X.; Yang, G.-C.; Lu, C.-F. Synthesis and Evaluation of a New Non-Cross-Linked Polystyrene Supported Hydantoin Chiral Auxiliary for

- Asymmetric Aldol Reactions. *Tetrahedron: Asymmetry* **2013**, *24* (20), 1331–1335. <https://doi.org/https://doi.org/10.1016/j.tetasy.2013.08.017>.
- (15) Abdollahi-Alibeik, M.; Zaghaghi, Z. 1,3-Dibromo-5,5-Dimethylhydantoin as a Useful Reagent for Efficient Synthesis of 3,4-Dihydropyrimidin-2-(1H)-Ones under Solvent-Free Conditions. *Chem. Pap.* **2009**, *63* (1), 97–101. <https://doi.org/10.2478/s11696-008-0084-1>.
- (16) Hernández-Torres, G.; Tan, B.; Barbas, C. F. Organocatalysis as a Safe Practical Method for the Stereospecific Dibromination of Unsaturated Compounds. *Org. Lett.* **2012**, *14* (7), 1858–1861. <https://doi.org/10.1021/ol300456x>.
- (17) Urech, F. XXI. Ueber Lacturaminsäure Und Lactylharnstoff. *Justus Liebigs Ann. Chem.* **1873**, *165* (1), 99–103. <https://doi.org/https://doi.org/10.1002/jlac.18731650110>.
- (18) Read, W. T. Researches on hydantoins. Synthesis of the soporific, 4,4-phenylethylhydantoin(nirvanol). *J. Am. Chem. Soc.* **1922**, *44* (8), 1746–1755. <https://doi.org/10.1021/ja01429a017>.
- (19) Biltz, H. Über Die Konstitution Der Einwirkungsprodukte von Substituierten Harnstoffen Auf Benzil Und Über Einige Neue Methoden Zur Darstellung Der 5.5-Diphenyl-Hydantoine. *Berichte der Dtsch. Chem. Gesellschaft* **1908**, *41* (1), 1379–1393. <https://doi.org/https://doi.org/10.1002/cber.190804101255>.
- (20) Bucherer, H. T.; Lieb, V. Über Die Bildung Substituierter Hydantoine Aus Aldehyden Und Ketonen. Synthese von Hydantoinen. *J. Fur Prakt. Chemie-chemiker-zeitung* **1934**, *141*, 5–43.
- (21) Tanwar, D. K.; Ratan, A.; Gill, M. S. Facile One-Pot Synthesis of Substituted Hydantoins from Carbamates. *Synlett* **2017**, *28* (17), 2285–2290.
- (22) Liu, H.; Yang, Z.; Pan, Z. Synthesis of Highly Substituted Imidazolidine-2,4-Dione (Hydantoin) through Tf<sub>2</sub>O-Mediated Dual Activation of Boc-Protected Dipeptidyl Compounds. *Org. Lett.* **2014**, *16* (22), 5902–5905. <https://doi.org/10.1021/ol502900j>.
- (23) Chen, Y.; Su, L.; Yang, X.; Pan, W.; Fang, H. Enantioselective Synthesis of 3,5-Disubstituted Thiohydantoins and Hydantoins. *Tetrahedron* **2015**, *71* (49), 9234–9239. <https://doi.org/https://doi.org/10.1016/j.tet.2015.10.041>.
- (24) Zhang, D.; Xing, X.; Cuny, G. D. Synthesis of Hydantoins from Enantiomerically Pure  $\alpha$ -Amino Amides without Epimerization. *J. Org. Chem.* **2006**, *71* (4), 1750–1753. <https://doi.org/10.1021/jo052474s>.

**CHAPTER FIVE: BENZOTHAZOLES FISSURE A NEW GATE FOR A DISCOVERY  
OF NOVEL DERIVATIVES REGULATING GABA RECEPTORS**

Marian N. Aziz<sup>1, 2</sup>, Kamal Awad<sup>3, 4</sup>, Jian Huang<sup>3</sup>, Zhiying Wang<sup>3</sup>, Venu Varanasi<sup>3</sup>, Marco  
Brotto<sup>3</sup>, Carl J. Lovely<sup>1</sup>

1. Department of Chemistry and Biochemistry, University of Texas-Arlington, Arlington, TX  
76019-0065, USA
2. Department of Pesticide Chemistry, National Research Centre, Dokki, Giza 12622, Egypt
3. Bone-Muscle Research Center, College of Nursing & Health Innovation, University of  
Texas at Arlington, Arlington, TX 76019, USA
4. Department of Ceramics, National Research Centre, Dokki, Giza 12622, Egypt

Corresponding author

Prof. Carl J. Lovely

Professor, Chemistry and Biochemistry Department

University of Texas at Arlington

Address: 700 Planetarium Place, Box 19065, UT Arlington, TX 76019-0065

Email: lovely@uta.edu

Phone: +1 817 272 5446

(Not Published)

## ABSTRACT

Drug discovery is considered one of the most intriguing stages in the treatment process of any disease which usually consumes time, effort, and expense. Thus, there are significant efforts from scientists to explore novel molecules as candidate drugs for various diseases. In this study, novel benzothiazole derivatives have been synthesized and their possible biological applications were investigated. Cell culture studies were performed using a C2C12 skeletal muscle cell line to test the cytotoxicity of the synthesized benzothiazoles and their effects on GABA regulation. Cell proliferation and differentiation, real time PCR analysis, and omics studies were performed. The cytotoxicity results indicated that the tested benzothiazoles are safe at low concentration of 5 to 10  $\mu$ M. The differentiation study revealed that one of the synthesized agents has potential myogenic effects. Omics and PCR analysis for GABA indicated that 2-((4-methoxybenzyl)(methylamino)benzo[d]thiazol-6-yl acetate (**7b**) induces more than 2-folds downregulation of *Gabrg2*, *Grm7*, *Gria1*, *Grin2a*, and *Slc17a7*, while 5-chloro-*N*-(4-methoxybenzyl)-*N*,6-dimethylbenzo[d]thiazol-2-amine (**7g**) induces more than 2-folds upregulation of *Gabrg1*, *Gabrg3*, *Slc7a11*, *Slc1a6*, and downregulation of *Slc7a7*. Since the *Gabrg2* gene is considered as epilepsy gene and is a potential molecular target for the discovery of novel therapeutic strategies, the synthesized benzothiazoles could have a potential application for diseases associated with mutation in GABAergic synapses.

## 5.1 INTRODUCTION

Since 1958, gamma-aminobutyric acid (GABA) has been classified as a major neurotransmitter inhibitor and GABA aminotransferase was identified as a therapeutic target for number of neurological diseases.<sup>1-3</sup> This small natural activator, GABA, mediates synaptic inhibition via binding to GABA receptors (A and B) which are known as receptor-gated chloride channels.<sup>4</sup> GABA regulated-chloride gates allow chloride ions to pass through neurons resulting

in hyperpolarization of these negative charges thus reducing the probability of changes in neuron action potentials.<sup>5</sup> GABA-A receptor is an ionotropic and heteropentameric channel consisting of five subunits (two  $\alpha_1$ , two  $\beta_2$ , one  $\gamma_2$ ). This subunit composition ( $\alpha_1$ ,  $\beta_2$ ,  $\gamma_2$ ) represents the most common GABA isoform in the mammalian central nervous system (CNS) and encoded by *Gabra1*, *Gabrb2*, and *Gabrg2* genes, respectively.<sup>5-8</sup> Tremendous attention is focused (particularly) on the GABA-A receptor due to the presence of at least three allosteric binding sites, making it a pharmacological rich receptor for the treatment of three different diseases of the central nervous system. These include the benzodiazepine site for reducing epileptic seizures, the sedative site for anxiety treatment, and the site of the depressant barbiturates.<sup>8</sup> The  $\gamma_2$  subunits of GABA type A gene play a chief role in maintenance of GABA-A receptors at mature synapses and its deletion resulted in the absence of benzodiazepine binding site.<sup>9</sup> Over half of the known epilepsy-associated mutations has been identified in the *GABAG2*.<sup>10,11</sup> Therefore, *Gabrg2* gene is considered as the epilepsy gene and is potential molecular target for discovery of novel therapeutic strategies for genetic and non-genetic epilepsy and other diseases associated with mutation in GABAergic synapses.<sup>12</sup> On the other hand, solute carrier family 7 member 11 (*SLC7a11*, system Xc-, glutamate transporter) is one of the important plasma membrane transporter systems in humans, regulating the intracellular glutathione level.<sup>13,14</sup> *SLC7a11* gene is a Na-independent antiporter/exchanger up taking and reducing extracellular L-cystine (dimer structure of cysteine) into cysteine, a key intermediate in intracellular L-glutathione synthesis, thus it protects the cells from reactive oxygen species (ROS) and converts toxic lipids into healthy lipids.<sup>13</sup> Furthermore, the neurotransmitter glutamate plays a significant role in the functioning of the central nervous system and its dysfunction is associated with number of CNS disorders.<sup>15-17</sup>

Benzothiazoles are class of heterocyclic molecules as a classical definition which contain a substituted phenyl ring fused with a five-member ring containing sulfur and nitrogen atoms called thiazole moiety.<sup>18</sup> Benzothiazoles are core structures in many numbers of bioactive and drug molecules with different pharmacological activities. Riluzole (**1**) is the most common and best known benzothiazole categorized under CNS medicines for amyotrophic lateral sclerosis (ALS) treatment (Figure 5.1).<sup>19</sup> Thus, numerous benzothiazole based analogues have been developed for improving their corresponding activity against ALS.<sup>19</sup> In addition, the benzothiazole motif serves as the core structure in number of approved drugs such as probenzole (**2**) (agrochemical drug),<sup>20</sup> ethoxazolamide (**3**) (carbonic anhydrase inhibitor for glaucoma treatment),<sup>21</sup> and zopolrestat (**4**) (aldose reductase inhibitor for treating diabetic complications).<sup>22</sup> Thus, there is great interest in developing and investigating biologically active benzothiazole derivatives, as a result there are numerous articles, and patents describing various derivatives based on the benzothiazole scaffold.<sup>18</sup> To name a few, benzothiazoles serve as anti-convulsants,<sup>23–27</sup> anti-inflammatories,<sup>28–30</sup> anti-proliferative agents,<sup>31–36</sup> anti-microbials,<sup>32,37,38</sup> anti-analgesics,<sup>39–41</sup> and antioxidant agents.<sup>42–44</sup> Due to the broad potential bioactivity of benzothiazoles, organic and medicinal chemists have an ongoing interest in discovering alternative synthetic methodologies and investigating bioactivity.

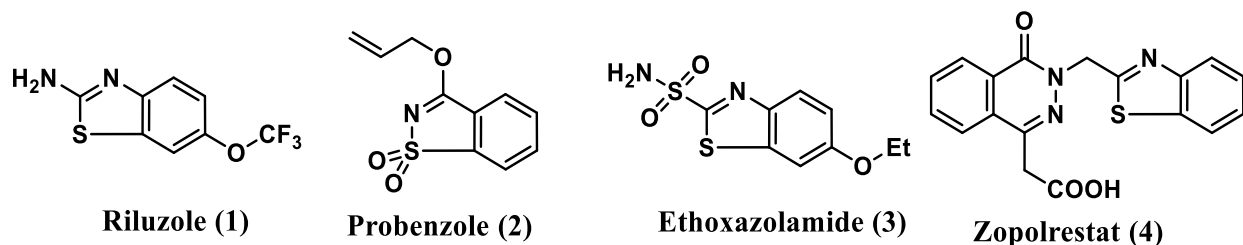


**Figure 5.1:** Marketed benzothiazole drugs (1-4).

Oxidative intermolecular/intramolecular *S*-cyclization of *N*-aryl urea derivatives deliver 2-aminobenzothiazoles which is one of the most potent benzothiazole families. Many approaches



have been studied for this direct transformation using metal catalyzed oxidative cyclization such as ruthenium chloride,<sup>45</sup> palladium acetate,<sup>45</sup> and nickel salts.<sup>46</sup> 2-Aminobenzothiazoles can also be synthesized using aniline derivatives with different type of amines and thiocarbonyl sources via various oxidative conditions. These conditions include iodine or bromine oxidations,<sup>46</sup> copper catalyzed Ullmann-type reactions,<sup>47</sup> thiocarbonyl as a source for thioamide group,<sup>48-50</sup> and three component reaction using potassium sulfide and mediated by copper chloride.<sup>51</sup> In the present study, new synthetic methodology towards synthesis of functionalized benzothiazoles has been developed, and investigation of the possible biological activity of these benzothiazole derivatives is reported.

## 5.2 RESULT AND DISCUSSION

### 5.2.1 Chemistry

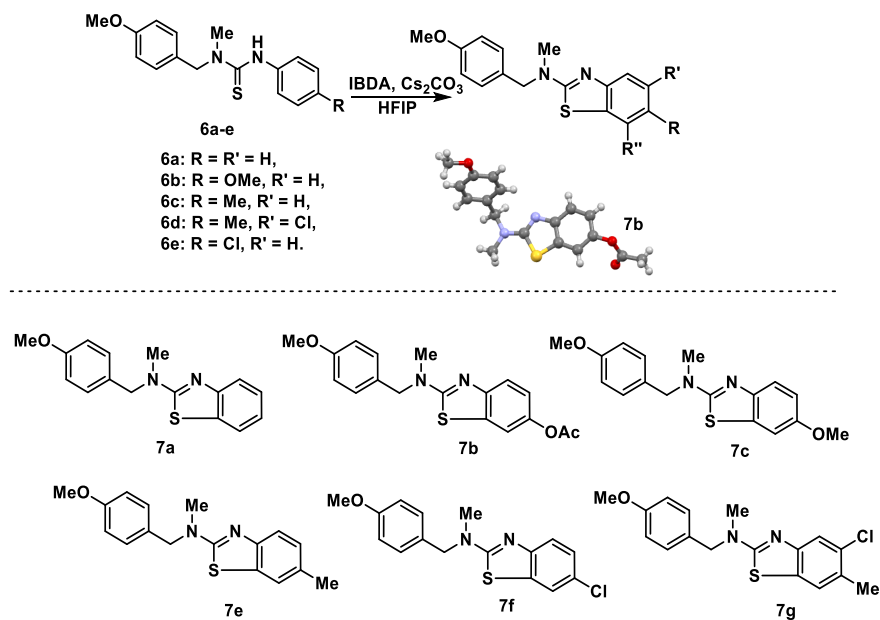
Most of the reported methods toward constructions of benzothiazole derivatives require harsh reaction conditions at elevated temperature, metal catalyzed transformations and long completion time. In this chapter, we report a fast and easy access to the benzothiazole scaffold through an environmentally benign condition developed in the Lovely lab for thioureas chemoselective cyclization. Selective oxidation reaction of the synthesized thiourea containing two aryl groups (**6a-e**) presumably through activation of sulfur followed by electrophilic aromatic substitution of the *N*-aryl group rather the *N*-benzyl group. However, the present methodology requires further optimization to discover its limitations, it offers a straightforward approach for construction of benzothiazole derivatives from simple thioureas to deliver the substituted core structure of benzothiazole scaffold. Subjecting the synthesized thioureas (**6a-e**) to iodobenzene diacetate (IBDA) in the presence of Cs<sub>2</sub>CO<sub>3</sub> in hexafluoroisopropanol as a solvent yielded the corresponding benzothiazoles as shown in **scheme 5.1**. Interestingly, the chemoselectivity of formation of acetylated benzothiazole depends mainly on molar equivalents of IBDA (Table 5.1).

Therefore, two acetated benzothiazoles (**7b** and **7d**) were isolated when 2.0 equiv of IBDA was used. The X-ray crystal structure of **7b** confirmed the chemical structures and other spectroscopic techniques as well. Initial optimization study was performed by lowering the equivalent of IBDA to one molar equivalent resulted in isolation of good to moderate yields for benzothiazoles **7a** and **7c**.

**Table 5.1:** Benzothiazoles derived from oxidation of thiourea mediated by hypervalent iodine.

	Thiourea derivative	IBDA molar equivalents	Benzothiazoles				Yield (%)*
			Code	R	R'	R''	
1	6a	2.0	7a	H	H	H	11
2	6a	1.0	7a	H	H	H	47
3	6a	2.0	7b	OAc	H	H	27
4	6b	2.0	15a	OMe	H	H	23
5	6b	2.0	15b	OMe	H	OAc	14
6	6b	1.0	15a	OMe	H	H	65
7	6c	2.0	16	Me	H	H	20
8	6c	1.0	16	Me	H	H	19
9	6d	1.0	17	Me	Cl	H	22
10	6e	1.0	18	Cl	H	H	30

\*) Isolated yields by column chromatography.



**Scheme 5.1:** Synthesis of the benzothiazoles **7a-g** via oxidation of thioureas **6a-e**.

## **5.2.2 Biological studies of benzothiazoles**

### *5.2.2.1 Antitumor Activity of benzothiazoles*

Initial attempts toward studying the possible bioactivity of the isolated benzothiazoles were testing their antitumor activity. Thus, the anti-proliferative activity of benzothiazole **7a** was investigated by the National Cancer Institute against 60 human cell line panel. The results showed that **7a** is probably a good inducer for cell growth and did not show any inhibition. Thus, we shifted our focus to investigate another possible bioactivity for the synthesized benzothiazoles. In line with riluzole drug, the simplest marketed benzothiazole drug, we decided to test the possible activity of the synthesized benzothiazole on the central nervous system (CNS), selectively one of the most common and contributed receptors to CNS which is GABA receptor.

### *5.2.2.2 Cytotoxicity of benzothiazoles*

To assist in establishing the cytotoxicity of benzothiazoles, C2C12 skeletal muscle cells were cultured, and the cells' viability was performed using MTS cell viability assay. C2C12 cell viability was measured after 24 hours of proliferation after treatment with various concentrations of each tested benzothiazole agent (5, 10, 50, 75, and 100  $\mu\text{M}$ ). All results are normalized to the dimethyl sulfoxide (DMSO) which was used as vehicle and compared to a positive control (normal growth medium) as shown in **Figure 5.2**. All tested compounds presented no cytotoxic effect at lower concentrations (5 and 10  $\mu\text{M}$ ), while significant decrease in C2C12 cell viability was observed at higher concentrations (50, 75, and 100  $\mu\text{M}$ ) for all tested compounds. Furthermore, low concentrations of agents **7b**, **7c**, **7e**, and **7g** showed a significant increase in the cell's viability after 24 hours of C2C12 cells' proliferation. Thus, and based on the cytotoxicity results, low doses of benzothiazoles (5 and 10  $\mu\text{M}$ ) were considered as nontoxic and safe doses and will be used for the myogenic and differentiation studies.

### 5.2.2.3 Myogenic effect of benzothiazoles

To study the myogenic effects of benzothiazoles, C2C12 skeletal muscle cells were cultured and allowed to differentiate for 5 days with 5  $\mu$ M and 10  $\mu$ M concentration of each benzothiazole agent as shown in **Figure 5.3**. Figure 3-A shows the differentiated C2C12 cells (myotubes) stained with Myosin Heavy Chain (MHC-green) antibodies and 4',6-diamidino-2-phenylindole dihydrochloride hydrate (DAPI-blue) stained the nuclei. Figure 3-B indicates quantitative analysis of the differentiation study. Bar graphs with data points distribution are used to compare the mean values of fusion index (FI) of all agents compared to the control and the vehicle (DMSO, 5-10  $\mu$ M). FI is considered a standard method to measure the muscle cell myotubule formation and quantify the differentiation phase as it measures the ratio of number of nuclei being fused and formed myotubes divided by the total number of nuclei. Thus, FI indicates the ability of mononucleated single cells to fuse and form multinucleated myotubes. Analysis indicated that DMSO groups have no significant effect on the FI compared to the positive control, while DMSO (10  $\mu$ M) slightly increased the FI. Low dose of benzothiazoles agents did not show any significant changes on the FI compared to the control except for **7b** (5  $\mu$ M) that induced a significant decrease in the FI compared to the positive control. While the high concentration 10  $\mu$ M of all benzothiazoles agents presented a significant decrease in the FI compared to the control except agent **7g** that indicated FI ratio similar to the positive control at both doses of 5 and 10  $\mu$ M.

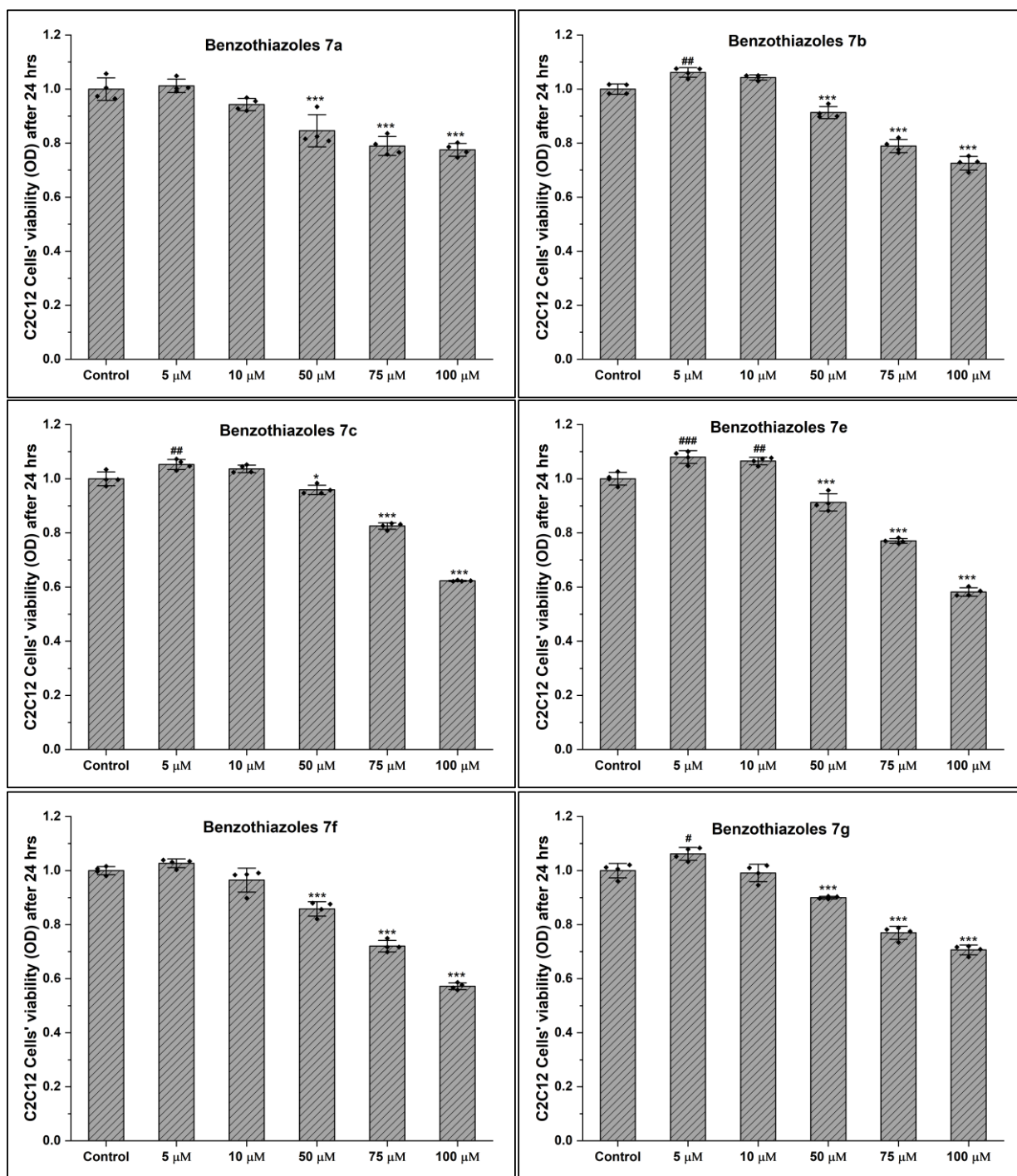


**Figure 5.2: Cytotoxicity of benzothiazoles.** Six different compounds of benzothiazoles derivatives were screened at different concentrations to test their cytotoxicity effect on C2C12 cells. Low concentrations of 5 μM to 10 μM showed no cytotoxicity while higher doses indicated significant decrease in cell's viability as shown \* $p < 0.05$ , \*\* $p < 0.01$ , \*\*\* $p < 0.001$ . Compounds **7b**, **7c**, **7e**, and **7g** indicated significant increase in cells viability at low dose of 5 μM as shown #  $p < 0.05$ , ##  $p < 0.01$ , ### $p < 0.001$ . The test was performed by Dr. Marco Brotto and Dr. Venu Varanasi laboratories.

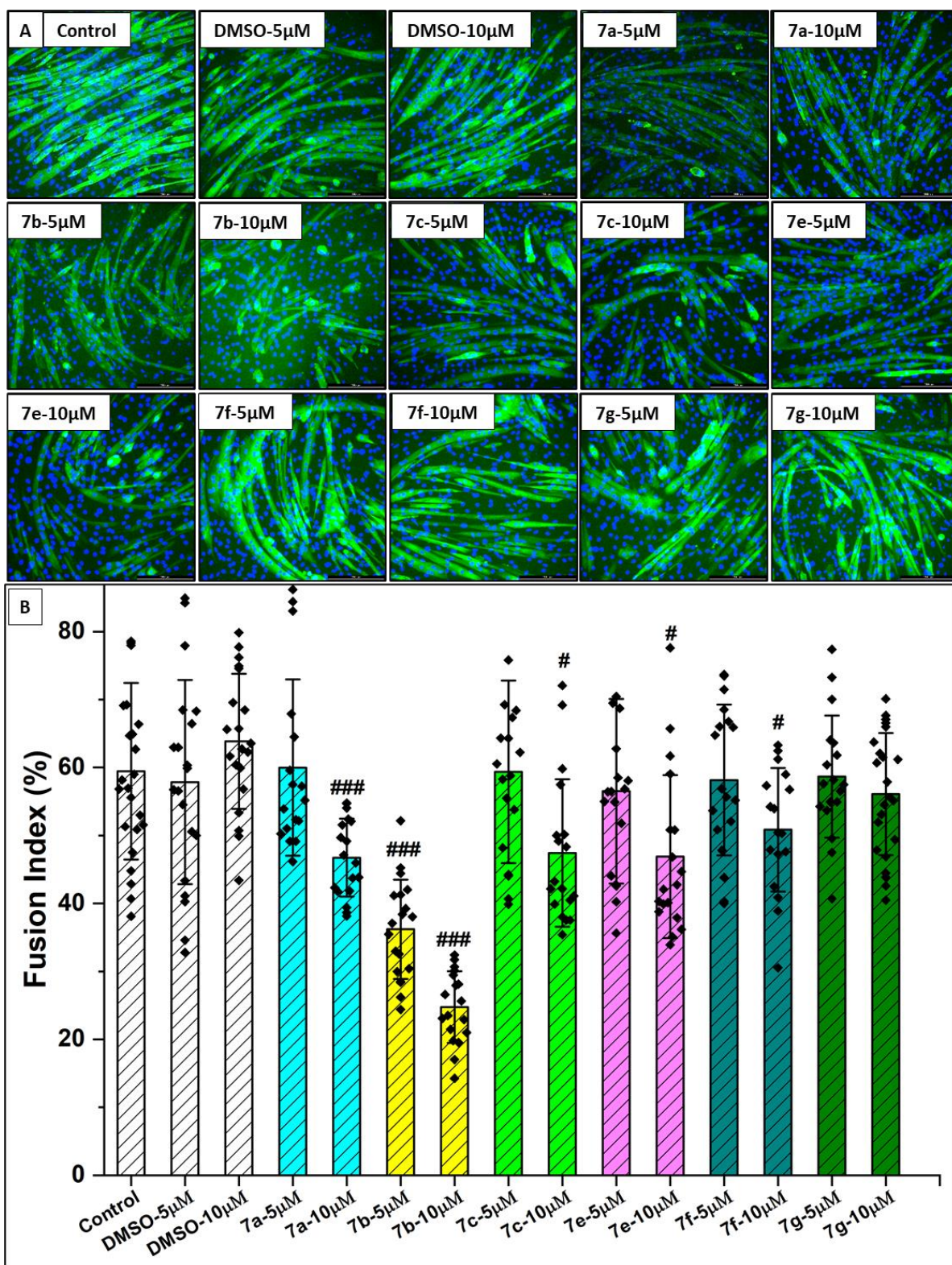


**Figure 5.3: Myogenic effects of benzothiazoles.** Six different compounds of benzothiazoles derivatives were studied at two concentrations to test their myogenic effect on C2C12 cells. A) Differentiated C2C12 cells (Myotubes) stained with Myosin Heavy Chain and DAPI. B) Calculated fusion index of tested benzothiazoles compared to positive control and DMSO, statistical analysis based on One-Way ANOVA with Tukey Post Hoc test; #  $p < 0.05$ , ##  $p < 0.01$ , ###  $p < 0.001$ . The test was performed by Dr. Marco Brotto and Dr. Venu Varanasi laboratories.

It is important to note that only agent **7b** presented a significant decrease in FI at both concentrations, while agent **7g** did not present a significant difference even at the high concentration. Thus, benzothiazoles **7b** and **7g** were selected for further omics and RT-PCR analysis.

#### 5.2.2.4 Effect of benzothiazoles on GABA

To investigate the effect of benzothiazoles on the levels of GABA and its isomers generated in C2C12 cells and conditioned media after the treatment of different concentrations of benzothiazole agents, a LC-MS/MS based analytical method were used. GABA,  $\alpha$ -aminobutyric acid (AABA, *L*- and *D*-),  $\beta$ -aminobutyric acid (BABA, *L*-), and  $\beta$ -aminoisobutyric acid (BAIBA, *L*- and *D*-) were measured and quantified in cells and conditioned media (CM). GABA was determined in C2C12 cells of the vehicles (DMSO), control cells, and cells treated with 10  $\mu$ M benzothiazole agents **7b** and **7g**, while L-BAIBA was detected only in cells treated with benzothiazoles as shown in Figure 4-A and B. Treating cells with benzothiazoles decreased the GABA concentration compared to the positive control as well as DMSO vehicle. Benzothiazole **7b** significantly decreased the GABA concentration ( $p = 0.04919$ ) while agent **7g** did not show any significant difference. On the other hand, only cells treated with agents **7b** presented a significant increase in the L-BAIBA concentration compared to the control and DMSO vehicle ( $p = 0.03055$ ). Furthermore, GABA, L-BAIBA and D-BAIBA were determined in the CM of C2C12 cells at the 5<sup>th</sup> day post-treated with 10  $\mu$ M benzothiazole agents **7b**, **7g**, and vehicle (DMSO) (Figure 5.4C-E). GABA was generated by C2C12 and released into CM (Figure 5.4C). After treatment with **7b** or **7g** (10  $\mu$ M), GABA concentration in CM was significantly lower than that from control and DMSO-5  $\mu$ M groups, but this reduction was not significant ( $p > 0.05$ ) when compared with DMSO-10  $\mu$ M group (Figure 5.4C).

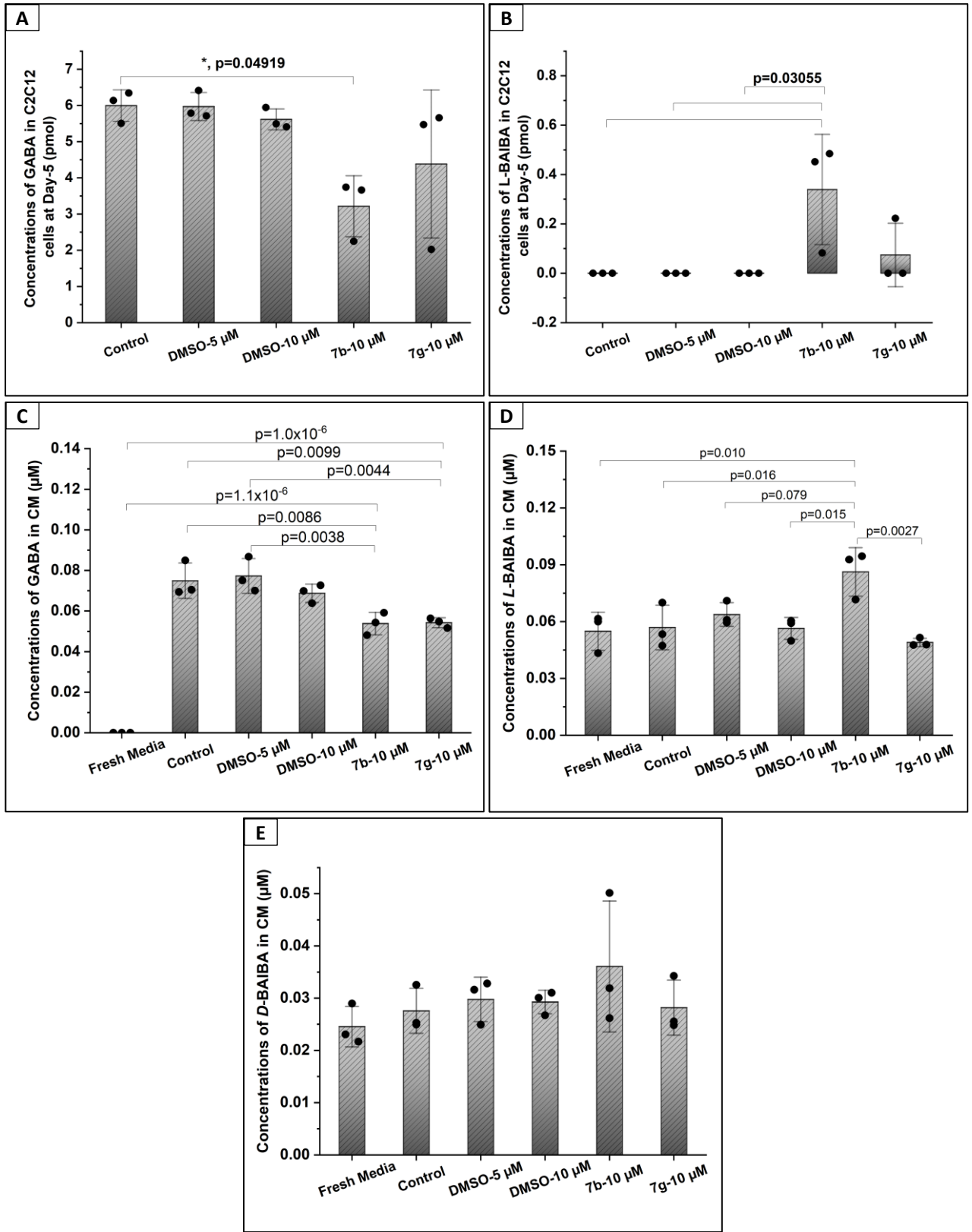


**Figure 5.4: Concentrations of aminobutyric acids in conditioned media (CM) and C2C12 cells at the 5<sup>th</sup> day post-treatment with 10 μM benzothiazole agents 7b and 7g.** (A) GABA in cells, (B) L-BAIBA in cells, (C) GABA in CM, (D) L-BAIBA in CM, and (E) D-BAIBA in CM. Mean ± SD (n=3). One-way ANOVA with Tukey's post-hoc test ( $\alpha=0.05$ ) was performed for multiple comparisons between groups. The test was performed by Dr. Marco Brotto laboratories.



While significantly higher *L*-BAIBA level was observed in CM at the 5<sup>th</sup> day when C2C12 was treated with 10  $\mu$ M of **7b** compared to all other groups of control, DMSO vehicle, and agent **7g** (Figure 5.4D). No significant alteration was observed in the *D*-BAIBA concentrations in CM (Figure 4E). These omics data indicated that benzothiazole agent **7b** significantly decrease the GABA and increase the *L*-BAIBA concentrations and secretions in C2C12 cells and media, respectively. Also, benzothiazole **7g** slightly decreased the GABA concentration in cells and did not significantly alter the *L*-, and *D*-BAIBA concentrations. Statistical analysis using One-way ANOVA with Tukey's post-hoc test ( $\alpha = 0.05$ ) was performed for multiple comparisons between groups in this study.

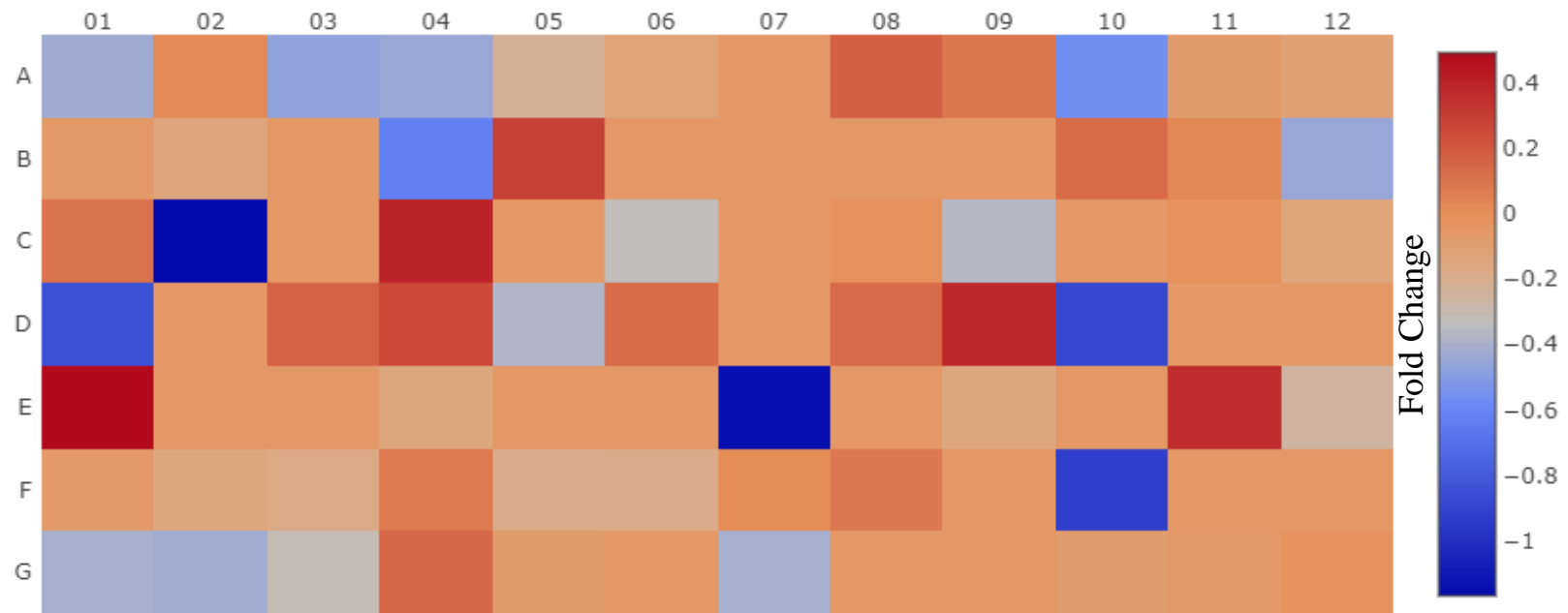
Based on the omics results, GABA RT<sup>2</sup> Profiler PCR Gene Array was performed to gain more insights on the effect of benzothiazoles on GABA genes regulations. For the GABA gene array experiments, differentiated C2C12 cells were treated with 10  $\mu$ M of benzothiazole agents **7b** and **7g** compared to control and 10  $\mu$ M DMSO. Then, mouse GABA and Glutamate RT<sup>2</sup> Profiler PCR Array was performed. This mouse GABA and glutamate profiler PCR array profiles 84 key genes of the GABA and glutamate neurotransmitter system. This array presents genes essential for the synthesis and transport of GABA and glutamate and the downstream signaling. The gene list of this array includes 17 GABAergic Synapse "Neurotransmitter Receptors", 9 Signaling Downstream of GABAergic Synapse, 20 Glutamatergic Synapse, 15 Signaling Downstream of Glutamatergic Synapse, 16 Transporters & Trafficking Proteins, and 7 metabolism genes. The results of this array indicated that benzothiazole **7b** significantly decreased the expression of GABA receptor *Gabrg2* (Fold change is -2.25,  $p=0.016$ ) compared to DMSO 10  $\mu$ M. Furthermore, agent **7b** decreased the expression of the neurotransmitter receptors *Gria1*, *Grin2a*, and *Grm7* (Fold change are -2.26, -2.33, -2.79, respectively) as well as the transporter and trafficking protein

*Slc17a7* (Fold change is -2.39), without significant differences compared to the DMSO-10  $\mu$ M. After treatment with benzothiazole **7g**, compared to DMSO-10  $\mu$ M, the expression of *Slc7a11* was significantly increased (Fold change is 4.39,  $p=0.0036$ ). It is important to note that *Slc7a11* encodes a member of a heteromeric, sodium-independent, anionic amino acid transport system that is highly specific for cysteine and glutamate. Also, agent **7g** increased the expression of GABA receptors *Gabrg1* and *Gabrg3* and the transporter and trafficking protein *Slc1a6* by more than 2-fold while no significant difference was observed compared to the control group. Benzothiazole **7g** also decreased the trafficking protein *Slc17a7* by more than 2-fold without significant differences compared to the DMSO-10  $\mu$ M. Thus, the results of this RT<sup>2</sup> Profiler PCR Array suggests that agent **7b** resulted in significant regulation of GABA receptor *Gabrg2* while agent **7g** can be a potential target for the regulation of *Slc7a11*. Considering that, these synthesized benzothiazoles could be potential targets for discovery of novel therapeutic strategies for genetic and non-genetic epilepsy and other diseases associated with mutation in GABAergic synapses and CNS disorders associated with glutamate dysfunction.

#### 5.2.2.5. Lipidomic analysis for the synthesized benzothiazoles **7b** and **7g**

The upregulation of *Slc7a11* via treatment with benzothiazole **7g** guided us to check the effect of the synthesized benzothiazoles on lipid profiling using an interesting analytical technique based on liquid chromatography/mass spectrometry (LC/MS) techniques. Totally 158 lipid mediator-related components can be analyzed simultaneously using 16 internal standard samples. The study showed that benzothiazole **7g** upregulated most of the detected lipid including arachidonic acid, eicosapentaenoic acid (EPA), docosahexaenoic acid (DHA) and Linoleic acid (LA). While benzothiazole **7b** decreased the expression of the detected lipids as shown in Table 5.2.

**A**



	01	02	03	04	05	06	07	08	09	10	11	12	GABA & Glutamate Gene List
<b>A</b>	Abat -1.34	Adcy7 1.01	Adora1 -1.39	Adora2a -1.36	Aldh5a1 -1.16	App -1.09	Avp -1.04	Bdnf 1.13	Cacna1a 1.07	Cacna1b -1.48	Cdk5r1 -1.05	Cln3 -1.08	
<b>B</b>	Dlg4 -1.04	Gabbr1 -1.1	Gabbr2 -1.04	Gabra1 -1.54	Gabra2 1.23	Gabra4 -1.04	Gabra5 -1.04	Gabra6 -1.04	Gabrb1 -1.04	Gabrb3 1.1	Gabrd 1.02	Gabre -1.37	
<b>C</b>	Gabrg1 1.08	<b>Gabrg2</b> <b>-2.25</b>	Gabrg3 -1.04	Gabrq 1.32	Gabrr1 -1.04	Gabrr2 -1.26	Gad1 -1.04	Gls -1.01	Glu 1 -1.29	Gnai1 -2.26	Gnaq -1.01	Gphn -1.1	
<b>D</b>	<b>Gria1</b> <b>-2.26</b>	Gria2 -1.04	Gria3 1.12	Gria4 1.2	Grik1 -1.3	Grik2 1.1	Grik4 -1.04	Grik5 1.1	Grin1 1.31	<b>Grin2a</b> <b>-2.33</b>	Grin2b -1.04	Grin2c -1.04	
<b>E</b>	Grm1 1.41	Grm2 -1.04	Grm3 -1.04	Grm4 -1.11	Grm5 -1.04	Grm6 -1.04	<b>Grm7</b> <b>-2.79</b>	Grm8 -1.04	Homer1 -1.11	Homer2 -1.04	I11b 1.29	Itpr1 -1.19	
<b>F</b>	Mapk1 -1.04	Nsf -1.11	P2rx7 -1.13	Phgdh 1.06	Pla2g6 -1.14	Plcb1 -1.13	Prodh 1.01	Shank2 1.06	Slc17a6 -1.04	<b>Slc17a7</b> <b>-2.39</b>	Slc17a8 -1.04	Slc1a1 -1.04	
<b>G</b>	Slc1a2 -1.33	Slc1a3 -1.34	Slc1a6 -1.24	Slc32a1 1.11	Slc38a1 -1.05	Slc6a1 -1.04	Slc6a11 -1.33	Slc6a12 -1.04	Slc6a13 -1.04	Slc7a11 -1.06	Sncg -1.04	Srr -1.02	

**B**

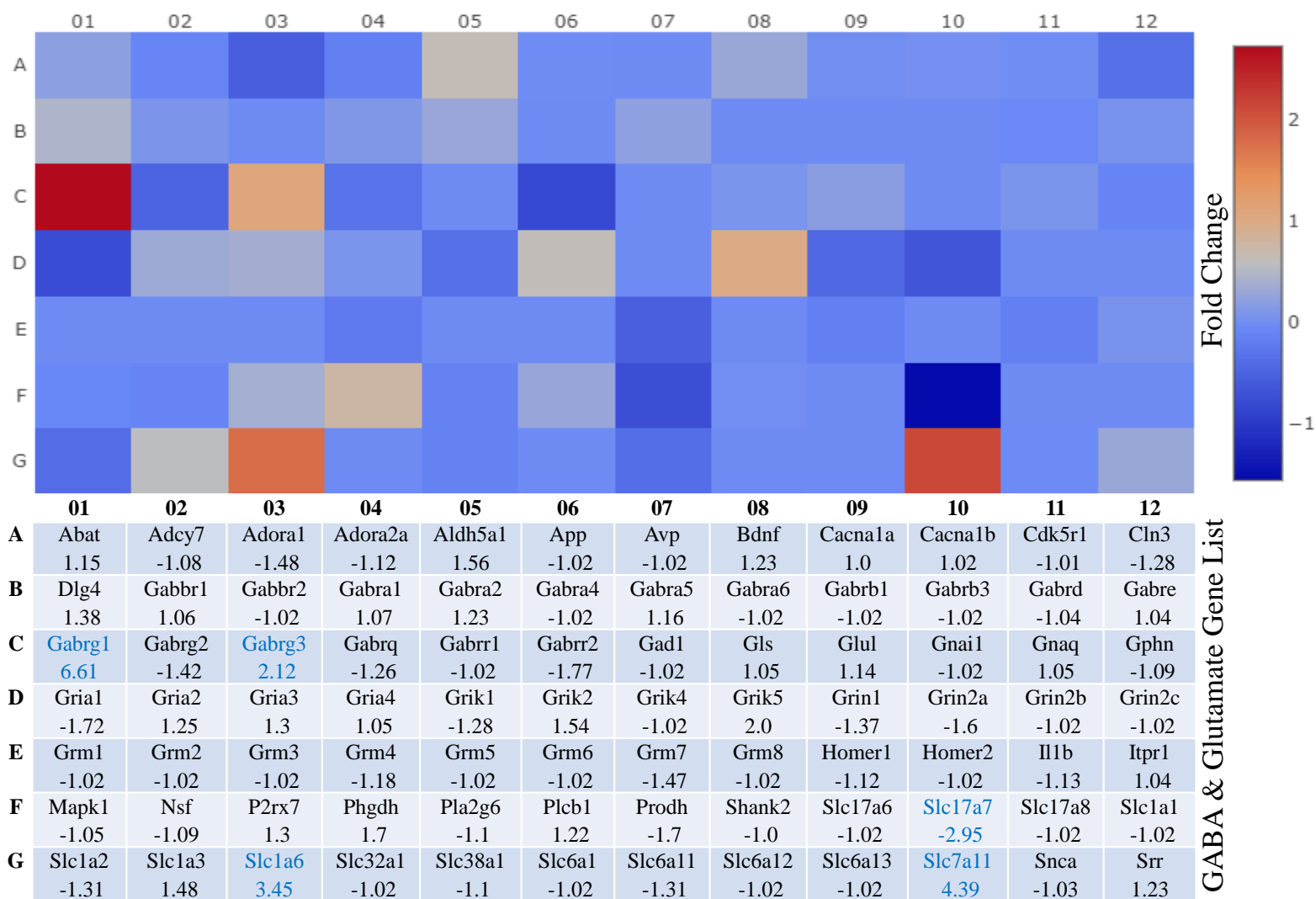


**Figure 5.5: Detection of GABA receptors by Mouse GABA & Glutamate RT<sup>2</sup> Profiler PCR Array.** A) GABA array for benzothiazole agent 7b indicated more than 2-folds downregulation of Gabrg2, Grm7, Gria1, Grin2a, and Slc17a7. B) GABA array for benzothiazole agent 7g indicated more than 2-folds upregulation of Gabrg1, Gabrg3, Slc7a11, Slc1a6, and downregulation of Slc7a7. The test was performed by Dr. Marco Brotto laboratories.

**Table 5.2:** Lipidomic analysis of the synthesized benzothiazoles **7b** and **7g**.

Quantified Analysis	ID	LM	Benzothiazole 7b	Benzothiazole 7g	DMSO	TCP
Arachidonic acid (AA), n-6 polyunsaturated fatty acid (PUFA)	12	6-keto-PGF1a	572.11	2031.65	1002.12	1226.84
	38	PGF2a	5.93	11.62	8.17	14.20
	43	PGE2	4.02	10.48	8.06	8.45
	51	PGD2	2.63	6.94	6.60	6.52
	97	12-HHT	276.20	1000.85	432.11	581.19
	174	AA	21.57	101.36	48.88	100.90
		TOTAL	882.46	3162.90	1505.95	1938.09
Linoleic acid (LA), n-6 PUFA	91	12,13-DiHOME	4.98	4.54	4.33	4.57
	92	9,10-DiHOME	0.00	0.00	0.00	0.00
	120	13-HODE	3135.45	2760.36	1985.19	2535.38
	121	9-HODE	6059.07	6252.32	3691.36	4583.22
		TOTAL	9199.50	9017.22	5680.88	7123.17
Docosahexaenoic acid (DHA), n-3 PUFA	172	DHA	634.29	1296.26	650.12	885.83
Endocannabinoids and congeners	162	AEA	0.00	0.00	0.00	0.00
	168	OEA	29.69	43.80	38.07	62.98
	177	PEA	58.30	74.72	53.00	86.99
	178	2-AG	65.95	112.12	110.42	209.62
		TOTAL	153.94	230.63	201.49	359.58
Eicosapentaenoic acid	170	EPA	316.15	1021.14	565.11	835.02
		AA/EPA	0.07	0.10	0.09	0.12

### 5.3 SUMMARY

In this chapter, the biological activity of a novel class of benzothiazole has been investigated. Six benzothiazole derivatives have been tested with C2C12 skeletal muscle cell line to test their cytotoxicity, their effect on cell proliferation and differentiation, and the GABA regulation. The results recommended the choice of acetylated derivative **7b** and benzothiazole **7g** for further investigation including omics and PCR analysis. Interestingly, benzothiazole **7b** decreased GABA expression and increased the expression of L-BAIBA in both cells and condition cell culture media. PCR gene array analysis showed that the acetylated benzothiazole downregulated *Gabrg2* gene which is associated to genetic and non-genetic epileptic disorders. While benzothiazole **7g** upregulated *Sc17a11* gene which regulates the glutathione pathway in our biological system. Therefore, the investigation of the possibility of antioxidant activity for the synthesized benzothiazoles is ongoing to test their ability as a scavenger for the free radical species and protect the cells from the oxidative stress/damage. In conclusion, the current work provides a start point for investigating a new biological activity for benzothiazole parent-based scaffolds.

## 5.4 REFERENCES

- (1) Mumford, J. P.; Cannon, D. J. Vigabatrin. *Epilepsia* **1994**, *35* (s5), S25–S28. <https://doi.org/https://doi.org/10.1111/j.1528-1157.1994.tb05962.x>.
- (2) Ben-Menachem, E.; Persson, L. I.; Mumford, J.; Haegele, K. D.; Huebert, N. Effect of Long-Term Vigabatrin Therapy on Selected Neurotransmitter Concentrations in Cerebrospinal Fluid. *J. Child Neurol.* **1991**, *Suppl 2*, S11–6.
- (3) Singh, K.; Kumar, P.; Bhatia, R.; Mehta, V.; Kumar, B.; Akhtar, M. J. Nipecotic Acid as Potential Lead Molecule for the Development of GABA Uptake Inhibitors; Structural Insights and Design Strategies. *Eur. J. Med. Chem.* **2022**, *234*, 114269. <https://doi.org/https://doi.org/10.1016/j.ejmech.2022.114269>.
- (4) Kaila, K.; Voipio, J. Postsynaptic Fall in Intracellular PH Induced by GABA-Activated Bicarbonate Conductance. *Nature* **1987**, *330* (6144), 163–165. <https://doi.org/10.1038/330163a0>.
- (5) Macdonald, R. L.; Olsen, R. W. GABAA Receptor Channels. *Annu. Rev. Neurosci.* **1994**, *17* (1), 569–602. <https://doi.org/10.1146/annurev.ne.17.030194.003033>.
- (6) Baumann, S. W.; Baur, R.; Sigel, E. Forced Subunit Assembly in GABA<sub>A</sub> Receptors: INSIGHT INTO THE ABSOLUTE ARRANGEMENT \*. *J. Biol. Chem.* **2002**, *277* (48), 46020–46025. <https://doi.org/10.1074/jbc.M207663200>.
- (7) Shivers, B. D.; Killisch, I.; Sprengel, R.; Sontheimer, H.; Köhler, M.; Schofield, P. R.; Seeburg, P. H. Two Novel GABA<sub>A</sub> Receptor Subunits Exist in Distinct Neuronal Subpopulations. *Neuron* **1989**, *3* (3), 327–337. [https://doi.org/10.1016/0896-6273\(89\)90257-2](https://doi.org/10.1016/0896-6273(89)90257-2).
- (8) Stephenson, F. A. Understanding the GABAA Receptor: A Chemically Gated Ion Channel. *Biochem. J.* **1988**, *249* (1), 21–32. <https://doi.org/10.1042/bj2490021>.
- (9) Schweizer, C.; Balsiger, S.; Bluethmann, H.; Mansuy, I. M.; Fritschy, J.-M.; Mohler, H.; Lüscher, B. The  $\Gamma 2$  Subunit of GABAA Receptors Is Required for Maintenance of Receptors at Mature Synapses. *Mol. Cell. Neurosci.* **2003**, *24* (2), 442–450. [https://doi.org/https://doi.org/10.1016/S1044-7431\(03\)00202-1](https://doi.org/https://doi.org/10.1016/S1044-7431(03)00202-1).
- (10) Baulac, S.; Huberfeld, G.; Gourfinkel-An, I.; Mitropoulou, G.; Beranger, A.; Prud'homme, J.-F.; Baulac, M.; Brice, A.; Bruzzone, R.; LeGuern, E. First Genetic Evidence of GABAA Receptor Dysfunction in Epilepsy: A Mutation in the  $\Gamma 2$ -Subunit Gene. *Nat. Genet.* **2001**, *28* (1), 46–48. <https://doi.org/10.1038/ng0501-46>.
- (11) Macdonald, R. L.; Kang, J.-Q. Molecular Pathology of Genetic Epilepsies Associated with GABAA Receptor Subunit Mutations. *Epilepsy Curr.* **2009**, *9* (1), 18–23. <https://doi.org/10.1111/j.1535-7511.2008.01278.x>.
- (12) Kang, J.-Q.; Macdonald, R. L. Molecular Pathogenic Basis for GABRG2 Mutations Associated With a Spectrum of Epilepsy Syndromes, From Generalized Absence Epilepsy to Dravet Syndrome. *JAMA Neurol.* **2016**, *73* (8), 1009–1016. <https://doi.org/10.1001/jamaneurol.2016.0449>.
- (13) Sun, L.; Dong, H.; Zhang, W.; Wang, N.; Ni, N.; Bai, X.; Liu, N. Lipid Peroxidation, GSH Depletion, and SLC7A11 Inhibition Are Common Causes of EMT and Ferroptosis in A549 Cells, but Different in Specific Mechanisms. *DNA Cell Biol.* **2021**, *40* (2), 172–183. <https://doi.org/10.1089/dna.2020.5730>.
- (14) Sato, H.; Tamba, M.; Kuriyama-Matsumura, K.; Okuno, S.; Bannai, S. Molecular Cloning and Expression of Human XCT, the Light Chain of Amino Acid Transport System Xc<sup>-</sup>. *Antioxidants & Redox Signal.* **2000**, *2* (4), 665–671. <https://doi.org/10.1089/ars.2000.2.4-665>.
- (15) Bridges, R.; Lutgen, V.; Lobner, D.; Baker, D. A. Thinking Outside the Cleft to Understand Synaptic Activity: Contribution of the Cystine-Glutamate Antiporter

- (System Xc-) to Normal and Pathological Glutamatergic Signaling. *Pharmacol. Rev.* **2012**, *64* (3), 780–802. <https://doi.org/10.1124/pr.110.003889>.
- (16) Lin, C.-H.; Lin, P.-P.; Lin, C.-Y.; Lin, C.-H.; Huang, C.-H.; Huang, Y.-J.; Lane, H.-Y. Decreased mRNA Expression for the Two Subunits of System Xc<sup>-</sup>, SLC3A2 and SLC7A11, in WBC in Patients with Schizophrenia: Evidence in Support of the Hypo-Glutamatergic Hypothesis of Schizophrenia. *J. Psychiatr. Res.* **2016**, *72*, 58–63. <https://doi.org/https://doi.org/10.1016/j.jpsychires.2015.10.007>.
- (17) Bridges, R. J.; Natale, N. R.; Patel, S. A. System Xc- Cystine/Glutamate Antiporter: An Update on Molecular Pharmacology and Roles within the CNS. *Br. J. Pharmacol.* **2012**, *165* (1), 20–34. <https://doi.org/https://doi.org/10.1111/j.1476-5381.2011.01480.x>.
- (18) Tariq, S.; Kamboj, P.; Amir, M. Therapeutic Advancement of Benzothiazole Derivatives in the Last Decennial Period. *Arch. Pharm. (Weinheim)*. **2019**, *352* (1), 1800170. <https://doi.org/https://doi.org/10.1002/ardp.201800170>.
- (19) Mignani, S.; Majoral, J.-P.; Desaphy, J.-F.; Lentini, G. From Riluzole to Dextramipexole via Substituted-Benzothiazole Derivatives for Amyotrophic Lateral Sclerosis Disease Treatment: Case Studies. *Molecules* **2020**, *25* (15). <https://doi.org/10.3390/molecules25153320>.
- (20) Wu, Z.; Wang, G.; Zhang, B.; Dai, T.; Gu, A.; Li, X.; Cheng, X.; Liu, P.; Hao, J.; Liu, X. Metabolic Mechanism of Plant Defense against Rice Blast Induced by Probenazole. *Metabolites* **2021**, *11* (4). <https://doi.org/10.3390/metabo11040246>.
- (21) Masini, E.; Carta, F.; Scozzafava, A.; Supuran, C. T. Antiglaucoma Carbonic Anhydrase Inhibitors: A Patent Review. *Expert Opin. Ther. Pat.* **2013**, *23* (6), 705–716. <https://doi.org/10.1517/13543776.2013.794788>.
- (22) Zhai, J.; Zhang, H.; Zhang, L.; Zhao, Y.; Chen, S.; Chen, Y.; Peng, X.; Li, Q.; Yuan, M.; Hu, X. Zopolrestat as a Human Glyoxalase I Inhibitor and Its Structural Basis. *ChemMedChem* **2013**, *8* (9), 1462–1464. <https://doi.org/https://doi.org/10.1002/cmdc.201300243>.
- (23) Kale, A.; Kakde, R.; Pawar, S.; Thombare, R. Recent Development in Substituted Benzothiazole as an Anticonvulsant Agent. *Mini-Reviews in Medicinal Chemistry*. 2021, pp 1017–1024. <https://doi.org/http://dx.doi.org/10.2174/1389557521666201222145236>.
- (24) Liu, D.-C.; Zhang, H.-J.; Jin, C.-M.; Quan, Z.-S. Synthesis and Biological Evaluation of Novel Benzothiazole Derivatives as Potential Anticonvulsant Agents. *Molecules* **2016**, *21* (3). <https://doi.org/10.3390/molecules21030164>.
- (25) Murtuja, S.; Shaquiquzzaman, M.; Amir, M. Design, Synthesis, and Screening of Hybrid Benzothiazolyl-Oxadiazoles as Anticonvulsant Agents. *Letters in Drug Design & Discovery*. 2018, pp 398–405. <https://doi.org/http://dx.doi.org/10.2174/1570180814666170526154914>.
- (26) Ali, R.; Siddiqui, N. New Benzo[d]Thiazol-2-Yl-Aminoacetamides as Potential Anticonvulsants: Synthesis, Activity and Prediction of Molecular Properties. *Arch. Pharm. (Weinheim)*. **2015**, *348* (4), 254–265. <https://doi.org/https://doi.org/10.1002/ardp.201400466>.
- (27) Amir, M.; Hassan, Z. M. Functional Roles of Benzothiazole Motif in Antiepileptic Drug Research. *Mini-Reviews in Medicinal Chemistry*. 2013, pp 2060–2075. <https://doi.org/http://dx.doi.org/10.2174/1389557513666131119203036>.
- (28) Shafi, S.; Mahboob Alam, M.; Mulakayala, N.; Mulakayala, C.; Vanaja, G.; Kalle, A. M.; Pallu, R.; Alam, M. S. Synthesis of Novel 2-Mercapto Benzothiazole and 1,2,3-Triazole Based Bis-Heterocycles: Their Anti-Inflammatory and Anti-Nociceptive Activities. *Eur. J. Med. Chem.* **2012**, *49*, 324–333. <https://doi.org/https://doi.org/10.1016/j.ejmech.2012.01.032>.



- (29) Khan, B.; Naiyer, A.; Athar, F.; Ali, S.; Thakur, S. C. Synthesis, Characterization and Anti-Inflammatory Activity Evaluation of 1,2,4-Triazole and Its Derivatives as a Potential Scaffold for the Synthesis of Drugs against Prostaglandin-Endoperoxide Synthase. *J. Biomol. Struct. Dyn.* **2021**, *39* (2), 457–475. <https://doi.org/10.1080/07391102.2019.1711193>.
- (30) Tariq, S.; Kamboj, P.; Alam, O.; Amir, M. 1,2,4-Triazole-Based Benzothiazole/Benzoxazole Derivatives: Design, Synthesis, P38 $\alpha$  MAP Kinase Inhibition, Anti-Inflammatory Activity and Molecular Docking Studies. *Bioorg. Chem.* **2018**, *81*, 630–641. <https://doi.org/10.1016/j.bioorg.2018.09.015>.
- (31) Chhabra, M.; Sinha, S.; Banerjee, S.; Paira, P. An Efficient Green Synthesis of 2-Arylbenzothiazole Analogues as Potent Antibacterial and Anticancer Agents. *Bioorg. Med. Chem. Lett.* **2016**, *26* (1), 213–217. <https://doi.org/10.1016/j.bmcl.2015.10.087>.
- (32) Sahu, P. K.; Sahu, P. K.; Samadhiya, P.; Sahu, P. L.; Agarwal, D. D. POM Analyses and Evaluation of in Vitro Antimicrobial, Antitumor Activity of 4H-Pyrimido[2,1-b]Benzothiazole Derivatives. *Med. Chem. Res.* **2016**, *25* (8), 1551–1563. <https://doi.org/10.1007/s00044-016-1589-8>.
- (33) Pathak, N.; Rathi, E.; Kumar, N.; Kini, G. S.; Rao, M. C. A Review on Anticancer Potentials of Benzothiazole Derivatives. *Mini-Reviews in Medicinal Chemistry*. 2020, pp 12–23. <https://doi.org/http://dx.doi.org/10.2174/1389557519666190617153213>.
- (34) Dadmal, T. L.; Appalanaidu, K.; Kumbhare, R. M.; Mondal, T.; Ramaiah, M. J.; Bhadra, M. P. Synthesis and Biological Evaluation of Triazole and Isoxazole-Tagged Benzothiazole/Benzoxazole Derivatives as Potent Cytotoxic Agents. *New J. Chem.* **2018**, *42* (19), 15546–15551. <https://doi.org/10.1039/C8NJ01249K>.
- (35) Sultana, F.; Saifi, M. A.; Syed, R.; Mani, G. S.; Shaik, S. P.; Osas, E. G.; Godugu, C.; Shahjahan, S.; Kamal, A. Synthesis of 2-Anilinopyridyl Linked Benzothiazole Hydrazones as Apoptosis Inducing Cytotoxic Agents. *New J. Chem.* **2019**, *43* (18), 7150–7161. <https://doi.org/10.1039/C8NJ06517A>.
- (36) Williams, N. S.; Gonzales, S.; Naidoo, J.; Rivera-Cancel, G.; Voruganti, S.; Mallipeddi, P.; Theodoropoulos, P. C.; Geboers, S.; Chen, H.; Ortiz, F.; Posner, B.; Nijhawan, D.; Ready, J. M. Tumor-Activated Benzothiazole Inhibitors of Stearoyl-CoA Desaturase. *J. Med. Chem.* **2020**, *63* (17), 9773–9786. <https://doi.org/10.1021/acs.jmedchem.0c00899>.
- (37) Shaikh, F. M.; Patel, N. B.; Sanna, G.; Busonera, B.; La Colla, P.; Rajani, D. P. Synthesis of Some New 2-Amino-6-Thiocyanato Benzothiazole Derivatives Bearing 2,4-Thiazolidinediones and Screening of Their in Vitro Antimicrobial, Antitubercular and Antiviral Activities. *Med. Chem. Res.* **2015**, *24* (8), 3129–3142. <https://doi.org/10.1007/s00044-015-1358-0>.
- (38) Sharma, C. P.; Bansal, K. K.; Deep, A.; Pathak, M. Benzothiazole Derivatives as Potential Anti-Infective Agents. *Current Topics in Medicinal Chemistry*. 2017, pp 208–237. <https://doi.org/http://dx.doi.org/10.2174/1568026616666160530152546>.
- (39) Ugwu, D. I.; Okoro, U. C.; Ukoha, P. O.; Gupta, A.; Okafor, S. N. Novel Anti-Inflammatory and Analgesic Agents: Synthesis, Molecular Docking and in Vivo Studies. *J. Enzyme Inhib. Med. Chem.* **2018**, *33* (1), 405–415. <https://doi.org/10.1080/14756366.2018.1426573>.
- (40) Kumar, G.; Singh, N. P. Synthesis, Anti-Inflammatory and Analgesic Evaluation of Thiazole/Oxazole Substituted Benzothiazole Derivatives. *Bioorg. Chem.* **2021**, *107*, 104608. <https://doi.org/10.1016/j.bioorg.2020.104608>.
- (41) Kamal, A.; Syed, M. A. H.; Mohammed, S. M. Therapeutic Potential of Benzothiazoles: A Patent Review (2010 – 2014). *Expert Opin. Ther. Pat.* **2015**, *25* (3), 335–349. <https://doi.org/10.1517/13543776.2014.999764>.

- (42) Mistry, B. M.; Patel, R. V.; Keum, Y.-S.; Kim, D. H. Chrysin–Benzothiazole Conjugates as Antioxidant and Anticancer Agents. *Bioorg. Med. Chem. Lett.* **2015**, *25* (23), 5561–5565. <https://doi.org/10.1016/j.bmcl.2015.10.052>.
- (43) Payaz, D. Ü.; Küçükbay, F. Z.; Küçükbay, H.; Angeli, A.; Supuran, C. T. Synthesis Carbonic Anhydrase Enzyme Inhibition and Antioxidant Activity of Novel Benzothiazole Derivatives Incorporating Glycine, Methionine, Alanine, and Phenylalanine Moieties. *J. Enzyme Inhib. Med. Chem.* **2019**, *34* (1), 343–349. <https://doi.org/10.1080/14756366.2018.1553040>.
- (44) Racané, L.; Ptiček, L.; Fajdetic, G.; Tralić-Kulenović, V.; Klobučar, M.; Kraljević Pavelić, S.; Perić, M.; Paljetak, H. Č.; Verbanac, D.; Starčević, K. Green Synthesis and Biological Evaluation of 6-Substituted-2-(2-Hydroxy/Methoxy Phenyl)Benzothiazole Derivatives as Potential Antioxidant, Antibacterial and Antitumor Agents. *Bioorg. Chem.* **2020**, *95*, 103537. <https://doi.org/10.1016/j.bioorg.2019.103537>.
- (45) Sharma, S.; Pathare, R. S.; Maurya, A. K.; Gopal, K.; Roy, T. K.; Sawant, D. M.; Pardasani, R. T. Ruthenium Catalyzed Intramolecular C–S Coupling Reactions: Synthetic Scope and Mechanistic Insight. *Org. Lett.* **2016**, *18* (3), 356–359. <https://doi.org/10.1021/acs.orglett.5b03185>.
- (46) Gao, M.-Y.; Li, J.-H.; Zhang, S.-B.; Chen, L.-J.; Li, Y.-S.; Dong, Z.-B. A Mild Synthesis of 2-Substituted Benzothiazoles via Nickel-Catalyzed Intramolecular Oxidative C–H Functionalization. *J. Org. Chem.* **2020**, *85* (2), 493–500. <https://doi.org/10.1021/acs.joc.9b02543>.
- (47) Zhu, H.; Zhang, S.-B.; Liu, X.; Cheng, Y.; Peng, H.-Y.; Dong, Z.-B. Copper(II)-Promoted Cascade Synthesis of 2-Aminobenzothiazoles Starting from 2-Iodoanilines and Sodium Dithiocarbamates. *European J. Org. Chem.* **2018**, *2018* (41), 5711–5716. <https://doi.org/10.1002/ejoc.201801122>.
- (48) Xu, W.; Zeng, M.-T.; Liu, M.; Liu, X.; Chang, C.-Z.; Zhu, H.; Li, Y.-S.; Dong, Z.-B. Palladium-Catalyzed Tandem Synthesis of 2-Aminobenzothiazoles Starting from Unreactive 2-Chloroanilines. *Chem. Lett.* **2017**, *46* (5), 641–643. <https://doi.org/10.1246/cl.170023>.
- (49) Chang, C.-Z.; Xu, W.; Zeng, M.-T.; Liu, M.; Liu, X.; Zhu, H.; Dong, Z.-B. Copper-Catalyzed Tandem Reaction of 2-Haloanilines with Thiocarbamoyl Chloride: Synthesis of 2-Aminobenzothiazoles. *Synth. Commun.* **2017**, *47* (13), 1262–1267. <https://doi.org/10.1080/00397911.2017.1324033>.
- (50) Xu, W.; Zeng, M.-T.; Liu, S.-S.; Li, Y.-S.; Dong, Z.-B. Copper Catalyzed Synthesis of Benzoxazoles and Benzothiazoles via Tandem Manner. *Tetrahedron Lett.* **2017**, *58* (45), 4289–4292. <https://doi.org/10.1016/j.tetlet.2017.09.089>.
- (51) Min, H.; Xiao, G.; Liu, W.; Liang, Y. Copper-Catalyzed Synthesis of 2-Aminobenzothiazoles from 2-Iodophenyl Isocyanides, Potassium Sulfide and Amines. *Org. Biomol. Chem.* **2016**, *14* (47), 11088–11091. <https://doi.org/10.1039/C6OB02413K>.
- (52) Awad, K.; Ahuja, N.; Fiedler, M.; Peper, S.; Wang, Z.; Aswath, P.; Brotto, M.; Varanasi, V. Ionic Silicon Protects Oxidative Damage and Promotes Skeletal Muscle Cell Regeneration. *International Journal of Molecular Sciences* . 2021. <https://doi.org/10.3390/ijms22020497>.
- (53) Wang, Z.; Bian, L.; Mo, C.; Shen, H.; Zhao, L. J.; Su, K.-J.; Kukula, M.; Lee, J. T.; Armstrong, D. W.; Recker, R.; Lappe, J.; Bonewald, L. F.; Deng, H.-W.; Brotto, M. Quantification of Aminobutyric Acids and Their Clinical Applications as Biomarkers for Osteoporosis. *Commun. Biol.* **2020**, *3* (1), 39. <https://doi.org/10.1038/s42003-020-0766-y>.

## **PART-II: NOVEL THIAZOLIDINES AS ANTI-APOPTOTIC AGENTS FOR CANCER DRUG DISCOVERY**

**In this part,** we discuss the design and synthesis of novel thiazolidines-based small molecules. The bioactivity of the synthesized thiazolidines was investigated as anti-proliferative agents. Two new thiazolidine libraries were synthesized and are discussed in chapters seven and eight based on the previous study described in chapter six. Utilization of the chemistry discovered in the Lovely lab was targeted to construct these new classes of thiazolidines and to improve their chemical stability and biological activity. The validation of the solid support synthetic method has been successfully performed. Computer-Assisted Drug Design (CADD, computational technique) approaches have been utilized to design new bioactive candidates and validate their observed activity, which include qualitative structure activity relationship (QSAR) and molecular docking. The biological activity of the first library (Chapter six) was investigated by our Egyptian colleagues from the national research center, while the second library was investigated by the Mandal lab (Department of Chemistry and Biochemistry, UTA). By synthesizing the third group of thiazolidines (Chapter eight), we isolated the most chemically stable derivatives, and their anticancer activity was performed by the Pan lab (Department of Graduate Nursing and Bone and Muscle Research Center, UTA).

**CHAPTER SIX: NOVEL THIAZOLIDINES: SYNTHESIS, ANTI-PROLIFERATIVE  
PROPERTIES AND 2D-QSAR STUDIES**

Ravi P. Singh<sup>1</sup>, Marian N. Aziz<sup>1,2</sup>, Delphine Gout<sup>1</sup>, Walid Fayad<sup>3</sup>, May A. El-Manawaty<sup>3</sup>,  
Carl J. Lovely<sup>1</sup>

1. Department of Chemistry and Biochemistry, 700 Planetarium Place, University of Texas at  
Arlington, TX 76019, USA

2. Department of Pesticide Chemistry, National Research Centre, Dokki, Giza 12622, Egypt

3. Drug Bioassay-Cell Culture Laboratory, Pharmacognosy Department, National Research  
Centre, Dokki, Giza, 12622. Egypt.

Corresponding author

Prof. Carl J. Lovely

Professor, Chemistry and Biochemistry Department

University of Texas at Arlington

Address: 700 Planetarium Place, Box 19065, UT Arlington, TX 76019-0065

Email: lovely@uta.edu

Phone: +1 817 272 5446

(Published)

## **ABSTRACT:**

A series of (Z)-2-imino-(5Z)-ylidene-N-substituted thiazolidines/thiazolidin-4-ones were synthesized and their anti-tumor activities against colon (HCT-116) and breast (MCF 7) cancer cell lines were evaluated utilizing an MTT growth assay. A qualitative structure activity relationship (2D-QSAR) investigation was conducted to probe and validate the obtained anti-tumor properties for the new synthesized thiazolidine derivatives. The majority of the thiazolidines exhibit higher potency against colon cancer relative to the standard reference. Compounds **16a** and **17a** exhibit the highest anti-proliferative activity against HCT116 relative to control ( $IC_{50} = 8.9$  and  $9.8 \mu\text{M}$  respectively compared to  $20.4 \mu\text{M}$  observed for 5-fluorouracil as positive control). An X-ray study confirmed the Z, Z'-configurations for the synthesized compounds.

## **6.1 INTRODUCTION**

Cancer and cardiovascular diseases are the major contributors to mortality rates globally; out of these two, cancer is predicted to be the single controlling factor for life expectancy worldwide in the 21<sup>st</sup> century. Globally, approximately 18.1 million new cancer cases were predicted to be diagnosed in 2018 in addition to 9.6 million deaths.<sup>1</sup> Among these statistical data, the estimated diagnosed cancer cases in the United States are 4700 per day which is approximately equivalent to 1.7 million cases, leading to 609,640 cancer deaths in 2018. Lung, prostate, colorectal, and breast cancers are the four most common cancers leading to death, accounting for 45% of the total number of cancer deaths.<sup>2</sup> Based on the GLOBOCAN database published in September 2018, colorectal cancer (CRC) is the third most common malignancy and the second leading cause of death from cancer. It was estimated that more than 1.8 million new CRC cases will occur in 2018 that relates to 881,000 deaths.

In the United States, CRC exhibits the fourth highest incidence rate in adults, and it was expected to affect more than 140,000 American lives in 2018.<sup>3</sup> The incidence and the mortality

rates of CRC in developed countries are 3-fold higher than developing countries.<sup>1</sup> These trends are related to the so-called “Western lifestyle” which is responsible for the major risk factors for increasing CRC incidence rates.<sup>3</sup> The International Classification of Diseases for Oncology classifies CRC as either colon or rectal cancer due to the misclassification of rectal cancer as colon in the mortality rates, therefore both of them are combined together in all the published statistical analyses.<sup>4</sup>

Colon cancer is a malignancy of the large intestine that starts by the formation of benign adenomatous polyps cells which transform into cancerous tumors by various genetic alternations including ras-gene mutation and allelic loss of chromosome 5, 17 and 18 sequences.<sup>5</sup> Surgery, chemotherapy, and radiation approaches are typically used in the CRC treatment modalities. 5-Fluorouracil is used as anticancer CRC drug along with others including irinotecan, oxaliplatin, trifluridine, and tipiracil.<sup>6</sup> Some of these combined drug regimens have achieved high efficacy in controlling tumor growth before surgical intervention for metastatic disease.<sup>7</sup> However, the unacceptable cytotoxicity and cytopenia with diarrhea are considered the major side effects which limit the drug dosages with the advanced CRC.<sup>8</sup> Moreover, metastatic colon and breast cancer cells are considered a lesion that causes secondary liver cancer.<sup>9</sup>

Therefore, the discovery of novel small molecules as antitumor drugs against colon and breast cancer remains the focus of several research groups worldwide. Candidate structures containing a thiazolidine framework have attracted the attention of many researchers due to the diversity of their biological activities, the generally short synthetic sequences required for their construction and the potential for rapid acquisition of diverse substitution patterns.<sup>10</sup> Specifically, for example, diverse biological/pharmacological activities including antibacterial and antifungal,<sup>11</sup> antihypertensive,<sup>12</sup> antidiabetic,<sup>13</sup> antidepressant, anticonvulsant,<sup>14</sup> anti-

inflammatory, analgesic, and antitumor properties have been described for synthetic 2-imino-5-arylidene-thiazolidin-4-ones.<sup>15</sup>

Special interest was recently directed towards 2-imino-5-arylidene-thiazolidines due to the antimetabolic activity revealed against various cancer cells.<sup>10b</sup> Teraishi *et al.* have explored the apoptotic activity of a series of 2-imino(amino)-5-ylidene-4-thiazolidinones against various drug resistant human cancer cell lines.<sup>15d, 15e</sup> Among these compounds, MMPT (**1**) and DBPT (**2**) induce cell death in drug resistant colon and lung cancer cells (Figure 6.1). These two thiazolidinones induce apoptosis by causing G2/M-phase arrest in p53-deficient H1299 (lung cancer) and HCT116 (colon cancer) cells.<sup>15d</sup> Ottanà *et al.* have demonstrated that 2-phenylimino-5-(3-methoxyphenyl-methylidene)-3-propyl-4-thiazolidindione (**3**) (Figure 6.1) inhibits the growth of HT-29 colon cancer cell lines with high COX-2 expression.<sup>15b</sup> Also, 2-[[4-(4-chlorophenyl)-1,3-thiazol-2-yl]imino]-5-(4-methoxybenzylidene)-1,3-thiazolidin-4-one (**4**) (Figure 6.1) was reported to exhibit antimetabolic activity against colon and breast cancers.<sup>15c</sup> Peroxisome proliferator activated receptors (PPARs) are overexpressed in various tumors including colon, breast, prostate, lung, pituitary, and thyroid cancers. HL005 (**5**) (Fig. 1) is reported as a PPAR $\gamma$  antagonist especially for breast cancer. Specifically, it antagonizes the rosiglitazone stimulated PPAR $\gamma$ /CBP interaction with 7.97  $\mu$ M (IC<sub>50</sub>), and also inhibits the proliferation of MCF-7 by inducing apoptosis at G2/M phase (IC<sub>50</sub> = 108  $\mu$ M).<sup>15a</sup> It is interesting to notice that most of the reported active 2-imino-5-arylidene-thiazolidines belong to a thiazolidinone scaffold; this may be a consequence of the paucity of available synthetic approaches for 2-imino-5-arylidene-thiazolidine compounds.

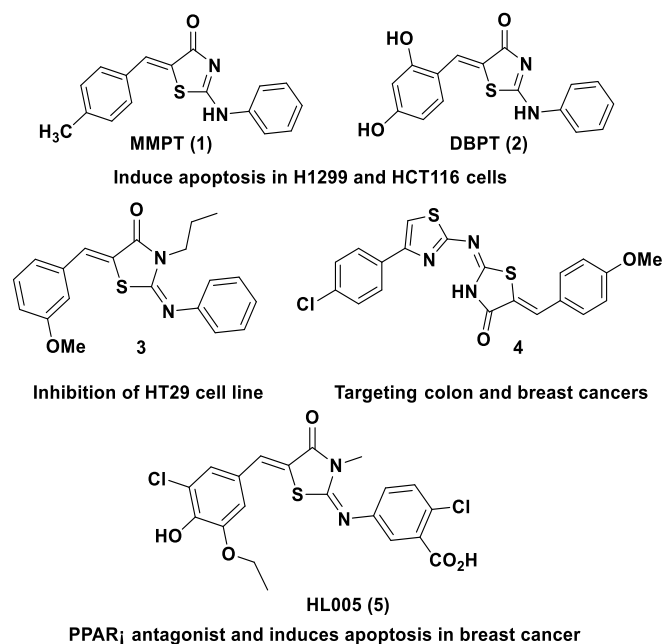


**Figure 6.1:** Structures of some anti-tumor thiazolidinones.

In this present chapter, we describe new 2-imino-5-ylidene-thiazolidinones and derived thiazolidinones through application of a new synthetic method developed by our research group, and an investigation of their antiproliferative properties against HCT-116 (colon) and MCF7 (breast) cancer cell lines using an MTT growth assay.

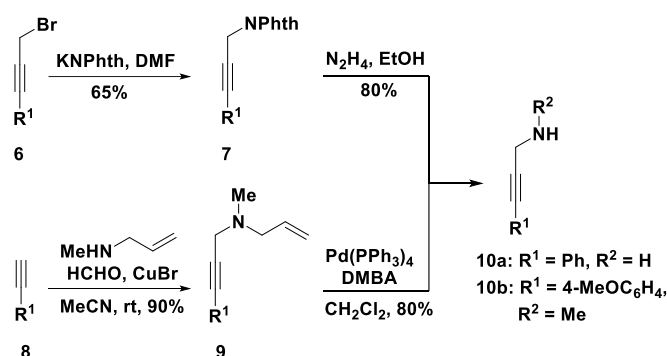
## 6.2 RESULTS AND DISCUSSION

### 6.2.1 Chemistry

Synthetic methods for the construction of thiazolidinones abound in the literature, but the synthesis of the corresponding thiazolidinones has received significantly less attention. Several synthetic protocols for the preparation of substituted thiazolidin-2-imines have been reported recently.<sup>16</sup> For example, Dethle and co-workers have described a method to synthesize thiazolidin-2-ylideneamine derivatives via thiol-yne coupling of propargylamine with isothiocyanate under metal- and solvent-free conditions, although there are some limitations in terms of substrate scope.<sup>17</sup> Herein, we report the formation of a variety of thiazolidinones in good to excellent yields via the tandem thioacylation-hydrosulfenylation of propargylamines and thiocyanates promoted by silica gel.<sup>18</sup>

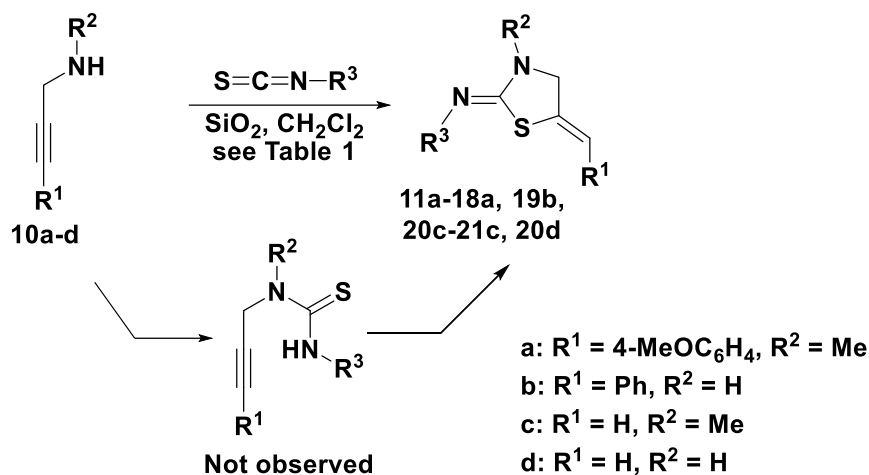


The two terminal alkynes **10c** and **10d** ( $R^1 = H$ ,  $R^2 = Me$ ;  $R^1 = R^2 = H$ ) used in this study were commercially available whereas the internal alkynes required synthesis. The primary propargylamine **10a** ( $R^1 = Ph$ ,  $R^2 = H$ ) was synthesized from the corresponding bromide via Gabriel chemistry using previously described procedures.<sup>9b</sup> The secondary propargylamine substrate **10b** ( $R^1 = 4\text{-MeOC}_6\text{H}_4$ ,  $R^2 = Me$ ) was synthesized using chemistry previously described by Looper and coworkers (Scheme 6.1).<sup>19</sup> Specifically, a copper-mediated, three-component coupling reaction of 4-ethynylanisole **8** with formaldehyde and the *N*-allyl amine was carried out to produce tertiary amine **9**. Pd-Catalyzed deallylation was employed to yield the requisite amine **10b**.



**Scheme 6.1:** Synthesis of 3-(substituted)-prop-2-yn-1-amines **10a-b**.

The (Z)-2-imino-5-(Z)-alkylidenethiazolidines **11a-18a**, **19b**, **20c-21c**, **20d** were readily synthesized by application of a recently described method utilizing silica gel-mediated tandem thio-acylation and subsequent anti-hydrosulfenylation of the alkyne. Propargyl amines **10a-d** were reacted on silica gel with several different isothiocyanates to afford the corresponding targeted thiazolidines in good yields (Scheme 6.2 and Table 6.1) via the intermediacy of the corresponding thiourea. The spectroscopic data (IR,  $^1\text{H}$  NMR,  $^{13}\text{C}$  NMR, and mass spectrometry) and X-ray crystallography corroborate the structures of **11a-18a**, **19b**, **20c-21c**, and **20d**.



**Scheme 6.2:** Synthesis of (Z)-2-imino-5-(Z)ylidene-N-substituted thiazolidines **11a-18a, 19b, 20c-21c, and 20d**.

For example, the  $^1\text{H}$  NMR spectrum of compound **15a** shows the diagnostic vinylic and methylene protons at  $\delta_{\text{H}} = 6.46$  (triplet) and  $\delta_{\text{H}} = 4.40$  (doublet) ppm respectively, with a small long-range coupling of  $J = 1.9$  Hz. An X-ray crystal structure study of compound **15a** (for more details, see below) confirms the geometry of the two exocyclic double bonds at C2 and C5 as possessing Z, Z'-configurations (Figure 6.2). 4-Thiazolidinones, have been known for a long time to possess a wide range of biological activities. Out of all types of thiazolidinones, 4-thiazolidinones and 2-imino-4-thiazolidinones are highly dominant.<sup>20</sup> There are several methods known for the synthesis of 2-imino-4-thiazolidinones from the corresponding thioureas.<sup>21</sup> However, in this context, we observed the formation of thiazolidinones from the corresponding thiazolidines via auto-oxidation. Interestingly, only the thiazolidine compounds which contained a 4-methoxybenzylidene moiety underwent air oxidation to the corresponding (Z)-2-imino substituted-5-((Z)-alkylidene)-thiazolidin-4-ones **28-38** upon standing at room temperature and open to the atmosphere for few days either neat or in solution (Scheme 6.3). The NMR spectra readily confirm the thiazolidin-4-one structures by, for example, disappearance of the methylene protons in the  $^1\text{H}$  NMR spectrum in addition to the  $^{13}\text{C}$  NMR data, which now exhibit an absorption due to the C4 carbonyl; for example, compound **22** exhibits a resonance at  $\delta_{\text{C}=\text{O}} = 167.1$  ppm. Also, IR spectra show a carbonyl stretching vibration

band for each member of the thiazolidinone family, Furthermore, a single crystal X-ray study confirms the structure of **31** (an example of the synthesized thiazolidinones) as shown in Fig. 2.

**Table 6.1:** Synthesis of (Z)-2-imino-(5Z)-ylidene-N-substituted thiazolidines **11a-18a**, **19b**, **20c-21c**, and **20d**.<sup>a</sup>

Entry	Cpd.	R <sup>1</sup>	R <sup>2</sup>	R <sup>3</sup>	Yield (%) <sup>b</sup>
1	11a	4-MeOC <sub>6</sub> H <sub>4</sub>	Me	4-MeC <sub>6</sub> H <sub>4</sub>	97
2	12a	4-MeOC <sub>6</sub> H <sub>4</sub>	Me	4-FC <sub>6</sub> H <sub>4</sub>	99
3	13a	4-MeOC <sub>6</sub> H <sub>4</sub>	Me	4-NO <sub>2</sub> C <sub>6</sub> H <sub>4</sub>	93
4	14a	4-MeOC <sub>6</sub> H <sub>4</sub>	Me	4-CF <sub>3</sub> C <sub>6</sub> H <sub>4</sub>	94
5	15a	4-MeOC <sub>6</sub> H <sub>4</sub>	Me	4-CH <sub>3</sub> OC <sub>6</sub> H <sub>4</sub>	99
6	16a	4-MeOC <sub>6</sub> H <sub>4</sub>	Me	4-BrC <sub>6</sub> H <sub>4</sub>	99
7	17a	4-MeOC <sub>6</sub> H <sub>4</sub>	Me	4-ClC <sub>6</sub> H <sub>4</sub>	99
8	18a	4-MeOC <sub>6</sub> H <sub>4</sub>	Me	4- <i>t</i> -BuC <sub>6</sub> H <sub>4</sub>	95
9	19b	C <sub>6</sub> H <sub>5</sub>	H	3,5-(CF <sub>3</sub> ) <sub>2</sub> C <sub>6</sub> H <sub>3</sub>	75
10	20c	H	H	C <sub>6</sub> H <sub>5</sub>	80
11	21c	H	H	Allyl	67
12	20d	H	Me	C <sub>6</sub> H <sub>5</sub>	78
13	22	C <sub>6</sub> H <sub>5</sub>	PhNHC=S	C <sub>6</sub> H <sub>5</sub>	9 <sup>c</sup>

<sup>a</sup> Reaction was performed with 200 mg of **10a-d** in CH<sub>2</sub>Cl<sub>2</sub> (0.2 mL/mmol) and isothiocyanate (1 equiv) on silica gel (1.75 g/mmol) for 2 h.

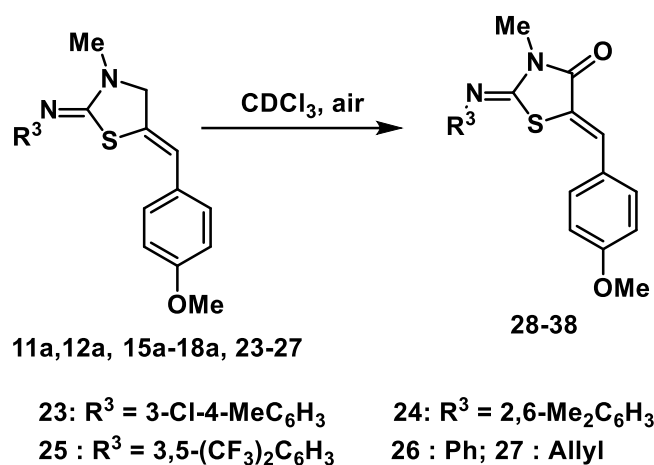
<sup>b</sup> Isolated yields after purification by column chromatography.

<sup>c</sup> Isolated as a minor byproduct.

### 6.2.2 Single crystal X-ray studies

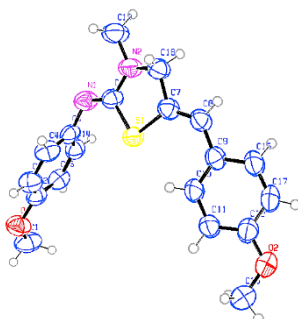
Analysis of compounds **15a** and **31** has been undertaken by single crystal X-ray diffraction to confirm the connectivity of these analogs. Thiazolidine **15a** crystallizes in a monoclinic space group P21/c with one molecule per asymmetric unit cell and 4 molecules per unit cell whereas compound **31** crystallizes in a triclinic space group P-1 with one molecule per asymmetric unit

cell and 2 molecules per unit cell. Molecules of compound **15a** are arranged in a zig-zag orientation and connected to each



**Scheme 6.3:** Synthesis of (Z)-2-substituted imino-5-((Z)-ylidene)-thiazolidin-4-ones **28-38**.

other through weak H-bonding stabilizing the crystallographic structure and forming a three-dimensional supramolecular arrangement. Similarly, molecules of compound **31** are arranged in a zig-zag shape linked with weak H bonds as well as Br...H bonds stabilizing the extended arrangement of the crystal structure. For molecule **31**, the bromophenyl group is found to have two statistically different orientations. Therefore, the atoms sites (C10/C13), (C11/C14), (C15/C17) and (C16/C18) are all half occupied. Fig. 2 illustrates the independent molecules of compounds **15a** and **31** as refined.



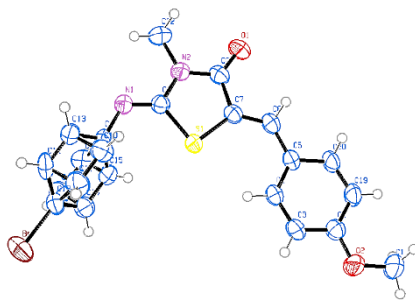


**Figure 6.2:** ORTEP views of compounds **15a** (top) and **31** (bottom) showing the atom-numbering scheme. Displacement ellipsoids are drawn at the 50% probability level and H atoms are shown as small spheres of arbitrary radii. Blue, red, yellow, purple and brown spheres refer to carbon, oxygen, sulfur, nitrogen and bromide atoms, respectively.

### 6.2.3 Anti-proliferative properties

An MTT growth assay<sup>22</sup> was utilized for evaluation of the antitumor activities of the synthetic 2-imino-5-alkylidene-thiazolidines/thiazolidinones (Table 6.1 and 6.2) against HCT-116 (colon), and MCF7 (breast) carcinoma cell lines using 5-fluorouracil as a positive control (approved drug against colon, breast and skin cancers).<sup>23</sup> It is observed from the data shown in Table 3 that several of the synthetic thiazolidine derivatives exhibit higher potency against colon cancer relative to the standard reference. Eleven analogs (**11a-13a**, **15a-17a**, **19b**, **29**, **31**, **32**, and **34**) out of the synthesized compounds are potentially promising antitumor hits, especially against colon cancer. All 11 of these compounds have higher antitumor activity than 5-fluorouracil with variable potency ( $IC_{50}$  values). It is noteworthy that most of these compounds belong to the thiazolidine library, while only four thiazolidinone-containing compounds display higher activity than standard reference. Compounds **16a**, **17a**, **12a**, **13a**, and **32** exhibit the highest anti-proliferative activity among this library against HCT116 relative to 5-fluorouracil ( $IC_{50}$  = 8.9, 9.8, 10.0, 10.2, and 10.4  $\mu$ M respectively in comparison to the corresponding 20.4  $\mu$ M observed for 5-fluorouracil). Compounds **11a**, **29**, **34**, **15a**, **19b**, and **31** display higher activities with mild potencies than that of 5-fluorouracil ( $IC_{50}$  = 11.1, 13.3, 14.1, 15.9, 16.1, 17.0  $\mu$ M, respectively, and 20.4  $\mu$ M corresponding to 5-fluorouracil).

**Table 6.2:** Synthesis of (Z)-2-substituted imino-5-((Z)-ylidene)-thiazolidin-4-ones **28-38**<sup>a</sup> via air oxidation.

Entry	Cpd.	R <sup>1</sup>	R <sup>2</sup>	R <sup>3</sup>	Yield (%) <sup>b</sup>
1	28	4-MeOC <sub>6</sub> H <sub>4</sub>	Me	4-CH <sub>3</sub> C <sub>6</sub> H <sub>4</sub>	23
2	29	4-MeOC <sub>6</sub> H <sub>4</sub>	Me	4-FC <sub>6</sub> H <sub>4</sub>	26
3	30	4-MeOC <sub>6</sub> H <sub>4</sub>	Me	4-MeOC <sub>6</sub> H <sub>4</sub>	22
4	31	4-MeOC <sub>6</sub> H <sub>4</sub>	Me	4-BrC <sub>6</sub> H <sub>4</sub>	17
5	32	4-MeOC <sub>6</sub> H <sub>4</sub>	Me	4-ClC <sub>6</sub> H <sub>4</sub>	16
6	33	4-MeOC <sub>6</sub> H <sub>4</sub>	Me	4- <sup>t</sup> BuC <sub>6</sub> H <sub>4</sub>	18
7	34	4-MeOC <sub>6</sub> H <sub>4</sub>	Me	3-Cl-4-MeC <sub>6</sub> H <sub>3</sub>	22
8	35	4-MeOC <sub>6</sub> H <sub>4</sub>	Me	2,6-Me <sub>2</sub> C <sub>6</sub> H <sub>3</sub>	20
9	36	4-MeOC <sub>6</sub> H <sub>4</sub>	Me	3,5-(CF <sub>3</sub> ) <sub>2</sub> C <sub>6</sub> H <sub>3</sub>	17
10	37	4-MeOC <sub>6</sub> H <sub>4</sub>	Me	C <sub>6</sub> H <sub>5</sub>	17
11	38	4-MeOC <sub>6</sub> H <sub>4</sub>	Me	Allyl	14

<sup>a</sup> Reaction was done with 100 mg of corresponding thiazolidine in CDCl<sub>3</sub> (1 mL) open to the atmosphere for 1-3 days.

<sup>b</sup> Isolated yields after purification by column chromatography (40-50% of the starting thiazolidine was also recovered).

In comparison, the antitumor activities of the synthesized compounds against MCF7 cell line (breast cancer) did not exhibit improved cytotoxicities over the standard reference used; however, they were still in low micromolar range. For example, the IC<sub>50</sub> values of **11a-13a** and **15a-17a** are 7.4-9.8 μM, whereas the 5-fluorouracil reference value is 3.15 μM. An analysis of the structure activity relationship (SAR) shows the substituent attached to the exocyclic 2-imino group of thiazolidines and thiazolidin-4-ones (mostly aryl groups) seems to be a controlling factor governing the antitumor properties. Antitumor activities of the synthetic thiazolidine derivatives against HCT116 are enhanced by the presence of an electron-deficient aryl system attached to the exocyclic amine rather than an electron-rich aryl group. Therefore,

it was observed that the activity of compound **19b** possessing a (3,5-bis(trifluoromethyl)phenyl) moiety exhibits twice the activity of compound **7** (4-trifluoromethylphenyl) against HCT116 ( $IC_{50} = 16.1, 34.3 \mu\text{M}$  for **19b** and **14a**, respectively). Of particular note is that thiazolidines containing phenyl rings substituted with halogens display the highest potency among all the synthesized compounds, exhibiting 8.9, 9.8, and 10.0  $\mu\text{M}$  for **16a**, **17a**, and **12a**, respectively. Although, when experimental error is considered, these values for **12a**, **16a** and **17a** are almost identical.

A comparable SAR analysis for the synthetic thiazolidinones against HCT116 reveals similar observations. Derivatives in which the exocyclic amine contains an electron deficient aryl moiety are much more active than those with electron rich systems. The effect of electron withdrawing groups is exemplified in compounds **32** (4-chloro) and **29** (4-fluoro) which exhibit higher activities than 5-fluorouracil ( $IC_{50} = 10.4$  and  $13.3 \mu\text{M}$ , respectively), while the impact of electron donating is shown in compounds **28** (*p*-tolyl) and **33** (4-(*t*-butyl)phenyl), significantly reducing the activity to  $>100 \mu\text{M}$  for both analogs. Additionally, an N-allyl amine group attached at C2 and methylene at C5 of thiazolidines and thiazolidinones attenuates the activity significantly such as observed for **38** and (**20c**, **21c**, and **20d**) ( $IC_{50} = 79.3$  and  $>100 \mu\text{M}$ , respectively).

Broadly similar SAR correlations for these derivatives in their antitumor activities against MCF7 cell line can be observed. The thiazolidines derivatives are more active than the corresponding thiazolidinone analogues but both groups exhibit attenuated activity in comparison to the positive control ( $IC_{50} = 3.15 \mu\text{M}$  for 5-fluorouracil). Also, a similar overall impact of electronegative substituents was noted along with within group trends. Bromine substitution on the iminophenyl ring results in the highest activity among the electronegative groups ( $IC_{50} = 7.4, 8.0$  and  $28.7 \mu\text{M}$  for **16a**, **12a**, and **18a** respectively).

All of the synthesized thiazolidines/thiazolidinones were tested against a normal (non-cancer) cell line (RPE1, retinal pigment epithelial). The observed data can explain and support the safety profile against normal cells. From the results observed, it has been noticed that most of the effective antitumor agents synthesized reveal safe cytotoxicity profile against normal cell line tested (high IC<sub>50</sub> values relative to that of the cancer cell lines tested).

#### 6.2.4 2D-QSAR study

Application of 2D-QSAR (quantitative structure-activity relationship) permits the expression of biological properties in mathematical equations in terms of descriptor values (physico-chemical parameters). This analysis provides some insight into the parameters controlling activity and simultaneously validating the observed data.<sup>24</sup> Thiazolidines/thiazolidinones (14 compounds) revealing variable anti-proliferative properties against HCT116 (colon) carcinoma cell line (**11a-18a**, **19b**, **29**, **31**, **32**, **34**, and **38**) were subjected to 2D-QSAR modeling by CODESSA-Pro software obeying the standard technique [42]. A robust two-descriptor QSAR model was obtained [ $R^2$  (correlation coefficient) = 0.941].

HA dependent HDCA-1/TMSA (MOPAC PC) (all) is a molecular type descriptor with  $t$  (criterion value) = 5.204. The high coefficient value (2556.82) of the descriptor is an indication for the potency of the tested compound(s) with high value and vice versa as exhibited in compounds **17a** and **37** that reveals IC<sub>50</sub>(estimated) values = 7.1, 76.6 due to descriptor values = 0.01923, 0.02354, respectively (Supplementary Tables S2,S3). Fractional hydrogen bonding donor ability of the molecule (FDCA-1) can be calculated from equations 1 and 2.<sup>25</sup>

$$\text{FHDCa-1} = (\text{HDCA-1})/\text{TMSA} \dots\dots\dots \text{Equation (1)}$$

Where, HDCA-1 stands for hydrogen bonding donor ability of atoms selected by threshold charge. TMSA is the total molecular surface area.

$$\text{HDCA-1} = \sum_D S_D \quad D \in H \text{ (H-donor)} \dots\dots\dots \text{Equation (2)}$$

Where, S<sub>D</sub> is the solvent accessible surface area of H-bonding donor H atoms selected by threshold charge



**Table 6.3:** Anti-proliferative properties of the synthesized thiazoline-containing compounds and 5-fluorouracil (standard reference).

Entry	Cpd	R1	R2	R3	IC <sub>50</sub> <sup>a</sup> (μM)		
					HCT116	MCF7	RPE1
1	11a	4-CH <sub>3</sub> OC <sub>6</sub> H <sub>4</sub>	Me	4-CH <sub>3</sub> C <sub>6</sub> H <sub>4</sub>	11.1	7.6	65.7
2	12a	4-CH <sub>3</sub> OC <sub>6</sub> H <sub>4</sub>	Me	4-FC <sub>6</sub> H <sub>4</sub>	10.0	8.0	42.8
3	13a	4-CH <sub>3</sub> OC <sub>6</sub> H <sub>4</sub>	Me	4-NO <sub>2</sub> C <sub>6</sub> H <sub>4</sub>	10.2	9.8	>100.0
4	14a	4-CH <sub>3</sub> OC <sub>6</sub> H <sub>4</sub>	Me	4-CF <sub>3</sub> C <sub>6</sub> H <sub>4</sub>	34.3	24.1	72.0
5	15a	4-CH <sub>3</sub> OC <sub>6</sub> H <sub>4</sub>	Me	4-CH <sub>3</sub> OC <sub>6</sub> H <sub>4</sub>	15.9	8.7	65.9
6	16a	4-CH <sub>3</sub> OC <sub>6</sub> H <sub>4</sub>	Me	4-BrC <sub>6</sub> H <sub>4</sub>	8.9	7.4	61.3
7	17a	4-CH <sub>3</sub> OC <sub>6</sub> H <sub>4</sub>	Me	4-ClC <sub>6</sub> H <sub>4</sub>	9.8	7.6	39.6
8	18a	4-CH <sub>3</sub> OC <sub>6</sub> H <sub>4</sub>	Me	4-Bu <sup>t</sup> C <sub>6</sub> H <sub>4</sub>	25.9	28.7	23.5
9	19b	C <sub>6</sub> H <sub>5</sub>	H	3, 5-(CF <sub>3</sub> ) <sub>2</sub> C <sub>6</sub> H <sub>3</sub>	16.1	13.5	32.8
10	20c	H	H	C <sub>6</sub> H <sub>5</sub>	>100.0	>100.0	>100.0
11	21c	H	H	Allyl	>100.0	>100.0	>100.0
12	20d	H	Me	C <sub>6</sub> H <sub>5</sub>	>100.0	>100.0	>100.0
13	22	C <sub>6</sub> H <sub>5</sub>	Ph-NH-C=S	C <sub>6</sub> H <sub>5</sub>	>100.0	>100.0	>100.0
14	28	4-CH <sub>3</sub> OC <sub>6</sub> H <sub>4</sub>	Me	4-CH <sub>3</sub> C <sub>6</sub> H <sub>4</sub>	>100.0	>100.0	>100.0
15	29	4-CH <sub>3</sub> OC <sub>6</sub> H <sub>4</sub>	Me	4-FC <sub>6</sub> H <sub>4</sub>	13.3	66.5	>100.0
16	30	4-CH <sub>3</sub> OC <sub>6</sub> H <sub>4</sub>	Me	4-CH <sub>3</sub> OC <sub>6</sub> H <sub>4</sub>	>100.0	>100.0	>100.0
17	31	4-CH <sub>3</sub> OC <sub>6</sub> H <sub>4</sub>	Me	4-BrC <sub>6</sub> H <sub>4</sub>	17.0	>100.0	>100.0
18	32	4-CH <sub>3</sub> OC <sub>6</sub> H <sub>4</sub>	Me	4-ClC <sub>6</sub> H <sub>4</sub>	10.4	39.3	>100.0
19	33	4-CH <sub>3</sub> OC <sub>6</sub> H <sub>4</sub>	Me	4-Bu <sup>t</sup> C <sub>6</sub> H <sub>4</sub>	>100.0	>100.0	46.7
20	34	4-CH <sub>3</sub> OC <sub>6</sub> H <sub>4</sub>	Me	3-Cl,4-CH <sub>3</sub> C <sub>6</sub> H <sub>3</sub>	14.1	>100.0	23.0
21	35	4-CH <sub>3</sub> OC <sub>6</sub> H <sub>4</sub>	Me	2,6-(CH <sub>3</sub> ) <sub>2</sub> C <sub>6</sub> H <sub>3</sub>	>100.0	>100.0	>100.0
22	36	4-CH <sub>3</sub> OC <sub>6</sub> H <sub>4</sub>	Me	3,5-(CF <sub>3</sub> ) <sub>2</sub> C <sub>6</sub> H <sub>3</sub>	>100.0	77.8	>100.0
23	37	4-CH <sub>3</sub> OC <sub>6</sub> H <sub>4</sub>	Me	C <sub>6</sub> H <sub>5</sub>	>100.0	>100.0	>100.0
24	38	4-CH <sub>3</sub> OC <sub>6</sub> H <sub>4</sub>	Me	Allyl	79.3	>100.0	>100.0
25	5-Fluorouracil	-	-	-	20.4	3.2	-

<sup>a</sup> IC<sub>50</sub> is the concentration required to produce 50% inhibition of cell growth compared to the control. The test was performed by the Egyptian colleagues.

The relative number of aromatic bonds is a constitutional descriptor indicating the global aromatic properties of the compound. This descriptor substantially enhances the activity of these analogs according to the QSAR model (coefficient = -473.528) contributing a high descriptor value (as a result of the high aromaticity of the molecule) and the ensuing high

antitumor potency as exhibited for example in compounds **17a** and **38** that reveals descriptor values = 0.28571, 0.16216, respectively. This is due to the presence of *p*-chlorophenylimino and allylimino residue in compounds **17a** and **38**, respectively. The appearance of this descriptor as a controlling physico-chemical factor governing the attained QSAR model is consistent with the reported SAR observations described above. The goodness of the 2D-QSAR model is supported by the statistical parameters revealed including leave one-out and leave many-out correlations relative to the main correlation coefficient of the model ( $R^2 = 0.941$ ,  $R^2_{cvOO} = 0.890$ ,  $R^2_{cvMO} = 0.865$ ) in addition to the Fisher and standard deviation values ( $F = 87.712$ ,  $s^2 = 24.015$ ). Estimated properties are also correlated to the experimental values.

### 6.3 SUMMARY

In summary, anti-proliferative thiazolidine derivatives are readily synthesized in good to excellent yields (67–99%) through a one-pot thio-acylation/anti-hydrosulfenylation of propargylamines and isothiocyanates on silica gel. The reaction is tolerant of the amine and the isothiocyanate thus offering a facile method for the construction of diversely substituted examples of this important heterocycle. In addition, these 4-methoxybenzylidene-substituted analogs undergo slow auto-oxidation at room temperature yielding the corresponding 4-thiazolidinones **28-38**. An X-ray study confirmed both the constitution and the *Z*, *Z'*-configurations for the synthesized compounds, considering compound **15a** and **31** as examples. Some of the synthetic derivatives reveal promising antitumor properties through in vitro growth inhibition against HCT-116 (colon) and MCF7 (breast) cancer cell lines exhibiting higher potency higher than 5-fluorouracil (positive control) in an MTT assay but were non-toxic in a normal cell line. The thiazolidines exhibited higher activity than the corresponding thiazolidinone analogues against colon cancer. Statistically significant 2D-QSAR using a two-descriptor model describes the antitumor properties against HCT-116. 2D-QSAR results show that the estimated properties are also correlated to the experimental values. We are continuing to explore this framework both in synthetic and medicinal chemistry contexts and will publish these data elsewhere.

## 6.4 REFERENCES

1. Bray, F.; Ferlay, J.; Soerjomataram, I.; Siegel, R. L.; Torre, L. A.; Jemal, A., Global cancer statistics 2018: GLOBOCAN estimates of incidence and mortality worldwide for 36 cancers in 185 countries. *CA Cancer J. Clin.* **2018**, *68*, 394-424.
2. Siegel, R. L.; Miller, K. D.; Jemal, A., Cancer statistics, 2018. *CA Cancer J. Clin.* **2018**, *68*, 7-30.
3. Wolf, A. M. D.; Fontham, E. T. H.; Church, T. R.; Flowers, C. R.; Guerra, C. E.; LaMonte, S. J.; Etzioni, R.; McKenna, M. T.; Oeffinger, K. C.; Shih, Y. T.; Walter, L. C.; Andrews, K. S.; Brawley, O. W.; Brooks, D.; Fedewa, S. A.; Manassaram-Baptiste, D.; Siegel, R. L.; Wender, R. C.; Smith, R. A., Colorectal cancer screening for average-risk adults: 2018 guideline update from the American Cancer Society. *CA Cancer J. Clin.* **2018**, *68*, 250-281.
4. (a) Siegel, R. L.; Miller, K. D.; Fedewa, S. A.; Ahnen, D. J.; Meester, R. G. S.; Barzi, A.; Jemal, A., Colorectal cancer statistics, 2017. *CA Cancer J. Clin.* **2017**, *67*, 177-193; (b) Yin, D.; Morris, C. R.; Bates, J. H.; German, R. R., Effect of misclassified underlying cause of death on survival estimates of colon and rectal cancer. *J. Natl. Cancer Inst.* **2011**, *103*, 1130-3.
5. (a) Aarons, C. B.; Shanmugan, S.; Bleier, J. I., Management of malignant colon polyps: current status and controversies. *World J Gastroenterol* **2014**, *20*, 16178-83; (b) Bos, J. L.; Fearon, E. R.; Hamilton, S. R.; Verlaan-de Vries, M.; van Boom, J. H.; van der Eb, A. J.; Vogelstein, B., Prevalence of ras gene mutations in human colorectal cancers. *Nature* **1987**, *327*, 293-7; (c) Forrester, K.; Almoguera, C.; Han, K.; Grizzle, W. E.; Perucho, M., Detection of high incidence of K-ras oncogenes during human colon tumorigenesis. *Nature* **1987**, *327*, 298-303; (d) Vogelstein, B.; Fearon, E. R.; Hamilton, S. R.; Kern, S. E.; Preisinger, A. C.; Leppert, M.; Nakamura, Y.; White, R.; Smits, A. M.; Bos, J. L., Genetic alterations during colorectal-tumor development. *New Eng. J. Med.* **1988**, *319*, 525-32.
6. (a) Misra, S.; Ghatak, S.; Patil, N.; Dandawate, P.; Ambike, V.; Adsule, S.; Unni, D.; Venkateswara Swamy, K.; Padhye, S., Novel dual cyclooxygenase and lipoxygenase inhibitors targeting hyaluronan-CD44v6 pathway and inducing cytotoxicity in colon cancer cells. *Bioorg. Med. Chem.* **2013**, *21*, 2551-9; (b) Nunes, R. C.; Ribeiro, C. J. A.; Monteiro, A.; Rodrigues, C. M. P.; Amaral, J. D.; Santos, M. M. M., In vitro targeting of colon cancer cells using spiropyrazoline oxindoles. *Eur J Med Chem* **2017**, *139*, 168-179.
7. Seium, Y.; Stupp, R.; Ruhstaller, T.; Gervaz, P.; Mentha, G.; Philippe, M.; Allal, A.; Trembleau, C.; Bauer, J.; Morant, R.; Roth, A. D., Oxaliplatin combined with irinotecan and 5-fluorouracil/leucovorin (OCFL) in metastatic colorectal cancer: a phase I-II study. *Ann. Oncol.* **2005**, *16*, 762-6.
8. Calvo, E.; Cortes, J.; Gonzalez-Cao, M.; Rodriguez, J.; Aramendia, J. M.; Fernandez-Hidalgo, O.; Martin-Algarra, S.; Salgado, J. E.; Martinez-Monge, R.; de Irala, J.; Brugarolas, A., Combined irinotecan, oxaliplatin and 5-fluorouracil in patients with advanced colorectal cancer. a feasibility pilot study. *Oncology* **2002**, *63*, 254-65.
9. (a) Blazquez, A. G.; Fernandez-Dolon, M.; Sanchez-Vicente, L.; Maestre, A. D.; Gomez-San Miguel, A. B.; Alvarez, M.; Serrano, M. A.; Jansen, H.; Efferth, T.; Marin, J. J.; Romero, M. R., Novel artemisinin derivatives with potential usefulness against liver/colon cancer and viral hepatitis. *Bioorg. Med. Chem.* **2013**, *21*, 4432-41; (b) Zhou, X.; Jiang, Z.; Xue, L.; Lu, P.; Wang, Y., Preparation of 1,2,5-Trisubstituted 1H-Imidazoles from Ketanimines and Propargylic Amines by Silver-Catalyzed or Iodine-Promoted Electrophilic Cyclization Reaction of Alkynes. *Eur. J. Org. Chem.* **2015**, *2015*, 5789-5797.

- 10.(a) Jain, A. K.; Vaidya, A.; Ravichandran, V.; Kashaw, S. K.; Agrawal, R. K., Recent developments and biological activities of thiazolidinone derivatives: a review. *Bioorg. Med. Chem.* **2012**, *20*, 3378-95; (b) Kaminsky, D.; Kryshchshyn, A.; Lesyk, R., 5-Ene-4-thiazolidinones - An efficient tool in medicinal chemistry. *Eur. J. Med. Chem.* **2017**, *140*, 542-594.
- 11.(a) Omar, K.; Geronikaki, A.; Zoumpoulakis, P.; Camoutsis, C.; Sokovic, M.; Ciric, A.; Glamoclija, J., Novel 4-thiazolidinone derivatives as potential antifungal and antibacterial drugs. *Bioorg. Med. Chem.* **2010**, *18*, 426-32; (b) Vicini, P.; Geronikaki, A.; Anastasia, K.; Incerti, M.; Zani, F., Synthesis and antimicrobial activity of novel 2-thiazolylimino-5-arylidene-4-thiazolidinones. *Bioorg. Med. Chem.* **2006**, *14*, 3859-64.
12. Bhandari, S. V.; Bothara, K. G.; Patil, A. A.; Chitre, T. S.; Sarkate, A. P.; Gore, S. T.; Dangre, S. C.; Khachane, C. V., Design, synthesis and pharmacological screening of novel antihypertensive agents using hybrid approach. *Bioorg. Med. Chem.* **2009**, *17*, 390-400.
13. Ottana, R.; Maccari, R.; Ciurleo, R.; Paoli, P.; Jacomelli, M.; Manao, G.; Camici, G.; Laggner, C.; Langer, T., 5-Arylidene-2-phenylimino-4-thiazolidinones as PTP1B and LMW-PTP inhibitors. *Bioorg. Med. Chem.* **2009**, *17*, 1928-37.
14. Shiradkar, M. R.; Ghodake, M.; Bothara, K. G.; Bhandari, S. V.; Nikalje, A.; Akula, K. C.; Desai, N. C.; Burange, P. J., Synthesis and anticonvulsant activity of clubbed thiazolidinone-barbituric acid and thiazolidinone-triazole derivatives. *ARKIVOC* **2007**, *XIV* 58-74.
- 15.(a) Lu, W.; Che, P.; Zhang, Y.; Li, H.; Zou, S.; Zhu, J.; Deng, J.; Shen, X.; Jiang, H.; Li, J.; Huang, J., HL005--a new selective PPARgamma antagonist specifically inhibits the proliferation of MCF-7. *J. Steroid Biochem. Mol. Biol.* **2011**, *124*, 112-20; (b) Ottana, R.; Carotti, S.; Maccari, R.; Landini, I.; Chiricosta, G.; Caciagli, B.; Vigorita, M. G.; Mini, E., In vitro antiproliferative activity against human colon cancer cell lines of representative 4-thiazolidinones. Part I. *Bioorg. Med. Chem. Lett.* **2005**, *15*, 3930-3; (c) Revelant, G.; Huber-Villaume, S.; Dunand, S.; Kirsch, G.; Schohn, H.; Hesse, S., Synthesis and biological evaluation of novel 2-heteroarylimino-1,3-thiazolidin-4-ones as potential anti-tumor agents. *Eur. J. Med. Chem.* **2015**, *94*, 102-12; (d) Teraishi, F.; Wu, S.; Sasaki, J.; Zhang, L.; Davis, J. J.; Guo, W.; Dong, F.; Fang, B., JNK1-dependent antimitotic activity of thiazolidin compounds in human non-small-cell lung and colon cancer cells. *Cell Mol. Life Sci.* **2005**, *62*, 2382-9; (e) Teraishi, F.; Wu, S.; Sasaki, J.; Zhang, L.; Zhu, H. B.; Davis, J. J.; Fang, B., P-glycoprotein-independent apoptosis induction by a novel synthetic compound, MMPT [5-[(4-methylphenyl)methylene]-2-(phenylamino)-4(5H)-thiazolone]. *J. Pharmacol. Exp. Ther.* **2005**, *314*, 355-62.
- 16.(a) Easton, N. R.; Cassady, D. R.; Dillard, R. D., Reactions of Acetylenic Amines. VIII. Cyclization of Acetylenic Ureas. *J. Org. Chem.* **1964**, *29*, 1851-1855; (b) Huang, S.; Shao, Y.; Liu, R.; Zhou, X., Facile access to oxazolidin-2-imine, thiazolidin-2-imine and imidazolidin-2-imine derivatives bearing an exocyclic haloalkylene via direct halocyclization between propargylamines, heterocumulenes and I<sub>2</sub> (NBS). *tetrahedron* **2015**, *71*, 4219-4226.
17. Ranjan, A.; Deore, A. S.; Yerande, S. G.; Dethle, D. H., Thiol-Yne Coupling of Propargylamine under Solvent-Free Conditions by Bond Anion Relay Chemistry: An Efficient Synthesis of Thiazolidin-2-ylideneamine. *Eur. J. Org. Chem.* **2017**, *2017*, 4130-4139.
18. Singh, R. P.; Gout, D.; Lovely, C. J., Tandem thioacylation-intramolecular hydrosulfenylation of propargyl amines – rapid access to 2-aminothiazolidines. *Eur. J. Org. Chem.* **2019**, 1726–1740.
19. Gainer, M. J.; Bennett, N. R.; Takahashi, Y.; Looper, R. E., Regioselective rhodium(II)-catalyzed hydroaminations of propargylguanidines. *Angew. Chem. Int. Ed.* **2011**, *50*, 684-687.

- 20.(a) Brown, F. C., 4-Thiazolidinones. *Chemical Reviews* **1961**, *61*, 463-521; (b) Singh, S. P.; Parmar, S. S.; Raman, K.; Stenberg, V. I., Chemistry and biological activity of thiazolidinones. *Chem. Rev.* **1981**, *81*, 175-203.
- 21.(a) Klika, Karel D.; Janovec, L.; Imrich, J.; Suchár, G.; Kristian, P.; Sillanpää, R.; Pihlaja, K., Regioselective Synthesis of 2-Imino-1,3-thiazolidin-4-ones by Treatment of N-(Anthracen-9-yl)-N'-ethylthiourea with Bromoacetic Acid Derivatives. *Eur. J. Org. Chem.* **2002**, *2002*, 1248-1255; (b) Mushtaque, M.; Avecilla, F.; Azam, A., Synthesis, characterization and structure optimization of a series of thiazolidinone derivatives as *Entamoeba histolytica* inhibitors. *Eur. J. Med. Chem.* **2012**, *55*, 439-48.
22. Ismail, N. S. M.; George, R. F.; Serya, R. A. T.; Baseliouis, F. N.; El-Manawaty, M.; Shalaby, E. S. M.; Girgis, A. S., Rational design, synthesis and 2D-QSAR studies of antiproliferative tropane-based compounds. *RSC Adv.* **2016**, *6*, 101911-101923.
- 24.(a) Katritzky, A. R.; Kuanar, M.; Slavov, S.; Hall, C. D.; Karelson, M.; Kahn, I.; Dobchev, D. A., Quantitative correlation of physical and chemical properties with chemical structure: utility for prediction. *Chem. Rev.* **2010**, *110*, 5714-89; (b) Srour, A. M.; Panda, S. S.; Salman, A. M. M.; El-Manawaty, M. A.; George, R. F.; Shalaby, E. M.; Fitch, A. N.; Fawzy, N. G.; Girgis, A. S., Synthesis & molecular modeling studies of bronchodilatory active indole-pyridine conjugates. *Future Med. Chem.* **2018**, *10*, 1787-1804.
25. Katritzky, A.R.; Petrukhin, R.; Petrukhina, I.; Lomaka, A.; Tatham, D.B.; Karelson, M., CODESSA-Pro software manual. **2005**, 63-66.
26. SADABS Version 2014/5, Bruker AXS Inc., Madison, WI, USA (2014).
27. SHELXTLPlus (6.14), Bruker AXS, Inc. Madison, WI, USA (2003).
28. JANA 2006, V. Petricek, M. Dusek, L. Palatinus, Z. Kristallogr. **2006**, *229* (2014) 345-352.

**CHAPTER SEVEN: ONE-POT SYNTHESIS OF NOVEL 2-IMINO-5-ARYLIDINE-  
THIAZOLIDINE ANALOGUES AND EVALUATION OF THEIR ANTI-  
PROLIFERATIVE ACTIVITY AGAINST MCF7 BREAST CANCER CELL LINE**

Marian N. Aziz<sup>1,2</sup>, Arzoo Patel<sup>1</sup>, Amany Iskander<sup>1</sup>, Avisankar Chini<sup>1</sup>, Delphine Gout<sup>1</sup>,  
Subhrangsu S. Mandal<sup>1</sup>, Carl J. Lovely<sup>1,\*</sup>

<sup>1</sup>Department of Chemistry and Biochemistry, University of Texas-Arlington, Arlington, TX  
76019-0065, USA.

<sup>2</sup>Department of Pesticide Chemistry, National Research Centre, Dokki, Giza 12622, Egypt.

Corresponding author

Prof. Carl J. Lovely

Professor, Chemistry and Biochemistry Department

University of Texas at Arlington

Address: 700 Planetarium Place, Box 19065, UT Arlington, TX 76019-0065

Email: lovely@uta.edu

Phone: +1 817 272 5446

(Published)

**ABSTRACT:**

An efficient surface-mediated synthetic method to facilitate access to a novel class of thiazolidines is described. The rationale behind the design of the targeted thiazolidines was to prepare stable thiazolidine analogues and evaluate their anti-proliferative activity against a breast cancer cell line (MCF7). Most of the synthesized analogues exhibit increased potency ranging from 2-15 fold higher compared to the standard reference, cisplatin. The most active thiazolidines contain a halogenated or electron withdrawing group attached to the *N*-phenyl ring of exocyclic 2-imino group. However, combination of the two substituents did not enhance the activity. The anti-proliferative activity was measured in terms of IC<sub>50</sub> values using an MTT assay.

**7.1 INTRODUCTION:**

Thiazolidines, five membered nitrogen and sulfur containing ring compounds, are among the most eminent heterocyclic classes due to their broad applications. Intriguing chemical applications of thiazolidine derivatives include site-specific peptide and protein modification and chemical protein synthesis.<sup>1-3</sup> Also, thiazolidines have been reported as potent agents against a number of ailments and these include diabetes, epilepsy, viral and bacterial diseases, and cancer, to name a few.<sup>4</sup> Cancer is considered the second death causing disease with a high mortality rate, exceeding more than 10 million annually worldwide.<sup>5</sup> Breast cancer is among the most feared of women's diseases due to the fact there are multiple genotypes and phenotypes and it is a metastatic and heterogenous solid tumor.<sup>6</sup> Therefore, there are number of published studies focused on developing novel lead/hit compounds containing thiazolidines targeting cancers.<sup>7-13</sup> Figure 7.1 shows three different compounds described in recently published studies, in which novel thiazolidine analogues are reported as anti-proliferative agents targeting breast cancer.<sup>14-16</sup> Interestingly, most of these derivatives contain on 4-methoxy benzylidene derivatives and show good selectivity towards breast cancer cell lines. Also, figure 7.2 depicts four examples of marketed drugs containing a



thiazolidine core structure, etozoline, troglitazone, rosiglitazone, and ralitoline. Etozoline is used as an antihypertensive and diuretic drug,<sup>17,18</sup> while troglitazone and rosiglitazone are used as remedies for type 2 diabetes mellitus *via* enhancing PPAR $\gamma$  activity.<sup>19–22</sup> In addition, (*E*)-*N*-(2-chloro-6-methylphenyl)-2-(3-methyl-4-oxothiazolidin-2-ylidene)acetamide (ralitoline) is used as an anticonvulsant-thiazolidinone drug.<sup>23,24</sup> Therefore thiazolidines exhibit a broad array of medicinal applications which have inspired researchers to develop novel methodologies for their synthesis. Acid- and base-catalyzed thiazolidine syntheses have been reported as approaches to these heterocycles, however, most of these synthetic methods require elevated temperatures and long reaction times and are characterized by low yields and moderate substrate scope.<sup>25–29</sup> Also, ionic-liquid assisted synthesis of thiazolidine is considered to be an efficient method but in some cases required introduction of additional catalysts, otherwise yields can be an issue.<sup>30</sup> Recently, nanoparticles have been used as catalysts because of their high surface-to-volume ratio which enhance the reactivity and selectivity of the reaction, especially nano-heterogenous catalysts. All reported nanoparticles used in thiazolidine synthesis are reusable but challenges remain with the scope limited to aryl derivatives<sup>31–33</sup> and long reaction times.<sup>32,34</sup> In addition to these promising methodologies, multi-step reactions, metal catalysis, ultrasonic irradiation, microwave conditions, catalyst free and solvent free approaches have been described for the synthesis various derivatives of thiazolidines.<sup>4</sup>

A previously reported on-surface synthesis has been developed for thiazolidinones but it required long reaction times and dichloromethane as solvent.<sup>35</sup> While in our earlier work, silica gel was investigated and shown to promote fast cyclization of thioureas formed in situ from propargyl amines and isothiocyanates. Therefore, we have focused on developing this interesting one-pot chemistry further to easily access bio-active thiazolidine based structures.<sup>36</sup> In 2019, our group

published the synthesis of a novel group of thiazolidines using this procedure, some of which were prone to oxidation at C4 upon exposure to the ambient atmosphere producing thiazolidinones (Scheme 1).<sup>37</sup> Interestingly, most of the reported compounds showed good anti-tumor activity against colon and breast cancers (*in-vitro* study using HCT116 and MCF7 cell lines) which inspired us to design new analogs belonging to thiazolidines system only. Therefore, in this present study, an efficient, fast, and convenient on-surface methodology is explored towards synthesis of 5-substituted thiazolidines in a one-pot reaction from propargyl amines and isothiocyanates. Since our previously prepared thiazolidines were more active against breast cancer in general, the anti-proliferative activity of the current new analogues against a breast cancer cell line (MCF7) is also described.

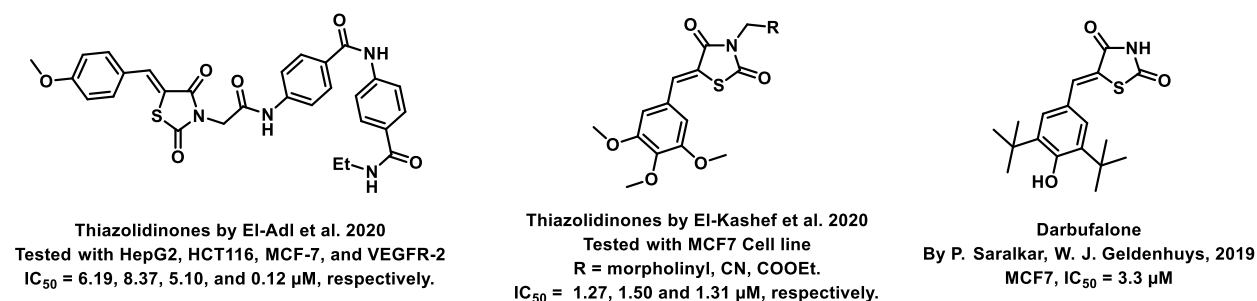


**Figure 7.1:** Recently published thiazolidinones targeting breast cancer.

## 7.2 RESULTS AND DISCUSSION:

### 7.2.1 Chemistry:

Initially, it was thought that blocking the oxidation hot spot in the thiazolidine structure, specifically the C4 methylene group, would mitigate the oxidation process. Therefore, we have designed these new derivatives by incorporating a methyl group at the C4 position and evaluated the stability and antiproliferative activity of these derivatives. Thiazolidines **5a-1** were synthesized

via reaction of propargyl amine **1** and various aryl isothiocyanates on silica gel at room temperature overnight.

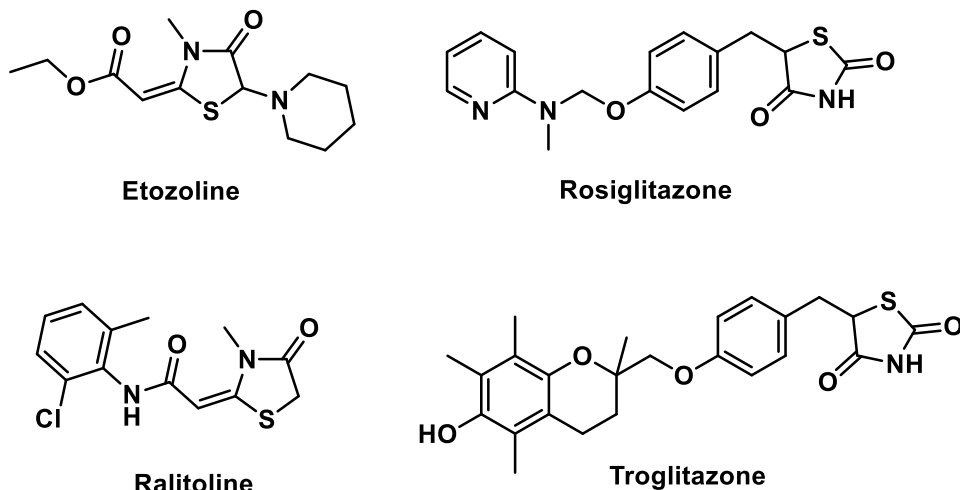
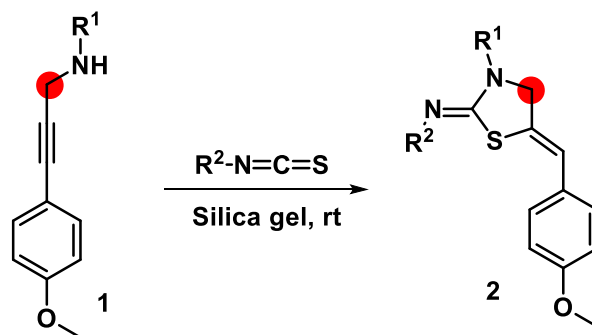


**Figure 7.2:** Approved drugs containing the thiazolidine core structure.



$R^1 = H, Me; R^2 = \text{aryl}$

13 examples

Anti-proliferative activity measured by  $IC_{50}$

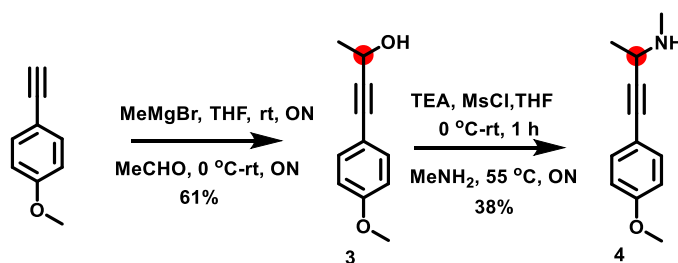
Breast Cancer (MCF7 7.4 - 28.7  $\mu\text{M}$ )

Colon cancer (HCT116 8.9 - 34.3  $\mu\text{M}$ )

**Scheme 7.1:** Previously synthesized and screened thiazolidines against breast and colon cancers.

Initially, several unsuccessful experiments were performed evaluating approaches for the synthesis of the targeted propargyl amine including a three component reaction (3CR) of 4-ethylanisole,

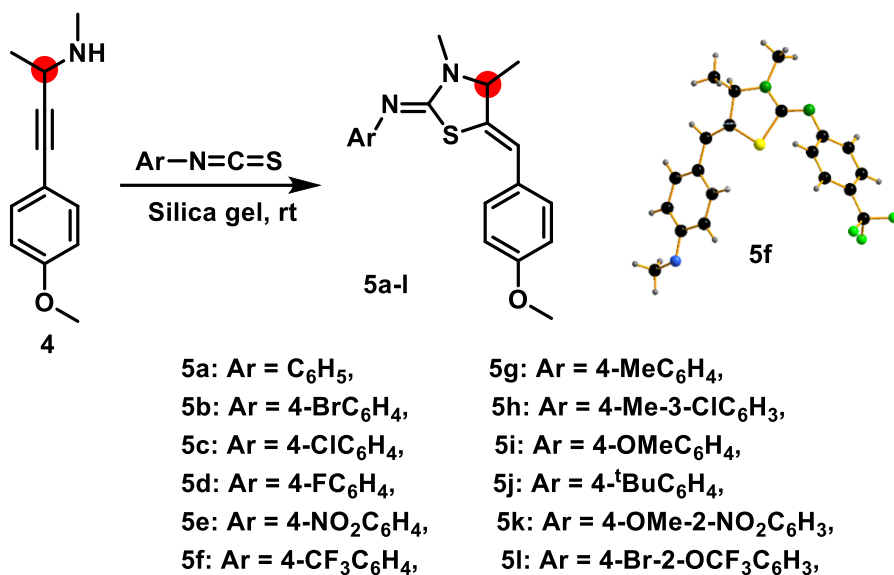
acetaldehyde, and methylamine catalyzed by CuI and/or CuBr.<sup>38-40</sup> Such conditions have worked well for us and others for the assembly of propargyl amines in other contexts. Also, palladium catalysts for C-N bond formation have been used in 3CR under different conditions but these were not successful either.<sup>41</sup> Therefore the approach was modified and propargyl alcohol **3** was synthesized first in good yield (61%) using a Grignard reaction from commercially available reagents (4-ethynylanisole, ethylmagnesium bromide and acetaldehyde). The propargyl amine **4** was prepared *via* an S<sub>N</sub>2 reaction by activating the alcohol first with methanesulfonyl chloride and then treating the corresponding sulfonate with methylamine in the presence of triethylamine as a base (Scheme 7.2).



**Scheme 7.2:** Synthesis of the targeted 4-(4-methoxyphenyl)-N-methylbut-3-yn-2-amine (ON = overnight).

An initial negative result was obtained by treating the synthesized propargyl amine with phenyl isothiocyanate in dichloromethane solution at room temperature for 12 h. While adding silica gel as a solid support makes a significant difference by bringing the two reagents together on its surface presumably through hydrogen bonding interactions with the hydroxyl groups on its surface. Therefore, silica gel helps in thiourea formation and mediates and/or catalyzes the cyclization process through these types of interactions. The fully substituted thiazolidines were synthesized through mixing 4-(4-methoxyphenyl)-N-methylbut-3-yn-2-amine (**4**) and different

aryl isothiocyanates (**5a-l**) in the presence of silica gel at room temperature with stirring overnight (Scheme 7.3). Solid starting materials were dissolved in a very small amount of dichloromethane and then added to the silica gel with stirring to evaporate the solvent. The reaction was monitored by TLC by taking tiny amount of silica gel reaction mixture and adding a few drops of dichloromethane. All of the isolated thiazolidines were purified by silica gel chromatography and the structures were confirmed by spectroscopic analysis (IR,  $^1\text{H}$  NMR,  $^{13}\text{C}$  NMR, HRMS).



**Scheme 7.3:** Synthesis of the fully substituted thiazolidines **5a-l**.

**Table 7.1:** The synthesized thiazolidines **5a-l** and their IC<sub>50</sub> against an MCF7 cell line.

	Compound	Ar	Yield (%)	IC <sub>50</sub> (μM±SMD)
<b>1</b>	5a	C <sub>6</sub> H <sub>5</sub>	60	0.50±0.21
<b>2</b>	5b	4-BrC <sub>6</sub> H <sub>4</sub>	61	0.62±0.24
<b>3</b>	5c	4-ClC <sub>6</sub> H <sub>4</sub>	61	0.27±0.14
<b>4</b>	5d	4-FC <sub>6</sub> H <sub>4</sub>	45	0.50±0.23
<b>5</b>	5e	4-NO <sub>2</sub> C <sub>6</sub> H <sub>4</sub>	95	1.15±0.18
<b>6</b>	5f	4-CF <sub>3</sub> C <sub>6</sub> H <sub>4</sub>	58	16.32±1.24
<b>7</b>	5g	4-MeC <sub>6</sub> H <sub>4</sub>	20	ND†
<b>8</b>	5h	4-Me-3-ClC <sub>6</sub> H <sub>3</sub>	46	1.82±0.17
<b>9</b>	5i	4-OMeC <sub>6</sub> H <sub>4</sub>	63	1.75±0.16
<b>10</b>	5j	4- <sup>t</sup> BuC <sub>6</sub> H <sub>4</sub>	95	12.61±3.71
<b>11</b>	5k	4-OMe-2-NO <sub>2</sub> C <sub>6</sub> H <sub>3</sub>	63	1.38±0.13
<b>12</b>	5l	4-Br-2-CF <sub>3</sub> C <sub>6</sub> H <sub>3</sub>	57	15.64±3.6
<b>13</b>	Cisplatin	-	-	4.14±1.14

†This compound was not stable and thus the cytotoxicity was not determined.

Analysis of compound **5f** via X-ray single crystal shows the constitution is as expected and that the geometry of the two exocyclic double bonds is exhibiting the same geometry of the previous reported thiazolidines, *Z*, *Z'*-configurations.<sup>37</sup> Colorless needle crystals of compound **5f** are crystallized in a monoclinic space group P2<sub>1</sub>/c with four molecules per unit cell. Further details about X-ray single crystal study of **5f** is shown in supplementary information file and experimental section. Also, the <sup>1</sup>H NMR spectrum shows long range coupling between the C4-methyl group (at the hot spot) and the vinylic proton also confirming the *Z*-configuration for the exocyclic double bond. The vinylic proton and carbon for compound **5f** appear at δ<sub>H</sub> = 6.49 ppm and δ<sub>C</sub> = 119.5 ppm, respectively.

The initial rationale behind developing this chemistry was to investigate the bioactivity of different derivatives of thiazolidine, especially against breast cancer, and ultimately discovering new hits/leads to serve as anti-tumor agents. Although, we have blocked the reactive methylene group using a methyl group, all the synthesized compounds were unstable decomposing after extended

periods at room temperature, and they were stored at -10 °C under an atmosphere of argon. TLC analysis showed formation of multiple components after leaving the molecules in deuterated chloroform or dichloromethane and exposure to the atmospheric air over the course of several days. Attempted purification of these mixtures by preparative TLC of the decomposed samples failed; however, while the isolated components appeared homogenous by TLC, we were unable to identify the decomposed product. While a <sup>1</sup>H NMR study of the reaction mixtures of these new derivatives after long term exposure to air was not helpful due to formation of unidentifiable peaks. The instability of our previously published thiazolidines was determined by isolation of the oxidized thiazolidinones. Our assumption is that hydroxylation occurs, and the resulting carbinolamine undergoes ring-opening and further oxidation. Therefore, samples for testing were synthesized immediately prior to their use in the MTT assays using breast cancer cell line (MCF7) to test their cytotoxicity with tumorous cell line. Compound **5g** has been excluded from biological screening due to its instability at - 10 °C. A year later, simple TLC experiments were done for all the derivatives stored in the freezer under argon, and they showed only one spot, referring to successful storage method for such unstable derivatives except **5g**. In addition, samples stored in DMSO at 4 °C exhibited good stability after a year especially compounds **5d** and **5e** which contain an electronic withdrawing group (F and NO<sub>2</sub>).

### ***7.2.2 Anti-proliferative activity:***

Evaluation of the biological activity of the targeted thiazolidines was the main motivation towards the synthesis and developing such interesting chemistry. Therefore, the synthesized compounds were tested with a breast cancer cell line (MCF7) using the MTT colorimetric assay using solutions of freshly prepared thiazolidines **5a-f** and **5h-l**. Cisplatin was used as a standard reference for the MTT obtained data. Figure 7.3A-C shows the cell viability using ten different concentrations of

thiazolidines and cisplatin, and all the compounds exhibited activity in a dose-dependent manner. Figure 7.3D shows the cytotoxicity of the thiazolidines represented as  $IC_{50}$  values which express the concentration required from each compound to inhibit the growth of the MCF7 cells by 50%. Figure 7.3A depicts the effect of compounds **5a-d**, all of them behave similarly and showing more potency compared to cisplatin activity. Figure 7.3B and 7.3C show that most of the compounds are more active compared to cisplatin except one compound in each graph, **5f** and **5j**, respectively. The bar graph (Figure 7.3D) indicates that most of synthesized compounds are more potent relative to the standard reference based on the calculated values of the corresponding  $IC_{50}$ . Regarding the structure activity relationship, generally, all the synthesized compounds have a common scaffold of the thiazolidine core and 4-methoxybenzylidene group, but different substituents attached to exocyclic aryl amine. It is of note that all the derivatives substituted with an electron withdrawing group exhibit higher potency ( $IC_{50}$  values) against MCF7 breast cancer cell lines compared to cisplatin. For instance, compounds **5a-e** exhibit the highest anti-proliferative activity among this library against MCF7 ( $IC_{50}$  = 0.50, 0.62, 0.27, 0.50, and 1.15  $\mu$ M for **5a-e** respectively, Table 7.1) in comparison to the corresponding 4.14  $\mu$ M observed for cisplatin. Compound **5a** with an unsubstituted phenyl ring on the exocyclic 2-imino group and thiazolidine **5d** *p*-fluorophenyl ring exhibit similar  $IC_{50}$  values (0.50  $\mu$ M), displaying more than 8-fold potency. Interestingly, replacing the fluoro group attached to exocyclic 2-imino group with a chloro group (**5c**) enhances the activity and increases the potency from 8 to 15-fold higher than cisplatin. Meanwhile, using a bromo group (**5b**) instead of a fluoro or chloro group doesn't show any improvement in the corresponding  $IC_{50}$ , and yet the activity is still better than cisplatin (Table 7.1, entry 2 and 13). (*Z*)-*N*-(4-chlorophenyl)-5-((*Z*)-4-methoxybenzylidene)-3,4-dimethylthiazolidin-2-imine (**5c**) is the most potent compound among the screened series of thiazolidines, exhibiting higher than 15-fold anti-proliferative



activity compared to the positive control. The electron donating groups attached to both phenyl rings (methoxy groups, compound **5i**) exhibited good activity higher than 2-fold. While trifluoromethyl and *tert*-butyl groups attached to phenyl ring, compounds **5f** and **5j**, lower the activity by 3-fold compared with cisplatin (16.32 and 12.61  $\mu\text{M}$  respectively). Interestingly, a compound bearing both an electron donating group with electron withdrawing groups on the same phenyl ring lower the activity compared to the corresponding analogues with only electron withdrawing groups. A clear example is compound **5l** in which the bromo group does not affect the influence of the trifluoromethoxy group, thus the corresponding  $\text{IC}_{50}$  value is 15.64  $\mu\text{M}$  and the halogen (Br) group did not improve the activity in comparison to compound **5b** ( $\text{IC}_{50} = 0.62$   $\mu\text{M}$ ). Combination of a methoxy and a nitro group in compound **5k** did not cause a significant effect on the corresponding potency (1.38  $\mu\text{M}$ ) which is still close to a single methoxy substituted phenyl group (compound **5i** with  $\text{IC}_{50} = 1.75$   $\mu\text{M}$ ) and nitro group (compound **5e** with  $\text{IC}_{50} = 1.15$   $\mu\text{M}$ ). The activity of the current library of thiazolidines is not only consistent with our previously published series, but it shows a good improvement in terms of  $\text{IC}_{50}$  values.<sup>37</sup> It is noteworthy that  $\text{IC}_{50}$  of the previously synthesized thiazolidines ranged from 7.4 - 28.7  $\mu\text{M}$  (Scheme 7.1), while the new derivatives ranged from 0.27 – 16.32  $\mu\text{M}$  (Table 7.1). Moreover, the present thiazolidine library appears to be one of the most active thiazolidines against breast cancer cell (MCF7). In comparison to other published data, our new library revealed excellent activity in terms of  $\text{IC}_{50}$  compared to the three studies shown in Figure 7.1. This figure presents the most active three examples derived from these three different studies,  $\text{IC}_{50}$  ranged from 3.3 to 5.1  $\mu\text{M}$ . Therefore, our group is interested to develop such kind of clean chemistry towards stable bio-active thiazolidines. Another novel and chemically stable series of thiazolidines are being prepared for publication in the near future with interesting anti-tumor activity.

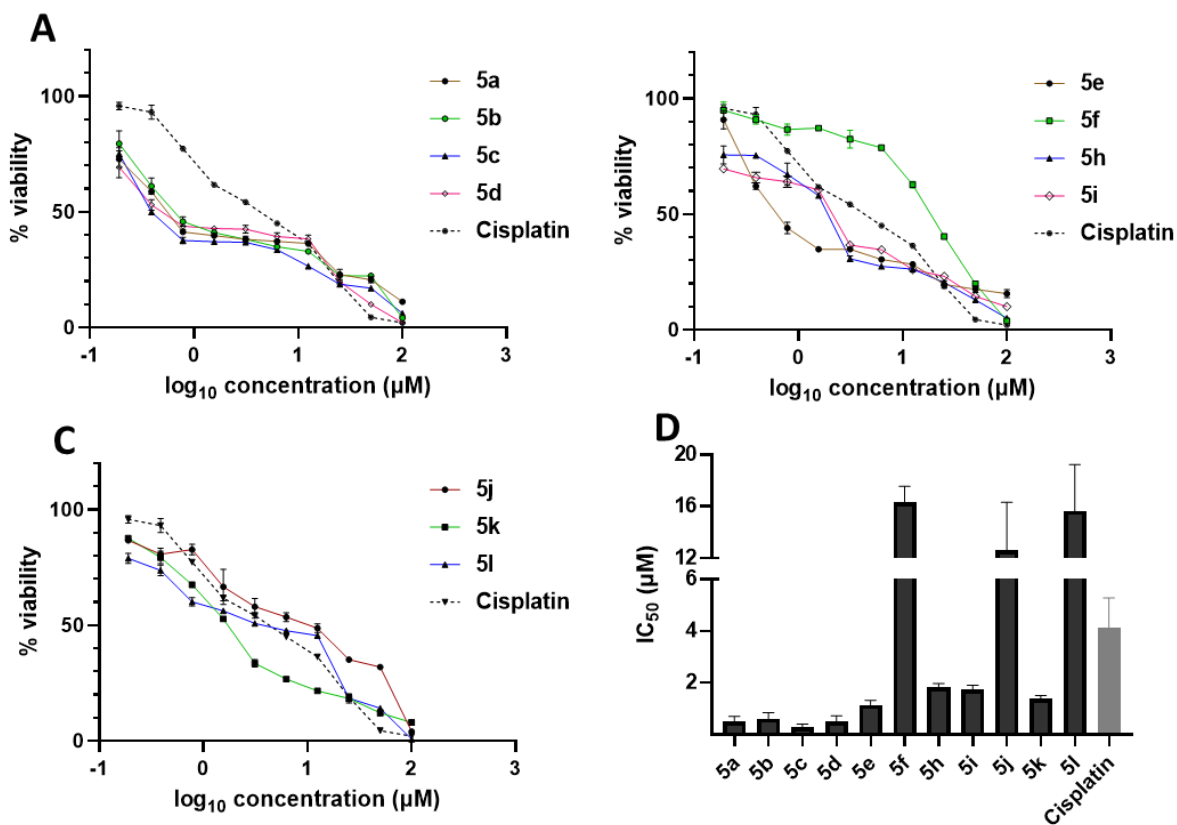


**Figure 7.3:** Anti-proliferative activity of thiazolidines **5a-f** and **5h-l**; A-C show the cell viability of MCF7 cell incubated with thiazolidine and tested by MTT assay after 96 h. Figure 3-D shows the calculated IC<sub>50</sub> based on non-linear data obtained from the cell viability study. The test was performed by Dr. Mandal lab.

### 7.3 SUMMARY:

A novel series of thiazolidines have been prepared via a convenient and efficient method using surface-mediated acceleration and their anti-proliferative activity evaluated. The substitution of methylene at position 4 in thiazolidine ring blocks the aerobic oxidation to the corresponding thiazolidinone but still resulted in compounds unstable at room temperature. All the compounds were analyzed through spectroscopic analysis and the exact configuration of the thiazolidines was confirmed by X-ray single crystal characterization for one compound **5f** as an example for the synthesized library. Freshly prepared thiazolidines were screened for their cytotoxicity against

breast cancer cell line (MCF7) using an MTT assay. Most of the synthesized library show potent cytotoxicity against a breast cancer cell line (MCF7). (*Z*)-*N*-(4-chlorophenyl)-5-((*Z*)-4-methoxybenzylidene)-3,4-dimethylthiazolidin-2-imine (**5c**) is the best analogues exhibiting a 15-fold higher potency compared to cisplatin. A study of structure activity relationship shows that electron withdrawing groups attached to the exocyclic 2-arylamine of thiazolidine exhibit the greatest activity among two synthesized libraries so far in the present work and previously published study in 2019. A stability study was performed for the compounds at room temperature, 4 °C and -10 °C, which illustrated the thiazolidines bearing an electron withdrawing groups show a good chemical stability and biological activity. Thus, the present report provides a promising approach towards the development of a new variety of thiazolidine scaffolds in terms of green/clean chemistry and biologically active molecules.

## 7.4 REFERENCES:

- (1) Bi, X.; Pasunooti, K. K.; Lescar, J.; Liu, C. F. Thiazolidine-Masked  $\alpha$ -Oxo Aldehyde Functionality for Peptide and Protein Modification. *Bioconjug. Chem.* **2017**, *28*, 325–329. <https://doi.org/10.1021/acs.bioconjchem.6b00667>.
- (2) Katayama, H.; Morisue, S. A Novel Ring Opening Reaction of Peptide N-Terminal Thiazolidine with 2,2'-Dipyridyl Disulfide (DPDS) Efficient for Protein Chemical Synthesis. *Tetrahedron* **2017**, *73* (25), 3541–3547. <https://doi.org/10.1016/j.tet.2017.05.041>.
- (3) Bi, X.; Pasunooti, K. K.; Tareq, A. H.; Takyi-Williams, J.; Liu, C. F. Genetic Incorporation of 1,2-Aminothiols Functionality for Site-Specific Protein Modification: Via Thiazolidine Formation. *Org. Biomol. Chem.* **2016**, *14* (23), 5282–5285. <https://doi.org/10.1039/c6ob00854b>.
- (4) Sahiba, N.; Sethiya, A.; Soni, J.; Agarwal, D. K.; Agarwal, S. Saturated Five-Membered Thiazolidines and Their Derivatives: From Synthesis to Biological Applications. *Topics in Current Chemistry*. 2020, pp 378 (2), 34. <https://doi.org/10.1007/s41061-020-0298-4>.
- (5) Zaimy, M. A.; Saffarzadeh, N.; Mohammadi, A.; Pourghadamyari, H.; Izadi, P.; Sarli, A.; Moghaddam, L. K.; Paschepari, S. R.; Azizi, H.; Torkamandi, S.; Tavakkoly-Bazzaz, J. New Methods in the Diagnosis of Cancer and Gene Therapy of Cancer Based on Nanoparticles. *Cancer Gene Ther.* **2017**, *24* (6), 233–243. <https://doi.org/10.1038/cgt.2017.16>.
- (6) Korkmaz, U.; Ustun, F. Experimental Breast Cancer Models: Preclinical Imaging Perspective. *Curr. Radiopharm.* **2021**, *14* (1), 5–14. <https://doi.org/10.2174/1874471013666200508080250>.
- (7) Gouda, M. A.; Abu-Hashem, A. A. Synthesis, Characterization, Antioxidant and Antitumor Evaluation of Some New Thiazolidine and Thiazolidinone Derivatives. *Arch. Pharm. (Weinheim)*. **2011**, *344*, 170–177. <https://doi.org/10.1002/ardp.201000165>.
- (8) Nishida, S.; Maruoka, H.; Yoshimura, Y.; Goto, T.; Tomita, R.; Masumoto, E.; Okabe, F.; Yamagata, K.; Fujioka, T. Synthesis and Biological Activities of Some New Thiazolidine Derivatives Containing Pyrazole Ring System. *J. Heterocycl. Chem.* **2012**, *49* (2), 303–309. <https://doi.org/https://doi.org/10.1002/jhet.834>.
- (9) Zhang, Q.; Zhou, H.; Zhai, S.; Yan, B. Natural Product-Inspired Synthesis of Thiazolidine and Thiazolidinone Compounds and Their Anticancer Activities. *Curr. Pharm. Des.* **2010**, *16* (16), 1826–1842. <https://doi.org/10.2174/138161210791208983>.
- (10) Havrylyuk, D.; Zimenkovsky, B.; Vasylenko, O.; Lesyk, R. Synthesis and Anticancer and Antiviral Activities of New 2-Pyrazoline-Substituted 4-Thiazolidinones. *J. Heterocycl. Chem.* **2013**, *50* (S1), E55–E62. <https://doi.org/https://doi.org/10.1002/jhet.1056>.
- (11) Osmaniye, D.; Levent, S.; Ardıç, C. M.; Atlı, Ö.; Özkay, Y.; Kaplancıklı, Z. A. Synthesis and Anticancer Activity of Some Novel Benzothiazole-Thiazolidine Derivatives. *Phosphorus. Sulfur. Silicon Relat. Elem.* **2018**, *193* (4), 249–256. <https://doi.org/10.1080/10426507.2017.1395878>.

- (12) El-Gaby, M. S. A.; Ismail, Z. H.; Abdel-Gawad, S. M.; Aly, H. M.; Ghorab, M. M. Synthesis of Thiazolidine and Thiophene Derivatives for Evaluation as Anticancer Agents. *Phosphorus. Sulfur. Silicon Relat. Elem.* **2009**, *184* (10), 2645–2654. <https://doi.org/10.1080/10426500802561096>.
- (13) Singh, R. P.; Aziz, M. N.; Gout, D.; Fayad, W.; El-Manawaty, M. A.; Lovely, C. J. Novel Thiazolidines: Synthesis, Antiproliferative Properties and 2D-QSAR Studies. *Bioorganic Med. Chem.* **2019**, *27* (20). <https://doi.org/10.1016/j.bmc.2019.115047>.
- (14) Saralkar, P.; Geldenhuys, W. J. Screening for Anticancer Properties of Thiazolidinedione Compounds in a Galactose Media Metastatic Breast Cancer Cell Model. *Med. Chem. Res.* **2019**, *28* (12), 2165–2170. <https://doi.org/10.1007/s00044-019-02444-z>.
- (15) El-Kashef, H.; Badr, G.; Abo El-Maali, N.; Sayed, D.; Melnyk, P.; Lebegue, N.; Abd El-Khalek, R. Synthesis of a Novel Series of (Z)-3,5-Disubstituted Thiazolidine-2,4-Diones as Promising Anti-Breast Cancer Agents. *Bioorg. Chem.* **2020**, *96*, 103569. <https://doi.org/10.1016/j.bioorg.2020.103569>.
- (16) El-Adl, K.; Sakr, H.; Nasser, M.; Alswah, M.; Shoman, F. M. A. 5-(4-Methoxybenzylidene)Thiazolidine-2,4-Dione-Derived VEGFR-2 Inhibitors: Design, Synthesis, Molecular Docking, and Anticancer Evaluations. *Arch. Pharm. (Weinheim)*. **2020**, *353* (9), e2000079. <https://doi.org/10.1002/ardp.202000079>.
- (17) Xie, Y.; Hou, W.; Song, X.; Yu, Y.; Huang, J.; Sun, X.; Kang, R.; Tang, D. Ferroptosis: Process and Function. *Cell Death Differ.* **2016**, *23* (3), 369–379. <https://doi.org/10.1038/cdd.2015.158>.
- (18) Reyes, A. J. Formal Comparison of the Antihypertensive Effects of Torasemide and Other Diuretics by the Montevideo Mathematical Model. *Arzneimittelforschung*. **1988**, *38* (1A), 194–199.
- (19) B G, M.; Manjappara, U. V. Obestatin and Rosiglitazone Differentially Modulate Lipid Metabolism Through Peroxisome Proliferator-Activated Receptor- $\gamma$  (PPAR $\gamma$ ) in Pre-Adipose and Mature 3T3-L1 Cells. *Cell Biochem. Biophys.* **2021**, *79* (1), 73–85. <https://doi.org/10.1007/s12013-020-00958-7>.
- (20) Wolffenbittel, B. H. R.; Sels, J. P.; Huijberts, M. S. P. Rosiglitazone. *Expert Opinion on Pharmacotherapy*. Treasure Island (FL) January 2001, pp 467–478. <https://doi.org/10.1517/14656566.2.3.467>.
- (21) Saito, M.; Fujita, Y.; Kuribayashi, N.; Uchida, D.; Komiyama, Y.; Fukumoto, C.; Hasegawa, T.; Kawamata, H. Troglitazone, a Selective Ligand for PPAR $\gamma$ , Induces Cell-Cycle Arrest in Human Oral SCC Cells. *Anticancer Res.* **2020**, *40* (3), 1247–1254. <https://doi.org/10.21873/anticancer.14066>.
- (22) Cheng-Lai, A.; Levine, A. Rosiglitazone: An Agent from the Thiazolidinedione Class for the Treatment of Type 2 Diabetes. *Heart Dis.* **2000**, *2* (4), 326–333.
- (23) Fischer, W.; Bodewei, R.; Satzinger, G. Anticonvulsant and Sodium Channel Blocking Effects of Ralitolone in Different Screening Models. *Naunyn. Schmiedeberg's. Arch. Pharmacol.* **1992**, *346* (4), 442–452. <https://doi.org/10.1007/BF00171088>.

- (24) Löscher, W.; von Hodenberg, A.; Nolting, B.; Fassbender, C. -P; Taylor, C. Ralitone: A Reevaluation of Anticonvulsant Profile and Determination of “Active” Plasma Concentrations in Comparison with Prototype Antiepileptic Drugs in Mice. *Epilepsia* **1991**, 32 (4), 560–568. <https://doi.org/10.1111/j.1528-1157.1991.tb04693.x>.
- (25) Hassan, R. M.; Abd-Allah, W. H.; Salman, A. M.; El-Azzouny, A. A.-S.; Aboul-Enein, M. N. Design, Synthesis and Anticancer Evaluation of Novel 1,3-Benzodioxoles and 1,4-Benzodioxines. *Eur. J. Pharm. Sci.* **2019**, 139, 105045. <https://doi.org/https://doi.org/10.1016/j.ejps.2019.105045>.
- (26) Yahiaoui, S.; Moliterni, A.; Corriero, N.; Cuocci, C.; Toubal, K.; Chouaih, A.; Djafri, A.; Hamzaoui, F. 2-Thioxo- 3*N*-(2-Methoxyphenyl) –5 [4'-Methyl -3'*N* -(2'-Methoxyphenyl) Thiazol-2'(3'H)-Ylidene] Thiazolidin-4-One: Synthesis, Characterization, X-Ray Single Crystal Structure Investigation and Quantum Chemical Calculations. *J. Mol. Struct.* **2019**, 1177, 186–192. <https://doi.org/https://doi.org/10.1016/j.molstruc.2018.09.052>.
- (27) Revelant, G.; Huber-Villaume, S.; Dunand, S.; Kirsch, G.; Schohn, H.; Hesse, S. Synthesis and Biological Evaluation of Novel 2-Heteroarylimino-1,3-Thiazolidin-4-Ones as Potential Anti-Tumor Agents. *Eur. J. Med. Chem.* **2015**, 94, 102–112. <https://doi.org/10.1016/j.ejmech.2015.02.053>.
- (28) Santeusano, S.; Majer, R.; Perrulli, F. R.; De Crescentini, L.; Favi, G.; Giorgi, G.; Mantellini, F. Divergent Approach to Thiazolylidene Derivatives: A Perspective on the Synthesis of a Heterocyclic Skeleton from  $\beta$ -Amidothioamides Reactivity. *J. Org. Chem.* **2017**, 82 (18), 9773–9778. <https://doi.org/10.1021/acs.joc.7b02135>.
- (29) da Silva, D. S.; da Silva, C. E. H.; Soares, M. S. P.; Azambuja, J. H.; de Carvalho, T. R.; Zimmer, G. C.; Frizzo, C. P.; Braganhol, E.; Spanevello, R. M.; Cunico, W. Thiazolidin-4-Ones from 4-(Methylthio)Benzaldehyde and 4-(Methylsulfonyl)Benzaldehyde: Synthesis, Antiglioma Activity and Cytotoxicity. *Eur. J. Med. Chem.* **2016**, 124, 574–582. <https://doi.org/10.1016/j.ejmech.2016.08.057>.
- (30) Subhedar, D. D.; Shaikh, M. H.; Arkile, M. A.; Yeware, A.; Sarkar, D.; Shingate, B. B. Facile Synthesis of 1,3-Thiazolidin-4-Ones as Antitubercular Agents. *Bioorganic Med. Chem. Lett.* **2016**, 26 (7), 1704–1708. <https://doi.org/10.1016/j.bmcl.2016.02.056>.
- (31) Azgomi, N.; Mokhtary, M. Nano-Fe<sub>3</sub>O<sub>4</sub>@SiO<sub>2</sub> Supported Ionic Liquid as an Efficient Catalyst for the Synthesis of 1,3-Thiazolidin-4-Ones under Solvent-Free Conditions. *J. Mol. Catal. A Chem.* **2015**, 398, 58–64. <https://doi.org/https://doi.org/10.1016/j.molcata.2014.11.018>.
- (32) Sadeghzadeh, S. M.; Daneshfar, F. Ionic Liquid Immobilized on FeNi<sub>3</sub> as Catalysts for Efficient, Green, and One-Pot Synthesis of 1,3-Thiazolidin-4-One. *J. Mol. Liq.* **2014**, 199, 440–444. <https://doi.org/10.1016/j.molliq.2014.07.039>.
- (33) Safaei-Ghomi, J.; Nazemzadeh, S. H.; Shahbazi-Alavi, H. Nano-CdZr<sub>4</sub>(PO<sub>4</sub>)<sub>6</sub> as a Reusable and Robust Catalyst for the Synthesis of Bis-Thiazolidinones by a Multicomponent Reaction of Aldehydes, Ethylenediamine and Thioglycolic Acid. *J. Sulfur Chem.* **2017**, 38 ((2)), 195–205. <https://doi.org/10.1080/17415993.2016.1267176>.
- (34) Safaei-Ghomi, J.; Navvab, M.; Shahbazi-Alavi, H. CoFe<sub>2</sub>O<sub>4</sub>@SiO<sub>2</sub>/PrNH<sub>2</sub> Nanoparticles as

- Highly Efficient and Magnetically Recoverable Catalyst for the Synthesis of 1,3-Thiazolidin-4-Ones. *J. Sulfur Chem.* **2016**, *37* (6), 601–612. <https://doi.org/10.1080/17415993.2016.1169533>.
- (35) Thakare, M. P.; Kumar, P.; Kumar, N.; Pandey, S. K. Silica Gel Promoted Environment-Friendly Synthesis of 2,3-Disubstituted 4-Thiazolidinones. *Tetrahedron Lett.* **2014**, *55* (15), 2463–2466. <https://doi.org/10.1016/j.tetlet.2014.03.007>.
- (36) Singh, R. P.; Gout, D.; Lovely, C. J. Tandem Thioacylation-Intramolecular Hydrosulfonylation of Propargyl Amines – Rapid Access to 2-Aminothiazolidines. *European J. Org. Chem.* **2019**, *8*, 1726–1740. <https://doi.org/10.1002/ejoc.201801505>.
- (37) Singh, R. P.; Aziz, M. N.; Gout, D.; Fayad, W.; El-Manawaty, M. A.; Lovely, C. J. Novel Thiazolidines: Synthesis, Antiproliferative Properties and 2D-QSAR Studies. *Bioorganic Med. Chem.* **2019**, *27* (20), 115047. <https://doi.org/10.1016/j.bmc.2019.115047>.
- (38) Jiang, Z.; Lu, P.; Wang, Y. Three-Component Reaction of Propargyl Amines, Sulfonyl Azides, and Alkynes: One-Pot Synthesis of Tetrasubstituted Imidazoles. *Org. Lett.* **2012**, *14* (24), 6266–6269. <https://doi.org/10.1021/ol303023y>.
- (39) Mo, J.-N.; Su, J.; Zhao, J. The Asymmetric A<sup>3</sup>(Aldehyde–Alkyne–Amine) Coupling: Highly Enantioselective Access to Propargylamines. *Molecules* **2019**, *24* (7). <https://doi.org/10.3390/molecules24071216>.
- (40) Gommermann, N.; Knochel, P. Practical Highly Enantioselective Synthesis of Propargylamines through a Copper-Catalyzed One-Pot Three-Component Condensation Reaction. *Chem. – A Eur. J.* **2006**, *12* (16), 4380–4392. <https://doi.org/https://doi.org/10.1002/chem.200501233>.
- (41) Olivi, N.; Spruyt, P.; Peyrat, J.-F.; Alami, M.; Brion, J.-D. Tandem Amine Propargylation-Sonogashira Reactions: New Three-Component Coupling Leading to Functionalized Substituted Propargylic Amines. *Tetrahedron Lett.* **2004**, *45* (12), 2607–2610. <https://doi.org/https://doi.org/10.1016/j.tetlet.2004.01.141>.

**CHAPTER EIGHT: NOVEL THIAZOLIDINES OF POTENTIAL ANTI-  
PROLIFERATION PROPERTIES AGAINST ESOPHAGEAL SQUAMOUS CELL  
CARCINOMA VIA ERK PATHWAY**

Marian N. Aziz<sup>1,2</sup>, Linh Nguyen<sup>3,4</sup>, Yan Chang<sup>4,5</sup>, Delphine Gout<sup>1</sup>, Zui Pan<sup>4,5</sup>, Carl J. Lovely<sup>1,\*</sup>

1. Department of Chemistry and Biochemistry, 700 Planetarium Place, University of Texas at  
Arlington, TX 76019, USA

2. Department of Pesticide Chemistry, National Research Centre, Dokki, Giza 12622, Egypt

3. Dept. of Biology, College of Science, University of Texas at Arlington, TX 76019, USA

4. Department of Graduate Nursing, College of Nursing and Health Innovation, University of  
Texas at Arlington, TX 76019, USA

5. Bone and Muscle Research Center, University of Texas at Arlington, TX 76019, USA

Corresponding author

Prof. Carl J. Lovely

Professor, Chemistry and Biochemistry Department

University of Texas at Arlington

Address: 700 Planetarium Place, Box 19065, UT Arlington, TX 76019-0065

Email: lovely@uta.edu

Phone: +1 817 272 5446

(Not published)



## **ABSTRACT:**

The discovery of a new class of extracellular-signal-regulated kinase (ERK) inhibitors has been achieved via developing novel 2-imino-5-arylidine-thiazolidine analogues. A novel synthetic method employing a solid support-mediated reaction was used to construct the targeted thiazolidines through a cascade reaction with good yields. The chemical and physical stability of the new thiazolidine library has successfully been achieved by blocking the labile C5-position to aerobic oxidation. A cell viability study was performed using esophageal carcinomic cell lines (KYSE-30, KYSE-150, HET-1A cells) through utilization of the MTT assay, revealing that (Z)-5-((Z)-4-bromobenzylidene)-N-(4-methoxy-2-nitrophenyl)-4,4-dimethylthiazolidin-2-imine (9g) is the best compound among the synthesized library in terms of selectivity. DAPI staining experiments were performed to visualize the morphological changes and to investigate the apoptotic activity, guiding to select for the KYSE-150 cell line. Moreover, qRT-PCR was used to identify the mechanism/pathway behind the observed activity/selectivity of thiazolidine 9g which established selective inhibition of the phosphorylation process of one of the major signaling cascades, ERK pathway. Molecular modeling techniques have been utilized to confirm the observed activity. A molecular docking study has emphasized similar binding interactions between the synthesized thiazolidines and reported co-crystallized inhibitors with ERK proteins. Thus, the present study provides a starting point for the development of an interesting bioactive 2-imino-5-arylidine-thiazolidines.

## **8.1 INTRODUCTION**

Cancer is one of the most feared diseases worldwide due to its devastating impact on human health and its related death rate. Based on statistics from the International Agency for Research on Cancer (IARC), cancer incidence and mortality are growing rapidly. Thus, it is expected that the number of new cases will increase from 19.3 million in 2020 to 28.4 million in 2040.<sup>1</sup> Tumor cells develop by deviation from the tightly controlled differentiation pathways of normal cells, through the loss or modification of normal regulatory growth mechanisms. There are over 200 different

kinds of cancer that are usually classified based on the organ or cell where the tumor originated.<sup>2</sup> Thus, cancer is not a single disease but rather a collection which require individual treatment regimes. Tumor metastasis, which results in the spread of the primary tumor to secondary location, is an additional complication, creating significant fear among patients. The metastasis process is mediated by a mechanism called “angiogenic-switch” in which a normal blood vessel becomes a dormant hyperplasia and then turns into a vascularized solid tumor acting as a lesion affecting surrounding organs.<sup>3</sup> Metastatic tumors are the real challenge in cancer treatment because a tumor cell in a specific organ may be converted into another tumor cell in other organs.<sup>4,5</sup> The complex mechanisms behind metastatic death-causing cancer are considered the most important question marks in metastasis cancer research.<sup>5,6</sup> Moreover, few of the approved drugs by the U.S. Food and Drug Administration (FDA) are targeted and effective against metastatic cancers.<sup>6</sup> Tumor cells can be characterized by their high death resistance, therefore searching for different approaches to induce cell death provides an intriguing approach to for the development of apoptotic drugs. Based on the morphological stereotyped appearance of tumor cells, the lethal mode, programmed cell death is categorized into three different types (apoptosis, autophagy, and necrosis).

Apoptosis is recognized by the appearance of several morphological features, including cell rounding, shrinking of cytoplasm, condensed chromatin starting from the nuclear membrane to the whole nucleus, nuclear fragmentation, and generation of other organelles called apoptotic bodies.<sup>7-10</sup> There are number of intrinsic and extrinsic factors that activate the apoptotic process. Apoptotic ligands and/or drugs activate the extrinsic pathway by binding to death receptors of the tumor necrosis factor (TNF) receptor superfamily like Fas receptor (CD95), Death Receptor 4 and 5 (DR4 and 5).<sup>11-14</sup> Thus, these ligands/drugs induce apoptosis by converting pro-caspases-8 and/or pro-caspases-10 into their active forms of death inducing signaling complex (DISC).<sup>14</sup>

Activation of caspase proteins is essential for the apoptotic process which cleave hundreds of proteins required for cellular functions, including nuclear and cytoskeletal proteins. Therefore, loss of these proteins causes plasma membrane changes and leads to shrinking in apoptotic cells.<sup>15</sup> However, apoptosis is an essential physiological process during development and aging stages, apoptotic anomalies are associated with a number of diseases including neurodegenerative, bacterial, viral, heart, autoimmune, and cancer diseases.<sup>16–20</sup>

Mitogen-activated protein kinases (MAPK) are autophosphorylation protein kinases which react at serine and threonine residues to stimulate or deactivate their targets. MAPKs regulate essential physiological processes such as proliferation, transformation, differentiation, apoptosis, stress response, and innate immunity.<sup>21–23</sup> There are three known kinase proteins belonging to the MAPK family, the extracellular signal-regulated protein kinases (ERK1/2), the p38 MAP kinases ( $\alpha$ ,  $\beta$ ,  $\delta$ , and  $\gamma$ ), and the c-Jun NH2-terminal kinases ((JNK1/2/3)).<sup>23,24</sup> ERK1/2 isoforms are dual-specificity kinases and are involved in the Ras-Raf-MEK-ERK signal transduction cascade. This cascade plays an important role in variety of cellular processes which are initiated by activation of RAS kinase, mediating the activation or phosphorylation of Raf-kinase and then MEK mediates the activation of ERKs. Ras mutations are common oncogenic alterations in many cancers and ultimately activate ERK1/2 pathway.<sup>14,21,22,25–27</sup> Therefore, discovering ERK inhibitors is a promising approach to cancer chemotherapy and some ERK inhibitors are reaching to clinical stages as potential anticancer agents. Figure 8.1 shows some ERK inhibitors in clinical trials.<sup>28,29</sup>

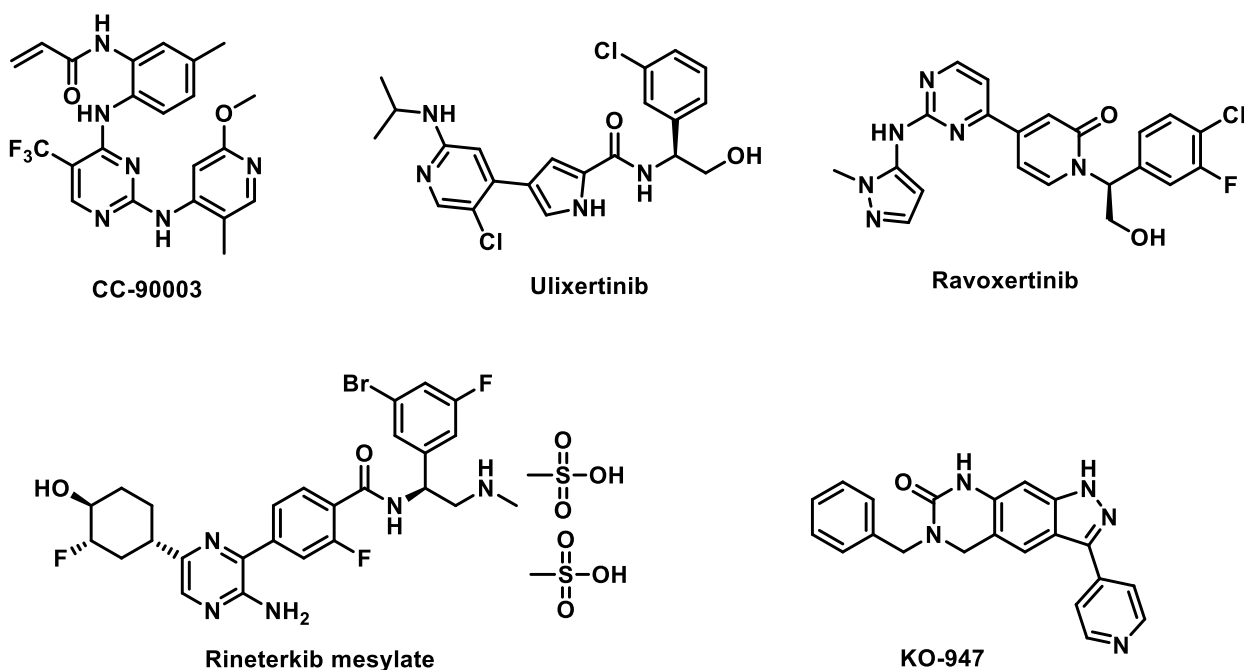


**Figure 8.1:** ERK1/2 inhibitors in the clinical stages.

Esophageal cancer, occurring in the upper gastrointestinal tract, is the 6<sup>th</sup> deadliest cancer with a total number of deaths numbering around 544,000 lives in 2020 globally.<sup>29</sup> It is one of the most common malignant neoplasms of the digestive tract and is characterized by high rate of incidence.<sup>32</sup> About 572,000 new cases were diagnosed as esophageal cancer worldwide in 2018, that increased to 604,000 cases in 2020.<sup>31</sup> There are mainly two types of esophageal cancer; squamous esophageal cell carcinoma (ESCC) which is the most common type worldwide, and adenocarcinoma that is the predominant type in the USA, Australia, UK, and Western Europe.<sup>34</sup> The poor diagnosis and low survival rate ( $\leq 20\%$ ) of esophageal cancer are due to unclear/unnoticeable symptoms in the early stages of tumor development.<sup>35</sup> The gold standard approach for esophageal cancer treatment is radiotherapy, chemotherapy (using cisplatin and 5-fluorouracil), surgical resection, and their combination. Sadly, these approaches are not sufficient with many patients who suffer from advanced, inoperable, and metastatic diseases, especially

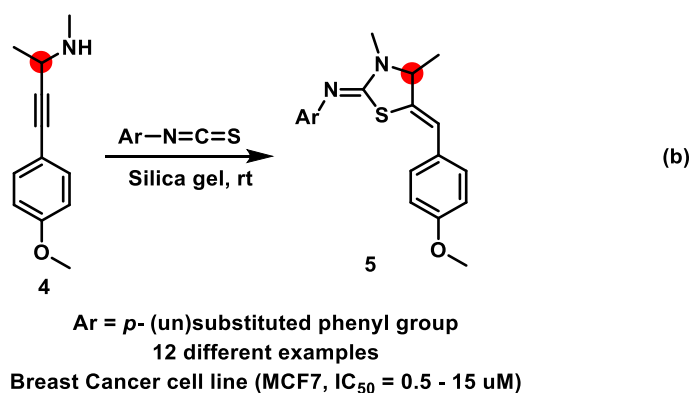
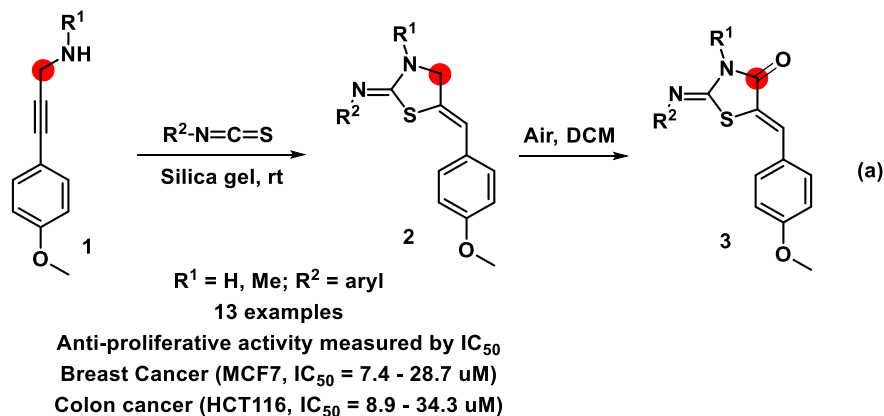
when the cases are diagnosed in the late stages of the disease.<sup>36,37</sup> Recent studies show that the importance of Ras/Raf/MEK/ERK pathway in esophageal carcinoma treatments and diagnosis especially for ESCC.<sup>38-42</sup> Therefore, our research group is interested in discovering and developing potent novel small molecules acting as ERK inhibitors. In the present study, we designed and synthesized novel small organic molecules, thiazolidines, then evaluated their anti-cancer activity in terms of induction of apoptosis and inhibition of ERK signaling pathway using *in-vitro* bioassays.

## **8.2 RESULT AND DISCUSSION:**

### ***8.2.1 Chemistry***

The thiazolidines class of heterocyclic compounds show broad bioactivity against global distribution of diseases. The thiazolidine core structure is found in various synthetic compounds acting as antiproliferative,<sup>43-49</sup> anti-inflammatory,<sup>50-52</sup> anti-diabetic,<sup>53</sup> anti-fungal,<sup>54</sup> anti-convulsant,<sup>55</sup> anti-parasitic,<sup>56,57</sup> anti-HIV,<sup>58,59</sup> and anti-microbial active agents.<sup>60,61</sup> Various synthetic methodologies have been developed for construction of the core thiazolidine ring structure. On-surface thiazolidine synthesis is one of the most efficient methods and environmentally favorable strategies reported to date. Our group has developed a silica gel-based technique as a solid support for thiourea cyclization to produce thiazolidines in a one-pot reaction directly from propargyl amines and thioureas.<sup>62</sup> Scheme 8.1 outlines the sequential stages of developing our targeted novel thiazolidine compounds. The encouraging cytotoxicity results obtained for our first thiazolidine library led us to develop the present chemistry using the solid support technique as a green methodology towards constructing the thiazolidine scaffolds.<sup>49</sup> Most of the synthesized thiazolidines in the first library showed good antiproliferative activity against colon and breast cancer cell lines. Interestingly however, the several of synthesized thiazolidines

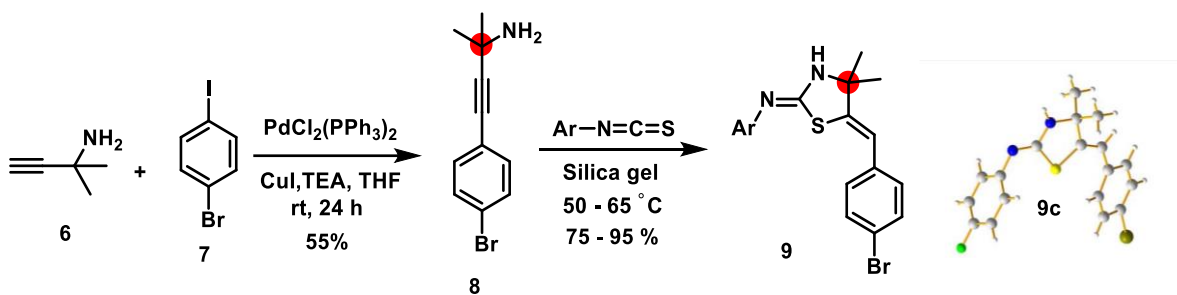
were prone to oxidation by exposure to the atmospheric air resulting in the formation of the corresponding thiazolidinones **3** (Scheme 8.1a).<sup>49</sup>



**Scheme 8.1:** Previous developed/published anti-proliferative thiazolidines **2**, **3**, and **5**.

Therefore, a second library of thiazolidines was developed in response as a means to enhance their chemical and physical stabilities. The core structure of thiazolidine ring was modified to block the oxidatively labile methylene group ( $\text{CH}_2$ ) by introducing a methyl group instead of a hydrogen atom (Scheme 8.1b) but retaining the other functional groups within the core structure.<sup>63</sup> They revealed interesting anti-proliferative activity that was sufficiently encouraging to continue developing such chemistry toward synthesizing a stable and bio-active novel thiazolidines. However, unless the fully substituted thiazolidines are protected from the anaerobic oxidation,

they were still unstable at room temperature over the course of several days. Thus, another methyl group was introduced at that same position, so the two hydrogen atoms in the first library were now replaced with two methyl groups in the new series of thiazolidines (Scheme 8.2). A second point, an initial thought was that a *N*-methyl group in the core structure of thiazolidines as in the first two libraries (Scheme 8.1a and b) might cause strain within the ring and affecting compound stability. Therefore, the *N*-methyl group was removed and replaced by NH group, providing another potential site for binding *via* a hydrogen bond donor. Moreover, a qualitative structure activity relationship (QSAR) study has been performed based on the published data to predict the bioactivity of new thiazolidine derivatives using CODESSA-Pro (comprehensive descriptors for structural and statistical analysis) software.<sup>64</sup> The results show that replacing the methoxy group in the benzylidene ring with an electron withdrawing group should improve their corresponding IC<sub>50</sub>. Therefore, the propargyl amine 4-(4-bromophenyl)-2-methylbut-3-yn-2-amine (**8**) was synthesized via a Sonogashira cross-coupling reaction using 2-methylbut-3-yn-2-amine (**6**) as an alkyne, 1-bromo-4-iodobenzene (**7**) (to incorporate a halogenated group instead of methoxy group into benzylidene ring) in the presence of PdCl<sub>2</sub>(PPh<sub>3</sub>)<sub>2</sub> and CuI in a THF/TEA mixture (Scheme 8.2).<sup>65</sup>



**Scheme 8.2:** Novel synthesized thiazolidines **9a-i** using on-surface methodology.

Then the synthesized propargyl amine **8** was mixed with isothiocyanate derivatives in presence of silica gel as a solid support, resulting in isolation of the targeted thiazolidines. Initial experiments with this propargyl amine were conducted at room temperature as had been used previously, which resulted in consumption of the starting materials after two to three days (monitoring by TLC experiment). Presumably, the loss of the methyl groups compared to the previously reported systems reduces the reactive rotamer population thereby slowing down the reaction.<sup>49,66</sup> Therefore, the impact of elevating the temperature was investigated which resulted in identification of conditions leading to improved yields; ultimately finalized conditions consisted of stirring the slurry at 50-65 °C for 24 h. The isolated thiazolidines were purified by flash column chromatography, followed by crystallization using toluene or ethanol (Table 8.1). All the final products are stable crystalline solids at room temperature therefore one goal of this study, namely preparation of chemically and physically stable novel thiazolidines using our on-surface technique, has been achieved. All synthesized compounds were characterized using spectroscopic techniques (IR, <sup>1</sup>H NMR, <sup>13</sup>C NMR, HRMS) and a single crystal X-ray structure was obtained for one sample. Our initial expectation of removing the N-methyl group attached to thiazolidine-nitrogen (*cf.* **7** vs **2** or **5**) was releasing of some strain and potentially inversion of the geometry of exocyclic aryl imine group. However, on the basis of the X-ray study, it actually exhibits the same double bond geometry as the two published libraries of thiazolidines and removing the *N*-methyl group does not affect the formation of (*Z*)-2-imino-(5*Z*)-ylidene thiazolidines.



**Table 8.1:** Synthesis of (Z)-5-((Z)-substituted benzylidene)-N-(4-bromophenyl)-4,4-dimethylthiazolidin-2-imine.

Entry	Cpd.	Ar	Yield (%) <sup>a</sup>	
			I	II
1	9a	4-BrC <sub>6</sub> H <sub>4</sub>	77	55
2	9b	4-ClC <sub>6</sub> H <sub>4</sub>	75	50
3	9c	4-FC <sub>6</sub> H <sub>4</sub>	77	46
4	9d	4-NO <sub>2</sub> C <sub>6</sub> H <sub>4</sub>	95	30
5	9e	C <sub>6</sub> H <sub>5</sub>	80	54
6	9f	4-MeC <sub>6</sub> H <sub>4</sub>	78	34
7	9g	4-OMe-2-NO <sub>2</sub> C <sub>6</sub> H <sub>3</sub>	94	44
8	9h	4-CH <sub>3</sub> -3-ClC <sub>6</sub> H <sub>3</sub>	80	40
9	9i	4-CH <sub>3</sub> C <sub>6</sub> H <sub>4</sub>	85	42

<sup>a</sup>Reaction was performed with 1.0 mmol of 4-(4-bromophenyl)-2-methylbut-3-yn-2-amine and 1.0 mmol of the corresponding aryl isothiocyanate in a vigorous stirred silica gel (1.75 g) at 65 °C for 24 h.

<sup>I</sup> Isolated yields after chromatography purification.

<sup>II</sup> Isolated yields after crystallization.

### 8.2.2 Anti-tumor activity:

#### *Inhibitory effects of thiazolidine compounds on ESCC cells*

The anti-cancer efficacy of thiazolidine compound in cultured human esophageal squamous cell carcinoma and normal epithelial cell lines was assessed using the gold standard MTT assay (3-(4,5-dimethylthiazol-2-yl)-2,5-diphenyl-2H-tetrazolium bromide).<sup>67</sup> The efficacy of the thiazolidines was measured initially as IC<sub>50</sub> values using eight different concentrations by incubation with EYSE-30 cells for 72 hours. The results of these experiments are shown in Figure 2 (IC<sub>50</sub> values for all the synthesized compounds against KYSE-30 cell line). For investigating the structure activity relationship (SAR) study, the thiazolidine structures were designed to have a variety of functional groups attached to exocyclic aryl amine such as electron withdrawing groups ((Br, Cl, F, NO<sub>2</sub>), **9a-d**, respectively), electron-donating groups (Me (**9f**), OMe (**9i**)), and bearing the two groups together as in compounds **9g** and **9h**. Comparing these derivatives with thiazolidine containing unsubstituted phenyl **9e** helps understanding SAR of the synthesized compounds. All the derivatives reveal good inhibitory activity except ones containing Cl (**9b**), Me (**9f**) groups and

combinations of both (**9h**). However, the negative and reverse effect of thiazolidines containing Cl group, the data are still compatible with the previously published data obtained for the two thiazolidine series.<sup>49,63</sup> Thiazolidines **9c**, **9a** and **9i** are considered more effective derivatives based on these initial data (10.6, 13.2, and 14.2  $\mu\text{M}$ , respectively) compared to unsubstituted exocyclic aryl amine **9d**. Interestingly, thiazolidines containing a methyl substituent group to the exocyclic aryl amine show good inhibitory effect (14.2  $\mu\text{M}$ ) and the combination of methyl and nitro group to exocyclic aryl amine **9g** retains the activity to be 16.8  $\mu\text{M}$ . It was noticeable that  $\text{IC}_{50}$  values of most of the effective compounds are close to 15  $\mu\text{M}$  and for the less effective ones are higher than 60  $\mu\text{M}$ .

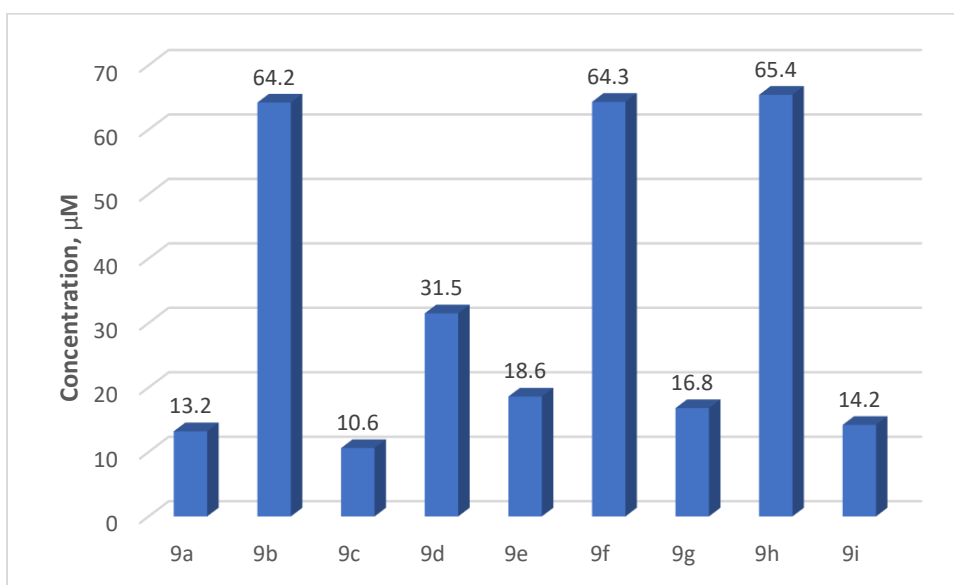


**Figure 8.2:**  $\text{IC}_{50}$  values of thiazolidines 9a-i tested with KYSE-30 cell line. The test was performed by Dr. Zui Pan Laboratory.

Therefore, the inhibitory effects for each compound using a single dose of 10  $\mu\text{M}$  concentration for 72 h was assessed using two tumorous esophageal cell lines (KYSE-30 and KYSE-150) and non-tumorous esophageal epithelial cell HET-1A cells (Figure 8.3). A general theme among all the tested compounds is the higher efficacy against KYSE-150 compared to KYSE-30 cell line. However, modest selectivity of thiazolidines towards tumorous and non-tumorous cell lines was observed, compounds **9e** and **9g** reveal the lowest toxicity toward HET-1A cells. Therefore, a cell viability study of **9e** and **9g** with KYSE-30 and KYSE-150 was conducted using eight different concentrations (Figure 8.4A). Compound **9g** displayed the highest efficacy against KYSE-150 cell line (71% inhibition of cell growth using 10  $\mu\text{M}$ ) among all the compounds. Also, the  $\text{IC}_{50}$  values support the choice of **9g** for further evaluation revealing inhibition of the proliferation of KYSE-30 and KYSE-150 using 16.8  $\mu\text{M}$  and 10.07  $\mu\text{M}$ , respectively. The  $\text{IC}_{50}$  of **9g** for HET-1A and NES-G4T, two non-tumorous esophageal epithelia cell lines, were calculated as 13  $\mu\text{M}$  and 202.2  $\mu\text{M}$ , respectively. In general, viability of all cell lines reduced in a dose-dependent manner during treatment of compound **9g** for 72 h as it is shown in Figure 8.4B. Data suggest that **9g** could selectively inhibit cancer cell growth, while normal cells remained relatively insensitive, hence **9g** was selected for further analysis.

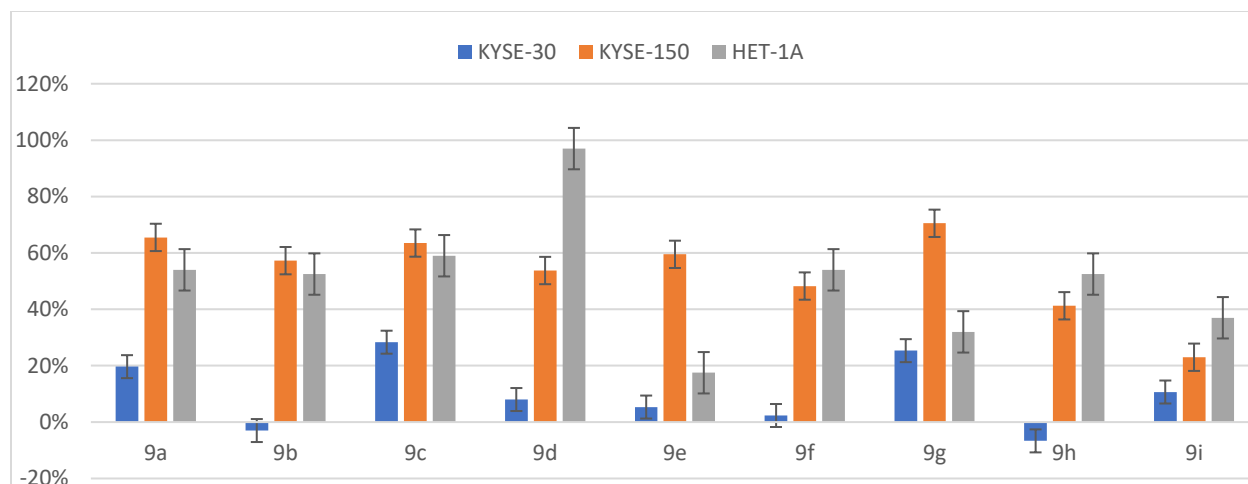


**Figure 8.3:** Inhibitory effects on cell proliferation by thiazolidine compounds variations. Cell viability with thiazolidine compounds at 10  $\mu$ M treatments for 72 h were calculated by MTT assay and normalized inhibitory effects were compared in KYSE-30, KYSE-150, HET-1A cells. Data were from 4 independent experiments with biological triplicates for each experiment. The test was performed by Dr. Zui Pan Laboratory.

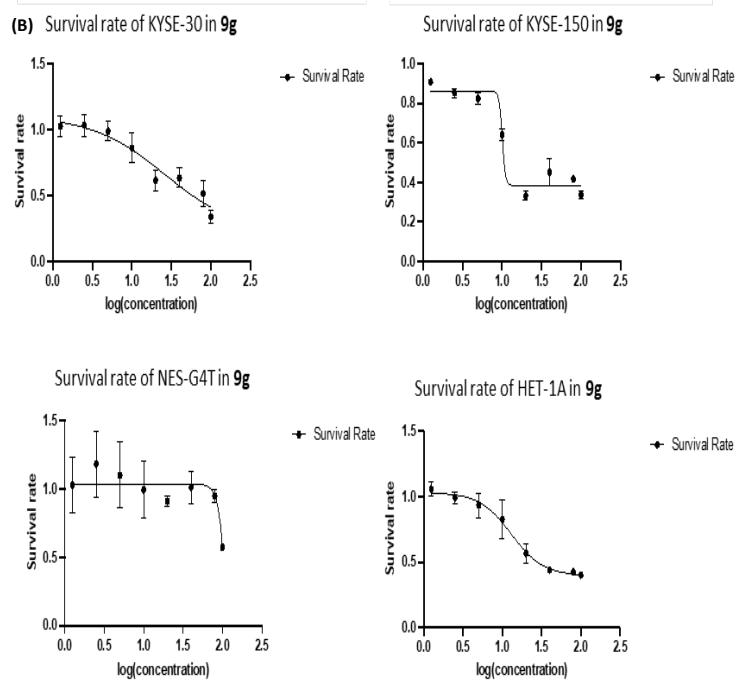
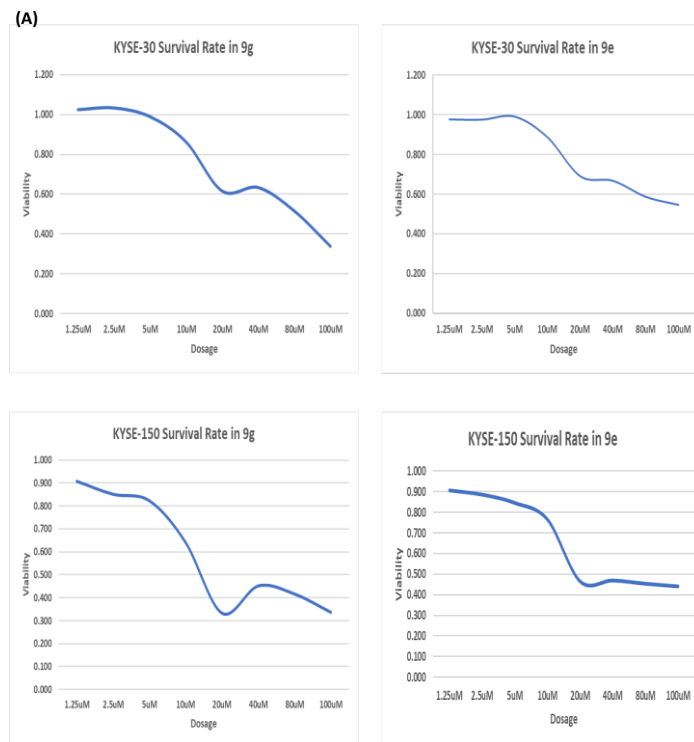


**Figure 8.4:** Compound 9g selectively inhibited cell proliferation in ESCC cells: (A) Cell viability of KYSE-30 and KYSE-150 with 9e and 9g compounds at eight different concentrations using MTT assay; (B) Cell viability with 9g treatment after 72 h were calculated by MTT assay in KYSE-30, KYSE-150, HET-1A, and NES-G4T. The test was performed by Dr. Zui Pan Laboratory.

### *Apoptosis analysis of 9g in KYSE-30 and KYSE-150 cells*

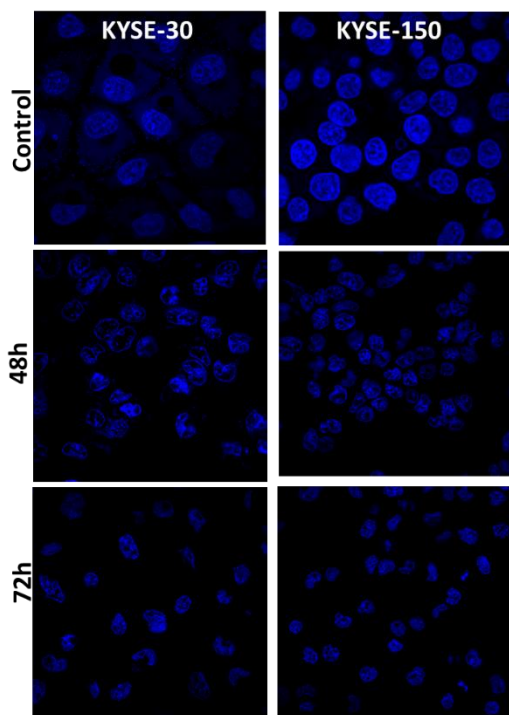


**Figure 8.5:** DAPI staining of KYSE-30 and KYSE-150 cells treated with **9g** for 48 h, and 72 h. The test was performed by Dr. Zui Pan Laboratory.

4',6-Diamidino-2-phenylindole dihydrochloride hydrate (DAPI) is a fluorescent sensitive staining dye that is useful for analyzing and visualizing nuclear changes and identifying cases of apoptosis. DAPI binds efficiently to adenine-thymine regions rich grooves in DNA. DAPI absorbs light at ultraviolet wavelength (359 nm) and emits a blue fluorescence at 461 nm. The measured fluorescence is proportional to the amount of DNA present in the stained cells. DAPI staining can help identify the nuclear morphology of apoptotic cells such as chromatin fragmentation and condensation.<sup>68,69</sup>

Therefore, nuclei staining of the cells treated with compound **9g** and stained with DAPI provided images that were obtained at various time points. As shown in Fig. 5, condensation of chromatin and fragmentation of nuclei membrane in both KYSE-30 and KYSE-150 when treated with **9g** at 10  $\mu$ M were noticeable at 48 h and 72 h compared to the control. After 72 h, loss of nuclei integrity was apparent. This result reveals **9g** could induce cell apoptosis.

### *Compound 9g induced apoptosis through the ERK pathway*

Since ERKs and protein kinase B (Akt) play a key role in a number of cellular processes such as proliferation, transcription and apoptosis, they are being targeting for developing novel inhibitors of cancer growth.<sup>14,70,71</sup> The potential mechanism of action of **9g** was examined *via* detecting expression of ERK and Akt proteins and their phosphorylated proteins by performing western blots on lysates of KYSE-150 and NES-G4T after treatment with 10  $\mu$ L of compound **9g** after 4 h, 8 h,

and 12 h. For KYSE-150, Figure 8.6A shows that **9g** down regulates pERK in a time dependent manner, while expression of Akt and pAkt seems similar from zero time till 12 h, compared to  $\beta$ -actin levels. Therefore, the ratio of pERK/ERK and pAkt/Akt were calculated and figure 6B shows a significant difference in the ratio pERK/ERK between 4 h and 12 h. Meanwhile, the pAkt/Akt ratio difference was insignificant as exposure duration increased. For NES-G4T, both pERK/ERK and pAKT/AKT ratio differences between 4 h and 12 h were not significant. These data demonstrate that treatment with **9g** induced apoptosis in ESSC cells through the ERK pathway but did not result in death of normal epithelial cells.

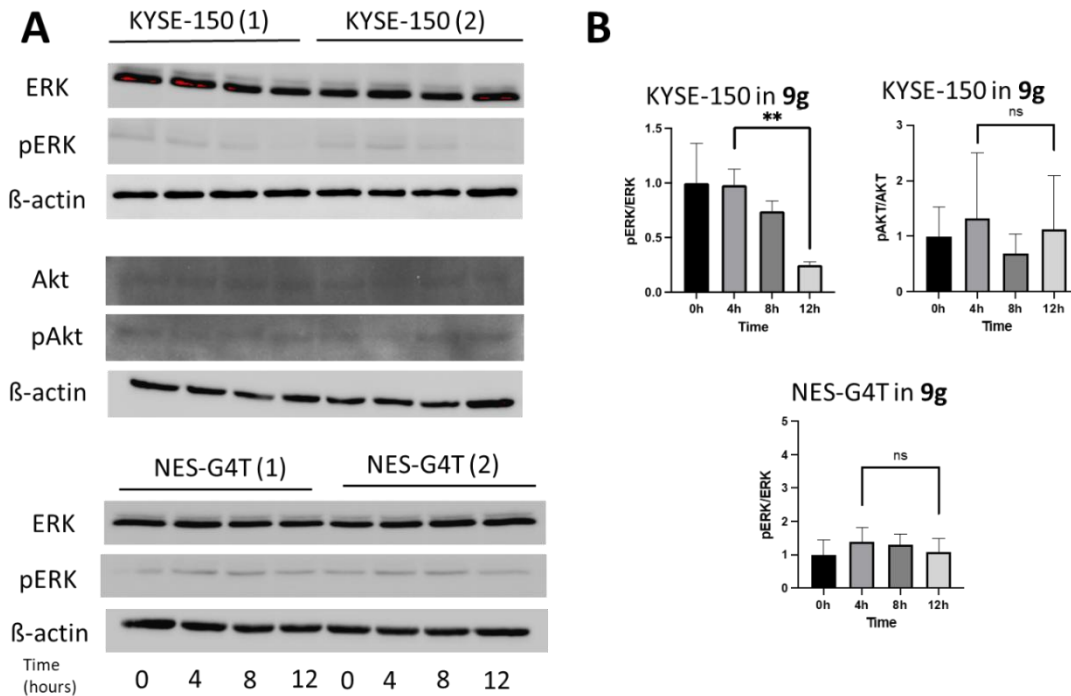


**Figure 8.6:** Induced apoptosis through the ERK pathway in KYSE-150 cells. (A) Western blots of proteins ERK, pERK, Akt, and pAkt in KYSE-150 and NES-G4T treated with **9g** (10  $\mu$ L) for 4 h, 8 h, and 12 h. Beta actin was used as the loading control. (B) Statistical data analysis of western blot results. Data is showed as mean  $\pm$  SEM. \*\* $p \leq 0.05$ . The test was performed by Dr. Zui Pan Laboratory.

### 8.2.3 Molecular Modeling Studies

Molecular modeling techniques are helpful approaches in medicinal chemistry assisting in identification of the parameters behind biological properties.<sup>66</sup> Computer-aided drug discovery (CADD) can be classified based on the targeted biological receptor whether it is known/isolated or unknown, therefore, it is categorized as structure- and ligand-based techniques.<sup>72</sup> Molecular docking is the most common approach for ligand-based technique, while pharmacophore and quantitative structure-activity relationship techniques are used for the unknown targets and based on previously reported studies.<sup>72,73</sup> Thus, drug design (CADD) approaches play a vital role in the pharmaceutical search to accelerate the process of discovering new lead compounds. Using the computational tools to analyze the actual facts and forming theoretical data helps in predicting the bioactivity of the designed molecules. It also provides us with rational ideas that help in modification and developing new novel compounds.

### 8.2.4 Molecular Docking Study

Molecular docking is a helpful tool in discovering novel candidates with improved potency based on previously isolated and co-crystallized lead/drug compound with targeted protein. There are number of discovered ERK inhibitors co-crystallized with ERK proteins (Figure 8.1 and 8.7) and some of them have been moved into clinical trials.<sup>74-76</sup>

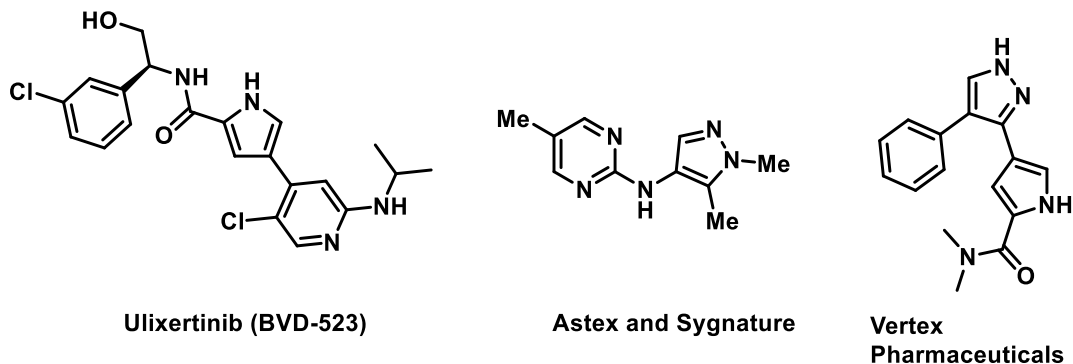


**Figure 8.7:** Important ERK inhibitors.



Molecular docking techniques have been useful for designing the targeted thiazolidines, confirming the observed biological activity and helping improve the activity for future designed thiazolidines and other derivatives. From recent studies done by pharmaceutical companies, it is obvious that the newly discovered ERK inhibitors bind to a number of amino acid residues in the target pocket with more hydrogen bond interactions thus improved and confirmed the

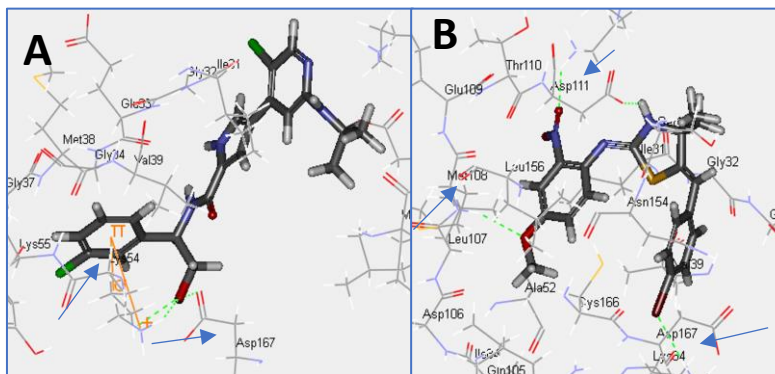


**Figure 8.8:** The docking study of 6gdq ERK protein with ulixertinib (A) and an example of thiazolidines (9g) (B).

corresponding activity compared to ulixertinib.<sup>74,76</sup> For instance, the Astex and Sygnature compound reveals hydrogen bonds with MET108 and LYS114 which is different from the clinical candidate ulixertinib. Similar observations have been made while running the standard CDOCKER technique (Discovery Studio 2.5 software, Accelrys Inc., San Diego, CA, USA) for our synthesized thiazolidines. Ulixertinib exhibits three hydrogen bond interactions due to the terminal alcohol moiety with LYS54 and ASP167,  $\pi$ -cation and  $\pi$ - $\sigma$  interactions between *p*-chlorophenyl and LYS54 with docking score -56.4471 kcal/mol. The thiazolidine docking studies show that the interactions with LYS54 are as expected and common among all the synthesized thiazolidine derivatives whether through hydrogen bond or  $\pi$ -cation interactions. Electron withdrawing groups attached to the aniline moiety makes the Br group attached to the benzylidene ring interact with LYS54 via a hydrogen bond interaction (**9a-b/g-h**) or  $\pi$ -cation interactions (**9c-d**). Derivatives containing electron-rich groups attached to aniline ring makes  $\pi$ -cation interactions with LYS54

with phenyl ring of aniline moiety (**9e-f**). The synthesized thiazolidines exhibit hydrogen bond interactions via the free NH thiazolyl group except compounds **9a-d**. As it is shown from the previously published work that interaction with MET108 is one of the main interactions corresponding to the observed activity,<sup>76</sup> similar observations were made with three of the synthesized thiazolidines (**9c-d** and **9g**) via anilinyll moiety substituted with electron withdrawing groups. Among all the synthesized thiazolidines, compound **9g** exhibits the best docking score (the lowest binding interactions) -47.5406 kcal/mol with the highest number of hydrogen bonds which supports its choice for further examinations among all other synthesized compounds and is consistent with the observed biodata. Also, the second two best thiazolidines in terms of binding interactions are **9c** and **9d**, showing close docking scores -42.6524, and -42.5816 kcal/mol, respectively. Thus, this docking study confirms that our novel thiazolidines match with the reported docking features of published and clinically valid ERK inhibitors. Moreover, all the previously mentioned observations support our initial design for this third thiazolidine library in which the electron deficient aryl rings were important for the expected activity based on the previous two studies of two thiazolidine libraries. To investigate is the importance of the imine group, we have removed the nitrogen from the exocyclic double bond and performed a docking study for all the compounds. Interestingly, only two common hydrogen bond interactions were noticed with ASP111 with thiazolyl NH and LYS54 with Br attached to benzyldiene system (example of **9g** without imine nitrogen). Thus, the imino nitrogen was crucial for MET108 interactions as it is shown from Figure 9B interactions of **9g** forming four different hydrogen bond interactions (thiazolyl NH – ASP111, NO<sub>2</sub> – LYS114, OMe – Met108, and Br – LYS54). Comparing compound **9g** with ulixertinib, thiazolidine **9g** reveals more hydrogen bond

interactions especially with MET108 which matches with other reported ERK inhibitors, and also, the docking scores for **9g** and ulixertinib are quite close in value.

### **8.2.5 3D-Pharmacophore study**

3D-Pharmacophoric approach can illuminate the parameters governing bio-properties in terms of molecular structural elements/functions with chemical feature interactions (hydrogen bonding, charge ionizable ... etc.) in 3D-array.<sup>67</sup> The synthesized thiazolidines **9a–i** were investigated using Discovery Studio 2.5 software obeying the standard protocol for assigning the 3D-pharmacophoric model.<sup>67</sup> Determination of the thiazolidinyl functional group interactions with the pharmacophoric features will assist in understanding the parameters necessary for bio-activity. Three pharmacophoric features (two hydrophobics “H-1, H-2” and a hydrogen-bonding acceptor) are the components of the 3D-array.

All the tested compounds show alignment of the phenyl group and its bromine substituent attached to the thiazolidinyl C-5 with H-1 and H-2, respectively. The sulfur heteroatom of the thiazolidinyl heterocycle is aligned with the hydrogen-bonding feature. The latter observation can explain the effect of the (un)substituted phenyl linked through imino linkage to the C-2 of thiazolidinyl heterocycle in controlling the antiproliferative activities. The different fits of the pharmacophoric features led to variable estimated bio-properties. The estimated antiproliferative properties of the effective agents synthesized **9a**, **9c** and **9i** ( $IC_{50} = 17.6–19.0 \mu M$ ) are consistent with their experimentally observed values ( $IC_{50} = 10.6–14.2 \mu M$ ). The same for the weak antiproliferative agents discovered.

### **8.2.6 QSAR study**

A mathematical equation obtained through QSAR techniques is capable of describing the biological properties in the form of physico-chemical/descriptor parameters which are the items

necessary for interpretation the bio-observations. QSAR model of the synthesized thiazolidines **9a-i** was assigned by CODESSA-Pro software utilizing BMLR (best multi-linear regression).<sup>68</sup> A two descriptor QSAR model was obtained with good correlation coefficient ( $R^2 = 0.852$ ). Hydrogen bonding acceptor dependent HDCA-1/TMSA (MOPAC PC) (all) is a charge-related descriptor ( $t = -3.778$ ). The appearance of this descriptor with its high coefficient value (-116.298) supports the observation due to the aforementioned 3D-pharmacophoric modeling technique revealing the alignment of hydrogen-bonding feature with the thiazolidinyl sulfur. The impact of this descriptor on the estimated antiproliferation properties is obvious due to its high coefficient value. This is easily revealed in compounds **9h** and **9i** which possess descriptor values = 0.01462, 0.01818 corresponding to estimated antiproliferative properties  $IC_{50} = 67.1, 11.2 \mu\text{M}$ , respectively. In other words, any slight/minor difference of descriptor value will greatly affect the estimated property due to high coefficient value of this descriptor. The molecular fractional hydrogen bonding donor ability can be calculated by equation (1).<sup>69</sup>

$$FHDC A1 = \frac{HDCA1}{TMSA} \dots\dots\dots \text{Equation (1)}$$

Since, *HDCA1* stands for to the hydrogen bonding donor ability of an atom. *TMSA* is corresponding to total molecular surface area.

Minimum one-electron reactivity index for atom *N* is a semi-empirical descriptor with negative coefficient value (-84.6416). Thus, the high mathematical descriptor value of an agent observes high estimated antiproliferative compound and vice versa as revealed by compounds **9a** and **9b** that possess descriptor values 0.00455, -0.00421 corresponding to estimated properties  $IC_{50} = 12.8$  and  $60.4 \mu\text{M}$ , respectively. The Fukui atomic one-electron reactivity index can be determined by equation (2).<sup>69</sup>

$$R_A = \sum_{i \in A} \sum_{j \in A} C_{iHOMO} C_{jLUMO} / (\epsilon_{LUMO} - \epsilon_{HOMO}) \dots\dots\dots \text{Equation (2)}$$

Since,  $C_{iHOMO}$  and  $C_{jLUMO}$  stand for the highest occupied and the lowest unoccupied molecular orbital coefficients. The  $\epsilon_{LUMO}$  and  $\epsilon_{HOMO}$  stand for the lowest unoccupied and the highest occupied molecular orbital energies.

Statistical internal validation parameters including standard deviation ( $s^2 = 0.021$ ) and Fisher criteria ( $F = 17.300$ ) support the goodness of the optimized QSAR model. The comparative cross-validation values of leave-one-out ( $R^2_{cvOO} = 0.729$ ) and leave-many-out ( $R^2_{cvMO} = 0.783$ ) to that of the QSAR equation ( $R^2 = 0.852$ ) also add evidence to the robust nature of the model. Additionally, the correlation due to the estimated and experimental observed antiproliferation properties of the tested thiazolidines preserving their potencies among each other is also a good sign for the success of the QSAR model. To conclude, the molecular modeling message is that QSAR model has confirmed the observed features analyzed by pharmacophore technique, revealing the importance of sulfur atom in the core structure of our designed and synthesized compounds. Moreover, existence of electron deficient aryl system attached to thiazolidinyl core motif is crucial for the expected activity and that supports the observed experimental values, in addition to the importance of the imine nitrogen (docking model). Thus, designing and discovering novel class of ERK inhibitors will be investigated in the near future based on the current molecular modeling techniques.

### 8.3 SUMMARY

In summary, a novel class of 2-imino-5-arylidine-thiazolidines has been discovered using an environmentally benign methodology. Discovery of stable thiazolidines has emerged through three stages by synthesizing three libraries of the targeted 2-imino-5-arylidine-thiazolidines via the chemistry developed in the Lovely lab. The reported library achieves the best chemical and

physical stabilities to date and establishes a new class of bioactive thiazolidines. The antiproliferative activity of the synthesized thiazolidines was tested using four different esophageal cancer cell lines, KYSE-30, KYSE-150, HET-1A, and NSE-G4T cells. The MTT assay was performed to study the cell viability under treatment with 10  $\mu$ M of synthesized thiazolidines, revealing two compounds (**9e** and **9g**) out of the nine synthesized thiazolidines are the best ones among the group. Further cell viability studies of eight different concentrations of the two compounds were performed for selecting the most toxic compound against carcinomic cell line and least effective against healthy cell lines, resulting in selection of **9g** for further investigations. DAPI staining was utilized to investigate the morphological changes as a result of cytotoxicity of **9g** against carcinomic KYSE-30 and KYSE-150 cell lines. The microscopic imaging guided us in selecting the KYSE-150 cell line which expresses antiapoptotic effect on the cell morphology. Therefore, two kinases (ERK and AKT) were targeted to be tested with thiazolidine **9g** using qRT-PCR, resulting in determining that the inhibition of the phosphorylation of ERK pathway is a possible mechanism behind the observed anticancer activity of **9g**. Molecular modeling techniques have been utilized on the designed thiazolidines confirm the observed activity. A QSAR study shows that the electron deficient aryl rings attached to the thiazolidine core ring might enhance their corresponding activity, and that is confirmed by the reported activity. The molecular docking study has emphasized the importance of attaching an electron withdrawing group to benzylidene moiety and existence of the exocyclic imine group. Thus, the molecular modeling techniques provide a guide to validate and confirm the observed activity.

#### 8.4 REFERENCES:

- (1) Sung, H.; Ferlay, J.; Siegel, R. L.; Laversanne, M.; Soerjomataram, I.; Jemal, A.; Bray, F. Global Cancer Statistics 2020: GLOBOCAN Estimates of Incidence and Mortality Worldwide for 36 Cancers in 185 Countries. *CA. Cancer J. Clin.* **2021**, *71* (3), 209–249. <https://doi.org/https://doi.org/10.3322/caac.21660>.
- (2) Naresh, R.; Nazeer, Y.; Palani, S. In Silico Evaluation of Modes of Action of Anticancer Compounds on Molecular Targets for Cancer. *Med. Chem. Res.* **2013**, *22* (4), 1938–1947. <https://doi.org/10.1007/s00044-012-0198-4>.
- (3) De Bock, K.; Mazzone, M.; Carmeliet, P. Antiangiogenic Therapy, Hypoxia, and Metastasis: Risky Liaisons, or Not? *Nature Reviews Clinical Oncology*. 2011, pp 8, 393–404. <https://doi.org/10.1038/nrclinonc.2011.83>.
- (4) Yang, S.; Zhang, J. J.; Huang, X. Y. Orai1 and STIM1 Are Critical for Breast Tumor Cell Migration and Metastasis. *Cancer Cell* **2009**, *15* (2), 124–134. <https://doi.org/10.1016/j.ccr.2008.12.019>.
- (5) Steeg, P. S. Targeting Metastasis. *Nat. Rev. Cancer* **2016**, *16* (4), 201–218. <https://doi.org/10.1038/nrc.2016.25>.
- (6) Qian, C.-N.; Mei, Y.; Zhang, J. Cancer Metastasis: Issues and Challenges. *Chin. J. Cancer* **2017**, *36* (1), 38. <https://doi.org/10.1186/s40880-017-0206-7>.
- (7) Galluzzi, L.; Maiuri, M. C.; Vitale, I.; Zischka, H.; Castedo, M.; Zitvogel, L.; Kroemer, G. Cell Death Modalities: Classification and Pathophysiological Implications. *Cell Death and Differentiation*. **2007**, pp 14, 1237–1243. <https://doi.org/10.1038/sj.cdd.4402148>.
- (8) Kroemer, G.; Galluzzi, L.; Vandenabeele, P.; Abrams, J.; Alnemri, E. S.; Baehrecke, E. H.; Blagosklonny, M. V.; El-Deiry, W. S.; Golstein, P.; Green, D. R.; Hengartner, M.; Knight, R. A.; Kumar, S.; Lipton, S. A.; Malorni, W.; Nuñez, G.; Peter, M. E.; Tschopp, J.; Yuan, J.; Piacentini, M.; Zhivotovsky, B.; Melino, G. Classification of Cell Death: Recommendations of the Nomenclature Committee on Cell Death 2009. *Cell Death and Differentiation*. **2009**, pp 16, 3–11. <https://doi.org/10.1038/cdd.2008.150>.
- (9) Galluzzi, L.; Bravo-San Pedro, J. M.; Vitale, I.; Aaronson, S. A.; Abrams, J. M.; Adam, D.; Alnemri, E. S.; Altucci, L.; Andrews, D.; Annicchiarico-Petruzzelli, M.; Baehrecke, E. H.; Bazan, N. G.; Bertrand, M. J.; Bianchi, K.; Blagosklonny, M. V.; Blomgren, K.; Borner, C.; Bredesen, D. E.; Brenner, C.; Campanella, M.; Candi, E.; Cecconi, F.; Chan, F. K.; Chandel, N. S.; Cheng, E. H.; Chipuk, J. E.; Cidlowski, J. A.; Ciechanover, A.; Dawson, T. M.; Dawson, V. L.; De Laurenzi, V.; De Maria, R.; Debatin, K. M.; Di Daniele, N.; Dixit, V. M.; Dynlacht, B. D.; El-Deiry, W. S.; Fimia, G. M.; Flavell, R. A.; Fulda, S.; Garrido, C.;

- Gougeon, M. L.; Green, D. R.; Gronemeyer, H.; Hajnoczky, G.; Hardwick, J. M.; Hengartner, M. O.; Ichijo, H.; Joseph, B.; Jost, P. J.; Kaufmann, T.; Kepp, O.; Klionsky, D. J.; Knight, R. A.; Kumar, S.; Lemasters, J. J.; Levine, B.; Linkermann, A.; Lipton, S. A.; Lockshin, R. A.; López-Otín, C.; Lugli, E.; Madeo, F.; Malorni, W.; Marine, J. C.; Martin, S. J.; Martinou, J. C.; Medema, J. P.; Meier, P.; Melino, S.; Mizushima, N.; Moll, U.; Muñoz-Pinedo, C.; Nuñez, G.; Oberst, A.; Panaretakis, T.; Penninger, J. M.; Peter, M. E.; Piacentini, M.; Pinton, P.; Prehn, J. H.; Puthalakath, H.; Rabinovich, G. A.; Ravichandran, K. S.; Rizzuto, R.; Rodrigues, C. M.; Rubinsztein, D. C.; Rudel, T.; Shi, Y.; Simon, H. U.; Stockwell, B. R.; Szabadkai, G.; Tait, S. W.; Tang, H. L.; Tavernarakis, N.; Tsujimoto, Y.; Vanden Berghe, T.; Vandenabeele, P.; Villunger, A.; Wagner, E. F.; Walczak, H.; White, E.; Wood, W. G.; Yuan, J.; Zakeri, Z.; Zhivotovsky, B.; Melino, G.; Kroemer, G. Essential versus Accessory Aspects of Cell Death: Recommendations of the NCCD 2015. *Cell Death and Differentiation*. **2015**, pp 22, 58–73. <https://doi.org/10.1038/cdd.2014.137>.
- (10) Méry, B.; Guy, J. B.; Vallard, A.; Espenel, S.; Ardail, D.; Rodriguez-Lafrasse, C.; Rancoule, C.; Magné, N. In Vitro Cell Death Determination for Drug Discovery: A Landscape Review of Real Issues. *Journal of Cell Death*. **2017**, pp 10, 1–8. <https://doi.org/10.1177/1179670717691251>.
- (11) Ocker, M.; Höpfner, M. Apoptosis-Modulating Drugs for Improved Cancer Therapy. *Eur. Surg. Res.* **2012**, 48 (3), 111–120. <https://doi.org/10.1159/000336875>.
- (12) Wajant, H.; Pfizenmaier, K.; Scheurich, P. Tumor Necrosis Factor Signaling. *Cell Death Differ.* **2003**, 10 (1), 45–65. <https://doi.org/10.1038/sj.cdd.4401189>.
- (13) Baud, V.; Karin, M. Signal Transduction by Tumor Necrosis Factor and Its Relatives. *Trends Cell Biol.* **2001**, 11 (9), 372–377. [https://doi.org/10.1016/s0962-8924\(01\)02064-5](https://doi.org/10.1016/s0962-8924(01)02064-5).
- (14) Mandal, R.; Raab, M.; Matthes, Y.; Becker, S.; Knecht, R.; Strebhardt, K. PERK 1/2 Inhibit Caspase-8 Induced Apoptosis in Cancer Cells by Phosphorylating It in a Cell Cycle Specific Manner. *Mol. Oncol.* **2014**, 8 (2), 232–249. <https://doi.org/https://doi.org/10.1016/j.molonc.2013.11.003>.
- (15) Pfeffer, C. M.; Singh, A. T. K. Apoptosis: A Target for Anticancer Therapy. *Int. J. Mol. Sci.* **2018**, 19 (2), 448. <https://doi.org/10.3390/ijms19020448>.
- (16) Kobayashi, S. D.; Voyich, J. M.; Whitney, A. R.; DeLeo, F. R. Spontaneous Neutrophil Apoptosis and Regulation of Cell Survival by Granulocyte Macrophage-Colony Stimulating Factor. *J. Leukoc. Biol.* **2005**, 78 (6), 1408–1418. <https://doi.org/https://doi.org/10.1189/jlb.0605289>.
- (17) Wang, M. L.; Tuli, R.; Manner, P. A.; Sharkey, P. F.; Hall, D. J.; Tuan, R. S. Direct and



- Indirect Induction of Apoptosis in Human Mesenchymal Stem Cells in Response to Titanium Particles. *J. Orthop. Res.* **2003**, *21* (4), 697–707. [https://doi.org/https://doi.org/10.1016/S0736-0266\(02\)00241-3](https://doi.org/https://doi.org/10.1016/S0736-0266(02)00241-3).
- (18) Hanahan, D.; Weinberg, R. A. The Hallmarks of Cancer. *Cell* **2000**, *100* (1), 57–70. [https://doi.org/https://doi.org/10.1016/S0092-8674\(00\)81683-9](https://doi.org/https://doi.org/10.1016/S0092-8674(00)81683-9).
- (19) Hanahan, D.; Weinberg, R. A. Hallmarks of Cancer: The Next Generation. *Cell* **2011**, *144* (5), 646–674. <https://doi.org/https://doi.org/10.1016/j.cell.2011.02.013>.
- (20) Norbury, C. J.; Hickson, I. D. Cellular Responses to DNA Damage. *Annu. Rev. Pharmacol. Toxicol.* **2001**, *41*, 367–401. <https://doi.org/10.1146/annurev.pharmtox.41.1.367>.
- (21) Soares-Silva, M.; Diniz, F. F.; Gomes, G. N.; Bahia, D. The Mitogen-Activated Protein Kinase (MAPK) Pathway: Role in Immune Evasion by Trypanosomatids. *Front. Microbiol.* **2016**, *7*, 183. <https://doi.org/10.3389/fmicb.2016.00183>.
- (22) Johnson, G. L.; Lapadat, R. Mitogen-Activated Protein Kinase Pathways Mediated by ERK, JNK, and P38 Protein Kinases. *Science* (80). **2002**, *298* (5600), 1911–1912. <https://doi.org/10.1126/science.1072682>.
- (23) Owens, D. M.; Keyse, S. M. Differential Regulation of MAP Kinase Signalling by Dual-Specificity Protein Phosphatases. *Oncogene* **2007**, *26* (22), 3203–3213. <https://doi.org/10.1038/sj.onc.1210412>.
- (24) Zhang, Y.; Dong, C. Regulatory Mechanisms of Mitogen-Activated Kinase Signaling. *Cell. Mol. Life Sci.* **2007**, *64* (21), 2771–2789. <https://doi.org/10.1007/s00018-007-7012-3>.
- (25) Dong, C.; Davis, R. J.; Flavell, R. A. MAP Kinases in the Immune Response. *Annu. Rev. Immunol.* **2002**, *20* (1), 55–72. <https://doi.org/10.1146/annurev.immunol.20.091301.131133>.
- (26) Roskoski, R. J. ERK1/2 MAP Kinases: Structure, Function, and Regulation. *Pharmacol. Res.* **2012**, *66* (2), 105–143. <https://doi.org/10.1016/j.phrs.2012.04.005>.
- (27) Wortzel, I.; Seger, R. The ERK Cascade: Distinct Functions within Various Subcellular Organelles. *Genes Cancer* **2011**, *2* (3), 195–209. <https://doi.org/10.1177/1947601911407328>.
- (28) Chin, H. M.; Lai, D. K.; Falhook, G. S. Extracellular Signal-Regulated Kinase (ERK) Inhibitors in Oncology Clinical Trials. *J. Immunother. Precis. Oncol.* **2020**, *2* (1), 10–16. [https://doi.org/10.4103/JIPO.JIPO\\_17\\_18](https://doi.org/10.4103/JIPO.JIPO_17_18).
- (29) Portelinha, A.; Thompson, S.; Smith, R. A.; Da Silva Ferreira, M.; Asgari, Z.; Knezevic,

- A.; Seshan, V.; de Stanchina, E.; Gupta, S.; Denis, L.; Younes, A.; Reddy, S. ASN007 Is a Selective ERK1/2 Inhibitor with Preferential Activity against RAS-and RAF-Mutant Tumors. *Cell Reports Med.* **2021**, *2* (7), 100350. <https://doi.org/https://doi.org/10.1016/j.xcrm.2021.100350>.
- (30) 6-Oesophagus-fact-sheet.pdf (iarc.fr) 6-Oesophagus-fact-sheet.pdf (iarc.fr).
- (31) Chen, Z.; Hu, X.; Wu, Y.; Cong, L.; He, X.; Lu, J.; Feng, J.; Liu, D. Long Non-Coding RNA XIST Promotes the Development of Esophageal Cancer by Sponging MiR-494 to Regulate CDK6 Expression. *Biomed. Pharmacother.* **2019**, *109*, 2228–2236. <https://doi.org/10.1016/j.biopha.2018.11.049>.
- (32) Li, J.; Wang, T.; Pei, L.; Jing, J.; Hu, W.; Sun, T.; Liu, H. Expression of VRK1 and the Downstream Gene BANF1 in Esophageal Cancer. *Biomed. Pharmacother.* **2017**. <https://doi.org/10.1016/j.biopha.2017.02.095>.
- (33) Arnold, M.; Ferlay, J.; Van Berge Henegouwen, M. I.; Soerjomataram, I. Global Burden of Oesophageal and Gastric Cancer by Histology and Subsite in 2018. *Gut* **2020**, *69* (9), 1564–1571. <https://doi.org/10.1136/gutjnl-2020-321600>.
- (34) Arnal, M. J. D.; Arenas, Á. F.; Arbeloa, Á. L. Esophageal Cancer: Risk Factors, Screening and Endoscopic Treatment in Western and Eastern Countries. *World Journal of Gastroenterology*. 2015. <https://doi.org/10.3748/wjg.v21.i26.7933>.
- (35) di Pietro, M.; Canto, M. I.; Fitzgerald, R. C. Endoscopic Management of Early Adenocarcinoma and Squamous Cell Carcinoma of the Esophagus: Screening, Diagnosis, and Therapy. *Gastroenterology* **2018**. <https://doi.org/10.1053/j.gastro.2017.07.041>.
- (36) Ying, J.; Zhang, M.; Qiu, X.; Lu, Y. The Potential of Herb Medicines in the Treatment of Esophageal Cancer. *Biomedicine and Pharmacotherapy*. **2018**. <https://doi.org/10.1016/j.biopha.2018.04.088>.
- (37) Higuchi, K.; Koizumi, W.; Tanabe, S.; Sasaki, T.; Katada, C.; Azuma, M.; Nakatani, K.; Ishido, K.; Naruke, A.; Ryu, T. Current Management of Esophageal Squamous-Cell Carcinoma in Japan and Other Countries. *Gastrointest. Cancer Res.* **2010**.
- (38) Chang, Y.-S.; Liu, J.-C.; Fu, H.-Q.; Yu, B.-T.; Zou, S.-B.; Wu, Q.-C.; Wan, L. [Roles of Targeting Ras/Raf/MEK/ERK Signaling Pathways in the Treatment of Esophageal Carcinoma]. *Yao Xue Xue Bao* **2013**, *48* (5), 635—641.
- (39) Zheng, S.-T.; Huo, Q.; Tuerxun, A.; Ma, W.-J.; Lv, G.-D.; Huang, C.-G.; Liu, Q.; Wang, X.; Lin, R.-Y.; Sheyhidin, I.; Lu, X.-M. The Expression and Activation of ERK/MAPK Pathway in Human Esophageal Cancer Cell Line EC9706. *Mol. Biol. Rep.* **2011**, *38* (2),

865–872. <https://doi.org/10.1007/s11033-010-0178-z>.

- (40) Yanchun, M.; Yi, W.; Lu, W.; Yu, Q.; Jian, Y.; Pengzhou, K.; Ting, Y.; Hongyi, L.; Fang, W.; Xiaolong, C.; Yongping, C. Triptolide Prevents Proliferation and Migration of Esophageal Squamous Cell Cancer via MAPK/ERK Signaling Pathway. *Eur. J. Pharmacol.* **2019**, *851*, 43–51. <https://doi.org/10.1016/j.ejphar.2019.02.030>.
- (41) Shi, H.; Ju, Q.; Mao, Y.; Wang, Y.; Ding, J.; Liu, X.; Tang, X.; Sun, C. TAK1 Phosphorylates RASSF9 and Inhibits Esophageal Squamous Tumor Cell Proliferation by Targeting the RAS/MEK/ERK Axis. *Adv. Sci.* **2021**, *8* (5), 2001575. <https://doi.org/https://doi.org/10.1002/advs.202001575>.
- (42) Wang, H.; Zhang, Y.; Yun, H.; Chen, S.; Chen, Y.; Liu, Z. ERK Expression and Its Correlation with STAT1 in Esophageal Squamous Cell Carcinoma. *Oncotarget* **2017**, *8* (28), 45249–45258. <https://doi.org/10.18632/oncotarget.16902>.
- (43) Gouda, M. A.; Abu-Hashem, A. A. Synthesis, Characterization, Antioxidant and Antitumor Evaluation of Some New Thiazolidine and Thiazolidinone Derivatives. *Arch. Pharm. (Weinheim)*. **2011**, *344*, 170–177. <https://doi.org/10.1002/ardp.201000165>.
- (44) Nishida, S.; Maruoka, H.; Yoshimura, Y.; Goto, T.; Tomita, R.; Masumoto, E.; Okabe, F.; Yamagata, K.; Fujioka, T. Synthesis and Biological Activities of Some New Thiazolidine Derivatives Containing Pyrazole Ring System. *J. Heterocycl. Chem.* **2012**, *49* (2), 303–309. <https://doi.org/https://doi.org/10.1002/jhet.834>.
- (45) Zhang, Q.; Zhou, H.; Zhai, S.; Yan, B. Natural Product-Inspired Synthesis of Thiazolidine and Thiazolidinone Compounds and Their Anticancer Activities. *Curr. Pharm. Des.* **2010**, *16* (16), 1826–1842. <https://doi.org/10.2174/138161210791208983>.
- (46) Havrylyuk, D.; Zimenkovsky, B.; Vasylenko, O.; Lesyk, R. Synthesis and Anticancer and Antiviral Activities of New 2-Pyrazoline-Substituted 4-Thiazolidinones. *J. Heterocycl. Chem.* **2013**, *50* (S1), E55–E62. <https://doi.org/https://doi.org/10.1002/jhet.1056>.
- (47) Osmaniye, D.; Levent, S.; Ardiç, C. M.; Atlı, Ö.; Özkay, Y.; Kaplancıklı, Z. A. Synthesis and Anticancer Activity of Some Novel Benzothiazole-Thiazolidine Derivatives. *Phosphorus. Sulfur. Silicon Relat. Elem.* **2018**, *193* (4), 249–256. <https://doi.org/10.1080/10426507.2017.1395878>.
- (48) El-Gaby, M. S. A.; Ismail, Z. H.; Abdel-Gawad, S. M.; Aly, H. M.; Ghorab, M. M. Synthesis of Thiazolidine and Thiophene Derivatives for Evaluation as Anticancer Agents. *Phosphorus. Sulfur. Silicon Relat. Elem.* **2009**, *184* (10), 2645–2654. <https://doi.org/10.1080/10426500802561096>.

- (49) Singh, R. P.; Aziz, M. N.; Gout, D.; Fayad, W.; El-Manawaty, M. A.; Lovely, C. J. Novel Thiazolidines: Synthesis, Antiproliferative Properties and 2D-QSAR Studies. *Bioorganic Med. Chem.* **2019**, *27* (20), 115047. <https://doi.org/10.1016/j.bmc.2019.115047>.
- (50) Geronikaki, A. A.; Lagunin, A. A.; Hadjipavlou-Litina, D. I.; Eleftheriou, P. T.; Filimonov, D. A.; Poroikov, V. V.; Alam, I.; Saxena, A. K. Computer-Aided Discovery of Anti-Inflammatory Thiazolidinones with Dual Cyclooxygenase/Lipoxygenase Inhibition. *J. Med. Chem.* **2008**, *51* (6), 1601–1609. <https://doi.org/10.1021/jm701496h>.
- (51) Ma, L.; Xie, C.; Ma, Y.; Liu, J.; Xiang, M.; Ye, X.; Zheng, H.; Chen, Z.; Xu, Q.; Chen, T.; Chen, J.; Yang, J.; Qiu, N.; Wang, G.; Liang, X.; Peng, A.; Yang, S.; Wei, Y.; Chen, L. Synthesis and Biological Evaluation of Novel 5-Benzylidenethiazolidine-2,4-Dione Derivatives for the Treatment of Inflammatory Diseases. *J. Med. Chem.* **2011**. <https://doi.org/10.1021/jm1011534>.
- (52) Barros, C. D.; Amato, A. A.; de Oliveira, T. B.; Iannini, K. B. R.; Silva, A. L. da; Silva, T. G. da; Leite, E. S.; Hernandez, M. Z.; Alves de Lima, M. do C.; Galdino, S. L.; Neves, F. de A. R.; Pitta, I. da R. Synthesis and Anti-Inflammatory Activity of New Arylidene-Thiazolidine-2,4-Diones as PPAR $\gamma$  Ligands. *Bioorg. Med. Chem.* **2010**, *18* (11), 3805–3811. <https://doi.org/10.1016/j.bmc.2010.04.045>.
- (53) Datar, P. A.; Aher, S. B. Design and Synthesis of Novel Thiazolidine-2,4-Diones as Hypoglycemic Agents. *J. Saudi Chem. Soc.* **2016**. <https://doi.org/10.1016/j.jscs.2012.10.010>.
- (54) Siddiqui, I. R.; Singh, P. K.; Singh, J.; Singh, J. Synthesis and Fungicidal Activity of Novel 4,4'-Bis(2''-Aryl-5''-Methyl/Unsubstituted-4''-Oxo-Thiazolidin-3''-Yl) Bibenzyl. *J. Agric. Food Chem.* **2003**. <https://doi.org/10.1021/jf0342324>.
- (55) Shiradkar, M. R.; Ghodake, M.; Bothara, K. G.; Bhandari, S. V.; Nikalje, A.; Akula, K. C.; Desai, N. C.; Burange, P. J. Synthesis and Anticonvulsant Activity of Clubbed Thiazolidinone-Barbituric Acid and Thiazolidinone-Triazole Derivatives. *Arkivoc* **2007**. <https://doi.org/10.3998/ark.5550190.0008.e08>.
- (56) Moreira, D. R. M.; Costa, S. P. M.; Hernandez, M. Z.; Rabello, M. M.; de Oliveira Filho, G. B.; de Melo, C. M. L.; da Rocha, L. F.; de Simone, C. A.; Ferreira, R. S.; Fradico, J. R. B.; Meira, C. S.; Guimarães, E. T.; Srivastava, R. M.; Pereira, V. R. A.; Soares, M. B. P.; Leite, A. C. L. Structural Investigation of Anti-Trypanosoma Cruzi 2-Iminothiazolidin-4-Ones Allows the Identification of Agents with Efficacy in Infected Mice. *J. Med. Chem.* **2012**, *55* (24), 10918–10936. <https://doi.org/10.1021/jm301518v>.
- (57) Zehetmeyr, F. K.; da Silva, M. A. M. P.; Pereira, K. M.; Berne, M. E. A.; Cunico, W.;

- Campos, J. C. J.; Gouvea, D. P.; da Silva Nascente, P.; de Oliveira Hübner, S.; Siqueira, G. M. Ovicidal in Vitro Activity of 2-Aryl-3-(2-Morpholinoethyl)Thiazolidin-4-Ones and 2-Aryl-3-(3-Morpholinopropyl)Thiazolidin-4-Ones against *Fasciola Hepatica* (Linnaeus, 1758). *Exp. Parasitol.* **2018**, *192*, 60–64. <https://doi.org/10.1016/j.exppara.2018.07.012>.
- (58) Jiang, S.; Tala, S. R.; Lu, H.; Abo-Dya, N. E.; Avan, I.; Gyanda, K.; Lu, L.; Katritzky, A. R.; Debnath, A. K. Design, Synthesis, and Biological Activity of Novel 5-((Arylfuran/1H-Pyrrol-2-Yl)Methylene)-2-Thioxo-3-(3-(Trifluoromethyl)Phenyl)Thiazolidin-4-Ones as HIV-1 Fusion Inhibitors Targeting Gp41. *J. Med. Chem.* **2011**, *54* (2), 572–579. <https://doi.org/10.1021/jm101014v>.
- (59) Barreca, M. L.; Balzarini, J.; Chimirri, A.; De Clercq, E.; De Luca, L.; Höltje, H. D.; Höltje, M.; Monforte, A. M.; Monforte, P.; Pannecouque, C.; Rao, A.; Zappalà, M. Design, Synthesis, Structure-Activity Relationships, and Molecular Modeling Studies of 2,3-Diaryl-1,3-Thiazolidin-4-Ones as Potent Anti-HIV Agents. *J. Med. Chem.* **2002**, *45* (24), 5410–5413. <https://doi.org/10.1021/jm020977+>.
- (60) Rajeswari, T.; Rekha, T.; Dinneswara Reddy, G.; Padmaja, A.; Padmavathi, V. Synthesis and Antibacterial Activity of Benzazolyl Azolyl Sulfamoyl Acetamides. *J. Heterocycl. Chem.* **2019**, *56* (9), 2449–2459. <https://doi.org/https://doi.org/10.1002/jhet.3634>.
- (61) Deep, A.; Kumar, P.; Narasimhan, B.; Ramasamy, K.; Mani, V.; Mishra, R. K.; Majeed, A. B. A. Synthesis, Antimicrobial, Anticancer Evaluation of 2-(Aryl)-4- Thiazolidinone Derivatives and Their QSAR Studies. *Curr. Top. Med. Chem.* **2015**, *15* (11), 990–1002. <https://doi.org/10.2174/1568026615666150317221849>.
- (62) Singh, R. P.; Gout, D.; Lovely, C. J. Tandem Thioacylation-Intramolecular Hydrosulfenylation of Propargyl Amines – Rapid Access to 2-Aminothiazolidines. *European J. Org. Chem.* **2019**, *8*, 1726–1740. <https://doi.org/10.1002/ejoc.201801505>.
- (63) Aziz, M. N.; Patel, A.; Iskander, A.; Chini, A.; Gout, D.; Mandal, S. S.; Lovely, C. J. One-Pot Synthesis of Novel 2-Imino-5-Arylidine-Thiazolidine Analogues and Evaluation of Their Anti-Proliferative Activity against MCF7 Breast Cancer Cell Line. *Molecules* **2022**, *27* (3), 841. <https://doi.org/10.3390/molecules27030841>.
- (64) Srour, A. M.; Panda, S. S.; M Salman, A. M.; El-Manawaty, M. A.; George, R. F.; Shalaby, E. M.; Fitch, A. N.; Fawzy, N. G.; Girgis, A. S. Synthesis & Molecular Modeling Studies of Bronchodilatory Active Indole-Pyridine Conjugates. *Future Med. Chem.* **2018**. <https://doi.org/10.4155/fmc-2018-0039>.
- (65) Ying, J.; Le, Z.; Wu, X.-F. Benzene-1,3,5-Triyl Triformate (TFBen)-Promoted Palladium-Catalyzed Carbonylative Synthesis of 2-Oxo-2,5-Dihydropyrroles from Propargyl Amines.

- Org. Lett.* **2020**, 22 (1), 194–198. <https://doi.org/10.1021/acs.orglett.9b04147>.
- (66) Marian N. Aziz, Arzoo Patel, Amany Iskander, Avisankar Chini, Delphine Gout, S. S. M.; Carl J. Lovely. One-Pot Synthesis of Novel 2-Imino-5-Arylidine-Thiazolidine Analogues and Evaluation of Their Anti-Proliferative Activity against MCF7 Breast Cancer Cell Line. *Molecules* **2022**, Inpress.
- (67) Mosmann, T. Rapid Colorimetric Assay for Cellular Growth and Survival: Application to Proliferation and Cytotoxicity Assays. *J. Immunol. Methods* **1983**, 65 (1), 55–63. [https://doi.org/https://doi.org/10.1016/0022-1759\(83\)90303-4](https://doi.org/https://doi.org/10.1016/0022-1759(83)90303-4).
- (68) Sreelatha, S.; Jeyachitra, A.; Padma, P. R. Antiproliferation and Induction of Apoptosis by Moringa Oleifera Leaf Extract on Human Cancer Cells. *Food Chem. Toxicol.* **2011**, 49 (6), 1270–1275. <https://doi.org/https://doi.org/10.1016/j.fct.2011.03.006>.
- (69) Choi, B.-Y.; Kim, H.-Y.; Lee, K.-H.; Cho, Y.-H.; Kong, G. Clofilium, a Potassium Channel Blocker, Induces Apoptosis of Human Promyelocytic Leukemia (HL-60) Cells via Bcl-2-Insensitive Activation of Caspase-3. *Cancer Lett.* **1999**, 147 (1), 85–93. [https://doi.org/https://doi.org/10.1016/S0304-3835\(99\)00280-3](https://doi.org/https://doi.org/10.1016/S0304-3835(99)00280-3).
- (70) Liang, Y.; Chen, J.; Yu, Q.; Ji, T.; Zhang, B.; Xu, J.; Dai, Y.; Xie, Y.; Lin, H.; Liang, X.; Cai, X. Phosphorylated ERK Is a Potential Prognostic Biomarker for Sorafenib Response in Hepatocellular Carcinoma. *Cancer Med.* **2017**, 6 (12), 2787–2795. <https://doi.org/10.1002/cam4.1228>.
- (71) Will, M.; Qin, A. C. R.; Toy, W.; Yao, Z.; Rodrik-Outmezguine, V.; Schneider, C.; Huang, X.; Monian, P.; Jiang, X.; de Stanchina, E.; Baselga, J.; Liu, N.; Chandarlapaty, S.; Rosen, N. Rapid Induction of Apoptosis by PI3K Inhibitors Is Dependent upon Their Transient Inhibition of RAS-ERK Signaling. *Cancer Discov.* **2014**, 4 (3), 334–347. <https://doi.org/10.1158/2159-8290.CD-13-0611>.
- (72) Wang, T.; Wu, M.-B.; Lin, J.-P.; Yang, L.-R. Quantitative Structure–Activity Relationship: Promising Advances in Drug Discovery Platforms. *Expert Opin. Drug Discov.* **2015**, 10 (12), 1283–1300. <https://doi.org/10.1517/17460441.2015.1083006>.
- (73) Sprou, D. G.; Palmer, R. K.; Swanson, J. T.; Lawless, M. QSAR in the Pharmaceutical Research Setting: QSAR Models for Broad, Large Problems. *Curr. Top. Med. Chem.* **2010**, 10 (6), 619–637. <https://doi.org/10.2174/156802610791111506>.
- (74) Aronov, A. M.; Baker, C.; Bemis, G. W.; Cao, J.; Chen, G.; Ford, P. J.; Germann, U. A.; Green, J.; Hale, M. R.; Jacobs, M.; Janetka, J. W.; Maltais, F.; Martinez-Botella, G.; Namchuk, M. N.; Straub, J.; Tang, Q.; Xie, X. Flipped Out: Structure-Guided Design of Selective Pyrazolopyrrole ERK Inhibitors. *J. Med. Chem.* **2007**, 50 (6), 1280–1287.

<https://doi.org/10.1021/jm061381f>.

- (75) Germann, U. A.; Furey, B. F.; Markland, W.; Hoover, R. R.; Aronov, A. M.; Roix, J. J.; Hale, M.; Boucher, D. M.; Sorrell, D. A.; Martinez-Botella, G.; Fitzgibbon, M.; Shapiro, P.; Wick, M. J.; Samadani, R.; Meshaw, K.; Groover, A.; DeCrescenzo, G.; Namchuk, M.; Emery, C. M.; Saha, S.; Welsch, D. J. Targeting the MAPK Signaling Pathway in Cancer: Promising Preclinical Activity with the Novel Selective ERK1/2 Inhibitor BVD-523 (Ulixertinib). *Mol. Cancer Ther.* **2017**, *16* (11), 2351–2363. <https://doi.org/10.1158/1535-7163.MCT-17-0456>.
- (76) Heightman, T. D.; Berdini, V.; Braithwaite, H.; Buck, I. M.; Cassidy, M.; Castro, J.; Courtin, A.; Day, J. E. H.; East, C.; Fazal, L.; Graham, B.; Griffiths-Jones, C. M.; Lyons, J. F.; Martins, V.; Muench, S.; Munck, J. M.; Norton, D.; O'Reilly, M.; Palmer, N.; Pathuri, P.; Reader, M.; Rees, D. C.; Rich, S. J.; Richardson, C.; Saini, H.; Thompson, N. T.; Wallis, N. G.; Walton, H.; Wilsher, N. E.; Woolford, A. J.-A.; Cooke, M.; Cousin, D.; Onions, S.; Shannon, J.; Watts, J.; Murray, C. W. Fragment-Based Discovery of a Potent, Orally Bioavailable Inhibitor That Modulates the Phosphorylation and Catalytic Activity of ERK1/2. *J. Med. Chem.* **2018**, *61* (11), 4978–4992. <https://doi.org/10.1021/acs.jmedchem.8b00421>.
- (77) Cui, C.; Chang, Y.; Zhang, X.; Choi, S.; Tran, H.; Penmetsa, K. V.; Viswanadha, S.; Fu, L.; Pan, Z. Targeting Orai1-Mediated Store-Operated Calcium Entry by RP4010 for Anti-Tumor Activity in Esophagus Squamous Cell Carcinoma. *Cancer Lett.* **2018**. <https://doi.org/10.1016/j.canlet.2018.06.006>.
- (78) Choi, S.; Cui, C.; Luo, Y.; Kim, S.-H.; Ko, J.; Huo, X.; Ma, J.; Fu, L.-W.; Souza, R. F.; Korichneva, I.; Pan, Z. Selective Inhibitory Effects of Zinc on Cell Proliferation in Esophageal Squamous Cell Carcinoma through Orai1. *FASEB J.* **2018**, *32*, 401–416.

## CHAPTER NINE: DISSERTATION CONCLUSION

In summary, we have investigated some of the “known knowns” about the phenolic oxidative dearomatization reactions and have discovered some of the “unknown unknowns”. In addition, we have designed and synthesized a stable bioactive new class of thiazolidines and investigated their anti-proliferative activity. Studying the application of oxidative dearomatization reactions for different classes of urea, thiourea, and guanidine molecules has confirmed the “known known” about the oxidative dearomatization reactions which is the formation of C-N/C-O/C-S bonds. We have performed the oxidative dearomatized spirocyclization reactions using environmentally benign hypervalent iodine reagents and electrochemical oxidation conditions. Interestingly, the oxidative dearomatization reactions of phenolic urea derivatives depend on substituted group to the anilinyll moiety affecting their corresponding pKa values. Substituting the urea and guanidine derivatives by *N*-alkoxy groups improved the yields and chemoselectivity of the spirocyclization compared to *N*-aryl groups. Discovery of a novel synthetic methodology towards hydantoin system was investigated using three component reaction of amine derivatives and carbodiimide. In addition, application of oxidative dearomatization reaction towards synthesis the core structure of a recently isolated natural product (KB343) has been investigated.

Moreover, construction of benzothiazole ring system was achieved using the oxidative chemistry of hypervalent iodine reagent with thiourea derivatives. The biological activity of the synthesized benzothiazole was investigated as modulators for genes regulating GABA receptors. Interestingly, acetylated benzothiazole downregulate Gabrg2 gene, which is associated with



epilepsy disease, fissuring a new gate to discover novel derivatives acting as anti-epileptic or convulsant agents. Also, we have intensively studied a solid support synthetic methodology for construction of novel class of thiazolidine derivatives using propargyl amines and isothiocyanate derivatives in the presence of silica gel. The discovery of chemically stable thiazolidines was achieved through synthesis of three libraries of thiazolidines. Also, we have tested the antiproliferative activity of the three synthesized libraries, and investigated the possible mechanism behind their antiproliferative effect, which resulted in blocking the phosphorylation of ERK pathway. In a word, this dissertation focused on organic synthetic methodologies and medicinal chemistry applications.

## CHAPTER TEN: EXPERIMENTAL SECTION

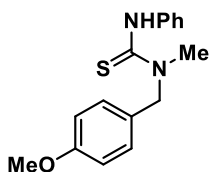
### 10.1. GENERAL PROCEDURE:

All chemicals were purchased from commercial suppliers, stored under the recommended conditions and used without any further purification. Reactions were carried out in oven-dried glassware and monitored by thin layer chromatography using silica gel 60F<sub>254</sub> aluminum precoated plates (0.25 mm layer) and visualized by a dual short/long wave UV lamp at 254 nm. Reactions were purified by crystallization and chromatography. NMR spectra were obtained at either 500 or 300 MHz (for <sup>1</sup>H NMR spectra) or 125 or 75 MHz (for <sup>13</sup>C NMR spectra) in CDCl<sub>3</sub> unless indicated otherwise. <sup>1</sup>H NMR spectra were referenced to residual protiosolvent unless indicated otherwise (CHCl<sub>3</sub> δ = 7.26 ppm). For spectra recorded in other solvents, residual MeOH (δ = 3.31 ppm) or DMSO (δ = 2.50 ppm) were used as internal references. <sup>13</sup>C NMR spectra were recorded in CDCl<sub>3</sub> (unless otherwise indicated) using residual CHCl<sub>3</sub> (δ = 77.2 ppm) as an internal reference. For spectra recorded in other solvents, residual MeOH (δ = 39.5 ppm) or DMSO (δ = 49.0 ppm) were used as internal references. The multiplicity of signals was being recorded and abbreviated as s = singlet, d = doublet, t = triplet, q = quartet, dd = doublet of doublets, br = broad singlet and m = multiplet. Data are reported here as follows: chemical shift (δ, ppm), multiplicity, coupling constant(s) in Hz, integration). Infrared (IR) spectra were obtained on neat samples (ATR spectroscopy). Flash column chromatography was performed with 230–400 silica gel. High resolution mass spectra (HRMS) were recorded by electrospray ionization (ESI-TOF).

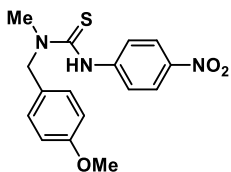
## 10.2 SYNTHESIS

### Chapter two

**General procedure for the preparation of thioureas derived from 1-(4-methoxyphenyl)-N-methylmethanamine:** To a solution of 1-(4-methoxyphenyl)-N-methylmethanamine (3.31 mmol, 0.51 ml, 1.0 equiv) in DCM (30 ml), triethylamine (3.97 mmol, 0.55 ml, 1.2 equiv) then stir reaction mixture at rt for 15 min, then the corresponding aryl isothiocyanate was added (3.31 mmol, 1.0 equiv) at rt and stirring continued at rt overnight. The solvent was evaporated and the crude thioureas were purified by chromatography or by crystallization.



**1-(4-Methoxybenzyl)-1-methyl-3-phenylthiourea (2.6a):** Obtained as a white solid (0.93 g, 98%), m.p. 126-129 °C, purified by chromatography (25% EtOAc/Hexanes). <sup>1</sup>H NMR (500 MHz, CDCl<sub>3</sub>) δ 7.37 – 7.08 (m, 7H), 6.90 (dd, *J* = 8.6, 1.7 Hz, 2H), 5.01 (s, 2H), 3.81 (s, 3H), 3.25 (s, 3H); <sup>13</sup>C NMR (125 MHz, CDCl<sub>3</sub>) δ 182.6, 159.4, 139.8, 128.8, 128.7, 127.9, 125.8, 125.3, 114.4, 56.6, 55.4, 38.9; FT-IR (neat, cm<sup>-1</sup>): 3260, 3042, 2996, 2924, 2831, 1610, 1592; HRMS (*m/z*): calc for [M+H]<sup>+</sup> C<sub>16</sub>H<sub>18</sub>N<sub>2</sub>OS 287.1152 found 287.1190.



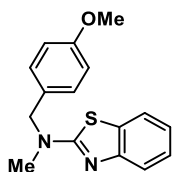
**1-(4-Methoxybenzyl)-1-methyl-3-(4-nitrophenyl)thiourea (2.6f):** Obtained as a yellow solid (0.86 g, 78%), m.p. 162-164 °C, crystallized from ethanol (60 ml concentrated into 30 ml). <sup>1</sup>H NMR (500 MHz, CDCl<sub>3</sub>) δ 8.10 (d, *J* = 8.5 Hz, 2H), 7.41 (d, *J* = 8.6 Hz, 2H), 7.21 (d, *J* = 8.3 Hz,

2H), 6.88 (d,  $J = 8.2$  Hz, 2H), 4.95 (s, 2H), 3.77 (s, 3H), 3.29 (s, 3H);  $^{13}\text{C}$  NMR (125 MHz,  $\text{CDCl}_3$ )  $\delta$  181.5, 159.7, 145.7, 143.9, 128.6, 127.1, 124.5, 123.0, 114.7, 56.7, 55.4; FT-IR (neat,  $\text{cm}^{-1}$ ): 3171, 3131, 3053, 3012, 2978, 2933, 2840, 1610, 1593, 1534; HRMS ( $m/z$ ): calc for  $[\text{M}+\text{H}]^+$   $\text{C}_{16}\text{H}_{17}\text{N}_3\text{O}_3\text{S}$  332.1063 found 332.1051.

### Oxidative dearomatization reactions of thioureas (2.4 and 2.10):

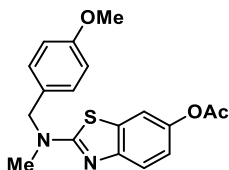
Method A: The thiourea (1.0 equiv, 0.2 g, 0.7 mmol of thiourea **2.4** and 0.6 mmol of thiourea **2.10**) was dissolved in 25 ml of HFIP then  $\text{Cs}_2\text{CO}_3$  (1.2 equiv) was added then stir it for 10 min, and then 2.0 equiv of DAIB was added and stir the reaction for 2 h.

Method B: The thiourea (1.0 equiv, 0.5 g and 1.64 mmol of thiourea **2.4**, 0.4 g and 1.2 mmol of thiourea **2.10**) was dissolved in 25 ml of HFIP then  $\text{Cs}_2\text{CO}_3$  (1.2 equiv) was added then stirred for 10 min, and then 1.0 equiv of DAIB was added and continue stirring for 2 h.

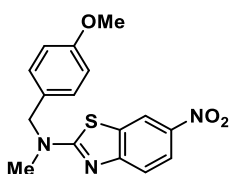


*N*-(4-Methoxybenzyl)-*N*-methylbenzo[*d*]thiazol-2-amine (**2.7a**): Obtained via oxidative dearomatization of 1-(4-methoxybenzyl)-1-methyl-3-phenylthiourea (**2.6a**) as white solid (9%, 18.0 mg, Method A), (47%, 220 mg, Method B), m.p. 74-76 °C, purified by chromatography (1% EtOAc/Hexanes).  $^1\text{H}$  NMR (500 MHz,  $\text{CDCl}_3$ )  $\delta$  7.58 (td,  $J = 7.7, 7.2, 1.2$  Hz, 2H), 7.30 (ddd,  $J = 7.9, 7.3, 1.3$  Hz, 1H), 7.27 – 7.20 (m, 2H), 7.06 (td,  $J = 7.5, 1.2$  Hz, 1H), 6.89 – 6.84 (m, 2H), 4.70 (s, 2H), 3.79 (s, 3H), 3.11 (s, 3H);  $^{13}\text{C}$  NMR (125 MHz,  $\text{CDCl}_3$ )  $\delta$  168.9, 159.3, 153.3, 131.1, 129.1, 128.5, 126.1, 121.2, 120.7, 118.9, 114.27, 114.2, 56.1, 55.4, 37.7, 29; FT-IR (neat,  $\text{cm}^{-1}$ ):

2960, 2917, 2853, 2832, 1596, 1543, 1410; HR-MS ( $m/z$ ): calc for  $[M+H]^+$   $C_{16}H_{16}N_2OS$  285.1056, found 285.1045.



**2-((4-Methoxybenzyl)(methyl)amino)benzo[d]thiazol-6-yl acetate (2.7b)**: Obtained via oxidative dearomatization of 1-(4-methoxybenzyl)-1-methyl-3-phenylthiourea (**2.6a**) as a white solid (27%, 66.0 mg, Method A), m.p. 100-102 °C, purified by chromatography (8% EtOAc/Hexanes).  $^1H$  NMR (500 MHz,  $CDCl_3$ )  $\delta$  7.52 (d,  $J = 8.7$  Hz, 1H), 7.34 (d,  $J = 2.4$  Hz, 1H), 7.22 (d,  $J = 8.7$  Hz, 2H), 7.00 (dd,  $J = 8.7, 2.4$  Hz, 1H), 6.88 – 6.84 (m, 2H), 4.68 (s, 2H), 3.79 (s, 3H), 3.09 (s, 3H), 2.30 (s, 3H);  $^{13}C$  NMR (126 MHz,  $CDCl_3$ )  $\delta$  170.1, 169.0, 159.4, 151.2, 144.8, 131.5, 129.1, 128.3, 119.8, 119.1, 114.2, 113.9, 56.1, 55.4, 37.7, 29.8, 21.2; FT-IR (neat,  $cm^{-1}$ ): 2920, 2850, 1758, 1602, 1574, 1509; HRMS ( $m/z$ ): calc for  $[M+H]^+$   $C_{16}H_{16}N_2OS$  285.1056, found 285.1045.

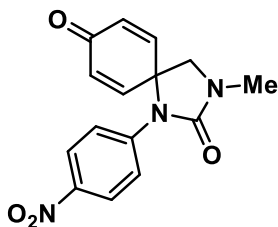


**N-(4-Methoxybenzyl)-N-methyl-6-nitrobenzo[d]thiazol-2-amine (2.11)**: Obtained via oxidative dearomatization of 1-(4-methoxybenzyl)-1-methyl-3-(4-nitrophenyl)thiourea (**2.6f**) as an impure yellow solid (~8%, 17.0 mg, Method A), m.p. 120-124 °C, purified by chromatography (3% EtOAc/Hexanes).  $^1H$  NMR (500 MHz,  $CDCl_3$ )  $\delta$  8.51 (d,  $J = 2.3$  Hz, 1H), 8.21 (dd,  $J = 8.9, 2.4$

Hz, 1H), 7.53 (d,  $J = 8.9$  Hz, 1H), 7.26 – 7.23 (m, 2H), 6.91 – 6.87 (m, 2H), 4.77 (s, 2H), 3.80 (s, 3H), 3.17 (s, 3H); FT-IR (neat,  $\text{cm}^{-1}$ ): 2925, 2854, 1621, 1568, 1488, 1327.



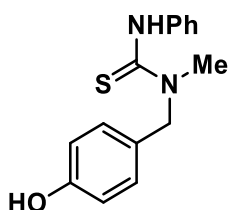
**4-Methoxyphenyl (E)-N-methyl-N'-(4-nitrophenyl)carbamimidothioate (2.12):** Obtained via oxidative dearomatization of 1-(4-methoxybenzyl)-1-methyl-3-(4-nitrophenyl)thiourea (**2.6f**) as a yellow solid (12%, Method A and 44%, Method B), m.p. 132-136 °C, purified by chromatography (10% EtOAc/Hexanes).  $^1\text{H}$  NMR (500 MHz,  $\text{CDCl}_3$ )  $\delta$  8.20 – 8.09 (m, 2H), 7.47 – 7.29 (m, 2H), 7.06 – 7.02 (m, 2H), 6.94 – 6.91 (m, 2H), 3.83 (s, 3H), 2.89 (s, 3H);  $^{13}\text{C}$  NMR (126 MHz,  $\text{CDCl}_3$ )  $\delta$  162.9, 161.7, 140.4, 137.8, 124.8, 123.7, 115.8, 55.6, 29.8; FT-IR (neat,  $\text{cm}^{-1}$ ): 2925, 2849, 1621, 1567, 1486, 1325; HRMS ( $m/z$ ): calc for  $[\text{M}+\text{H}]^+$  318.0907 found 318.0891.



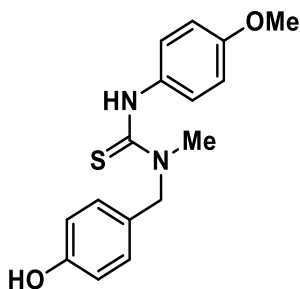
**3-Methyl-1-(4-nitrophenyl)-1,3-diazaspiro[4.5]deca-6,9-diene-2,8-dione (2.13):** Obtained via oxidative dearomatization of 1-(4-methoxybenzyl)-1-methyl-3-(4-nitrophenyl)thiourea (**2.6f**) as a yellow solid (38%, Method A and 5%, Method B), m.p. 168-171 °C, purified by chromatography (20% EtOAc/Hexanes).  $^1\text{H}$  NMR (500 MHz,  $\text{CDCl}_3$ )  $\delta$  8.13 (d,  $J = 9.3$  Hz, 2H), 7.52 (d,  $J = 9.3$  Hz, 2H), 7.07 (d,  $J = 10.1$  Hz, 2H), 6.47 (d,  $J = 10.1$  Hz, 2H), 3.51 (s, 2H), 2.99 (s, 3H);  $^{13}\text{C}$  NMR

(125 MHz, CDCl<sub>3</sub>)  $\delta$  183.5, 156.6, 148.5, 144.1, 143.8, 131.3, 124.7, 120.8, 59.0, 54.8, 31.4; FT-IR (neat, cm<sup>-1</sup>): 2922, 2853, 1714, 1664, 1591, 1492, 1317; HRMS (*m/z*): calc for [M+H]<sup>+</sup> C<sub>15</sub>H<sub>13</sub>N<sub>3</sub>O<sub>4</sub> 300.0967 found 300.0979.

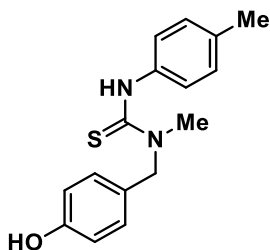
**General procedure for preparation of thioureas 22a-e:** 4-[(Methylamino)methyl]phenol (1.0 equiv, 0.7 mmol) was dissolved in THF (10 mL), then trimethylamine (1.2 equiv) was added and mixture was stirred for 10 min then aryl isothiocyanate was added dropwise (1.0 equiv, 0.7 mmol), then the mixture was stirred for 2 h at rt. The solvent was evaporated then the crude thioureas were purified by chromatography or by crystallization.



**1-(4-Hydroxybenzyl)-1-methyl-3-phenylthiourea (2.22a):** Colorless semisolid, (1.0 g, 98%), purified by chromatography (20% EtOAc/Hexanes). <sup>1</sup>H NMR (500 MHz, CDCl<sub>3</sub>)  $\delta$  7.32 (dd, *J* = 8.4, 7.3 Hz, 2H), 7.25 – 7.21 (m, 2H), 7.20 – 7.16 (m, 3H), 7.16 (s, 1H), 6.84 – 6.78 (m, 2H), 4.98 (s, 2H), 3.26 (s, 3H); <sup>13</sup>C NMR (125 MHz, CDCl<sub>3</sub>)  $\delta$  182.5, 155.8, 139.7, 128.9, 128.8, 127.7, 126.0, 125.5, 116.1, 56.7, 53.6; FT-IR (neat, cm<sup>-1</sup>): 3389, 3165, 2920, 2852, 2673, 1611, 1594, 1511, 1331; HR-MS (*m/z*): calc for [M+H]<sup>+</sup> C<sub>15</sub>H<sub>16</sub>N<sub>2</sub>OS 273.1056 found 273.1027.



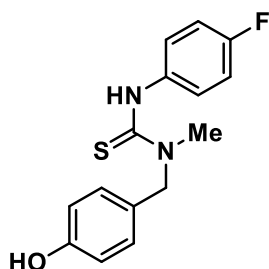
**1-(4-Hydroxybenzyl)-3-(4-methoxyphenyl)-1-methylthiourea (2.22b):** Colorless crystals, (0.22 g, 98%), m.p. 118-121 °C, purified by chromatography (25% EtOAc/Hexanes).  $^1\text{H}$  NMR (500 MHz,  $\text{CDCl}_3$ )  $\delta$  7.14 – 7.10 (m, 4H), 7.09 (s, 1H), 6.84 (d,  $J = 8.9$  Hz, 2H), 6.80 (d,  $J = 8.5$  Hz, 2H), 4.96 (s, 2H), 3.77 (s, 3H), 3.24 (s, 3H);  $^{13}\text{C}$  NMR (125 MHz,  $\text{CDCl}_3$ )  $\delta$  182.8, 157.9, 155.8, 132.6, 128.7, 127.8, 127.7, 116.0, 114.1, 56.6, 55.5, 46.1; FT-IR (neat,  $\text{cm}^{-1}$ ): 3219, 2957, 2936, 2837, 1612, 1514, 1335; HRMS ( $m/z$ ): calc for  $[\text{M}+\text{H}]^+$   $\text{C}_{16}\text{H}_{18}\text{N}_2\text{O}_2\text{S}$  303.1162 found 303.1141.



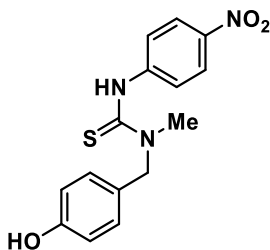
**1-(4-Hydroxybenzyl)-1-methyl-3-(p-tolyl)thiourea (2.22c):** White solid (0.18 g, 90%), m.p. 138-142 °C, purified by chromatography (30% EtOAc/Hexanes).  $^1\text{H}$  NMR (300 MHz,  $\text{CDCl}_3$ )  $\delta$  7.40 (d,  $J = 1.8$  Hz, 1H), 7.36 – 7.28 (m, 2H), 7.23 (m, 3H), 6.97 (dd,  $J = 8.5, 1.9$  Hz, 2H), 5.67 (s, 1H), 5.13 (s, 2H), 3.40 (s, 3H), 2.46 (s, 3H);  $^{13}\text{C}$  NMR (75 MHz,  $\text{CDCl}_3$ )  $\delta$  182.8, 155.7, 137.1, 136.1,



129.6, 128.8, 127.9, 125.8, 116.1, 56.7, 21.2; FT-IR (neat,  $\text{cm}^{-1}$ ): 3301, 3139, 2912, 1612, 1514, 1346; HR-MS ( $m/z$ ): calc for  $[\text{M}+\text{H}]^+$   $\text{C}_{16}\text{H}_{18}\text{N}_2\text{OS}$  287.1213 found 287.1191.



**3-(4-Fluorophenyl)-1-(4-hydroxybenzyl)-1-methylthiourea (2.22d):** White solid, (0.19 g, 95%), m.p. 150-154 °C, purified by chromatography (40% EtOAc/Hexanes).  $^1\text{H}$  NMR (300 MHz,  $\text{DMSO}-d_6$ )  $\delta$  9.39 (s, 1H), 9.15 (s, 1H), 7.33 (ddd,  $J = 7.0, 5.5, 2.8$  Hz, 2H), 7.15 (dd,  $J = 9.8, 8.0$  Hz, 5H), 6.75 (d,  $J = 8.5$  Hz, 2H), 5.04 (s, 2H), 3.13 (s, 3H);  $^{13}\text{C}$  NMR (125 MHz,  $\text{CD}_3\text{OD}$ )  $\delta$  182.3, 161.6, 159.7, 156.7, 137.0, 128.7, 128.6, 128.5, 127.6, 115.0, 114.5, 114.3, 56.0, 36.3; FT-IR (neat,  $\text{cm}^{-1}$ ): 3405, 3176, 3077, 3050, 2922, 1607, 1500; HR-MS ( $m/z$ ): calc for  $[\text{M}+\text{H}]^+$   $\text{C}_{15}\text{H}_{15}\text{FN}_2\text{OS}$  291.0962 found 291.0924.

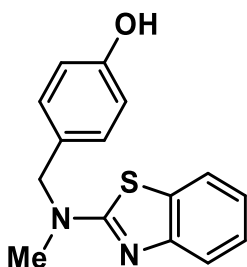


**1-(4-Hydroxybenzyl)-1-methyl-3-(4-nitrophenyl)thiourea (2.22e):** Yellow gum material, (0.22 g, 96%), purified by chromatography (25% EtOAc/Hexanes).  $^1\text{H}$  NMR (500 MHz,  $\text{CD}_3\text{OD}$ )  $\delta$  8.26 (d,  $J = 9.1$  Hz, 2H), 7.74 (d,  $J = 9.2$  Hz, 2H), 7.33 (d,  $J = 8.2$  Hz, 2H), 6.91 (d,  $J = 8.6$  Hz, 2H),

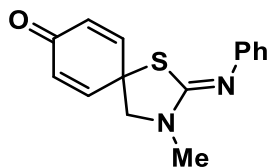
4.98 (s, 2H), 2.27 (s, 3H);  $^{13}\text{C}$  NMR (125 MHz,  $\text{CD}_3\text{OD}$ )  $\delta$  181.8, 156.8, 147.3, 143.5, 128.9, 127.2, 123.8, 123.5, 115.1, 56.1, 29.5; FT-IR (neat,  $\text{cm}^{-1}$ ): 3267, 2928, 2856, 1596, 1538, 1503, 1292; HRMS ( $m/z$ ): calc for  $[\text{M}+\text{H}]^+$   $\text{C}_{15}\text{H}_{15}\text{N}_3\text{O}_3\text{S}$  318.0907 found 318.0870.

#### Oxidative dearomatization of thioureas (2.22a-e):

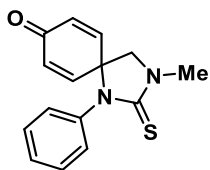
Oxidative dearomatization of 1-(4-hydroxybenzyl)-1-methyl-3-phenylthiourea (**2.22a**): To a solution of synthesized thiourea (0.74 mmol, 0.20 g) in 5-7 ml of HFIP, 0.24 g of PIDA (0.74 mmol) was added at rt. The reaction was complete after few minutes (tlc analysis). Three different cyclic systems were isolated using column chromatography.



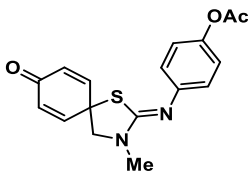
**4-((Benzo[d]thiazol-2-yl(methyl)amino)methyl)phenol (2.24)**: White solid (12 mg, 6%), m.p. 180-182 °C, purified by chromatography by (10% EtOAc/Hexanes).  $^1\text{H}$  NMR (500 MHz,  $\text{CDCl}_3$ )  $\delta$  7.58 (ddd,  $J = 8.1, 4.7, 1.2$  Hz, 2H), 7.28 (ddd,  $J = 8.4, 7.3, 1.3$  Hz, 1H), 7.11 – 7.02 (m, 3H), 6.68 (d,  $J = 8.5$  Hz, 2H), 4.64 (s, 2H), 3.10 (s, 3H);  $^{13}\text{C}$  NMR (125 MHz,  $\text{CDCl}_3$ )  $\delta$  169.3, 156.1, 128.9, 126.3, 121.5, 120.8, 118.7, 115.9, 56.5, 37.9; FT-IR (neat,  $\text{cm}^{-1}$ ): 3069, 2960, 2917, 2904, 1588, 1540, 1506; HRMS ( $m/z$ ): calc for  $[\text{M}+\text{H}]^+$   $\text{C}_{15}\text{H}_{14}\text{N}_2\text{OS}$  271.0900 found 271.0881.



**(Z)-3-Methyl-2-(phenylimino)-1-thia-3-azaspiro[4.5]deca-6,9-dien-8-one (2.23a):** Colorless solid, (100 mg, 45%), m.p. 116-120 °C, purified by chromatography (20% EtOAc/Hexanes). <sup>1</sup>H NMR (500 MHz, CDCl<sub>3</sub>) δ 7.31 – 7.16 (m, 2H), 7.11 – 6.98 (m, 3H), 6.91 (dd, *J* = 8.5, 1.2 Hz, 1H), 6.24 (d, *J* = 10.1 Hz, 1H), 3.59 (s, 2H), 3.08 (s, 3H); <sup>13</sup>C NMR (125 MHz, CDCl<sub>3</sub>) δ 184.5, 156.4, 151.3, 146.9, 129.3, 129.1, 123.9, 121.8, 60.3, 50.7, 34.2; FT-IR (neat, cm<sup>-1</sup>): 3050, 2925, 2856, 1666, 1628, 1620; HRMS (*m/z*): calc for [M+H]<sup>+</sup> C<sub>15</sub>H<sub>14</sub>N<sub>2</sub>OS 271.0900 found 271.0871.



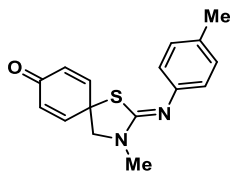
**3-Methyl-1-phenyl-1,3-diazaspiro[4.5]deca-6,9-diene-2,8-dione (2.25):** Colorless solid, (16 mg, 8%), m.p. 193-196 °C, purified by chromatography (25% EtOAc/Hexanes). <sup>1</sup>H NMR (500 MHz, CDCl<sub>3</sub>) δ 7.37 – 7.30 (m, 3H), 7.18 (dd, *J* = 8.0, 1.7 Hz, 2H), 7.00 (d, *J* = 10.1 Hz, 2H), 6.24 (d, *J* = 10.1 Hz, 2H), 3.79 (s, 2H), 3.29 (s, 3H); <sup>13</sup>C NMR (125 MHz, CDCl<sub>3</sub>) δ 184.1, 183.5, 146.2, 137.6, 131.0, 129.6, 129.2, 128.8, 63.0, 58.3, 35.4; FT-IR (neat, cm<sup>-1</sup>): 3026, 2925, 2853, 1674, 1636, 1498; HRMS (*m/z*): calc for [M+H]<sup>+</sup> C<sub>15</sub>H<sub>14</sub>N<sub>2</sub>OS 271.0900 found 271.0873.



**(Z)-4-((3-Methyl-8-oxo-1-thia-3-azaspiro[4.5]deca-6,9-dien-2-ylidene)amino)phenyl acetate**

**(2.26):** Obtained as a main product using 2.0 equivalents of IBDA, colorless solid (57 mg, 31%), m.p. 174-176 °C, purified by chromatography (30% EtOAc/Hexanes). <sup>1</sup>H NMR (500 MHz, DMSO) δ 7.25 (d, *J* = 10.0 Hz, 2H), 7.00 (d, *J* = 8.8 Hz, 1H), 6.86 (d, *J* = 8.7 Hz, 2H), 6.24 (d, *J* = 10.0 Hz, 1H), 3.79 (s, 2H), 3.02 (s, 3H), 2.23 (s, 3H); <sup>13</sup>C NMR (125 MHz, DMSO) δ 185.1, 170.2, 156.6, 149.4, 148.5, 146.7, 128.8, 122.8, 122.8, 59.3, 51.2, 34.1, 21.3; FT-IR (neat, cm<sup>-1</sup>): 3397, 3056, 2970, 2925, 1751, 1660, 1623; HRMS (*m/z*): calc for [M+H]<sup>+</sup> C<sub>17</sub>H<sub>16</sub>N<sub>2</sub>O<sub>3</sub>S 329.0954 found 329.0916.

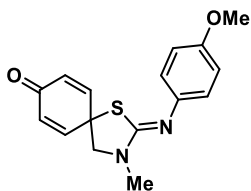
Oxidative dearomatization of *1-(4-hydroxybenzyl)-1-methyl-3-(p-tolyl)thiourea*: To a solution of thiourea (**22c**) (0.19 mmol, 55 mg) in 5-7 ml of HFIP, 95 mg of PIDA (0.29 mmol, 1.5 molar equiv) was added at rt. The reaction was complete after few minutes and the following spiro compound was isolated as major product.



**(Z)-3-Methyl-2-(p-tolylimino)-1-thia-3-azaspiro[4.5]deca-6,9-dien-8-one (2.23b):** Pale yellow solid (33 mg, 60%), m.p. 110-114 °C, purified by chromatography (20% EtOAc/Hexanes). <sup>1</sup>H NMR (300 MHz, CDCl<sub>3</sub>) δ 7.09 – 7.03 (m, 4H), 6.83 (d, *J* = 8.2 Hz, 2H), 6.26 (d, *J* = 10.0 Hz, 2H), 3.59 (s, 2H), 3.09 (s, 3H), 2.28 (s, 3H); <sup>13</sup>C NMR (75 MHz, CDCl<sub>3</sub>) δ 184.6, 156.4, 148.8,

147.1, 133.4, 129.7, 129.2, 121.6, 60.3, 50.6, 34.2, 21.0; FT-IR (neat,  $\text{cm}^{-1}$ ): 3050, 2954, 2914, 2872 ; HRMS ( $m/z$ ): calc for  $[\text{M}+\text{H}]^+$   $\text{C}_{16}\text{H}_{16}\text{N}_2\text{OS}$  285.1056 found 285.1036.

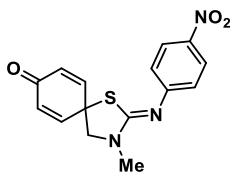
Oxidative dearomatization of *1-(4-hydroxybenzyl)-3-(4-methoxyphenyl)-1-methylthiourea* (**2.22b**): To a solution of the synthesized thiourea (0.57 mmol, 172 mg) in 5-7 ml of HFIP, 280 mg of PIDA (0.86 mmol, 1.5 molar equiv) was added at rt. The reaction was complete after few minutes and the following spiro compound was isolated as major product.



**(Z)-2-((4-Methoxyphenyl)imino)-3-methyl-1-thia-3-azaspiro[4.5]deca-6,9-dien-8-one** (**2.23c**):

Yellow gummy material (80 mg, 47%), purified by chromatography (30% EtOAc/Hexanes).  $^1\text{H}$  NMR (300 MHz,  $\text{CDCl}_3$ )  $\delta$  7.04 (d,  $J = 10.2$  Hz, 2H), 6.89 – 6.70 (m, 4H), 6.23 (d,  $J = 10.1$  Hz, 2H), 3.74 (s, 3H), 3.57 (s, 2H), 3.06 (s, 3H);  $^{13}\text{C}$  NMR (75 MHz,  $\text{CDCl}_3$ )  $\delta$  184.6, 156.6, 156.2, 147.1, 144.7, 129.2, 122.7, 114.3, 60.3, 55.5, 50.7, 34.2, 29.8; FT-IR (neat,  $\text{cm}^{-1}$ ): 3037, 2930, 2832, 1660, 1618, 1498; HRMS ( $m/z$ ): calc for  $[\text{M}+\text{H}]^+$   $\text{C}_{16}\text{H}_{16}\text{N}_2\text{O}_2\text{S}$  301.1005 found 301.0989.

**Oxidative dearomatization of 1-(4-hydroxybenzyl)-1-methyl-3-(4-nitrophenyl)thiourea (2.22e):** To a solution of the synthesized thiourea (**15e**) (0.284 mmol, 90 mg) in 5-7 ml of HFIP, 137 mg of PIDA (0.426 mmol, 1.5 molar equiv) was added at rt. The reaction was complete after few minutes and the following spiro compound was isolated as major product.



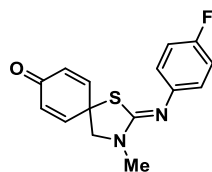
**(Z)-3-Methyl-2-((4-nitrophenyl)imino)-1-thia-3-azaspiro[4.5]deca-6,9-dien-8-one (2.23d):**

Yellow solid (72 mg, 80%), m.p. 140-143 °C, purified by chromatography (45% EtOAc/Hexanes).

<sup>1</sup>H NMR (300 MHz, CDCl<sub>3</sub>) δ 8.15 (d, *J* = 9.0 Hz, 2H), 7.04 (dd, *J* = 13.0, 9.5 Hz, 4H), 6.31 (d, *J* = 10.0 Hz, 2H), 3.70 (s, 2H), 3.14 (s, 3H); <sup>13</sup>C NMR (75 MHz, CDCl<sub>3</sub>) δ 184.2, 157.1, 156.9, 146.1, 143.0, 137.8, 129.7, 125.2, 122.4, 60.4, 51.1, 34.2; FT-IR (neat, cm<sup>-1</sup>): 3082, 2922, 2853, 1666, 1623, 1570; HRMS (*m/z*): calc for [M+H]<sup>+</sup> C<sub>15</sub>H<sub>13</sub>N<sub>3</sub>O<sub>3</sub>S 316.0750 found 316.0736.

**Oxidative dearomatization of 3-(4-fluorophenyl)-1-(4-hydroxybenzyl)-1-methylthiourea (2.22d):**

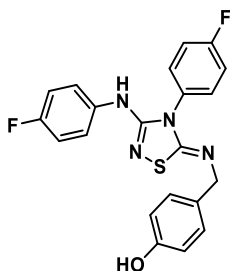
To a solution of the synthesized thiourea (**2.15d**) (0.345 mmol, 100 mg) in 5-7 ml of HFIP, 170 mg of PIDA (0.517 mmol, 1.5 molar equiv) was added at rt. The reaction was complete after few minutes and the following spiro compound was isolated as major product.



**(Z)-2-((4-Fluorophenyl)imino)-3-methyl-1-thia-3-azaspiro[4.5]deca-6,9-dien-8-one (2.23e):**

Pale yellow solid (67 mg, 68%), m.p. 114-118 °C, purified by chromatography (25% EtOAc/Hexanes). <sup>1</sup>H NMR (300 MHz, CDCl<sub>3</sub>) δ 7.06 (d, *J* = 10.0 Hz, 2H), 7.00 – 6.84 (m, 4H), 6.27 (d, *J* = 10.0 Hz, 2H), 3.62 (s, 2H), 3.09 (s, 3H); <sup>13</sup>C NMR (75 MHz, CDCl<sub>3</sub>) δ 184.5, 161.2, 158.0, 156.9, 147.4, 146.8, 129.3, 123.1, 123.0, 115.9, 115.6, 60.4, 50.7, 34.2; FT-IR (neat, cm<sup>-1</sup>): 3053, 2957, 2928, 2856, 1655, 1639, 1620, 1500; HRMS (*m/z*): calc for [M+H]<sup>+</sup> C<sub>15</sub>H<sub>13</sub>FN<sub>2</sub>OS 289.0805 found 289.0785.

**Oxidative dearomatization of 1-(4-fluorophenyl)-3-(4-hydroxybenzyl)thiourea (2.22d):** To a solution of the synthesized thiourea (0.36 mmol, 100 mg) in 5-7 ml of HFIP, 143 mg of Cs<sub>2</sub>CO<sub>3</sub> (1.2 equiv) was added then stir reaction mixture for 10 minutes then 119 mg of PIDA (0.36 mmol, 1.0 molar equiv) was added at rt. The reaction was complete after few minutes and the following spiro compound was isolated as major product.



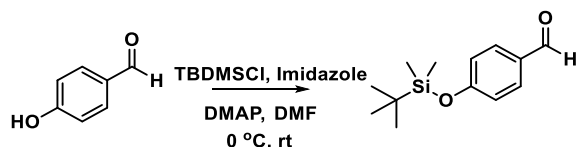
**(Z)-4-(((4-(4-Fluorophenyl)-3-((4-fluorophenyl)amino)-1,2,4-thiadiazol-5(4H)-**

**ylidene)amino)methyl)phenol (2.29):** Colorless solid (24.0 mg, 32%), m.p. 218-220 °C, purified using prep TLC. (30% EtOAc/Hexanes). <sup>1</sup>H NMR (500 MHz, CD<sub>3</sub>OD) δ 7.40 (dtd, *J* = 9.2, 4.7,

2.3 Hz, 4H), 7.26 (ddd,  $J = 8.8, 5.5, 3.2$  Hz, 2H), 7.03 – 6.97 (m, 2H), 6.92 (dtd,  $J = 8.9, 4.5, 2.2$  Hz, 2H), 6.70 – 6.60 (m, 2H), 4.06 (s, 2H);  $^{13}\text{C}$  NMR (125 MHz,  $\text{CD}_3\text{OD}$ )  $\delta$  156.1, 150.0, 131.4, 128.6, 122.7, 117.1, 116.8, 114.6, 56.5;  $^{19}\text{F}$  NMR (283 MHz)  $\delta$  -113.04, -121.59; FT-IR (neat,  $\text{cm}^{-1}$ ): 3323, 2928, 2853, 1663, 1543, 1503, 1212; HRMS ( $m/z$ ): calc for  $[\text{M}+\text{H}]^+$   $\text{C}_{21}\text{H}_{16}\text{F}_2\text{N}_4\text{OS}$  411.1087 found 411.1070.

### 3.5- General procedure for preparation of urea derivatives (2.34a-e):

#### 3.5.1- Formation of the protected benzaldehyde using silyl chloride (2.31):



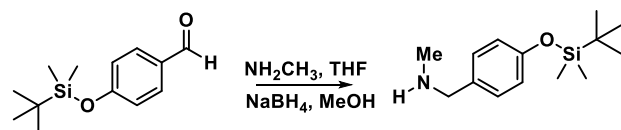
A solution of 4-hydroxy benzaldehyde (5.6 g, 45 mmol) in 50 ml DMF was cooled in an ice bath for 15 min then imidazole (6.12 g, 90 mmol) and 0.1 g of DMAP were added respectively. After a few minutes TBDMSCl (10.2 g, 67.5 mmol) was added and stirring continued at 0 °C for one hour then stirred at rt for 3 h. The reaction was quenched with 25 ml water, then 25 ml EtOAc added. The aqueous layer was washed with EtOAc (3x2 5ml). The combined organic extracts were dried over  $\text{Na}_2\text{SO}_4$ , filtered and concentrated by rotary evaporation. The crude aldehyde was purified chromatographically using 25% EtOAc in hexanes, yielding a yellow oil (7.0 g, 64%). The spectroscopic data matched that found in the literature.<sup>1</sup>  $^1\text{H}$  NMR (300 MHz,  $\text{CDCl}_3$ )  $\delta$  9.8 (s,

<sup>1</sup> Bastos, E.; Ciscato, L. F. M. L.; Baader, W. J. *Synth. Commun.* **2005**, *35*, 1501-1509.



1H), 7.84 – 7.66 (m, 2H), 7.03 – 6.83 (m, 2H), 1.07 – 0.80 (m, 9H), 0.27 – 0.13 (m, 6H); <sup>13</sup>C NMR (75 MHz, CDCl<sub>3</sub>) δ 191.4, 161.8, 132.6, 130.1, 116.1, 25.7, 1.2, -3.0.

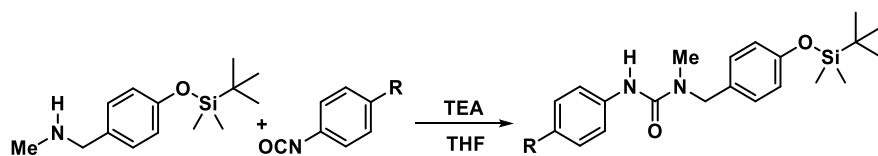
### Synthesis of the targeted masked amine (2.32):



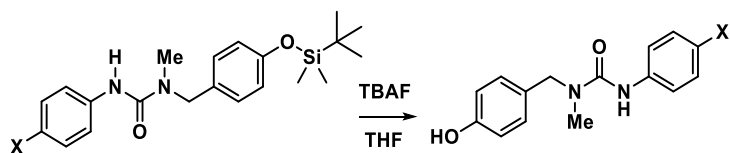
To a solution of the protected benzaldehyde (1.3 g, 5.5 mmol) in 6 ml of CHCl<sub>3</sub>/MeOH (5:1), 6.1 ml of methylamine in THF (2.0 equiv) was diluted with CHCl<sub>3</sub> (6 ml) and added to the aldehyde solution. Then anhydrous Na<sub>2</sub>SO<sub>4</sub> (15 g, 2-3 g/mmol) was added and stirring of the mixture continued at rt for 90 min under argon. Glacial acetic acid (0.13 ml) was added, then after 15 min 5.5 g of anhydrous Na<sub>2</sub>SO<sub>4</sub> was added then stirring was continued at rt for two days. Any remaining solids were filtered from the reaction mixture, then the filtrate was concentrated. The residue was dissolved in methanol (50 ml) and the resulting solution cooled in ice for 30 min. NaBH<sub>4</sub> (0.315 g, 8.25 mmol, 1.5 equiv) was added and then stirred for 15 min while cooling in ice. The ice-bath was removed and stirring was continued for 30 min. The mixture was concentrated and partitioned between EtOAc (20 ml) and NaHCO<sub>3</sub> (20 ml), then the aqueous layer was extracted with EtOAc (3x15 ml). The combined organic extracts were dried over Na<sub>2</sub>SO<sub>4</sub>, then concentrated. The resulting red liquid (1.16 g, 83%) was used without any further purification. <sup>1</sup>H NMR (300 MHz, CDCl<sub>3</sub>) δ 7.24 – 7.06 (m, 2H), 6.79 (m, 2H), 3.68 (s, 3H), 2.43 (s, 2H), 0.98 (s, 9H), 0.25 (m, 6H);

$^{13}\text{C}$  NMR (125 MHz,  $\text{CDCl}_3$ )  $\delta$  154.9, 130.6, 129.6, 120.1, 55.2, 35.4, 25.7, 18.1, -3.5; HRMS ( $m/z$ ): calc for  $[\text{M}+\text{H}]^+$   $\text{C}_{14}\text{H}_{25}\text{NOSi}$  252.1778 found 252.2251.

### 3.5.3- General procedure for urea formation using the masked amine:

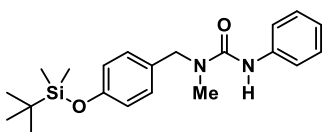


To a solution of 1-(4-((*tert*-butyldimethylsilyloxy)phenyl)-*N*-methylmethanamine (1 equiv) in THF, 1.2 equiv of triethylamine was added and kept the reaction mixture stir for 15 min in ice bath then the corresponding isocyanate (1.0 equiv) was added and continue stirring for 3 h at the same temperature then kept it stirring at rt overnight. The reaction mixture was absorbed over silica gel and subjected for column purification.

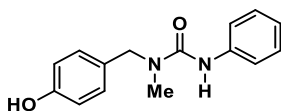


To a solution of THF containing 1.0 equiv of the masked synthesized ureas, TBAF (1.2 equiv) was added in ice bath while stirring, then warm the reaction mixture up to rt and continue stirring overnight. The reaction was quenched using aqueous solution of ammonium chloride then followed by work-up using DCM then washed with brine solution then dried over sodium sulfate. All the reactions were purified chromatography over  $\text{SiO}_2$ .

**Synthesis of 1-(4-Hydroxybenzyl)-1-methyl-3-phenylurea (2.34a):**



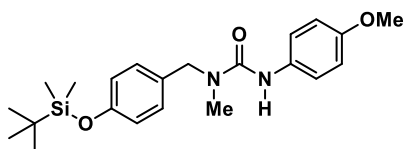
**1-(4-((tert-Butyldimethylsilyl)oxy)benzyl)-1-methyl-3-phenylurea:** Obtained through reaction of the synthesized amine and phenyl isocyanate as white solid (200 mg, 72%), m.p. 108-110 °C, purified chromatography (20% EtOAc/Hexanes). <sup>1</sup>H NMR (500 MHz, CDCl<sub>3</sub>) δ 7.27 (d, *J* = 7.3 Hz, 2H), 7.15 (t, *J* = 7.9 Hz, 2H), 7.06 (d, *J* = 8.2 Hz, 2H), 6.92 (t, *J* = 7.5 Hz, 1H), 6.75 (d, *J* = 8.5 Hz, 1H), 6.61 (s, 1H), 4.39 (s, 2H), 2.87 (s, 3H), 0.93 (s, 9H), 0.14 (s, 6H); <sup>13</sup>C NMR (125 MHz, CDCl<sub>3</sub>) δ 156.0, 155.2, 153.5, 139.5, 139.3, 130.2, 128.8, 128.7, 128.6, 123.1, 122.2, 120.5, 120.3, 119.2, 53.6, 51.9, 34.7, 25.8, 18.3, -4.3; FT-IR (neat, cm<sup>-1</sup>): 3328, 3053, 3038, 2953, 2929, 2856, 1641, 1593, 1508; HR-MS (*m/z*): calc for [M+H]<sup>+</sup> C<sub>21</sub>H<sub>30</sub>N<sub>2</sub>O<sub>2</sub>Si 371.2145 found 371.2109.



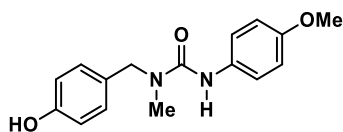
**1-(4-Hydroxybenzyl)-1-methyl-3-phenylurea (2.35a):** White solid (72 mg, 58%), m.p. 128-130 °C, purified by chromatography (25% EtOAc/Hexanes). <sup>1</sup>H NMR (500 MHz, CD<sub>3</sub>OD) δ 7.38 (d, *J* = 8.0 Hz, 2H), 7.25 (t, *J* = 7.7 Hz, 2H), 7.11 (d, *J* = 8.0 Hz, 2H), 7.01 (td, *J* = 7.4, 1.2 Hz, 1H), 6.77 (d, *J* = 8.6 Hz, 2H), 4.89 (s, 2H), 2.91 (s, 3H). <sup>13</sup>C NMR (125 MHz, CD<sub>3</sub>OD) δ 157.4, 156.5,

139.6, 128.6, 128.4, 128.2, 122.9, 121.2, 115.1, 51.0, 33.1. FT-IR (neat,  $\text{cm}^{-1}$ ): 3307, 2960, 2928, 2856, 4, 1594, 1511; HR-MS ( $m/z$ ): calc for  $[\text{M}+\text{H}]^+$   $\text{C}_{15}\text{H}_{16}\text{N}_2\text{O}_2$  257.1285 found 257.1249.

### 3.5.3.3. Synthesis of *1-(4-(tert-Butyldimethylsilyloxy)benzyl)-3-(4-methoxyphenyl)-1-methylurea (2.34b)*:



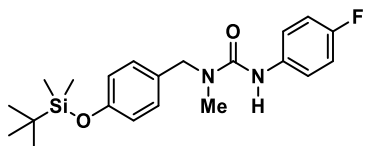
***1-(4-((tert-Butyldimethylsilyl)oxy)benzyl)-3-(4-methoxyphenyl)-1-methylurea***: Obtained through reaction of the amine and *p*-methoxyphenyl isocyanate as white solid (0.27 g, 42%), m.p. 90-92 °C, purified by chromatography (12.5% EtOAc/Hexanes).  $^1\text{H}$  NMR (500 MHz,  $\text{CDCl}_3$ )  $\delta$  7.22 (d,  $J = 9.0$  Hz, 2H), 7.16 (d,  $J = 8.5$  Hz, 2H), 6.82 (dd,  $J = 8.8, 2.2$  Hz, 4H), 6.22 (s, 1H), 4.49 (s, 2H), 3.77 (s, 3H), 3.00 (s, 3H), 1.02 – 0.94 (m, 9H), 0.26 – 0.14 (m, 6H);  $^{13}\text{C}$  NMR (125 MHz,  $\text{CDCl}_3$ )  $\delta$  156.2, 155.8, 155.3, 154.7, 132.2, 130.2, 128.6, 122.2, 120.5, 114.1, 55.6, 52.0, 34.8, 25.7, 18.3, -4.3; FT-IR (neat,  $\text{cm}^{-1}$ ): 3336, 2954, 2930, 2856, 1644, 1508, 1236; HRMS ( $m/z$ ): calc for  $[\text{M}+\text{H}]^+$   $\text{C}_{22}\text{H}_{32}\text{N}_2\text{O}_3\text{Si}$  401.2249 found 401.2255.



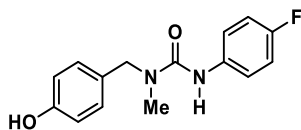
***1-(4-hydroxybenzyl)-3-(4-methoxyphenyl)-1-methylurea (2.35b)***: White solid (0.13 g, 90%), m.p. 139-142 °C, purified by chromatography (50% EtOAc/Hexanes).  $^1\text{H}$  NMR (500 MHz,  $\text{CDCl}_3$ )  $\delta$  7.21 (d,  $J = 8.9$  Hz, 2H), 7.13 (d,  $J = 8.2$  Hz, 2H), 6.82 (d,  $J = 9.1$  Hz, 2H), 6.78 (d,  $J = 8.6$  Hz, 2H), 6.22 (s, 1H), 4.49 (s, 2H), 3.77 (s, 3H), 3.01 (s, 3H);  $^{13}\text{C}$  NMR (126 MHz,  $\text{CDCl}_3$ )  $\delta$

156.3, 155.5, 129.2, 128.7, 122.4, 115.8, 114.2, 55.6, 52.0, 34.9; FT-IR (neat,  $\text{cm}^{-1}$ ): 3213, 2957, 2936, 2872, 1647, 1511; HRMS ( $m/z$ ): calc for  $[\text{M}+\text{H}]^+$   $\text{C}_{16}\text{H}_{18}\text{N}_2\text{O}_3$  287.1390 found 287.1378.

**Synthesis of 3-(4-fluorophenyl)-1-(4-hydroxybenzyl)-1-methylurea (2.34c):**



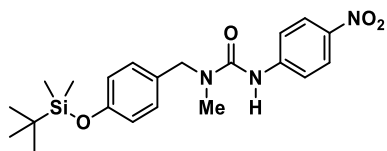
**1-(4-((tert-Butyl)dimethylsilyloxy)benzyl)-3-(4-fluorophenyl)-1-methylurea:** Obtained through reaction of the amine and *p*-fluorophenyl isocyanate as pale yellow solid (0.2 g, 33%), m.p. 80-84 °C, purified by chromatography (7% EtOAc/Hexanes).  $^1\text{H}$  NMR (500 MHz,  $\text{CDCl}_3$ )  $\delta$  7.25 (ddd,  $J = 9.1, 4.8, 2.3$  Hz, 2H), 7.16 (d,  $J = 6.5, 2.1$  Hz, 2H), 6.95 (ddt,  $J = 8.9, 6.5, 2.1$  Hz, 2H), 6.83 (dd,  $J = 8.5, 2.1$  Hz, 2H), 6.35 (s, 1H), 4.49 (d,  $J = 2.0$  Hz, 2H), 3.01 (d,  $J = 2.0$  Hz, 3H), 1.01 – 0.93 (m, 9H), 0.24 – 0.13 (m, 6H);  $^{13}\text{C}$  NMR (125 MHz,  $\text{CDCl}_3$ )  $\delta$  158.0, 155.9, 155.3, 135.0, 129.8, 128.6, 122.0, 121.9, 120.5, 115.5, 115.4, 52.0, 34.9, 25.7, 18.3, -4.4; FT-IR (neat,  $\text{cm}^{-1}$ ): 3325, 2960, 2928, 2858; HRMS ( $m/z$ ): calc for  $[\text{M}+\text{H}]^+$   $\text{C}_{21}\text{H}_{29}\text{FN}_2\text{O}_2\text{Si}$  389.2055 found 389.2040.



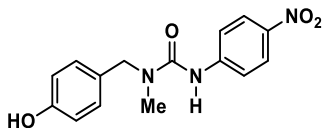
**3-(4-Fluorophenyl)-1-(4-hydroxybenzyl)-1-methylurea (2.35c):** White solid (96 mg, 65%), m.p. 134-138 °C, purified by chromatography (30% EtOAc/Hexanes).  $^1\text{H}$  NMR (500 MHz,  $\text{CDCl}_3$ )  $\delta$  7.29 – 7.22 (m, 2H), 7.11 (d,  $J = 8.5$  Hz, 2H), 7.00 – 6.90 (m, 2H), 6.78 (d,  $J = 8.5$  Hz, 2H), 6.31 (s, 1H), 5.97 (s, 1H), 4.49 (s, 2H), 3.02 (s, 3H);  $^{13}\text{C}$  NMR (126 MHz,  $\text{CDCl}_3$ )  $\delta$  160.0, 158.1, 156.0, 155.4, 134.9, 129.4, 128.9, 122.0, 122.0, 115.9, 115.6, 115.5, 52.0, 34.9, 29.8; FT-IR (neat,  $\text{cm}^{-1}$ )

<sup>1</sup>): 3349, 3123, 2925, 2848, 1636, 1503, 1212; HRMS (*m/z*): calc for [M+H]<sup>+</sup> C<sub>15</sub>H<sub>15</sub>FN<sub>2</sub>O<sub>2</sub> 275.1190 found 275.1174.

**Synthesis of 1-(4-hydroxybenzyl)-1-methyl-3-(4-nitrophenyl)urea (2.34d):**

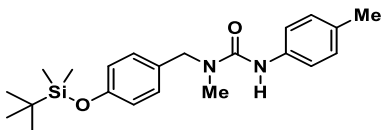


*1-(4-((tert-butyldimethylsilyl)oxy)benzyl)-1-methyl-3-(4-nitrophenyl)urea*: Obtained through reaction of the synthesized amine and *p*-nitrophenyl isocyanate as yellow solid (0.2 g, 30%), m.p. 104-108 °C, purified by chromatography (10% EtOAc/Hexanes). <sup>1</sup>H NMR (500 MHz, CDCl<sub>3</sub>) δ 8.13 (d, *J* = 9.2 Hz, 2H), 7.48 (d, *J* = 9.2 Hz, 2H), 7.16 (d, *J* = 8.4 Hz, 2H), 6.85 (d, *J* = 8.4 Hz, 2H), 6.75 (s, 1H), 4.52 (s, 2H), 3.07 (s, 3H), 0.96 (s, 9H), 0.19 (s, 6H); <sup>13</sup>C NMR (126 MHz, CDCl<sub>3</sub>) δ 155.6, 154.7, 145.4, 142.5, 129.3, 128.6, 125.1, 120.7, 118.4, 52.2, 35.2, 25.7, 18.3, -4.3; FT-IR (neat, cm<sup>-1</sup>): 3320, 2952, 2933, 2861, 1650, 1506; HRMS (*m/z*): calc for [M+H]<sup>+</sup> C<sub>21</sub>H<sub>29</sub>N<sub>3</sub>O<sub>4</sub>Si 416.2000 found 416.1992.

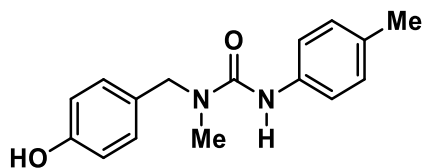


*1-(4-Hydroxybenzyl)-1-methyl-3-(4-nitrophenyl)urea (2.35d)*: Yellow solid (68 mg, 62%), m.p. 182-186 °C, purified by chromatography (20% EtOAc/Hexanes). <sup>1</sup>H NMR (500 MHz, CD<sub>3</sub>OD) δ 8.16 (d, *J* = 9.0 Hz, 2H), 7.66 (d, *J* = 9.0 Hz, 2H), 7.13 (d, *J* = 8.2 Hz, 2H), 6.77 (d, *J* = 8.2 Hz, 2H), 4.52 (s, 2H), 2.97 (s, 3H). <sup>13</sup>C NMR (125 MHz, CD<sub>3</sub>OD) δ 156.6, 156.2, 146.6, 142.2, 128.7, 128.0, 124.2, 119.0, 115.1, 51.1, 33.2. FT-IR (neat, cm<sup>-1</sup>): 3424, 3133, 3082, 2917, 2850, 1636, 1610, 1498, 1452, 1226.

**Synthesis of 1-(4-Hydroxybenzyl)-1-methyl-3-(p-tolyl)urea (2.34e):**



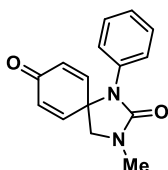
**1-(4-((tert-Butyldimethylsilyl)oxy)benzyl)-1-methyl-3-(p-tolyl)urea:** Obtained through reaction of the synthesized amine and *p*-tolyl isocyanate as white solid (230 mg, 75%), m.p. 120-122 °C, purified by chromatography (15% EtOAc/Hexanes). <sup>1</sup>H NMR (500 MHz, CDCl<sub>3</sub>) δ 7.18 (d, *J* = 8.4 Hz, 2H), 7.08 (d, *J* = 8.4 Hz, 2H), 6.99 (d, *J* = 7.9 Hz, 2H), 6.77 (d, *J* = 8.6 Hz, 2H), 6.58 (s, 1H), 4.40 (s, 2H), 2.88 (s, 3H), 2.23 (s, 3H), 0.96 (s, 9H), 0.16 (s, 6H); <sup>13</sup>C NMR (125 MHz, CDCl<sub>3</sub>) δ 156.2, 155.1, 136.7, 132.5, 130.3, 129.3, 129.2, 128.6, 120.5, 120.4, 119.3, 51.8, 34.6, 25.8, 20.8, 18.3, -4.3; FT-IR (neat, cm<sup>-1</sup>): 3307, 2957, 2930, 2853, 1634, 1591, 1508, 1244; HR-MS (*m/z*): calc for [M+H]<sup>+</sup> C<sub>22</sub>H<sub>32</sub>N<sub>2</sub>O<sub>2</sub>Si 385.2306 found 385.2257.



**1-(4-Hydroxybenzyl)-1-methyl-3-(p-tolyl)urea (2.35e):** White solid (80 mg, 57%), m.p. 170-173 °C, purified by chromatography (50% EtOAc/Hexanes). <sup>1</sup>H NMR (500 MHz, CD<sub>3</sub>OD) δ 7.22 (dd, *J* = 8.5, 2.5 Hz, 2H), 7.08 (ddd, *J* = 16.3, 8.6, 2.5 Hz, 4H), 6.74 (dd, *J* = 8.6, 2.6 Hz, 2H), 4.46 (s, 2H), 2.89 (s, 3H), 2.26 (s, 3H); <sup>13</sup>C NMR (125 MHz, CD<sub>3</sub>OD) δ 157.6, 156.5, 136.8, 132.5,

128.7, 128.6, 128.5, 121.5, 115.0, 51.0, 33.0, 19.5; FT-IR (neat,  $\text{cm}^{-1}$ ): 3324, 3111, 3014, 2919, 1627, 1607, 1509; HRMS ( $m/z$ ): calc for  $[\text{M}+\text{H}]^+$   $\text{C}_{16}\text{H}_{18}\text{N}_2\text{O}_2$  271.1441 found 271.1391.

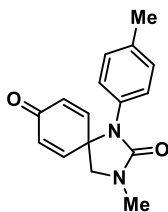
**Oxidative dearomatization of the synthesized ureas (2.36a-e):**



**3-Methyl-1-phenyl-1,3-diazaspiro[4.5]deca-6,9-diene-2,8-dione (2.36a):** To a solution of the synthesized urea (**2.35a**) (0.195 mmol, 50 mg) in 5-7 ml of HFIP, 77 mg of  $\text{Cs}_2\text{CO}_3$  (1.2 equiv) was added then stir reaction mixture for 10 minutes then 64 mg of PIDA (0.195 mmol, 1.0 molar equiv) was added at rt. The reaction was complete after few minutes and the following spiro compound was isolated as major product. Pale yellow semi-solid (18 mg, 36%), purified using by TLC prep. (25% EtOAc/Hexanes).  $^1\text{H}$  NMR (500 MHz,  $\text{CDCl}_3$ )  $\delta$  7.28 (d,  $J = 8.5$  Hz, 2H), 7.23 – 7.20 (m, 2H), 7.17 (ddt,  $J = 8.5, 6.8, 1.3$  Hz, 1H), 7.06 (d,  $J = 10.1$  Hz, 2H), 6.34 – 6.28 (m, 2H), 3.47 (s, 2H), 2.95 (s, 3H);  $^{13}\text{C}$  NMR (125 MHz,  $\text{CDCl}_3$ )  $\delta$  184.2, 148.5, 144.0, 130.4, 129.6, 128.7, 126.1, 124.8, 58.9, 53.2, 29.5; FT-IR (neat,  $\text{cm}^{-1}$ ): 3056, 2954, 2922, 2850, 1703, 1668, 1490; HRMS ( $m/z$ ): calc for  $[\text{M}+\text{H}]^+$   $\text{C}_{15}\text{H}_{14}\text{N}_2\text{O}_2$  255.1128 found 255.1117.

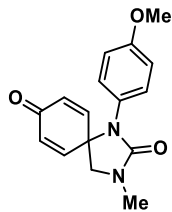
Oxidative dearomatization of 1-(4-hydroxybenzyl)-1-methyl-3-(*p*-tolyl)urea (**2.35e**): To a solution of the synthesized urea (**2.35e**) (0.185 mmol, 50 mg) in 5-7 ml HFIP, 73 mg of  $\text{Cs}_2\text{CO}_3$  (1.2 equiv) was added then stir reaction mixture for 10 minutes then 61 mg of PIDA (0.185 mmol, 1.0 molar equiv) was added at rt. The reaction was complete after few minutes and the following spiro compound was isolated as major product.





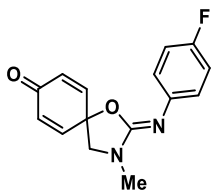
**3-Methyl-1-(p-tolyl)-1,3-diazaspiro[4.5]deca-6,9-diene-2,8-dione (2. 36b):** Yellow solid (28 mg, 56%), m.p. 115-119 °C, purified by chromatography (60% EtOAc/Hexanes). <sup>1</sup>H NMR (500 MHz, CDCl<sub>3</sub>) δ 7.04 (d, *J* = 8.0 Hz, 2H), 6.99 – 6.91 (m, 4H), 6.29 (d, *J* = 10.1 Hz, 2H), 3.53 (s, 2H), 3.05 (s, 3H), 2.27 (s, 3H); <sup>13</sup>C NMR (125 MHz, CDCl<sub>3</sub>) δ 184.3, 162.4, 144.4, 132.2, 130.1, 129.3, 123.3, 74.8, 56.3, 32.9, 20.9; FT-IR (neat, cm<sup>-1</sup>): 3020, 2919, 2874, 2854, 1685, 1670, 1508; HRMS (*m/z*): calc for [M+H]<sup>+</sup> C<sub>16</sub>H<sub>16</sub>N<sub>2</sub>O<sub>2</sub> 269.1285 found 269.1259.

Oxidative dearomatization of 1-(4-hydroxybenzyl)-3-(4-methoxyphenyl)-1-methylurea (**2. 35b**): To a solution of the synthesized urea (**2. 35b**) (0.35 mmol, 100 mg, 1.0 equiv) in 5-7 ml of HFIP, 139 mg of Cs<sub>2</sub>CO<sub>3</sub> (1.2 equiv) was added then stir reaction mixture for 10 minutes then 135 mg of PIDA (0.42 mmol, 1.2 molar equiv) was added at rt. The reaction was complete after few minutes and the following spiro compound was isolated as major product.



**1-(4-Methoxyphenyl)-3-methyl-1,3-diazaspiro[4.5]deca-6,9-diene-2,8-dione (2.36c):** Colorless solid (16 mg, 16%), m.p. 120-124 °C, purified by chromatography (25% EtOAc/Hexanes). <sup>1</sup>H NMR (500 MHz, CDCl<sub>3</sub>) δ 7.06 (d, *J* = 9.0 Hz, 2H), 7.00 (d, *J* = 10.1 Hz, 2H), 6.77 (d, *J* = 9.0 Hz, 2H), 6.24 (d, *J* = 10.1 Hz, 2H), 3.73 (s, 3H), 3.43 (s, 2H), 2.91 (s, 3H); <sup>13</sup>C NMR (125 MHz, CDCl<sub>3</sub>) δ 184.5, 159.1, 158.5, 148.3, 130.7, 129.5, 128.2, 114.3, 59.4, 55.5, 54.5, 31.6; FT-IR (neat, cm<sup>-1</sup>): 3050, 2920, 2850, 1709, 1665, 1554; HRMS (*m/z*): calc for [M+H]<sup>+</sup> C<sub>16</sub>H<sub>16</sub>N<sub>2</sub>O<sub>3</sub> 285.1234 found 285.1226.

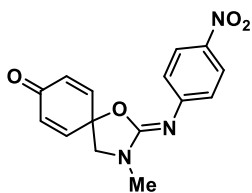
Oxidative dearomatization of 3-(4-fluorophenyl)-1-(4-hydroxybenzyl)-1-methylurea (**2.35c**): To a solution of the synthesized urea (**2.35c**) (0.29 mmol, 80 mg, 1.0 equiv) in 5-7 ml of HFIP, 115 mg of Cs<sub>2</sub>CO<sub>3</sub> (0.35 mmol, 1.2 equiv) was added then stir reaction mixture for 10 minutes then 95 mg of PIDA (0.29 mmol, 1.0 molar equiv) was added at rt. The reaction was complete after 30 minutes and the following spiro compound was isolated as major product.



**(Z)-2-((4-Fluorophenyl)imino)-3-methyl-1-oxa-3-azaspiro[4.5]deca-6,9-dien-8-one (2.36d):** Red solid (30 mg, 37%), m.p. 90-94 °C, purified chromatography (40% EtOAc/Hexanes). <sup>1</sup>H NMR (500 MHz, CDCl<sub>3</sub>) δ 7.00 (dd, *J* = 9.0, 5.0 Hz, 2H), 6.97 – 6.85 (m, 4H), 6.30 (d, *J* = 10.1 Hz, 2H),

3.52 (s, 2H), 3.01 (s, 3H);  $^{13}\text{C}$  NMR (125 MHz,  $\text{CDCl}_3$ )  $\delta$  184.3, 159.7, 157.8, 151.3, 144.3, 142.6, 142.5, 130.2, 124.6, 124.5, 123.2, 116.0, 115.8, 115.3, 115.1, 74.7, 56.2, 32.7; FT-IR (neat,  $\text{cm}^{-1}$ ): 2925, 2858, 1642, 1508, 1407, 1207; HRMS ( $m/z$ ): calc for  $[\text{M}+\text{H}]^+$   $\text{C}_{15}\text{H}_{13}\text{FN}_2\text{O}_2$  273.1034 found 273.1020.

**Oxidative dearomatization** of 1-(4-hydroxybenzyl)-1-methyl-3-(4-nitrophenyl)urea (**2.35d**): To a solution of the synthesized urea (**2.35d**) (0.183 mmol, 55 mg) in 5-7 ml of HFIP, 60 mg of  $\text{Cs}_2\text{CO}_3$  (1.2 equiv) was added then stir reaction mixture for 10 minutes then 60 mg of PIDA (0.183 mmol, 1.0 molar equiv) was added at rt. The reaction was complete after seconds and the following spiro compound was isolated as major product.



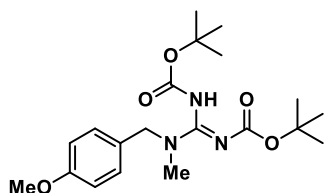
**(Z)-3-Methyl-2-((4-nitrophenyl)imino)-1-oxa-3-azaspiro[4.5]deca-6,9-dien-8-one** (**2.36e**):

Yellow solid (52 mg, 95%), m.p. 125-128 °C, purified chromatography (30% EtOAc/Hexanes).  $^1\text{H}$  NMR (500 MHz,  $\text{CDCl}_3$ )  $\delta$  8.04 (d,  $J = 9.0$  Hz, 2H), 7.07 (d,  $J = 9.0$  Hz, 2H), 6.90 (d,  $J = 10.1$  Hz, 2H), 6.29 (d,  $J = 10.1$  Hz, 2H), 3.58 (s, 2H), 3.03 (s, 3H);  $^{13}\text{C}$  NMR (125 MHz,  $\text{CDCl}_3$ )  $\delta$  184.0, 153.8, 152.4, 148.6, 143.5, 142.5, 130.5, 124.7, 123.9, 120.9, 75.3, 55.9, 32.5; FT-IR (neat,  $\text{cm}^{-1}$ ): 2928, 2890, 1658, 1639, 1575, 1492, 1319; HRMS ( $m/z$ ): calc for  $[\text{M}+\text{H}]^+$   $\text{C}_{15}\text{H}_{13}\text{N}_3\text{O}_4$  300.0979 found 300.0965.

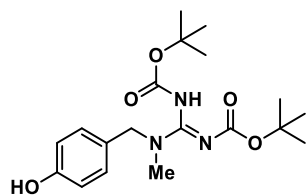
### Synthetic methodologies toward the synthesized guanidine derivatives:

Three different 2-methyl-2-thiopseudoureas were used for synthesis of the targeted guanidine derivatives. 1,3-diboc-2-methylisothiourea is commercially available and was used as it is. S-methylisothiourea hemi sulfate was used as precursor for the synthesis of 1,3-bis(2-trimethylsilylethoxycarbonyl)-2-methyl-2-thiopseudourea<sup>2</sup> and 1,3-diCbz-2-methylisothiourea.<sup>3</sup>

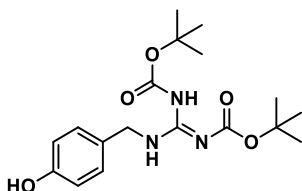
### Synthesis of guanidine derivatives:



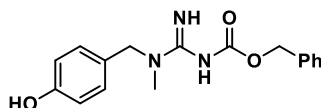
**(E)-2,3-diboc-1-(4-methoxybenzyl)-N-methyl-guanidine (2.45a):** To a solution of 1,3-diboc-2-methylisothiourea (3.31 mmol, 1.0 g), mercury oxide (3.31 mmol, 0.73 g) and triethyl amine (3.31 mmol, 0.47 g) in DCM (15 ml), 1-(4-methoxyphenyl)-N-methylmethanamine (3.31 mmol, 0.51 g) was added and stir the reaction mixture at rt overnight. Then the solvent was evaporated, and reaction mixture was subjected to column purification using 20% EtOAc/Hexanes. Obtained as a white solid (1.1 g, 85%, m.p. 84 - 86 °C). <sup>1</sup>H NMR (500 MHz, CDCl<sub>3</sub>) δ 10.10 (s, 1H), 7.13 (d, *J* = 8.2 Hz, 2H), 6.79 (d, *J* = 8.7 Hz, 2H), 4.56 (s, 2H), 3.71 (s, 3H), 2.79 (s, 3H), 1.44 (s, 18H); <sup>13</sup>C NMR (125 MHz, CDCl<sub>3</sub>) δ 162.8, 159.2, 156.3, 150.8, 129.9, 129.5, 128.5, 128.2, 114.3, 114.1, 81.9, 79.4, 55.3, 53.5, 36.5, 31.3, 28.2; FT-IR (neat, cm<sup>-1</sup>): 3412, 3320, 3128, 2982, 2933, 2878, 1720, 1648; HRMS (*m/z*): calc for [M+H]<sup>+</sup> C<sub>20</sub>H<sub>31</sub>N<sub>3</sub>O<sub>5</sub>, 394.2336, found: 394.2326.



**(E)-2,3-diBoc-1-(4-hydroxybenzyl)-1-methylguanidine (2. 45b):** To a solution of 1,3-diboc-2-methylisothiourea (2.0 mmol, 0.60 g), mercury oxide (2.0 mmol, 0.44 g) and triethylamine (2.0 mmol, 0.28 g) in dry THF (15 ml), 4-[(methylamino)methyl]phenol (2.0 mmol, 0.29 g) was added and stir the reaction mixture at rt overnight. Then the solvent was evaporated, and reaction mixture was subjected to column purification using 20% EtOAc/Hexanes and it was obtained as a white solid (0.4 g, 50%, m.p. 108–110 °C). <sup>1</sup>H NMR (500 MHz, CD<sub>3</sub>OD) δ 7.10 (d, *J* = 8.1 Hz, 2H), 6.77 (d, *J* = 8.2 Hz, 2H), 4.52 (s, 2H), 2.85 (s, 3H), 1.47 (s, 18H); <sup>13</sup>C NMR (125 MHz, CD<sub>3</sub>OD) δ 156.9, 154.2, 129.0, 128.6, 126.8, 121.8, 115.3, 80.1, 53.6, 53.2, 35.3, 27.4, 27.2, 27.1; FT-IR (neat, cm<sup>-1</sup>): 3199, 2977, 2931, 1745, 1649, 1586, 1139; HRMS (*m/z*): calc for [M+H]<sup>+</sup> C<sub>19</sub>H<sub>29</sub>N<sub>3</sub>O<sub>5</sub>, 380.2180, found: 380.2163.

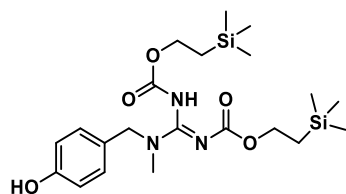


**(E)-2,3-diboc-1-(4-hydroxybenzyl)-guanidine (2.45c):** To a solution of 1,3-diboc-2-methylisothiourea (4.0 mmol, 1.2 g), mercury oxide (4.0 mmol, 0.87 g) and triethyl amine (4.0 mmol, 0.56 g) in DCM (15 ml), 4-(aminomethyl)phenol (4.0 mmol, 0.51 g) was added and stir the reaction mixture at rt overnight. Then the solvent was evaporated, and reaction mixture was subjected to column purification using 50% EtOAc/Hexanes and it was obtained as a white solid (1.0 g, 67%, m.p. 170-174 °C).  $^1\text{H}$  NMR (500 MHz,  $\text{CDCl}_3$ )  $\delta$  8.54 (t,  $J = 5.3$  Hz, 1H), 7.05 (d,  $J = 7.9$  Hz, 2H), 6.72 (d,  $J = 7.7$  Hz, 2H), 4.49 (d,  $J = 5.2$  Hz, 2H), 1.47 (s, 9H), 1.48 (s, 9H);  $^{13}\text{C}$  NMR (125 MHz,  $\text{CDCl}_3$ )  $\delta$  163.5, 156.1, 155.8, 153.2, 129.0, 128.5, 115.7, 83.4, 79.8, 44.5, 28.3, 28.1; FT-IR (neat,  $\text{cm}^{-1}$ ): 3412, 3320, 3128, 2982, 2933, 2878, 1720, 1648, 1609; HR-MS ( $m/z$ ): calc for  $[\text{M}+\text{H}]^+$   $\text{C}_{18}\text{H}_{27}\text{N}_3\text{O}_5$ , 366.2023, found: 366.2009.



**(E)-2-(benzyloxycarbonyl)-1-(4-hydroxybenzyl)-guanidine (2.49):** To a solution of 1,3-bis(benzyloxycarbonyl)-2-methyl-2-thiopseudourea (1.0 mmol, 358 mg), mercury oxide (1.0 mmol, 218 mg) and triethyl amine (1.0 mmol, 158 mg) in THF (15 ml), 4-(aminomethyl)phenol (1.0 mmol, 141 mg) was added and stir the reaction mixture at rt overnight. Then the solvent was evaporated, and reaction mixture was subjected to column purification using 50% EtOAc/Hexanes

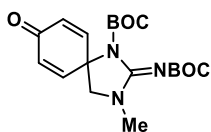
and it was obtained as a white solid (100 mg, 55%).  $^1\text{H}$  NMR (500 MHz,  $\text{CD}_3\text{OD}$ )  $\delta$  7.29 (d,  $J = 7.6$  Hz, 2H), 7.27 – 7.21 (m, 2H), 7.21 – 7.16 (m, 1H), 6.98 (d,  $J = 8.1$  Hz, 2H), 6.67 (d,  $J = 7.0$  Hz, 2H), 5.04 (s, 2H), 4.50 (s, 2H), 2.79 (s, 3H);  $^{13}\text{C}$  NMR (125 MHz,  $\text{CD}_3\text{OD}$ )  $\delta$  163.7, 161.6, 156.6, 137.8, 128.6, 128.0, 127.7, 127.3, 127.3, 115.0, 66.6, 51.3, 33.3; FT-IR (neat,  $\text{cm}^{-1}$ ): 3410, 3304, 2956, 2916, 1648, 1580; HR-MS ( $m/z$ ): calc for  $[\text{M}+\text{H}]^+$   $\text{C}_{17}\text{H}_{19}\text{N}_3\text{O}_3$ , 314.1499, found: 314.1461.



**(E)-2,3- bis(2-Trimethylsilylethoxycarbonyl)-1-(4-hydroxybenzyl)-guanidine (2.53):** To a solution of 1,3- bis(2-trimethylsilylethoxycarbonyl)-2-methylisothiourea (0.4 mmol, 160 mg), mercury oxide (0.4 mmol, 86 mg) and triethyl amine (0.4 mmol, 57 mg) in THF (15 ml), 4-(aminomethyl)phenol (0.4 mmol, 57 mg) was added and stir the reaction mixture at rt overnight. Then the solvent was evaporated, and reaction mixture was subjected to column purification using 25% EtOAc/Hexanes and it was obtained as a white solid (186 mg, 96%).  $^1\text{H}$  NMR (500 MHz,  $\text{CDCl}_3$ )  $\delta$  6.98 (d,  $J = 8.0$  Hz, 2H), 6.68 (d,  $J = 8.1$  Hz, 2H), 4.51 (s, 2H), 4.19 – 4.06 (m, 4H), 2.79 (s, 3H), 1.01 – 0.86 (m, 4H), -0.07 (s, 18H);  $^{13}\text{C}$  NMR (125 MHz,  $\text{CDCl}_3$ )  $\delta$  171.7, 156.4, 156.3, 129.4, 126.7, 115.7, 64.5, 60.6, 36.7, 21.1, 17.5, -1.5; FT-IR (neat,  $\text{cm}^{-1}$ ): 3400, 3197, 3150, 3064, 2954, 2922, 2896, 2855, 1724, 1670, 1596; HRMS ( $m/z$ ): calc for  $[\text{M}+\text{H}]^+$   $\text{C}_{21}\text{H}_{37}\text{N}_3\text{O}_5\text{Si}_2$ , 468.2345, found: 468.2292.

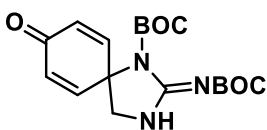
### Oxidative dearomatization of the guanidine derivatives

Oxidative dearomatization of (*E*)-2,3-diboc-1-(4-hydroxybenzyl)-1-methylguanidine: To a solution of the synthesized guanidine (**2.24**) (0.5 mmol, 173 mg) in 5-7 ml of HFIP, 178 mg of Cs<sub>2</sub>CO<sub>3</sub> (1.2 equiv) was added then stir reaction mixture for 10 minutes then 149 mg of PIDA (0.5 mmol, 1.0 molar equiv) was added at rt. The reaction was complete after seconds and the following spiro compound was isolated as major product.



*tert*-Butyl (Z)-2-((*tert*-butoxycarbonyl)imino)-3-methyl-8-oxo-1,3-diazaspiro[4.5]deca-6,9-diene-1-carboxylate (**2.46b**): White crystals (43 mg, 25%, mp 185-189 °C), purified chromatography (80% EtOAc in hexane) then crystalized from ethanol. <sup>1</sup>H NMR (500 MHz, CDCl<sub>3</sub>) δ 6.92 (d, *J* = 10.1 Hz, 1H), 6.28 (d, *J* = 10.0 Hz, 2H), 3.43 (s, 2H), 2.91 (s, 3H), 1.47 (s, 9H), 1.31 (s, 9H); <sup>13</sup>C NMR (126 MHz, CDCl<sub>3</sub>) δ 184.4, 159.1, 151.0, 149.2, 148.0, 147.3, 129.4, 129.3, 84.1, 79.4, 59.4, 55.2, 32.5, 28.3, 27.8; FT-IR (neat, cm<sup>-1</sup>): 2972, 2931, 1748, 1660, 1616, 1491, 1240, 1151, 1134, 841, 745; HRMS (*m/z*): calc for [M+H]<sup>+</sup> C<sub>19</sub>H<sub>27</sub>N<sub>3</sub>O<sub>5</sub>, 378.2023, found: 378.2018.

**Oxidative dearomatization** of (*E*)-2,3-diboc-1-(4-hydroxybenzyl)-guanidine (**2.26**) : To a solution of the synthesized guanidine (**2.26**) (0.55 mmol, 200 mg) in 5-7 ml of HFIP, 216 mg of

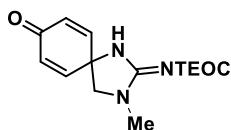




Cs<sub>2</sub>CO<sub>3</sub> (1.2 equiv) was added then stir reaction mixture for 10 minutes then 180 mg of PIDA (1.0 molar equiv) was added at rt. The reaction was complete after seconds and the following spiro compound was isolated as major product.

***tert*-Butyl (Z)-2-((*tert*-butoxycarbonyl)imino)-8-oxo-1,3-diazaspiro[4.5]deca-6,9-diene-1-carboxylate (2.46c):** Colorless crystals (30 mg, 15%, m.p. 260-264 °C), purified by chromatography (50% EtOAc/hexane). <sup>1</sup>H NMR (500 MHz, CDCl<sub>3</sub>) δ 9.73 (s, 1H), 6.86 (dd, *J* = 10.3, 2.4 Hz, 2H), 6.24 (dd, *J* = 10.3, 2.3 Hz, 2H), 3.93 (s, 2H), 1.49 (s, 9H), 1.34 (s, 9H); <sup>13</sup>C NMR (125 MHz, CDCl<sub>3</sub>) δ 184.7, 151.9, 149.9, 148.4, 146.7, 128.4, 85.2, 82.3, 62.2, 62.0, 28.1, 27.8; FT-IR (neat, cm<sup>-1</sup>): 3336, 1674, 1625, 1064, 1015, 443; HRMS (*m/z*): calc for [M+H]<sup>+</sup> C<sub>18</sub>H<sub>25</sub>N<sub>3</sub>O<sub>5</sub>, 364.1867, found: 364.1857.

**Oxidative dearomatization** of (*E*)-2,3-bis(2-trimethylsilyloxyethyl)-1-(4-hydroxybenzyl)-guanidine (**2.53**): To a solution of the synthesized guanidine (**2.53**) (0.35 mmol, 166 mg) in 5-7 ml of HFIP, 137 mg of Cs<sub>2</sub>CO<sub>3</sub> (1.2 equiv) was added, then after 2 min 116 mg of PIDA (1.0 molar equiv) was added and continue stirring at rt. After 2 h stirring, 29 mg of PIDA \_equivalent to 0.25 molar equiv\_ was added and continue stirring at rt. After 30 min, TLC showed the starting material was consumed. HFIP was evaporated and the reaction mixture was absorbed onto silica gel and subjected for column purification.

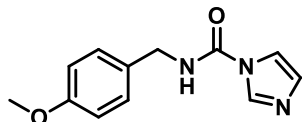


**2-(trimethylsilyl)ethyl (E)-(3-methyl-8-oxo-1,3-diazaspiro[4.5]deca-6,9-dien-2-ylidene)carbamate (2.54):** Colorless solid (10 mg, 9%, m.p. 140-144 °C), purified flash column chromatography using 50% EtOAc/Hexanes, followed by prep TLC technique using same

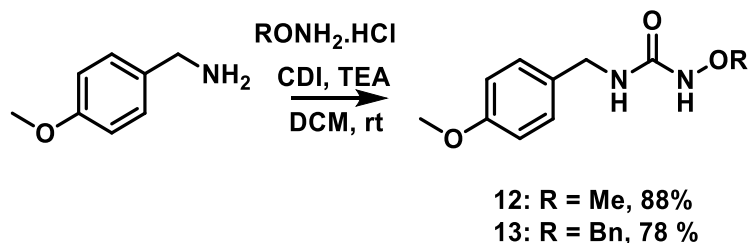
concentration.  $^1\text{H}$  NMR (500 MHz,  $\text{CDCl}_3$ )  $\delta$  8.05 (s, 1H), 6.87 (d,  $J = 10.1$  Hz, 2H), 6.29 (d,  $J = 9.9$  Hz, 2H), 4.25 – 4.07 (m, 2H), 3.50 (s, 2H), 3.02 (s, 3H), 1.12 – 0.98 (m, 2H), 0.03 (s, 9H);  $^{13}\text{C}$  NMR (125 MHz,  $\text{CDCl}_3$ )  $\delta$  184.0, 161.6, 146.3, 129.9, 64.0, 56.7, 56.5, 32.2, 17.8, -1.5; FT-IR (neat,  $\text{cm}^{-1}$ ): 3354, 2953, 2925, 2855, 1677, 1616, 1471; HRMS ( $m/z$ ): calc for  $[\text{M}+\text{H}]^+$   $\text{C}_{15}\text{H}_{23}\text{N}_3\text{O}_3\text{Si}$  322.1581 found 322.1558.

## 9.2.2. Chapter two and three:

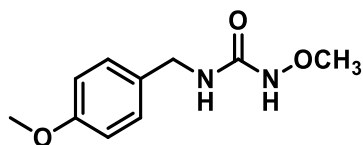
### Chapter Two



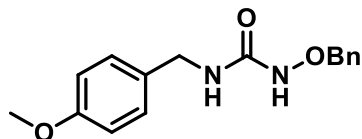
***N*-(4-methoxybenzyl)-1H-imidazole-1-carboxamide (3. 11):** To a solution of 4-methoxybenzylamine (65.0  $\mu$ L, 0.50 mmol, 1.0 equiv) in dichloromethane (2.0 ml), hydrochloric acid was added (100  $\mu$ L) then the reaction formed a white precipitate which was stirred for 5 minutes before addition of 1,1'-Carbonyldiimidazole (CDI) (98.0 mg, 0.55 mmol, 1.1 equiv) and DMF (0.8 ml). The solution was stirred for 2 h and then the solvent was evaporated. The crude product was purified chromatography using 2% methanol in dichloromethane, yielding the desired product as white material (60.0 mg, 55%, m.p. 118 – 120  $^{\circ}$ C).  $^1\text{H}$  NMR (500 MHz,  $\text{CDCl}_3$ )  $\delta$  8.21 (t,  $J = 5.7$  Hz, 1H), 8.04 (s, 1H), 7.41 (d,  $J = 1.6$  Hz, 1H), 7.14 (d,  $J = 7.0$  Hz, 2H), 6.78 – 6.74 (m, 3H), 4.37 (d,  $J = 5.6$ , 2H), 3.69 (s, 3H).  $^{13}\text{C}$  NMR (126 MHz,  $\text{CDCl}_3$ )  $\delta$  159.3, 149.1, 136.0, 129.4, 129.4, 116.8, 114.2, 55.3, 44.4. FT-IR (neat,  $\text{cm}^{-1}$ ): 3314, 3036, 3001, 2833, 1609, 1508, 1228; HRMS ( $m/z$ ): 301.1546, 321.1364, 339.1097, 359.2071.



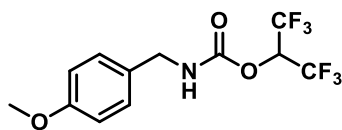
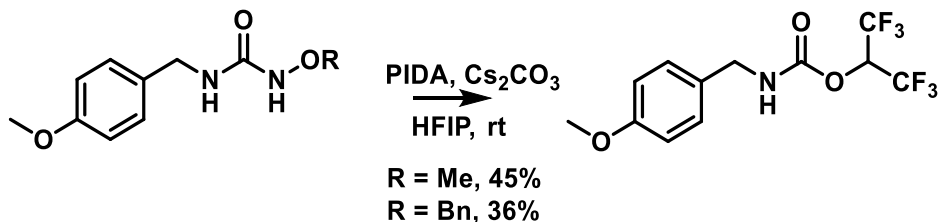
General Procedure of synthesis the *N*-methoxy urea derivatives: To a solution of the corresponding alkoxy amine (hydroxy methyl amine hydrochloride (1.0 equiv, 10.0 mmol, 0.83 g)) or benzyl hydroxy amine (1.0 equiv, 10.0 mmol, 1.3 ml) in dichloromethane (30 ml), triethyl amine (1.0 equiv, 10.0 mmol, 1.40 ml) was added at rt and the solution was stirred for 10 min after forming a white precipitate. Then 1,1'-Carbonyldiimidazole (CDI) (1.0 equiv, 10.0 mmol, 1.70 g) was added and stir the reaction at rt overnight. Then 4-methoxybenzylamine (**2. 10**) (1.0 equiv, 10.0 mmol, 1.4 g) was added to the mixture and stirred for 12 h. The solvent was evaporated, and the product was purified chromatography using 2% methanol in dichloromethane.



**1-methoxy-3-(4-methoxybenzyl)urea (3.12):** Obtained as a white solid (1.9 g, 88%, m.p. 112 – 114 °C). <sup>1</sup>H NMR (500 MHz, CDCl<sub>3</sub>) δ 7.16 (dd, *J* = 8.7, 2.3 Hz, 2H), 6.79 (dd, *J* = 8.8, 2.5 Hz, 2H), 5.98 (s, 1H), 4.31 (s, 2H), 3.71 (s, 3H), 3.57 (s, 3H). <sup>13</sup>C NMR (126 MHz, CDCl<sub>3</sub>) δ 160.3, 159.0, 130.7, 129.0, 114.1, 64.2, 55.3, 43.0. FT-IR (neat, cm<sup>-1</sup>): 3342, 3175, 2957, 2920, 2840, 1649, 1539, 1508, 1238; HRMS (*m/z*): calc for C<sub>10</sub>H<sub>14</sub>N<sub>2</sub>O<sub>3</sub> [M+H]<sup>+</sup> 211.1075 found 211.1077.

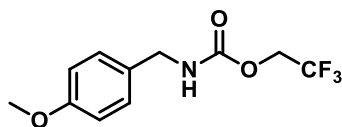


**1-(Benzyloxy)-3-(4-methoxybenzyl)urea (3.13):** Obtained as colorless crystals (2.2 g, 78%, m.p. 98 – 100 °C). <sup>1</sup>H NMR (500 MHz, CDCl<sub>3</sub>) δ 7.29 (d, *J* = 1.3 Hz, 5H), 7.07 (d, *J* = 8.7 Hz, 2H), 6.80 (d, *J* = 7.7 Hz, 2H), 4.71 (s, 2H), 4.25 (s, 2H), 3.74 (s, 3H). <sup>13</sup>C NMR (126 MHz, CDCl<sub>3</sub>) δ 160.2, 159.0, 135.5, 135.3, 130.6, 129.3, 129.3, 128.9, 128.9, 128.8, 128.8, 128.7, 114.1, 78.8, 78.7, 55.4, 43.0. FT-IR (neat, cm<sup>-1</sup>): 3321, 3060, 3032, 2928, 2918, 2835, 1655, 1537, 1510, 1249; HRMS (*m/z*): calc for [M+Na]<sup>+</sup> C<sub>16</sub>H<sub>18</sub>N<sub>2</sub>O<sub>3</sub> 309.1210 found 309.1188.

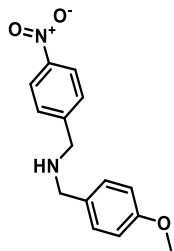


**(1,1,1,3,3,3-hexafluoropropan-2-yl (4-methoxybenzyl)carbamate (3.14):** To a solution of the synthesized thiourea (**3.12**) (1.0 equiv, 0.53 mmol, 112.0 mg) in HFIP (7 ml), Cs<sub>2</sub>CO<sub>3</sub> (1.2 equiv, 0.64 mmol, 211 mg) was added and followed by IBDA (1.0 equiv, 0.53 mmol, 175 mg) at rt. The

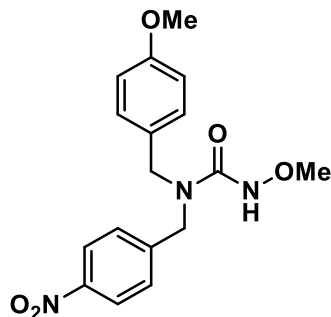
reaction was completed after 2 h and the new carbamate compound **14** was purified by column chromatography (20% EtOAc/Hexanes). Obtained as colorless solid (80 mg, 45%, m.p. 68 – 70 °C). <sup>1</sup>H NMR (500 MHz, CDCl<sub>3</sub>) δ 7.15 (d, *J* = 6.7 Hz, 2H), 6.83 (d, *J* = 6.5 Hz, 2H), 5.66 (sep, *J* = 8.5, 6.3, 3.3 Hz, 1H), 5.37 (s, 1H), 4.30 (d, *J* = 5.7 Hz, 1H), 3.75 (s, 3H). <sup>13</sup>C NMR (126 MHz, CDCl<sub>3</sub>) δ 159.4, 152.6, 129.1, 129.0, 121.8, 119.6, 114.3, 68.0, 67.7, 67.4, 67.2, 55.3, 45.2. HRMS (*m/z*): 391.2832, 413.2656.



**2,2,2-Trifluoroethyl (4-methoxybenzyl)carbamate (3.84)**: Obtained via constant current electrolysis using undivided electronic cell. Iodobenzene (PhI, 102 mg, 0.5 mmol, 2.0 equiv.) was added to a solution of LiClO<sub>4</sub> (53.0 mg, 0.5 mmol, 2.0 equiv) in trifluoroethanol (5 ml) as an electrolyte and subjected to electrolysis for 1 h to (in situ) generate hypervalent iodine reagent. Then, 1-methoxy-3-(4-methoxybenzyl)urea (**3.12**) (52.5 mg, 0.25 mmol, 1.0 equiv) was added and continued the electrolysis reaction for more 15 minutes. The solvent was evaporated, and the crude product was purified by column chromatography (30% EtOAc/Hexanes). Obtained as a colorless solid (27 mg, 42%, m.p. 80 – 82 °C). <sup>1</sup>H NMR (500 MHz, CDCl<sub>3</sub>) δ 7.15 (d, *J* = 8.7 Hz, 2H), 6.81 (d, *J* = 8.7 Hz, 2H), 5.18 (s, 1H), 4.41 (q, *J* = 8.6 Hz, 2H), 4.26 (d, *J* = 5.9 Hz, 2H), 3.74 (s, 3H). <sup>13</sup>C NMR (126 MHz, CDCl<sub>3</sub>) δ 159.3, 154.5, 129.8, 129.0, 124.3, 122.1, 114.2, 61.4, 61.1, 60.8, 60.6, 55.3, 44.9. FT-IR (neat, cm<sup>-1</sup>): 3315, 2996, 2976, 2941, 2843, 1703, 1586, 1536, 1242, 1146; HRMS (*m/z*): 238, 278, 300, 315, 337, 344.

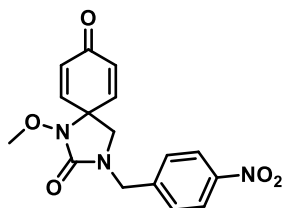


***N*-(4-methoxybenzyl)-1-(4-nitrophenyl)methanamine (3.16)**: A solution of 4-methoxy benzyl amine (1.0 equiv, 3.80 mmol, 0.51 ml) in acetonitrile (15 ml), K<sub>2</sub>CO<sub>3</sub> (1.5 equiv, 5.7 mmol, 0.79 g) was added and followed by 4-nitrobenzyl chloride (1.2 equiv, 4.54 mmol, 0.79 g). The mixture was stirred overnight at room temperature. The solvent was concentrated then the mixture was purified chromatography (50% EtOAc/Hexanes) to afford the desired secondary amine (0.80 g, 80%, yellow liquid). <sup>1</sup>H NMR (500 MHz, CDCl<sub>3</sub>) δ 8.03 (d, *J* = 8.9 Hz, 2H), 7.41 (d, *J* = 8.9 Hz, 2H), 7.18 (d, *J* = 8.7 Hz, 2H), 6.79 (d, *J* = 8.7 Hz, 2H), 3.78 (s, 2H), 3.69 (s, 3H), 3.65 (s, 2H). <sup>13</sup>C NMR (126 MHz, CDCl<sub>3</sub>) δ 158.8, 148.6, 146.9, 132.1, 129.4, 128.7, 123.5, 113.9, 55.2, 52.7, 52.2. FT-IR (neat, cm<sup>-1</sup>): 2933, 2835, 1605, 1508, 1456, 1340, 1242; HRMS (*m/z*): calc for C<sub>15</sub>H<sub>17</sub>N<sub>2</sub>O<sub>3</sub> [M+H]<sup>+</sup> 273.1234 found 273.1219.

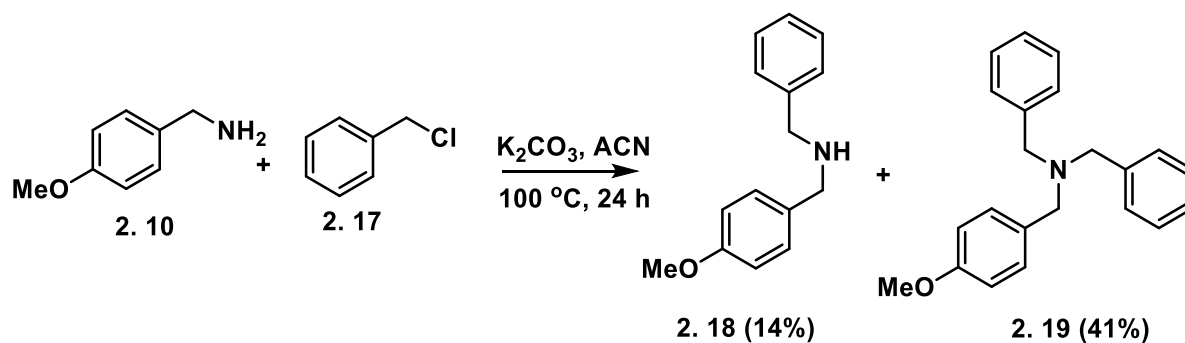


**3-Methoxy-1-(4-methoxybenzyl)-1-(4-nitrobenzyl)urea (3.22):** To a solution of methoxy amine hydrochloride (1.0 equiv, 2.75 mmol, 0.23 g) in dichloromethane (20 ml), triethyl amine (1.0 equiv, 2.75 mmol, 0.387 ml) was added at room temperature and stirred the solution for 10 min. Then 1,1'-carbonyldiimidazole (CDI) (1.0 equiv, 2.75 mmol, 0.47 g) was added and stir the mixture overnight. N-(4-methoxybenzyl)-1-(4-nitrophenyl)methanamine (**3.16**) (1.0 equiv, 2.75 mmol, 0.75 g) was added to the mixture and stirred at rt overnight. The solvent was evaporated, and the product was chromatography purified (70% EtOAc/hexanes) to afford the desired urea derivative as a brown liquid (0.64 g, 67%). <sup>1</sup>H NMR (500 MHz, CDCl<sub>3</sub>) δ 8.18 (d, *J* = 8.7 Hz, 2H), 7.41 (d, *J* = 8.5 Hz, 2H), 7.10 (d, *J* = 8.6 Hz, 2H), 6.87 (d, *J* = 8.6 Hz, 2H), 4.60 (s, 2H), 4.32 (s, 2H), 3.81 (s, 3H), 3.70 (s, 3H). <sup>13</sup>C NMR (76 MHz, CDCl<sub>3</sub>) δ 159.8, 159.6, 147.5, 144.9, 128.5, 128.4, 127.6, 124.1, 114.7, 64.5, 55.5, 50.0, 49.8. FT-IR (neat, cm<sup>-1</sup>): 2920, 2849, 1605, 1460, 1341, 1301, 1174. HRMS (*m/z*): calc for C<sub>17</sub>H<sub>20</sub>N<sub>3</sub>O<sub>5</sub> 346.1397 found 346.1372.

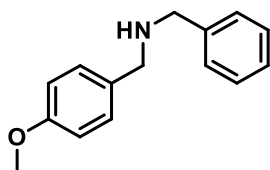




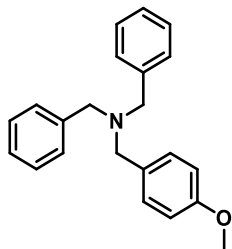
**1-Methoxy-3-(4-nitrobenzyl)-1,3-diazaspiro[4.5]deca-6,9-diene-2,8-dione (3.25):** To a solution of 3-methoxy-1-(4-methoxybenzyl)-1-(4-nitrobenzyl)urea (**2.22**) (200 mg, 0.58 mmol, 1.0 equiv) in HFIP (7 ml), was added  $\text{Cs}_2\text{CO}_3$  (228 mg, 0.70 mmol, 1.2 equiv) followed by stirring for 10 minutes then IBDA (95 mg, 0.24 mmol, 1.3 molar equiv) was added at rt. The reaction was complete after 2 hours and the product was purified chromatography (50% EtOAc/Hexanes). Obtained as a pale-yellow solid (110 mg, 52%, m.p. 168 - 172 °C).  $^1\text{H}$  NMR (500 MHz,  $\text{CDCl}_3$ )  $\delta$  8.19 (d,  $J = 6.7$  Hz, 2H), 7.40 (d,  $J = 6.9$  Hz, 2H), 6.84 (d,  $J = 10.1$  Hz, 2H), 6.33 (d,  $J = 9.9$  Hz, 2H), 4.49 (s, 2H), 3.72 (s, 3H), 3.13 (s, 2H).  $^{13}\text{C}$  NMR (126 MHz,  $\text{CDCl}_3$ )  $\delta$  184.4, 160.1, 145.2, 142.7, 132.3, 129.0, 124.3, 77.3, 77.1, 76.8, 65.9, 61.3, 49.3, 47.6. FT-IR (neat,  $\text{cm}^{-1}$ ): 3114, 3040, 2977, 2936, 1729, 1669, 1631, 1607, 1424; HRMS ( $m/z$ ): calc for  $[\text{M}+\text{Na}]^+$   $\text{C}_{16}\text{H}_{15}\text{N}_3\text{O}_5\text{Na}$  352.0904 found 352.0885.



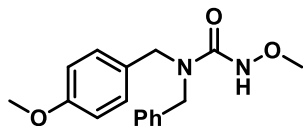
To a solution of 4-methoxybenzyl amine (**3.10**) (1.0 equiv, 30.0 mmol, 4.2 ml) in acetonitrile (30 ml),  $\text{K}_2\text{CO}_3$  (1.5 equiv, 45 mmol, 6.3 g) was added followed by benzyl chloride (**2.17**) (1.2 equiv, 36 mmol, 4.2 ml). The reaction was refluxing at  $100\text{ }^\circ\text{C}$  for 24 h. The solvent was concentrated, and the mixture was subjected to column purification to isolate the following products.



**N-benzyl-1-(4-methoxyphenyl)methanamine (3.18):** Obtained as a yellow liquid (1.0 g, 14% (30% EtOAc/Hexanes)).  $^1\text{H}$  NMR (300 MHz,  $\text{CDCl}_3$ )  $\delta$  7.17 (m, 4H), 7.09 (d,  $J = 8.6$  Hz, 2H), 6.70 (d,  $J = 8.7$  Hz, 2H), 3.61 (s, 2H), 3.57 (s, 3H), 3.55 (s, 2H).  $^{13}\text{C}$  NMR (76 MHz,  $\text{CDCl}_3$ )  $\delta$  158.6, 140.3, 132.3, 129.3, 128.4, 128.2, 126.9, 113.7, 55.1, 53.0, 52.5. FT-IR (neat,  $\text{cm}^{-1}$ ): 3061, 3001, 2931, 2833, 1610, 1509, 1441, 1031; HRMS ( $m/z$ ): calc for  $[\text{M}+\text{H}]^+$   $\text{C}_{15}\text{H}_{18}\text{NO}$  228.1383 found 228.1364.

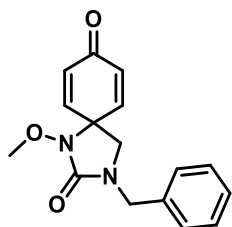


***N,N*-dibenzyl-1-(4-methoxyphenyl)methanamine (3. 19):** Obtained as a yellow liquid (4.0 g, 41%, (10% EtOAc/Hexanes)).  $^1\text{H}$  NMR (500 MHz,  $\text{CDCl}_3$ )  $\delta$  7.47 (d,  $J = 7.3$  Hz, 4H), 7.37 (t,  $J = 7.7$  Hz, 6H), 7.27 (t,  $J = 7.3$  Hz, 2H), 6.92 (d,  $J = 8.6$  Hz, 2H), 3.81 (s, 3H), 3.60 (s, 4H), 3.56 (s, 2H).  $^{13}\text{C}$  NMR (126 MHz,  $\text{CDCl}_3$ )  $\delta$  158.8, 139.9, 131.7, 130.0, 128.9, 128.4, 127.0, 113.8, 57.9, 57.4, 55.4. FT-IR (neat,  $\text{cm}^{-1}$ ): 3061, 2930, 2792, 2711, 1610, 1584, 1245; HRMS ( $m/z$ ): calc for  $[\text{M}+\text{H}]^+$   $\text{C}_{22}\text{H}_{23}\text{NO}$  318.1852 found 318.1829.

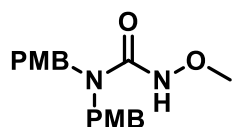


**1-Benzyl-3-methoxy-1-(4-methoxybenzyl)urea (3.24):** To a solution of methoxy amine hydrochloride (1.3 equiv, 4.88 mmol, 0.41 g) in dichloromethane (0.2 M, 19 ml), triethyl amine (1.3 equiv, 4.88 mmol, 0.69 ml) was added at room temperature and stirred the solution for 10 min. Then 1,1'-carbonyldiimidazole (CDI) (1.3 equiv, 4.88 mmol, 0.92 g) was added and stir the mixture overnight. *N*-benzyl-1-(4-methoxyphenyl)methanamine (**3. 18**) (1.0 equiv, 3.75 mmol, 0.84 g) was added to the mixture and stirred at rt overnight. The solvent was evaporated, and the product was chromatography purified (30% EtOAc/hexanes) to afford the desired urea derivative as a white solid (0.90 g, 80%, m.p. 58 – 60 °C).  $^1\text{H}$  NMR (500 MHz,  $\text{CDCl}_3$ )  $\delta$  7.29 – 7.18 (m, 3H), 7.15 (d,  $J = 6.9$  Hz, 2H), 7.07 (d,  $J = 8.6$  Hz, 2H), 6.79 (d,  $J = 8.7$  Hz, 2H), 4.36 (s, 2H), 4.32 (s, 2H), 3.72 (s, 3H), 3.62 (s, 3H).  $^{13}\text{C}$  NMR (126 MHz,  $\text{CDCl}_3$ )  $\delta$  159.8, 159.3, 136.8, 129.0,

128.8, 128.7, 127.8, 127.4, 114.3, 64.3, 55.3, 49.8, 49.5. FT-IR (neat,  $\text{cm}^{-1}$ ): 3262, 3237, 3029, 2931, 2834, 1644, 1584, 1248; HRMS ( $m/z$ ): calc for  $[\text{M}+\text{Na}]^+$   $\text{C}_{17}\text{H}_{20}\text{N}_2\text{O}_3\text{Na}$  323.1366 found 323.1342.

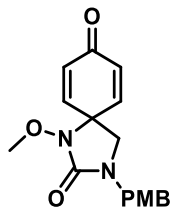


**3-benzyl-1-methoxy-1,3-diazaspiro[4.5]deca-6,9-diene-2,8-dione (3.27):** To a solution of 1-benzyl-3-methoxy-1-(4-methoxybenzyl)urea (**3.24**) (300 mg, 1.0 mmol, 1.0 equiv) in HFIP (10 ml), was added  $\text{Cs}_2\text{CO}_3$  (394 mg, 1.0 mmol, 1.0 equiv) followed by stirring for 10 minutes then IBDA (657 mg, 2.0 mmol, 2.0 molar equiv) was added at rt. The reaction was completed after 2 h and the crude product **3.27** was purified by chromatography (50% EtOAc/Hexanes). Obtained as brown gummy material (130 mg, 45%).  $^1\text{H}$  NMR (500 MHz,  $\text{CDCl}_3$ )  $\delta$  7.29 (m, 5H), 7.07 (d,  $J = 8.7$  Hz, 2H), 6.80 (d,  $J = 7.7$  Hz, 1H), 4.71 (s, 2H), 4.25 (s, 2H), 3.71 (s, 3H). FT-IR (neat,  $\text{cm}^{-1}$ ): 2936, 1722, 1667, 1610, 1176, 1030; HRMS ( $m/z$ ): calc for  $[\text{M}+\text{Na}]^+$   $\text{C}_{16}\text{H}_{15}\text{N}_3\text{O}_5$  352.0904 found 352.0885.

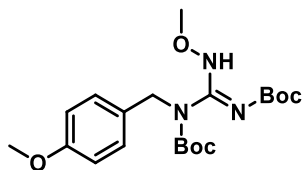


**3-Methoxy-1,1-bis(4-methoxybenzyl)urea (3.23):** To a solution of methoxy amine hydrochloride (1.3 equiv, 10.14 mmol, 0.85 g) in dichloromethane (40 ml), triethyl amine (1.3 equiv, 10.14 mmol, 1.5 ml) was added at room temperature and the solution was stirred for 10 minutes. Then 1,1'-carbonyldiimidazole (CDI) (1.3 equiv, 10.14 mmol, 1.73 g) was added and stir

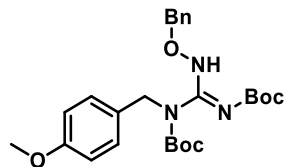
the mixture overnight. Bis(4-methoxybenzyl)amine (**3.21**) (1.0 equiv, 7.8 mmol, 2.0 g) was added to the mixture and stirred at rt overnight. The solvent was evaporated and then product was chromatography purified (50% EtOAc/hexanes). Obtained as a shiny white solid (1.95 g, 76%, m.p. 82-84 °C). <sup>1</sup>H NMR (301 MHz, CDCl<sub>3</sub>) δ 8.18 (s, 1H), 7.03 (d, *J* = 8.6 Hz, 4H), 6.74 (d, *J* = 8.7 Hz, 2H), 4.26 (s, 4H), 3.67 (s, 6H), 3.60 (s, 4H). <sup>13</sup>C NMR (76 MHz, CDCl<sub>3</sub>) δ 160.0, 159.1, 129.0, 114.1, 64.1, 55.2, 48.6. FT-IR (neat, cm<sup>-1</sup>): 3207, 3009, 2996, 2931, 2900, 2835, 1644, 1613, 1506, 1235; HRMS (*m/z*): calc for [M+H]<sup>+</sup> C<sub>18</sub>H<sub>23</sub>N<sub>2</sub>O<sub>4</sub> [M+H]<sup>+</sup> 331.1652 found 331.1630.



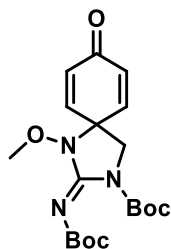
**1-Methoxy-3-(4-methoxybenzyl)-1,3-diazaspiro[4.5]deca-6,9-diene-2,8-dione (3.26):** To a solution of 3-methoxy-1,1-bis(4-methoxybenzyl)urea (**3.23**) (359mg, 1.0 mmol, 1.0 equiv) in HFIP (10 ml), Cs<sub>2</sub>CO<sub>3</sub> (418 mg, 1.2 mmol, 1.2 equiv) was added and followed by stirring for 10 minutes, then IBDA (1.04 g, 2.0 mmol, 2.0 molar equiv) was added at rt. The starting material was completely consumed after 10 minutes and the spiro compound (**3.26**) was purified chromatography (50% EtOAc/Hexanes). Obtained as a pale-yellow solid (280 mg, 89%, m.p. 106 – 108 °C). <sup>1</sup>H NMR (301 MHz, CDCl<sub>3</sub>) δ 7.09 (d, *J* = 8.6 Hz, 2H), 6.79 (t, *J* = 9.4 Hz, 4H), 6.23 (d, *J* = 10.2 Hz, 2H), 4.28 (s, 2H), 3.69 (s, 3H), 3.64 (s, 3H), 3.04 (s, 2H). <sup>13</sup>C NMR (76 MHz, CDCl<sub>3</sub>) δ 184.7, 160.1, 159.5, 146.0, 131.9, 129.7, 127.1, 114.3, 65.7, 61.4, 55.3, 48.6, 47.5. FT-IR (neat, cm<sup>-1</sup>): 3043, 3001, 2966, 2932, 2837, 1720, 1667, 1632, 1609, 1029; HRMS (*m/z*): calc for C<sub>17</sub>H<sub>18</sub>N<sub>2</sub>O<sub>4</sub>Na [M+Na]<sup>+</sup> 337.1159 found 337.1133.



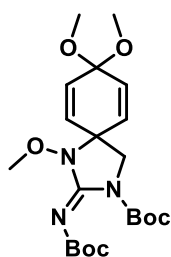
**(Z)-1,2-diboc-3-methoxy-1-(4-methoxybenzyl)-guanidine (3.35):** To a solution of tert-butyl (Z)-(((tert-butoxycarbonyl)imino)(methylthio)methyl)(4-methoxybenzyl)carbamate (**3.34**) (3.44 mmol, 1.42 g, 1.0 equiv), mercury oxide (3.78 mmol, 0.82 g, 1.1 equiv) and triethylamine (4.13 mmol, 0.6 g, 1.2 equiv) in dry THF (15 ml), methoxy amine hydrochloride (6.88 mmol, 0.57 g, 2.0 equiv) was added and the reaction was stirred at 40 °C overnight. Then the solvent was evaporated, and the crude product was purified chromatography (20% EtOAc/Hexanes). Obtained as a colorless solution (1.13 g, 79%). <sup>1</sup>H NMR (500 MHz, CDCl<sub>3</sub>) δ 7.25 (d, *J* = 6.7 Hz, 2H), 6.75 (d, *J* = 6.7 Hz, 2H), 4.47 (s, 2H), 3.70 (s, 6H), 1.38 (s, 9H), 1.34 (s, 9H). <sup>13</sup>C NMR (126 MHz, CDCl<sub>3</sub>) δ 158.9, 153.5, 149.0, 130.3, 113.5, 81.5, 81.4, 61.9, 55.2, 28.2, 28.1. FT-IR (neat, cm<sup>-1</sup>): 2977, 2934, 1748, 1716, 1642, 1613, 1513, 1245; HRMS (*m/z*): calc for C<sub>20</sub>H<sub>32</sub>N<sub>3</sub>O<sub>6</sub> [M+H]<sup>+</sup> 410.2286 found 410.2273.



**(Z)-1,2-diboc-3-benzyloxy-1-(4-methoxybenzyl)-guanidine (3.36):** To a solution of tert-butyl (Z)-(((tert-butoxycarbonyl)imino)(methylthio)methyl)(4-methoxybenzyl)carbamate (**3.34**) (0.73 mmol, 0.3 g, 1.0 equiv), mercury oxide (0.73 mmol, 0.16 g, 1.0 equiv) and triethylamine (0.73 mmol, 102  $\mu$ L, 1.0 equiv) in dry THF (15 ml), benzyloxy amine (0.73 mmol, 92 mg, 1.0 equiv) was added and the reaction mixture was stirred at rt overnight. The solvent was evaporated, and the product was purified chromatography (20% EtOAc/Hexanes). Obtained as a colorless solution (0.25 g, 70%).  $^1\text{H}$  NMR (500 MHz,  $\text{CDCl}_3$ )  $\delta$  7.35 – 7.22 (m, 6H), 7.17 (d,  $J = 8.6$  Hz, 2H), 6.72 (d,  $J = 8.7$  Hz, 2H), 4.95 (s, 2H), 4.46 (s, 2H), 3.72 (s, 3H), 1.39 (s, 9H), 1.37 (s, 9H).  $^{13}\text{C}$  NMR (126 MHz,  $\text{CDCl}_3$ )  $\delta$  158.9, 153.6, 149.0, 137.3, 130.4, 128.4, 128.1, 113.5, 81.6, 81.4, 76.2, 55.2, 52.0, 28.2, 28.1. FT-IR (neat,  $\text{cm}^{-1}$ ): 3315, 2976, 2931, 1752, 1730, 1637, 1363, 1282, 1147; HRMS ( $m/z$ ): calc for  $\text{C}_{26}\text{H}_{36}\text{N}_3\text{O}_6$   $[\text{M}+\text{H}]^+$  486.2599 found 486.2608.



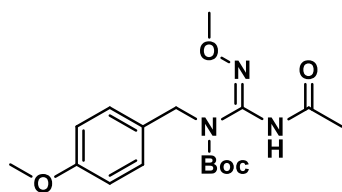
**tert-butyl (E)-2-((tert-butoxycarbonyl)imino)-1-methoxy-8-oxo-1,3-diazaspiro[4.5]deca-6,9-diene-3-carboxylate (3.37):** To a solution of (Z)-1,2-diboc-3-methoxy-1-(4-methoxybenzyl)-guanidine (**3.35**) (0.22 mmol, 1.0 equiv, 89 mg) in HFIP (2 ml, 0.1 M), Cs<sub>2</sub>CO<sub>3</sub> (0.22 mmol, 1.0 equiv, 72 mg) and IBDA (0.33 mmol, 1.5 equiv, 35.6 mg) were added with stirring at rt for 3h. The crude product was subjected to column purification (30% EtOAc/Hexanes). Obtained as a pale-yellow solid (26 mg, 30%, m.p. 84 – 86 °C). Also, it was isolated as a major product from the electrolysis reaction of (Z)-1,2-diboc-3-methoxy-1-(4-methoxybenzyl)-guanidine (**2.35**) (30%). <sup>1</sup>H NMR (500 MHz, CDCl<sub>3</sub>) δ 6.89 (d, *J* = 10.1 Hz, 2H), 6.37 (d, *J* = 10.1 Hz, 1H), 3.61 (s, 3H), 3.60 (s, 2H), 1.44 (s, 18H). <sup>13</sup>C NMR (126 MHz, CDCl<sub>3</sub>) δ 184.3, 147.0, 144.7, 132.5, 129.7, 84.1, 81.0, 65.0, 62.4, 49.6, 28.1, 28.0. FT-IR (neat, cm<sup>-1</sup>): 2978, 2928, 1755, 1671, 1634, 1140; HRMS (*m/z*): calc for C<sub>19</sub>H<sub>28</sub>N<sub>3</sub>O<sub>6</sub> [M+H]<sup>+</sup> 394.1973 found 394.1953.



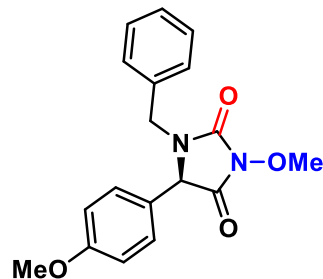
**tert-butyl (E)-2-((tert-butoxycarbonyl)imino)-1,8,8-trimethoxy-1,3-diazaspiro[4.5]deca-6,9-diene-3-carboxylate (3.82):** The (Z)-1,2-diboc-3-methoxy-1-(4-methoxybenzyl)-guanidine (**3.35**) (1.0 equiv, 0.25 mmol, 102 mg), tBuNOAc (1.0 equiv, 0.25 mmol, 75.3 mg) were placed in an undivided bottle containing methanol (10 ml). The bottle was equipped with a stir bar, and two



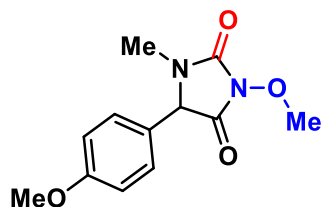
Pt rods. The reaction mixture was stirred and electrolyzed at a constant current of 10 mA at room temperature for 3 h. The reaction was monitored by TLC and the crude product was purified chromatography (40% EtOAc/Hexanes). The ketal product was obtained as a brown solid (67%, m.p. 174 – 176 °C). <sup>1</sup>H NMR (500 MHz, CDCl<sub>3</sub>) δ 6.05 (s, 4H), 3.57 (s, 3H), 3.43 (s, 2H), 3.20 (s, 6H), 1.38 (s, 9H), 1.37 (s, 9H). <sup>13</sup>C NMR (126 MHz, CDCl<sub>3</sub>) δ 158.9, 149.0, 147.6, 131.1, 130.9, 93.0, 83.4, 80.5, 64.4, 61.3, 51.3, 50.2, 49.7, 28.1, 28.0, 27.9. FT-IR (neat, cm<sup>-1</sup>); HRMS (*m/z*): calc for C<sub>21</sub>H<sub>34</sub>N<sub>3</sub>O<sub>7</sub> [M+H]<sup>+</sup> 439.2319 found 440.2368.



tert-butyl (Z)-(N-acetyl-N'-methoxycarbamimidoyl)(4-methoxybenzyl)carbamate (**3.39**): To a solution of (Z)-1,2-diboc-3-methoxy-1-(4-methoxybenzyl)-guanidine (**3.35**) (0.12 mmol, 1.0 equiv, 47 mg) in dry acetonitrile (1.5 ml) containing Cs<sub>2</sub>CO<sub>3</sub> (0.17 mmol, 1.5 equiv, 56.2 mg) and IBDA (0.35 mmol, 3.0 equiv, 111.1 mg) with stirring at 100 °C for 2 days. The solvent was concentrated, and the crude product was purified chromatography (20% EtOAc/Hexanes). Obtained as a white solid (14 mg, 35%, m.p. 100 – 102 °C). <sup>1</sup>H NMR (500 MHz, CDCl<sub>3</sub>) δ 7.79 (s, 1H), 7.25 (dd, *J* = 8.7, 2.7 Hz, 2H), 6.77 (dd, *J* = 8.7, 2.9 Hz, 2H), 4.48 (s, 2H), 3.75 (s, 3H), 3.73 (s, 3H), 2.00 (s, 3H), 1.35 (s, 9H). <sup>13</sup>C NMR (126 MHz, CDCl<sub>3</sub>) δ 158.9, 153.5, 142.8, 138.4, 130.2, 113.5, 107.8, 81.6, 74.0, 62.1, 55.3, 28.2. FT-IR (neat, cm<sup>-1</sup>): 3309, 2979, 2925, 2850, 1754, 1731, 1693, 1281, 1249; HR-MS (*m/z*): calc for [M+Na]<sup>+</sup> C<sub>17</sub>H<sub>25</sub>N<sub>3</sub>O<sub>5</sub>Na 374.1794 found 374.1676.



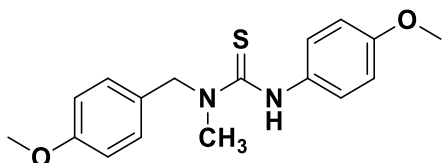
Synthesis of (R)-1-benzyl-3-methoxy-5-(4-methoxyphenyl)imidazolidine-2,4-dione (**4.42**): To a solution of methoxy amine hydrochloride (1.0 equiv, 0.35 mmol, 29 mg) in dichloromethane (6 ml), triethyl amine (1.0 equiv, 0.35 mmol, 100  $\mu$ l) was added at room temperature and stirred the solution for 10 min. Then 1,1'-carbonyldiimidazole (CDI) (1.0 equiv, 0.35 mmol, 60 mg) was added and stir the mixture overnight. Methyl (S)-2-(benzylamino)-2-(4-methoxyphenyl)acetate (**4.41**) (1.0 equiv, 0.35 mmol, 100 mg) was added to the mixture and stirred at rt overnight. The solvent was evaporated, and the product was chromatography purified (30% EtOAc/hexanes) to afford the isolated hydantoin derivative as a white solid (61 g, 54%, 96 – 98  $^{\circ}$ C).  $^1\text{H}$ NMR (500 MHz,  $\text{CDCl}_3$ )  $\delta$  7.29 (m, 3H), 7.08 (m, 4H), 6.91 (m, 2H), 5.06 (dd,  $J = 15.0, 5.2$  Hz, 1H), 4.53 (d,  $J = 5.3$  Hz, 1H), 3.99 (s, 3H), 3.68 (s, 3H), 3.67 (dd,  $J = 15.8, 4.6$  Hz, 1H).  $^{13}\text{C}$  NMR (126 MHz,  $\text{CDCl}_3$ )  $\delta$  166.0, 160.7, 152.6, 134.9, 129.1, 128.7, 128.4, 123.2, 115.0, 65.5, 60.6, 60.5, 55.5, 44.6, 14.3. FT-IR (neat,  $\text{cm}^{-1}$ ): 2927, 2839, 1782, 1727, 1512, 1496, 699; HRMS ( $m/z$ ): calc for  $\text{C}_{18}\text{H}_{19}\text{N}_2\text{O}_4$  327.1339 found 327.1325.



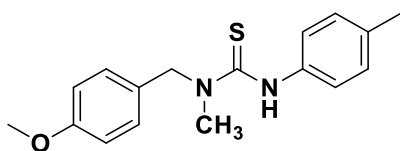
Synthesis of 3-methoxy-5-(4-methoxyphenyl)-1-methylimidazolidine-2,4-dione (**4.47**): To a solution of methoxy amine hydrochloride (1.0 equiv, 0.24 mmol, 20 mg) in dichloromethane (5 ml), triethyl amine (1.0 equiv, 0.24 mmol, 33  $\mu$ l) was added at room temperature and stirred the solution for 10 min. Then 1,1'-carbonyldiimidazole (CDI) (1.0 equiv, 0.24 mmol, 39 mg) was added and stir the mixture overnight. Methyl (S)-2-(4-methoxyphenyl)-2-(methylamino)acetate (**4.46**) (1.0 equiv, 0.24 mmol, 50 mg) was added to the mixture and stirred at rt overnight. The solvent was evaporated, and the product was chromatography purified (30% EtOAc/hexanes) to afford the isolated hydantoin derivative as a semi-solid (87 g, 83%).  $^1\text{H}$ NMR (500 MHz,  $\text{CDCl}_3$ )  $\delta$  7.11 (dd,  $J = 8.7, 1.6$  Hz, 2H), 6.88 (dd,  $J = 8.7, 1.6$  Hz, 2H), 4.66 (s, 1H), 3.94 (s, 3H), 3.75 (s, 3H), 2.79 (s, 3H).  $^{13}\text{C}$  NMR (126 MHz,  $\text{CDCl}_3$ )  $\delta$  165.8, 160.7, 152.8, 128.7, 123.3, 115.0, 65.5, 63.6, 55.4, 28.2. FT-IR (neat,  $\text{cm}^{-1}$ ): 2971, 2942, 2830, 1650, 1448, 1413, 816, 630.

### 9.2.3. Chapter five

General procedure for synthesizing thioureas derived from 1-(4-methoxyphenyl)-N-methylmethanamine and their cyclization is described in section 9.2.1:

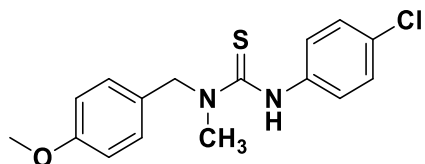


**1-(4-methoxybenzyl)-3-(4-methoxyphenyl)-1-methylthiourea (5.6b):** Obtained as white solid (0.95 g, 90%), m.p. 108-110 °C, purified chromatography (15% EtoAc/Hexanes). <sup>1</sup>H NMR (500 MHz, CDCl<sub>3</sub>) δ 7.21 (d, *J* = 8.7 Hz, 2H), 7.11 (d, *J* = 8.9 Hz, 2H), 6.84 (d, *J* = 8.6 Hz, 2H), 6.80 (d, *J* = 8.9 Hz, 2H), 4.96 (s, 2H), 3.75 (s, 3H), 3.73 (s, 3H), 3.19 (s, 3H). <sup>13</sup>C NMR (125 MHz, CDCl<sub>3</sub>) δ 182.9, 159.4, 157.9, 132.7, 128.7, 128.0, 127.8, 114.4, 114.0, 56.5, 55.5, 55.4. FT-IR (neat, cm<sup>-1</sup>): 3315, 3010, 2950, 2916, 2831, 1610, 1594; HR-MS (*m/z*): calc for [M+H]<sup>+</sup> C<sub>17</sub>H<sub>20</sub>N<sub>2</sub>O<sub>2</sub>S 317.1318 found 317.1302.

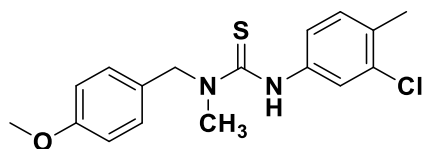


**1-(4-methoxybenzyl)-1-methyl-3-(p-tolyl)thiourea (5.6c):** Obtained as white solid (0.89 g, 90%), m.p. 142 -144 °C, purified chromatography (15% EtoAc/Hexanes). <sup>1</sup>H NMR (500 MHz, CDCl<sub>3</sub>) δ 7.25 (d, *J* = 8.7 Hz, 2H), 7.18 – 7.09 (m, 4H), 6.89 (d, *J* = 8.6 Hz, 2H), 4.99 (s, 2H), 3.80 (s, 3H), 3.15 (s, 3H), 2.33 (s, 3H). <sup>13</sup>C NMR (126 MHz, CDCl<sub>3</sub>) δ 182.6, 159.3, 137.3, 135.7, 129.3, 128.8, 128.2, 126.0, 114.3, 56.5, 55.4, 29.8, 21.1. FT-IR (neat, cm<sup>-1</sup>): 3324, 3261, 2999,

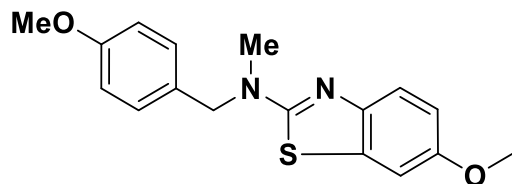
2918, 2834, 1611, 1589, 1510; HR-MS (m/z): calc for  $[M+H]^+$   $C_{17}H_{20}N_2OS$  301.1369 found 301.1353.



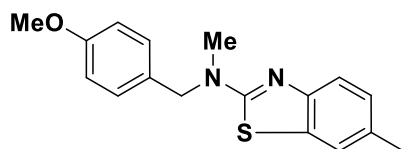
**3-(4-chlorophenyl)-1-(4-methoxybenzyl)-1-methylthiourea (5.6e):** Obtained as yellow solid (0.9 g, 85%), m.p. 148-150 °C, purified chromatography (30% EtOAc/Hexanes).  $^1H$  NMR (500 MHz,  $CDCl_3$ )  $\delta$  7.36 – 7.11 (m, 7H), 6.91 (d,  $J = 8.5$  Hz, 2H), 5.00 (s, 2H), 3.82 (s, 3H), 3.23 (s, 3H).  $^{13}C$  NMR (125 MHz,  $CDCl_3$ )  $\delta$  182.3, 159.4, 138.4, 131.1, 128.7, 128.7, 127.8, 127.0, 114.4, 56.5, 55.4. FT-IR (neat,  $cm^{-1}$ ): 3235, 3036, 3010, 2963, 2926, 2781, 1610, 1587, 1510, 1325; HR-MS (m/z): calc for  $[M+H]^+$   $C_{16}H_{17}ClN_2OS$  321.0823 found 321.0788.



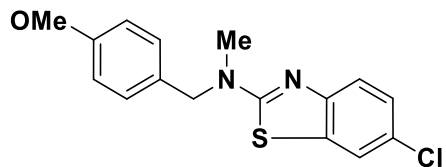
**3-(3-chloro-4-methylphenyl)-1-(4-methoxybenzyl)-1-methylthiourea (5.6d):** obtained as a white solid (0.78 g, 71%), m.p. 146 – 148 °C, purified by ethanolic crystallization and dried at room temperature.  $^1H$  NMR (500 MHz,  $CDCl_3$ )  $\delta$  7.24 – 7.13 (m, 4H), 7.08 (d,  $J = 8.0$  Hz, 1H), 7.01 (d,  $J = 8.2$  Hz, 1H), 6.83 (d,  $J = 7.3$  Hz, 2H), 4.92 (s, 2H), 3.74 (s, 3H), 3.12 (s, 3H), 2.26 (s, 3H).  $^{13}C$  NMR (126 MHz,  $CDCl_3$ )  $\delta$  182.4, 159.4, 138.6, 133.9, 133.6, 130.7, 128.7, 127.9, 126.2, 124.4, 114.4, 56.6, 55.4, 38.6, 19.7. FT-IR (neat,  $cm^{-1}$ ): 3230, 3083, 3000, 2956, 2829, 1577, 1509, 1491, 1395, 882; HR-MS (m/z): calc for  $[M+H]^+$   $C_{16}H_{20}ClN_2OS$  335.0979 found 335.0957.



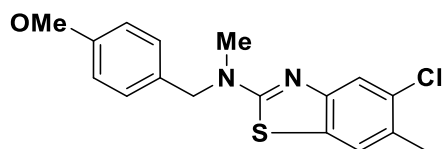
**6-Methoxy-N-(4-methoxybenzyl)-N-methylbenzo[d]thiazol-2-amine (5.7c):** Obtained as white solid (23%, 70.0 mg, Method A), (65%, 0.321 gm, Method B), m.p. 86-88 °C, purified chromatography (10% EtOAc/Hexanes).  $^1\text{H}$  NMR (500 MHz,  $\text{CDCl}_3$ )  $\delta$  7.59 (d,  $J = 8.8$  Hz, 1H), 7.41 – 7.32 (m, 2H), 7.26 (d,  $J = 2.6$  Hz, 1H), 7.02 (dd,  $J = 8.8, 2.6$  Hz, 1H), 6.98 (d,  $J = 8.7$  Hz, 2H), 4.78 (s, 2H), 3.93 (s, 3H), 3.91 (s, 3H), 3.20 (s, 3H).  $^{13}\text{C}$  NMR (125 MHz,  $\text{CDCl}_3$ )  $\delta$  167.5, 159.3, 154.9, 147.5, 132.0, 129.1, 128.6, 119.3, 114.2, 113.6, 105.4, 56.1, 56.0, 55.4, 37.6, 29.8. FT-IR (neat,  $\text{cm}^{-1}$ ): 2920, 2854, 1605, 1546, 1508, 1211; HR-MS (m/z): calc for  $[\text{M}+\text{H}]^+$   $\text{C}_{17}\text{H}_{18}\text{N}_2\text{O}_2\text{S}$  315.1162 found 315.1153.



**N-(4-methoxybenzyl)-N,6-dimethylbenzo[d]thiazol-2-amine (5.7e):** Obtained as white solid (20%, Method A), m.p. 80 - 82 °C, purified chromatography (25% EtOAc/Hexanes).  $^1\text{H}$  NMR (500 MHz,  $\text{CDCl}_3$ )  $\delta$  7.44 (d,  $J = 8.2$  Hz, 1H), 7.34 (s, 1H), 7.18 (d,  $J = 8.7$  Hz, 2H), 7.07 (dd,  $J = 8.2, 1.7$  Hz, 1H), 6.81 (d,  $J = 8.6$  Hz, 2H), 4.63 (s, 2H), 3.74 (s, 3H), 3.05 (s, 3H), 2.35 (s, 3H).  $^{13}\text{C}$  NMR (125 MHz,  $\text{CDCl}_3$ )  $\delta$  182.6, 159.3, 137.3, 135.7, 129.3, 128.8, 128.2, 126.0, 114.3, 56.5, 55.4, 38.2, 21.1. FT-IR (neat,  $\text{cm}^{-1}$ ): 2994, 2924, 2850, 1629, 1602, 1494; HR-MS (m/z): calc for  $[\text{M}+\text{H}]^+$   $\text{C}_{17}\text{H}_{18}\text{N}_2\text{OS}$  299.1213 found 299.1194.



**6-chloro-N-(4-methoxybenzyl)-N-methylbenzo[d]thiazol-2-amine (5.7f):** Obtained as white solid (60 mg, 30%, Method B), m.p. 72-73 °C, purified chromatography (8% EtOAc/Hexanes). <sup>1</sup>H NMR (500 MHz, CDCl<sub>3</sub>) δ 7.54 (dd, *J* = 2.2, 1.0 Hz, 1H), 7.47 (dd, *J* = 8.6, 1.0 Hz, 1H), 7.26 (dd, *J* = 2.1, 1.0 Hz, 1H), 7.23 (d, *J* = 8.6 Hz, 2H), 6.87 (d, *J* = 7.8 Hz, 2H), 4.68 (s, 2H), 3.79 (s, 3H), 3.10 (s, 3H). <sup>13</sup>C NMR (125 MHz, CDCl<sub>3</sub>) δ 168.9, 159.4, 151.6, 132.1, 129.1, 128.1, 126.5, 126.2, 120.4, 119.5, 114.2, 56.1, 55.3, 37.7. FT-IR (neat, cm<sup>-1</sup>): 3010, 2961, 2924, 2836, 1593, 1560, 1509, 1448, 1412, 856; HR-MS (m/z): calc for [M+H]<sup>+</sup> C<sub>16</sub>H<sub>16</sub>ClN<sub>2</sub>OS 319.0650 found 319.0666.

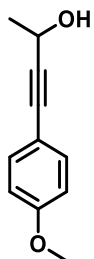


**5-chloro-N-(4-methoxybenzyl)-N,6-dimethylbenzo[d]thiazol-2-amine (5.7g):** Obtained as white solid (44 mg, 22%, Method B), m.p. 104-106 °C, purified chromatography (5% EtOAc/Hexanes). <sup>1</sup>H NMR (500 MHz, CDCl<sub>3</sub>) δ 7.52 (s, 1H), 7.35 (s, 1H), 7.17 (d, *J* = 8.7 Hz, 2H), 6.81 (d, *J* = 8.3 Hz, 2H), 4.63 (s, 2H), 3.75 (s, 3H), 3.04 (s, 2H), 2.34 (s, 2H). <sup>13</sup>C NMR (126 MHz, CDCl<sub>3</sub>) δ 169.2, 159.3, 132.3, 130.2, 129.1, 128.6, 128.1, 121.9, 119.0, 114.2, 114.0, 56.1, 55.3, 37.7, 20.1. FT-IR (neat, cm<sup>-1</sup>): 3056, 3032, 2990, 2918, 2849, 2834, 1737, 1606, 1561, 1176, 1098, 868; HR-MS (m/z): calc for [M+H]<sup>+</sup> C<sub>17</sub>H<sub>18</sub>ClN<sub>2</sub>OS 333.0823 found 333.0799.

#### 9.2.4. Chapter seven and eight:

##### Procedures for the synthesis of the propargyl alcohol and amine:

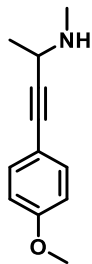
##### Synthesis of 4-(4-methoxyphenyl)but-3-yn-2-ol (7.3):



To a 500 ml flask containing 120 ml THF, 1-ethynyl-4-methoxybenzene (10.58 ml, 80 mmol, 1.0 equiv) was added while stirring at rt under argon. Then EtMgBr (26.1 ml, 80 mmol, 1.0 equiv) was added and the mixture was stirred under argon overnight. Acetaldehyde was then added (6.81 ml, 120 mmol, 1.5 equiv) while stirring at 0 °C forming a golden yellow solution. Then the solution was warmed to rt and stirring continued overnight. The reaction was quenched with saturated aqueous NaHCO<sub>3</sub> (30 ml) and then extracted with ethyl acetate (3x50 ml). The combined organic extracts were washed with brine solution (50 ml) then dried over sodium sulfate. The solvent was evaporated, and the crude product was purified by the flash column chromatography using 0-20% ethyl acetate/hexanes to afford the desired alcohol in good yield (9.5 g, 63%). <sup>1</sup>H NMR (500 MHz, CDCl<sub>3</sub>) δ 7.28 (d, *J* = 8.9 Hz, 2H), 6.75 (d, *J* = 8.9 Hz, 2H), 4.67 (q, *J* = 6.6, 1H), 3.73 (s, 3H), 1.47 (d, *J* = 6.6 Hz, 3H). <sup>13</sup>C NMR (126 MHz, CDCl<sub>3</sub>) δ 159.7, 133.2, 114.7, 113.9, 89.7, 83.9, 58.9, 55.3, 24.5. FT-IR (neat, cm<sup>-1</sup>): 3353, 2985, 2840, 2226, 1605, 1566, 1506, 1371, 1076, 835. HRMS (*m/z*): calc for C<sub>11</sub>H<sub>13</sub>O<sub>2</sub> [M+H]<sup>+</sup> 177.0910 found 177.0904.

##### Synthesis of 4-(4-methoxyphenyl)-N-methylbut-3-yn-2-amine (7.4):

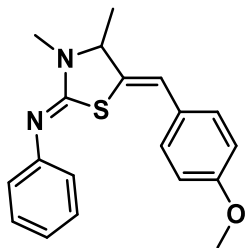




To a solution of 4-(4-methoxyphenyl)but-3-yn-2-ol (**7.3**) (0.34 g, 1.9 mmol, 1.0 equiv) in THF (5 ml, 2.5/mmol), triethylamine (1.32 ml, 9.5 mmol, 5.0 equiv) was added at rt then the mixture cooled in ice bath for 15 min. Then methane sulfonyl chloride (0.29 ml, 3.8 mmol, 2.0 equiv) was added dropwise at 0 °C and the mixture was stirring for more 15 min then warmed up to the room temperature for 1 h. Methyl amine in THF solution (5.3 ml, 9.5 mmol, 5.0 equiv) was added and the mixture was heated up to 50 °C and allowed to stir for 24 h. The reaction mixture was concentrated and then the gummy material was dissolved in ethyl acetate (30 ml) and washed with aqueous NaHCO<sub>3</sub> (20 ml). The aqueous layer was extracted with CH<sub>2</sub>Cl<sub>2</sub> (3x30 ml) then the combined organic extracts were dried over sodium sulfate. The solvent was removed by rotary evaporation and then the crude product was purified by flash column chromatography using 7% methanol in dichloromethane to afford the desired amine in a modest yield (0.12 g, 34%). <sup>1</sup>H NMR (500 MHz, CDCl<sub>3</sub>) δ 7.34 (d, *J* = 8.9 Hz, 2H), 6.80 (d, *J* = 8.9 Hz, 2H), 3.78 (s, 3H), 3.66 (q, *J* = 6.8 Hz, 1H), 2.78 (s, 1H), 2.55 (s, 3H), 1.44 (d, *J* = 6.8 Hz, 3H). <sup>13</sup>C NMR (126 MHz, CDCl<sub>3</sub>) δ 159.5, 133.2, 115.3, 113.9, 89.2, 83.4, 55.3, 47.5, 33.7, 22.0. FT-IR (neat, cm<sup>-1</sup>): 2962, 2934, 2835, 2767, 2458, 2229, 1603, 1507, 1290, 1243, 1026, 832. HRMS (*m/z*): calc for C<sub>12</sub>H<sub>16</sub>ON [M+H]<sup>+</sup> 190.1226 found 190.1228.

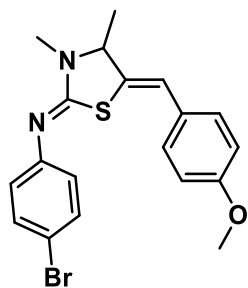
**General procedure for the synthesis of thiazolidine derivatives:**

To a 50 ml RBF containing 1.0 g of silica gel, 4-(4-methoxyphenyl)-*N*-methylbut-3-yn-2-amine (**7.4**) (1.0 equiv, 0.5 - 0.7 mmol) and the corresponding isothiourea derivative (1.0 equiv, 0.5 - 0.7 mmol) were added while stirring. The resulting slurry was placed under an argon atmosphere while stirring was continued at rt overnight. The silica gel containing the reaction mixture was poured directly onto a packed silica gel column followed elution with the appropriate solvent mixtures to afford the desired thiazolidines in good yield.



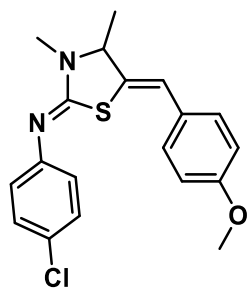
**(Z)-5-((Z)-4-methoxybenzylidene)-3,4-dimethyl-N-phenylthiazolidin-2-imine (7.5a):**

Obtained from reaction of 4-(4-methoxyphenyl)-*N*-methylbut-3-yn-2-amine (0.54 mmol, 103 mg) and phenyl isothiocyanate (0.54 mmol, 75.3 mg) as a semi-solid yellow material (34.0 mg, 60%), purified by chromatography (25% EtOAc/Hexanes). <sup>1</sup>H NMR (500 MHz, CDCl<sub>3</sub>) δ 7.36 (t, *J* = 7.6 Hz, 2H), 7.26 (d, *J* = 8.5 Hz, 2H), 7.13 (t, *J* = 7.4 Hz, 1H), 7.07 (d, *J* = 8.3 Hz, 2H), 6.92 (d, *J* = 8.6 Hz, 2H), 6.50 (d, *J* = 1.6 Hz, 1H), 4.57 (qd, *J* = 6.3, 1.5 Hz, 1H), 3.84 (s, 3H), 3.18 (s, 3H), 1.58 (d, *J* = 6.3 Hz, 3H). <sup>13</sup>CNMR (125 MHz, CDCl<sub>3</sub>) δ 158.6, 155.8, 151.3, 133.2, 132.5, 129.3, 129.0, 128.7, 123.3, 122.5, 119.6, 114.0, 114.0, 65.1, 55.3, 31.8, 21.0; FT-IR (neat, cm<sup>-1</sup>): 2959, 2920, 2850, 1614, 1584, 1508, 1247, 1176, 1027, 765; HRMS (*m/z*): calc for C<sub>19</sub>H<sub>21</sub>N<sub>2</sub>OS [M+H]<sup>+</sup> 325.1369 found 325.1345.



**(Z)-N-(4-bromophenyl)-5-((Z)-4-methoxybenzylidene)-3,4-dimethylthiazolidin-2-imine**

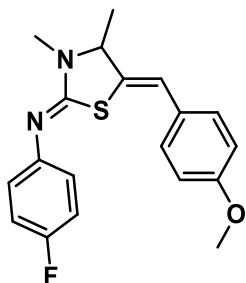
**(7.5b):** Obtained from reaction of 4-(4-methoxyphenyl)-*N*-methylbut-3-yn-2-amine (0.73 mmol, 136 mg) and *p*-bromophenyl isothiocyanate (0.73 mmol, 160 mg) as a semi-solid yellow material (41.7 mg, 61%), purified by chromatography (20% EtOAc/Hexanes). <sup>1</sup>H NMR (500 MHz, CDCl<sub>3</sub>) δ 7.39 (dd, *J* = 8.5, 1.8 Hz, 2H), 7.19 (dd, *J* = 8.6, 1.8 Hz, 2H), 6.87 (d, *J* = 8.7 Hz, 4H), 6.45 (s, 1H), 4.52 (q, *J* = 6.4 Hz, 1H), 3.78 (s, 3H), 3.11 (s, 3H), 1.52 (d, *J* = 6.3 Hz, 3H). <sup>13</sup>CNMR (125 MHz, CDCl<sub>3</sub>) δ 158.7, 132.0, 131.9, 129.3, 128.5, 124.4, 120.0, 116.2, 114.1, 65.3, 55.3, 31.8, 21.0; FT-IR (neat, cm<sup>-1</sup>): 2957, 2923, 2851, 2834, 1604, 1573, 1508, 1481, 1247, 1175, 1029, 858; HRMS (*m/z*): calc for C<sub>19</sub>H<sub>20</sub>N<sub>2</sub>OSBr [M+H]<sup>+</sup> 403.0474 found 403.0451.



**(Z)-N-(4-chlorophenyl)-5-((Z)-4-methoxybenzylidene)-3,4-dimethylthiazolidin-2-imine**

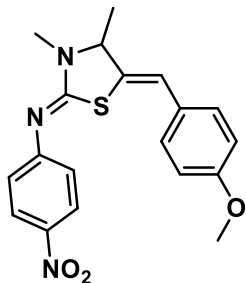
**(7.5c):** Obtained from reaction of 4-(4-methoxyphenyl)-*N*-methylbut-3-yn-2-amine (0.63 mmol, 118 mg) and *p*-chlorophenyl isothiocyanate (0.63 mmol, 108 mg) as a semi-solid yellow material

(68.3 mg, 61%), purified by chromatography (25% EtOAc/Hexanes).  $^1\text{H}$  NMR (500 MHz,  $\text{CDCl}_3$ ) 7.27 (d,  $J = 8.6$  Hz, 2H), 7.22 (d,  $J = 8.8$  Hz, 2H), 6.94 (d,  $J = 8.5$  Hz, 2H), 6.89 (d,  $J = 8.9$  Hz, 2H), 6.46 (s, 1H), 4.51 (q,  $J = 6.6$  Hz, 1H), 3.79 (s, 3H), 3.1 (s, 3H), 1.52 (d,  $J = 6.5$  Hz, 3H).  $^{13}\text{C}$  NMR (125 MHz,  $\text{CDCl}_3$ )  $\delta$  158.7, 156.1, 150.3, 132.2, 129.3, 129.1, 128.6, 128.3, 123.8, 119.9, 114.1, 65.2, 55.4, 31.7, 21.1. FT-IR (neat,  $\text{cm}^{-1}$ ): 2956, 2922, 2851, 1722, 1606, 1508, 1461, 1202, 832; HRMS ( $m/z$ ): calc for  $\text{C}_{19}\text{H}_{20}\text{N}_2\text{OSCl}$   $[\text{M}+\text{H}]^+$  359.0979 found 359.0946.



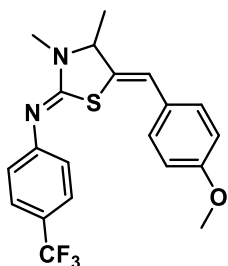
**(Z)-N-(4-fluorophenyl)-5-((Z)-4-methoxybenzylidene)-3,4-dimethylthiazolidin-2-imine (7.5d)**

**5d):** Obtained from reaction of 4-(4-methoxyphenyl)-N-methylbut-3-yn-2-amine (0.53 mmol, 100 mg) and *p*-fluorophenyl isothiocyanate (0.53 mmol, 80 mg) as a white solid (81.4 mg, 45%), m.p. 122-123 °C, purified by chromatography (25% EtOAc/Hexanes).  $^1\text{H}$  NMR (500 MHz,  $\text{CDCl}_3$ )  $\delta$  7.19 (dd,  $J = 8.7, 1.9$  Hz, 2H), 7.02 – 6.90 (m, 3H), 6.86 (dd,  $J = 6.8, 1.9$  Hz, 2H), 6.46 (s 1H), 4.53 (q,  $J = 6.4$  Hz, 1H), 3.79 (s, 3H), 3.13 (s, 3H), 1.53 (d,  $J = 6.5$  Hz, 3H).  $^{13}\text{C}$  NMR (126 MHz,  $\text{CDCl}_3$ )  $\delta$  158.7, 158.5, 132.0, 129.3, 128.5, 123.8, 123.7, 120.0, 115.7, 115.5, 114.1, 65.4, 55.3, 31.8, 21.0. FT-IR (neat,  $\text{cm}^{-1}$ ): 2981, 2956, 2928, 2833, 1605, 1572, 1497, 1449, 1308, 1286, 1251, 1087, 1031, 861. HRMS ( $m/z$ ): calc for  $\text{C}_{19}\text{H}_{20}\text{N}_2\text{OFS}$   $[\text{M}+\text{H}]^+$  343.1275 found 343.1248.



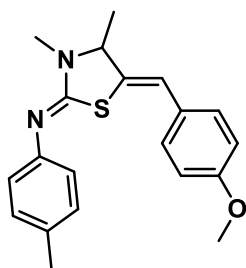
**(Z)-5-((Z)-4-methoxybenzylidene)-3,4-dimethyl-N-(4-nitrophenyl)thiazolidin-2-imine**

**(7.5e):** Obtained from reaction of 4-(4-methoxyphenyl)-N-methylbut-3-yn-2-amine (0.56 mmol, 106 mg) and *p*-nitrophenyl isothiocyanate (0.56 mmol, 104 mg) as a yellow solid (57.0 mg, 95%), m.p. 120-122 °C, purified by chromatography (25% EtOAc/Hexanes). <sup>1</sup>H NMR (500 MHz, CDCl<sub>3</sub>) δ 8.17 (dd, *J* = 9.0, 1.5 Hz, 2H), 7.18 (dd, *J* = 8.7, 1.5 Hz, 2H), 7.08 (d, *J* = 8.5 Hz, 2H), 6.87 (dd, *J* = 8.8, 1.5 Hz, 2H), 6.50 (s, 1H), 4.59 (q, *J* = 6.3 Hz, 1H), 3.79 (s, 3H), 3.16 (s, 3H), 1.56 (d, *J* = 6.3 Hz, 3H). <sup>13</sup>C NMR (126 MHz, CDCl<sub>3</sub>) δ 158.9, 129.3, 128.1, 125.1, 122.9, 120.8, 114.2, 65.5, 55.3, 31.9, 21.1. FT-IR (neat, cm<sup>-1</sup>): 2981, 2958, 2921, 2833, 1615, 1576, 1507, 1392, 1284, 1214, 851; HRMS (*m/z*): calc for C<sub>19</sub>H<sub>20</sub>N<sub>3</sub>O<sub>3</sub>S [M+H]<sup>+</sup> 370.1220 found 370.1196.



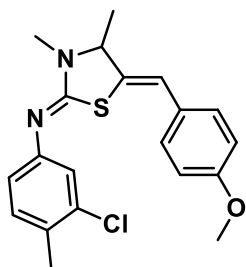
**(Z)-5-((Z)-4-methoxybenzylidene)-3,4-dimethyl-N-(4-(trifluoromethyl)phenyl)thiazolidin-2-imine (7.5f):** Obtained from reaction of 4-(4-methoxyphenyl)-N-methylbut-3-yn-2-amine (0.47 mmol, 89 mg) and *p*-(trifluoromethyl)phenyl isothiocyanate (0.47 mmol, 106 mg) as a pale yellow solid (33.0 mg, 58%), m.p. 120-121 °C, purified by chromatography (25% EtOAc/Hexanes). <sup>1</sup>H

NMR (500 MHz, CDCl<sub>3</sub>) δ 7.55 (dd, *J* = 8.6, 2.4 Hz, 2H), 7.18 (dd, *J* = 8.9, 2.5 Hz, 2H), 7.11 (d, *J* = 8.2 Hz, 2H), 6.90 – 6.86 (m, 2H), 6.49 (s, 1H), 4.59 (m, 1H), 3.78 (s, 3H), 3.20 (s, 3H), 1.55 (d, *J* = 6 Hz, 3H). <sup>13</sup>C NMR (126 MHz, CDCl<sub>3</sub>) δ 158.8, 156.1, 154.5, 131.8, 129.3, 128.5, 126.3, 126.3, 126.2, 126.2, 125.1, 123.7, 122.6, 120.1, 114.1, 65.2, 55.3, 31.7, 21.1.; FT-IR (neat, cm<sup>-1</sup>): 2958, 2925, 2851, 2838, 1625, 1590, 1509, 1318, 1250, 1101, 1062, 846; HRMS (*m/z*): calc for C<sub>20</sub>H<sub>20</sub>N<sub>2</sub>O<sub>F</sub><sub>3</sub>S [M+H]<sup>+</sup> 393.1243 found 393.1220.

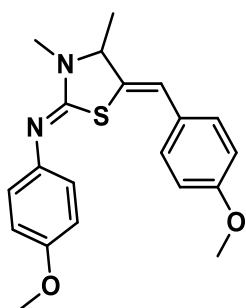


**(Z)-5-((Z)-4-methoxybenzylidene)-3,4-dimethyl-N-(*p*-tolyl)thiazolidin-2-imine (7.5g):**

Obtained from reaction of 4-(4-methoxyphenyl)-*N*-methylbut-3-yn-2-amine (0.53 mmol, 100 mg) and *p*-tert-butylphenyl isothiocyanate (0.53 mmol, 75 mg) as a pale yellow solid (35 mg, 20 %), m.p. 110 – 111 °C, purified by chromatography (25% EtOAc/Hexanes). <sup>1</sup>H NMR (500 MHz, CDCl<sub>3</sub>) δ 7.28 (d, *J* = 8.5 Hz, 2H), 7.20 (d, *J* = 8.8 Hz, 2H), 6.89 (d, *J* = 8.5 Hz, 2H), 6.83 (d, *J* = 8.0 Hz, 2H), 6.41 (s, 1H), 4.49 – 4.42 (m, 1H), 3.75 (s, 3H), 3.08 (s, 3H), 1.49 (d, *J* = 7.2 Hz, 3H), 1.31 (s, 3H). <sup>13</sup>C NMR (126 MHz, CDCl<sub>3</sub>) δ 158.7, 156.2, 150.5, 134.3, 132.3, 131.2, 130.4, 129.4, 128.6, 123.0, 120.8, 119.9, 114.1, 65.2, 55.4, 31.7, 21.1, 19.6. FT-IR (neat, cm<sup>-1</sup>): 2935, 2914, 2855, 1593, 1509, 1355, 1243, 1179, 1129, 838. HRMS (*m/z*): calc for C<sub>20</sub>H<sub>23</sub>N<sub>2</sub>O<sub>S</sub> [M+H]<sup>+</sup> 339.1515 found 339.1514.

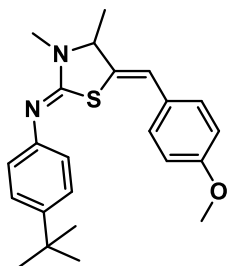


**(Z)-N-(3-chloro-4-methylphenyl)-5-((Z)-4-methoxybenzylidene)-3,4-dimethylthiazolidin-2-imine (7.5h):** Obtained from reaction of 4-(4-methoxyphenyl)-*N*-methylbut-3-yn-2-amine (0.53 mmol, 100 mg) and 3-chloro-4-methylphenyl isothiocyanate (0.53 mmol, 89 mg) as a pale-yellow solid (90.6 mg, 46%), m.p. 109-111 °C, purified by chromatography (25% EtOAc/Hexanes). <sup>1</sup>H NMR (500 MHz, CDCl<sub>3</sub>) δ 7.33 – 7.23 (m, 2H), 7.18 (dd, *J* = 8.3, 4.1 Hz, 1H), 7.06 (t, *J* = 2.6 Hz, 1H), 6.99 – 6.90 (m, 2H), 6.85 (dt, *J* = 8.1, 2.5 Hz, 1H), 6.50 (s, 1H), 4.56 (q, *J* = 6.2 Hz, 1H), 3.84 (s, 3H), 3.15 (s, 3H), 2.40 (s, 3H), 1.58 (d, *J* = 5.9 Hz, 3H). <sup>13</sup>C NMR (126 MHz, CDCl<sub>3</sub>) δ 158.7, 156.4, 150.1, 134.3, 132.1, 131.1, 130.5, 129.3, 128.5, 123.1, 120.8, 119.9, 114.1, 65.3, 55.3, 31.8, 21.1, 19.5; FT-IR (neat, cm<sup>-1</sup>): 2960, 2916, 2834, 1591, 1507, 1248, 1177, 1025, 866; HRMS (*m/z*): calc for C<sub>20</sub>H<sub>22</sub>N<sub>2</sub>OSCl [M+H]<sup>+</sup> 373.1136 found 373.1115.



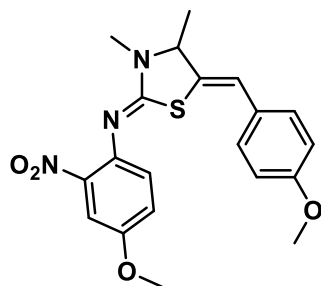
**(Z)-5-((Z)-4-methoxybenzylidene)-N-(4-methoxyphenyl)-3,4-dimethylthiazolidin-2-imine (7.5i):** Obtained from reaction of 4-(4-methoxyphenyl)-*N*-methylbut-3-yn-2-amine (0.59 mmol,

113 mg) and *p*-methoxyphenyl isothiocyanate (0.59 mmol, 100 mg) as a semi-solid yellow material (40.0 mg, 63%), purified by chromatography (25% EtOAc/Hexanes). <sup>1</sup>H NMR (500 MHz, CDCl<sub>3</sub>) δ 7.20 (d, *J* = 8.8 Hz, 2H), 6.92 (d, *J* = 8.8 Hz, 2H), 6.85 (dd, *J* = 8.8, 3.5 Hz, 4H), 6.43 (s, 1H), 4.50 (q, *J* = 6.3 Hz, 1H), 3.80 (s, 3H), 3.78 (s, 3H), 3.11 (s, 3H), 1.52 (d, *J* = 6.3 Hz, 3H). <sup>13</sup>C NMR (126 MHz, CDCl<sub>3</sub>) δ 158.6, 156.3, 155.9, 132.6, 129.3, 128.7, 123.3, 119.6, 114.2, 114.0, 65.2, 55.5, 55.3, 31.8, 21.0. FT-IR (neat, cm<sup>-1</sup>): 3033, 2954, 2925, 2833, 1602, 1502, 1236, 1133, 1028, 830; HRMS (*m/z*): calc for C<sub>20</sub>H<sub>23</sub>N<sub>2</sub>O<sub>2</sub>S [M+H]<sup>+</sup> 355.1475 found 355.1437.

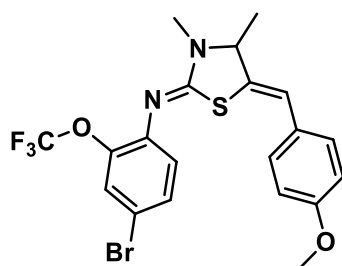


**(Z)-N-(4-(tert-butyl)phenyl)-5-((Z)-4-methoxybenzylidene)-3,4-dimethylthiazolidin-2-imine (7.5j):** Obtained from reaction of 4-(4-methoxyphenyl)-*N*-methylbut-3-yn-2-amine (0.47 mmol, 89 mg) and *p*-tert-butylphenyl isothiocyanate (0.47 mmol, 95 mg) as a pale yellow solid (27.4 mg, 95%), m.p. 122-123 °C, purified by chromatography (25% EtOAc/Hexanes). <sup>1</sup>H NMR (500 MHz, CDCl<sub>3</sub>) δ 7.32 (d, *J* = 8.3 Hz, 2H), 7.19 (d, *J* = 8.4 Hz, 2H), 7.02 (d, *J* = 8.1 Hz, 2H), 6.87 (d, *J* = 8.5 Hz, 2H), 6.49 (s, 1H), 4.60 (m, 1H), 3.79 (s, 3H), 3.28 (s, 3H), 1.56 (d, *J* = 6.4 Hz, 3H), 1.32 (s, 9H). <sup>13</sup>C NMR (126 MHz, CDCl<sub>3</sub>) δ 158.6, 155.2, 148.6, 145.8, 133.0, 129.3, 128.8, 125.9, 121.8, 119.5, 114.1, 64.9, 55.4, 34.4, 31.8, 31.6, 21.1.; FT-IR (neat, cm<sup>-1</sup>): 2957, 2929, 2853, 2836, 1597, 1508, 1248, 1176, 837; HRMS (*m/z*): calc for C<sub>23</sub>H<sub>29</sub>N<sub>2</sub>OS [M+H]<sup>+</sup> 381.1995 found 381.1967.





**(Z)-N-(4-methoxy-2-nitrophenyl)-5-((Z)-4-methoxybenzylidene)-3,4-dimethylthiazolidin-2-imine (7.5k):** Obtained from reaction of 4-(4-methoxyphenyl)-*N*-methylbut-3-yn-2-amine (0.53 mmol, 100 mg) and 4-methoxy-2-nitrophenyl isothiocyanate (0.53 mmol, 118 mg) as a semi-solid yellow material (43.0 mg, 63%), purified by chromatography (25% EtOAc/Hexanes). <sup>1</sup>H NMR (500 MHz, CDCl<sub>3</sub>) δ 7.43 (dd, *J* = 2.3 Hz, 1H), 7.16 (dd, *J* = 8.7, 2.0 Hz, 2H), 7.07 (ddd, *J* = 8.9, 3.0, 1.8 Hz, 1H), 7.00 (dd, *J* = 8.8, 1.8 Hz, 1H), 6.84 (dd, *J* = 8.7, 2.0 Hz, 2H), 6.46 (s, 1H), 4.58 (q, *J* = 6.3 Hz, 1H), 3.84 (s, 3H), 3.78 (s, 3H), 3.12 (s, 3H), 1.55 (d, *J* = 6.4 Hz, 3H). <sup>13</sup>C NMR (126 MHz, CDCl<sub>3</sub>) δ 158.7, 155.3, 131.6, 129.3, 128.4, 126.3, 121.0, 120.2, 114.1, 108.8, 65.8, 55.9, 55.3, 31.7, 21.2; FT-IR (neat, cm<sup>-1</sup>): 2965, 2929, 2836, 1604, 1508, 1247, 1176, 1029, 856; HRMS (*m/z*): calc for C<sub>20</sub>H<sub>22</sub>N<sub>3</sub>O<sub>4</sub>S [M+H]<sup>+</sup> 400.1326 found 400.1302.

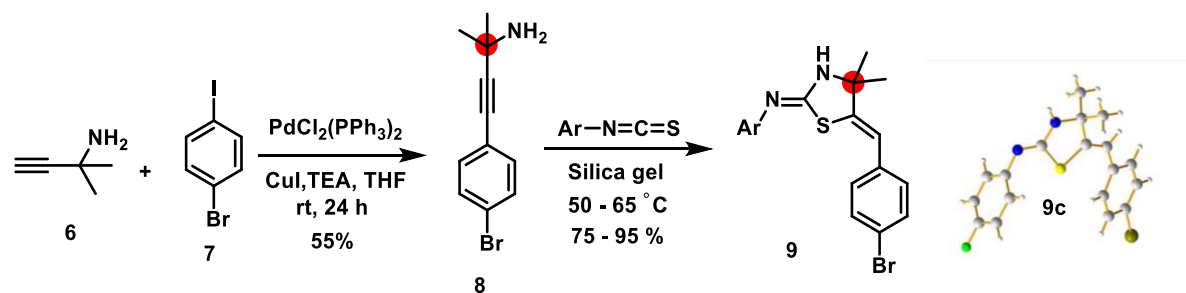


**(Z)-N-(4-bromo-2-(trifluoromethoxy)phenyl)-5-((Z)-4-methoxybenzylidene)-3,4-dimethylthiazolidin-2-imine (7.5l):** Obtained from reaction of 4-(4-methoxyphenyl)-*N*-methylbut-3-yn-2-amine (0.56 mmol, 106 mg) and 4-bromo-2-(trifluoromethoxy)phenyl isothiocyanate (0.56 mmol, 178 mg) as a semi-solid yellow material (47.0 mg, 57%), purified by

chromatography (25% EtOAc/Hexanes).  $^1\text{H}$  NMR (500 MHz,  $\text{CDCl}_3$ )  $\delta$  7.38 (dd,  $J = 2.5, 1.2$  Hz, 1H), 7.34 (ddd,  $J = 8.5, 2.3, 1.2$  Hz, 1H), 7.19 (d,  $J = 8.6$  Hz, 2H), 6.95 (dd,  $J = 8.5, 1.1$  Hz, 1H), 6.88 (dd,  $J = 7.6, 1.2$  Hz, 2H), 6.46 (s, 1H), 4.59 – 4.52 (m, 1H), 3.79 (s, 3H), 3.12 (s, 3H), 1.53 (d,  $J = 6.4$  Hz, 3H).  $^{13}\text{C}$  NMR (126 MHz,  $\text{CDCl}_3$ )  $\delta$  158.8, 157.0, 143.6, 142.1, 131.5, 130.6, 129.3, 128.4, 125.5, 125.3, 121.6, 120.1, 115.1, 114.1, 65.6, 55.3, 31.6, 21.1; FT-IR (neat,  $\text{cm}^{-1}$ ): 2957, 2923, 2853, 1612, 1509, 1245, 1214, 1161, 1032, 937, 819; HRMS ( $m/z$ ): calc for  $\text{C}_{20}\text{H}_{19}\text{BrF}_3\text{N}_2\text{O}_2\text{S}$   $[\text{M}+\text{H}]^+$  487.0297 found 487.0307.

## Chapter eight:

### Synthesis of 4-(4-bromophenyl)-2-methylbut-3-yn-2-amine:

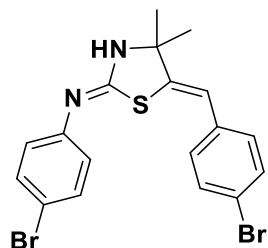


To an oven-dried flask, 2-methylbut-3-yn-2-amine (**8. 6**) (25 mmol, 1.0 equiv, 2.1 g), 1-bromo-4-iodobenzene (**8. 7**) (27.5 mmol, 1.1 equiv, 7.9 g), PdCl<sub>2</sub>(PPh<sub>3</sub>)<sub>2</sub> (0.5 mmol, 2.0 mol%, 0.35 g), CuI (1.0 mmol, 4.0 mol%, 0.2 g) and then THF/TEA mixture (4:1, 60 ml:15 ml) were added. The reaction mixture was stirred at room temperature under argon for 24 h. Ammonium chloride (20 ml) was used to quench the reaction, followed by extraction using ether (3 × 15 ml), then the combined organic extracts were further washed with brine solution (15 ml) and dried over sodium sulfate. The solvent was removed by rotary evaporation and then the crude residue was subjected to silica gel chromatography using 50% ethyl acetate in hexanes to afford the desired 4-(4-bromophenyl)-2-methylbut-3-yn-2-amine (**8. 8**) (brown oil, 3.2 g, 55%).<sup>65</sup> <sup>1</sup>H NMR (500 MHz, CDCl<sub>3</sub>) δ 7.43 – 7.29 (m, 2H), 7.27 – 7.12 (m, 2H), 1.84 (s, 2H), 1.42 (s, 3H), 1.41 (s, 3H). <sup>13</sup>C NMR (126 MHz, CDCl<sub>3</sub>) δ 133.0, 131.5, 128.6, 128.5, 122.4, 122.0, 98.1, 79.2, 45.8, 31.7. FT-IR (neat, cm<sup>-1</sup>): 3359, 3281, 2929, 2867, 2221, 1482, 1261, 1170, 818.

### 3.4.2. Synthesis of thiazolidines 9a-i:

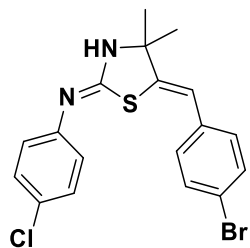
**General procedure:** To vigorously stirred silica gel (1.75 g) in 25 ml Erlenmeyer Flask, 4-(4-bromophenyl)-2-methylbut-3-yn-2-amine (0.24 g, 1.0 mmol, 1.0 equiv) and the corresponding phenyl isothiocyanates (0.12 – 0.22 g, 1.0 mmol, 1.0 equiv) were added, then stirred the slurry at 65 °C for 24 h. The reaction was monitored by TLC (by taking a small portion of silica gel mixture and adding few drops of dichloromethane). The slurry was subjected to the flash column

chromatography to afford the desired products which further crystallized using appropriate solvents to isolate the crystallized products in high grade of purity for biological examinations.



(*Z*)-5-((*Z*)-4-bromobenzylidene)-*N*-(4-bromophenyl)-4,4-dimethylthiazolidin-2-imine (**8.9a**):

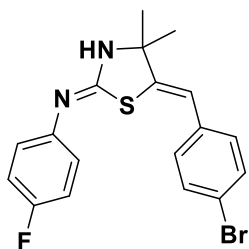
Obtained by using *p*-bromophenyl isothiocyanate (0.22 g, 1.0 mmol, 1.0 equiv) as colorless needles (0.25 g, 55%, m.p. 226-229 °C) by ethanolic crystallization of white solid (0.35 g, 77%) isolated by flash chromatography using 15% ethyl acetate in hexanes. <sup>1</sup>H NMR (500 MHz, CDCl<sub>3</sub>) δ 7.39 (d, *J* = 7.0 Hz, 2H), 7.36 (d, *J* = 7.0 Hz, 2H), 7.08 (d, *J* = 7.0 Hz, 2H), 6.97 (d, *J* = 8.1 Hz, 2H), 6.32 (s, 1H), 1.45 (s, 6H). <sup>13</sup>C NMR (126 MHz, CDCl<sub>3</sub>) δ 165.8, 157.9, 144.0, 135.2, 132.2, 131.7, 129.5, 123.5, 120.8, 117.6, 116.5, 80.1, 30.4. FT-IR (neat, cm<sup>-1</sup>): 3060, 2965, 2846, 2770, 1644, 1613, 1577, 1435, 1166, 840. HRMS (m/z): calc for C<sub>18</sub>H<sub>17</sub>N<sub>2</sub>SBr<sub>2</sub> [M+1]<sup>+</sup> 450.9474 found 450.9474.



(*Z*)-5-((*Z*)-4-bromobenzylidene)-*N*-(4-chlorophenyl)-4,4-dimethylthiazolidin-2-imine (**8.9b**):

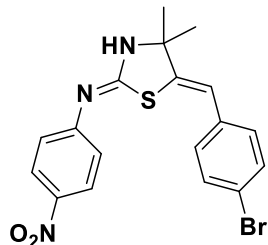
Obtained by using *p*-chlorophenyl isothiocyanate (0.17 g, 1.0 mmol, 1.0 equiv) as colorless

needles (0.20 g, 50%, 196-198 °C) by toluene crystallization of white solid (0.30 g, 75%) isolated by flash chromatography using 15% ethyl acetate in hexanes. <sup>1</sup>H NMR (500 MHz, CDCl<sub>3</sub>) δ 7.39 (dd, *J* = 8.5, 1.9 Hz, 2H), 7.25 – 7.16 (m, 2H), 7.08 (dd, *J* = 8.5, 1.8 Hz, 2H), 7.02 (dd, *J* = 8.6, 1.8 Hz, 2H), 6.32 (s, 1H), 1.45 (s, 6H). <sup>13</sup>C NMR (126 MHz, CDCl<sub>3</sub>) δ 176.6, 156.6, 145.6, 144.0, 135.2, 131.7, 129.5, 129.3, 129.1, 128.8, 128.3, 125.4, 123.1, 120.8, 117.5, 69.9, 30.4. FT-IR (neat, cm<sup>-1</sup>): 3062, 3021, 2964, 2867, 2854, 1645, 1583, 1505, 1166, 847. HRMS (*m/z*): calc for C<sub>18</sub>H<sub>17</sub>N<sub>2</sub>SClBr [M+1]<sup>+</sup> 406.9979 found 406.9954.



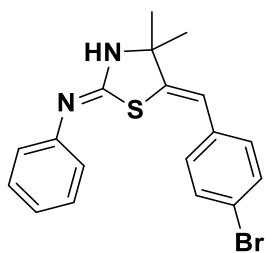
**(Z)-5-((Z)-4-bromobenzylidene)-N-(4-fluorophenyl)-4,4-dimethylthiazolidin-2-imine (8. 9c):**

Obtained by using *p*-fluorophenyl isothiocyanate (0.18 g, 1.2 mmol, 1.2 equiv) as colorless needles (0.18 g, 46%, m. p. 222-224 °C) by toluene crystallization of white solid (0.30 g, 77%) isolated by flash chromatography using 15% ethyl acetate in hexanes. <sup>1</sup>H NMR (500 MHz, CDCl<sub>3</sub>) δ 7.39 (d, *J* = 8.5 Hz, 2H), 7.15 – 7.01 (m, 4H), 7.00 – 6.91 (m, 2H), 6.32 (s, 1H), 1.46 (s, 6H). <sup>13</sup>C NMR (126 MHz, CDCl<sub>3</sub>) δ 158.4, 145.9, 143.7, 135.3, 131.7, 129.4, 129.1, 128.3, 125.4, 123.3, 123.2, 120.7, 117.4, 115.9, 115.8, 71.5, 30.4. FT-IR (neat, cm<sup>-1</sup>): 3061, 3019, 2990, 2948, 2868, 1649, 1615, 1248, 1175, 850. HRMS (*m/z*): calc for C<sub>18</sub>H<sub>17</sub>N<sub>2</sub>SFBr [M+1]<sup>+</sup> 391.0274 found 391.0264.



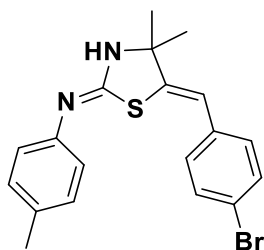
**(Z)-5-((Z)-4-bromobenzylidene)-4,4-dimethyl-N-(4-nitrophenyl)thiazolidin-2-imine (8.9d):**

Obtained by using *p*-nitrophenyl isothiocyanate (0.22 g, 1.2 mmol, 1.2 equiv) as shiny yellow crystals (0.11 g, 30%, 212-214 °C) by methanolic crystallization of the yellow crude product (0.36 g, 95%). <sup>1</sup>H NMR (500 MHz, CDCl<sub>3</sub>) δ 8.14 (dd, *J* = 8.9, 1.6 Hz, 2H), 7.41 (dd, *J* = 8.5, 1.6 Hz, 2H), 7.26 (d, *J* = 8.5 Hz, 2H), 7.11 – 7.02 (m, 2H), 6.38 (s, 1H), 1.51 (s, 3H), 1.50 (s, 3H). <sup>13</sup>C NMR (126 MHz, CDCl<sub>3</sub>) δ 169.9, 167.8, 150.9, 143.1, 135.3, 131.8, 129.4, 129.1, 128.3, 125.4, 120.9, 118.2, 67.5, 30.3. FT-IR (neat, cm<sup>-1</sup>): 3079, 3037, 2961, 2870, 2819, 1648, 1615, 1486, 1379, 1248, 1106, 851. HRMS (*m/z*): calc for C<sub>18</sub>H<sub>17</sub>N<sub>3</sub>O<sub>2</sub>SBr [M+1]<sup>+</sup> 418.0213 found 418.0219.

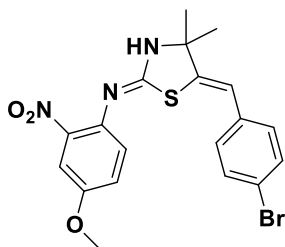


**(Z)-5-((Z)-4-bromobenzylidene)-4,4-dimethyl-N-phenylthiazolidin-2-imine (8.9e):** Obtained by using phenyl isothiocyanate (0.12 g, 1.0 mmol, 1.0 equiv) as colorless tiny needles (0.2 g, 54%, m. p. 216-220 °C) by toluene crystallization of the white solid (0.30 g, 80%) isolated by flash chromatography using 15% ethyl acetate in hexanes. <sup>1</sup>H NMR (500 MHz, CDCl<sub>3</sub>) δ 7.39 (d, *J* = 8.5 Hz, 2H), 7.31 – 7.23 (m, 2H), 7.17 (d, *J* = 7.9 Hz, 2H), 7.10 (d, *J* = 8.5 Hz, 2H), 7.04 (t, *J* =

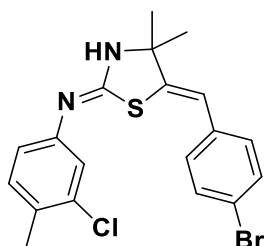
7.4 Hz, 1H), 6.33 (s, 1H), 1.49 (s, 6H).  $^{13}\text{C}$  NMR (126 MHz,  $\text{CDCl}_3$ )  $\delta$  153.9, 153.0, 150.7, 135.5, 131.7, 129.4, 129.2, 123.7, 121.3, 120.5, 117.1, 106.3, 100.0, 48.7, 30.5. FT-IR (neat,  $\text{cm}^{-1}$ ): 3017, 2963, 2855, 2800, 1652, 1615, 1587, 1483, 1195, 836. HRMS ( $m/z$ ): calc for  $\text{C}_{18}\text{H}_{18}\text{N}_2\text{SBr}$   $[\text{M}+1]^+$  373.0354 found 373.0369.



**(Z)-5-((Z)-4-bromobenzylidene)-4,4-dimethyl-N-(p-tolyl)thiazolidin-2-imine (8. 9f):** Obtained by using *p*-tolyl isothiocyanate (0.15 g, 1.0 mmol, 1.0 equiv) as colorless powders (0.13 g, 34%, 206-208 °C) by toluene crystallization of white solid (0.3 g, 78%) isolated by flash chromatography using 20% ethyl acetate in hexanes.  $^1\text{H}$  NMR (500 MHz,  $\text{CDCl}_3$ )  $\delta$  7.40 (ddd,  $J = 8.8, 4.1, 1.8$  Hz, 2H), 7.17 – 7.01 (m, 6H), 6.34 (s, 1H), 2.30 (s, 3H), 1.5 (s, 6H).  $^{13}\text{C}$  NMR (126 MHz,  $\text{CDCl}_3$ )  $\delta$  171.1, 142.1, 135.6, 133.5, 131.6, 129.8, 129.4, 127.3, 121.5, 120.5, 117.0, 110.8, 70.0, 30.5, 21.0. FT-IR (neat,  $\text{cm}^{-1}$ ): 3089, 3022, 3010, 2905, 1641, 1601, 1506, 1484, 1247, 1173, 831. HRMS ( $m/z$ ): calc for  $\text{C}_{19}\text{H}_{20}\text{N}_2\text{SBr}$   $[\text{M}+1]^+$  387.0499 found 387.0525.



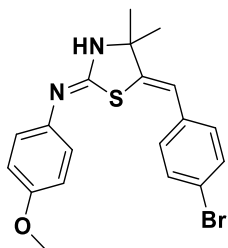
**(Z)-5-((Z)-4-bromobenzylidene)-N-(4-methoxy-2-nitrophenyl)-4,4-dimethylthiazolidin-2-imine (8.9g):** Obtained by using 4-methoxy-2-nitrophenyl isothiocyanate (0.21 g, 1.0 mmol, 1.0 equiv) as yellow powder (0.20 g, 44%, 252-254 °C) by toluene crystallization of the yellow solid (0.42 g, 94%) isolated by flash chromatography using 15% ethyl acetate in hexanes. <sup>1</sup>H NMR (500 MHz, CDCl<sub>3</sub>) δ 8.63 (s, 1H), 7.60 (t, *J* = 2.9 Hz, 1H), 7.44 (dd, *J* = 8.6, 2.5 Hz, 2H), 7.19 (dq, *J* = 9.4, 3.0 Hz, 1H), 7.13 (dd, *J* = 8.6, 2.5 Hz, 2H), 6.39 (s, 1H), 3.80 (s, 3H), 1.53 (s, 3H), 1.52 (s, 3H). <sup>13</sup>C NMR (126 MHz, CDCl<sub>3</sub>) δ 153.8, 146.8, 143.8, 135.7, 131.7, 129.3, 128.4, 124.3, 123.2, 120.6, 117.1, 108.1, 55.9, 30.4. FT-IR (neat, cm<sup>-1</sup>): 3086, 3030, 3006, 2961, 2868, 2835, 1614, 1561, 1518, 1478, 1397, 1288, 1256, 882. HRMS (*m/z*): calc for C<sub>18</sub>H<sub>20</sub>N<sub>2</sub>BrS [M+1]<sup>+</sup> 373.0369 found 373.0354.



**(Z)-5-((Z)-4-bromobenzylidene)-N-(3-chloro-4-methylphenyl)-4,4-dimethylthiazolidin-2-imine (8.9h):** Obtained by using 3-chloro-4-methylphenyl isothiocyanate (0.18 g, 1.0 mmol, 1.0 equiv) as colorless powder (0.16 g, 40%, m.p. 208-210 °C) by toluene crystallization of white solid (0.33 g, 80%) isolated by flash chromatography using 15% ethyl acetate in hexanes. <sup>1</sup>H NMR (500 MHz, CDCl<sub>3</sub>) δ 7.73 (s, 1H), 7.39 (d, *J* = 8.4 Hz, 2H), 7.14 – 7.03 (m, 4H), 6.89 (dd, *J* = 8.2, 2.3 Hz, 1H), 6.33 (s, 1H), 2.29 (s, 3H), 1.48 (s, 6H). <sup>13</sup>C NMR (126 MHz, CDCl<sub>3</sub>) δ 156.8, 144.6, 143.5, 135.1, 134.6, 131.7, 131.6, 131.4, 129.5, 128.3, 125.4, 122.6, 120.9, 120.4, 117.8, 70.0,



30.4, 19.6. FT-IR (neat,  $\text{cm}^{-1}$ ): 3110, 3043, 3031, 2926, 2874, 1649, 1599, 1552, 1484, 1276, 1008, 850. HRMS ( $m/z$ ): calc for  $\text{C}_{19}\text{H}_{19}\text{N}_2\text{SClBr}$   $[\text{M}+1]^+$  421.0135 found 421.0128.

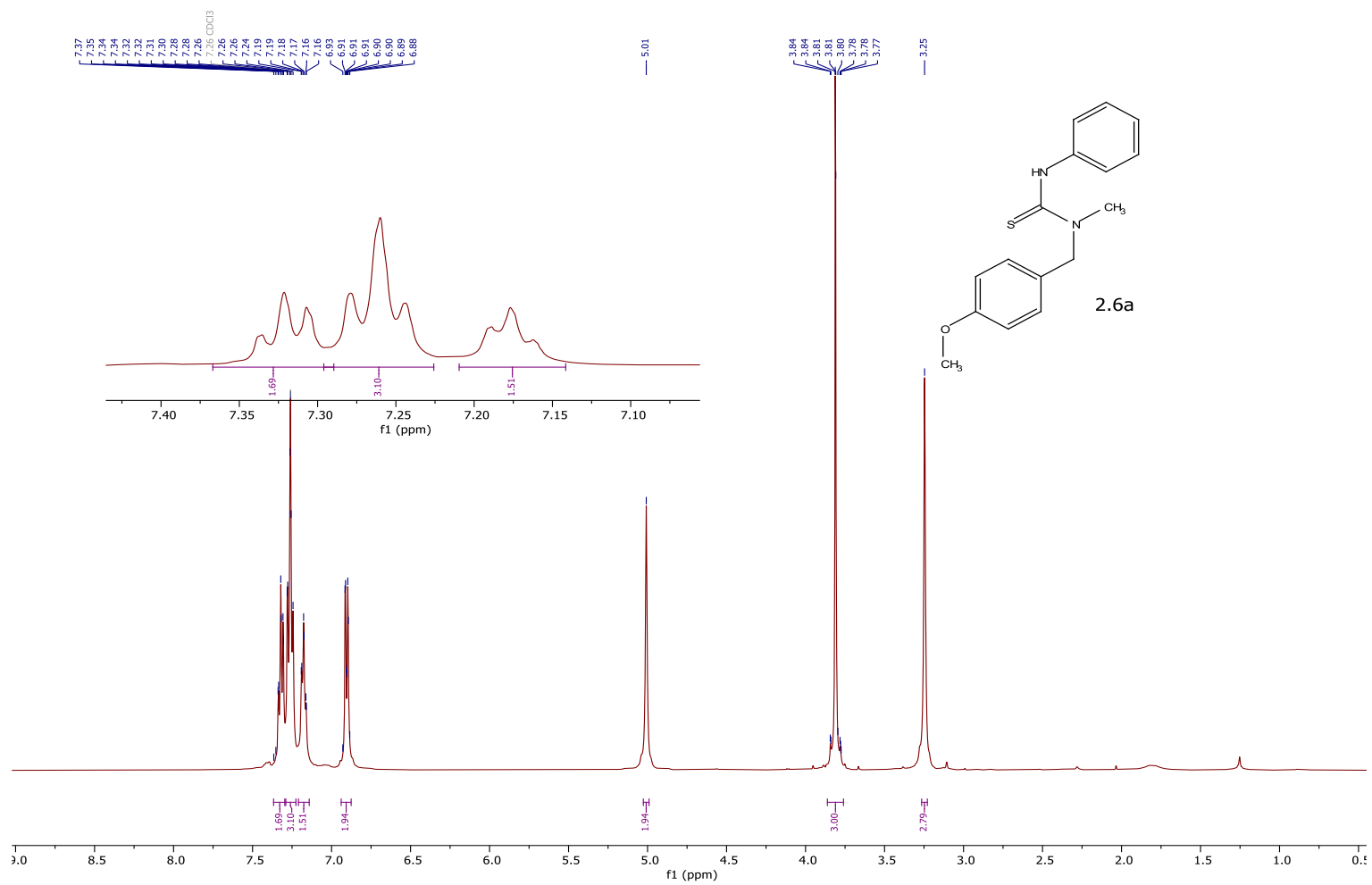


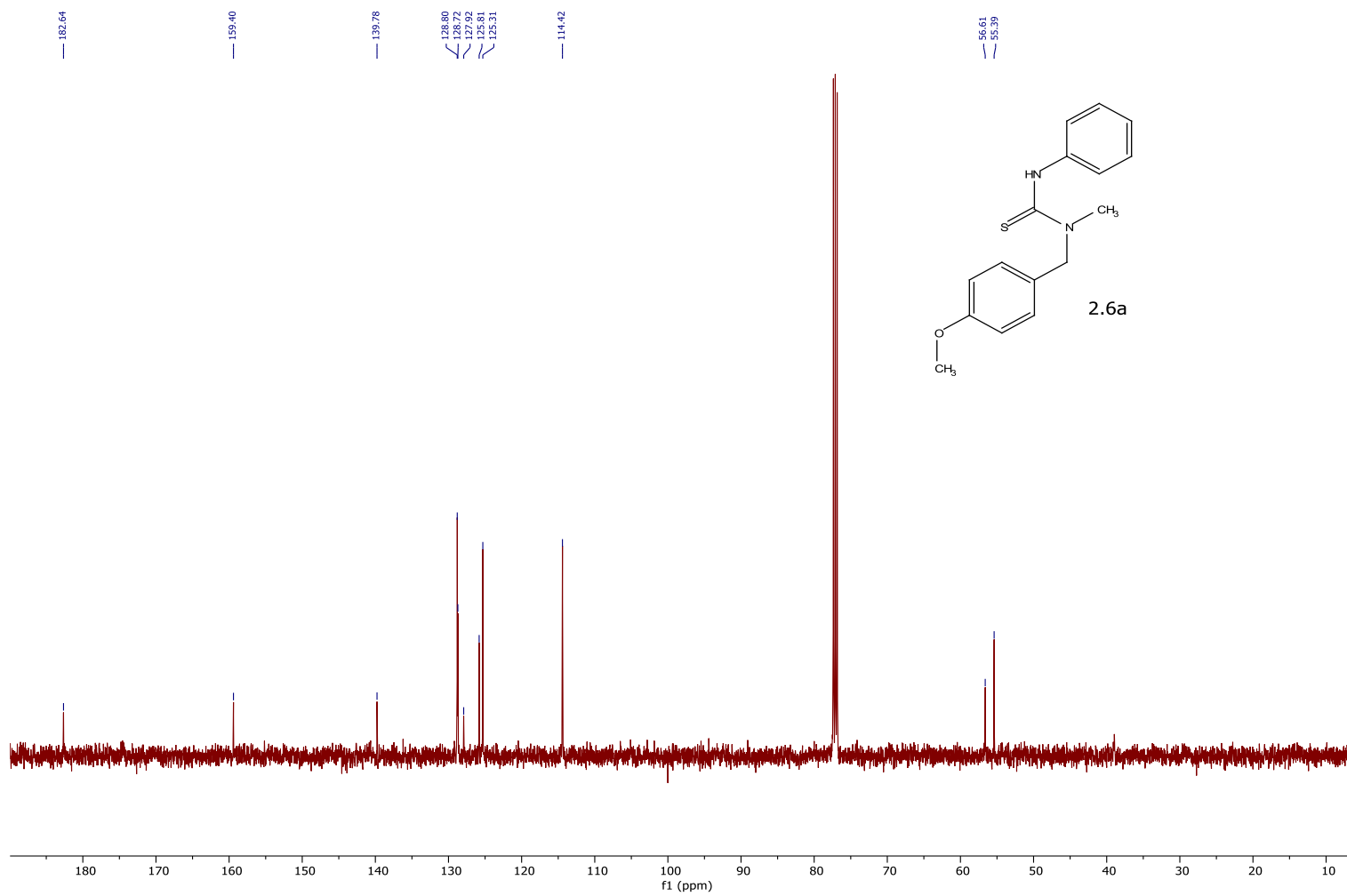
**(Z)-5-((Z)-4-bromobenzylidene)-N-(4-methoxyphenyl)-4,4-dimethylthiazolidin-2-imine**

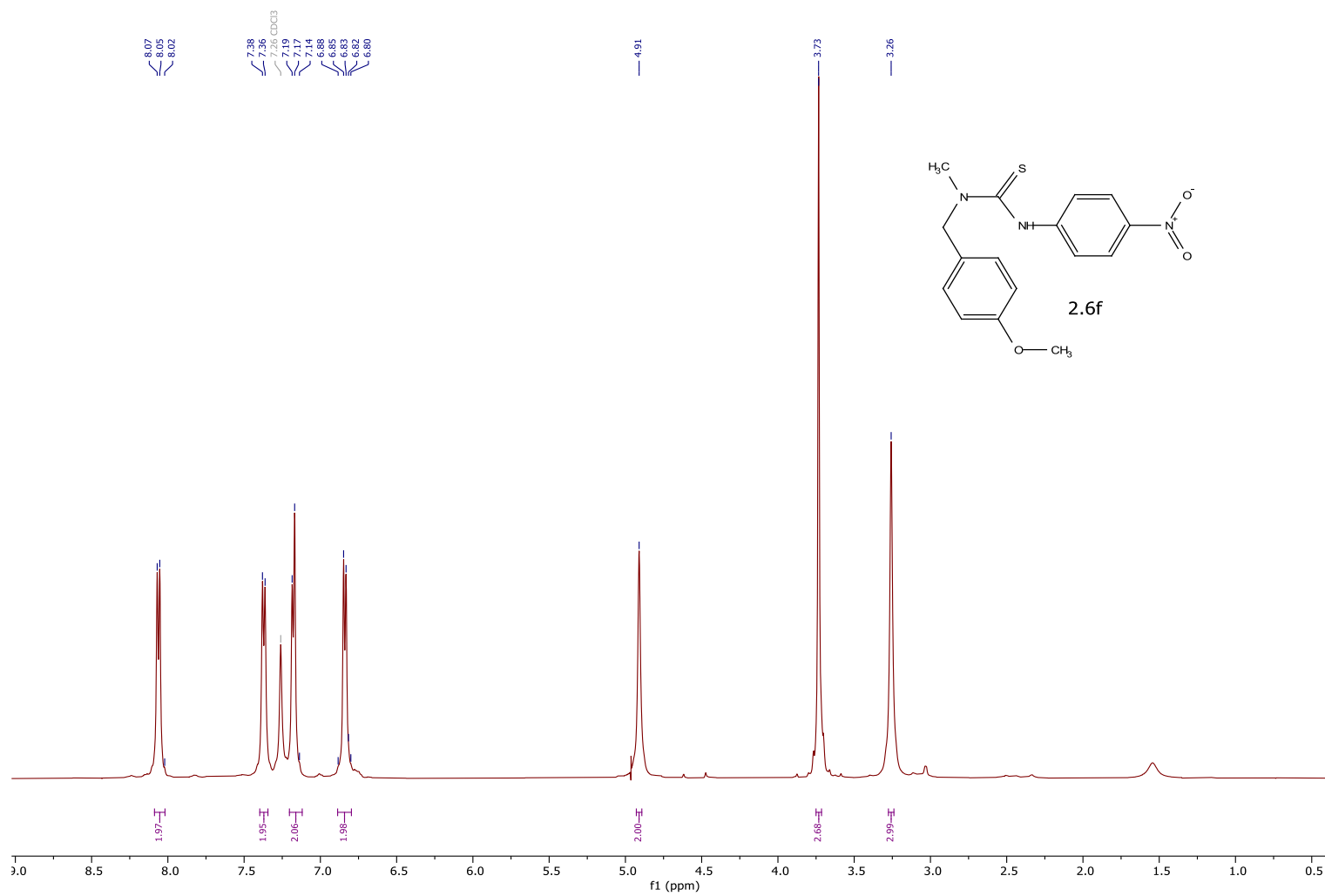
**(8.9i)**: Obtained by using 4-methoxyphenyl isothiocyanate (0.19 g, 1.0 mmol, 1.0 equiv) as shiny colorless needles (0.17 g, 42%, m.p. 170-172 °C) by toluene crystallization of the white solid (0.32 g, 85%) isolated by flash chromatography using 15% ethyl acetate in hexanes.  $^1\text{H}$  NMR (500 MHz,  $\text{CDCl}_3$ )  $\delta$  7.37 (d,  $J = 8.5$  Hz, 2H), 7.15 – 7.02 (m, 4H), 6.81 (d,  $J = 8.9$  Hz, 2H), 6.31 (s, 1H), 3.75 (s, 3H), 1.46 (s, 6H).  $^{13}\text{C}$  NMR (126 MHz,  $\text{CDCl}_3$ )  $\delta$  156.7, 156.6, 145.1, 138.3, 137.9, 135.4, 131.7, 129.4, 129.1, 128.3, 125.4, 123.9, 120.6, 117.2, 114.4, 71.8, 55.5, 30.5. FT-IR (neat,  $\text{cm}^{-1}$ ): 3021, 2960, 2829, 2777, 2657, 1657, 1613, 1501, 1209, 850. HRMS ( $m/z$ ): calc for  $\text{C}_{19}\text{H}_{20}\text{N}_2\text{OSBr}$   $[\text{M}+1]^+$  403.0474 found 403.0468.

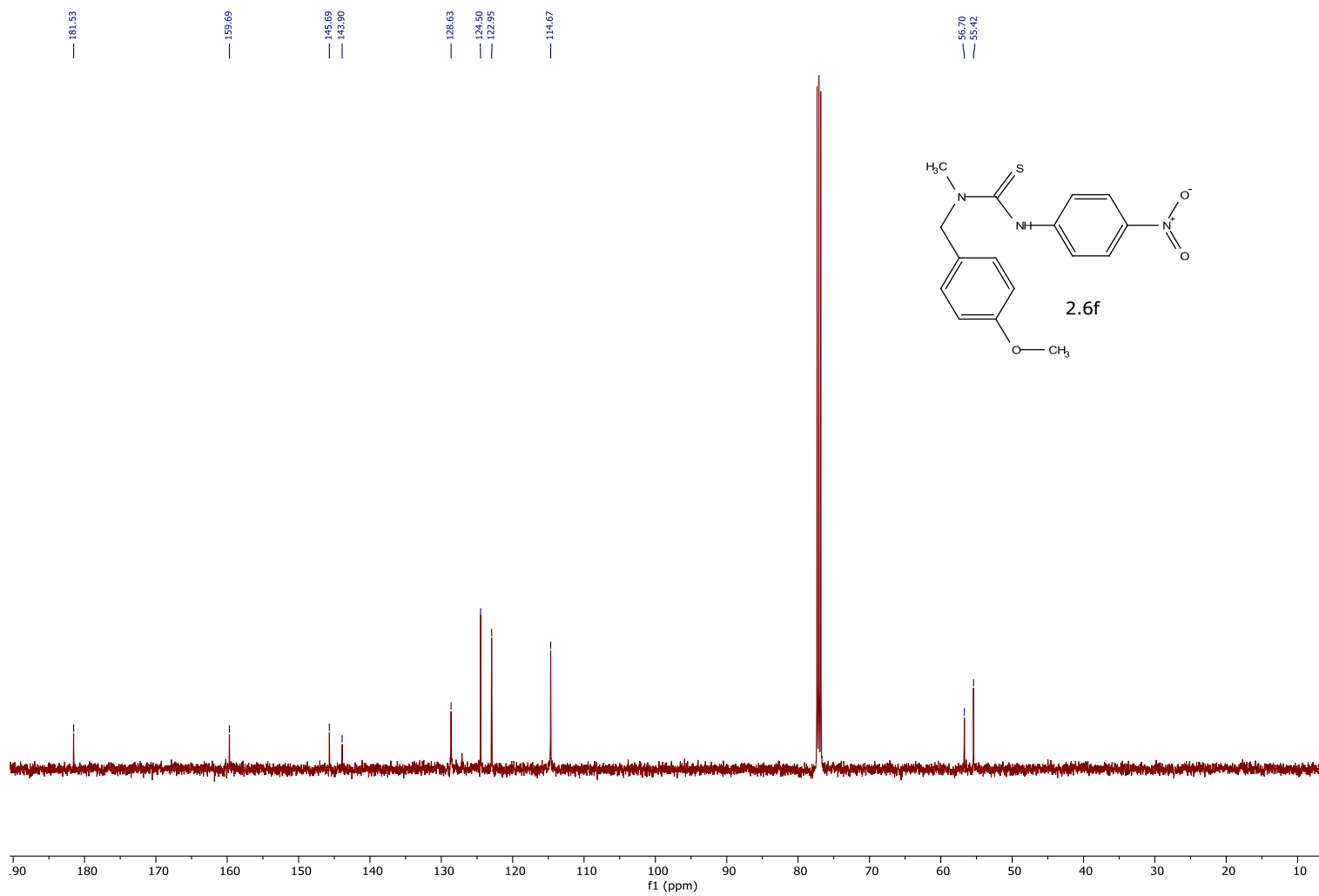
**Appendix:  $^1\text{H}$  and  $^{13}\text{C}$  NMR spectra**

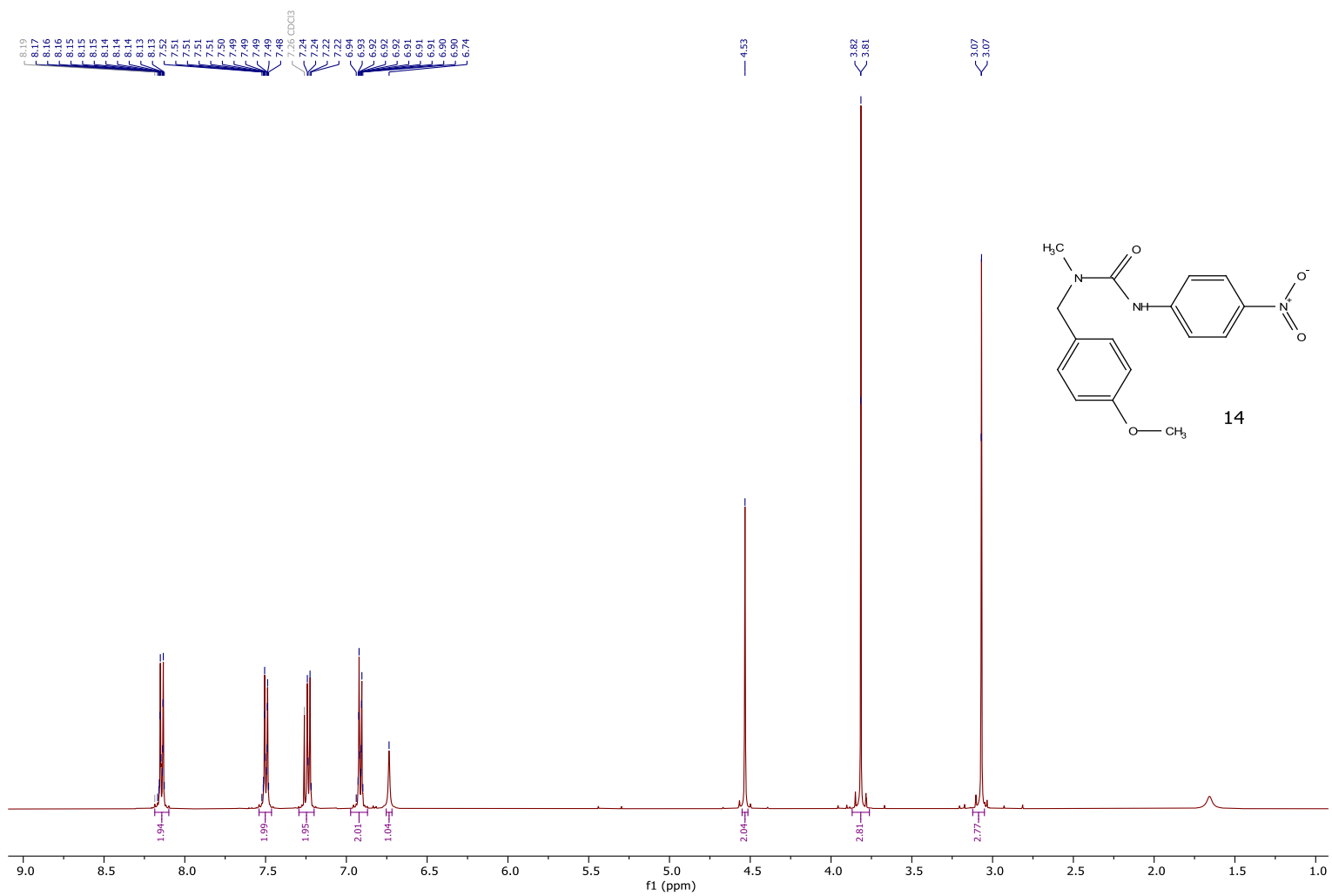




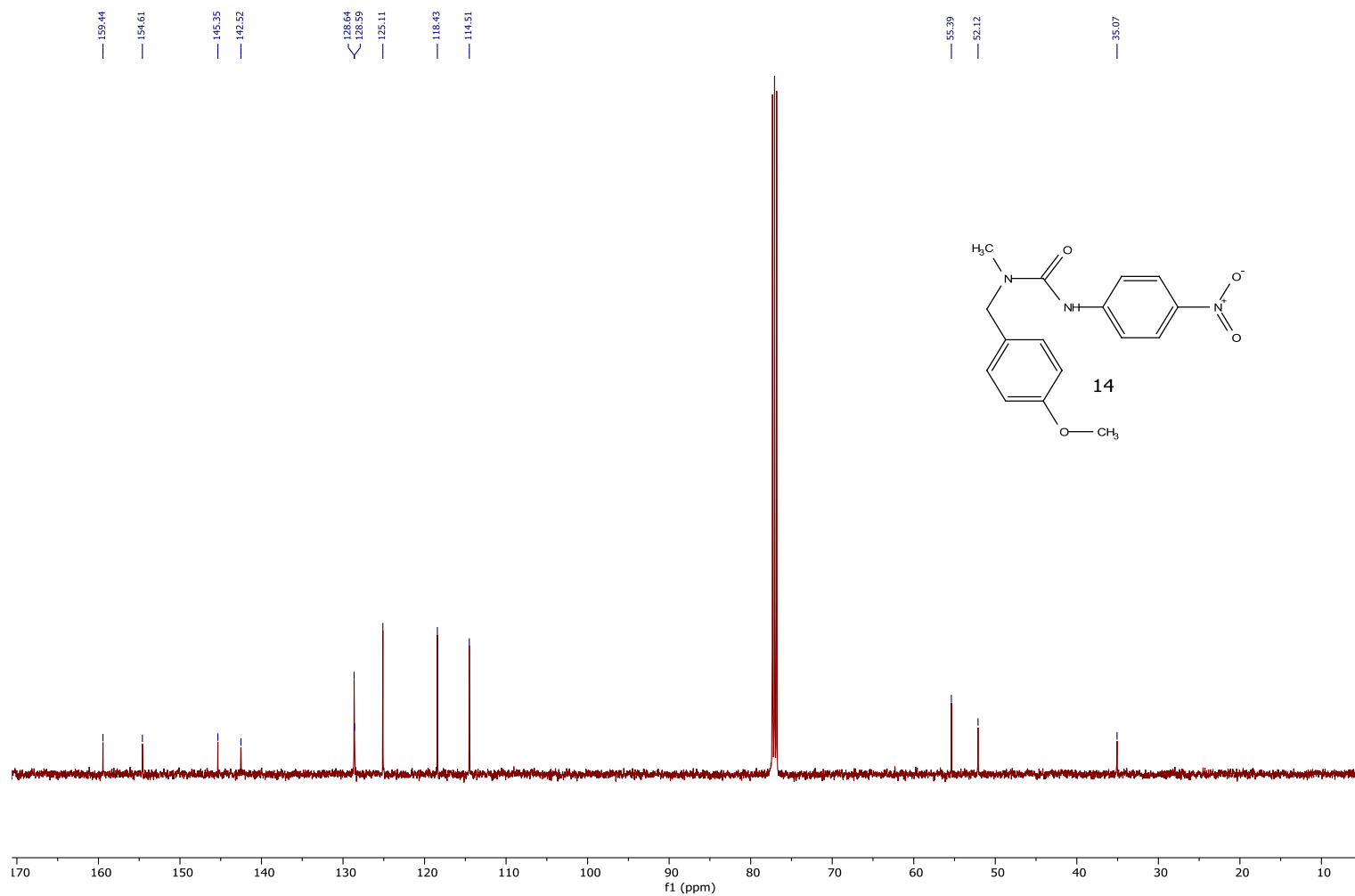


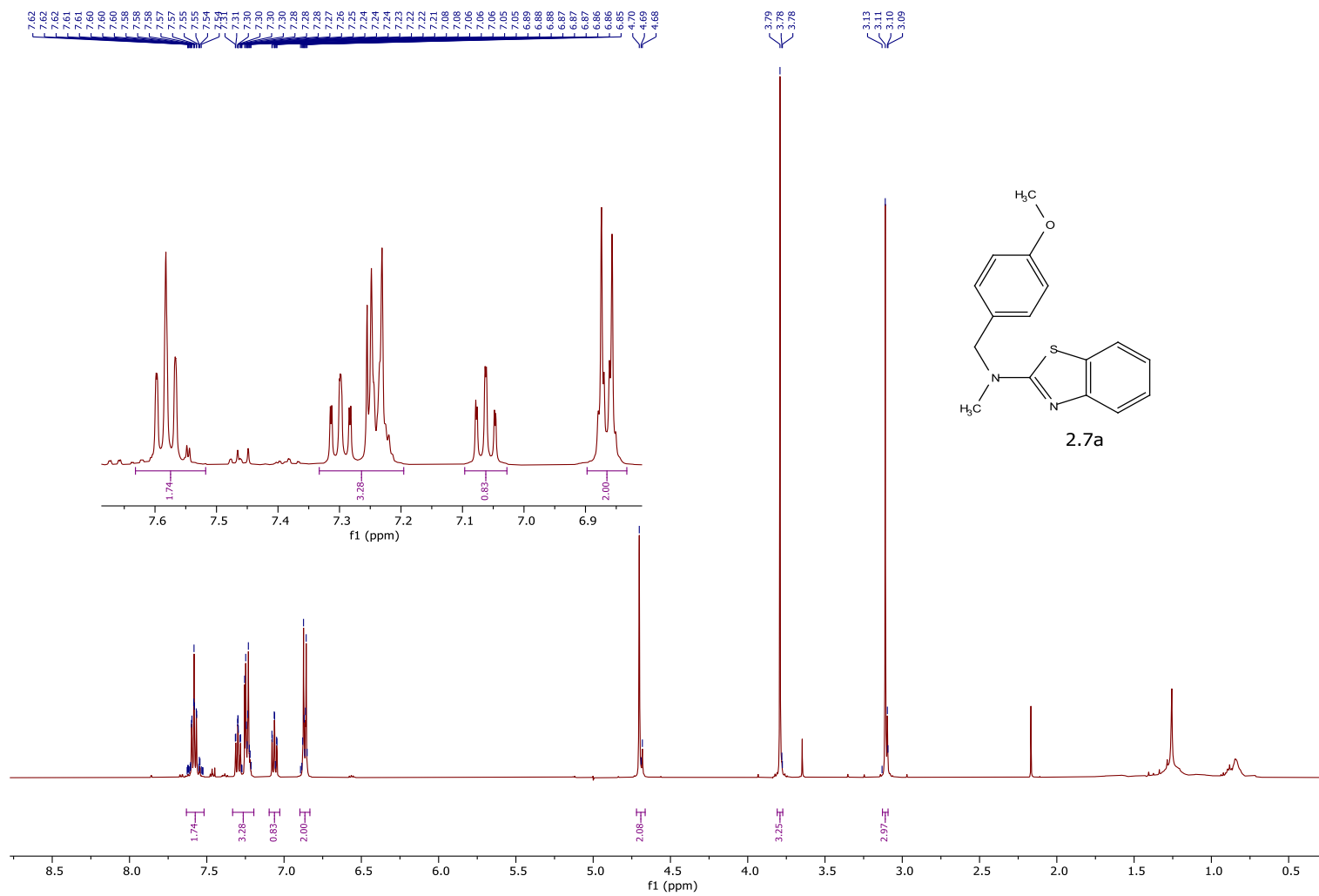


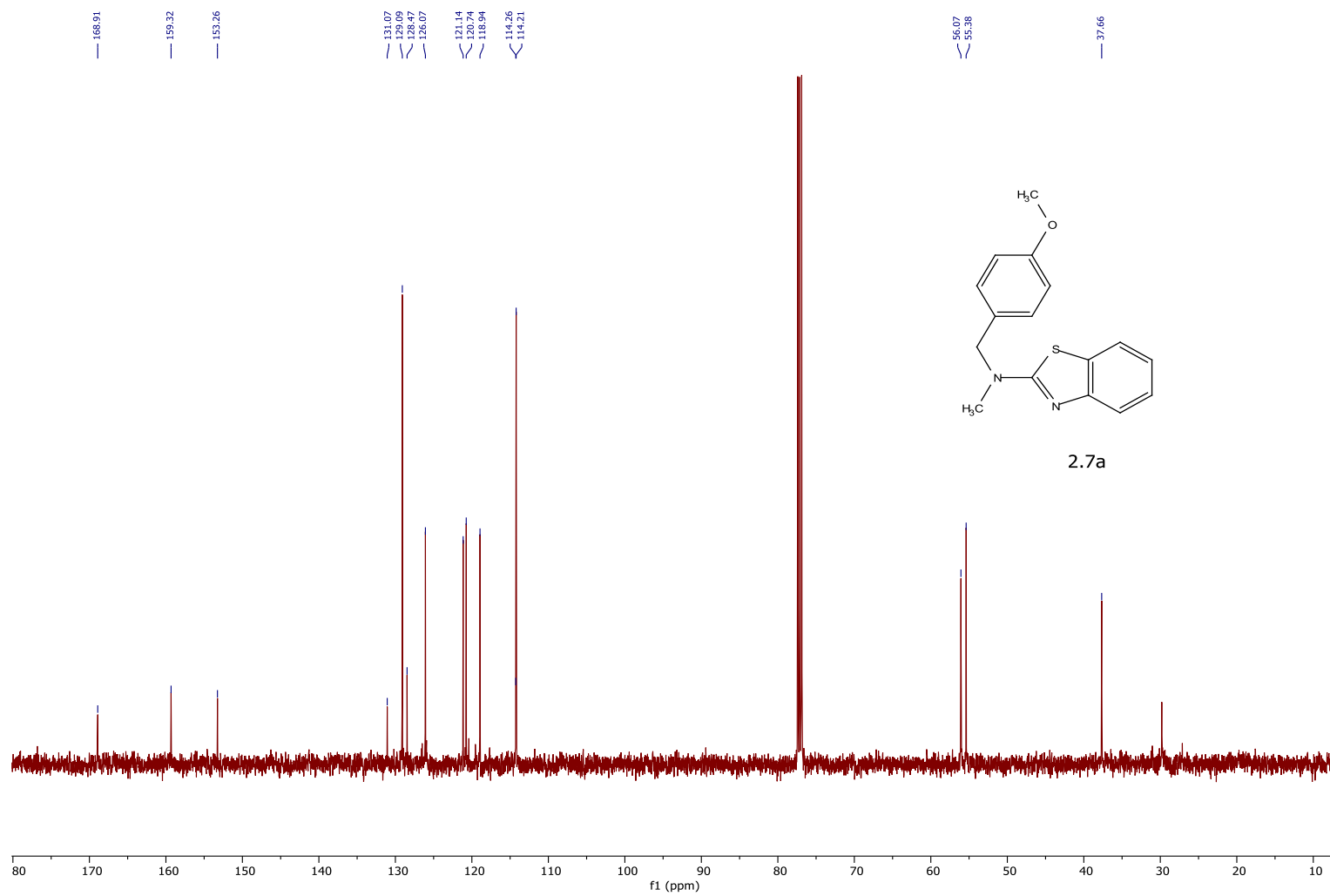


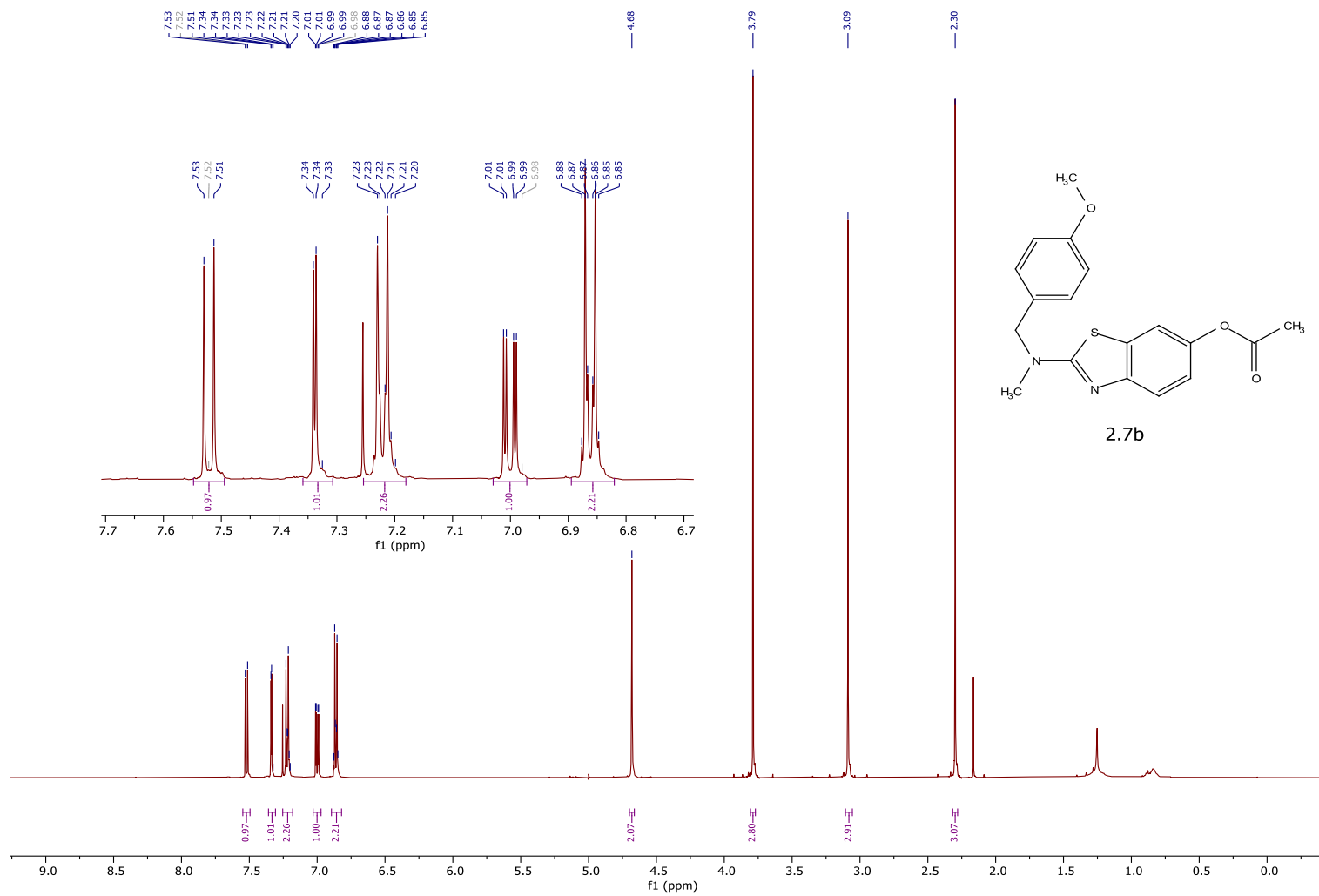


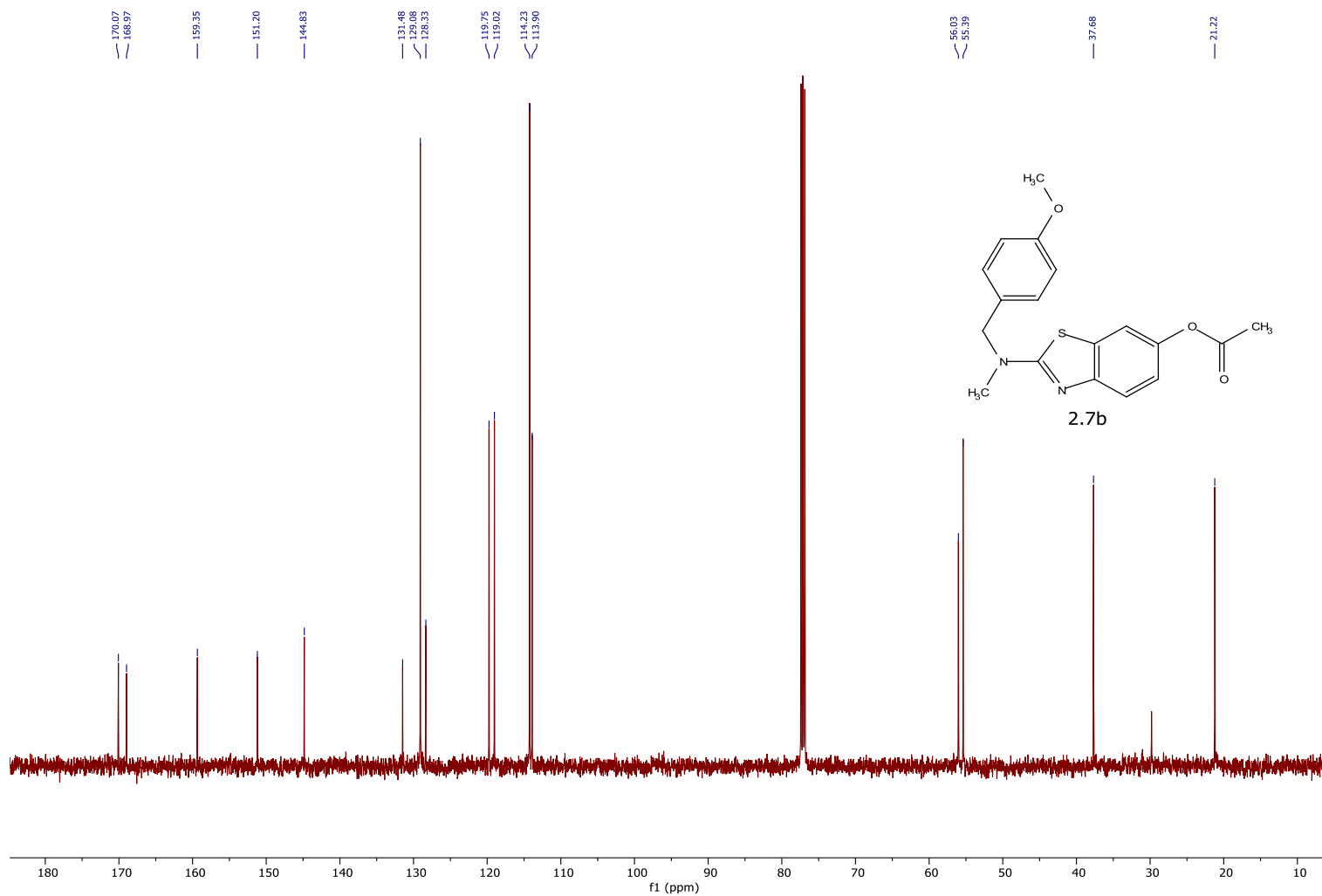


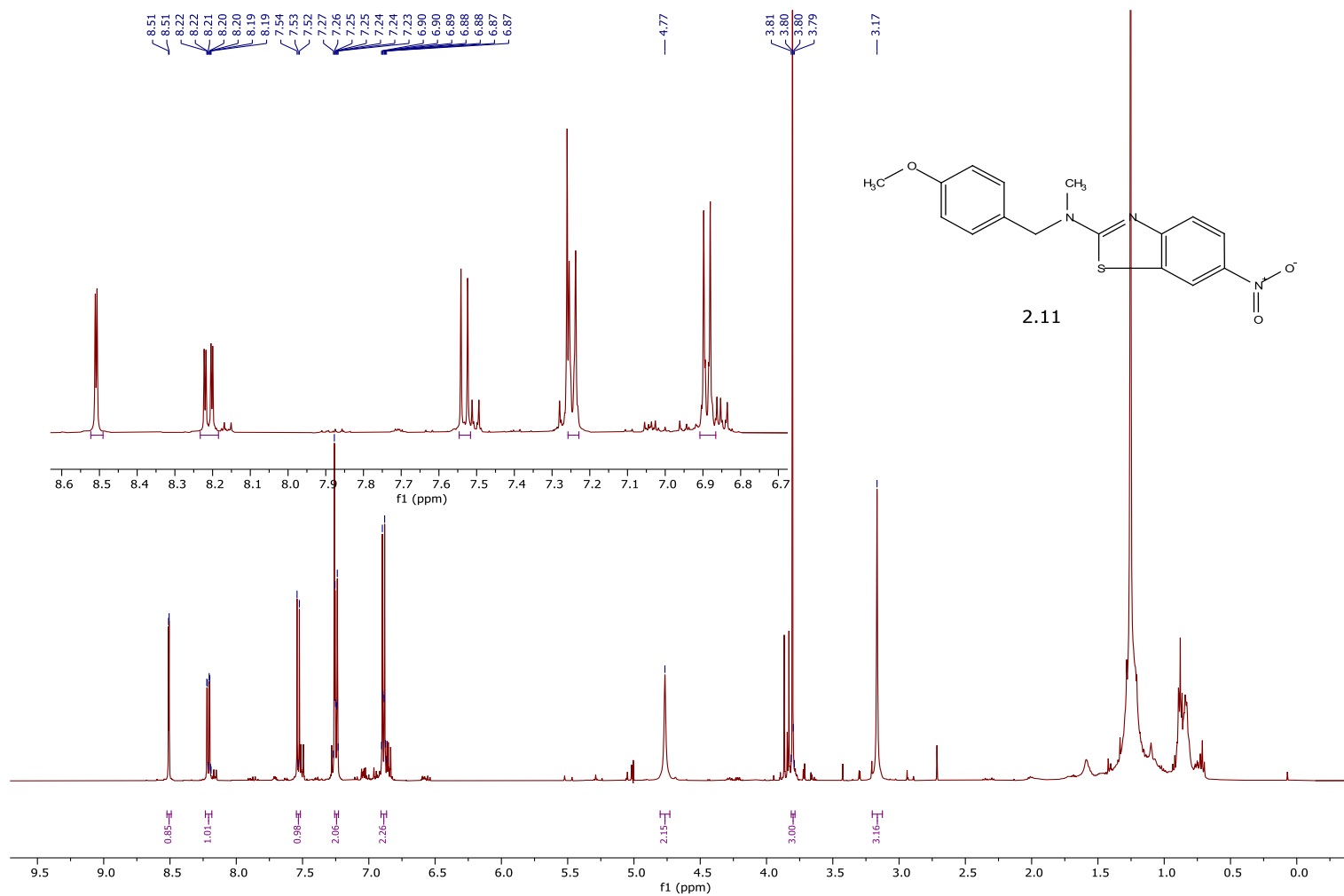


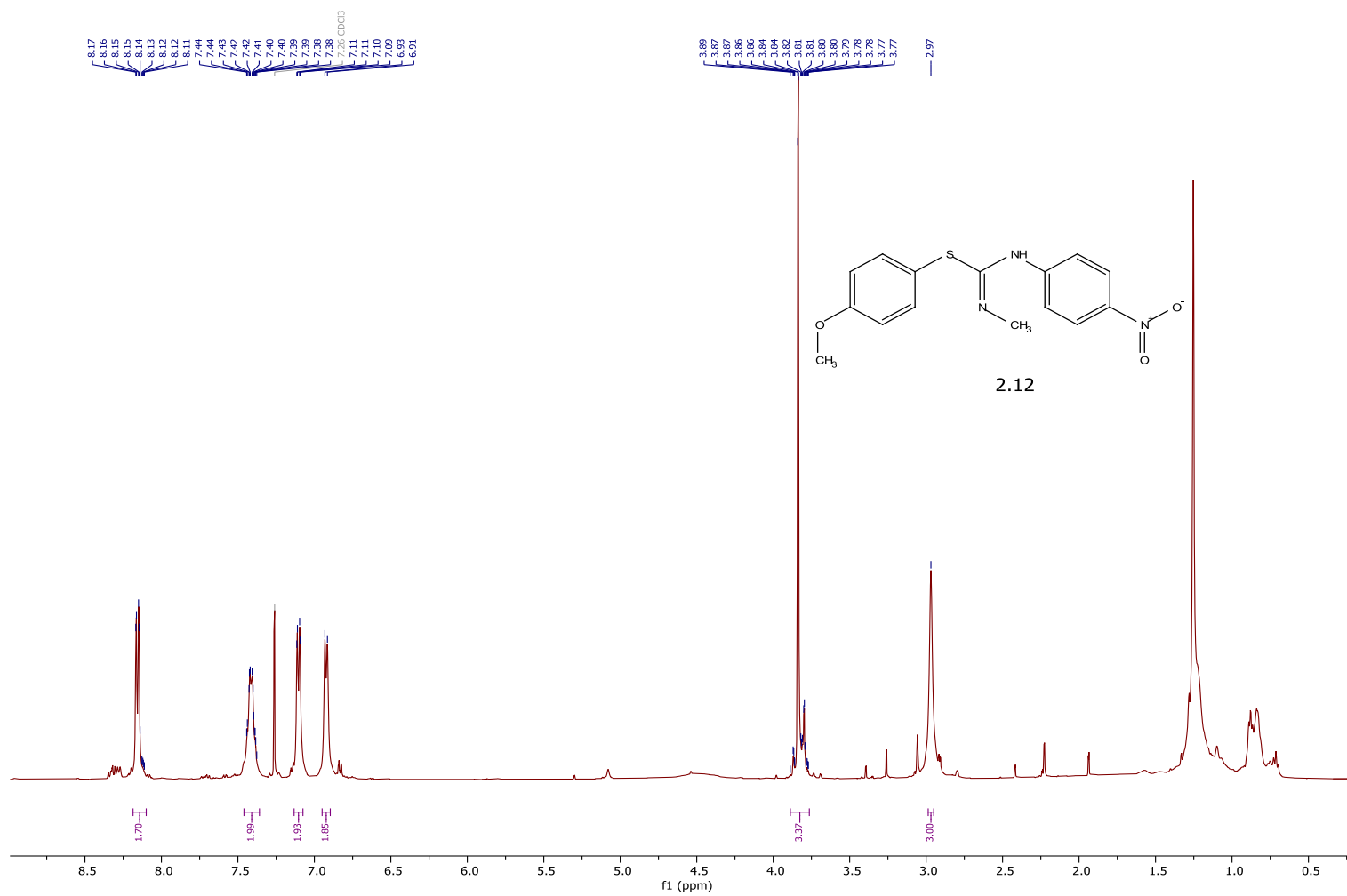


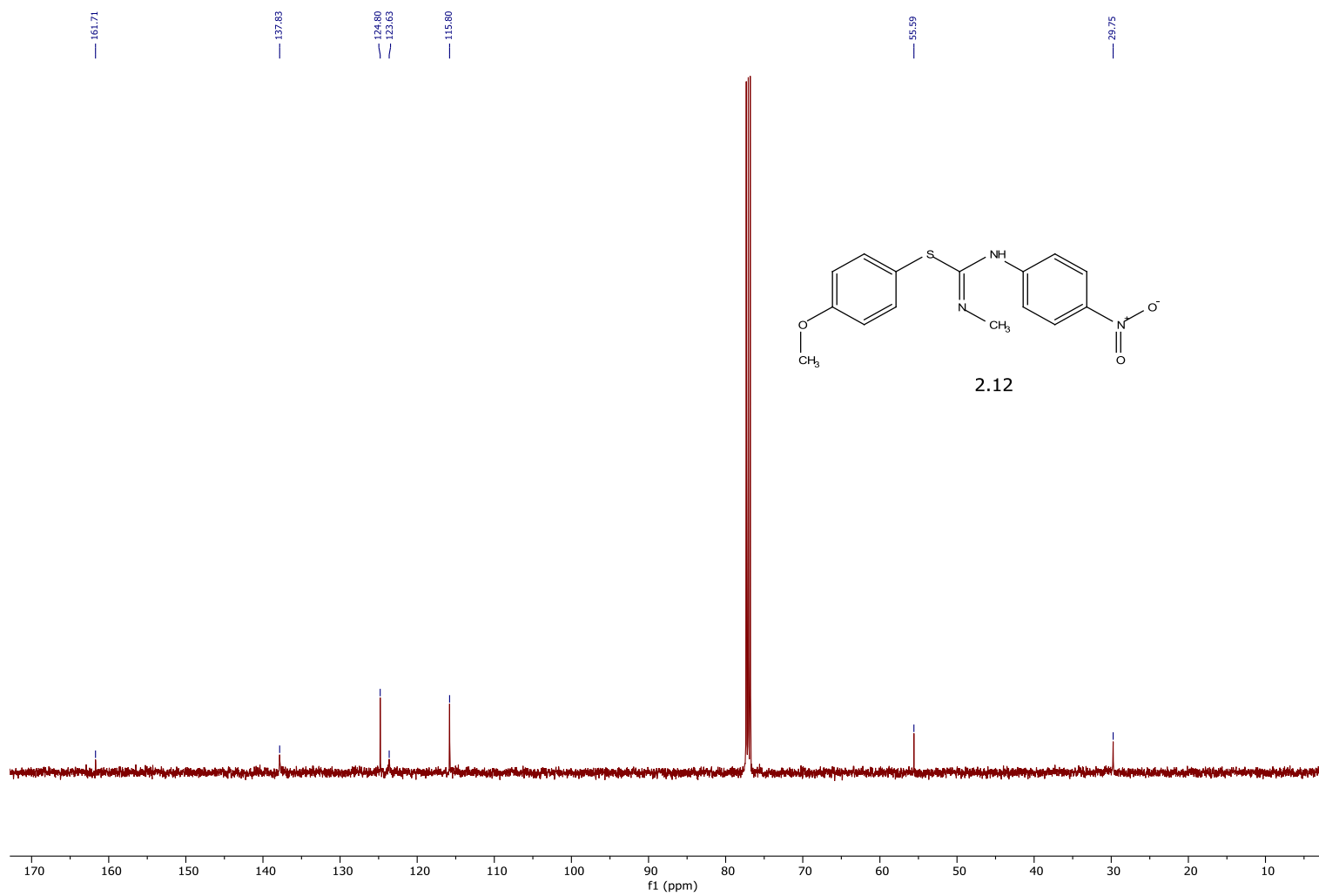




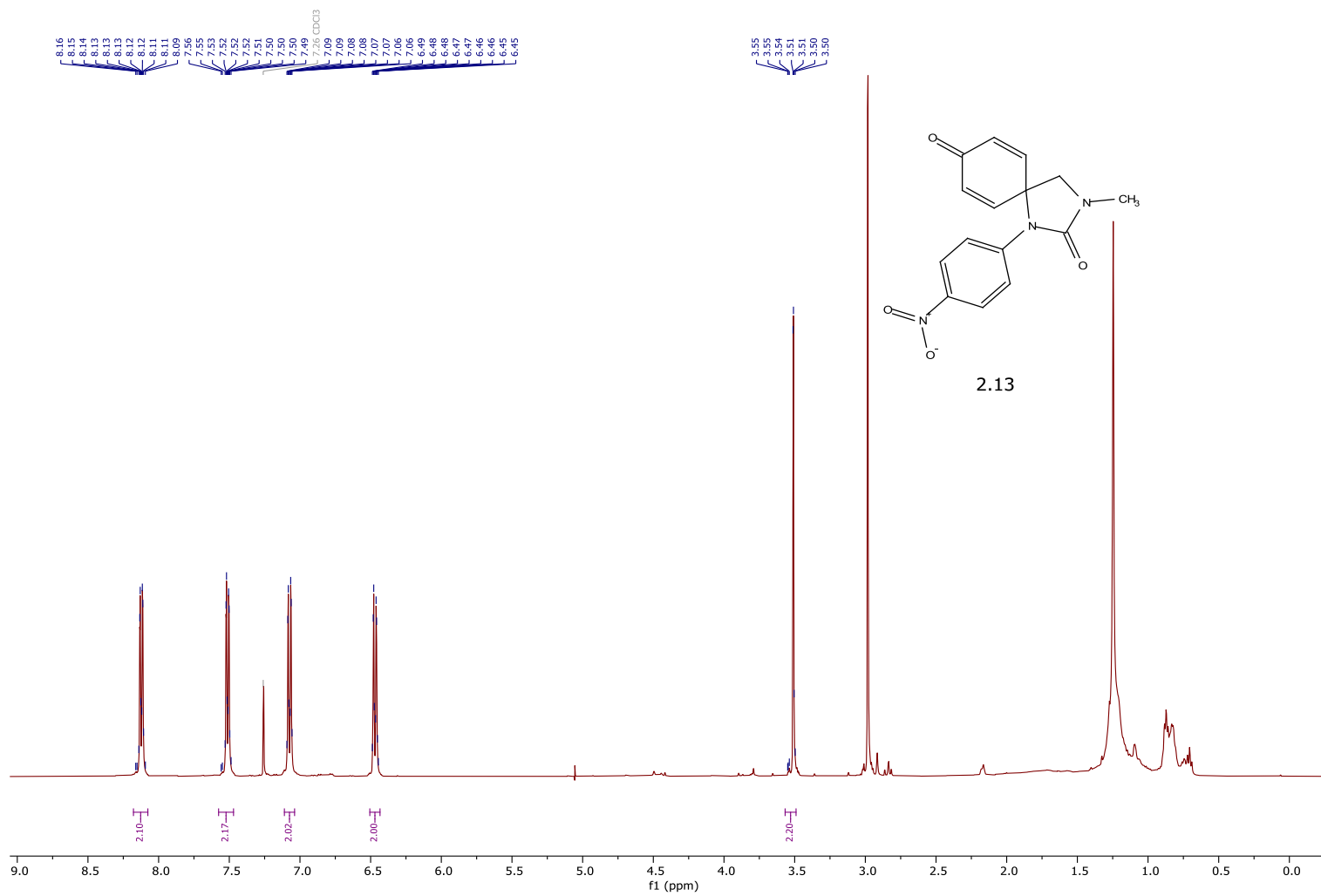


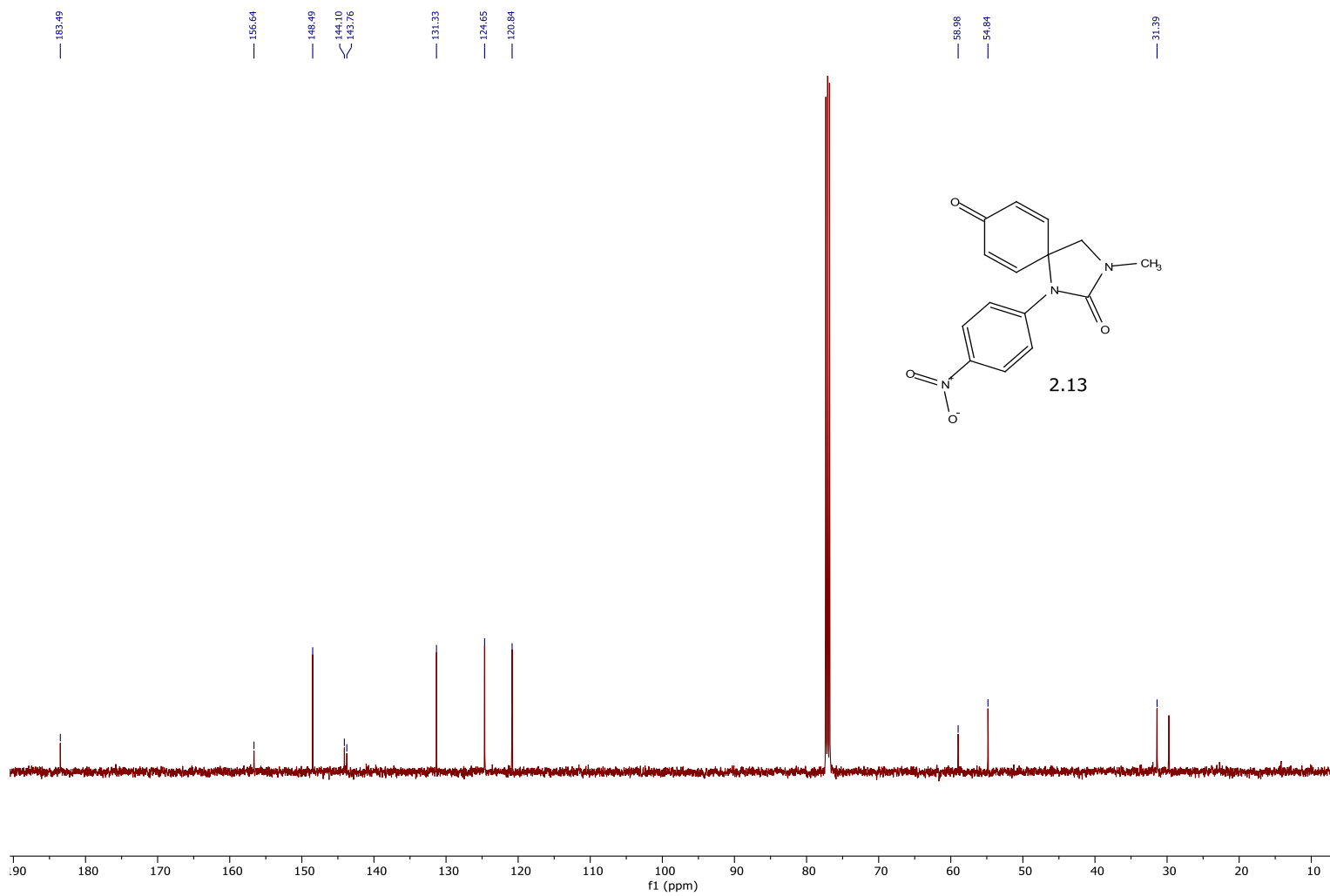


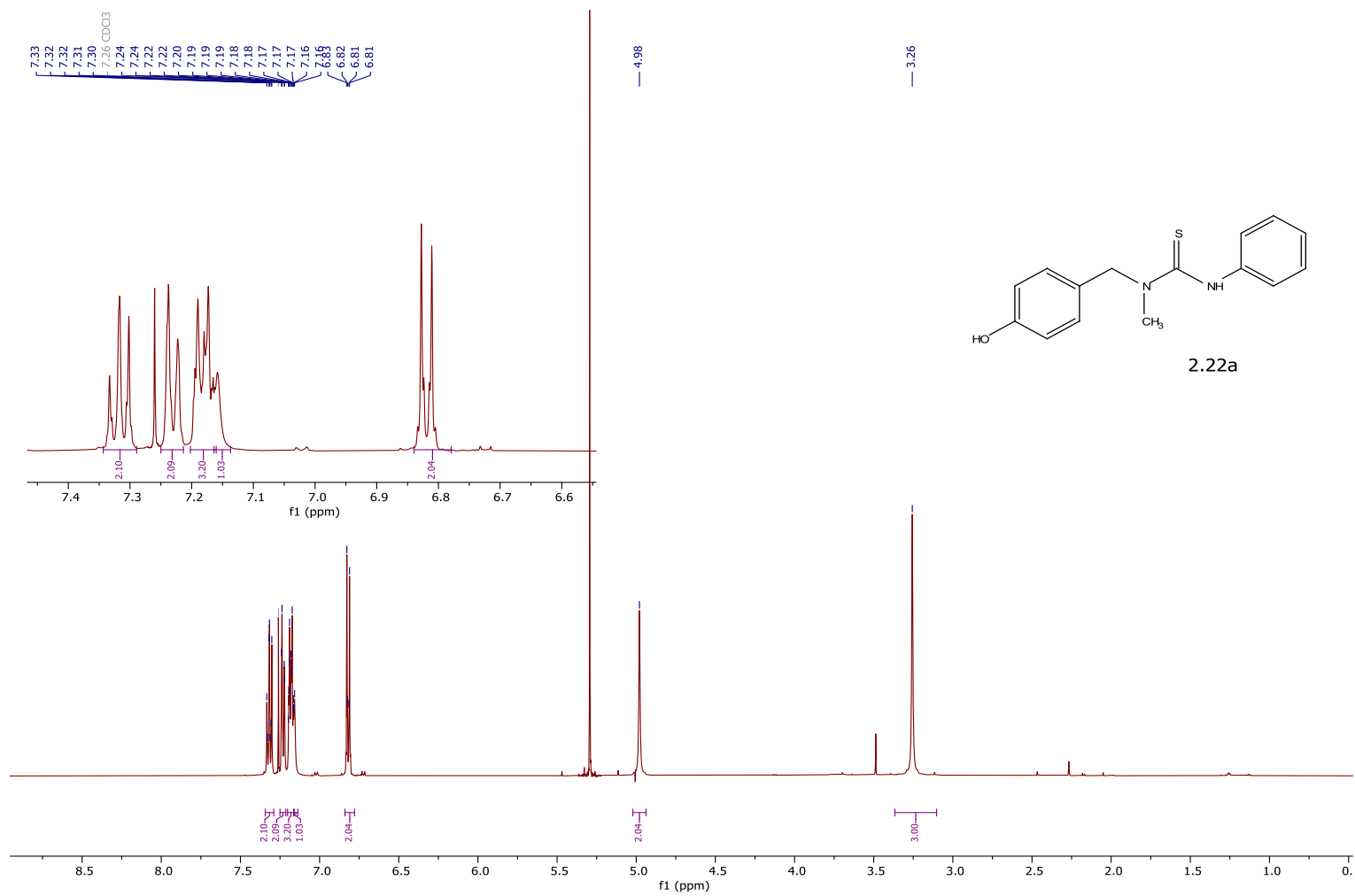


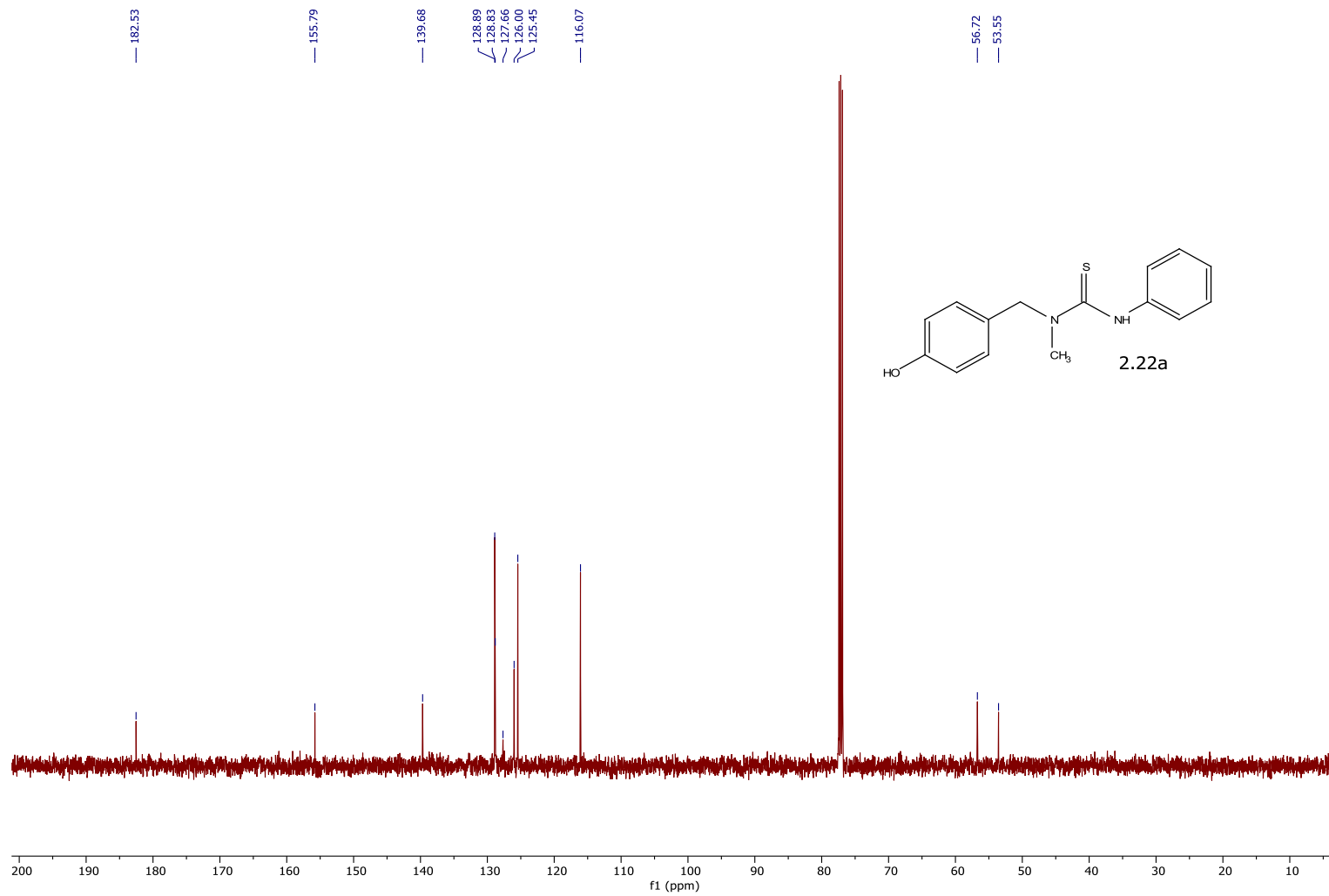


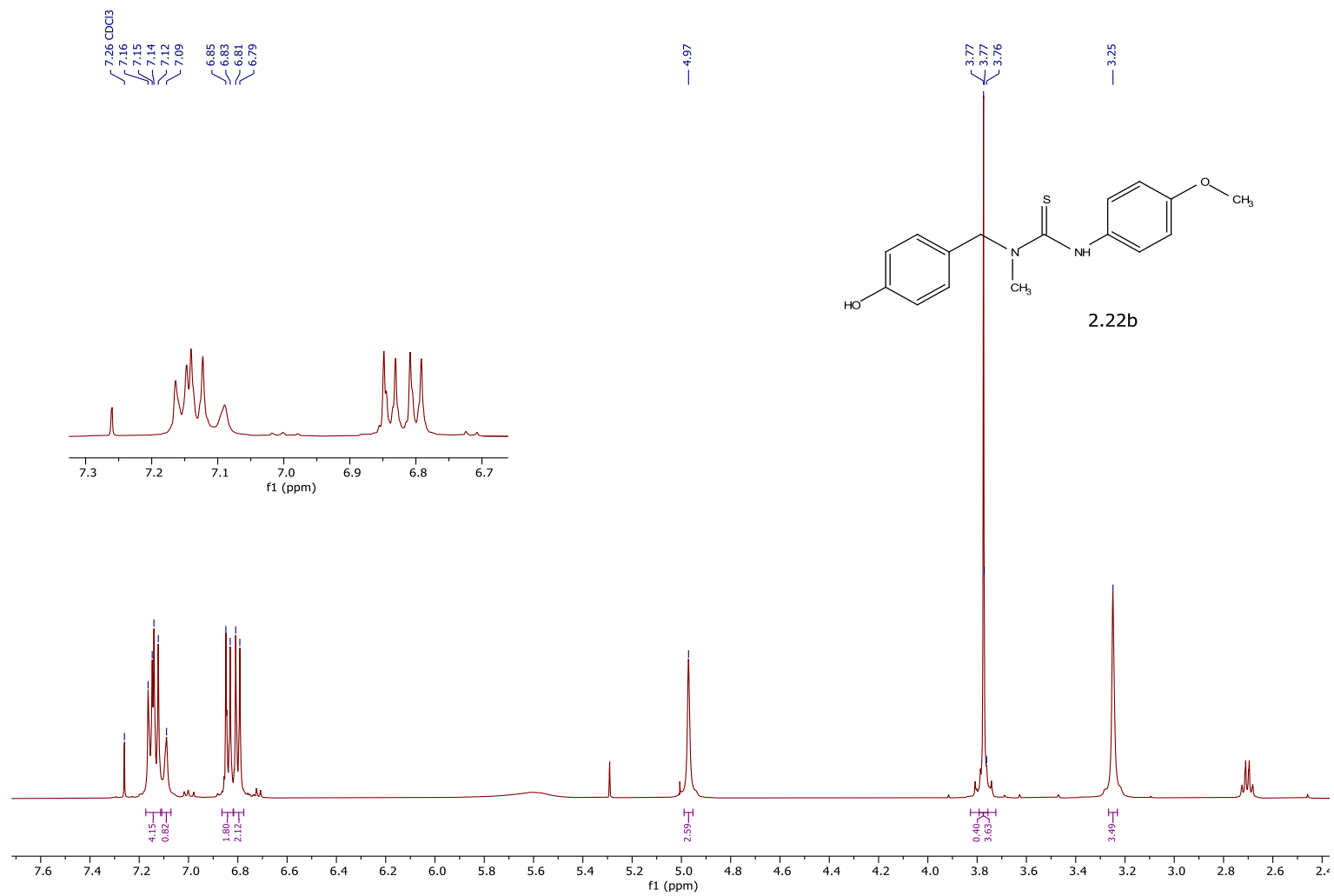


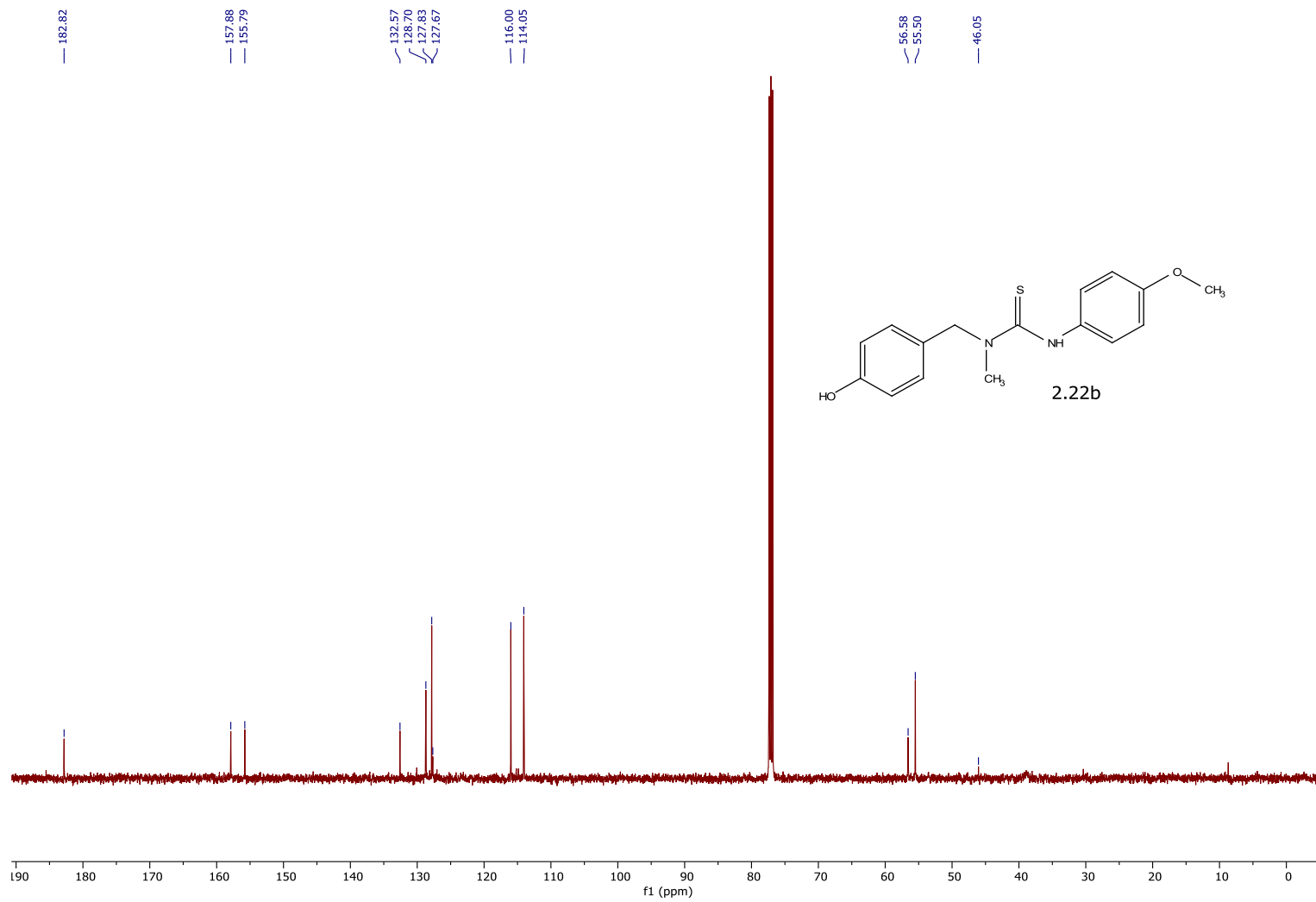


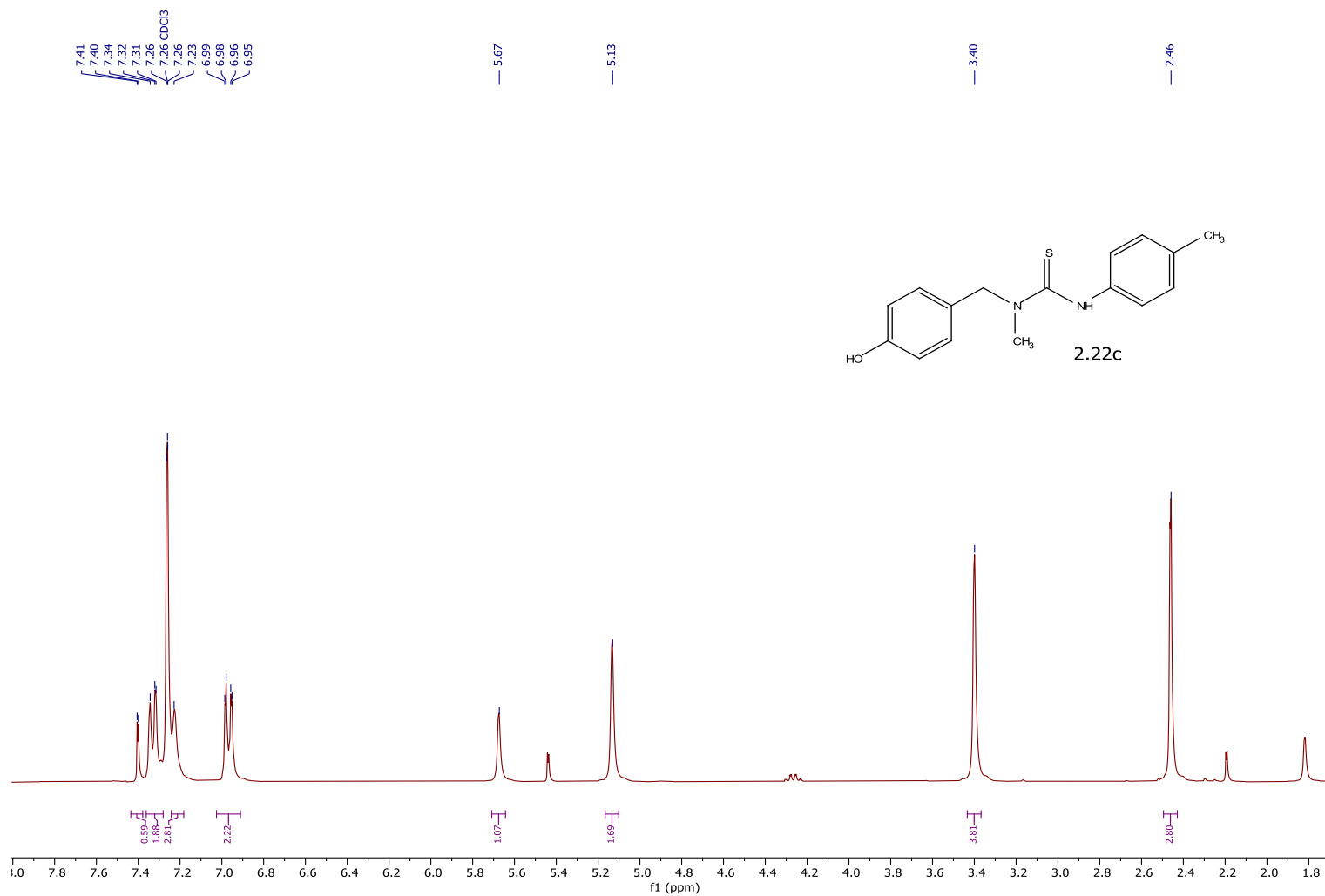


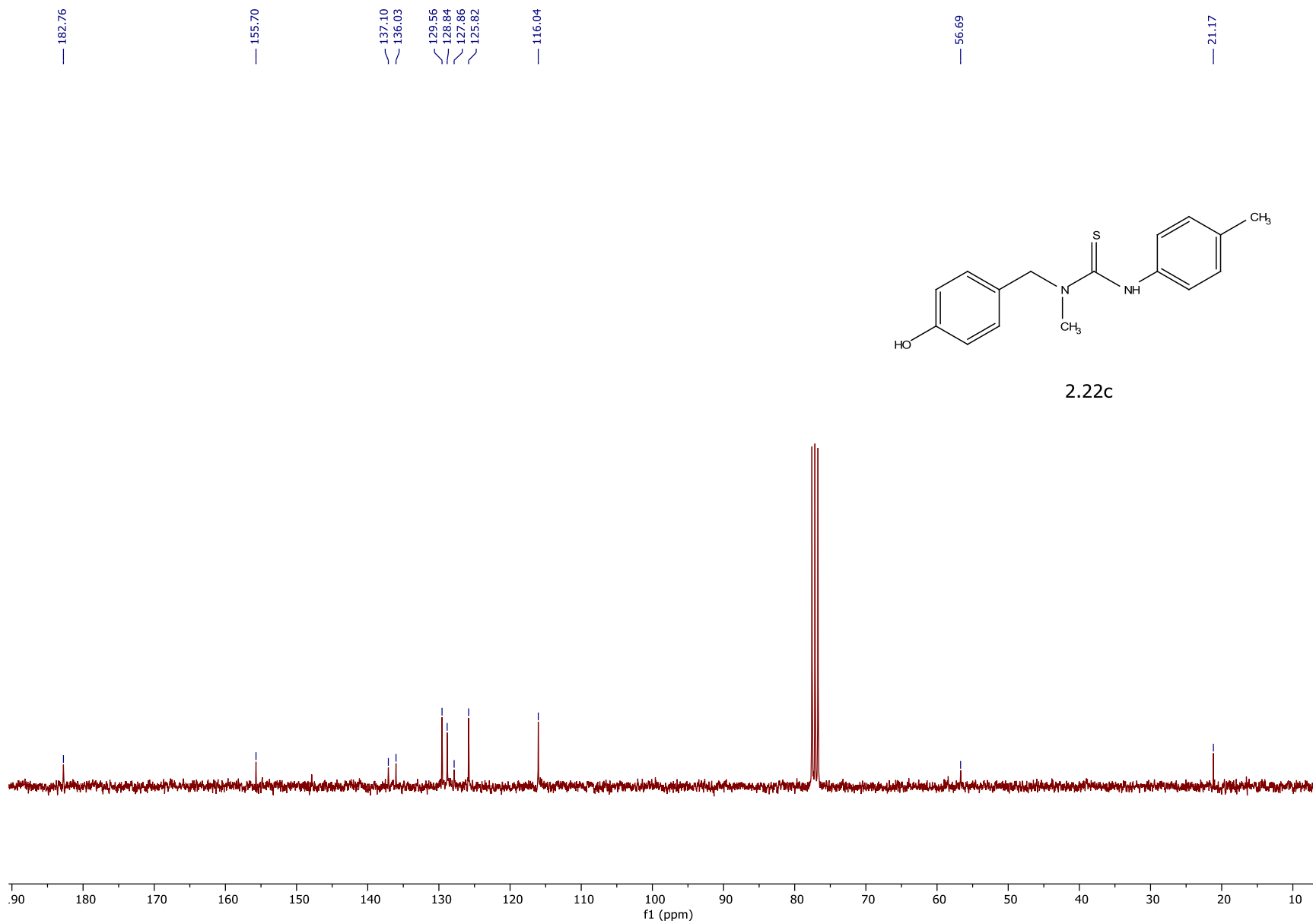




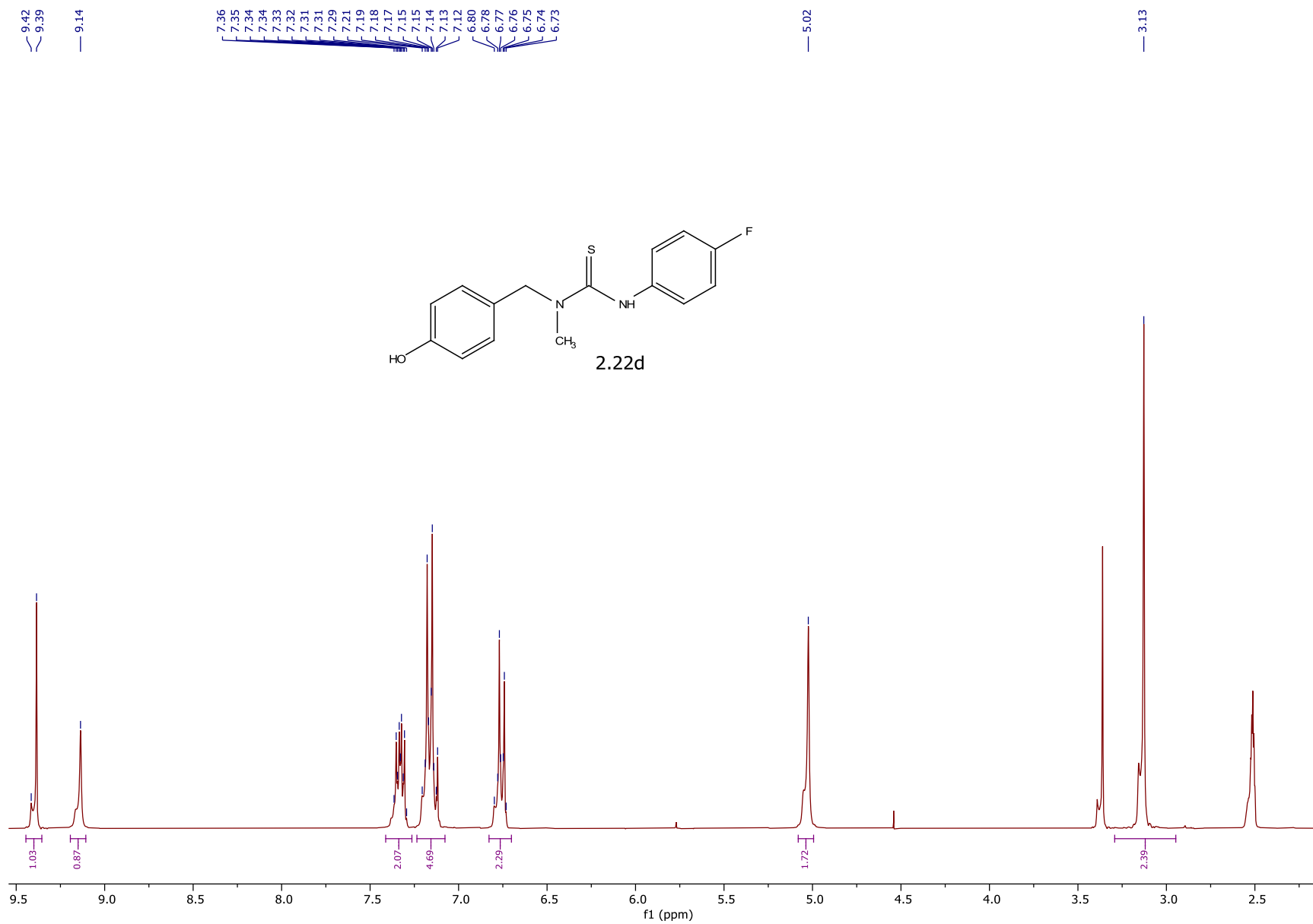


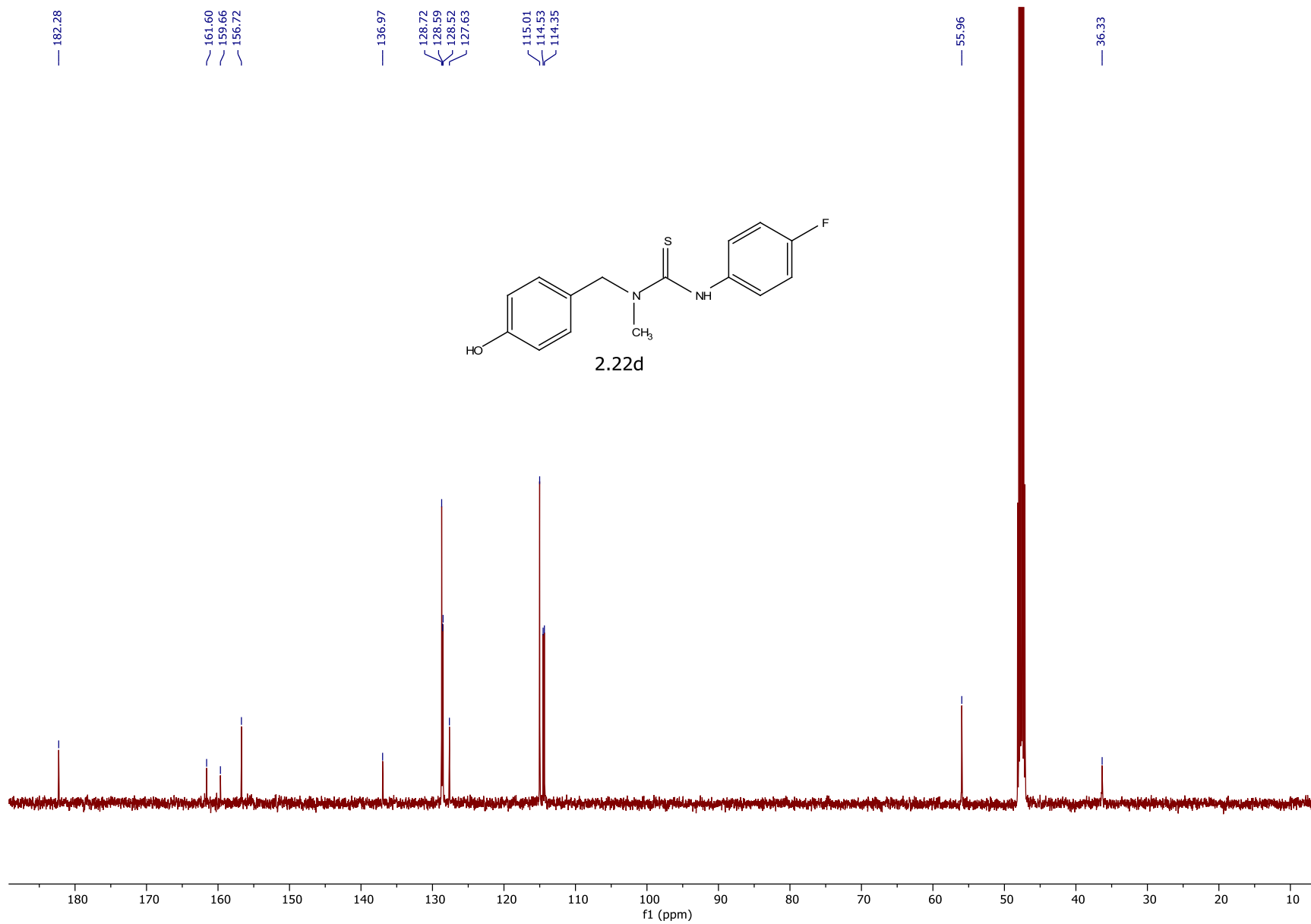


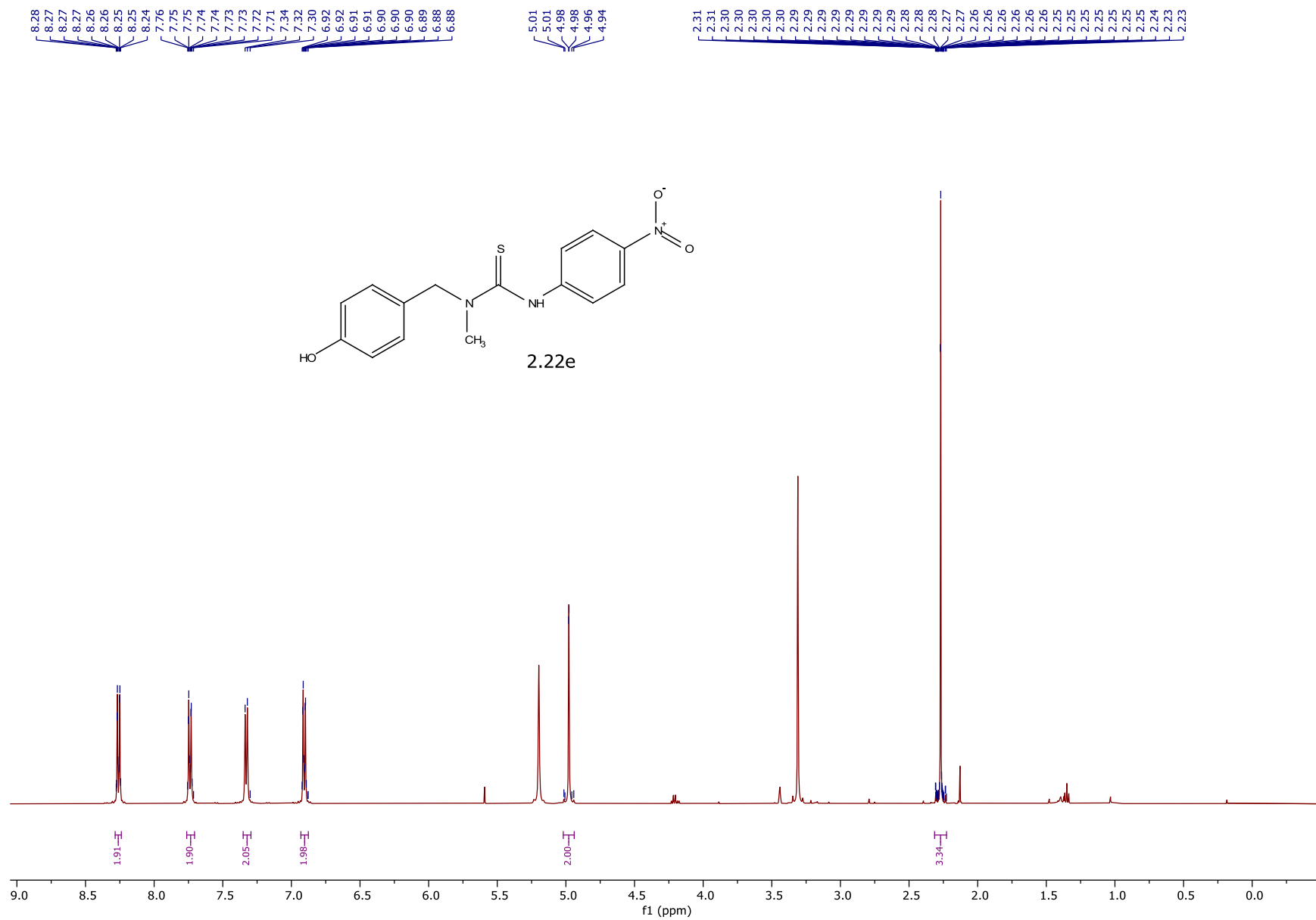


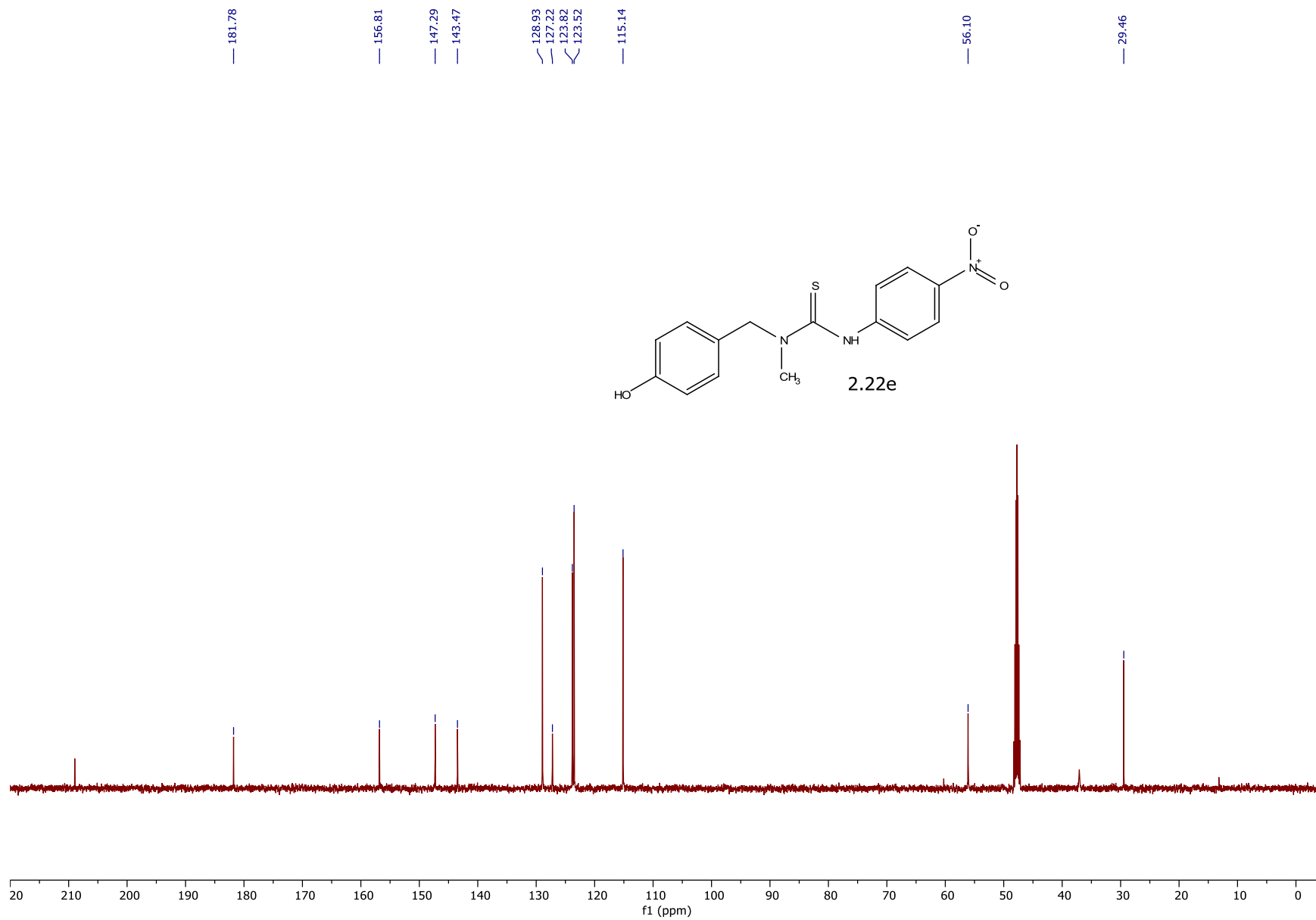








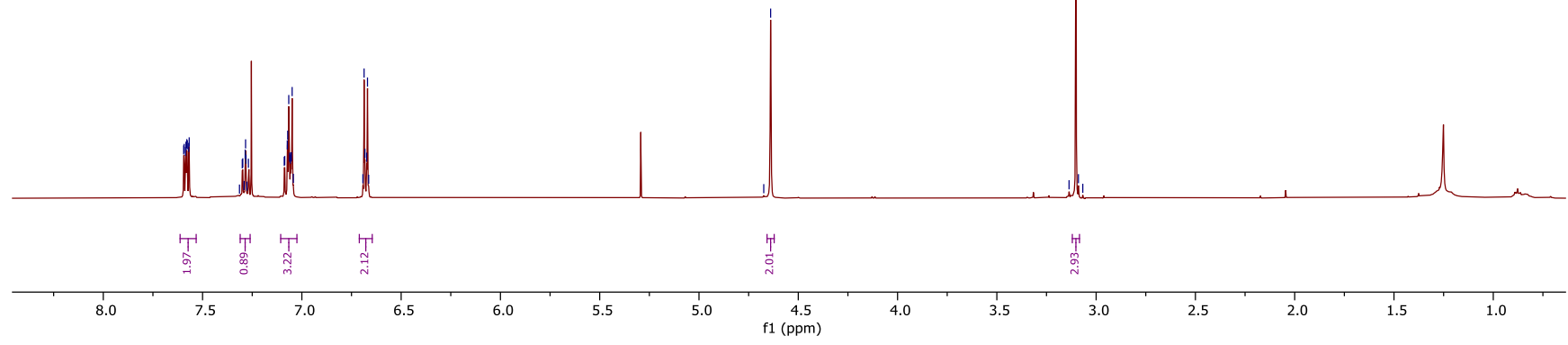
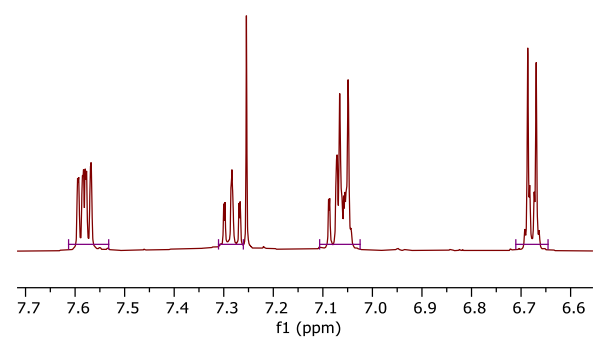
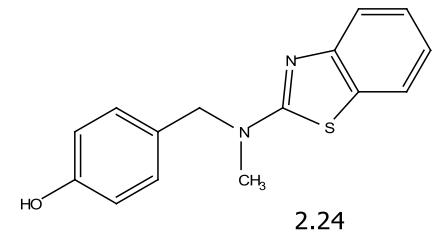


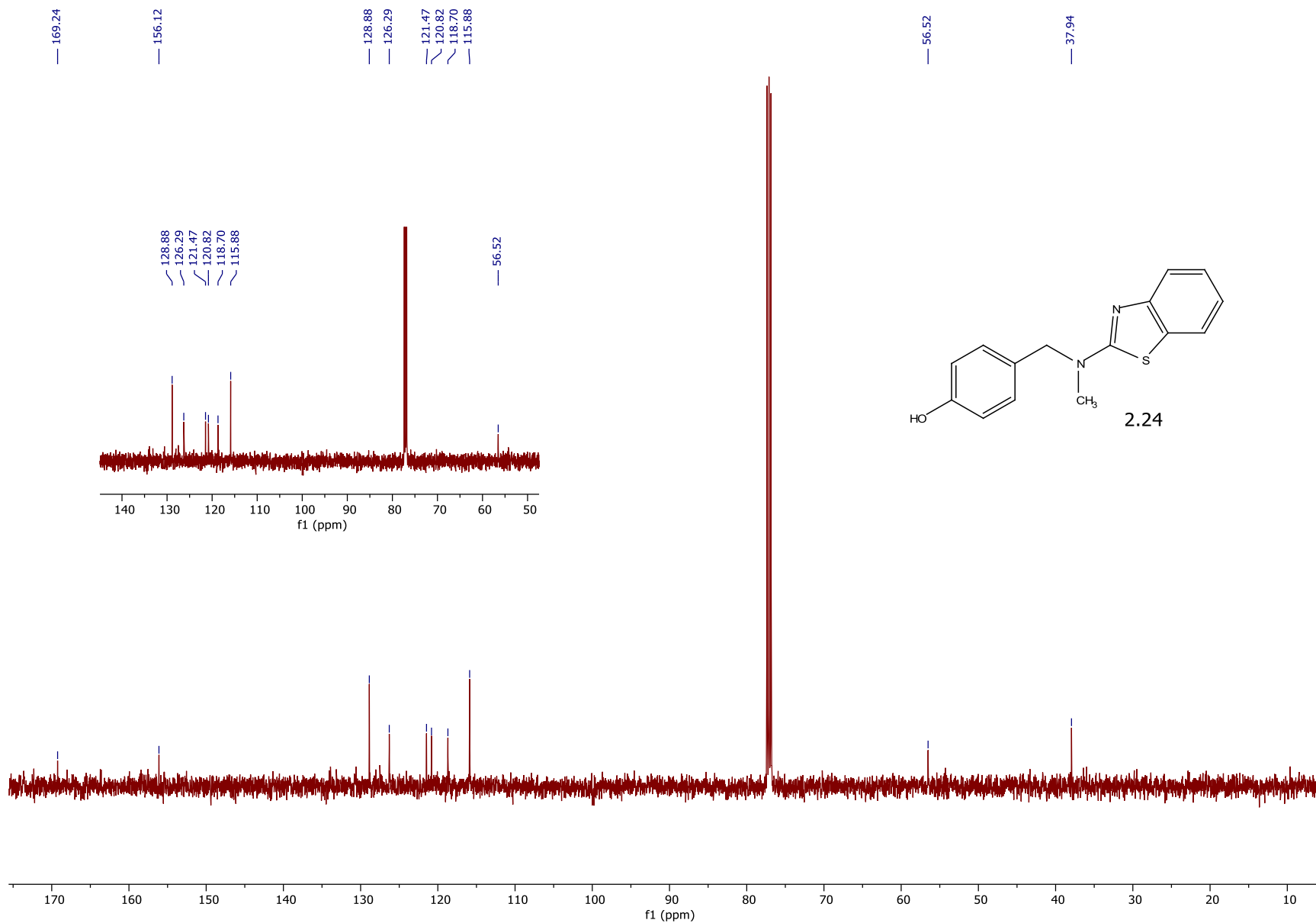


7.60  
7.59  
7.58  
7.57  
7.56  
7.31  
7.30  
7.29  
7.28  
7.27  
7.09  
7.07  
7.06  
7.05  
7.04  
6.69  
6.68  
6.67  
6.66

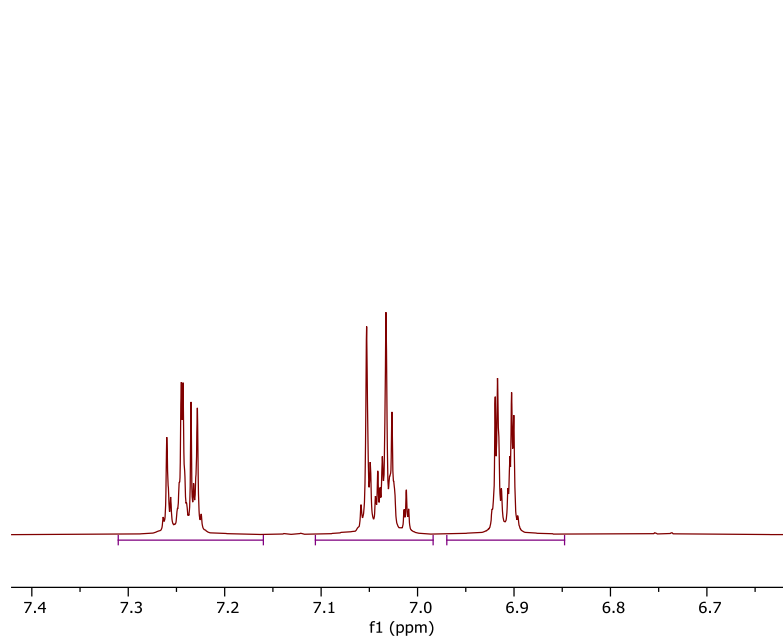
4.67  
4.64

3.14  
3.10  
3.07



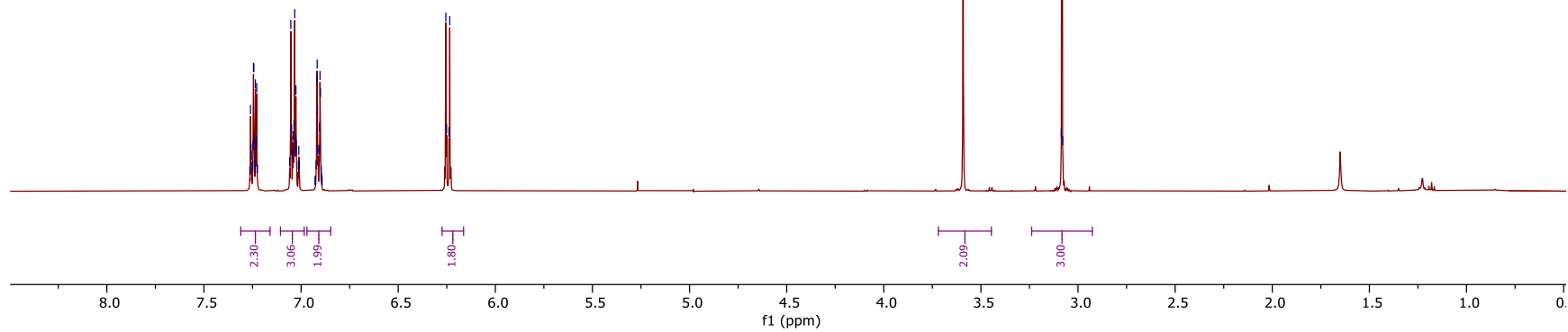
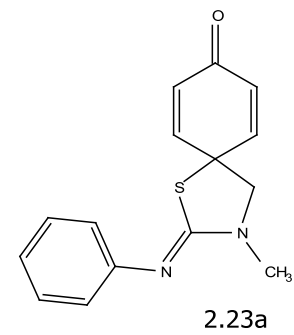


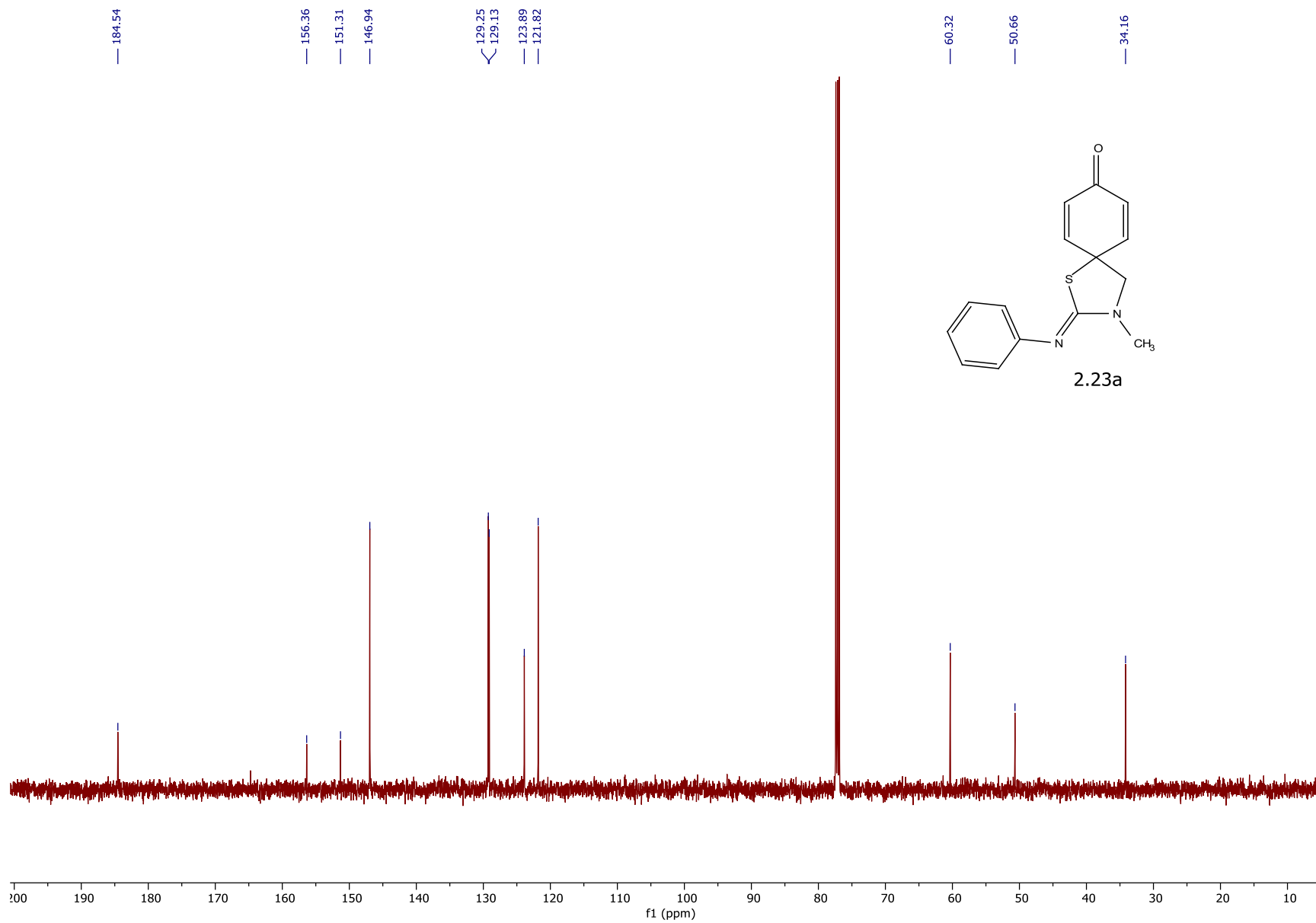
7.26  
7.26  
7.26  
7.25  
7.25  
7.24  
7.24  
7.24  
7.23  
7.23  
7.22  
7.06  
7.05  
7.05  
7.04  
7.04  
7.04  
7.03  
7.03  
7.02  
7.02  
7.01  
7.01  
7.01  
6.93  
6.93  
6.92  
6.92  
6.92  
6.92  
6.91  
6.91  
6.90  
6.90  
6.90  
6.90  
6.89  
6.89  
6.89  
6.25  
6.25  
6.24  
6.23



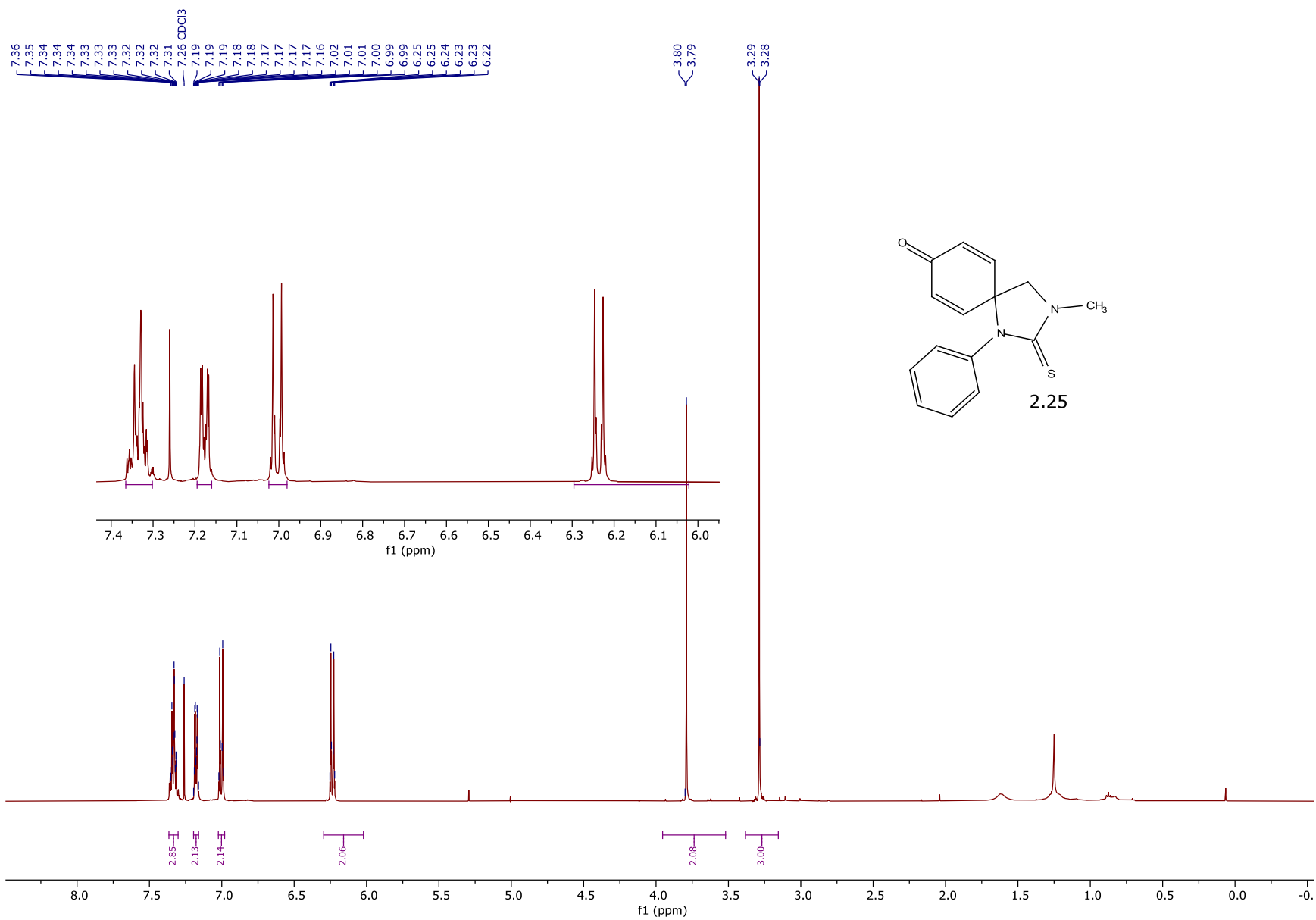
3.59

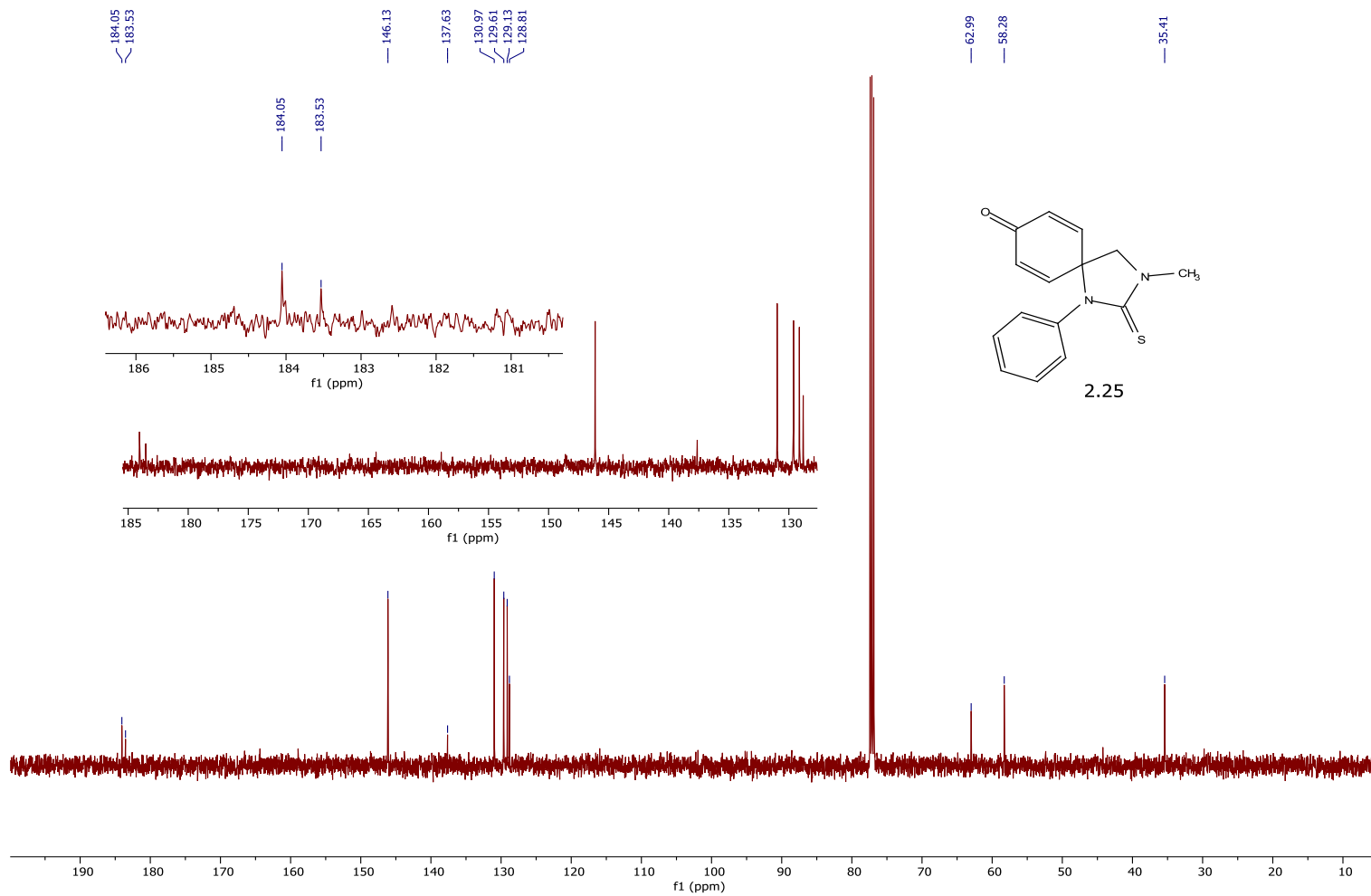
3.09  
3.08  
3.08

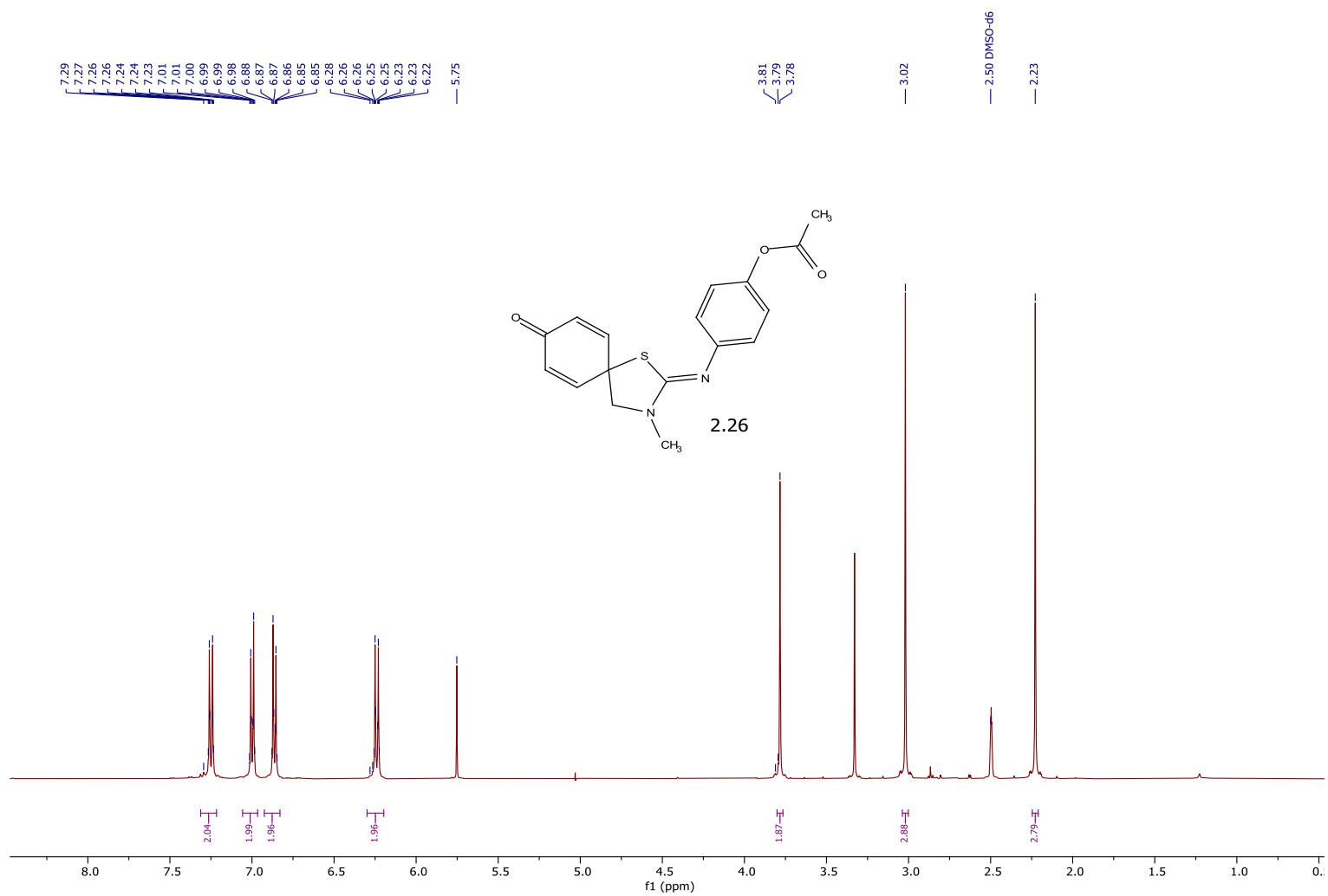


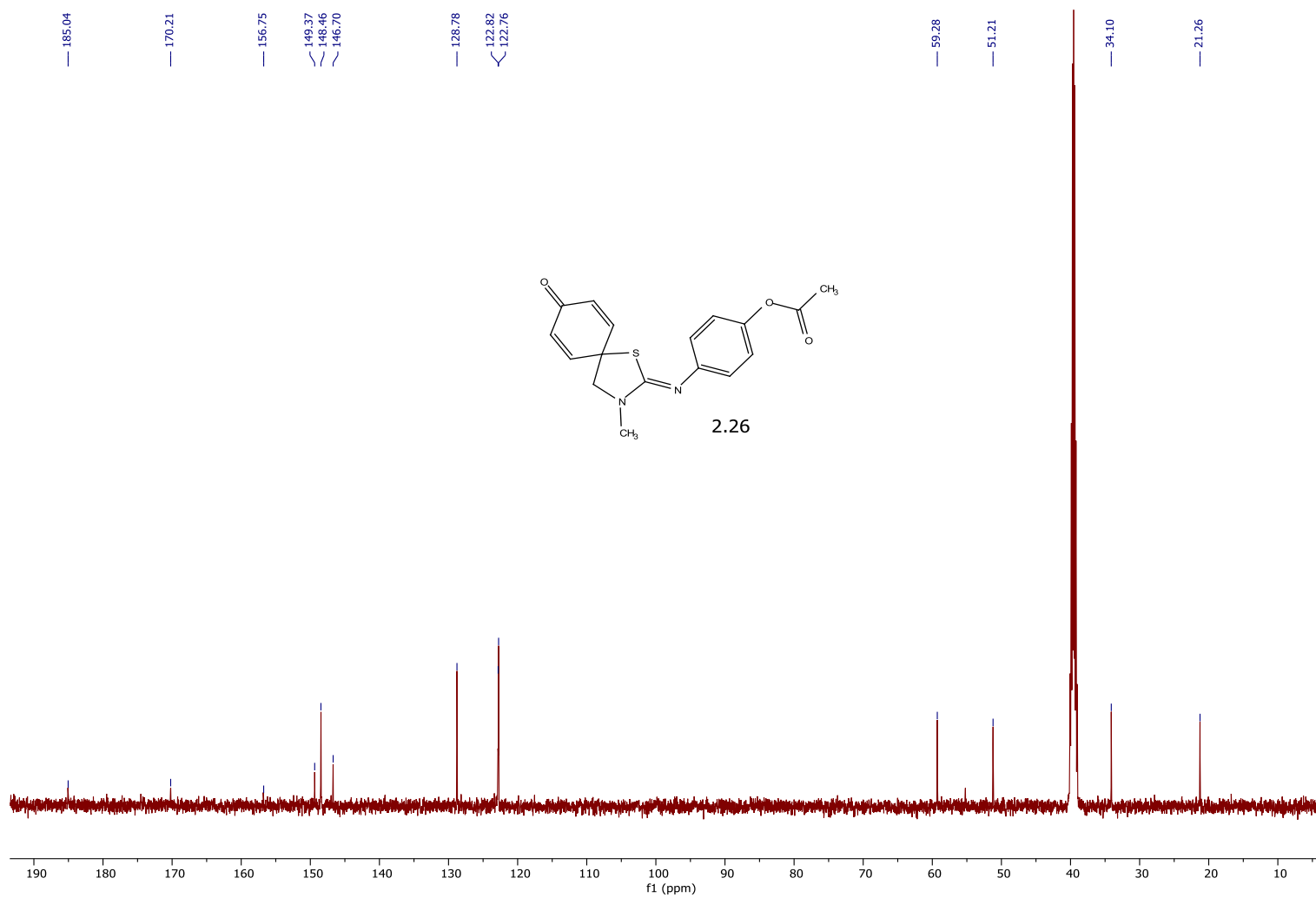




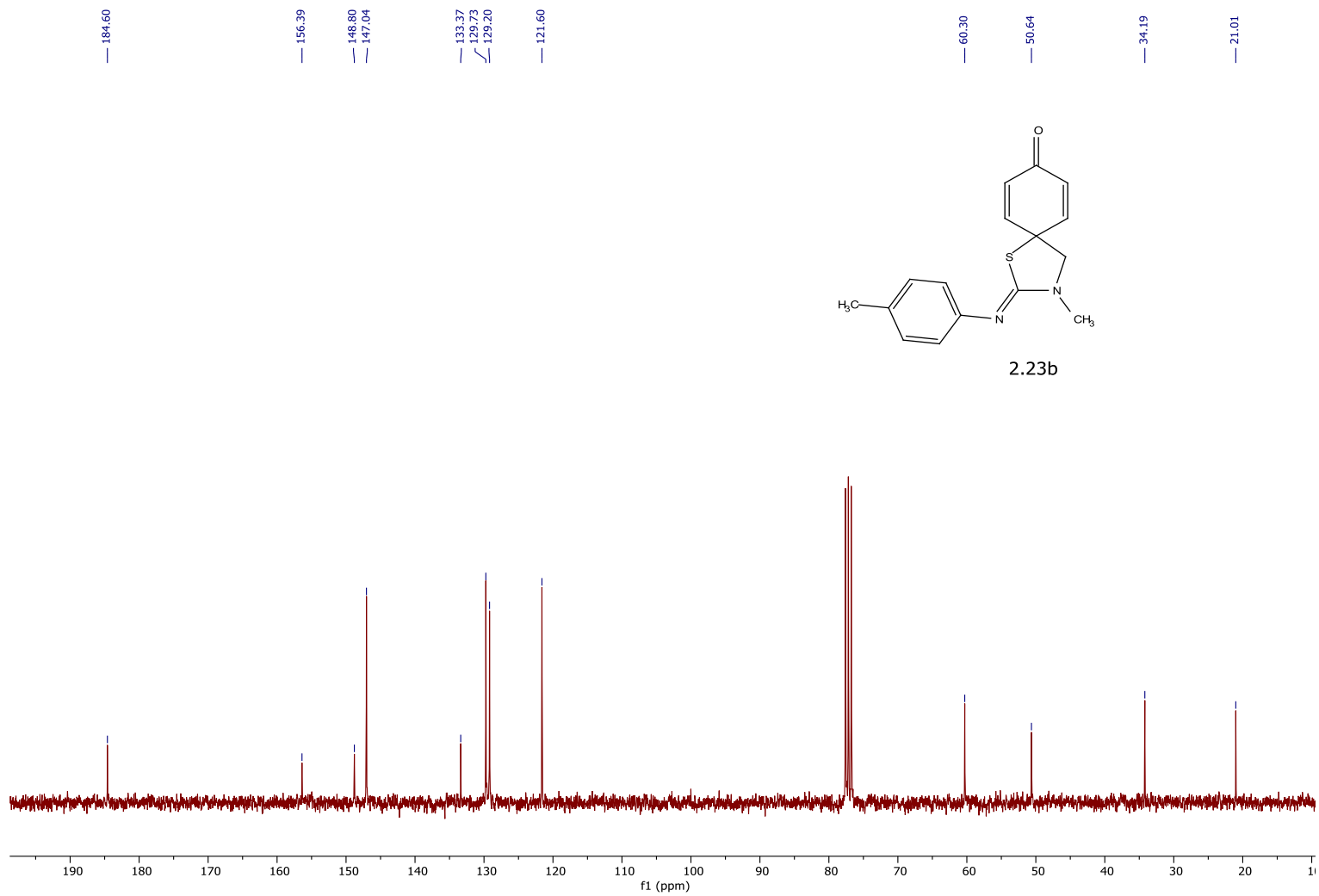


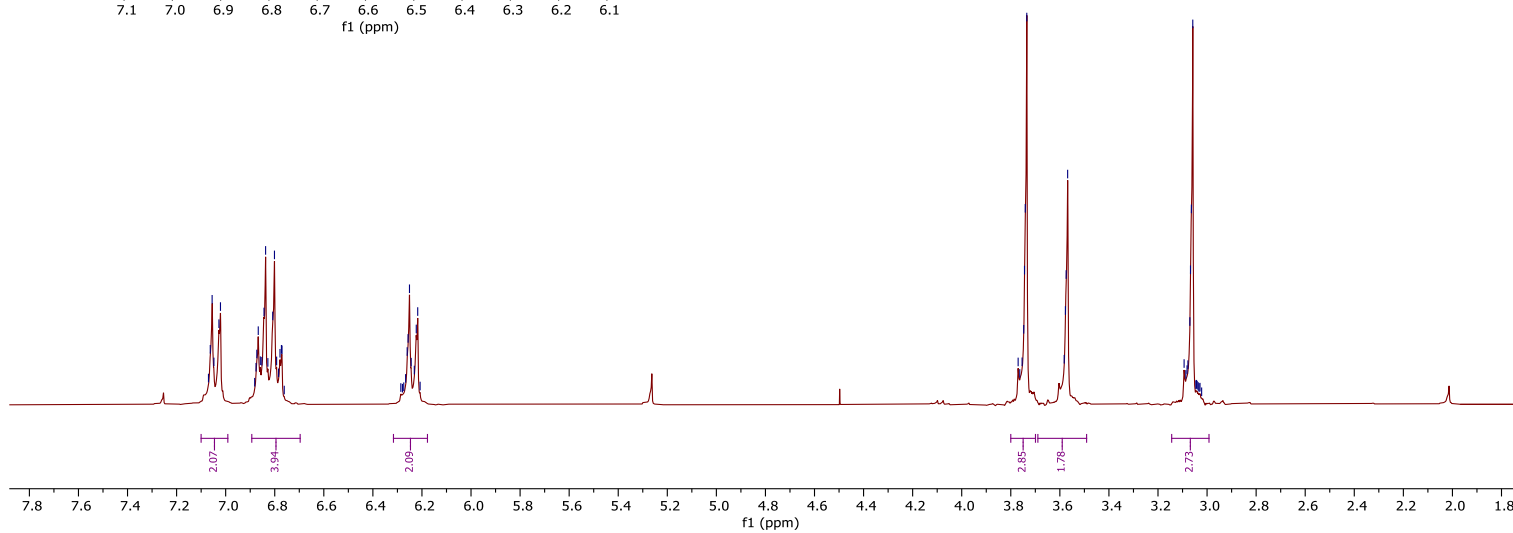
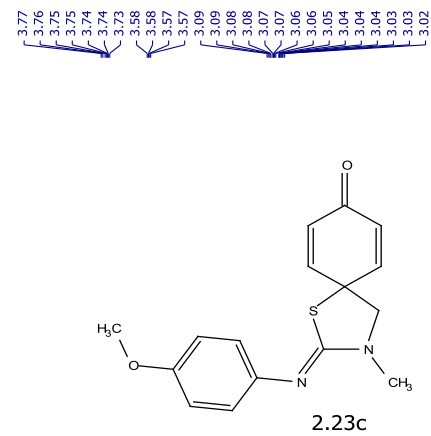
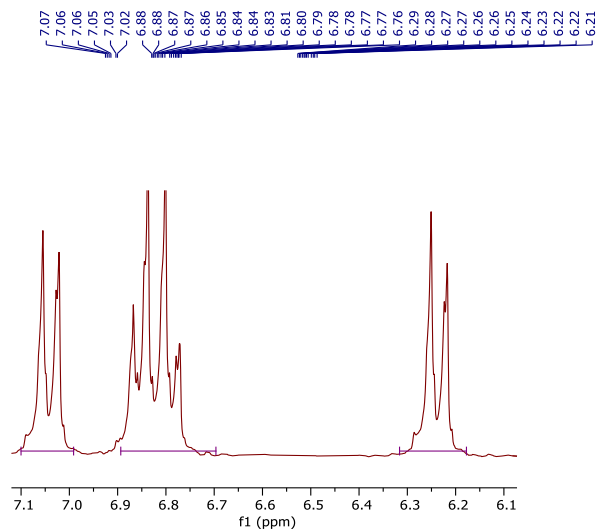


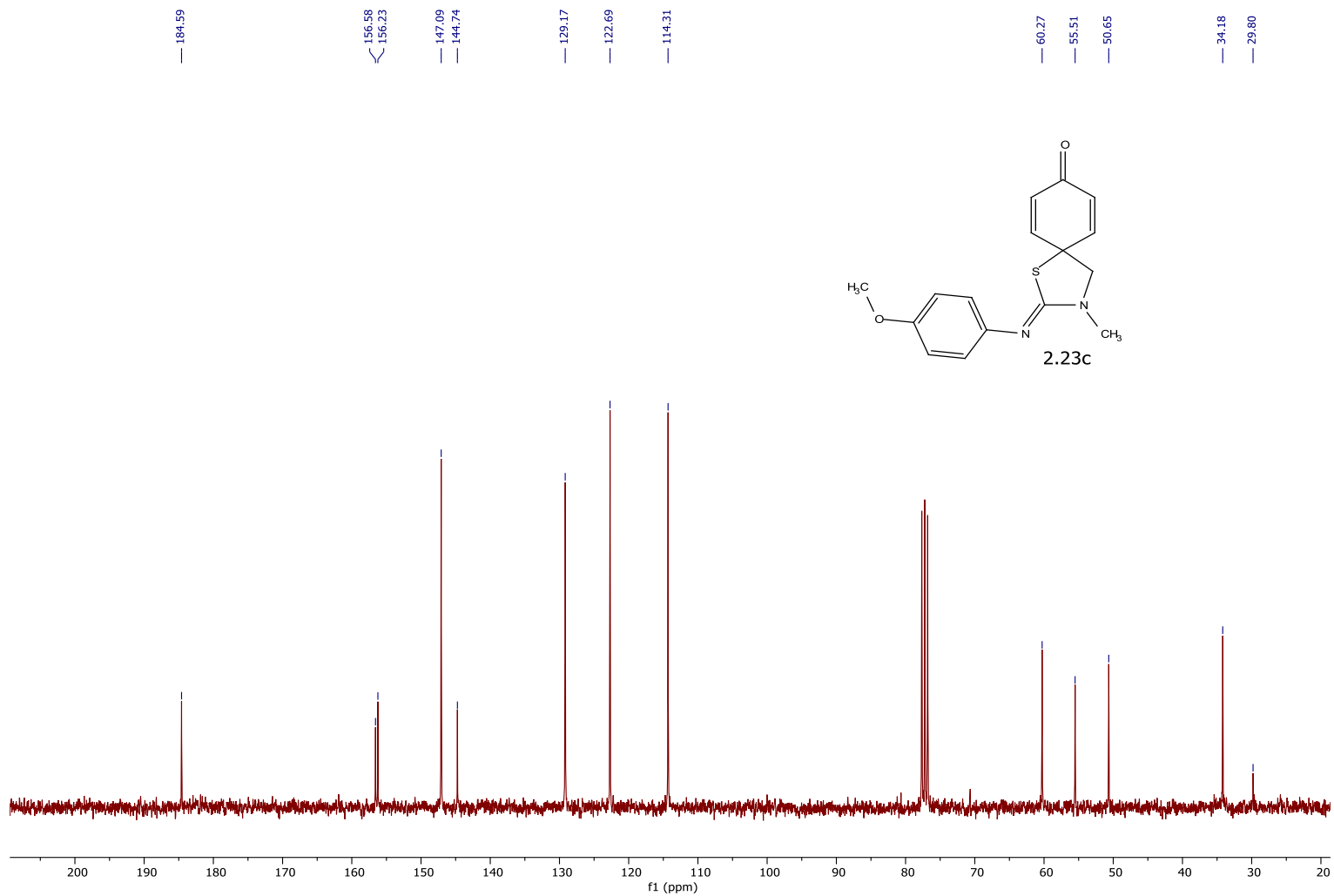














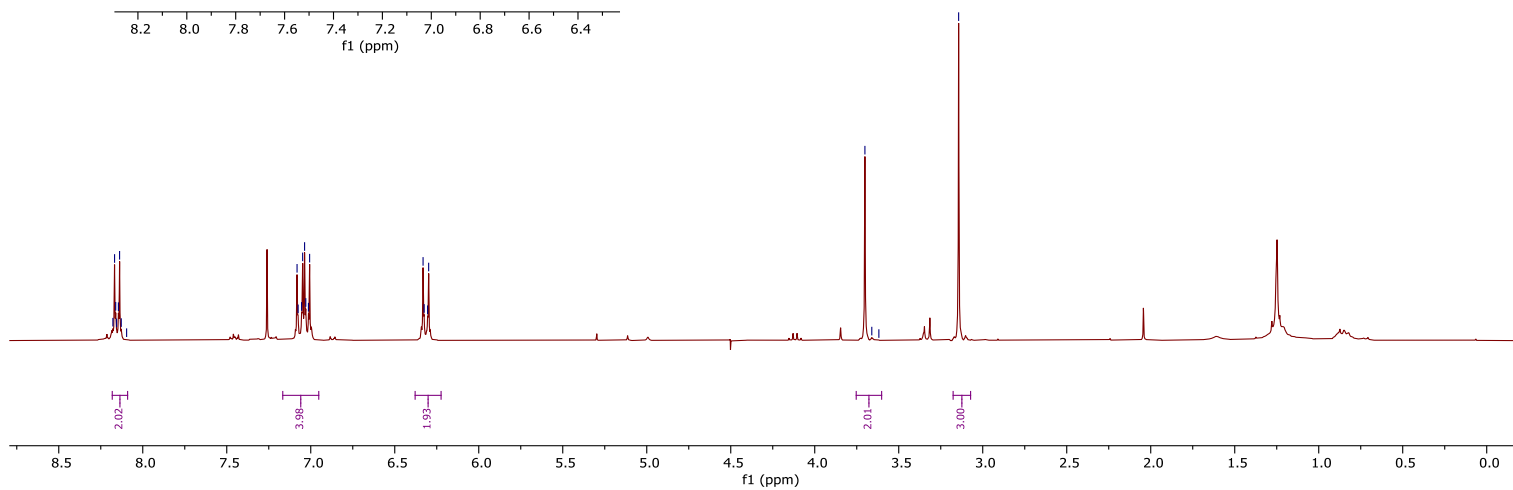
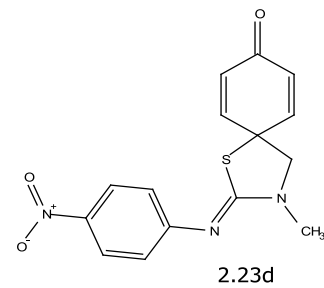
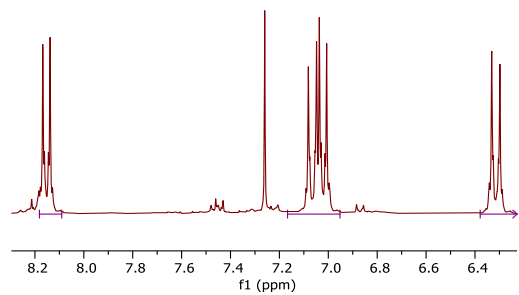
8.18  
8.17  
8.16  
8.16  
8.14  
8.14  
8.13  
8.10

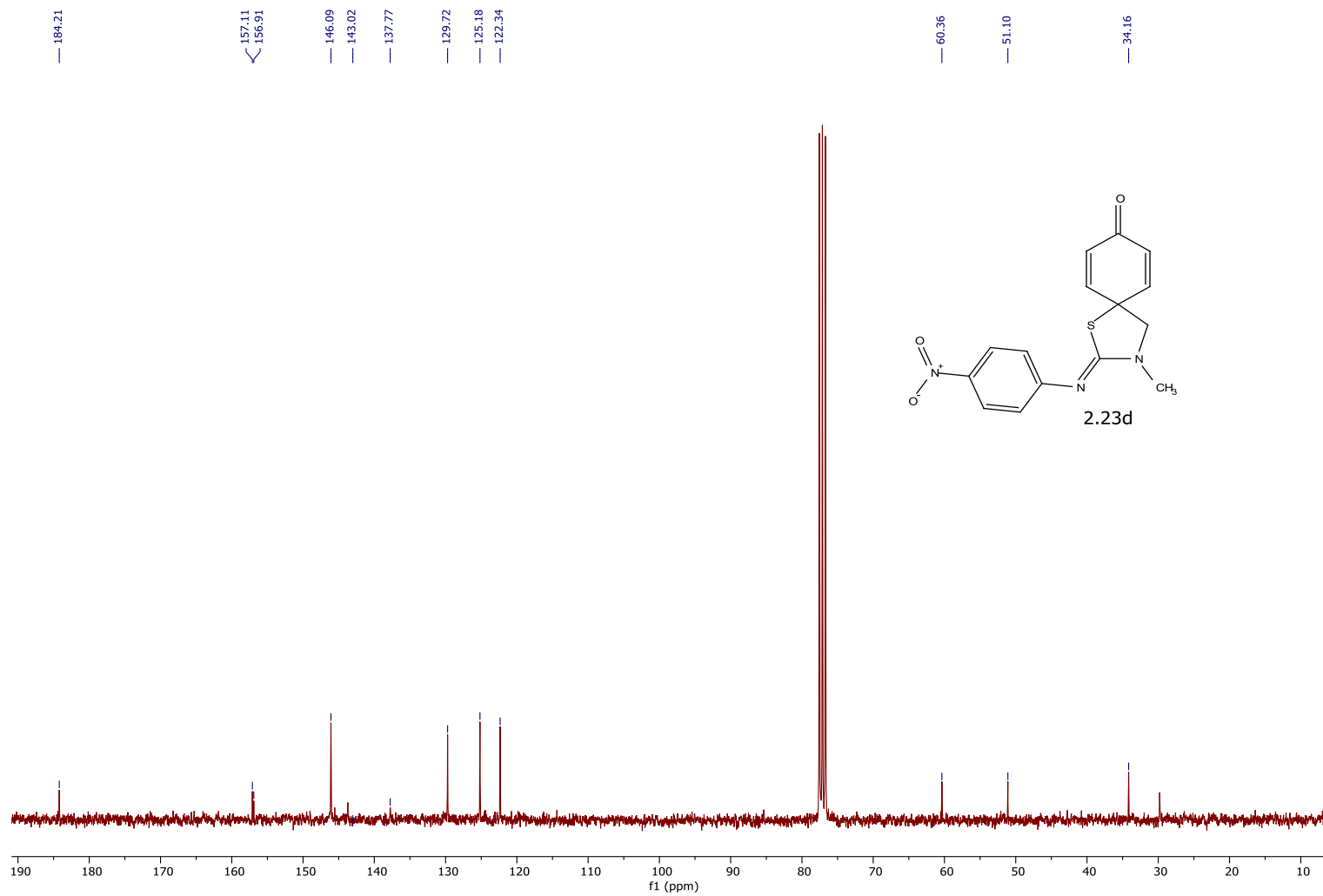
7.08  
7.08  
7.05  
7.05  
7.04  
7.03  
7.01  
7.01

6.33  
6.33  
6.30  
6.30

3.70  
3.66  
3.62

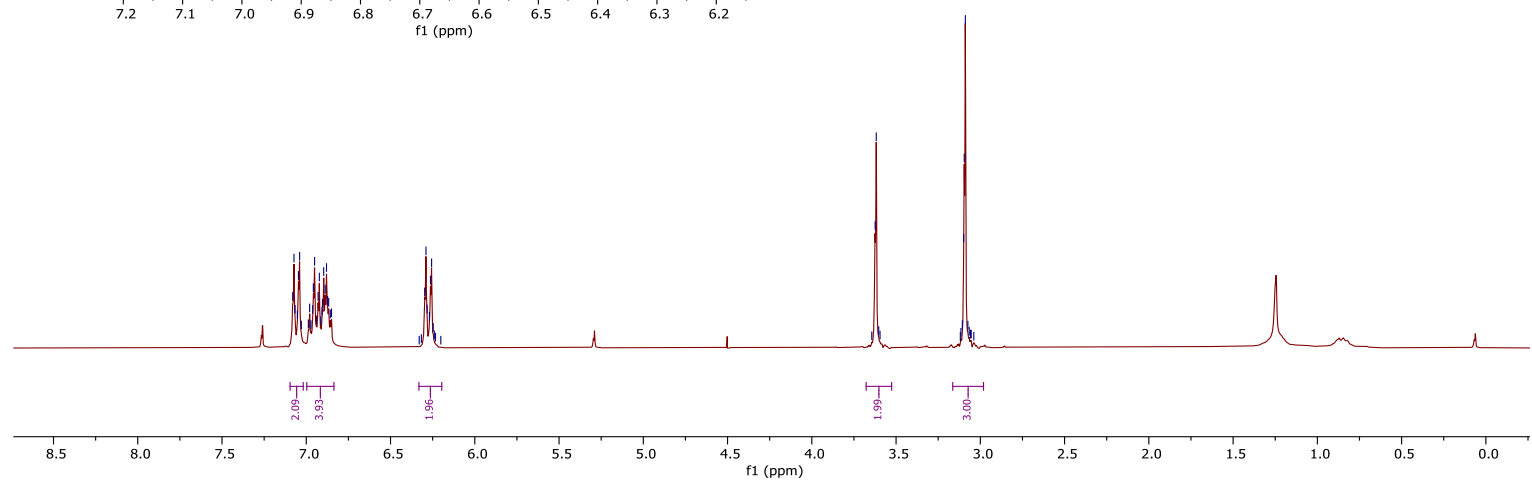
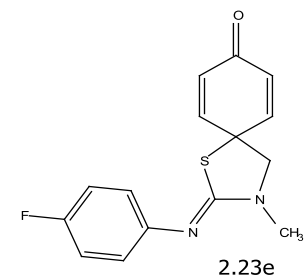
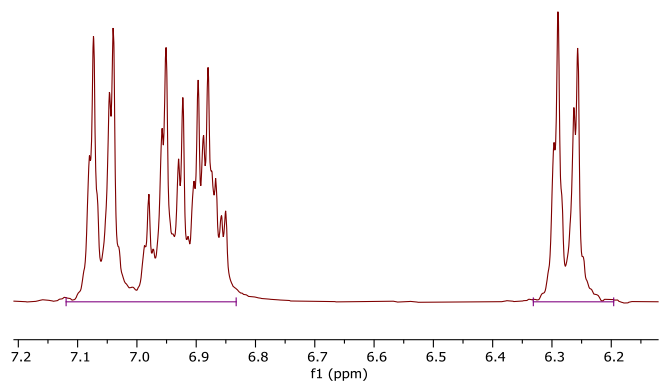
3.14

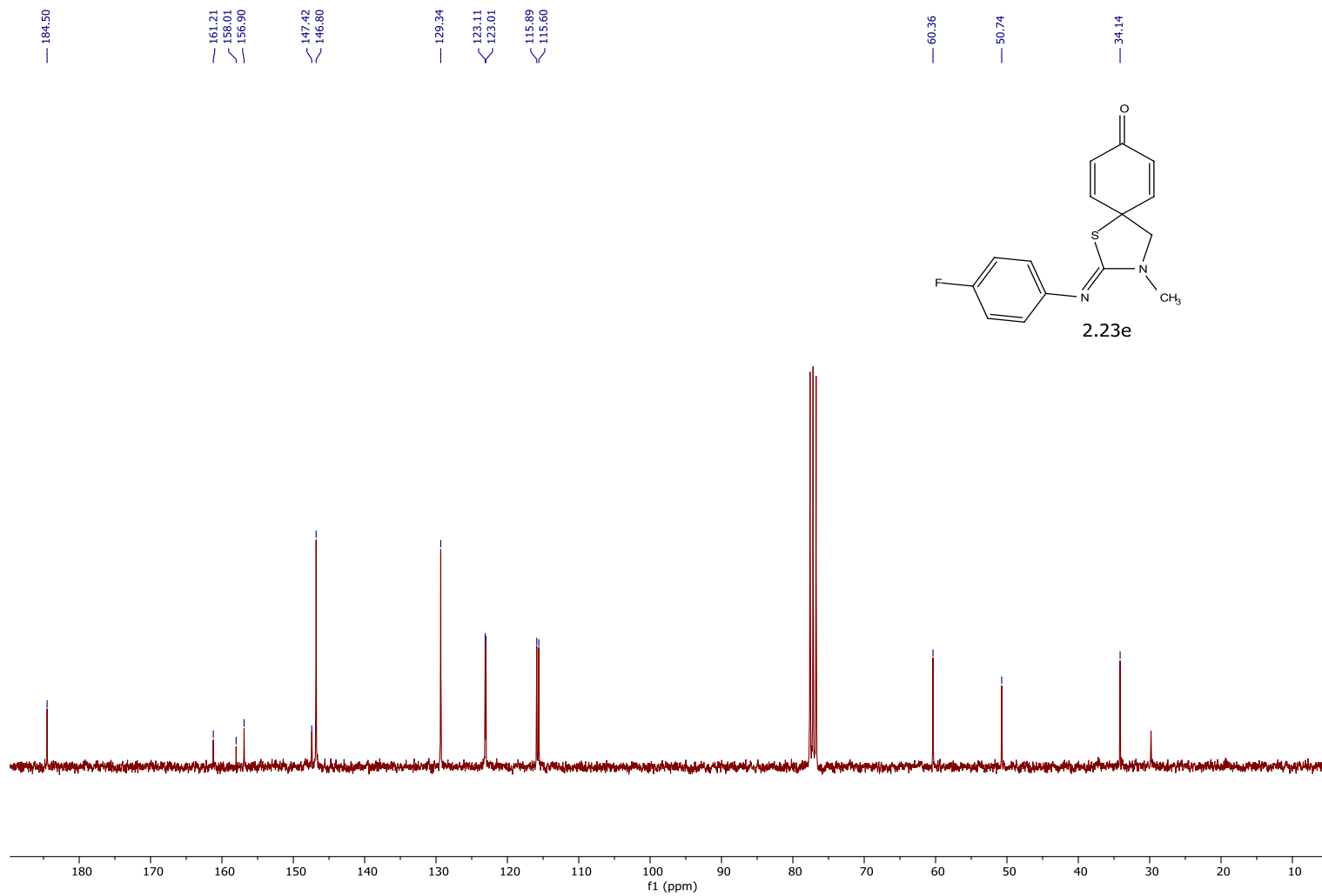


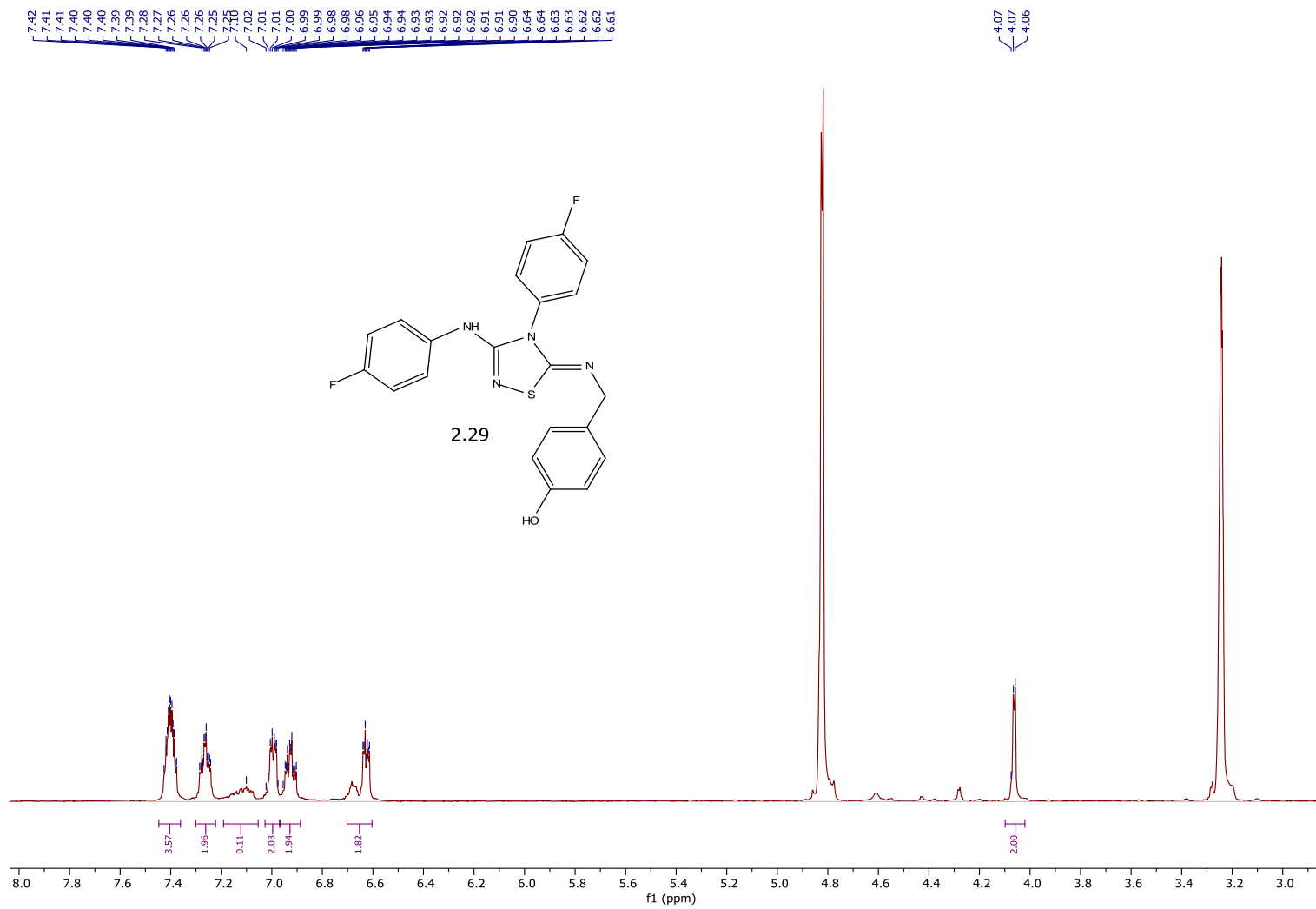


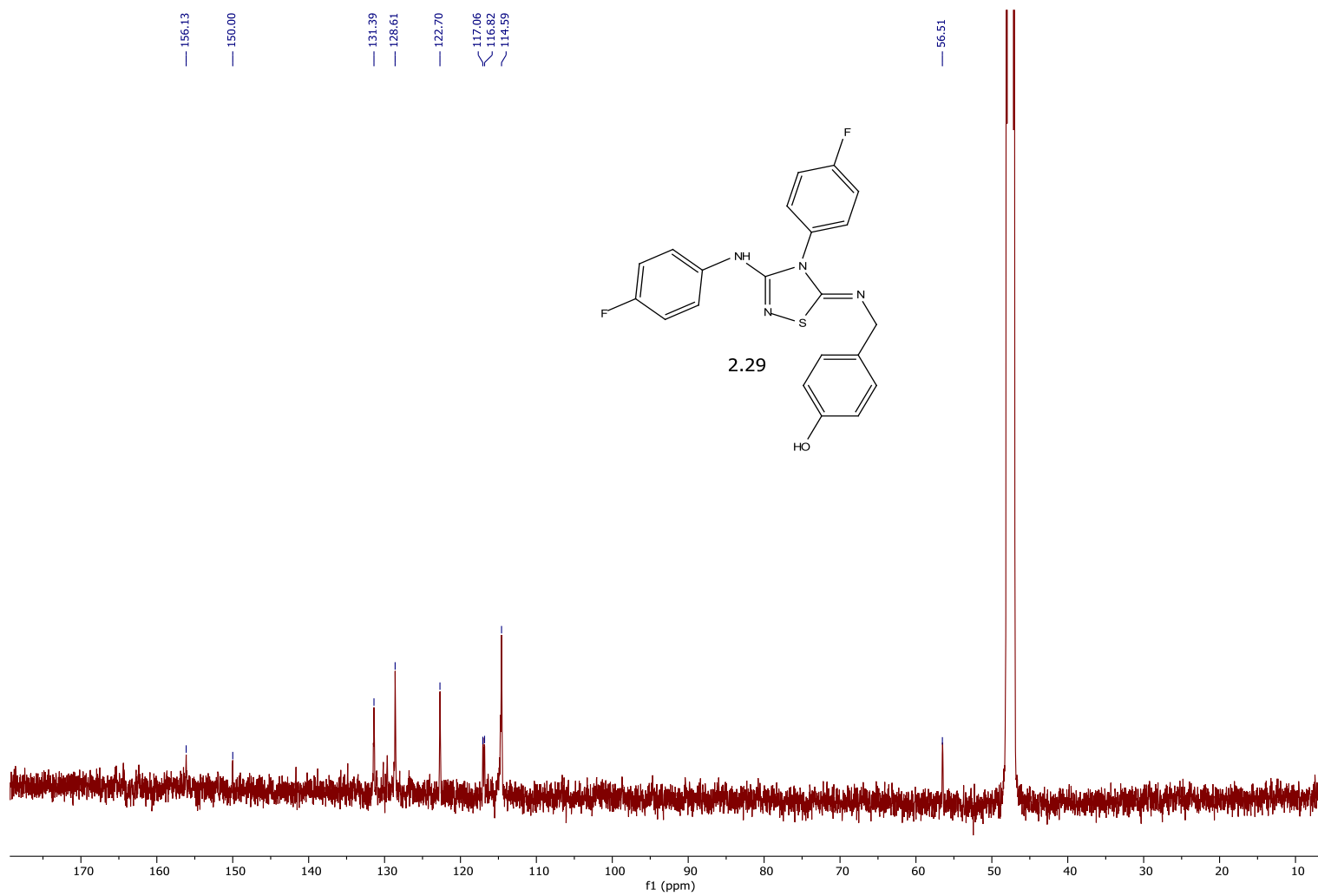
7.08  
7.07  
7.07  
7.05  
7.05  
7.04  
6.98  
6.96  
6.95  
6.94  
6.93  
6.92  
6.91  
6.90  
6.89  
6.88  
6.87  
6.86  
6.85  
6.85  
6.80  
6.79  
6.78  
6.77  
6.76  
6.75  
6.74  
6.73  
6.72

3.64  
3.62  
3.62  
3.60  
3.60  
3.12  
3.12  
3.11  
3.10  
3.10  
3.09  
3.07  
3.06  
3.05  
3.04



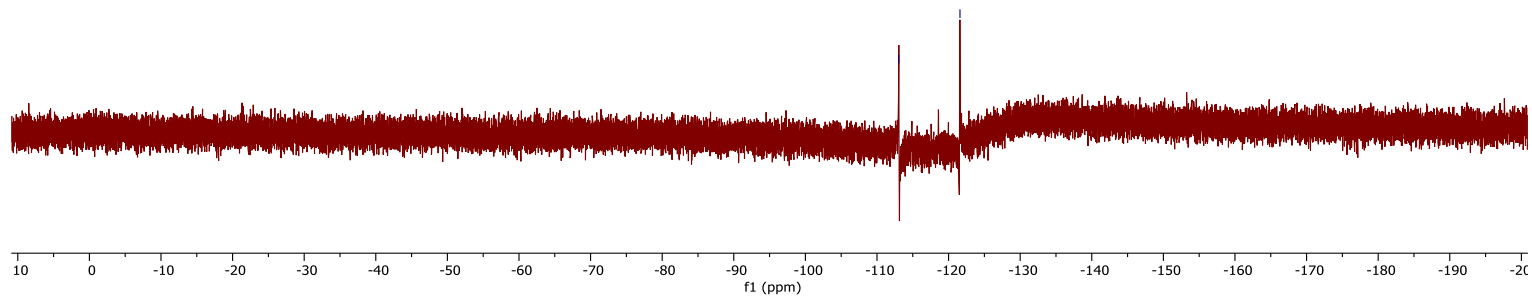
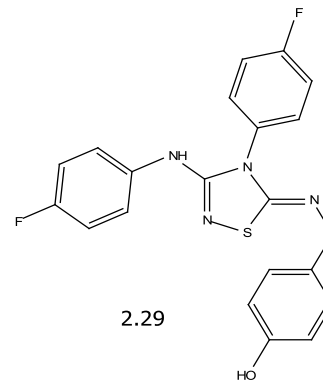


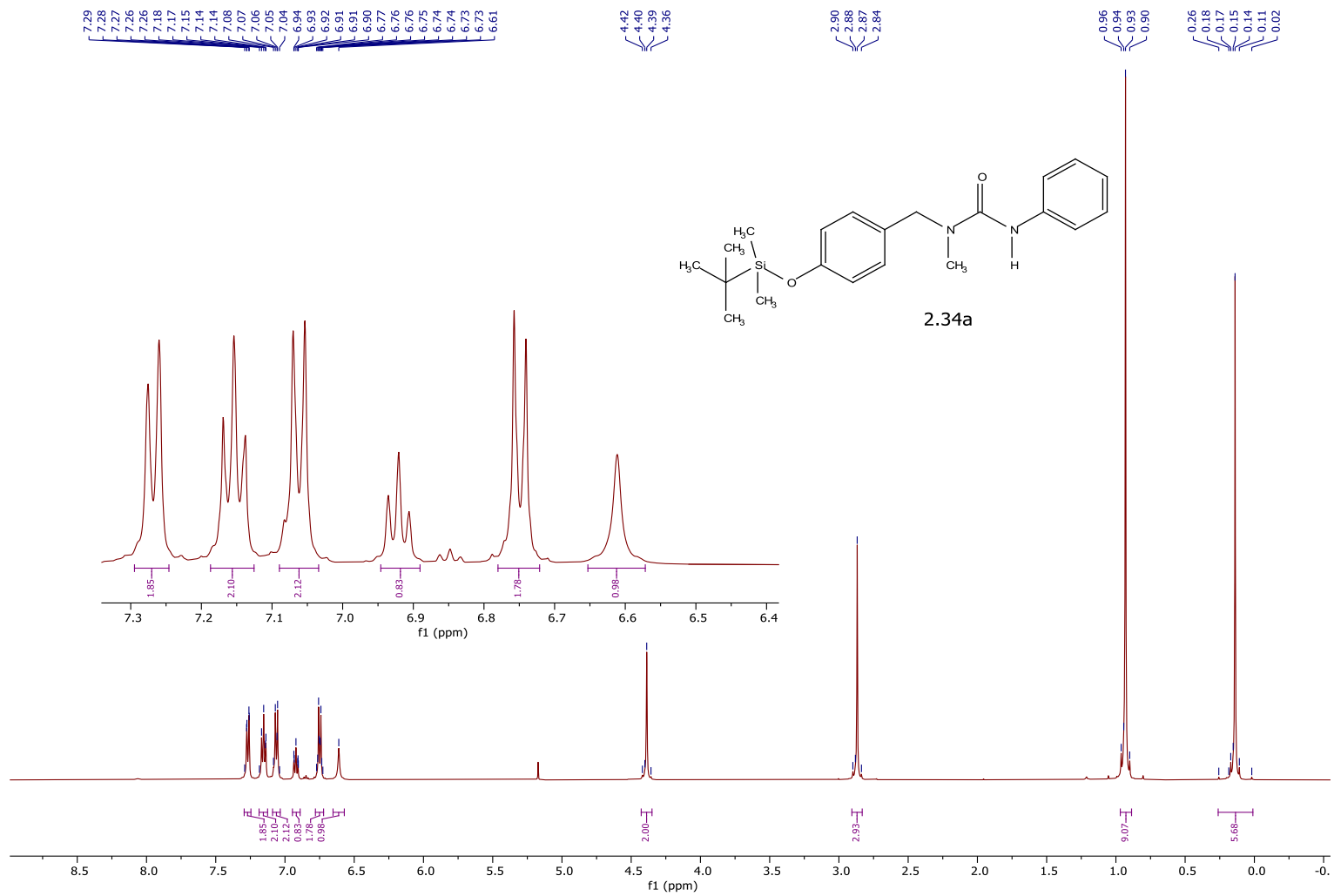




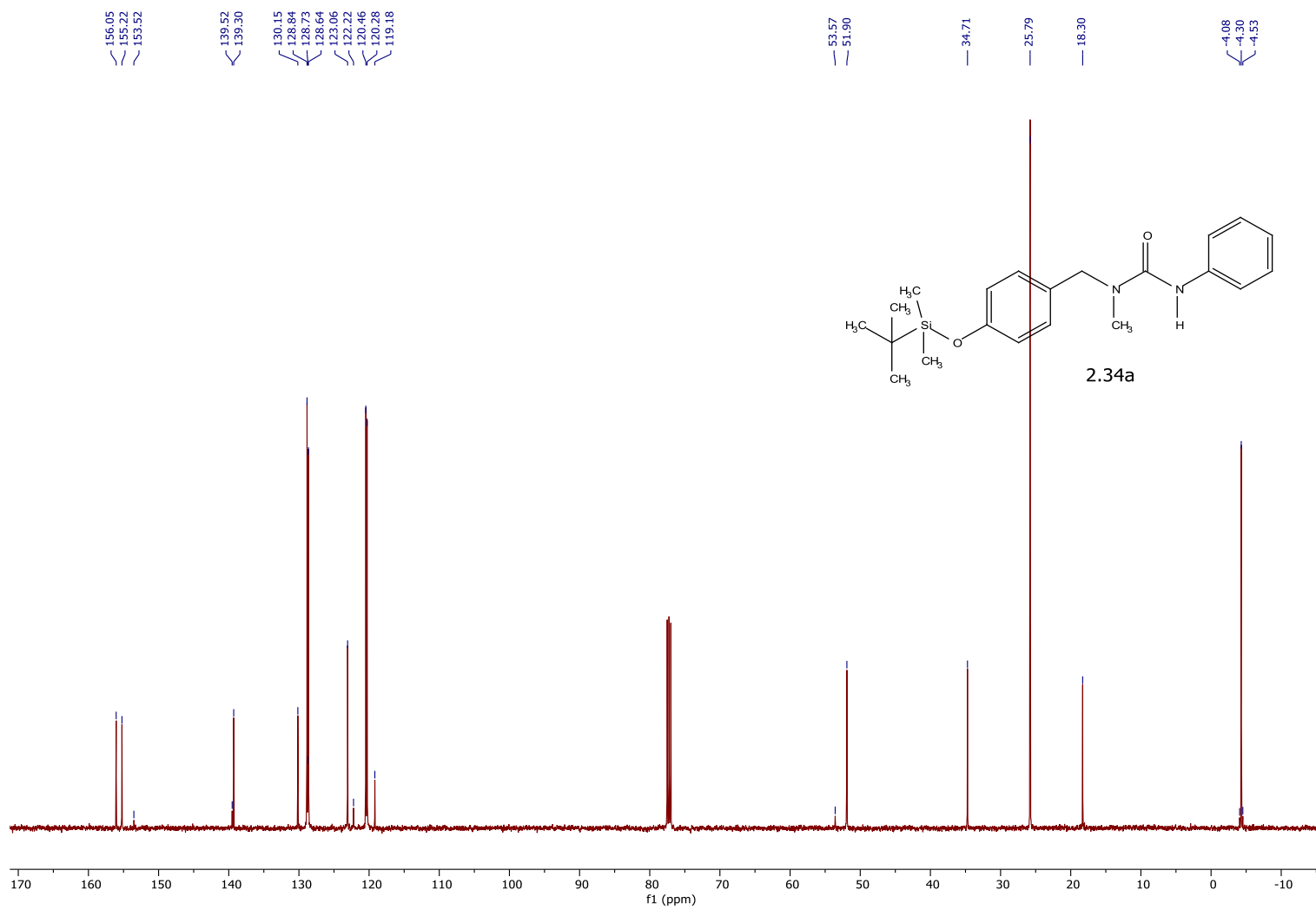
<sup>19</sup>F  
NMR

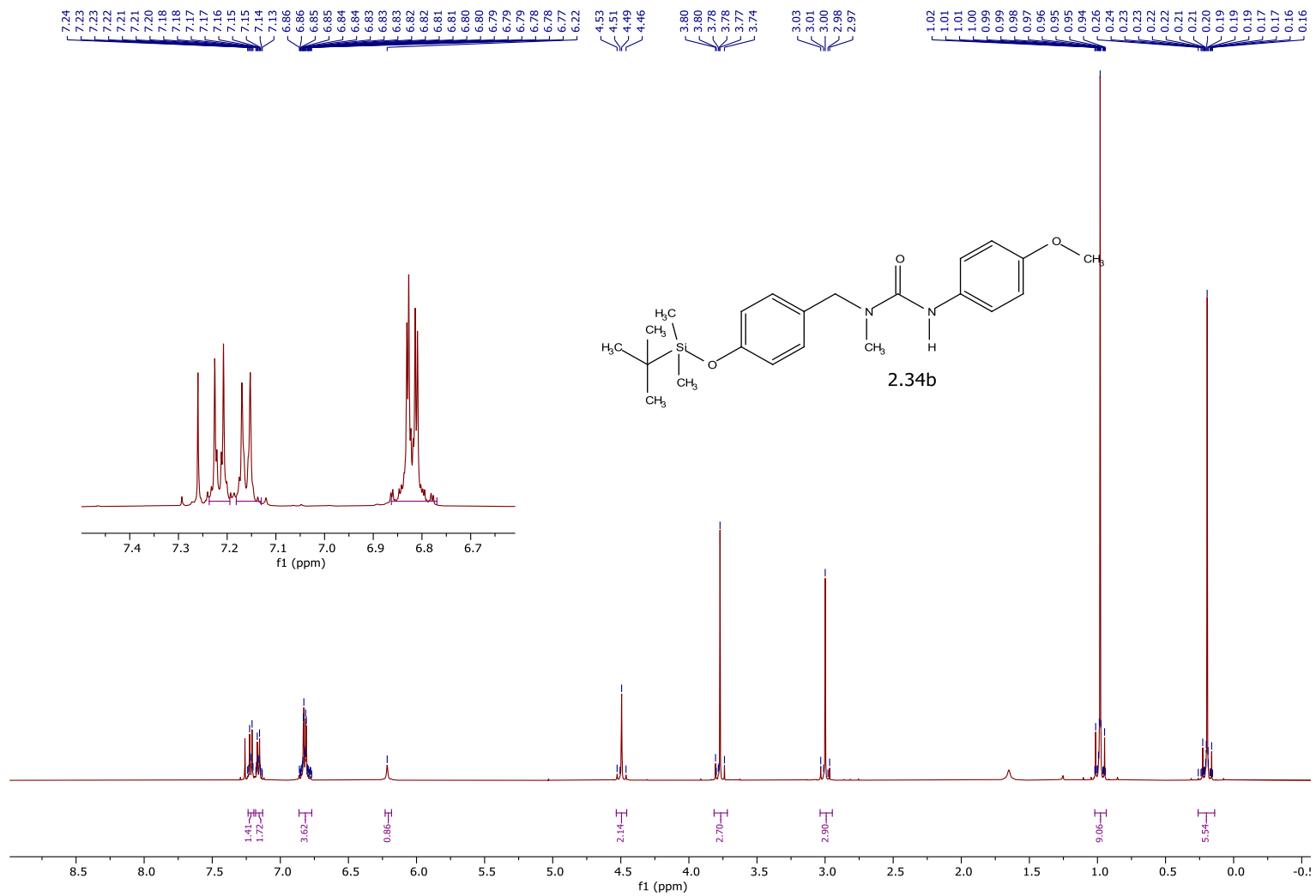
-113.04  
-121.99

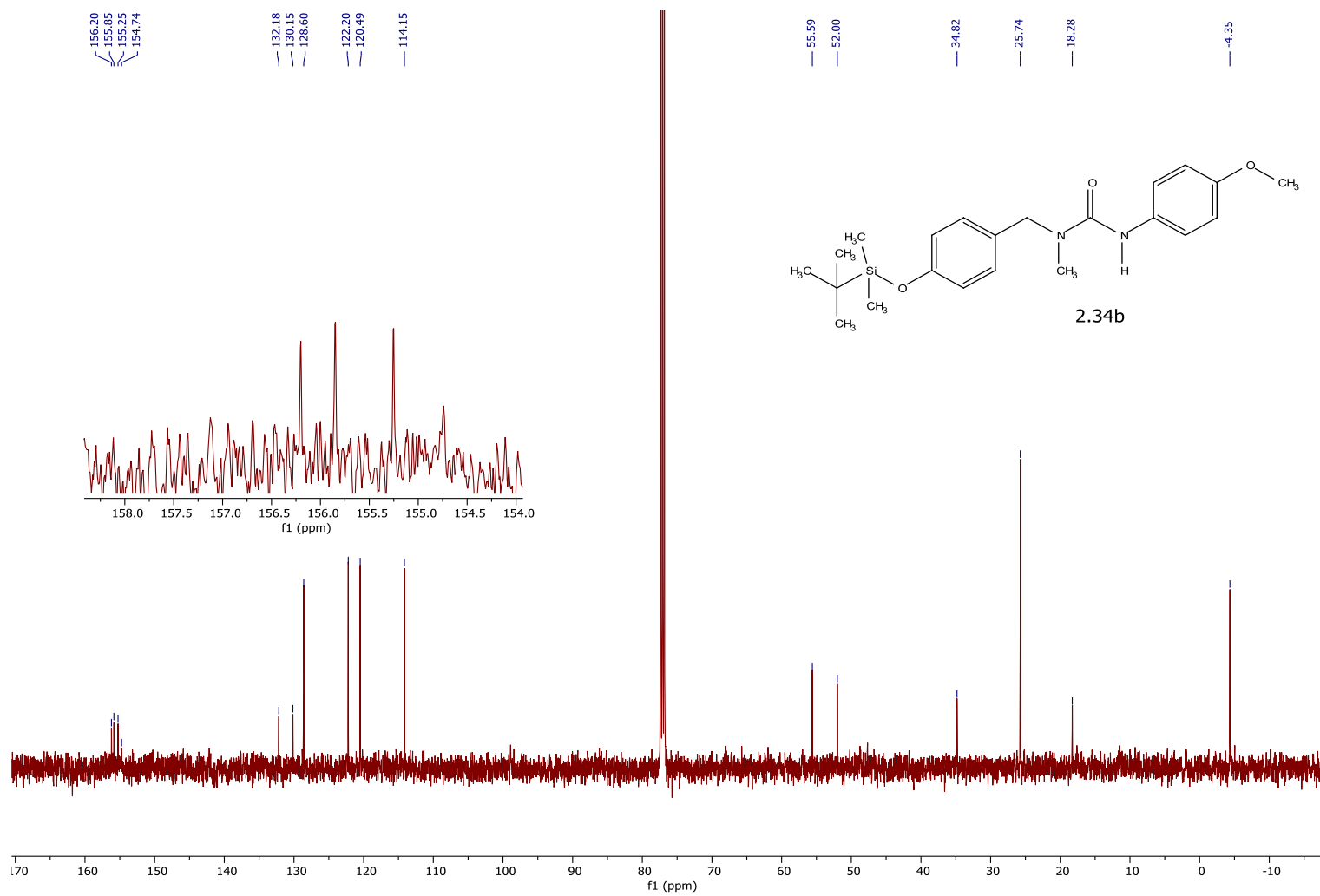






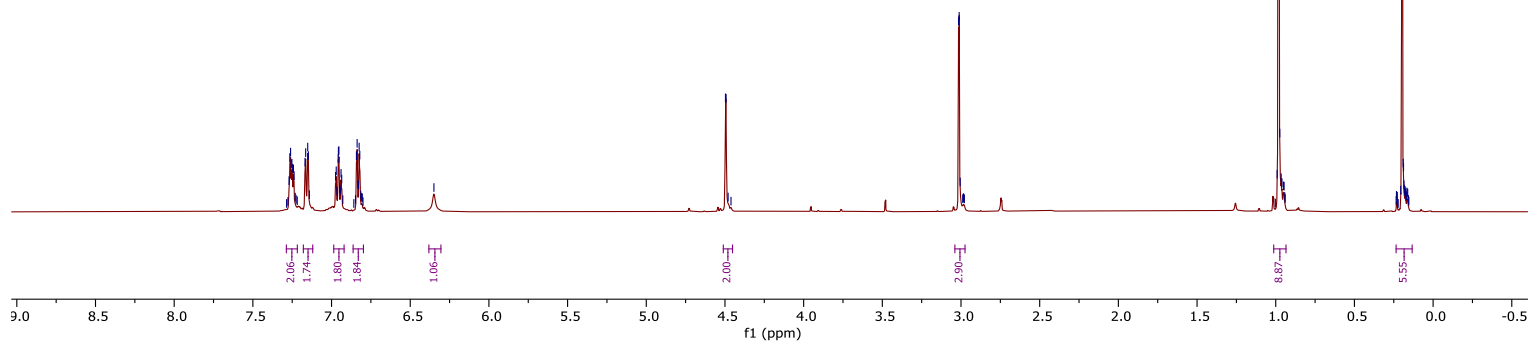
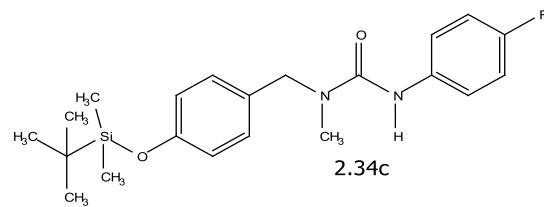
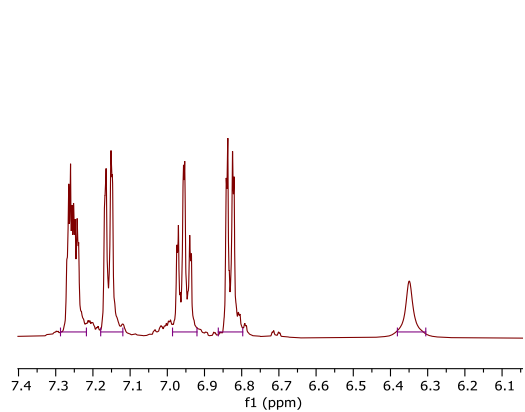


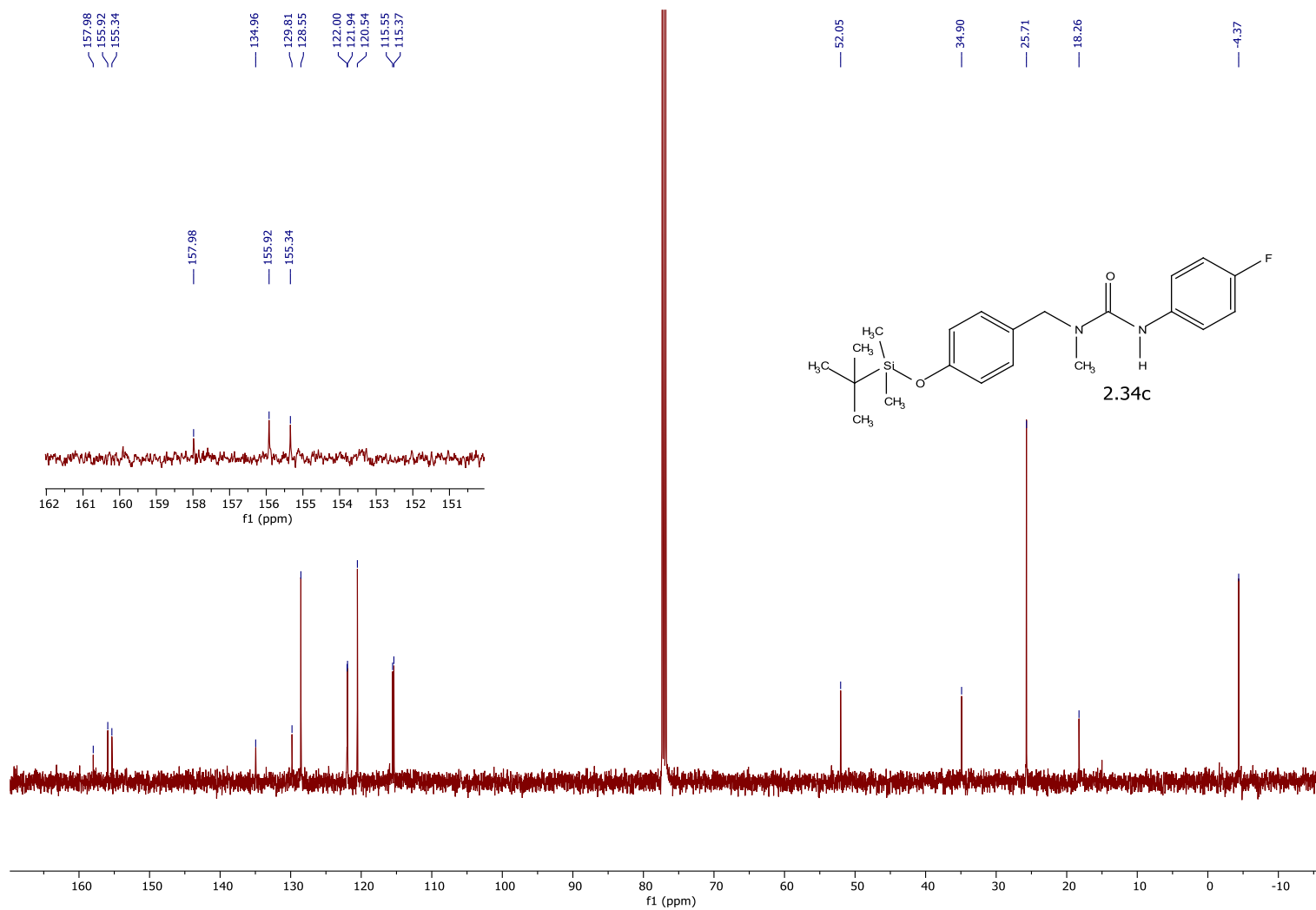


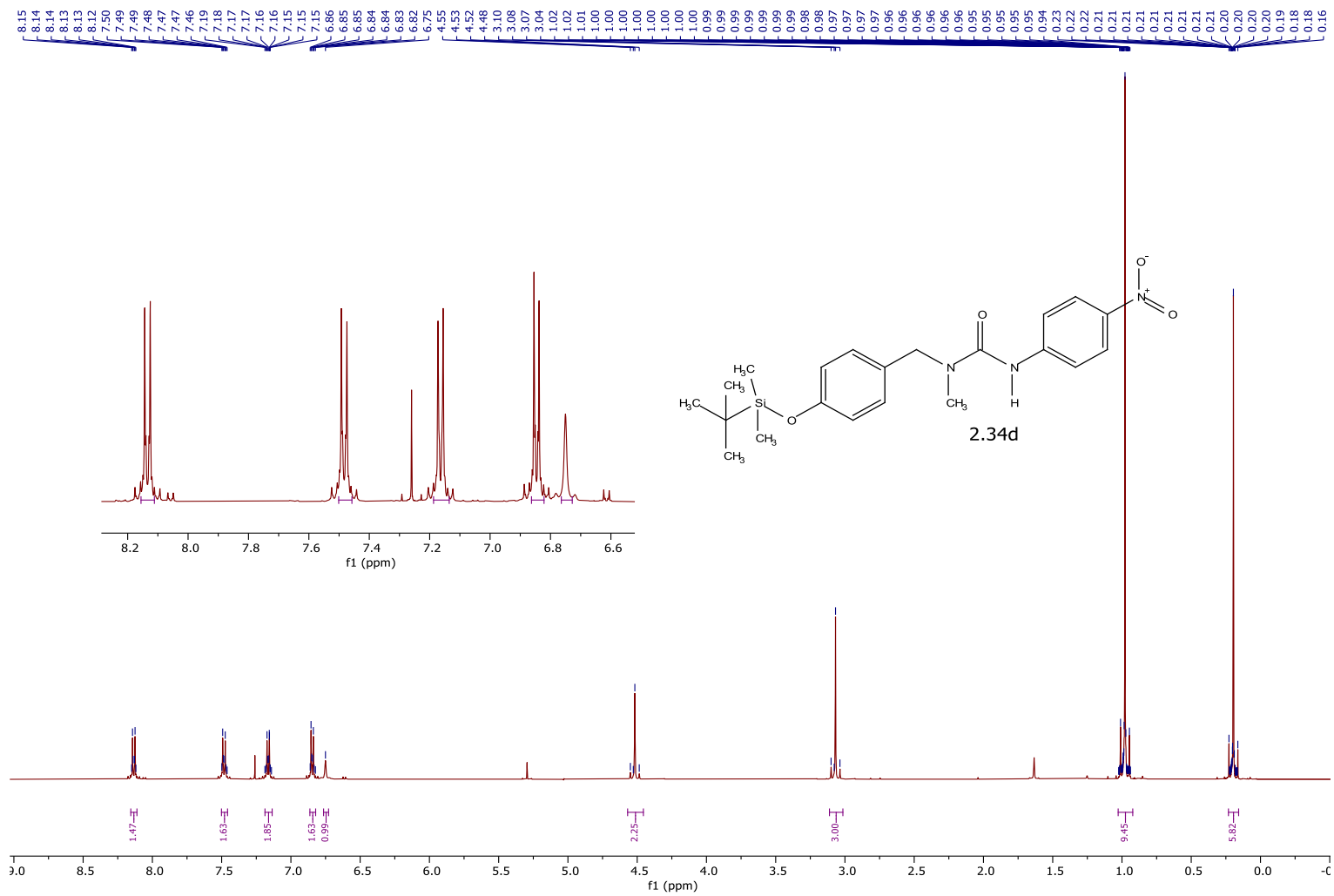


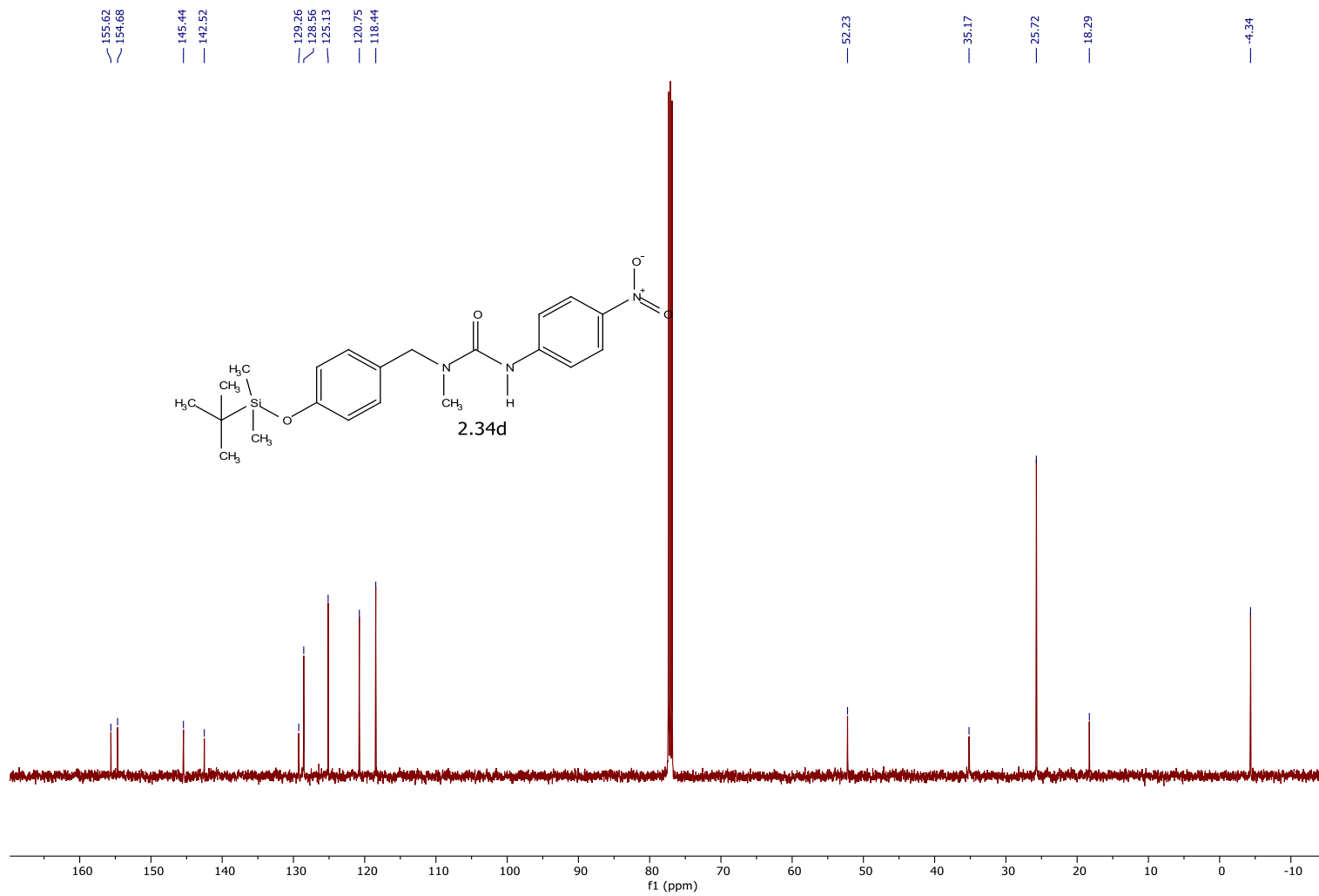
7.29  
7.28  
7.27  
7.27  
7.26  
7.26  
7.25  
7.25  
7.24  
7.24  
7.23  
7.23  
7.22  
7.22  
7.17  
7.16  
7.15  
7.15  
7.14  
6.97  
6.97  
6.96  
6.96  
6.95  
6.95  
6.94  
6.94  
6.94  
6.93  
6.93  
6.88  
6.88  
6.84  
6.84  
6.83  
6.83  
6.82  
6.82  
6.81  
6.81  
6.80  
6.80  
6.35  
4.50  
4.49  
4.48  
4.46

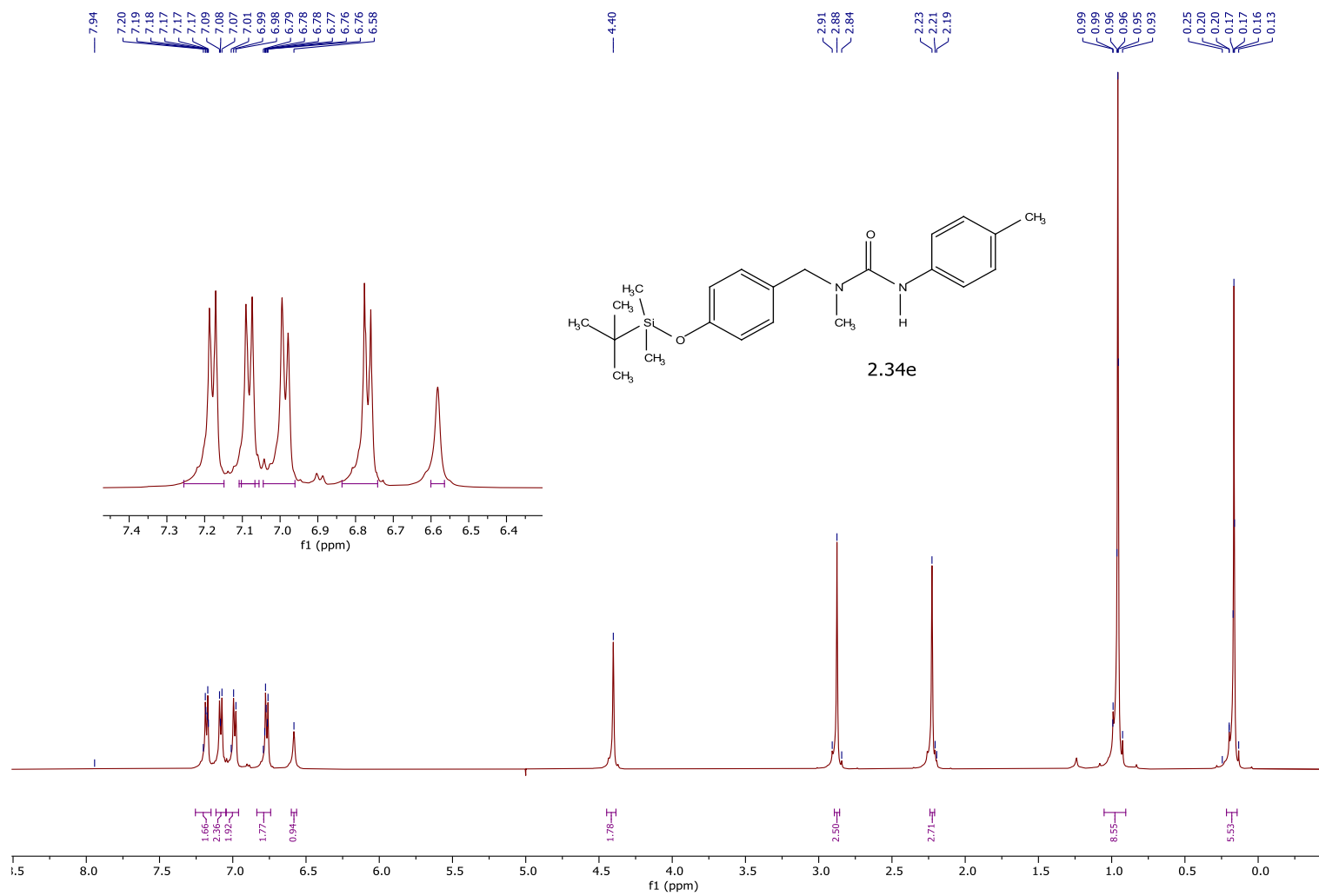
3.02  
3.01  
3.01  
2.99  
2.98  
2.98  
2.96  
1.00  
0.99  
0.98  
0.98  
0.96  
0.97  
0.96  
0.96  
0.95  
0.95  
0.94  
0.94  
0.23  
0.23  
0.23  
0.23  
0.22  
0.22  
0.21  
0.20  
0.20  
0.19  
0.19  
0.19  
0.18  
0.18  
0.18  
0.18  
0.17  
0.17  
0.16  
0.16  
0.16  
0.15



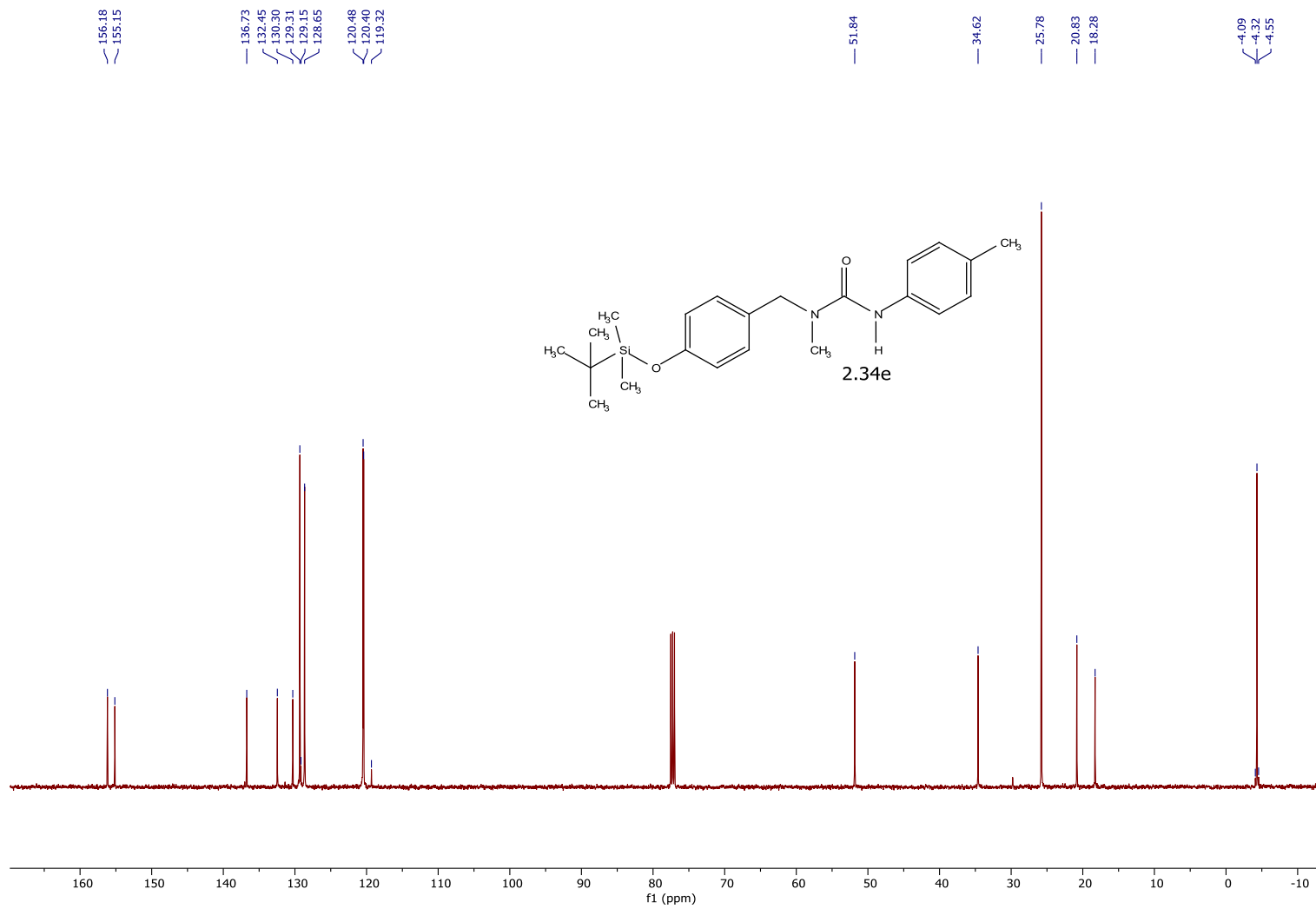


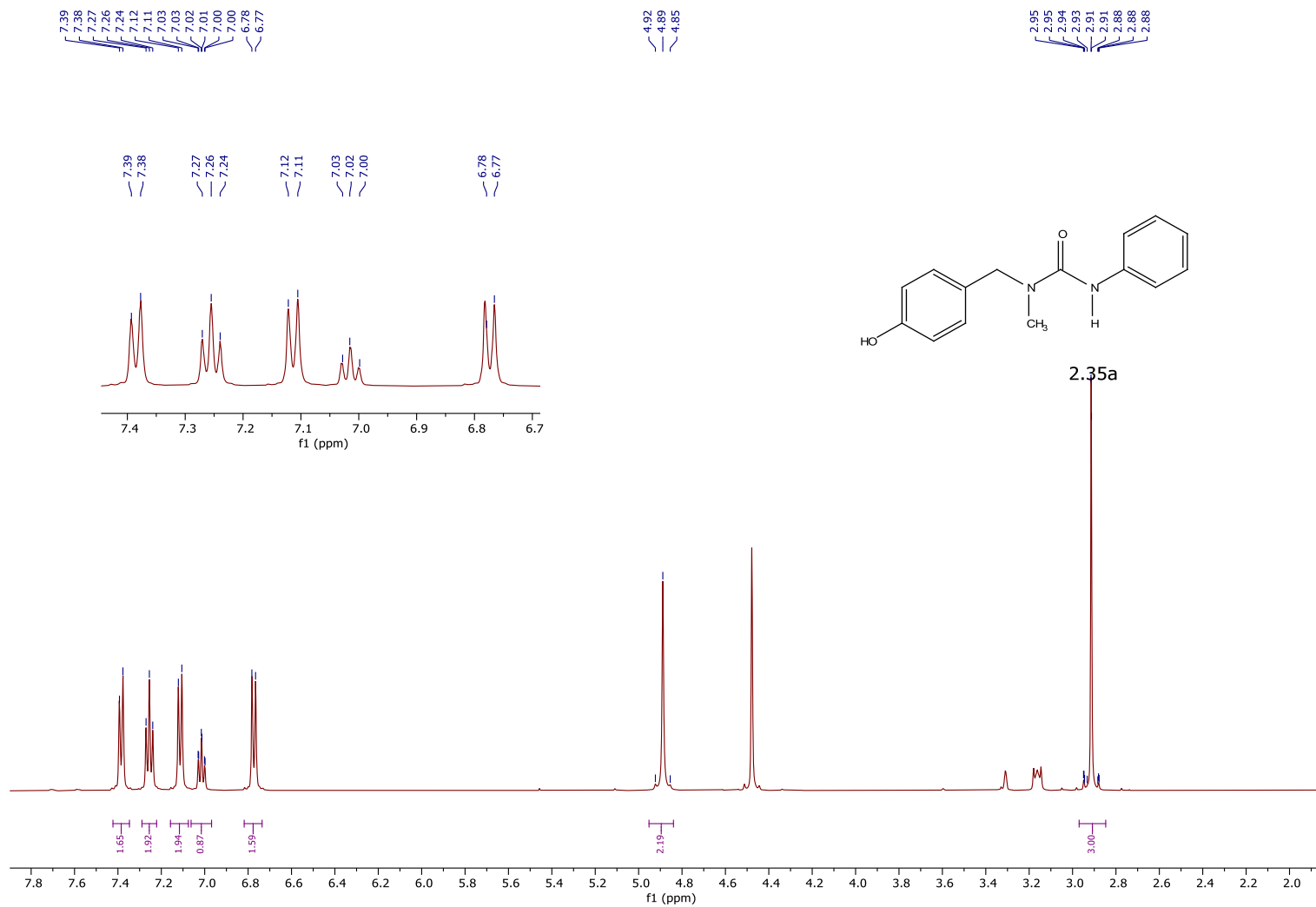


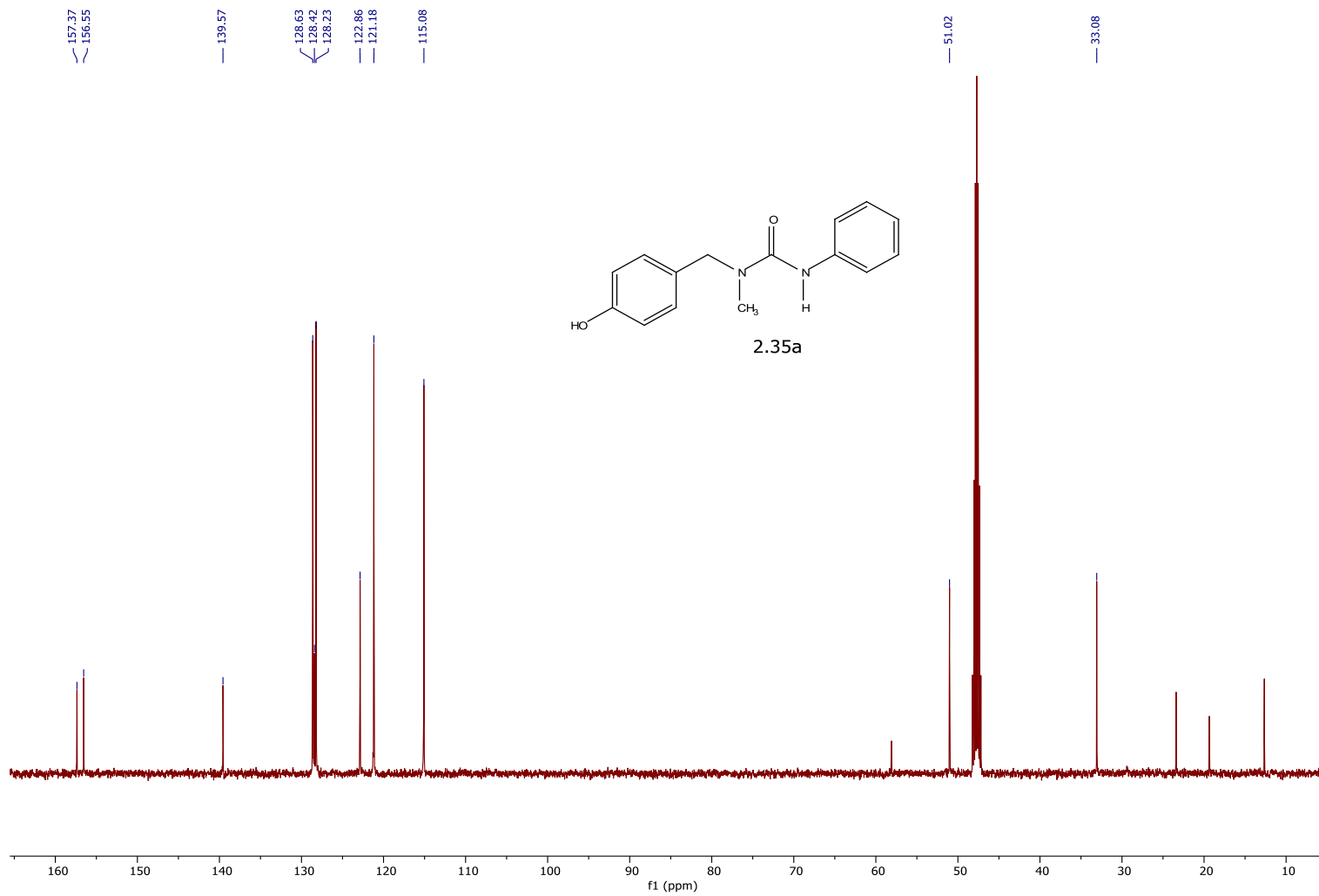


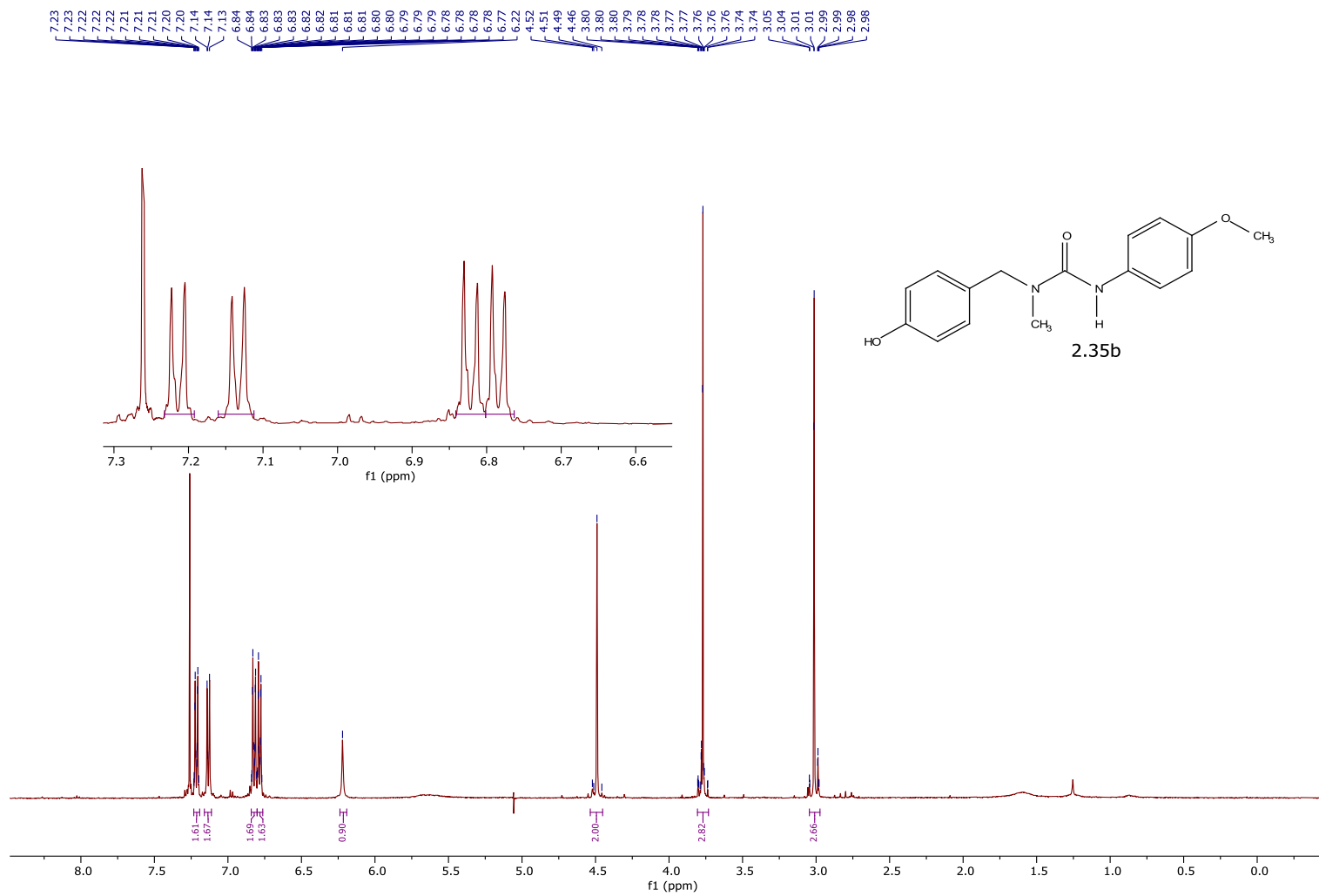


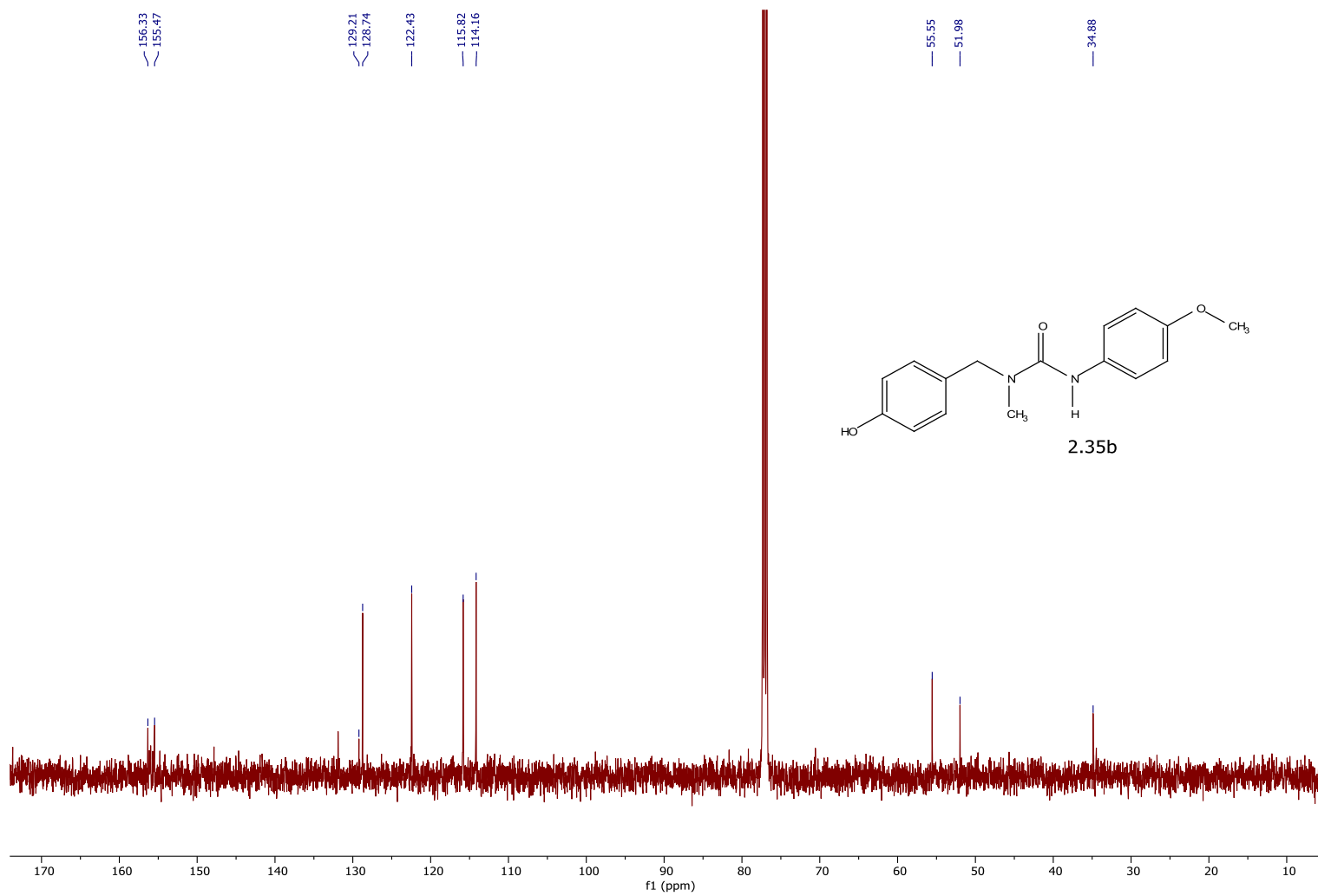


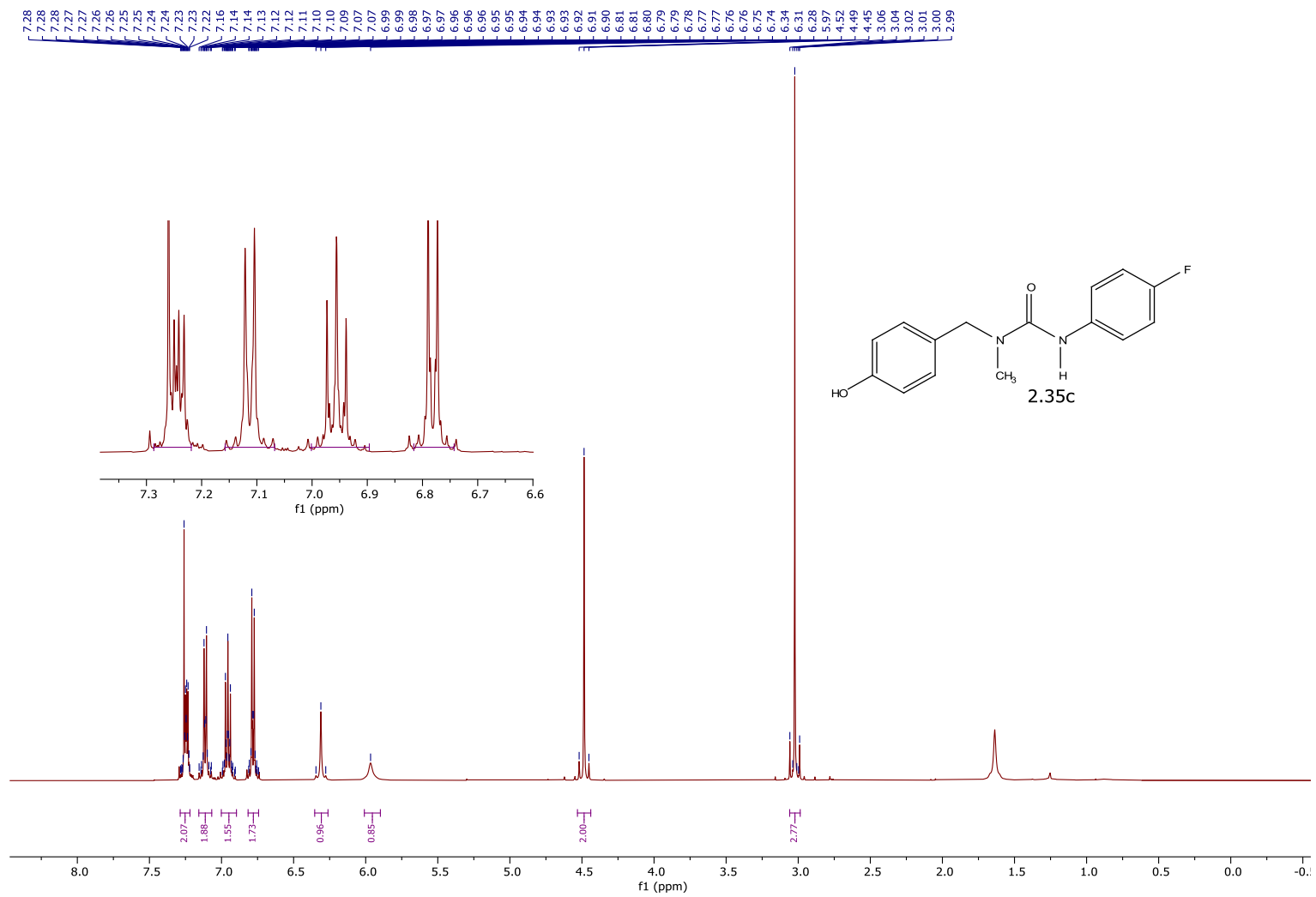


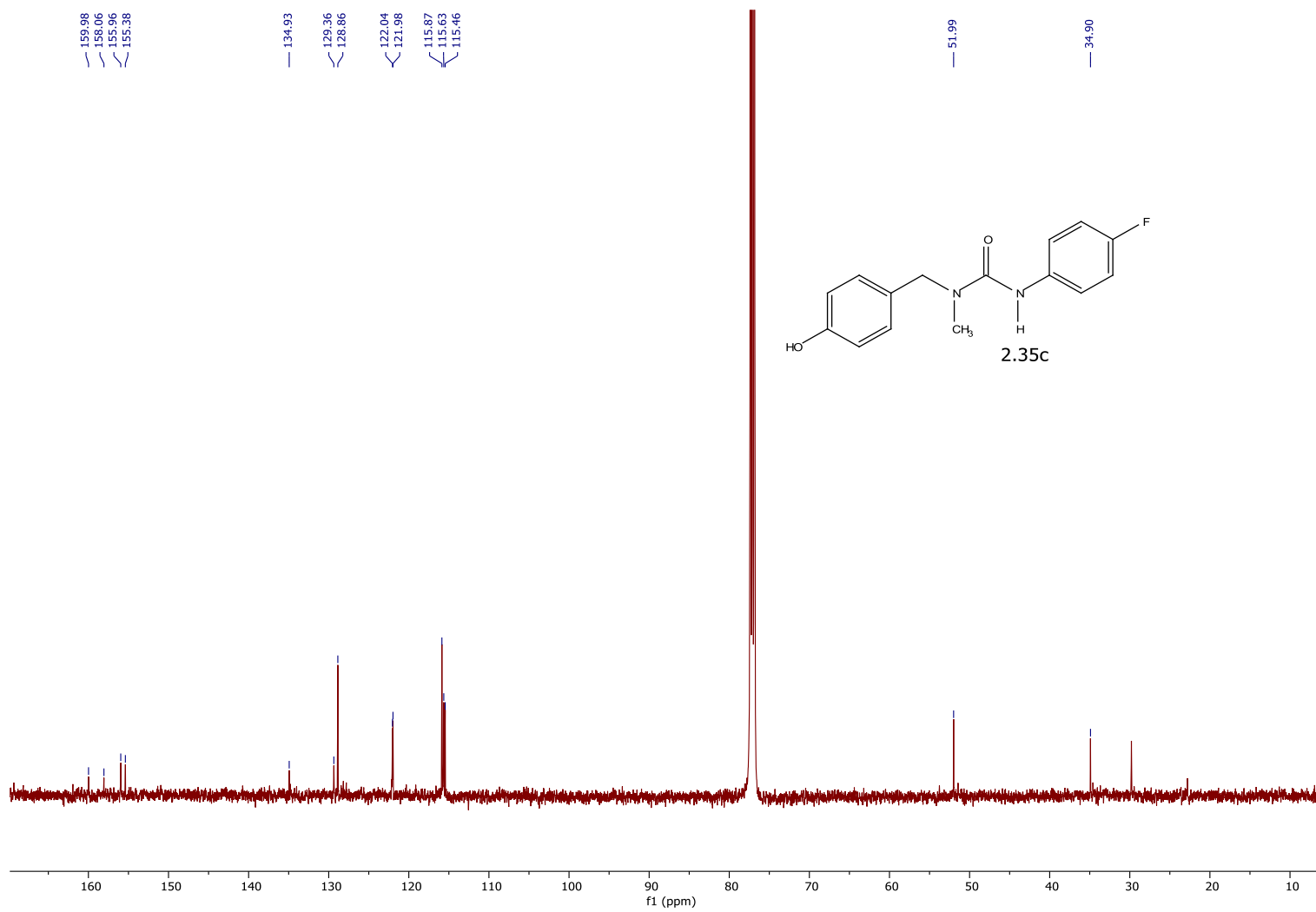


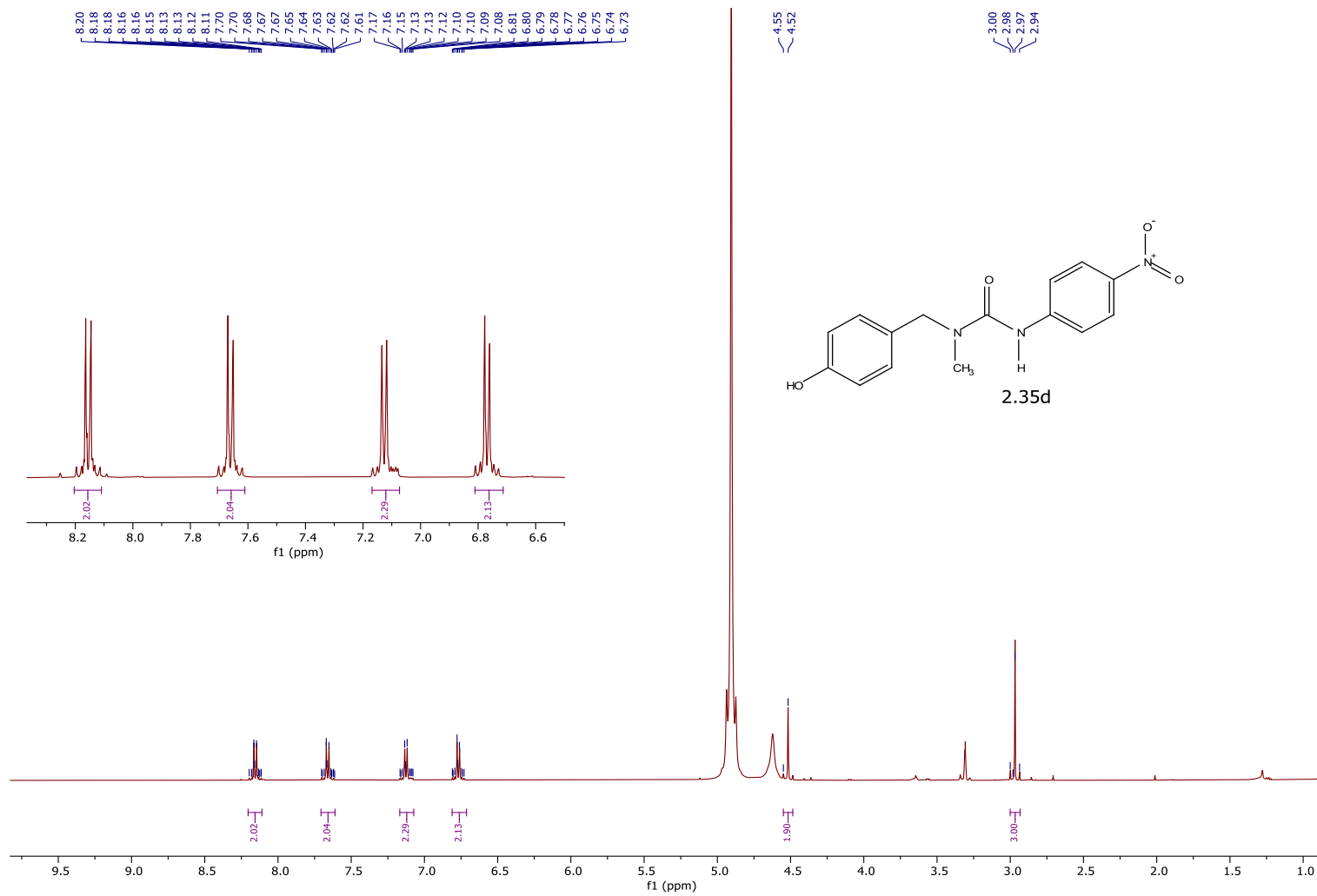




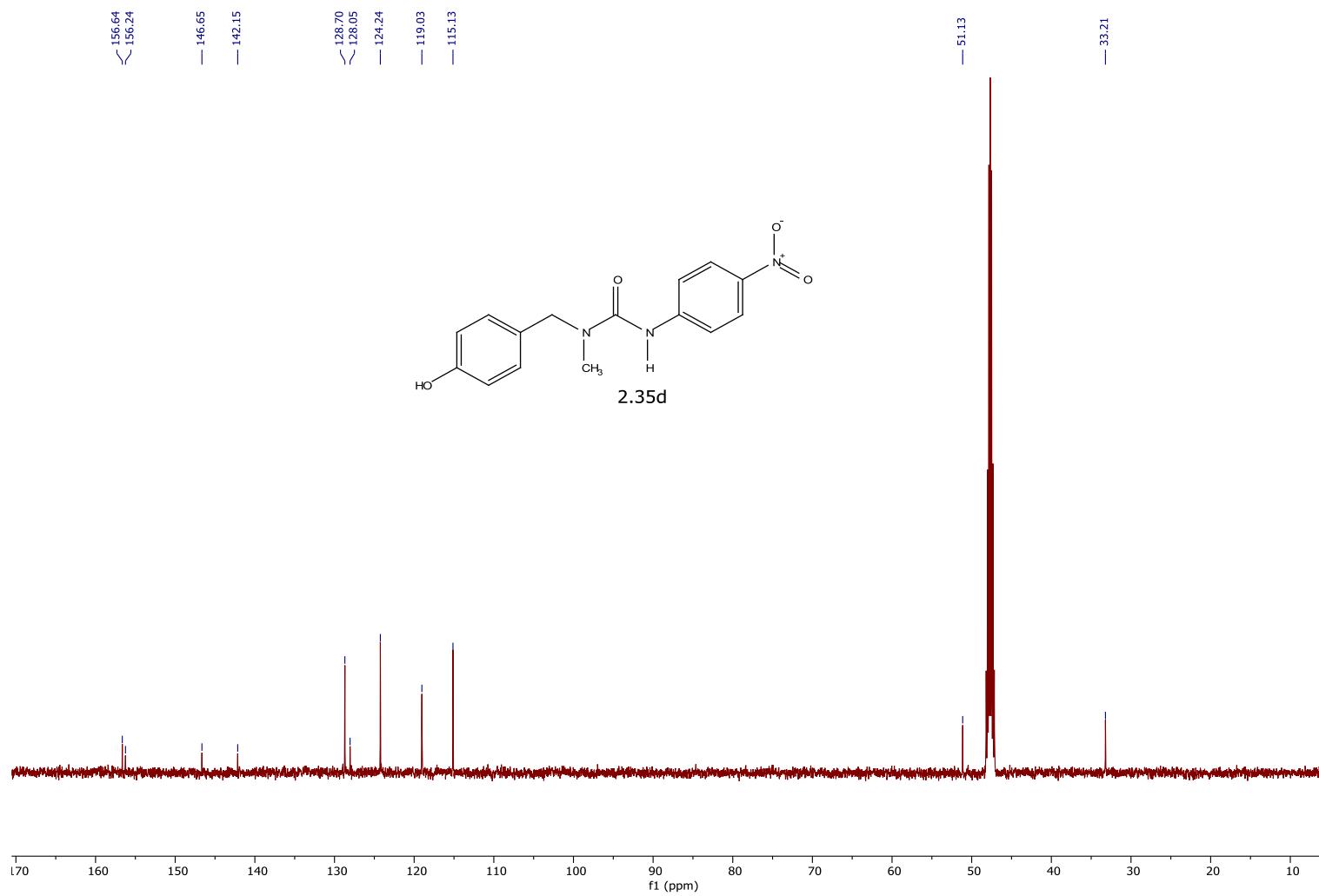








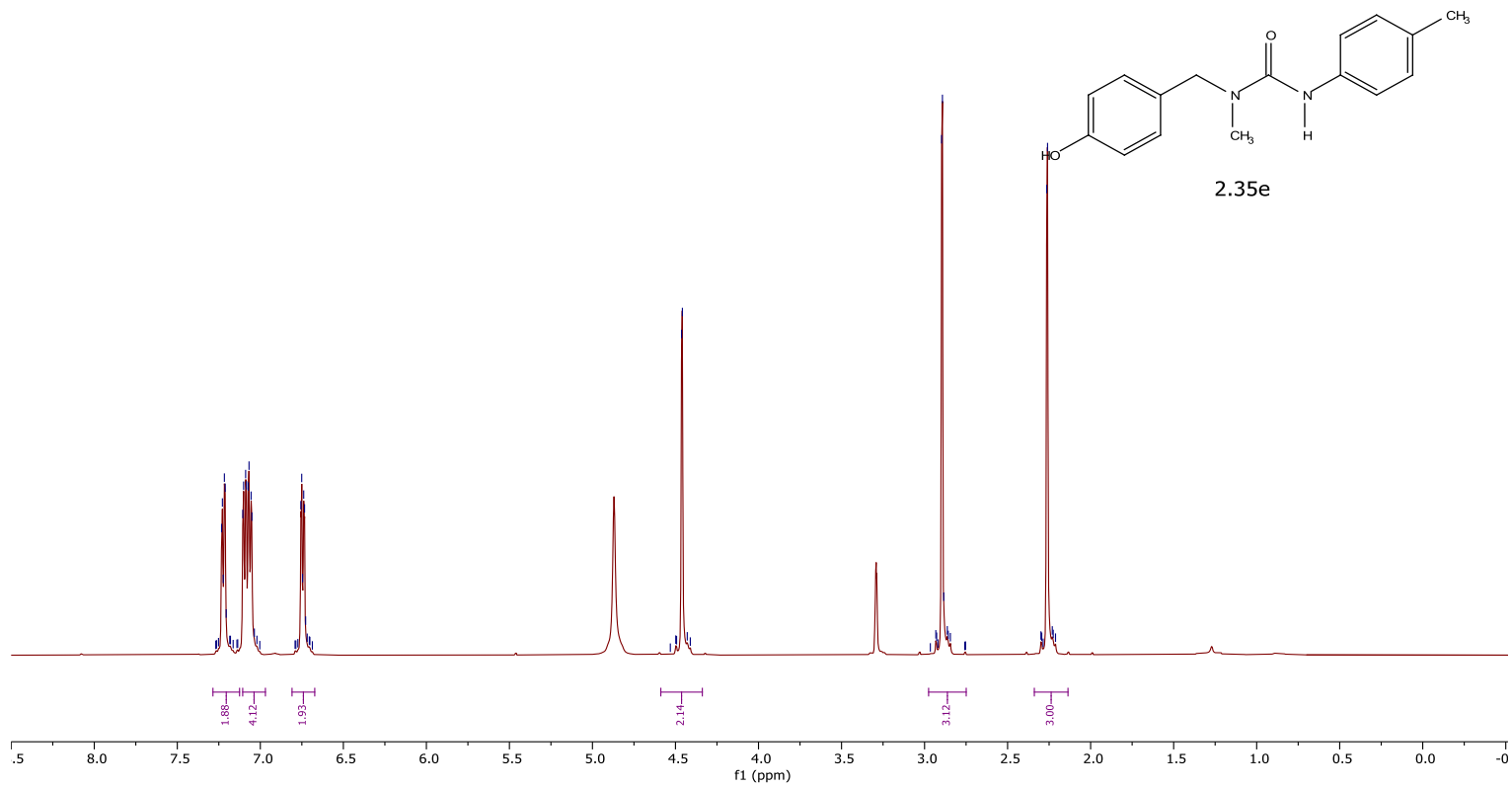


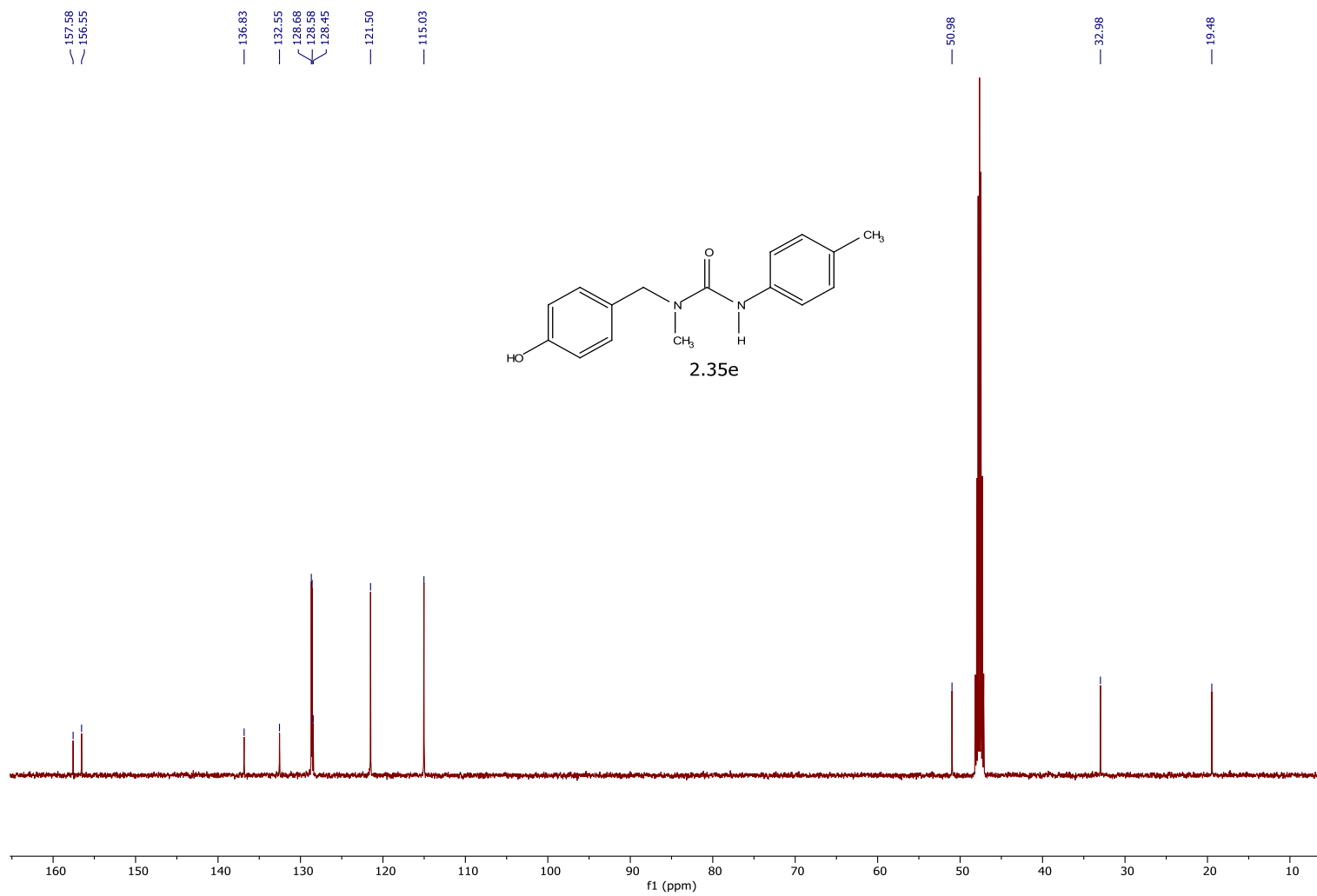


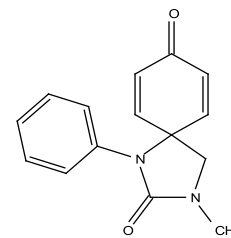
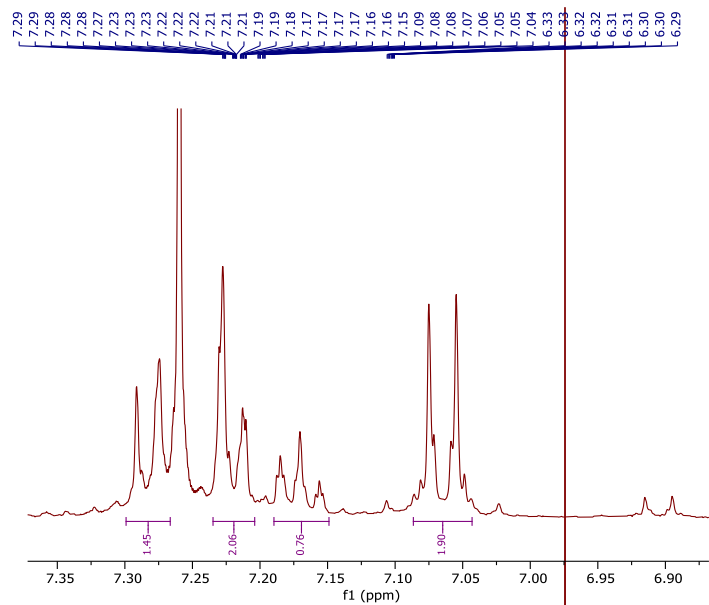
7.23  
7.23  
7.22  
7.22  
7.21  
7.21  
7.11  
7.10  
7.09  
7.07  
7.06  
7.05  
7.04  
6.99  
6.79  
6.77  
6.76  
6.75  
6.74  
6.73  
6.72  
6.71  
6.70  
6.69

4.53  
4.50  
4.49  
4.46  
4.43  
4.41

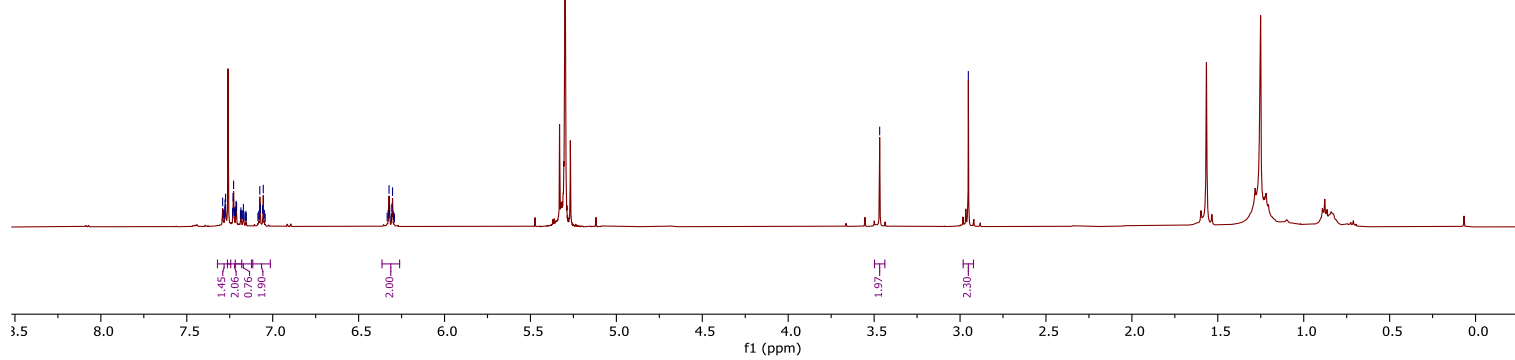
2.97  
2.93  
2.93  
2.92  
2.90  
2.89  
2.88  
2.86  
2.84  
2.76  
2.75  
2.30  
2.29  
2.29  
2.26  
2.26  
2.23  
2.23  
2.21

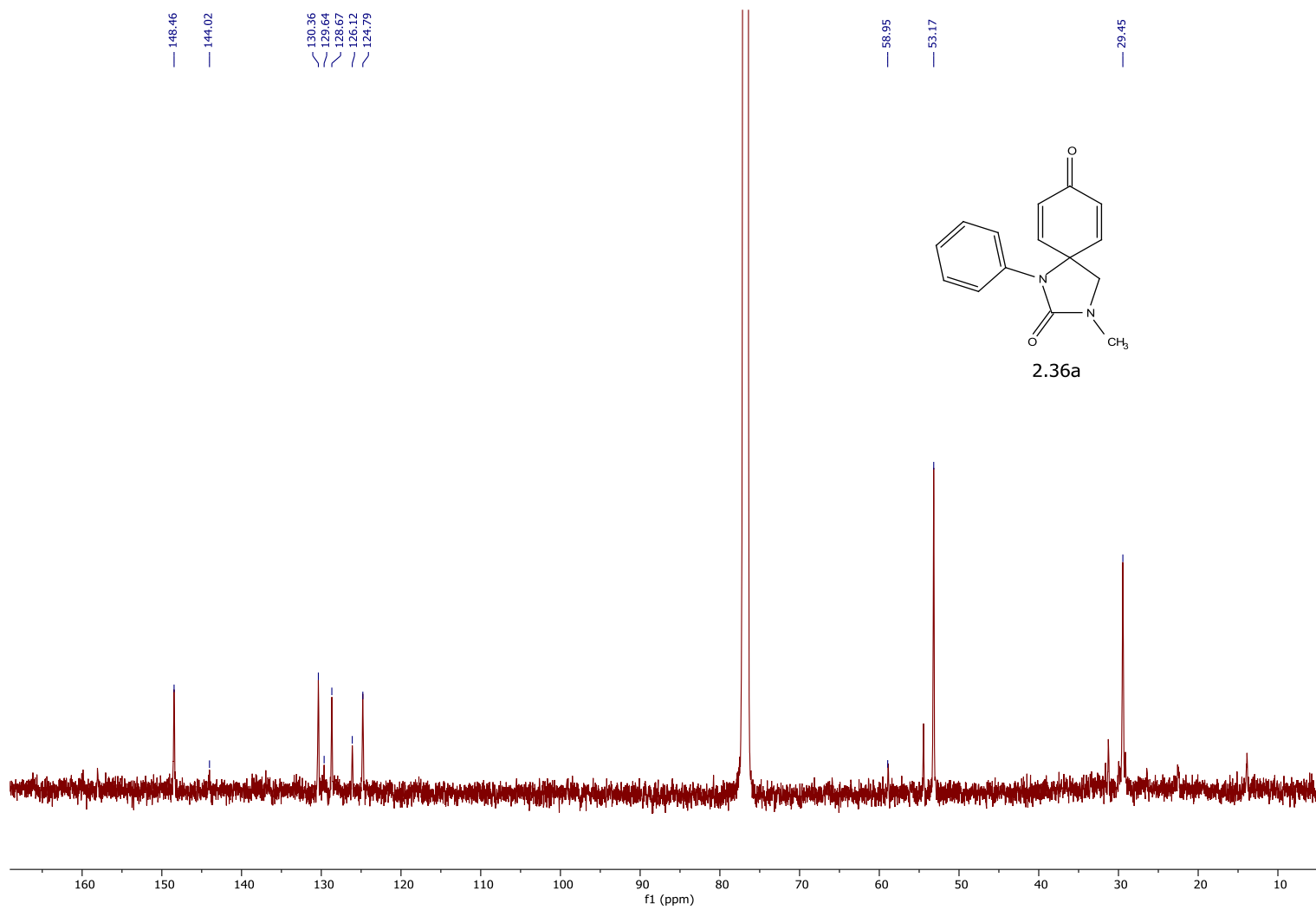


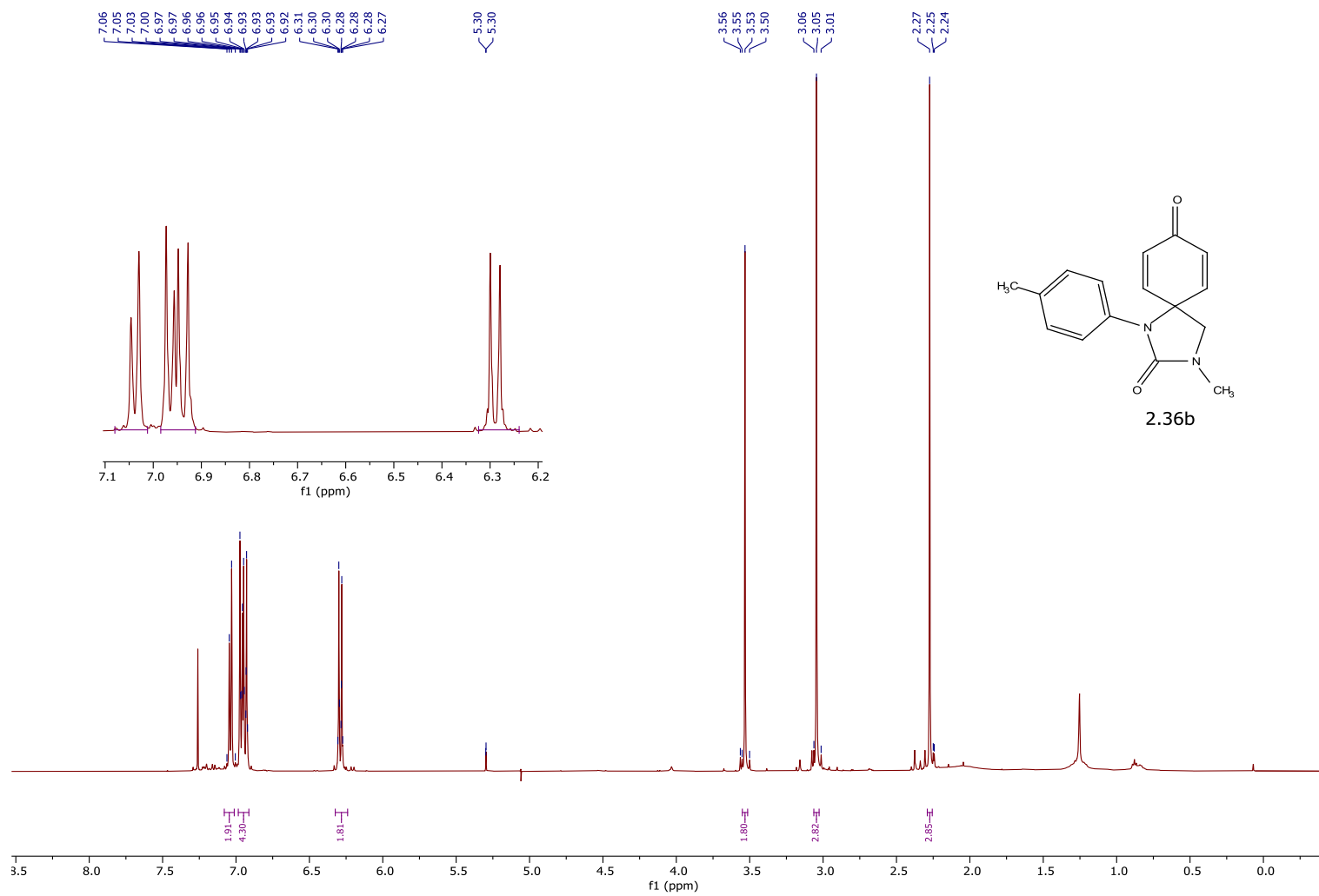


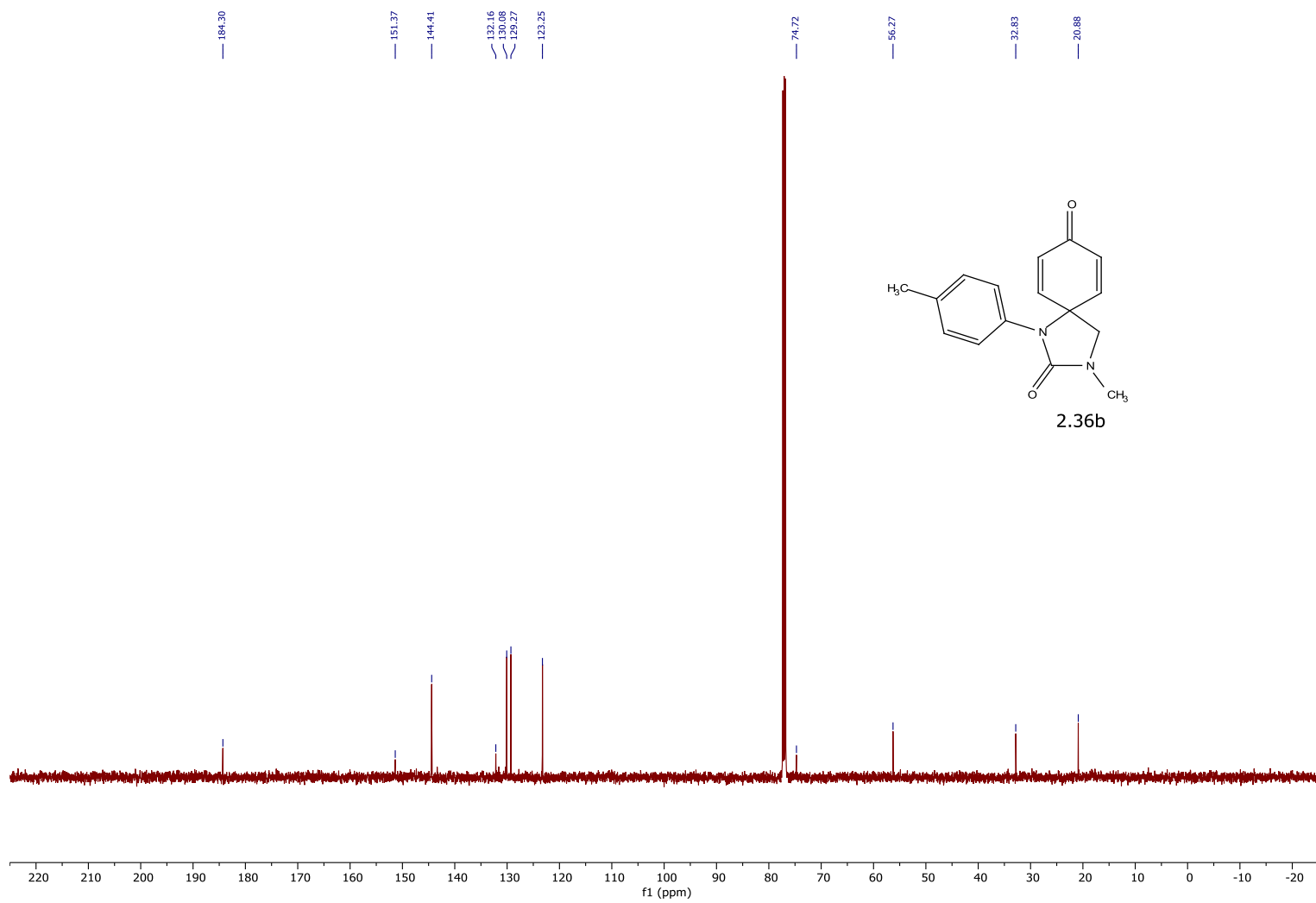


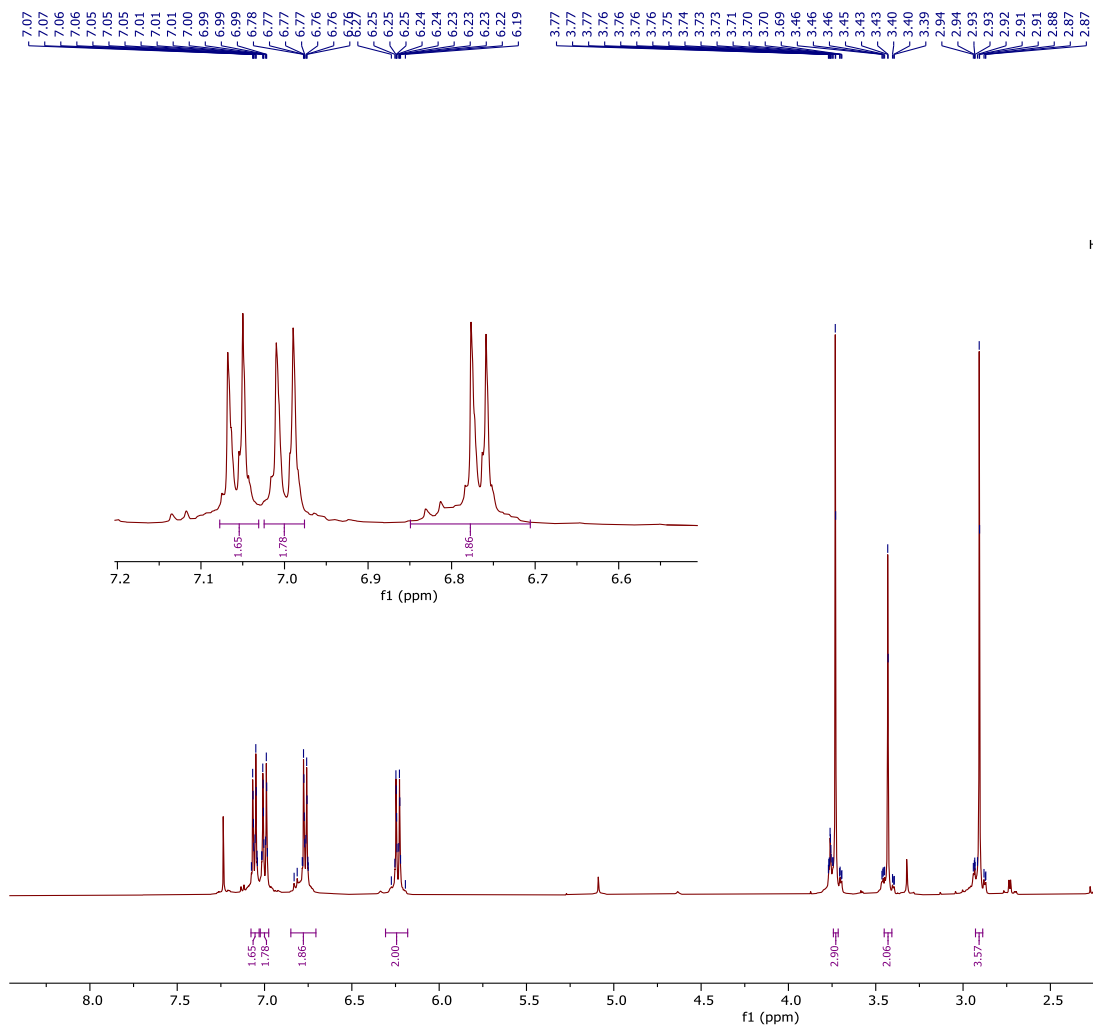
2.36a



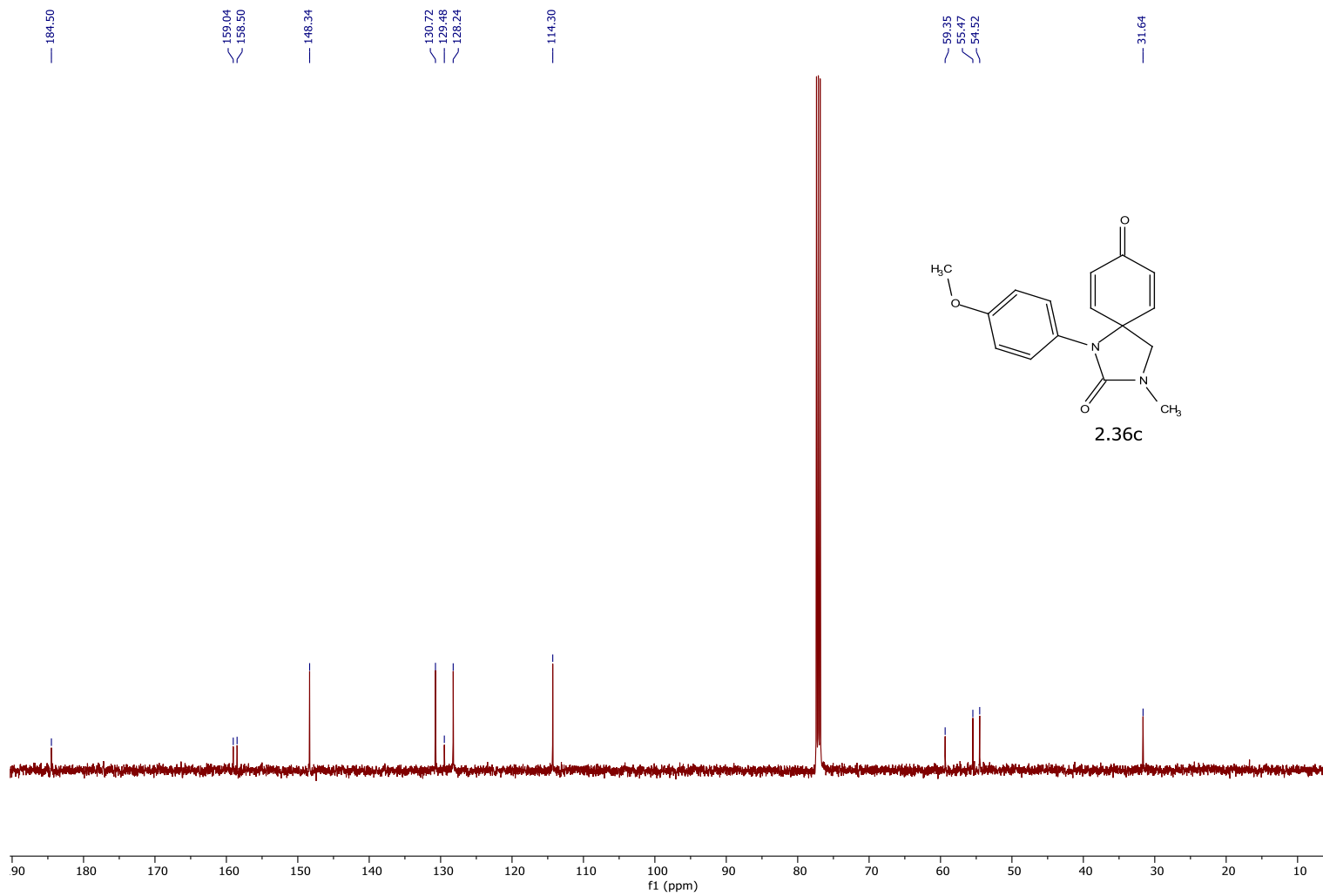


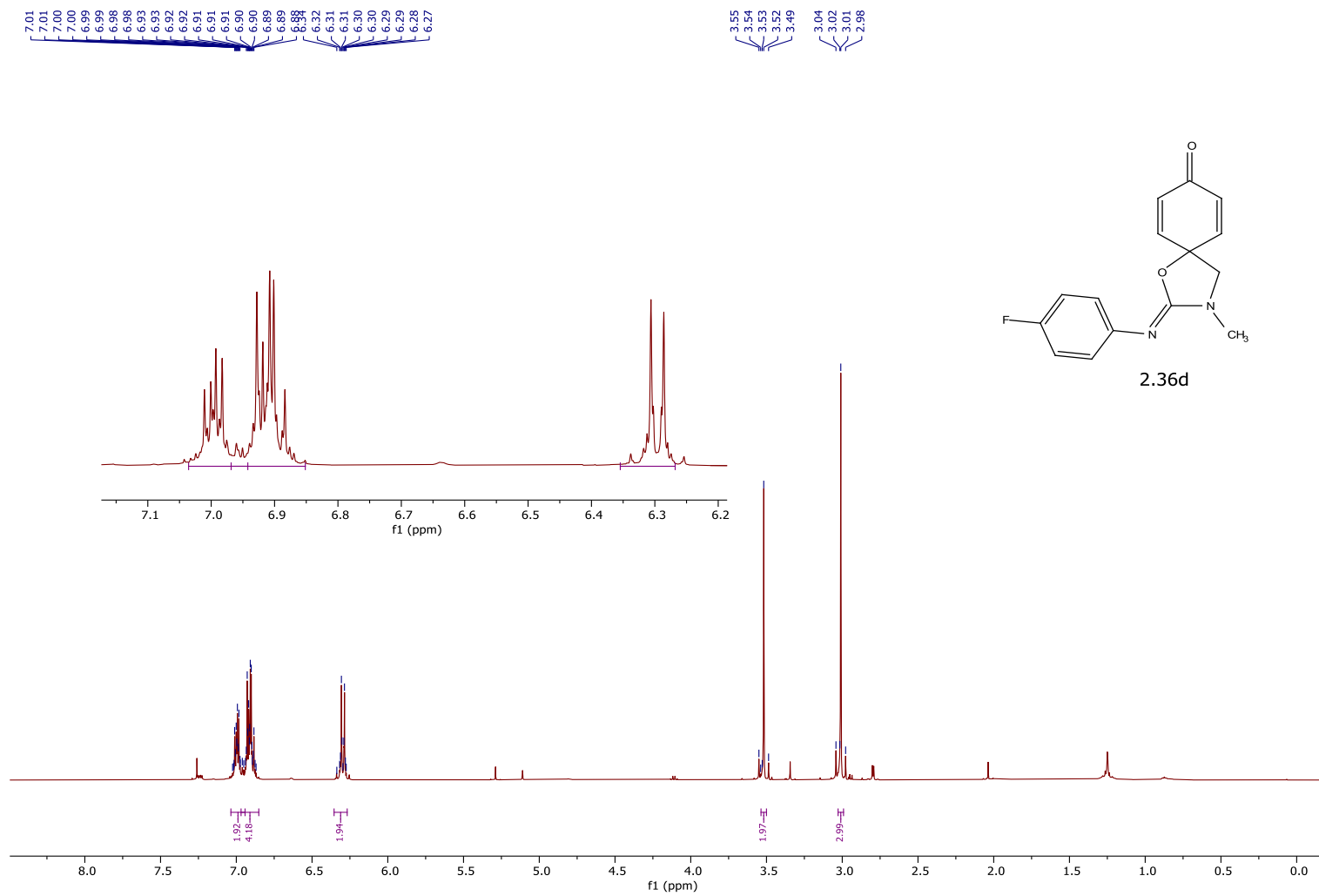


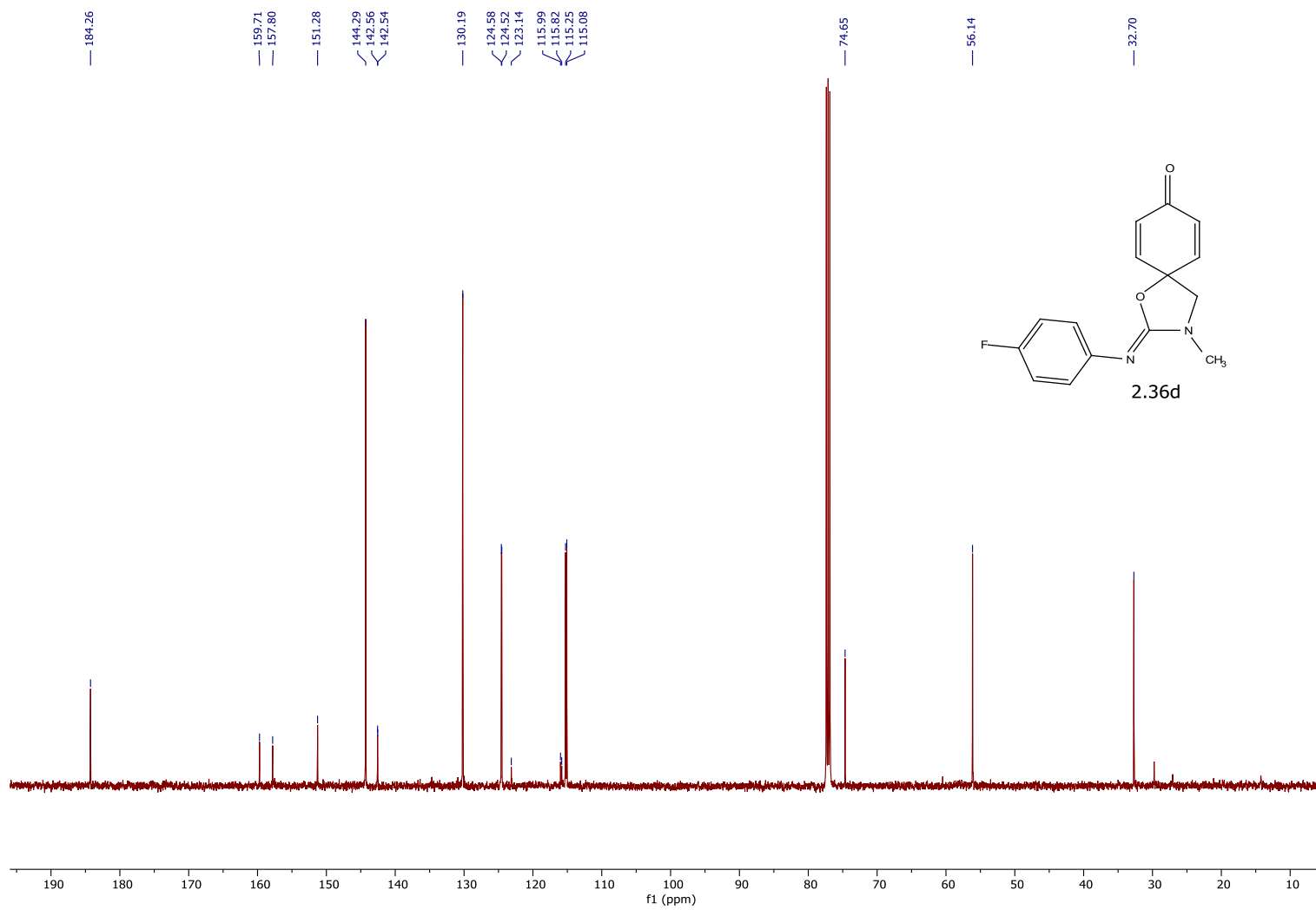






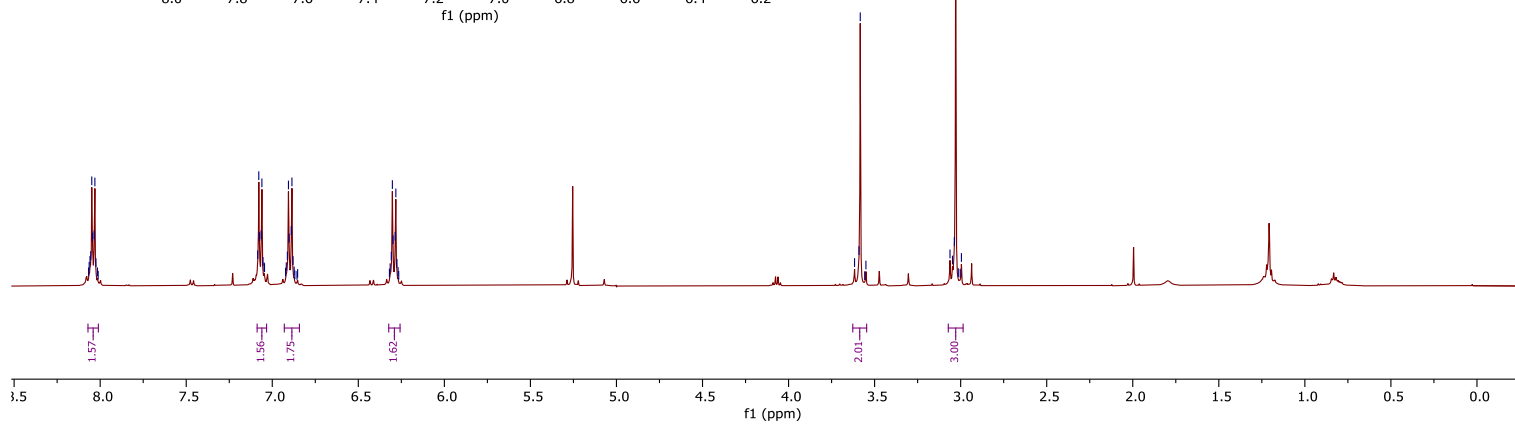
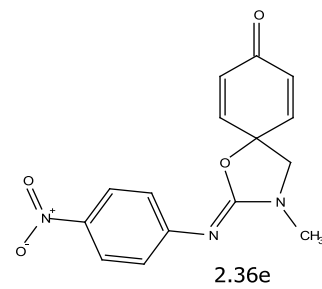
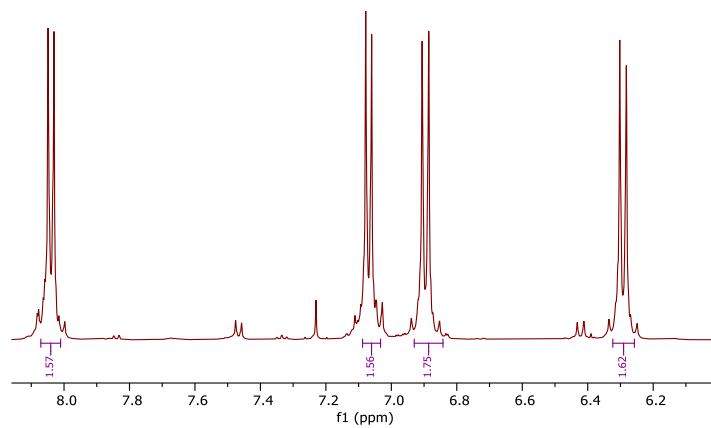


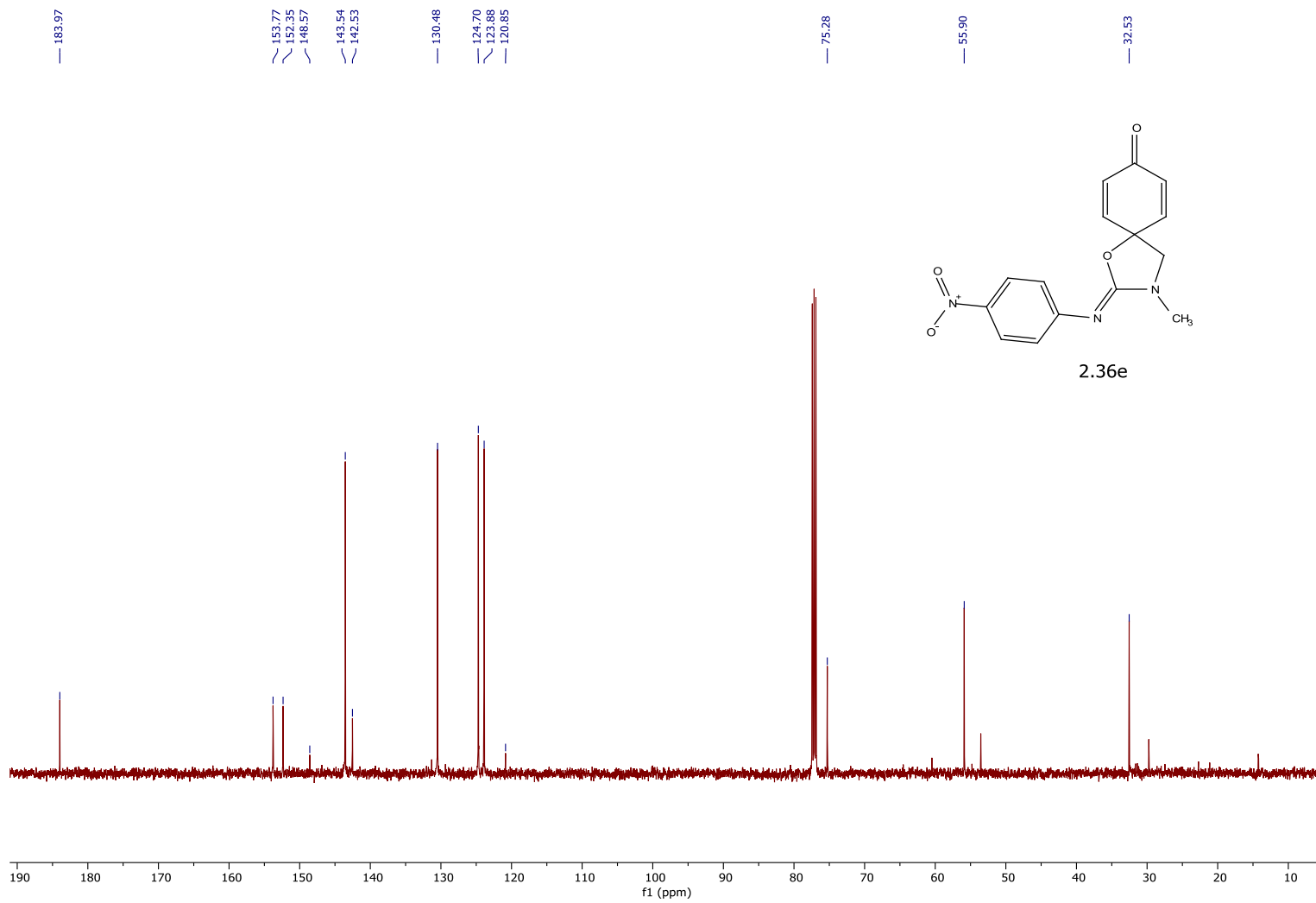


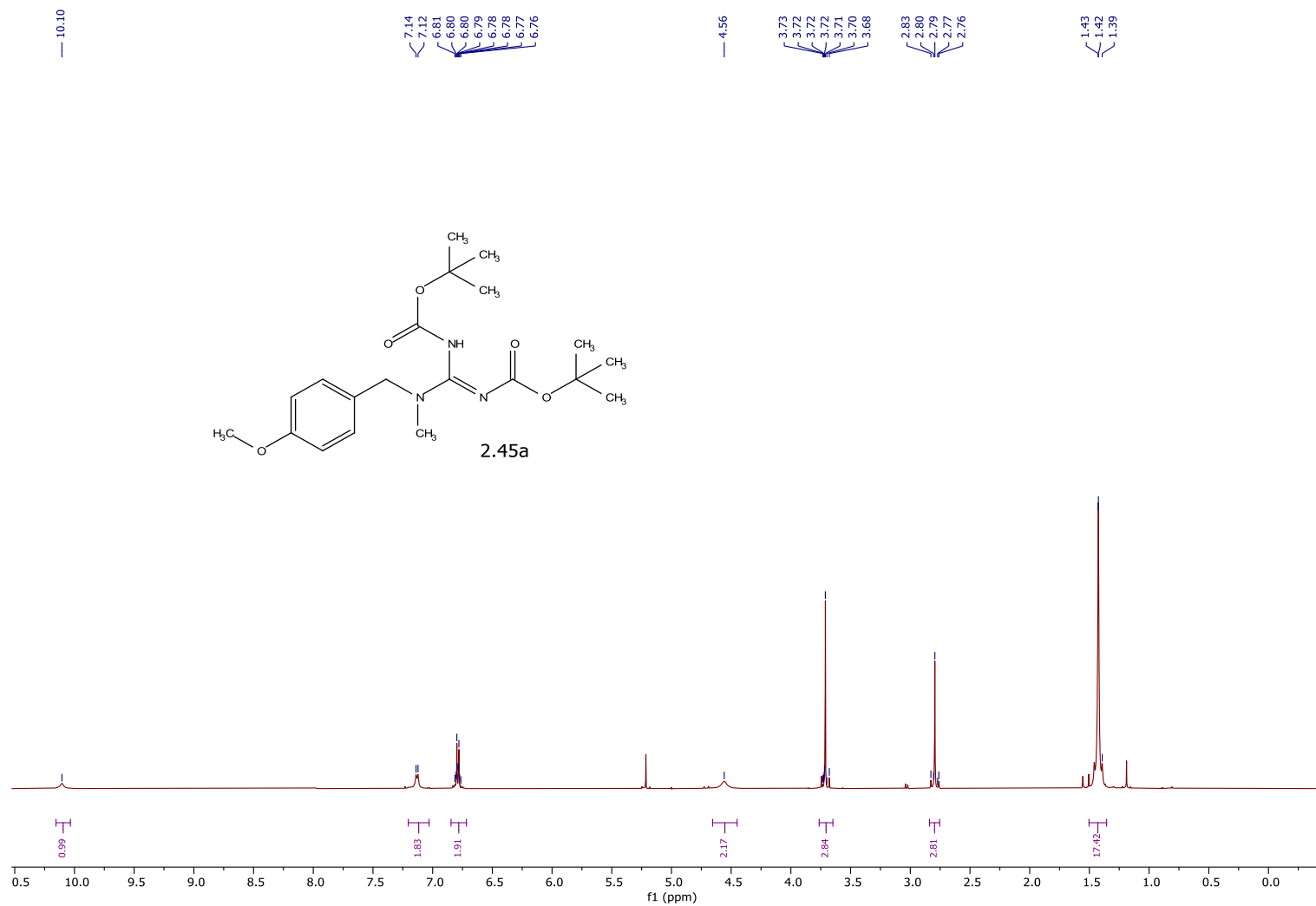


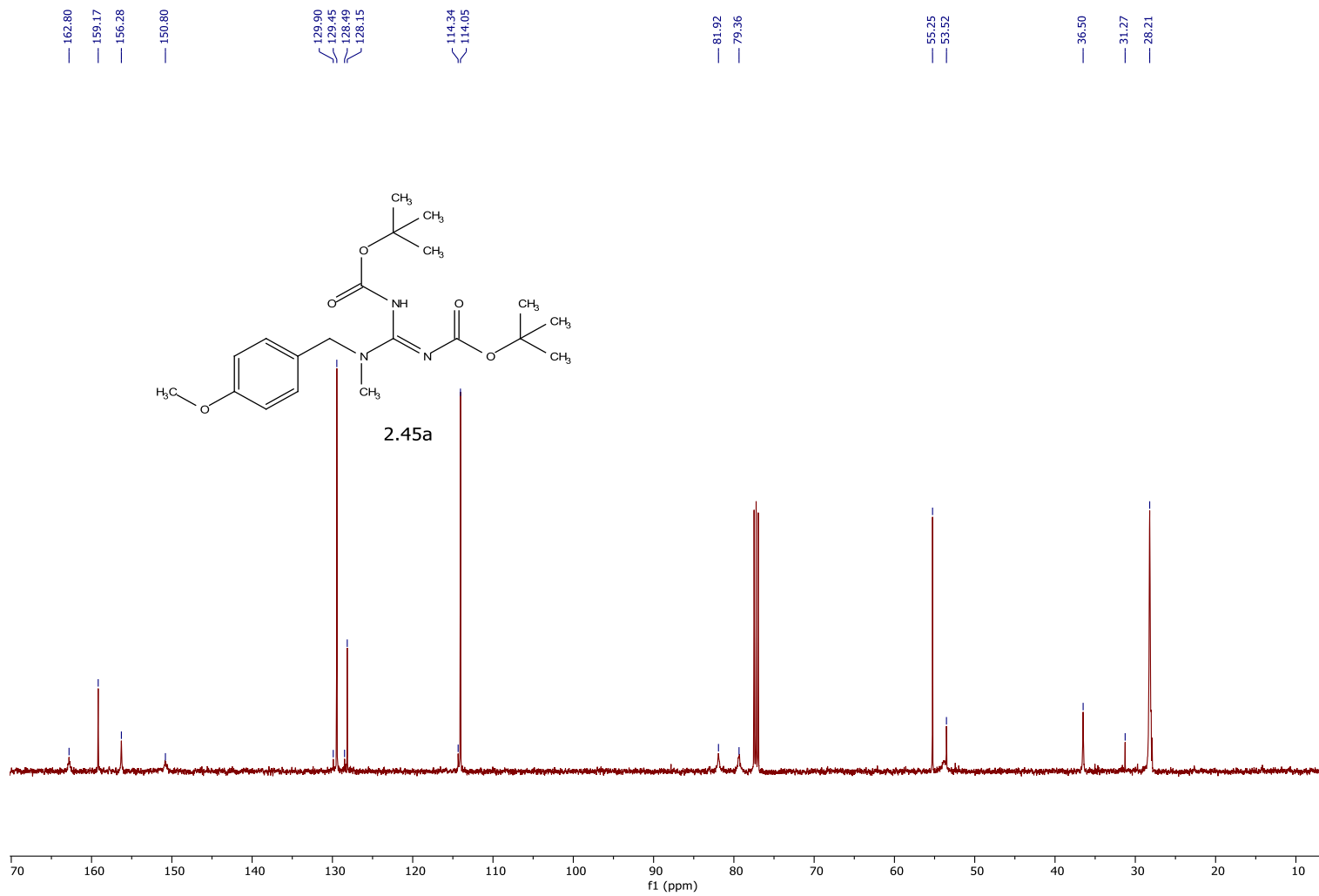
8.07  
8.06  
8.06  
8.05  
8.05  
8.04  
8.03  
8.03  
8.02  
8.01  
7.98  
7.98  
7.07  
7.06  
7.06  
7.05  
7.05  
7.05  
6.92  
6.92  
6.91  
6.91  
6.90  
6.89  
6.89  
6.88  
6.87  
6.86  
6.85  
6.85  
6.32  
6.31  
6.31  
6.30  
6.30  
6.29  
6.28  
6.28  
6.27  
6.27

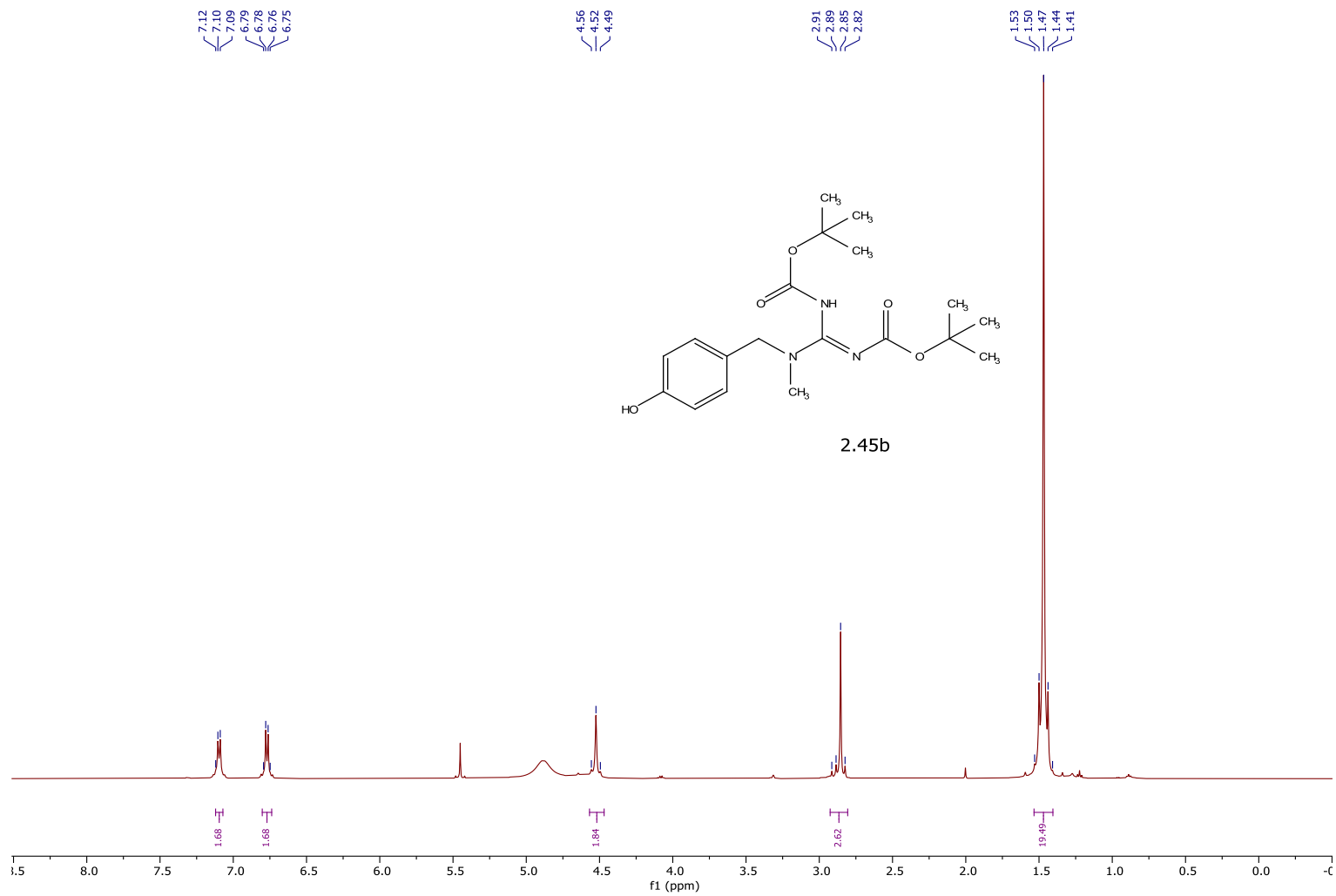
3.62  
3.59  
3.58  
3.56  
3.55  
3.06  
3.05  
3.04  
3.03  
3.01  
3.00  
3.00



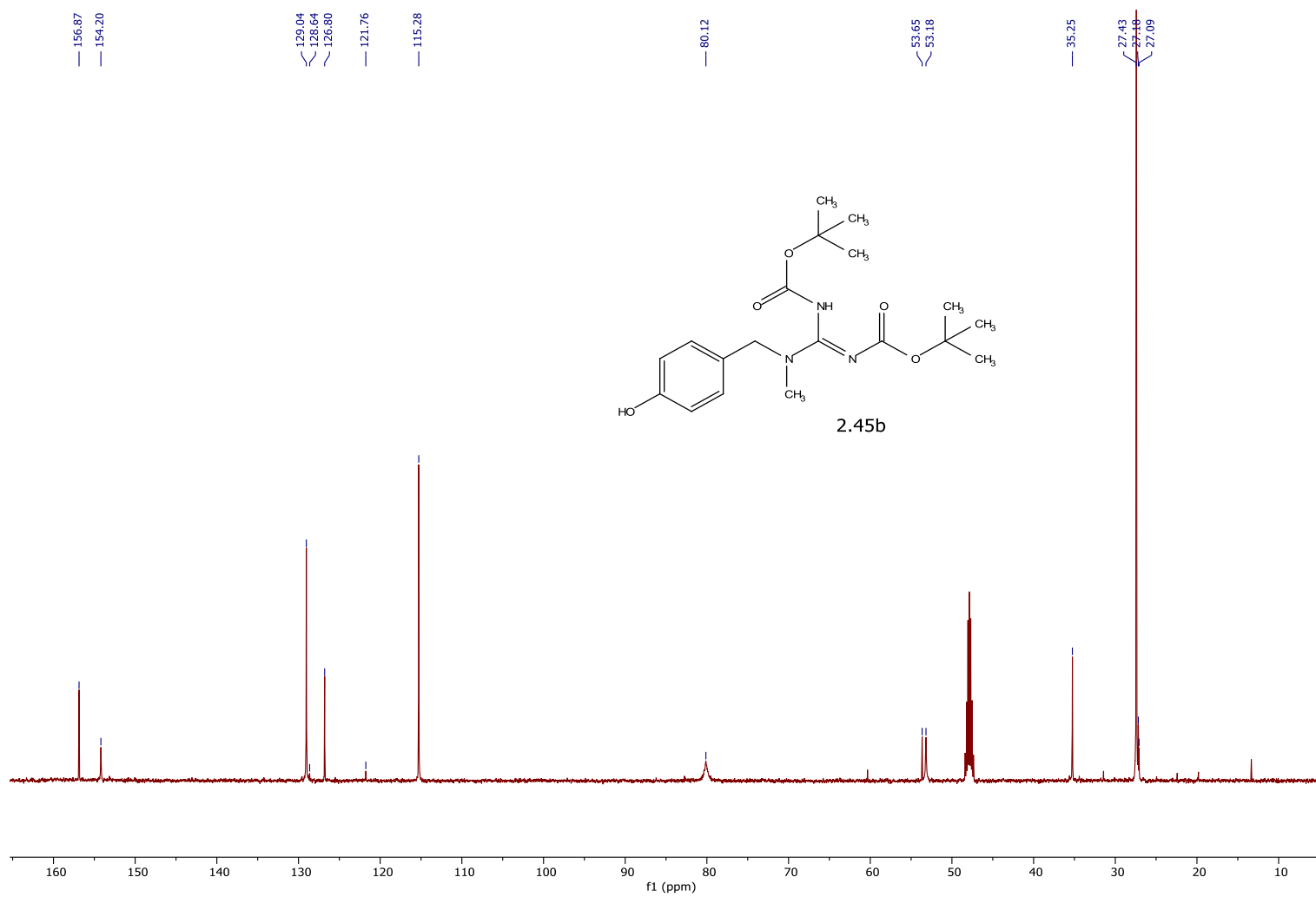


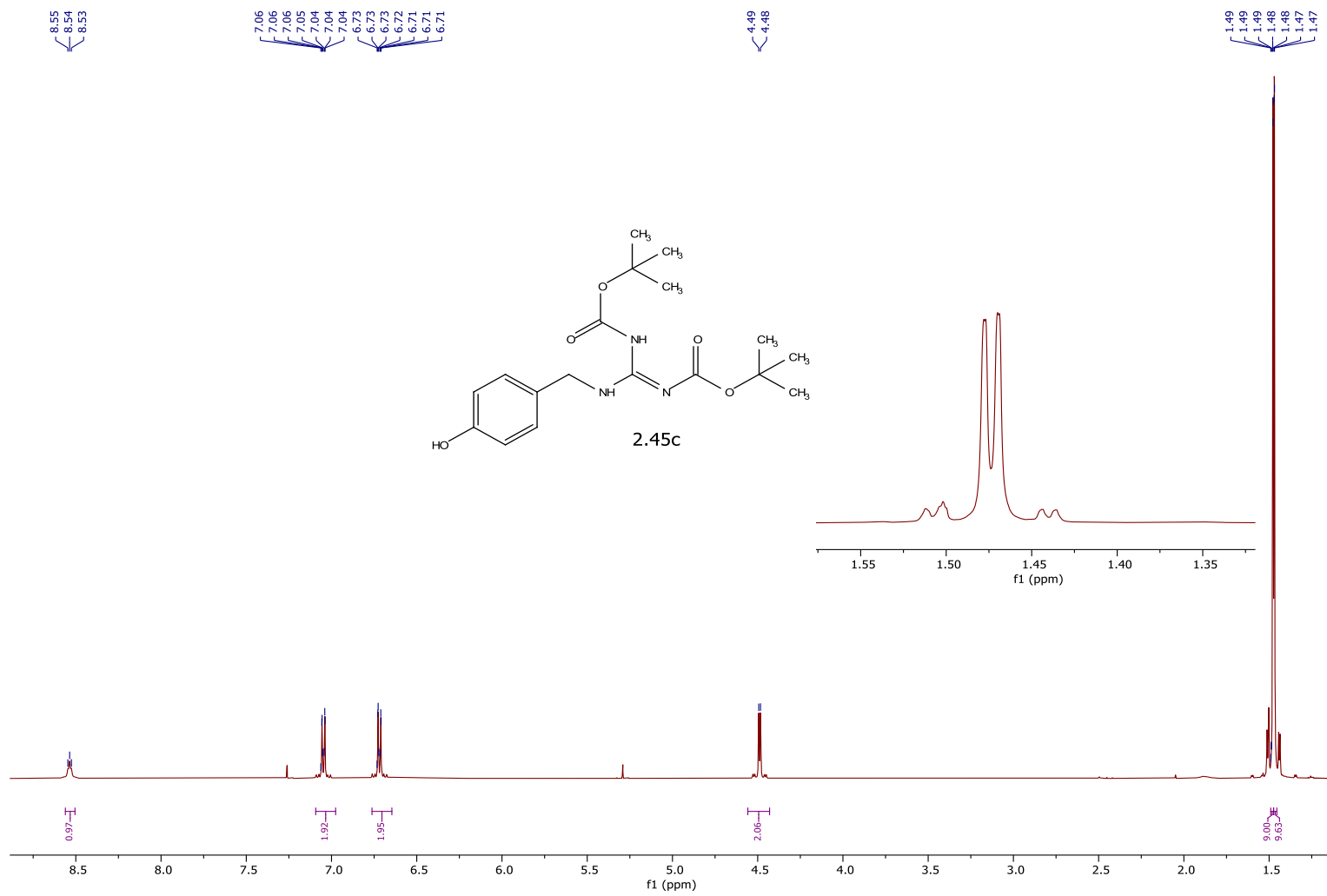


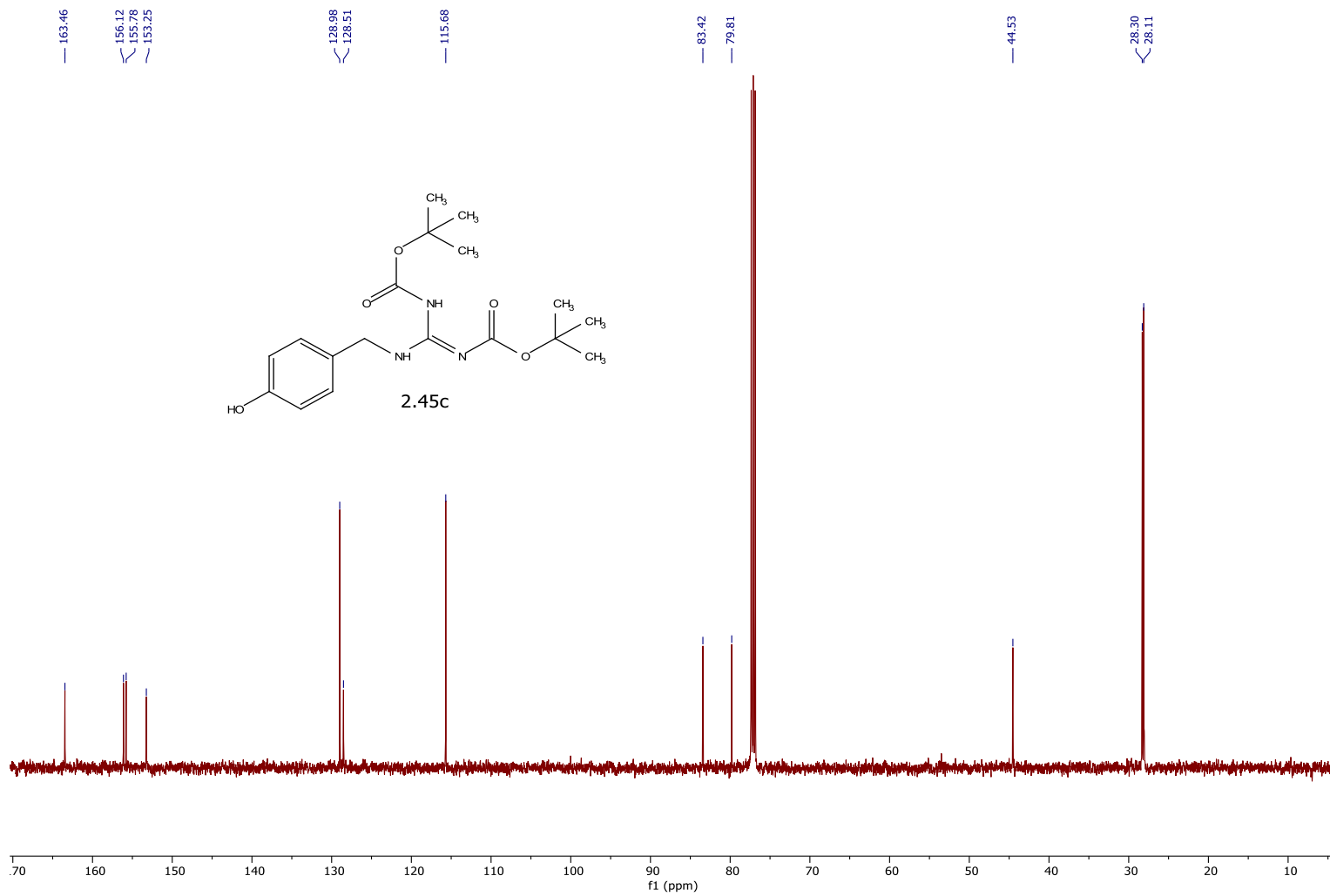


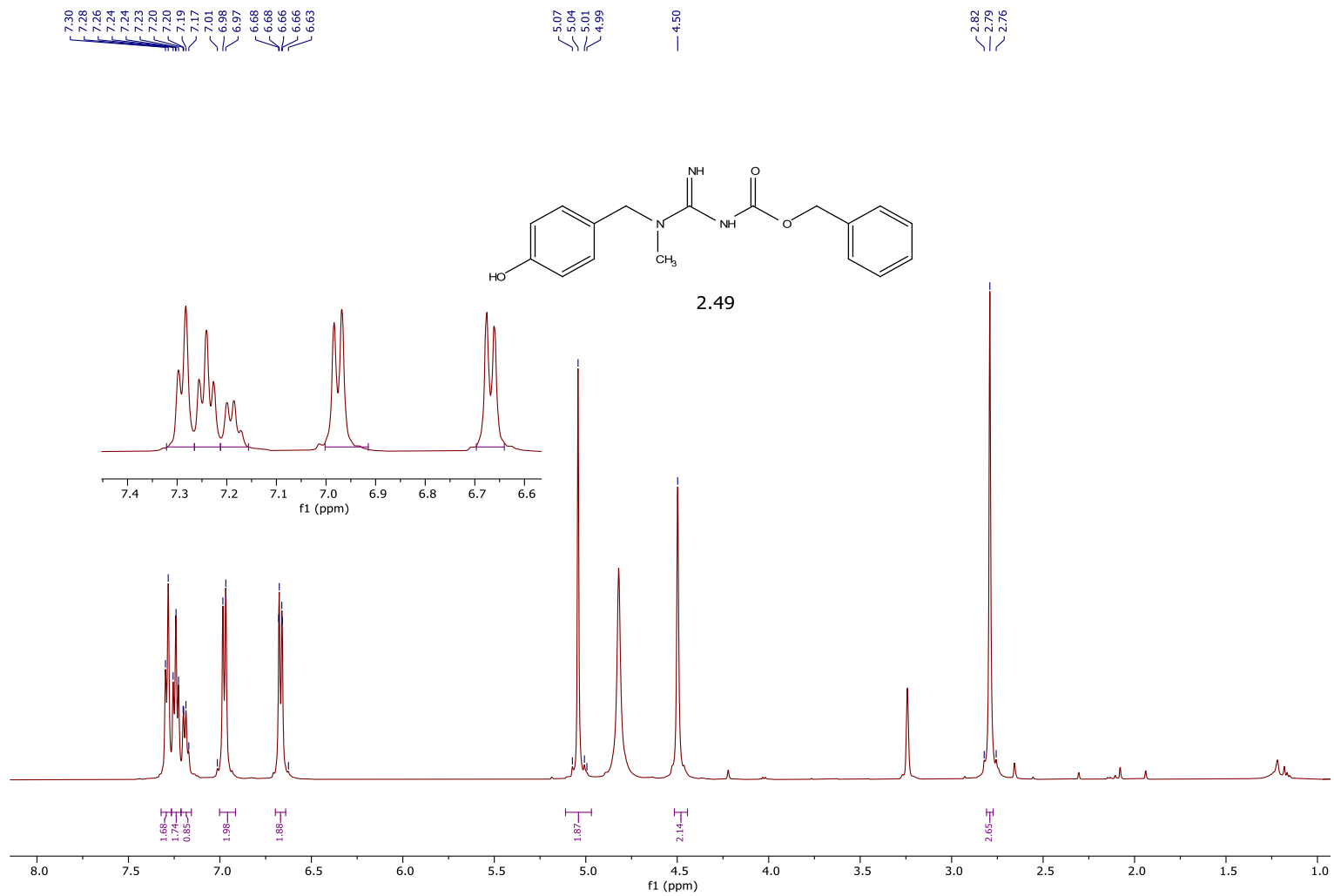


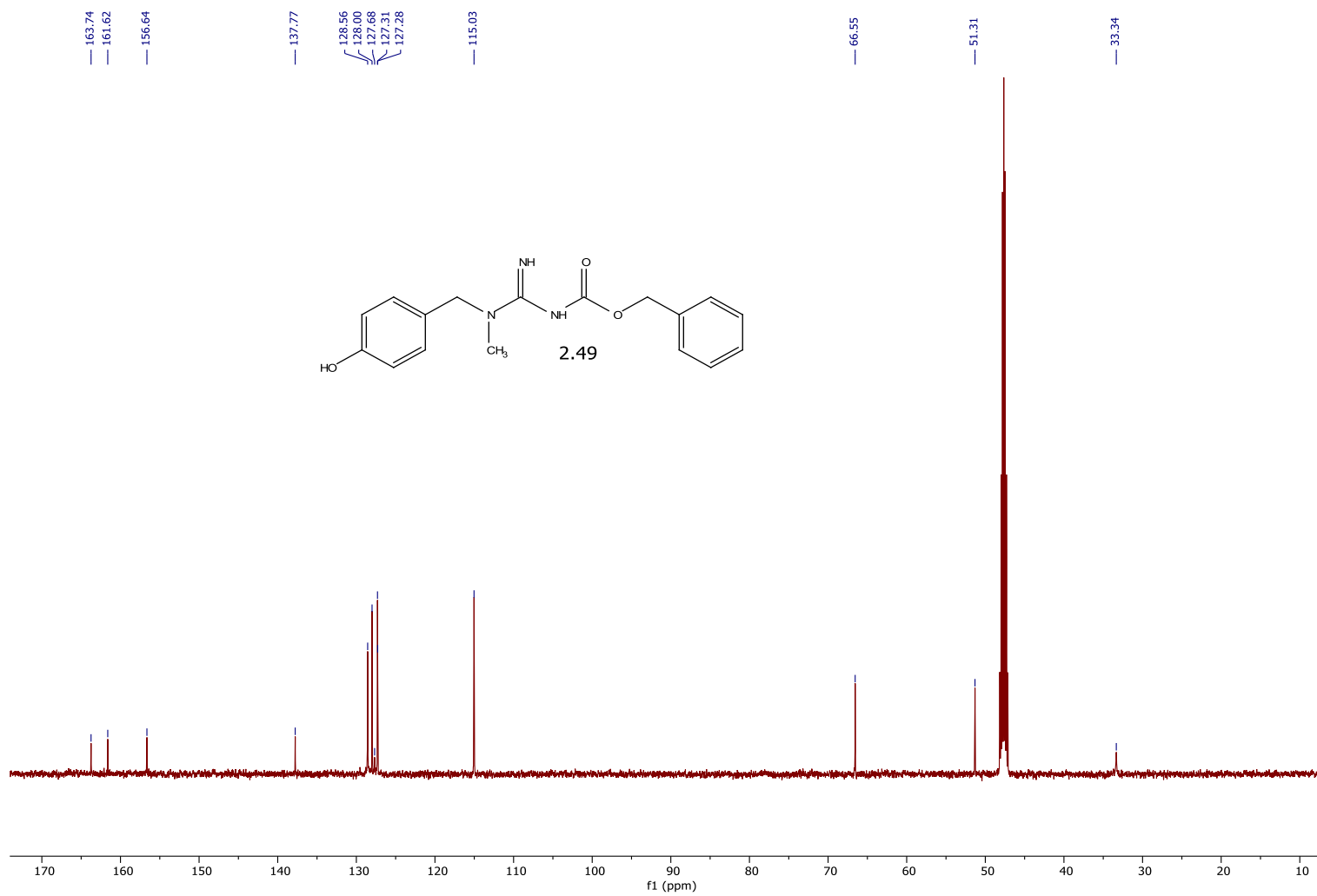




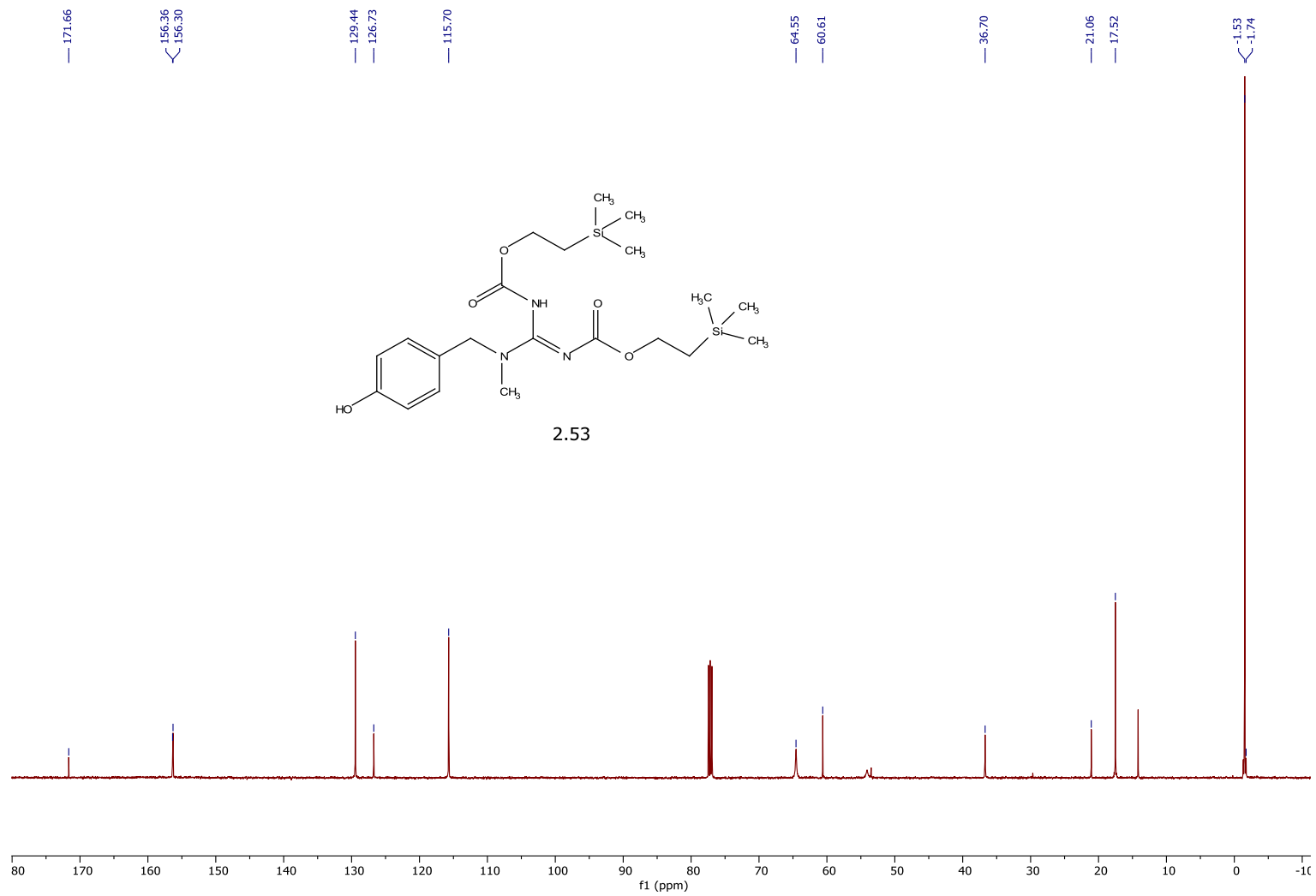










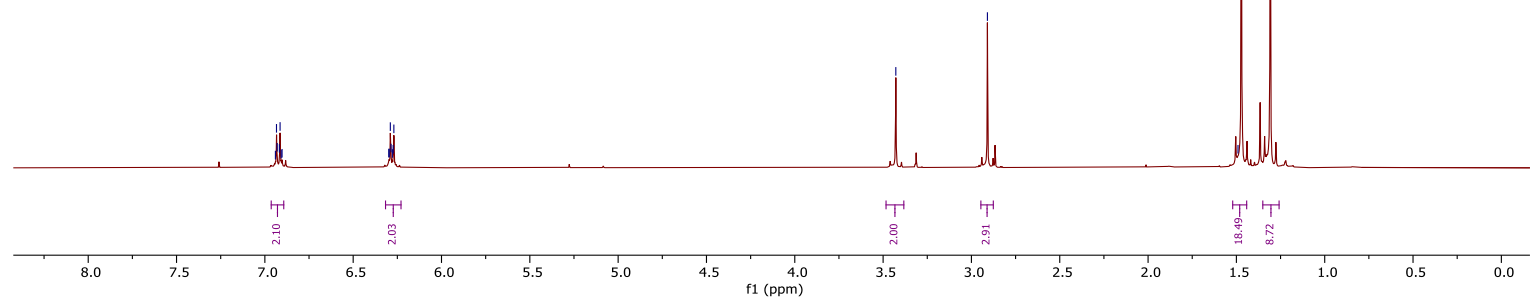
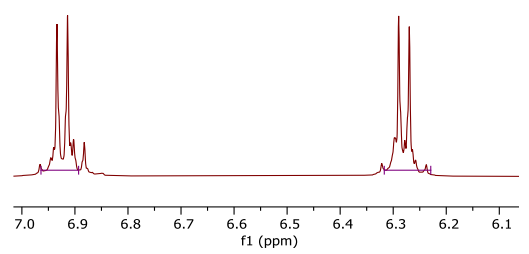
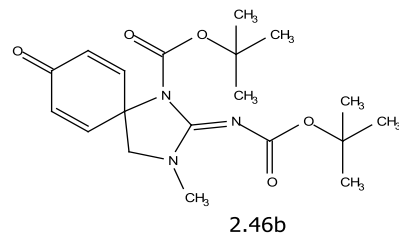


6.94  
6.93  
6.92  
6.91  
6.90  
6.30  
6.29  
6.28  
6.27

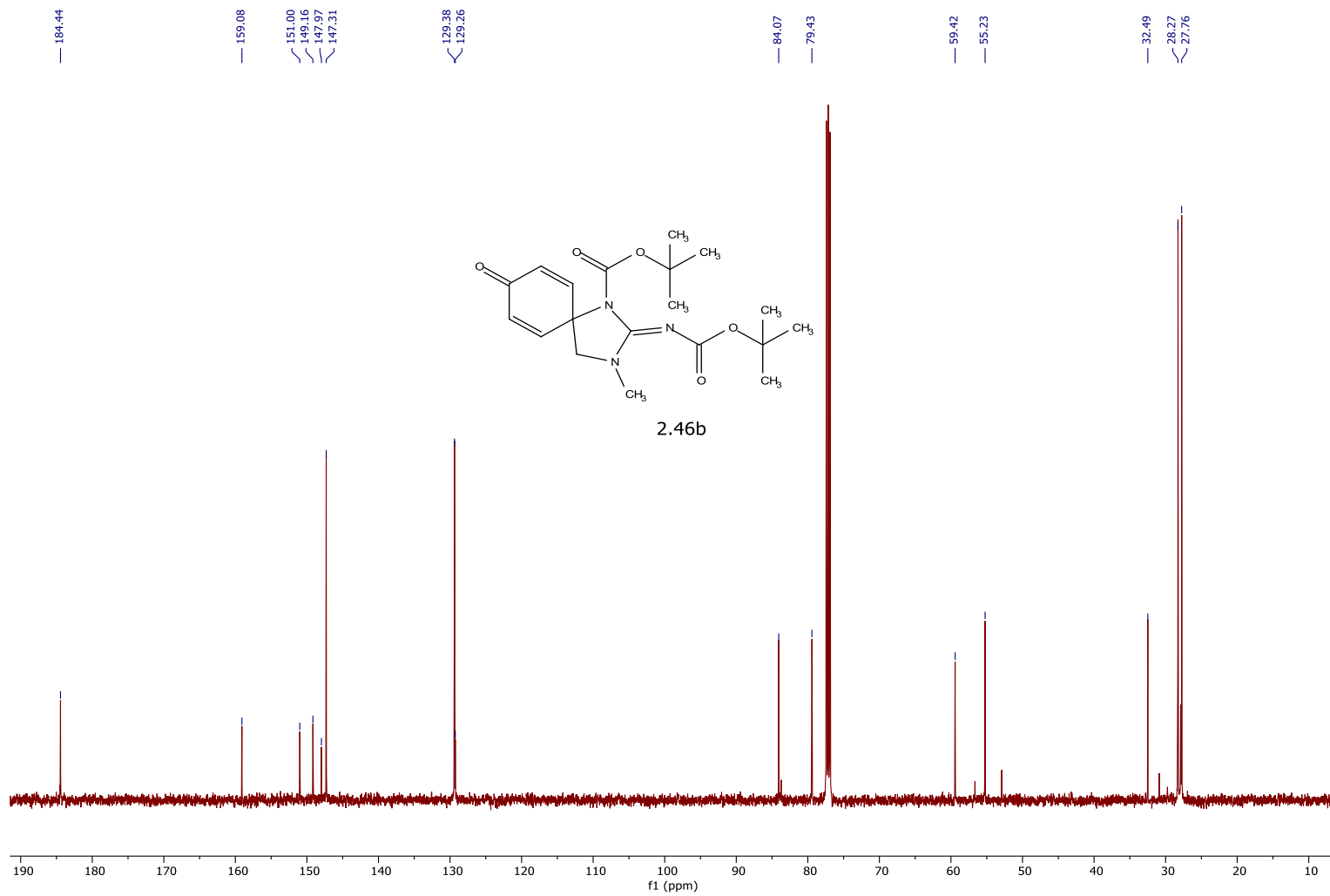
3.43

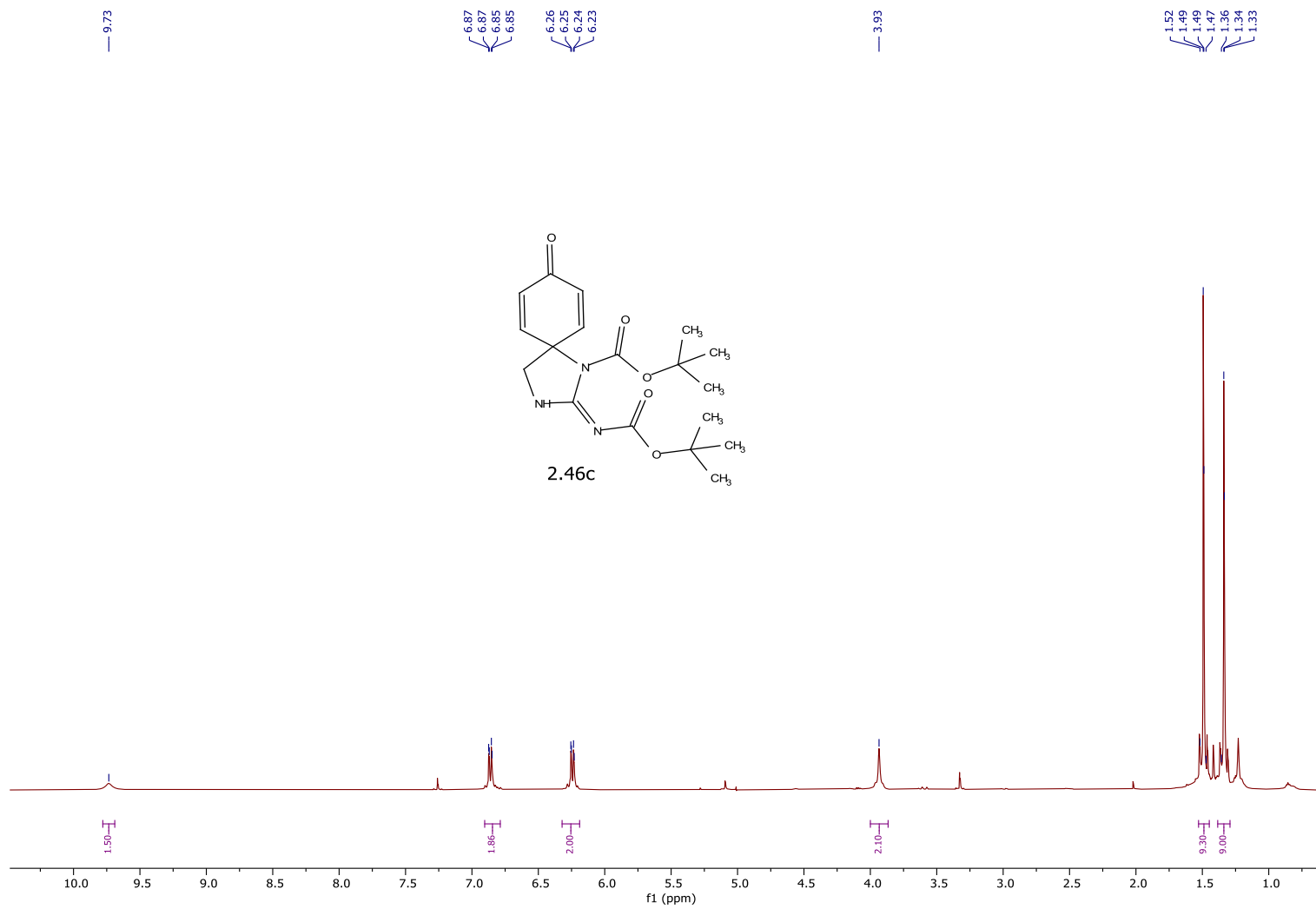
2.91

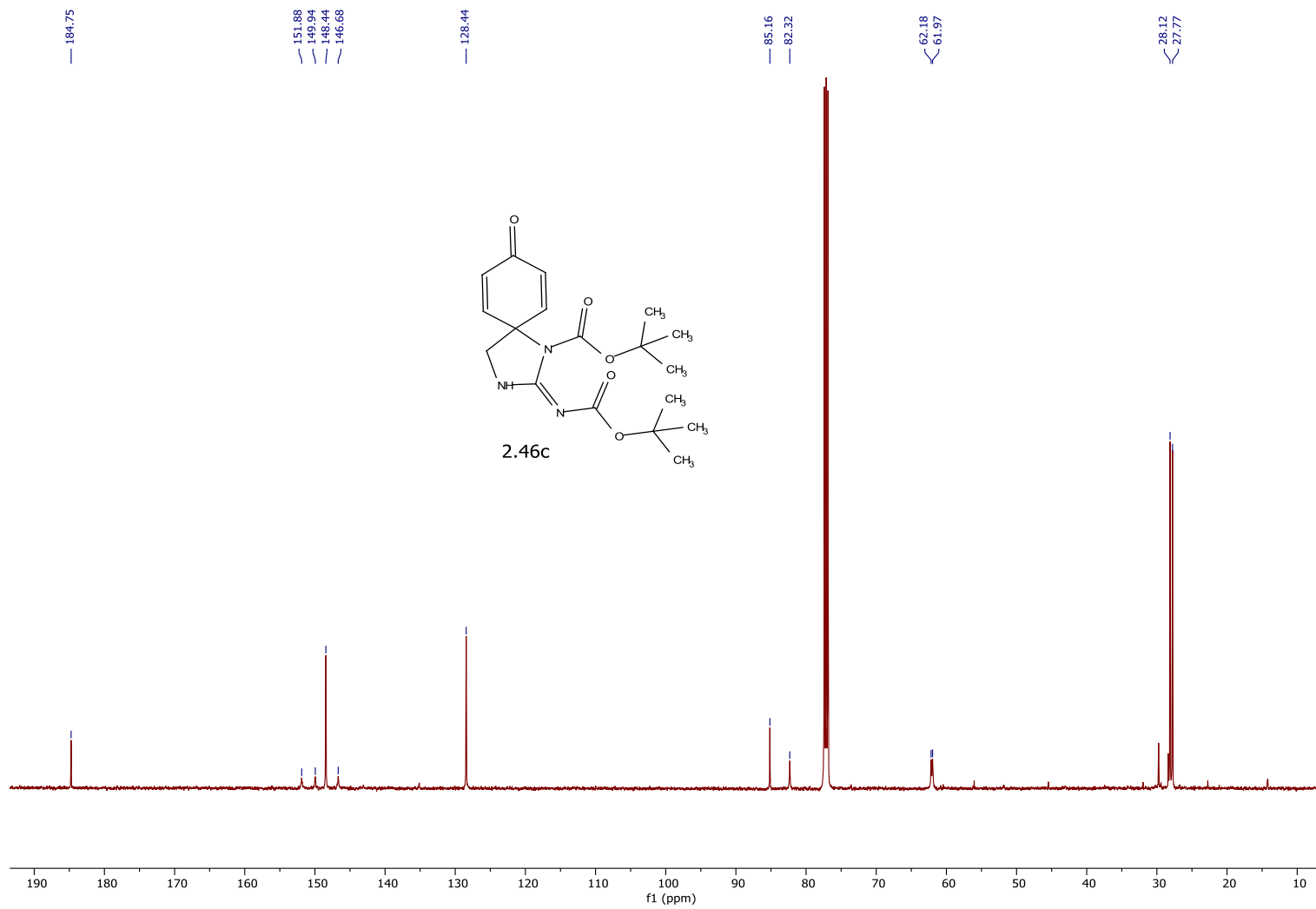
1.49  
1.47  
1.47  
1.31

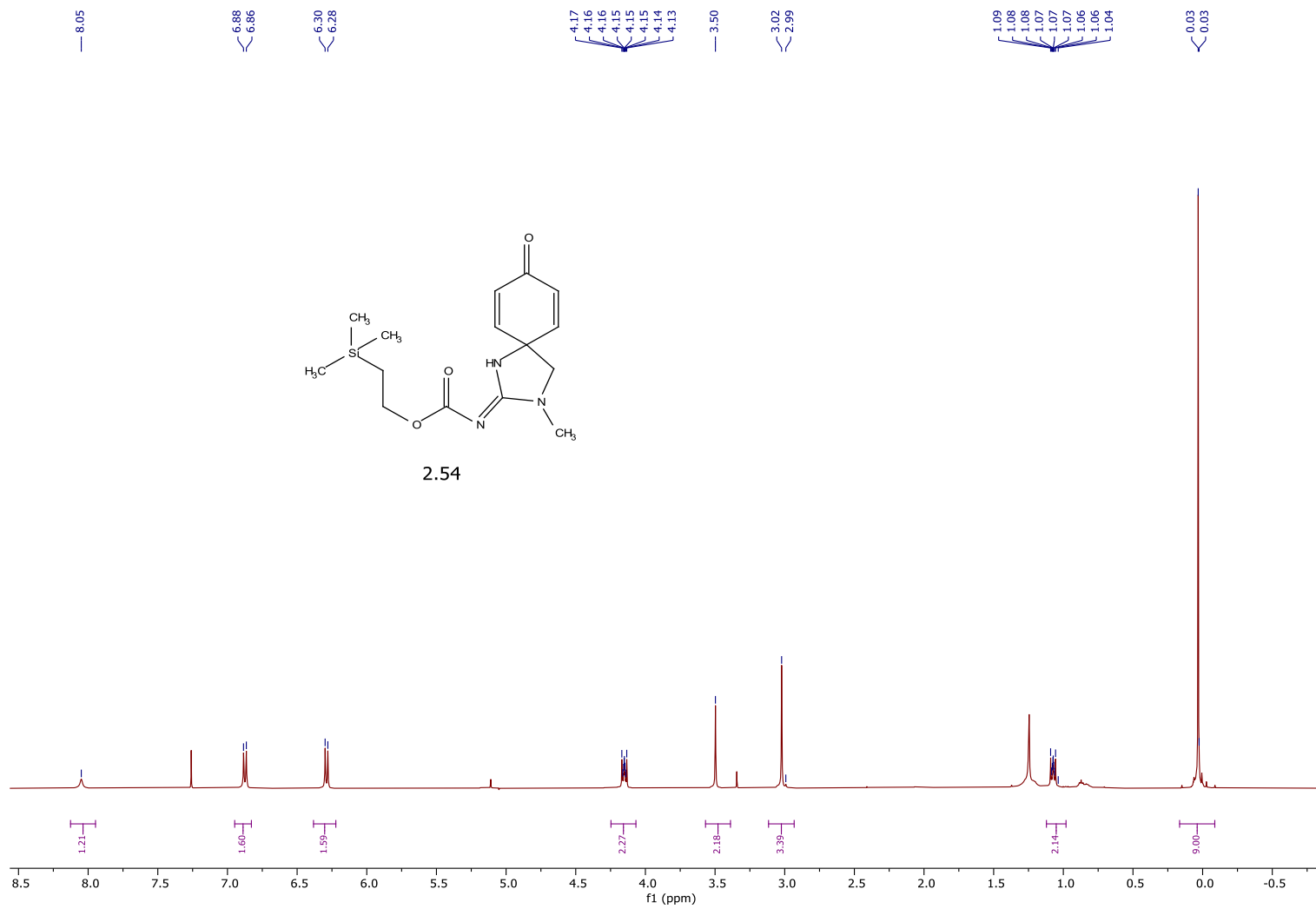


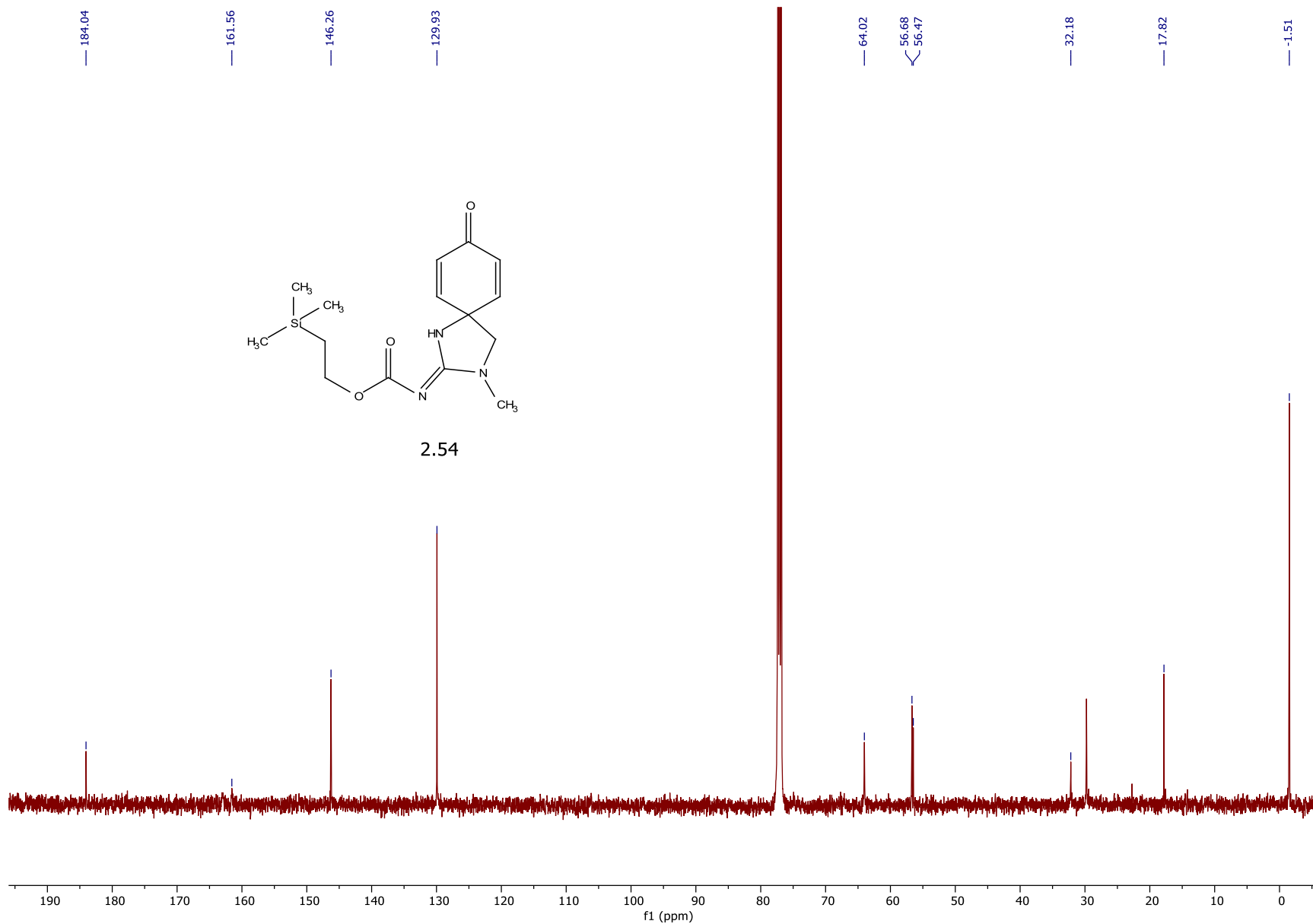




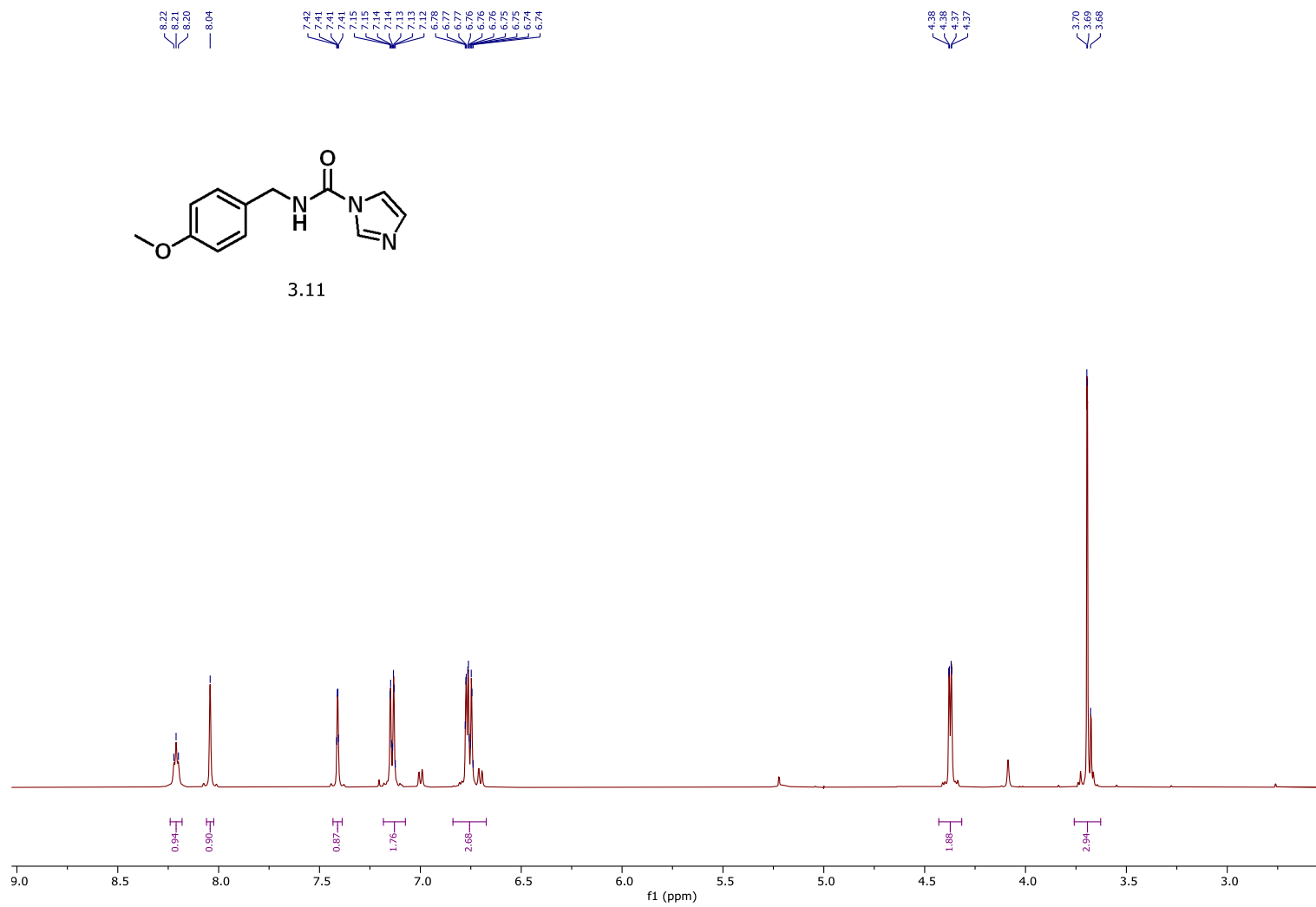
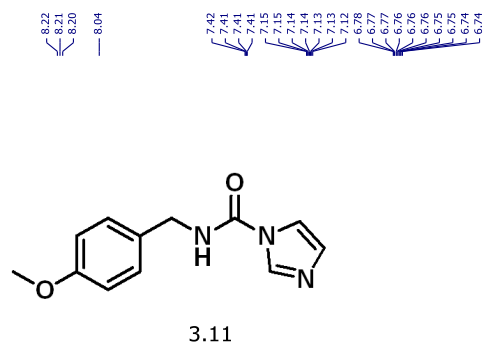


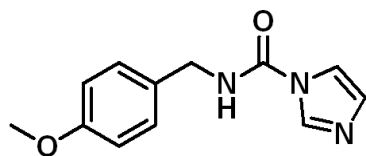




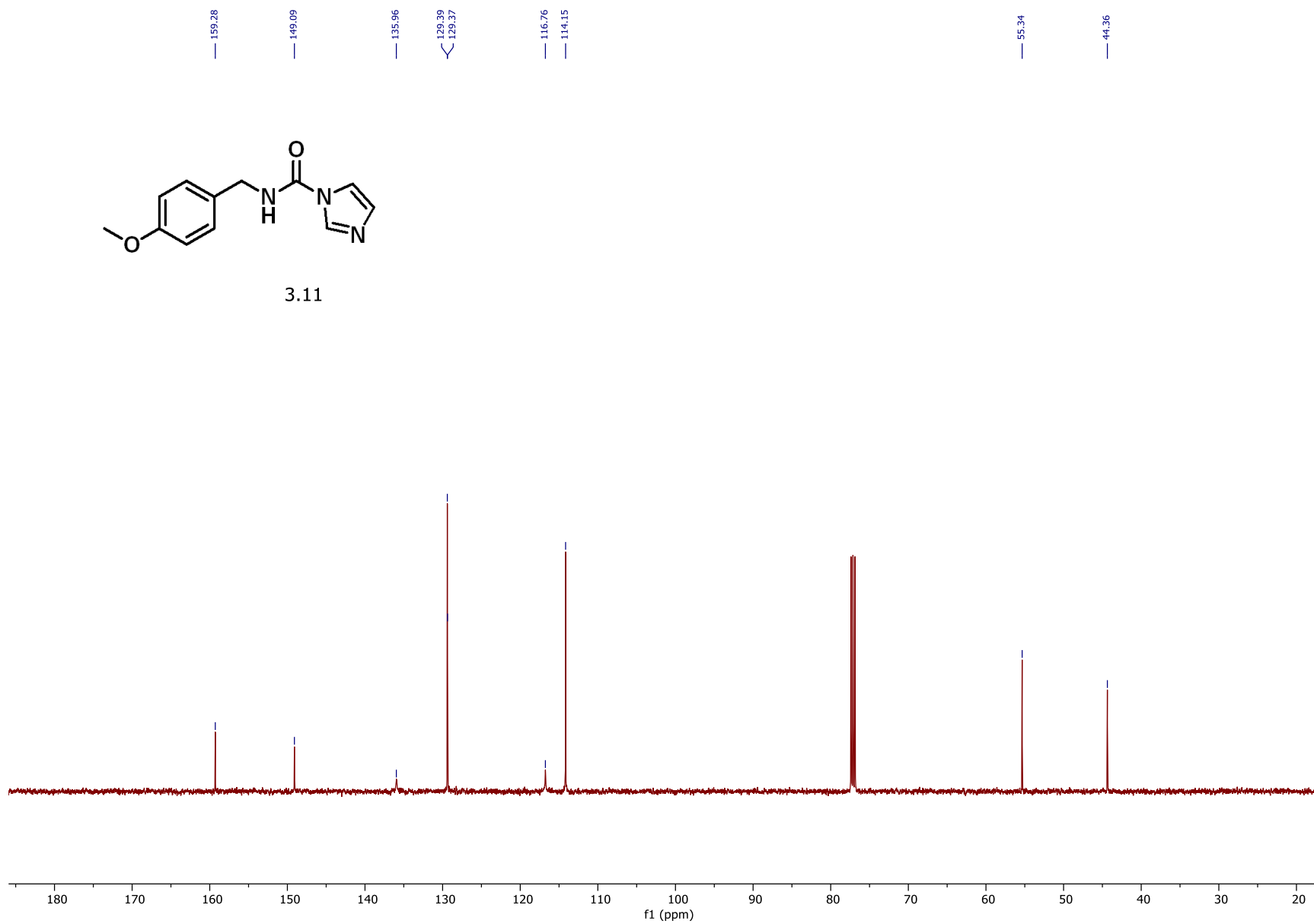


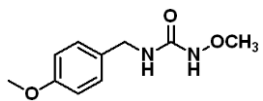
# Chapter Three



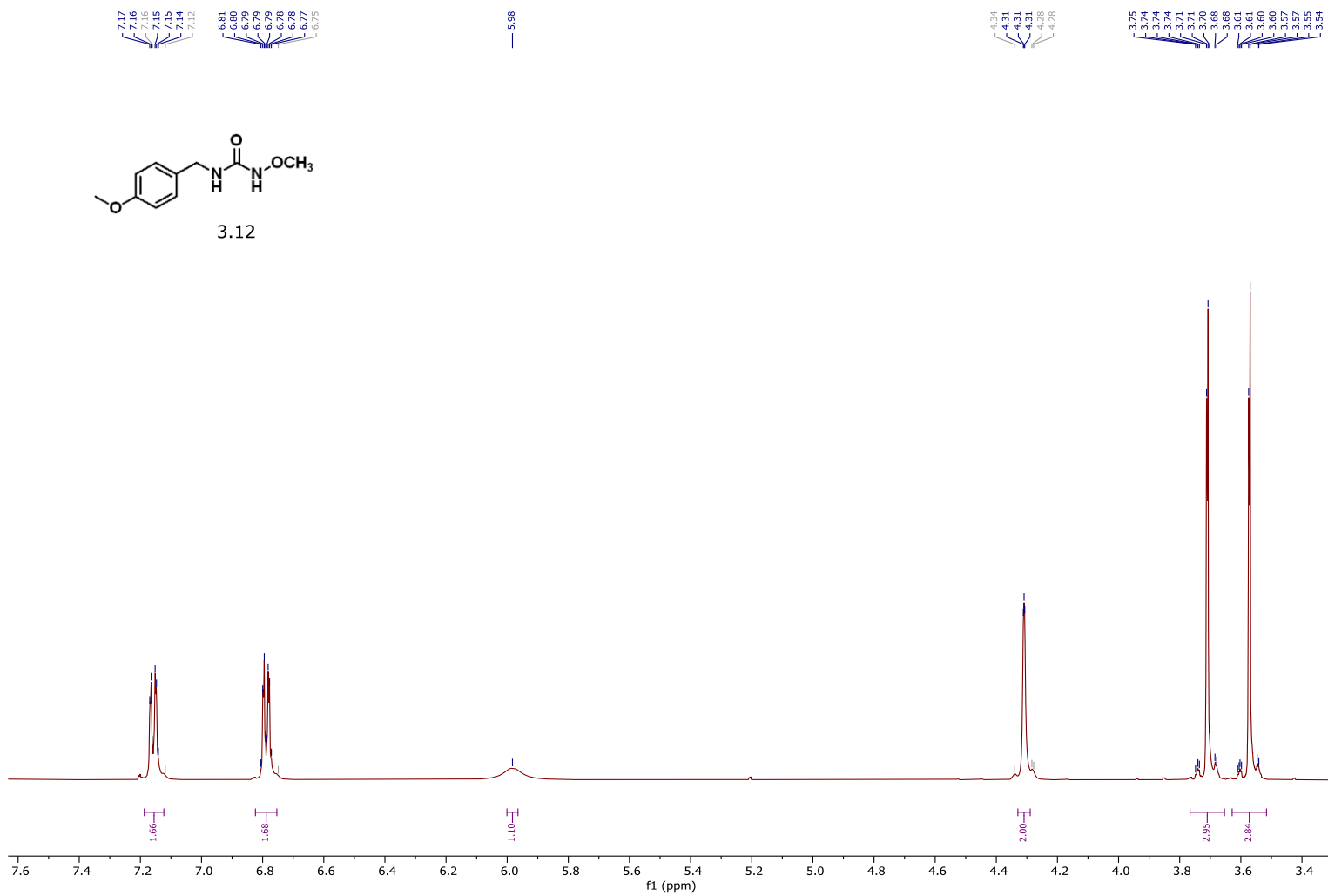


3.11

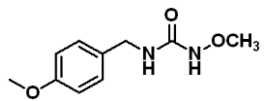




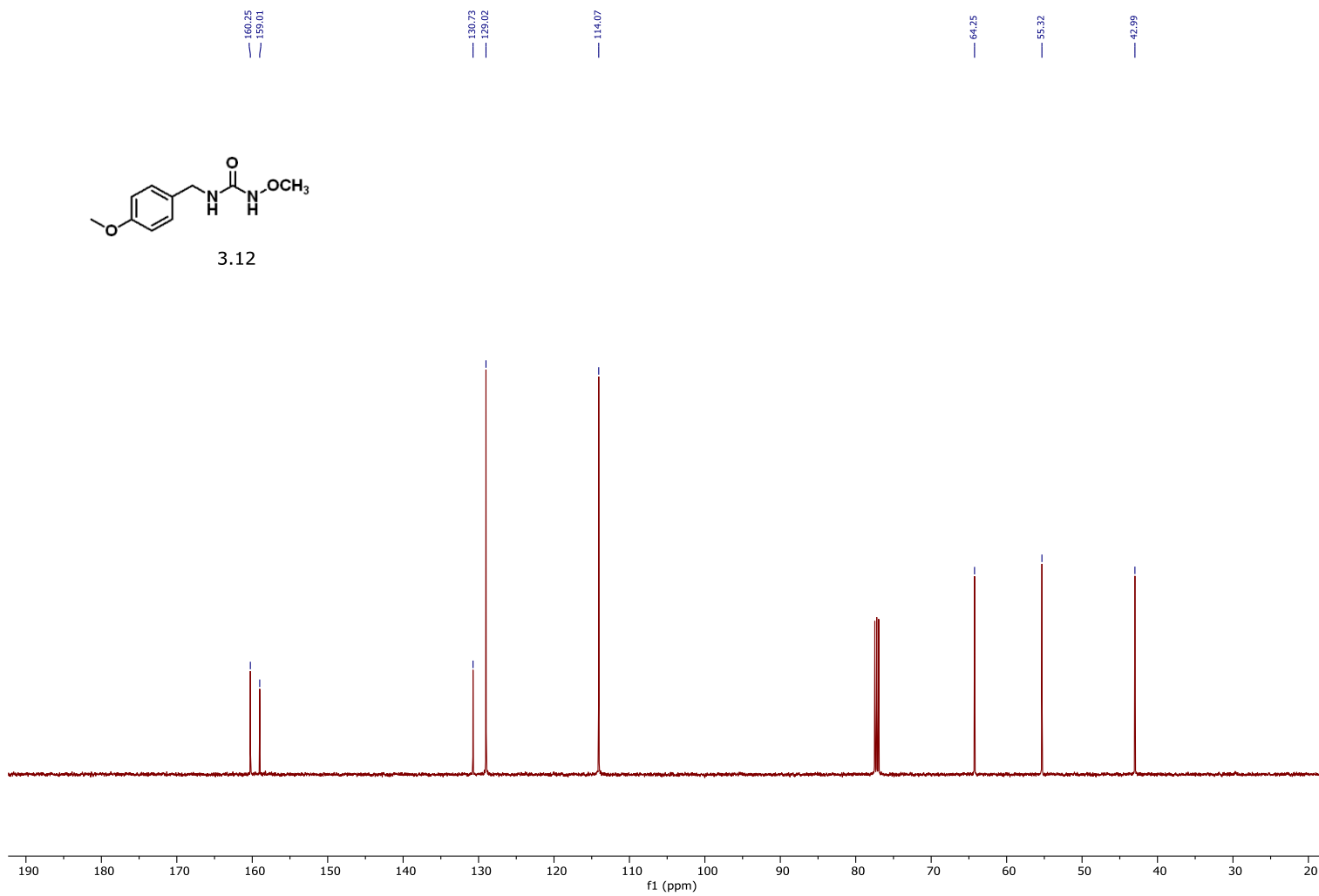
3.12

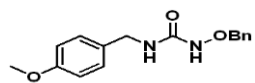




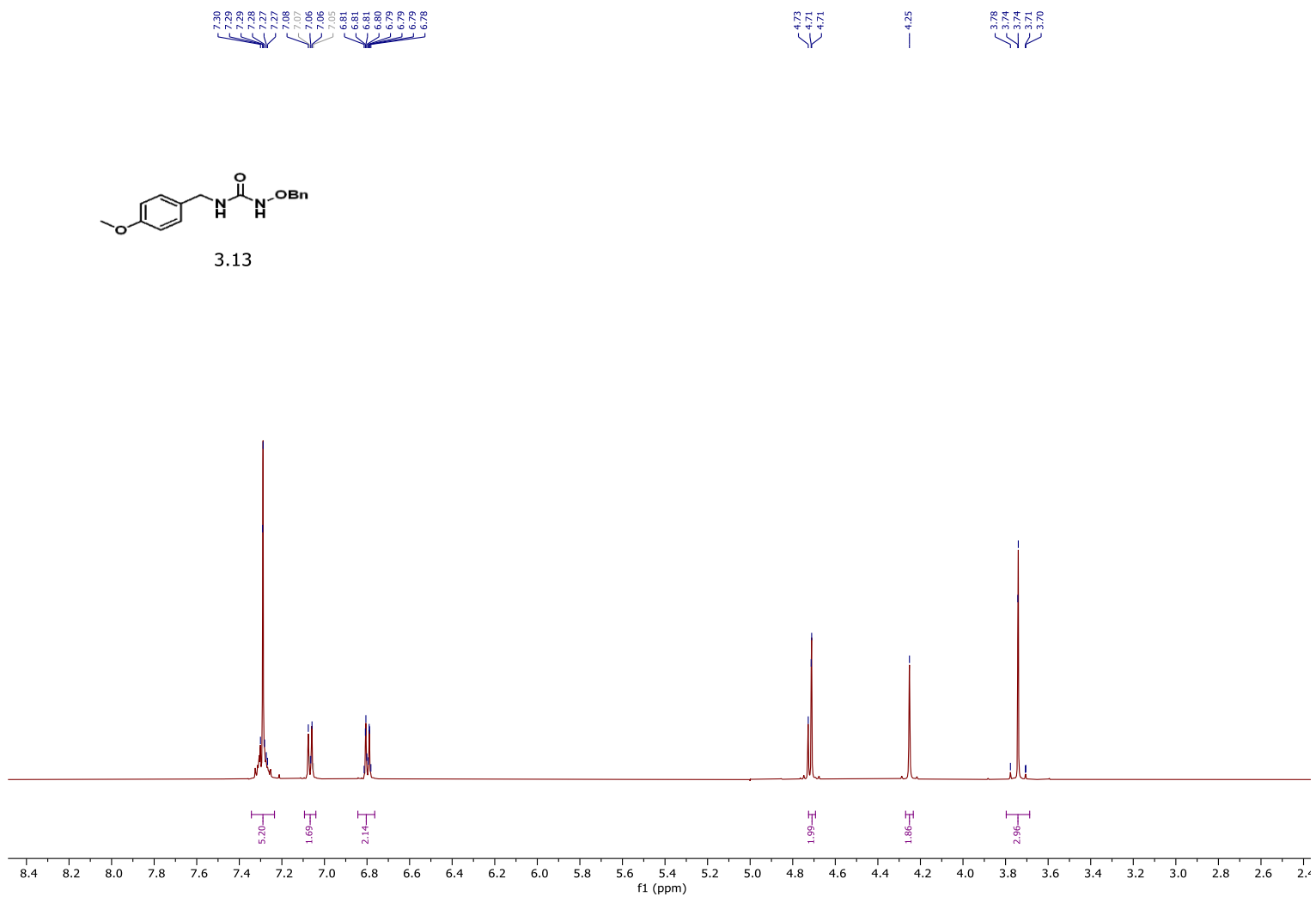


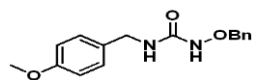
3.12



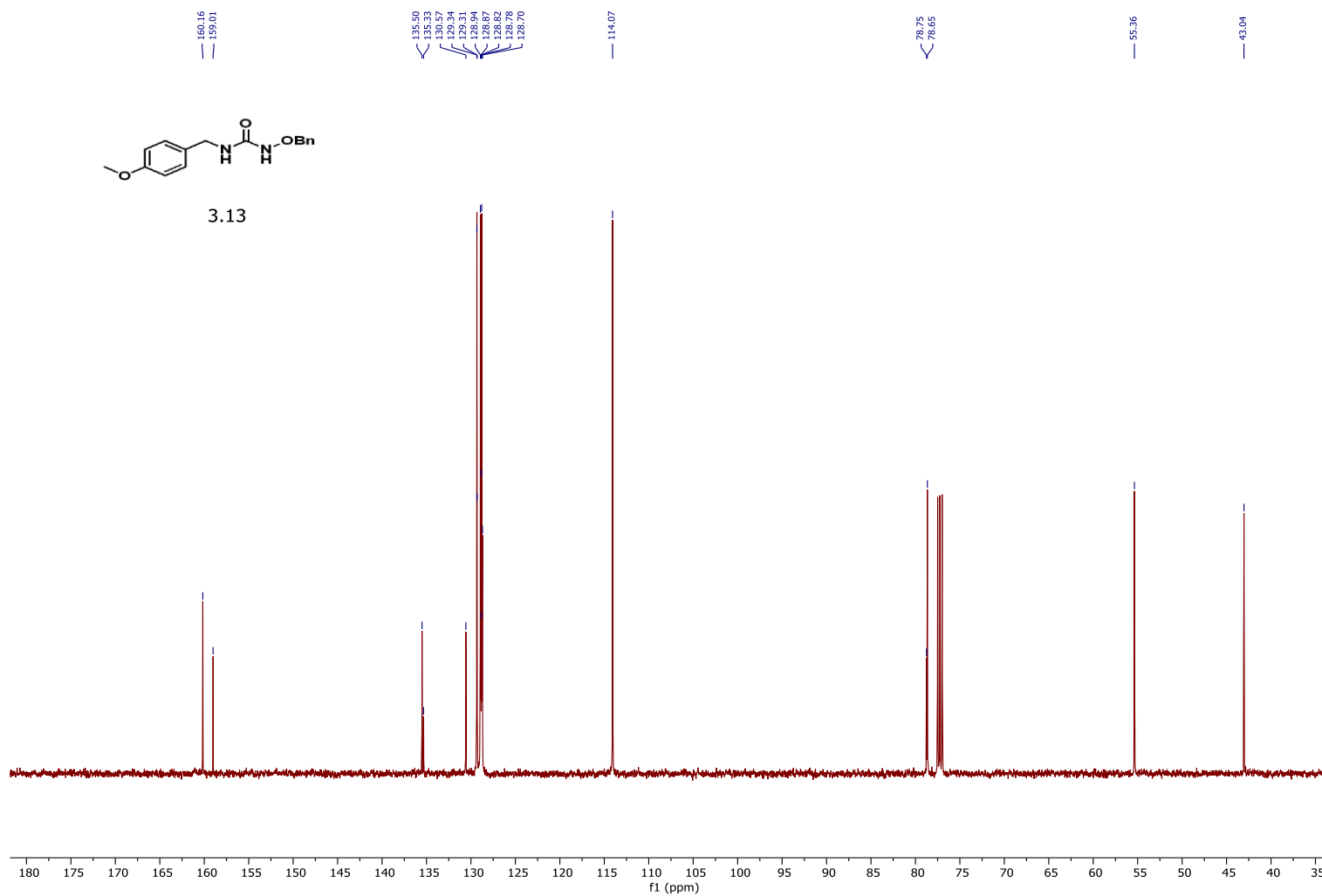


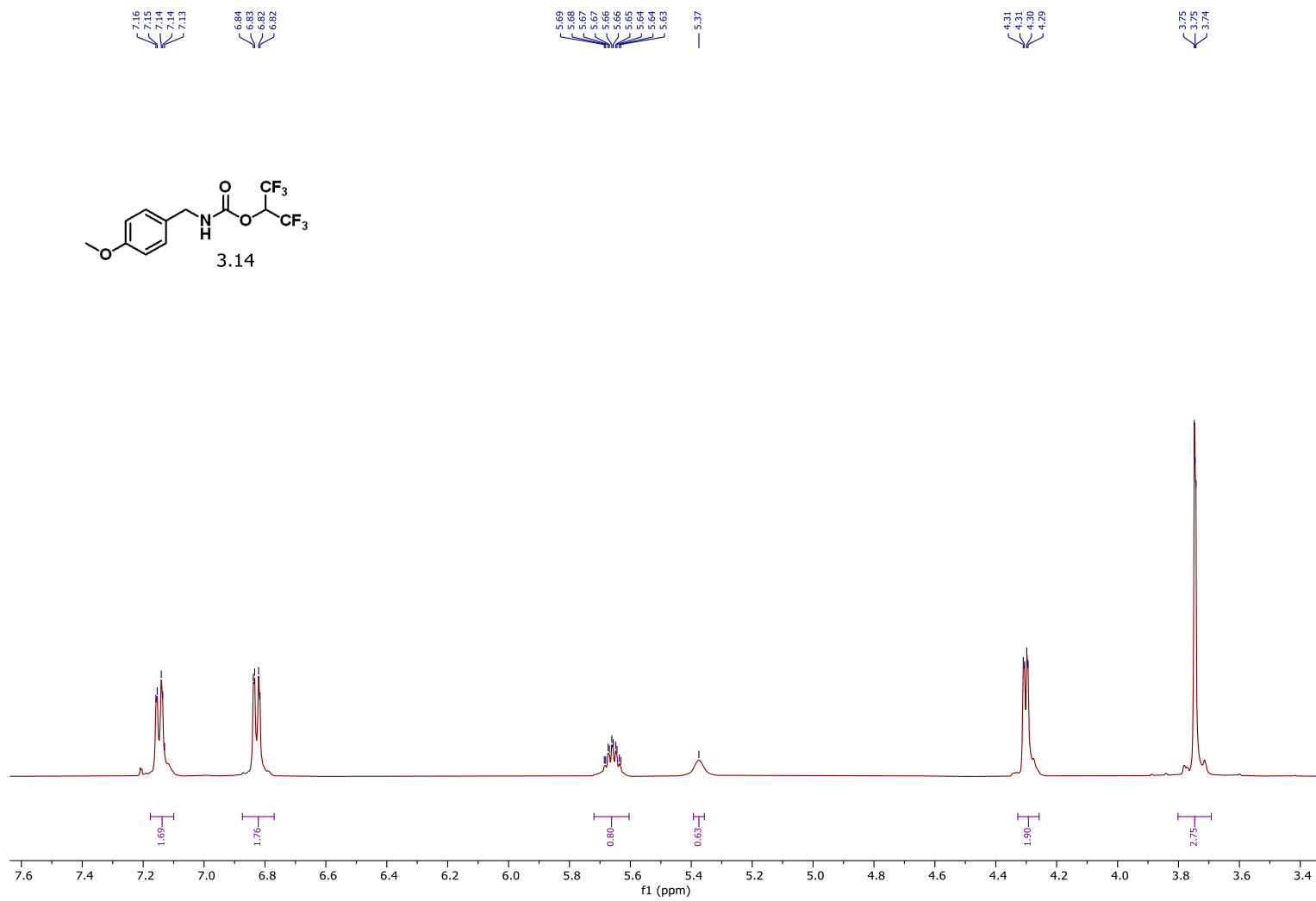
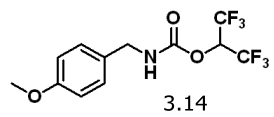
3.13

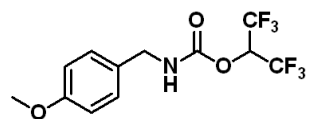




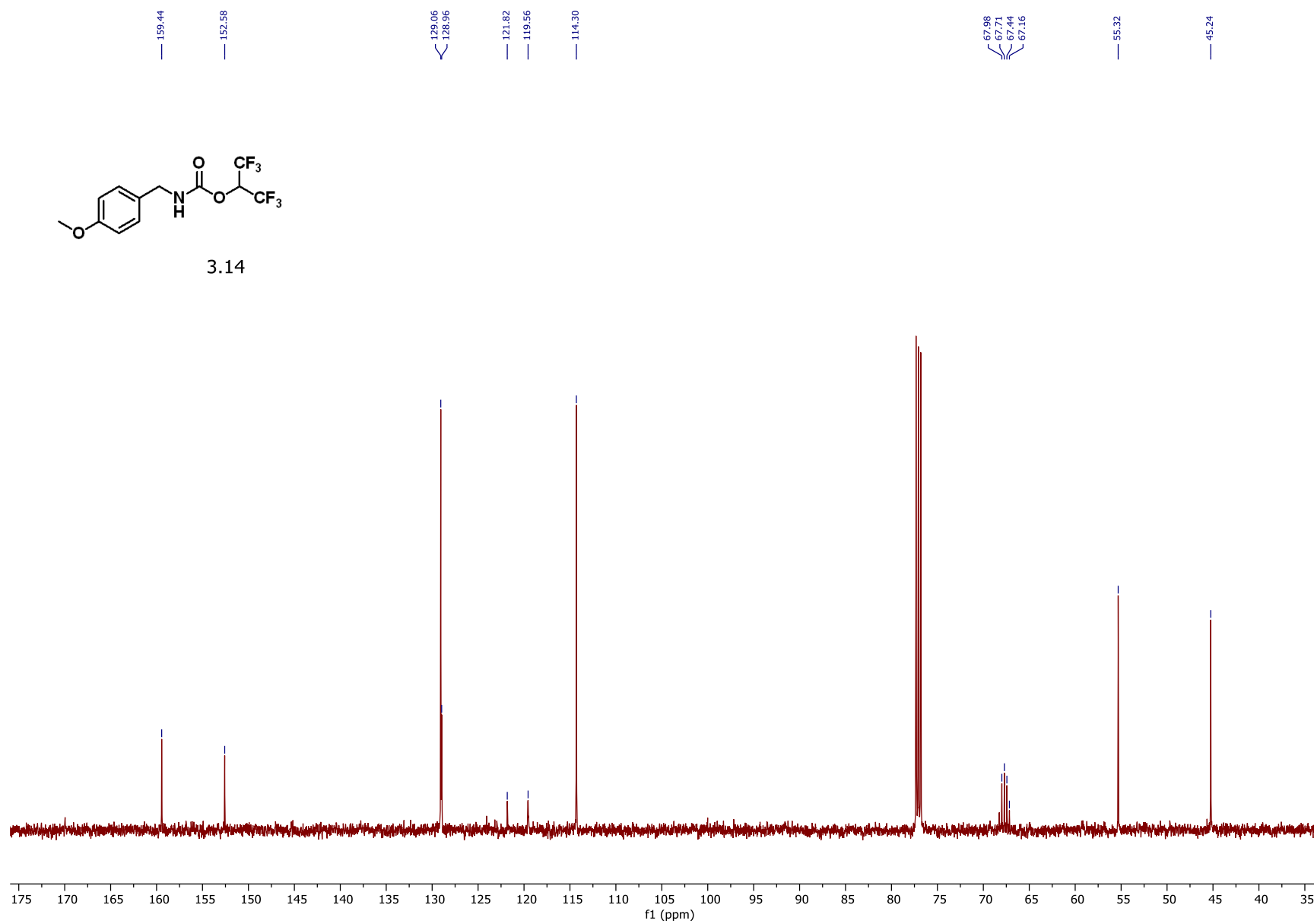
3.13

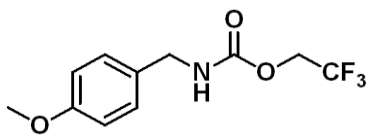




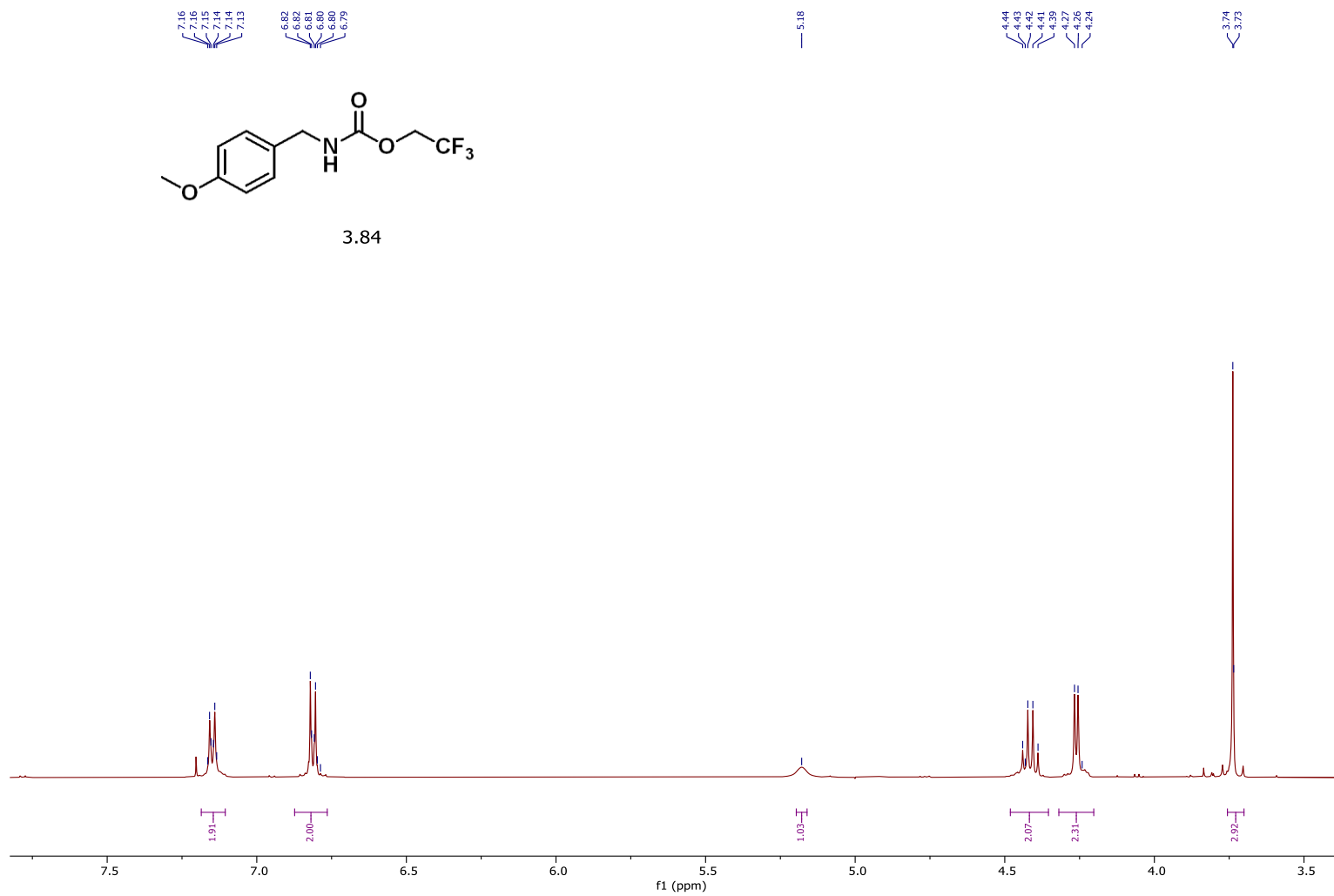


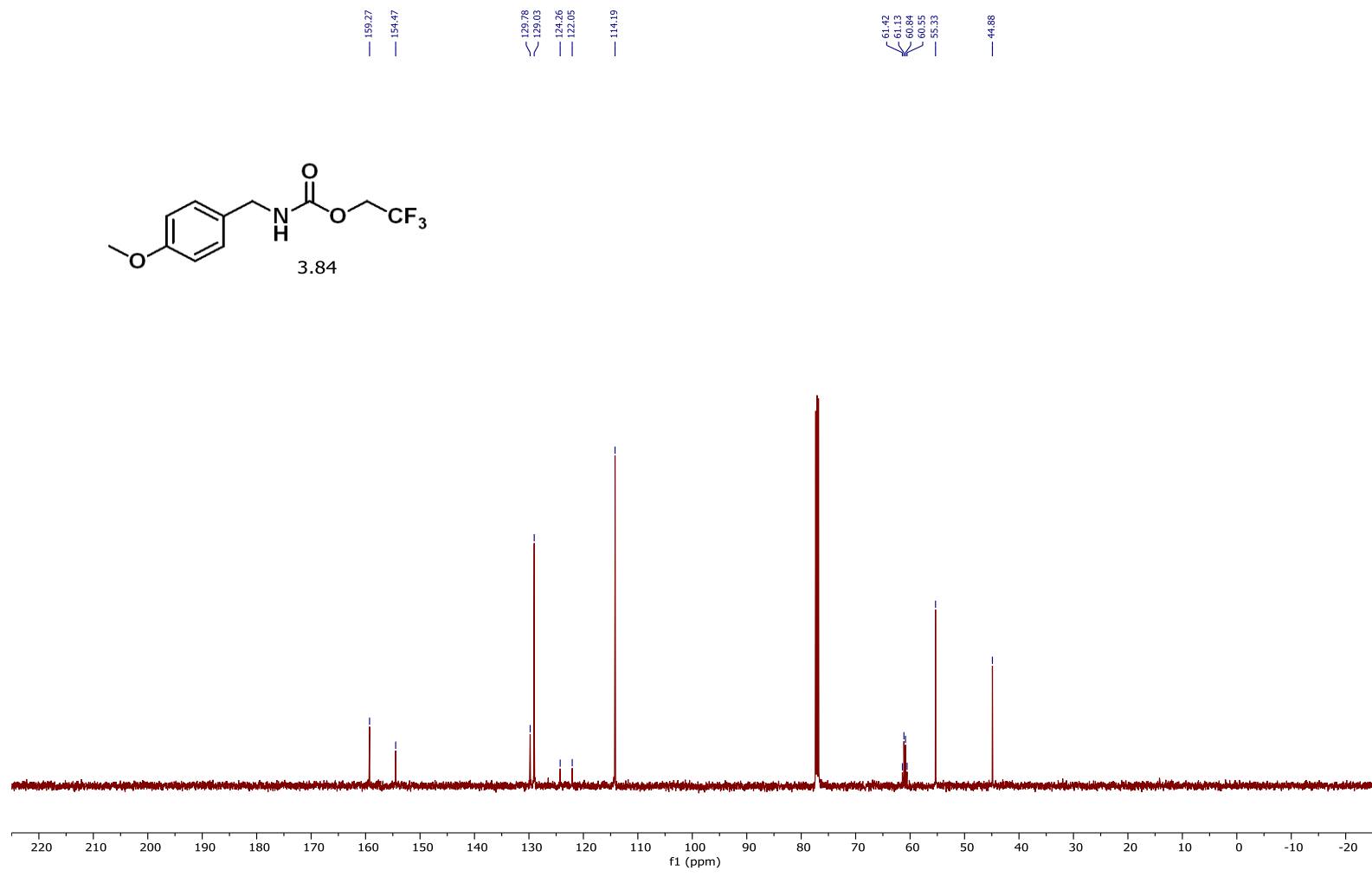
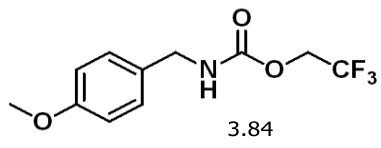
3.14

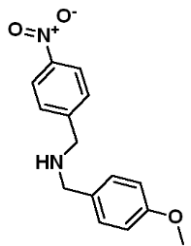




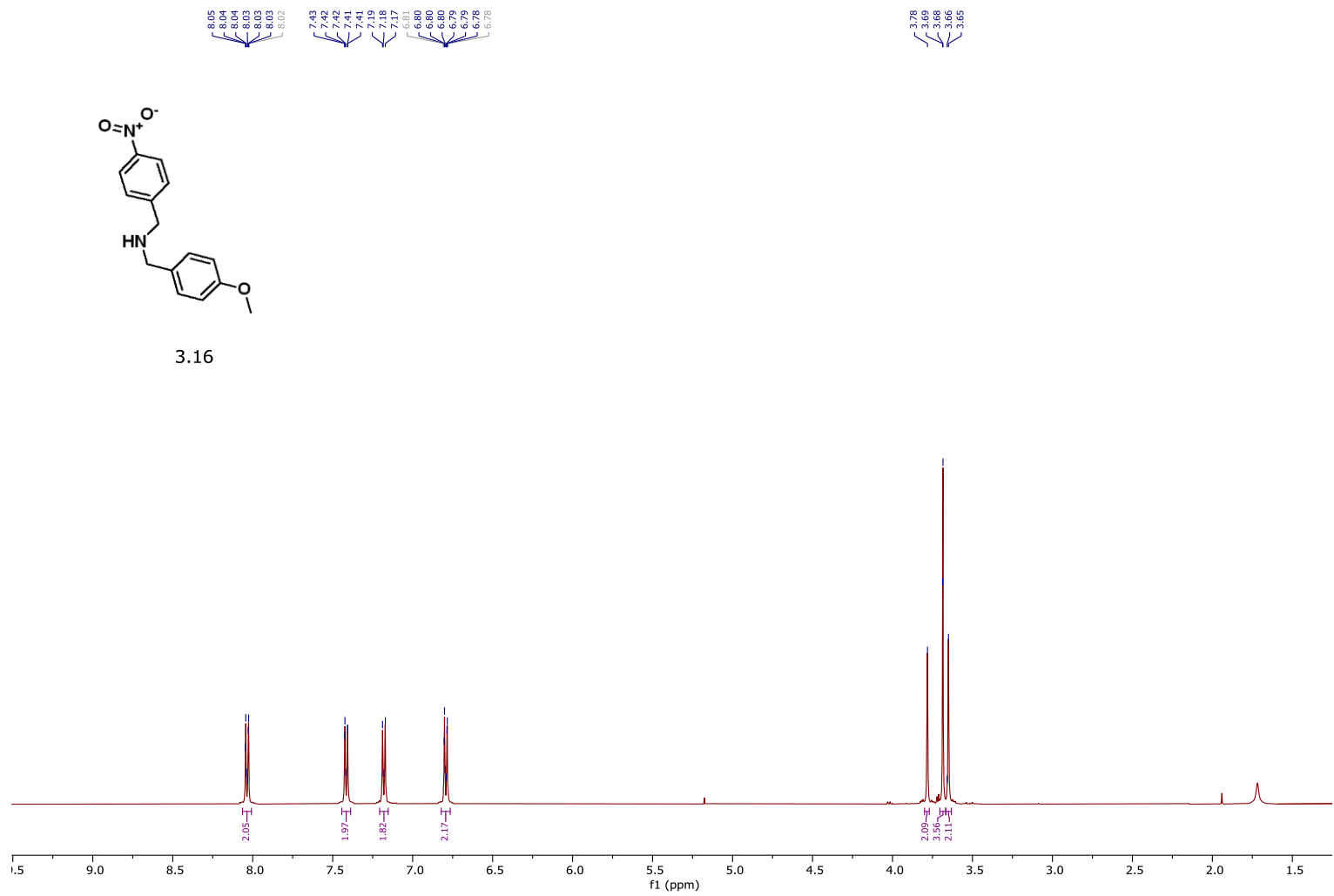
3.84



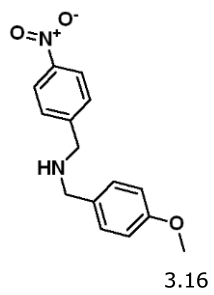




3.16







158.83

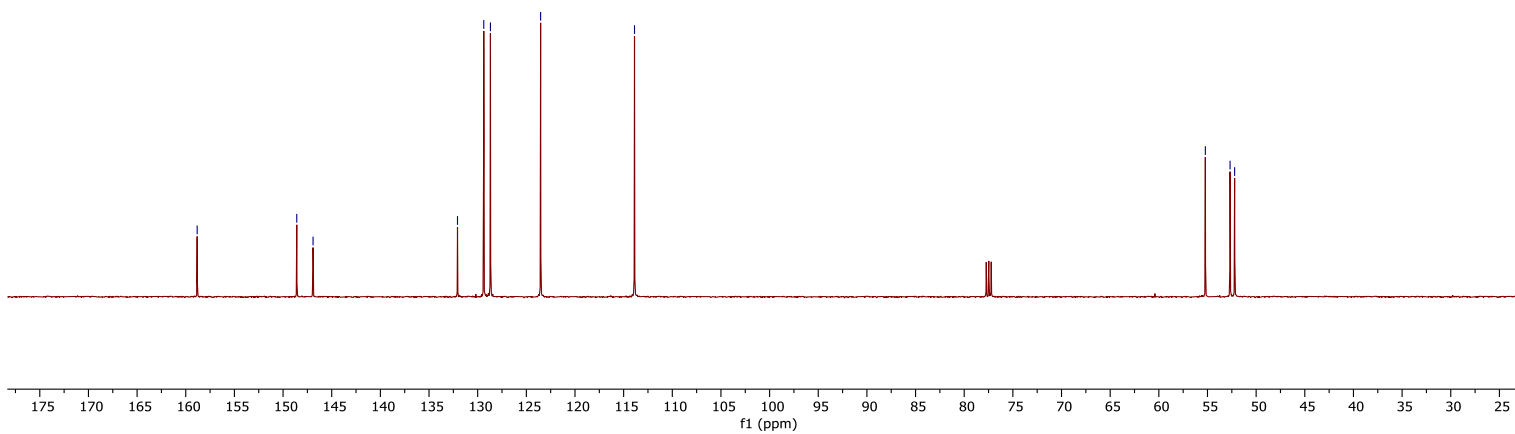
148.59  
146.92

132.07  
128.87  
128.69

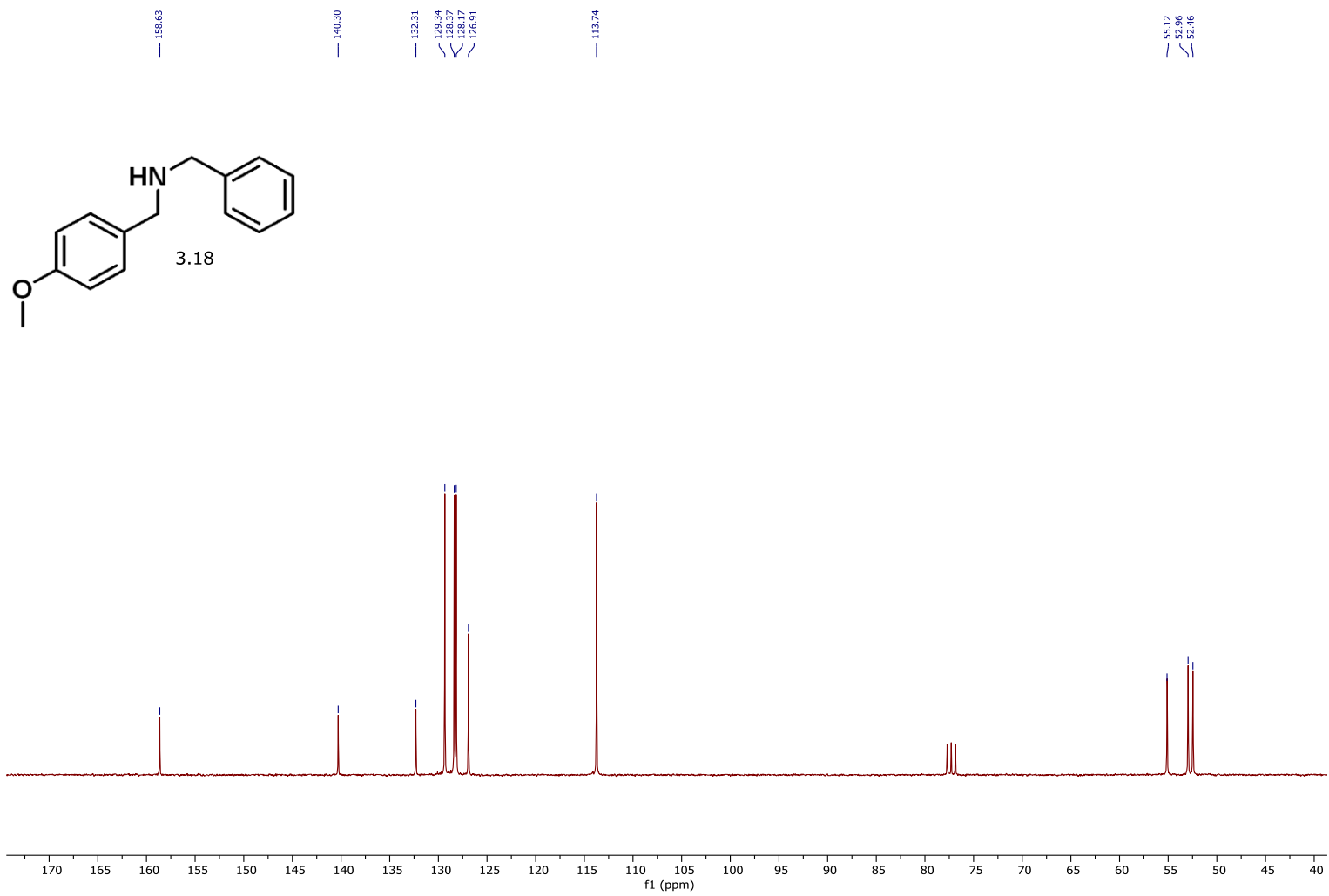
123.53

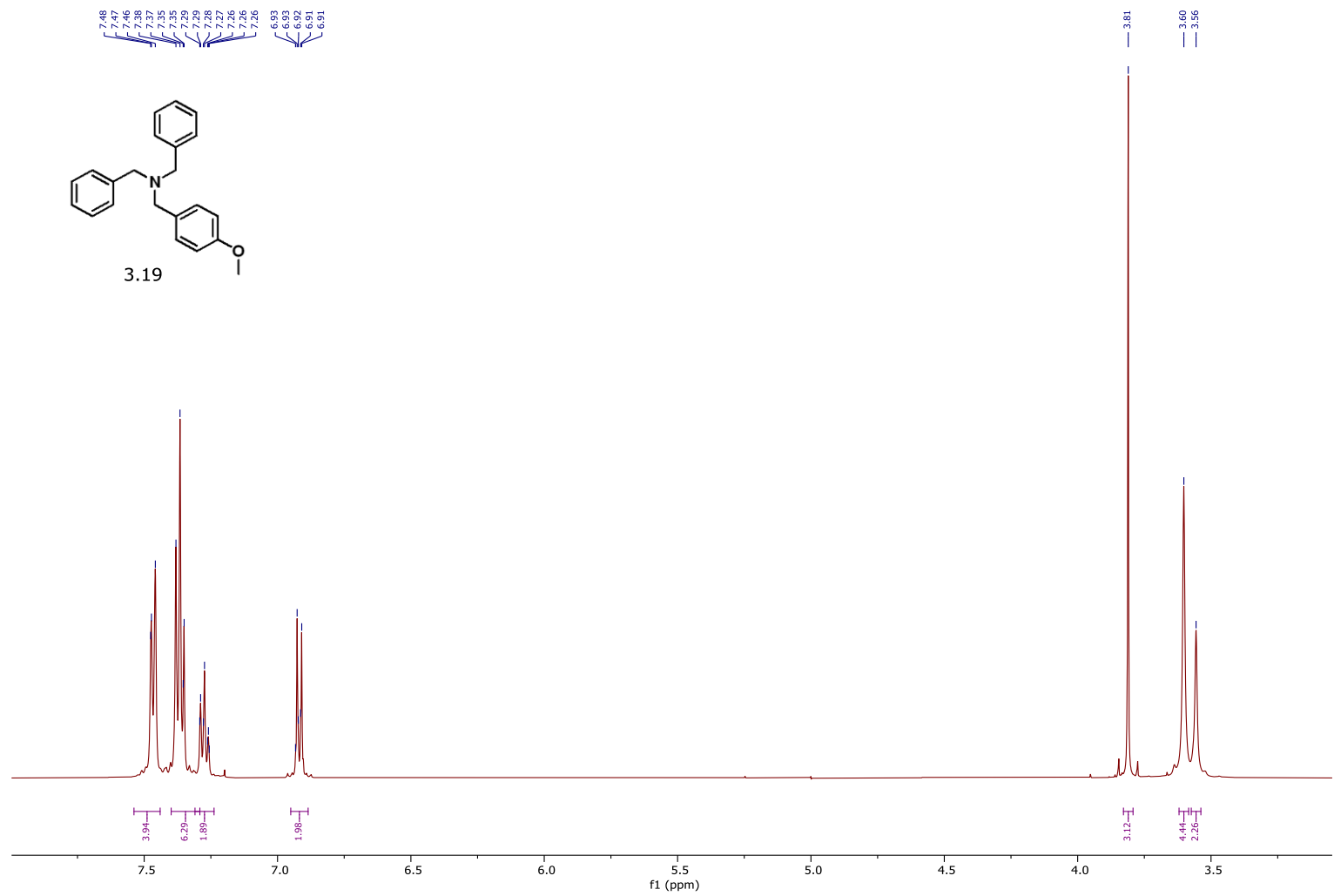
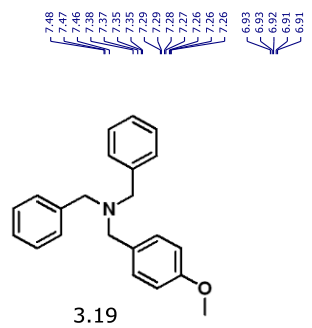
113.88

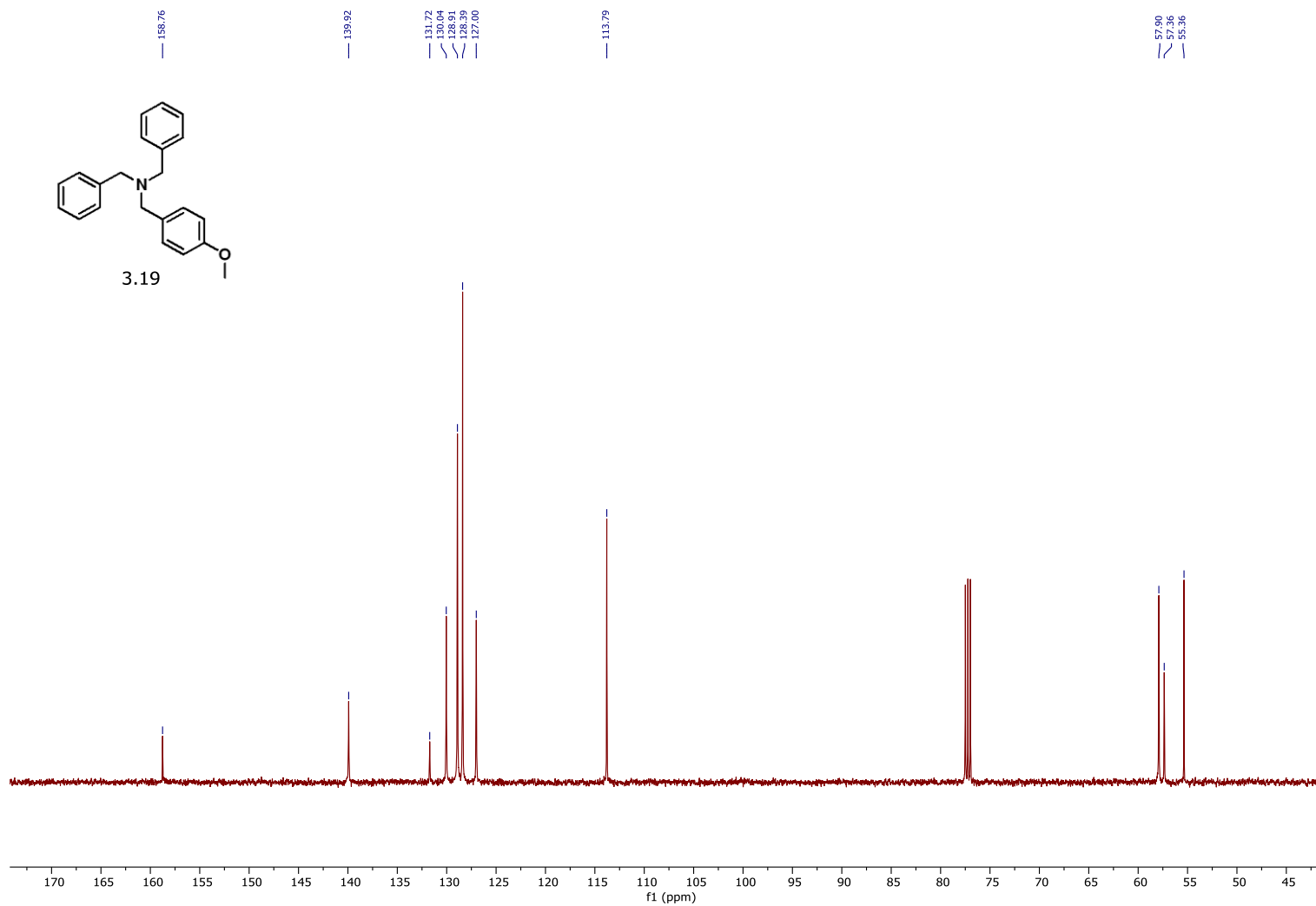
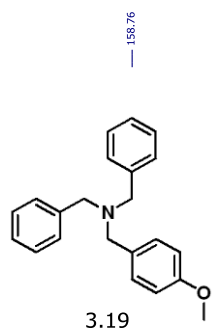
55.22  
52.68  
52.21



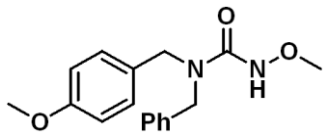




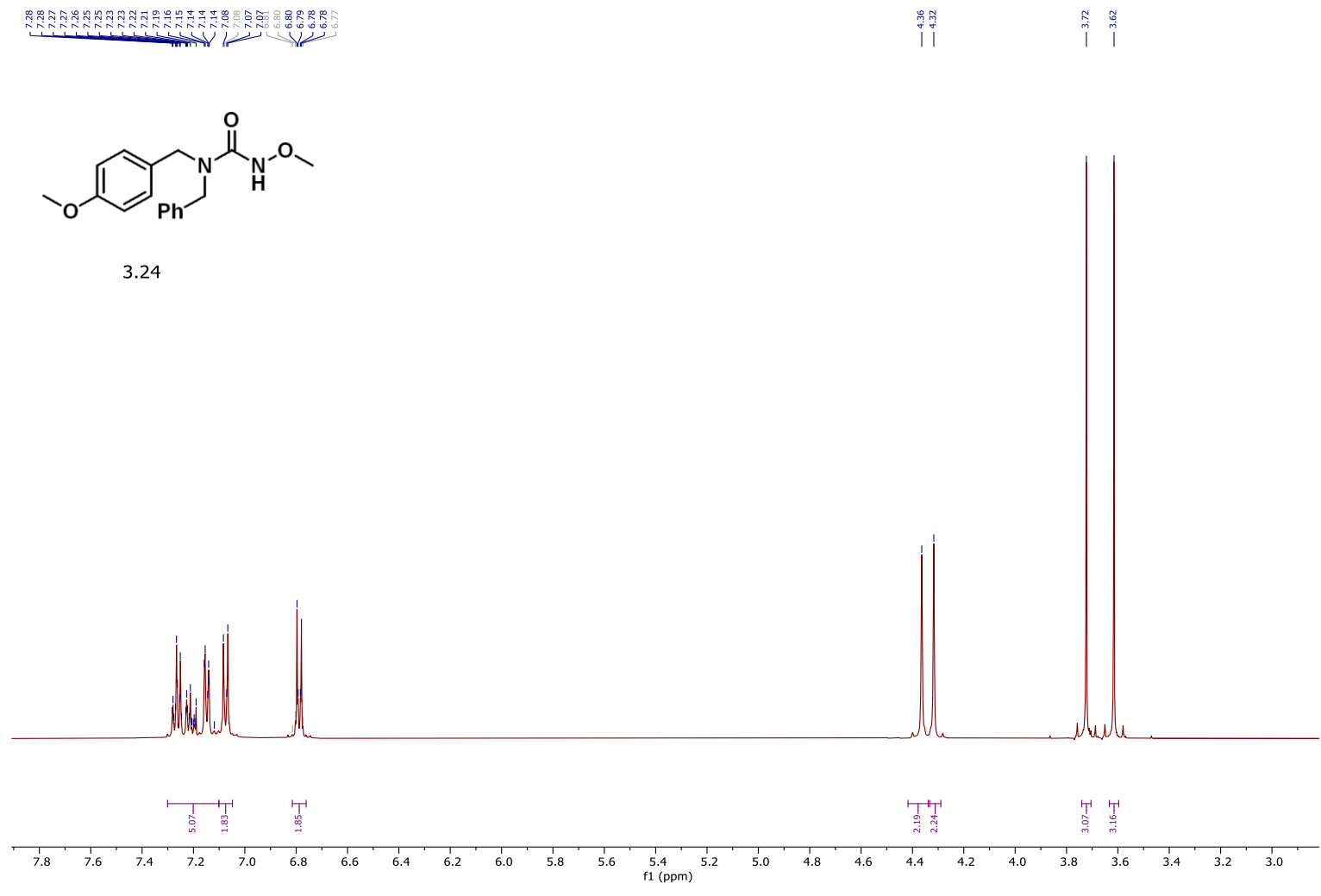


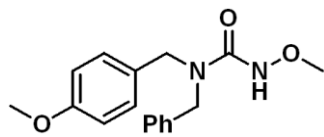


7.28  
7.27  
7.26  
7.25  
7.25  
7.25  
7.23  
7.22  
7.21  
7.19  
7.16  
7.15  
7.14  
7.14  
7.08  
7.07  
6.91  
6.80  
6.79  
6.78  
6.77

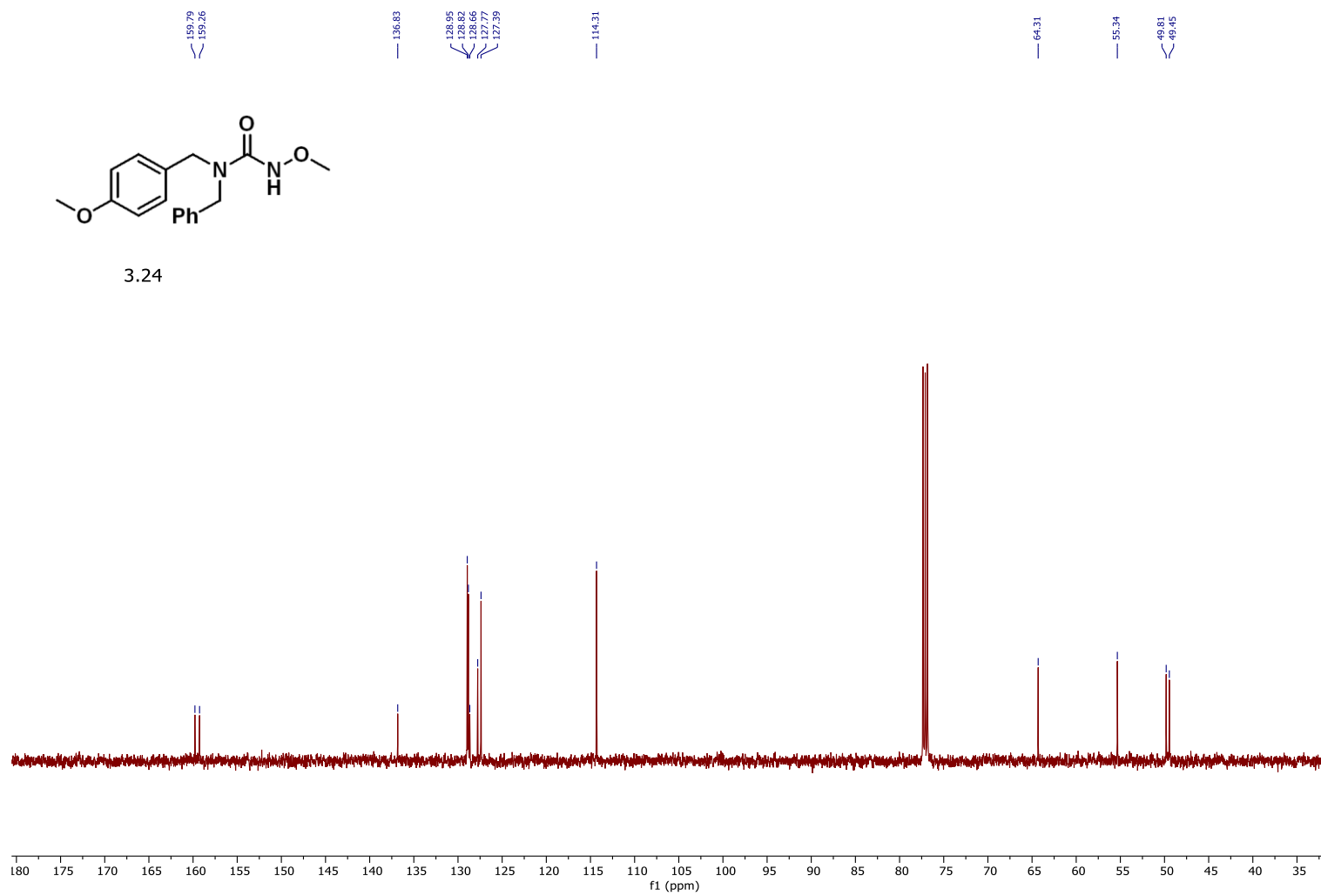


3.24





3.24

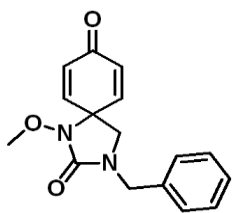


7.30  
7.29  
7.29  
7.29  
7.27  
7.08  
7.07  
7.06  
7.05  
6.81  
6.81  
6.81  
6.80  
6.79  
6.79  
6.78

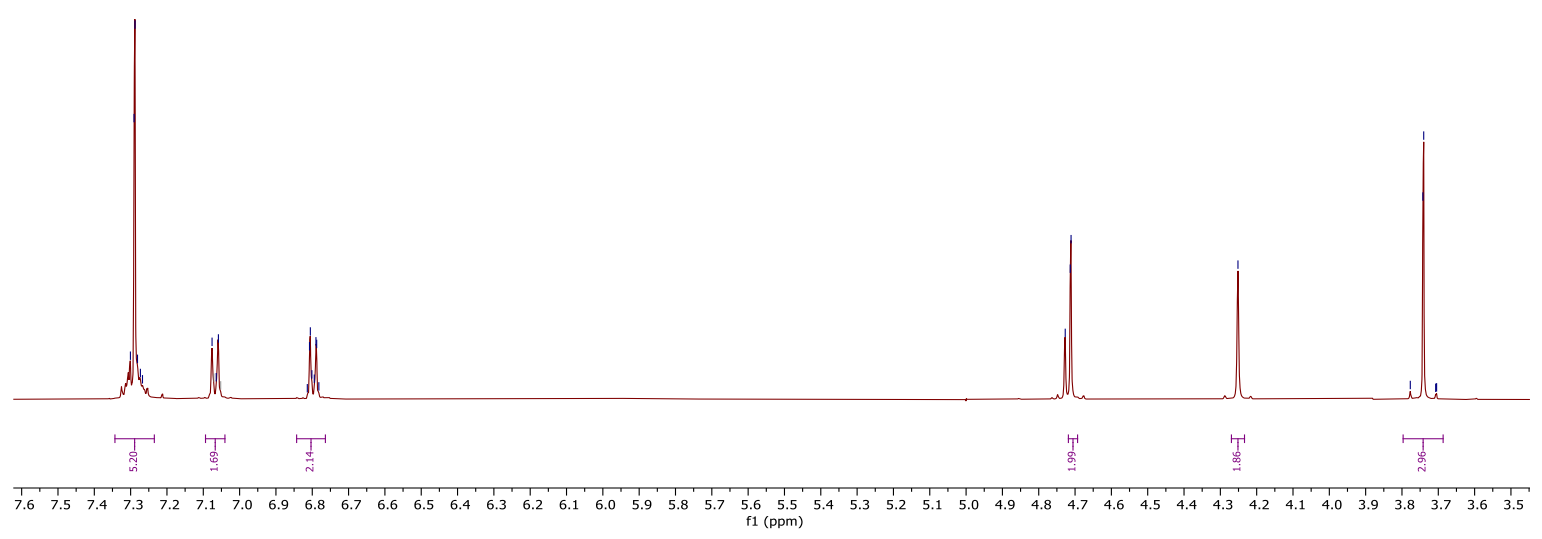
4.72  
4.71

4.25

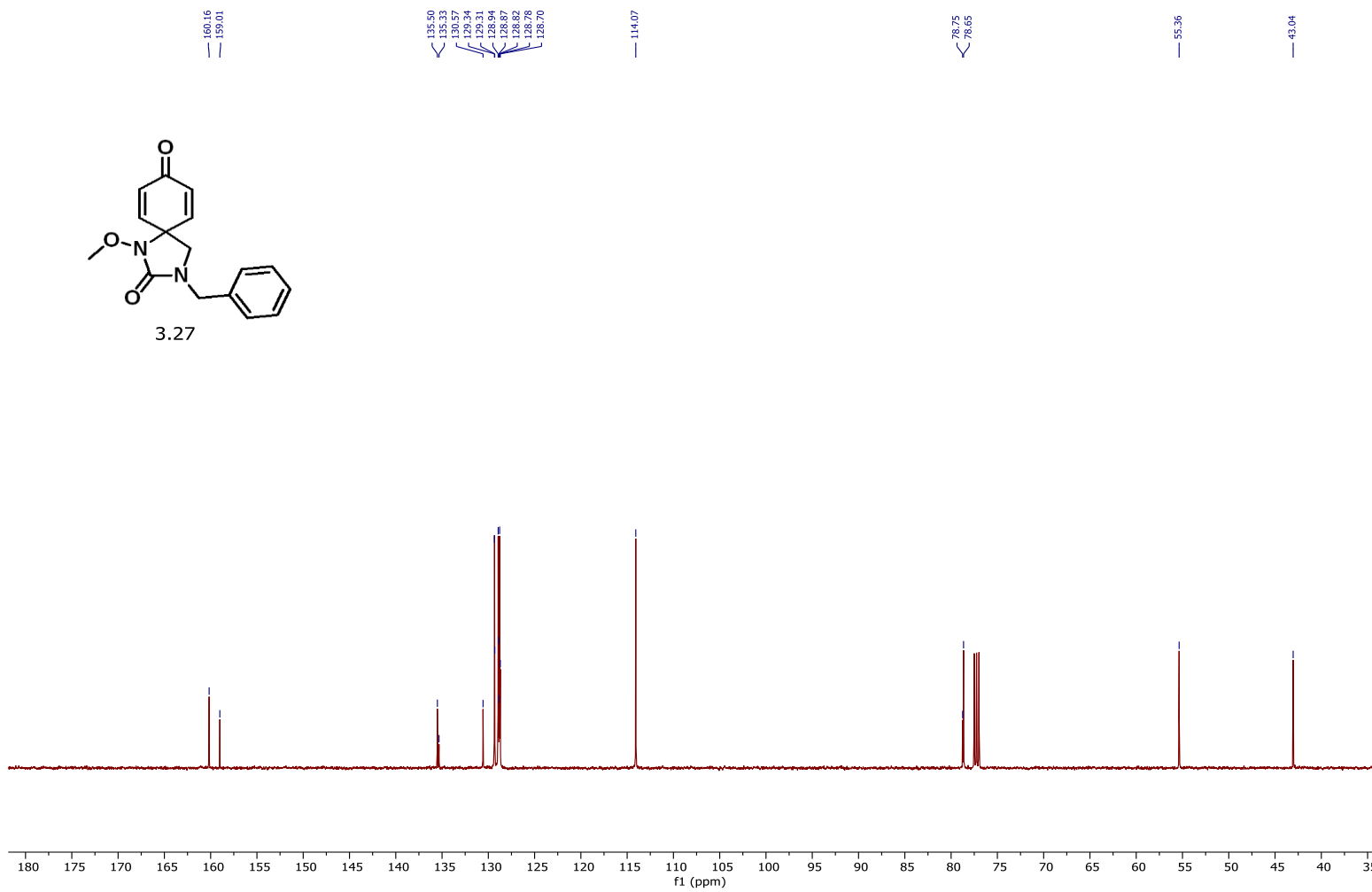
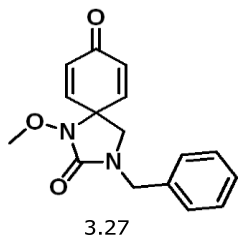
3.78  
3.74  
3.71  
3.70

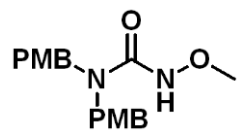


3.27

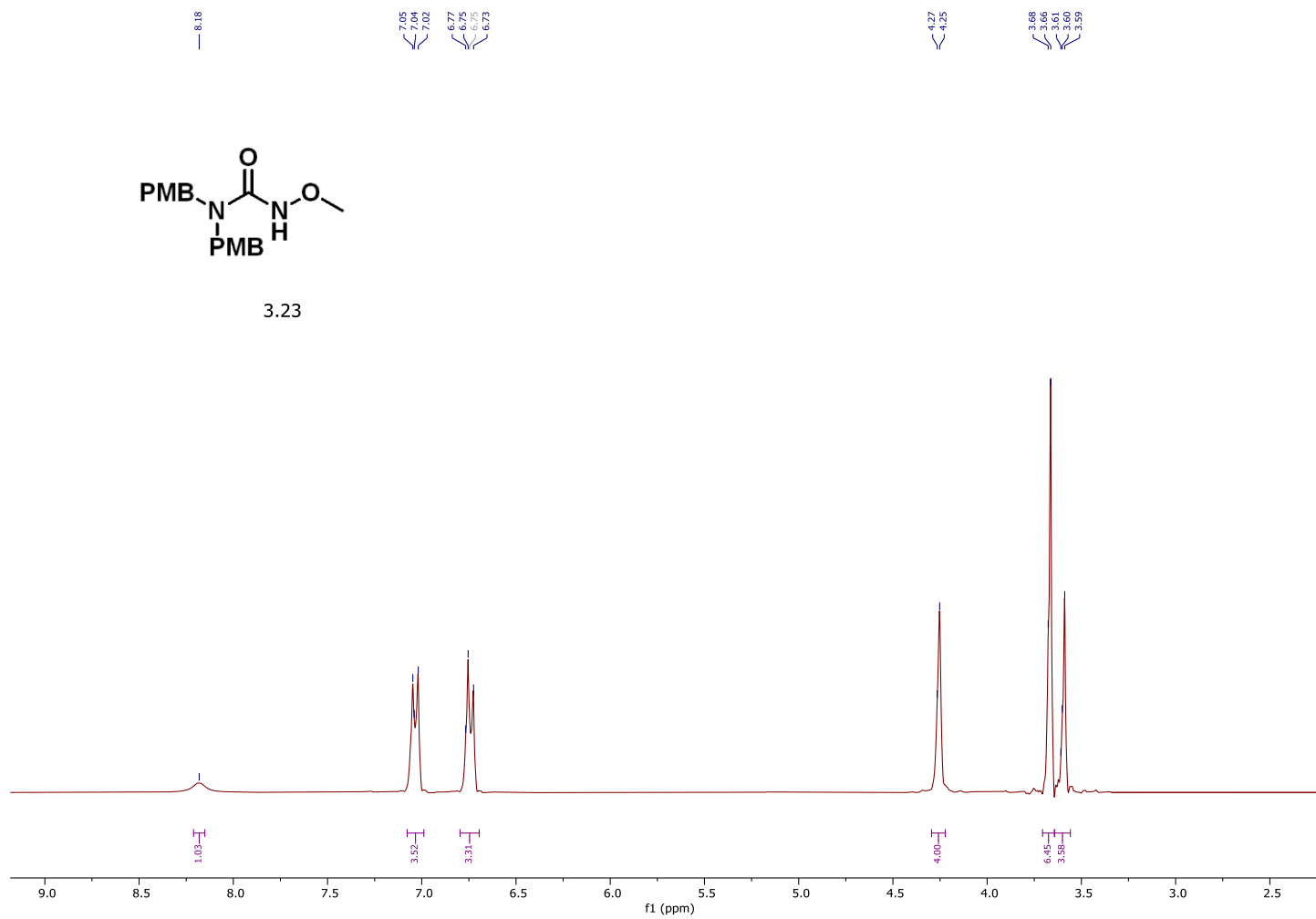


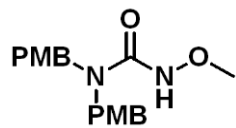




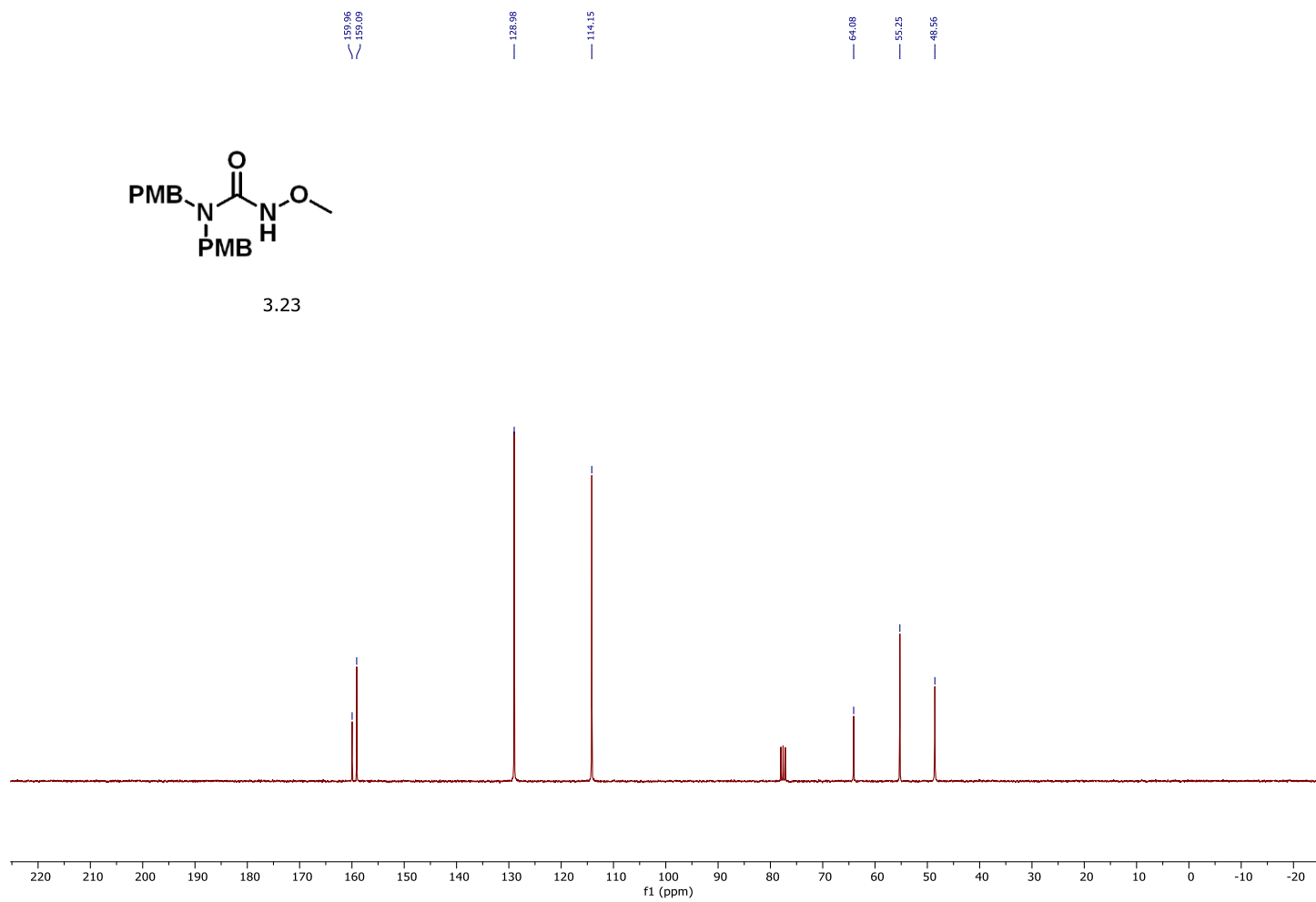


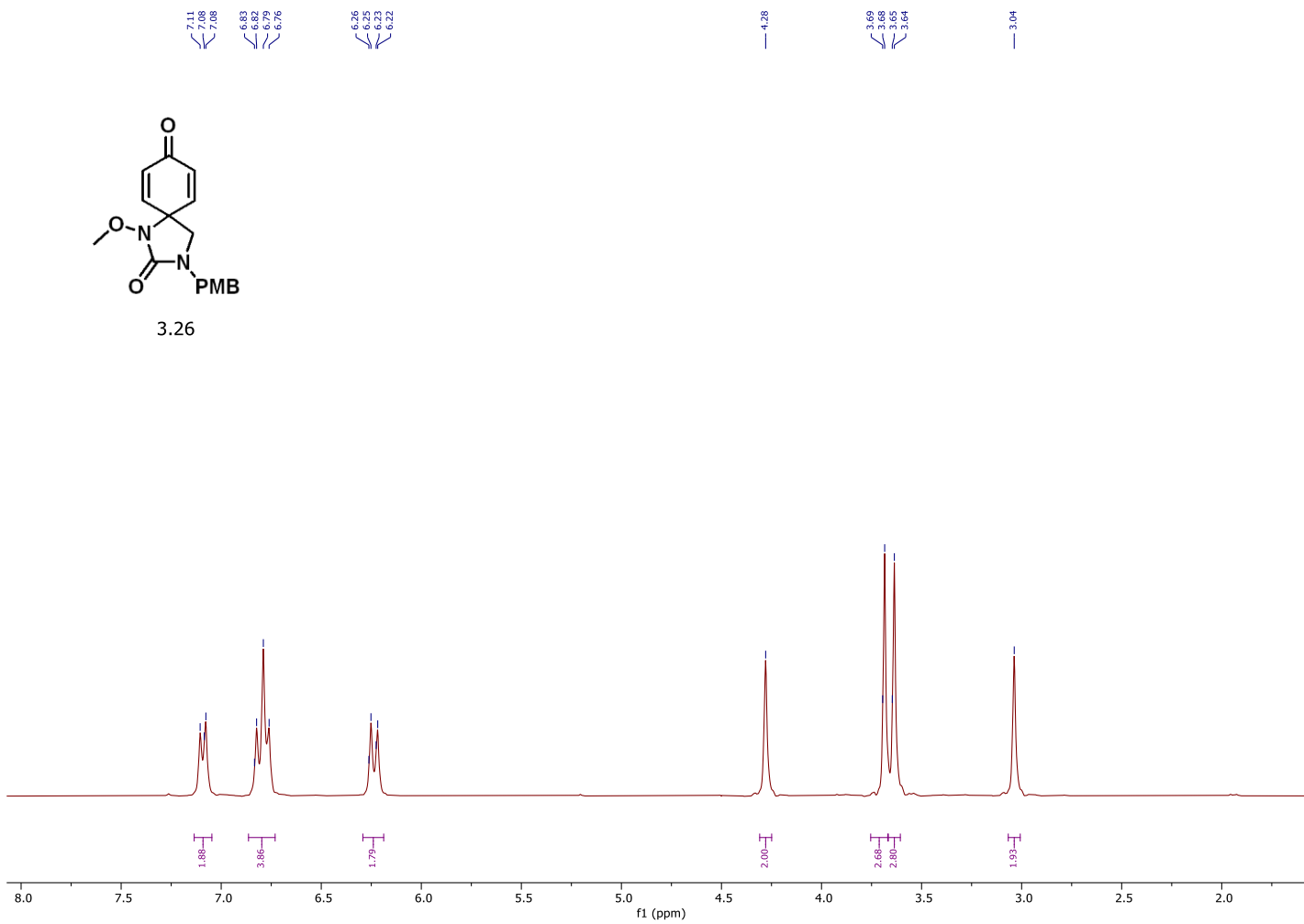
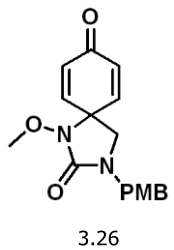
3.23

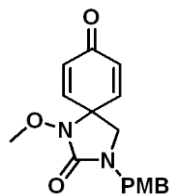




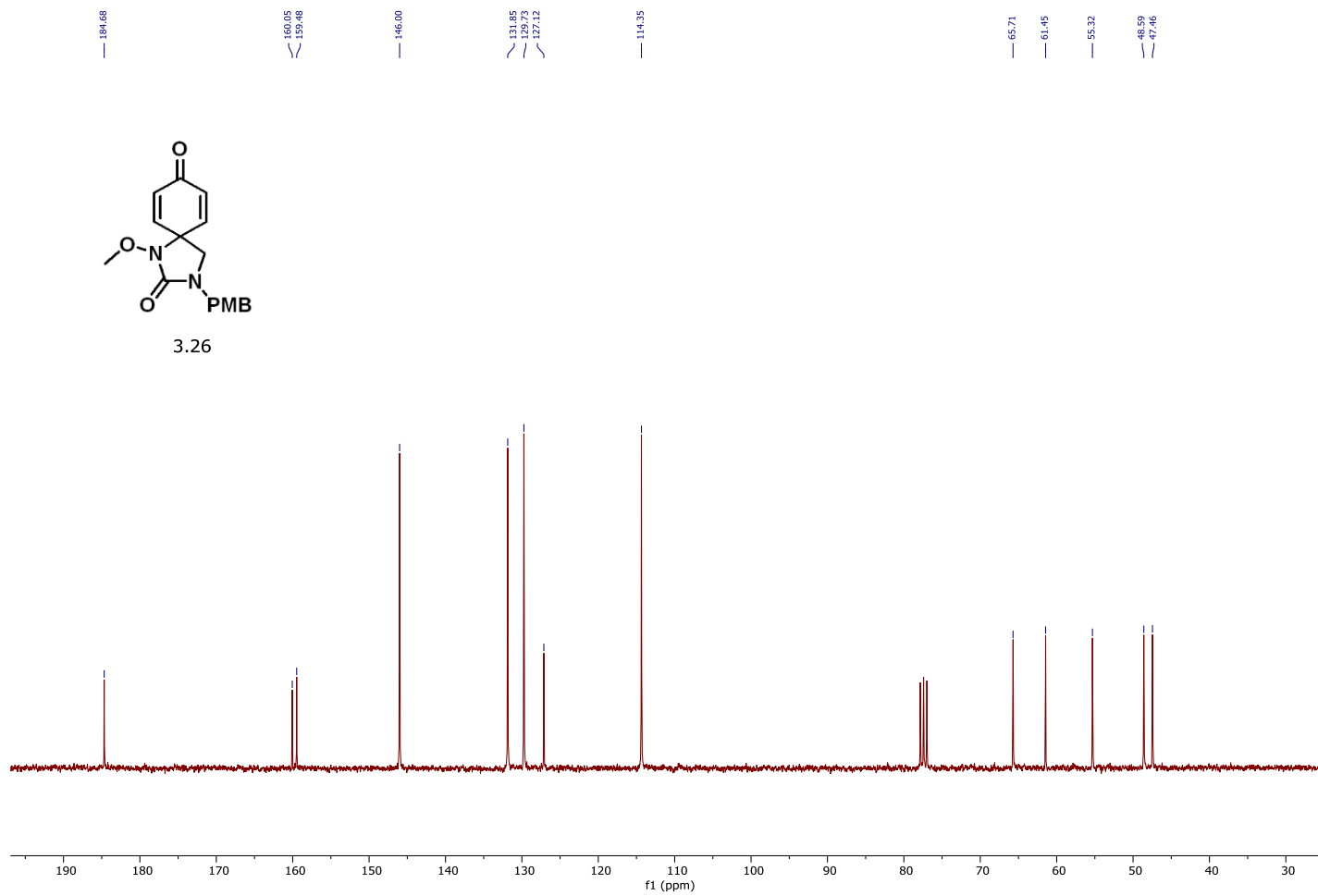
3.23

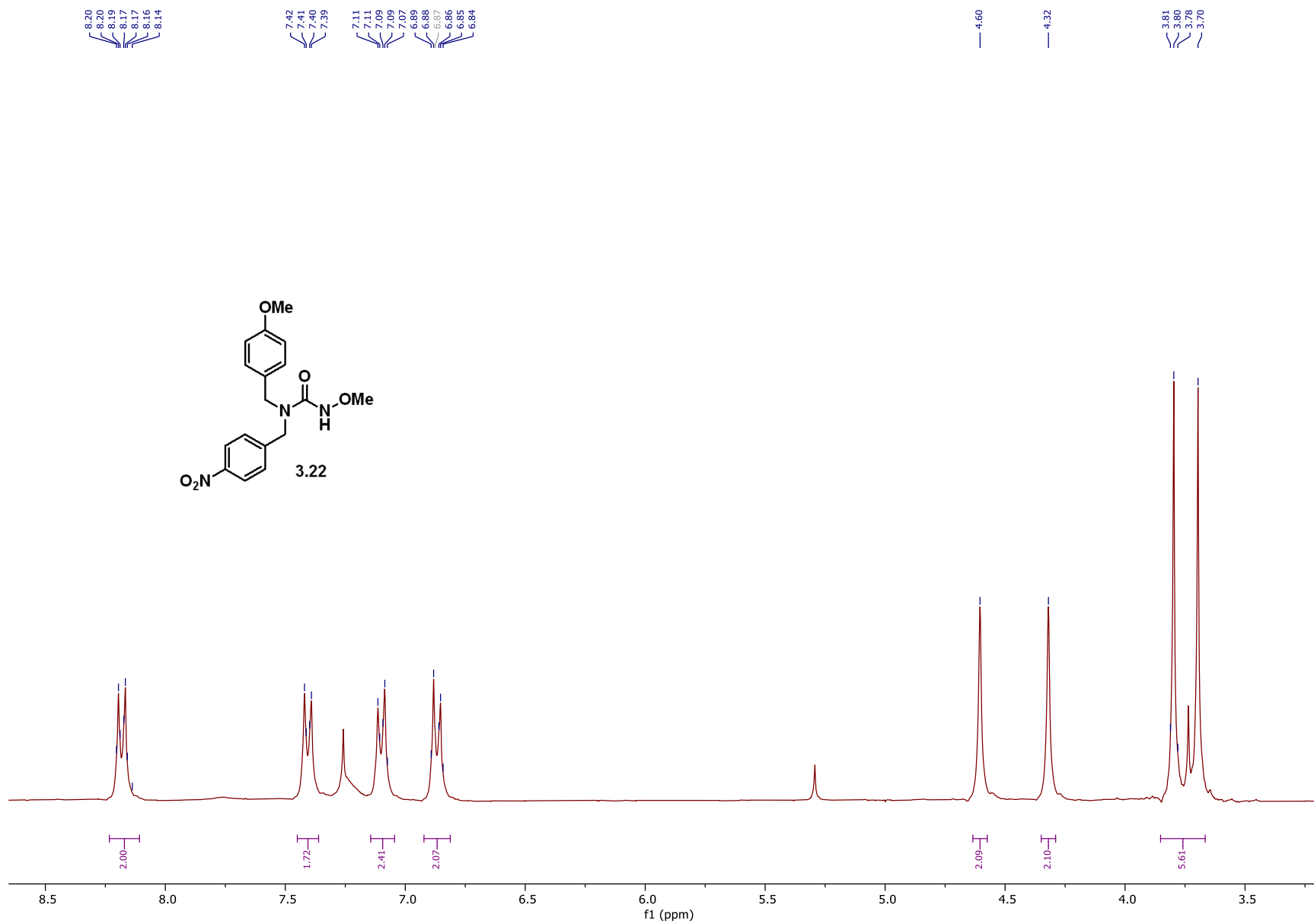


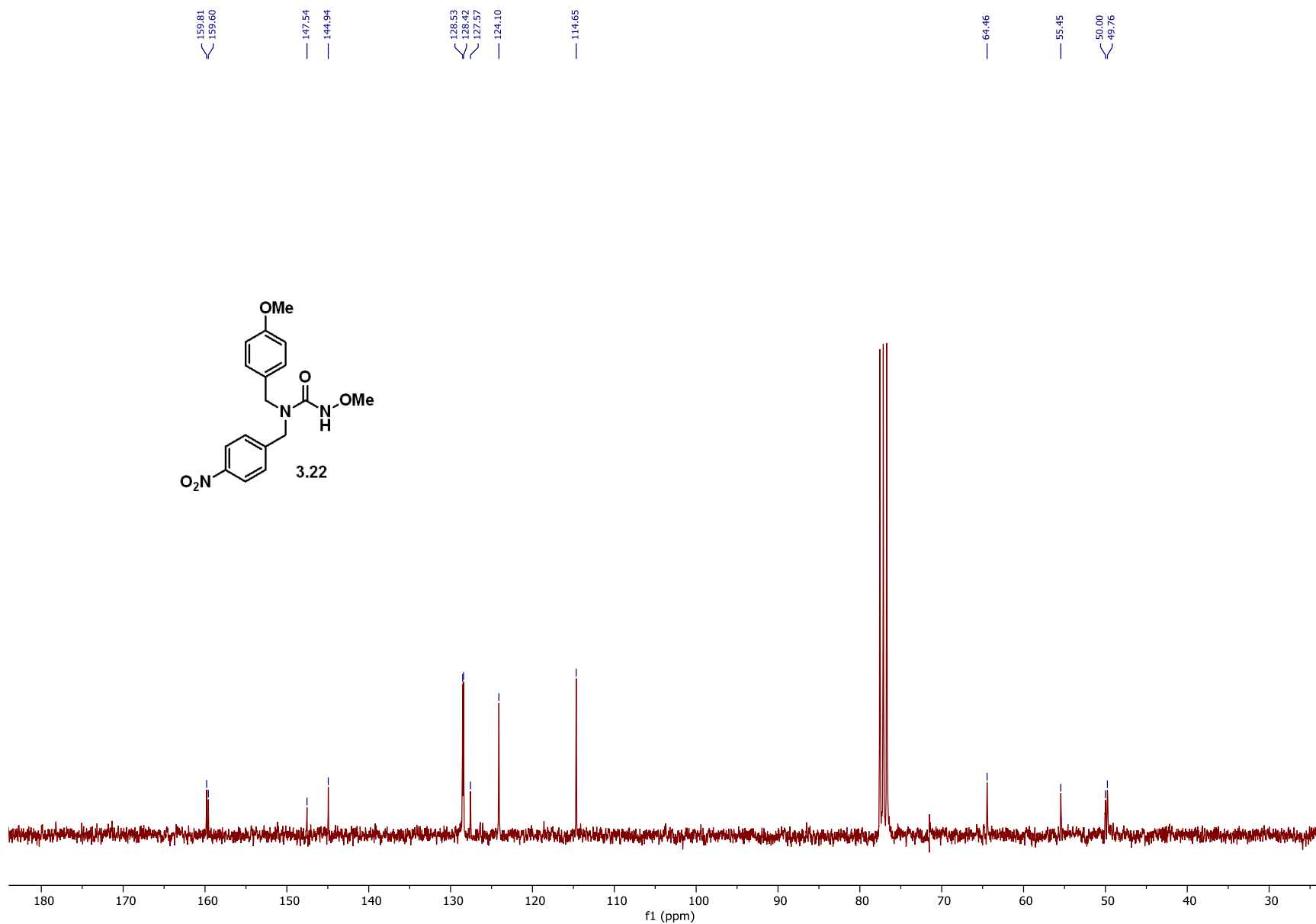
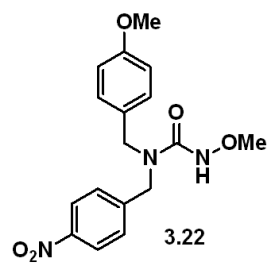


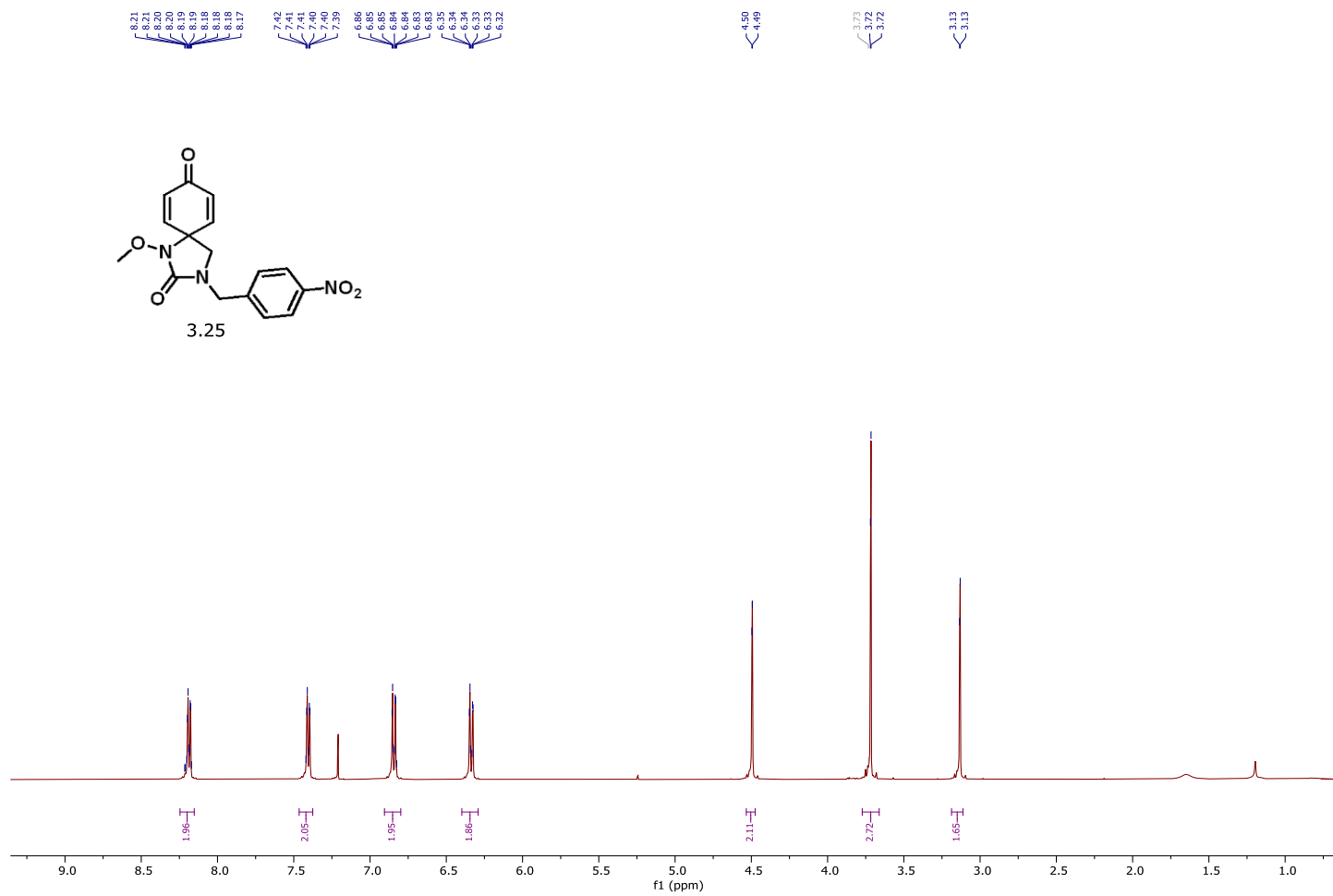


3.26

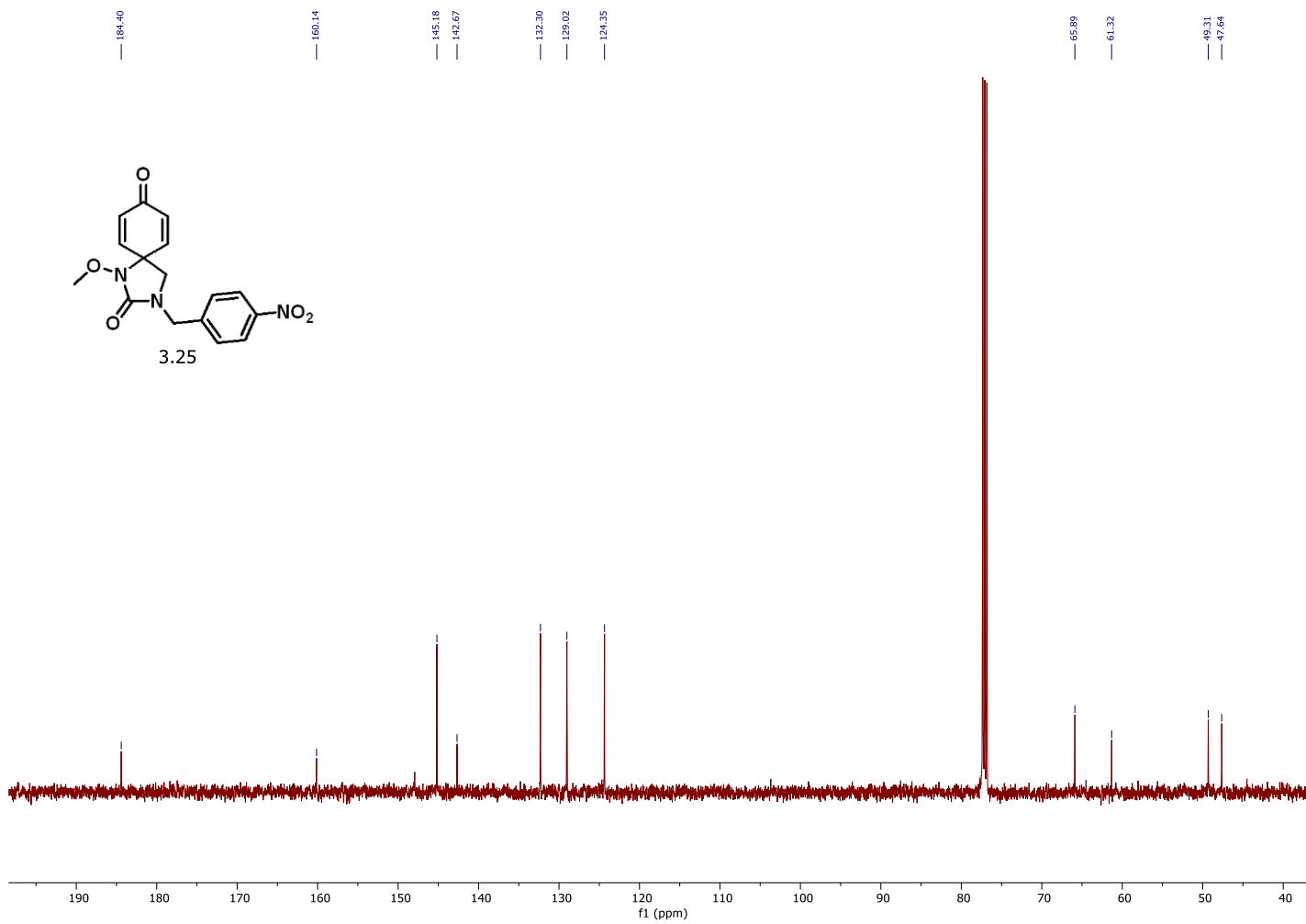
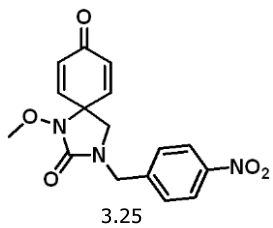












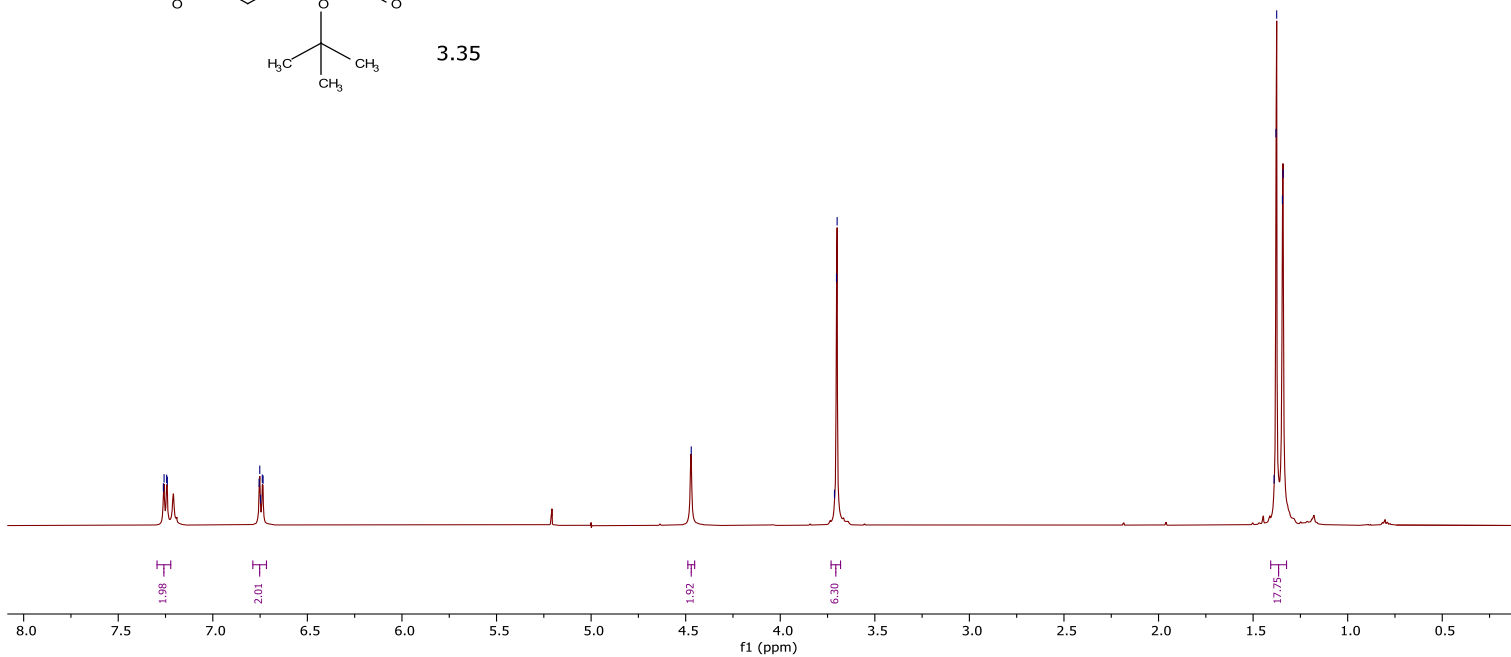
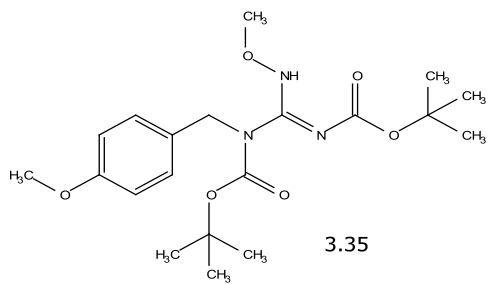
7.26  
7.26  
7.24  
7.24

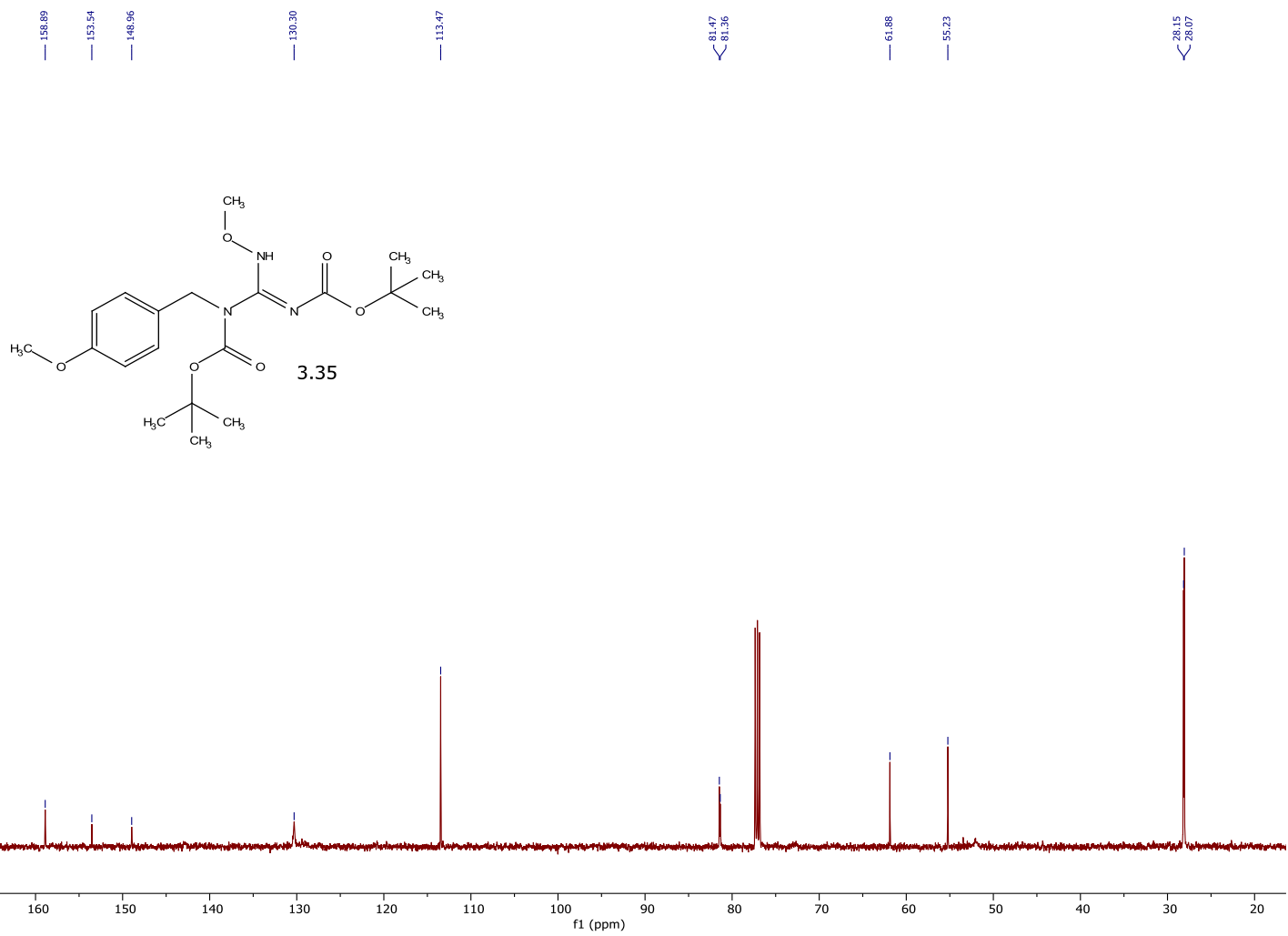
6.96  
6.95  
6.95  
6.94  
6.94  
6.93

4.47

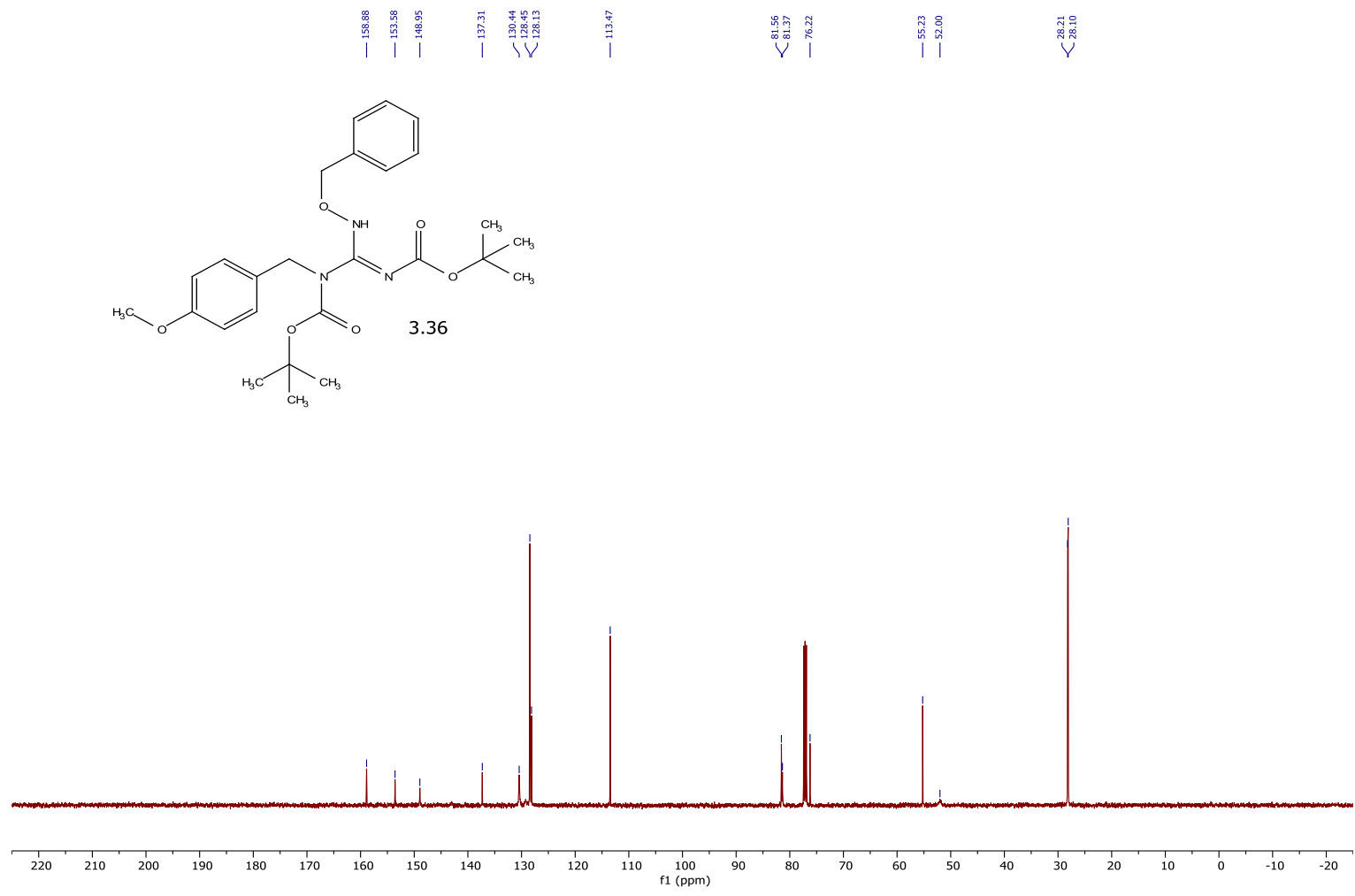
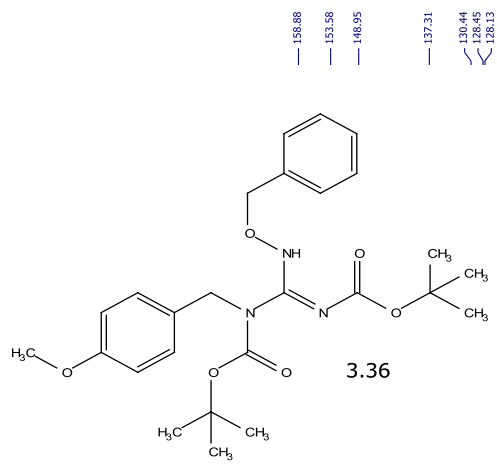
3.71  
3.70  
3.70

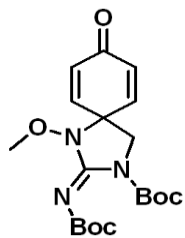
1.39  
1.38  
1.38  
1.35  
1.34



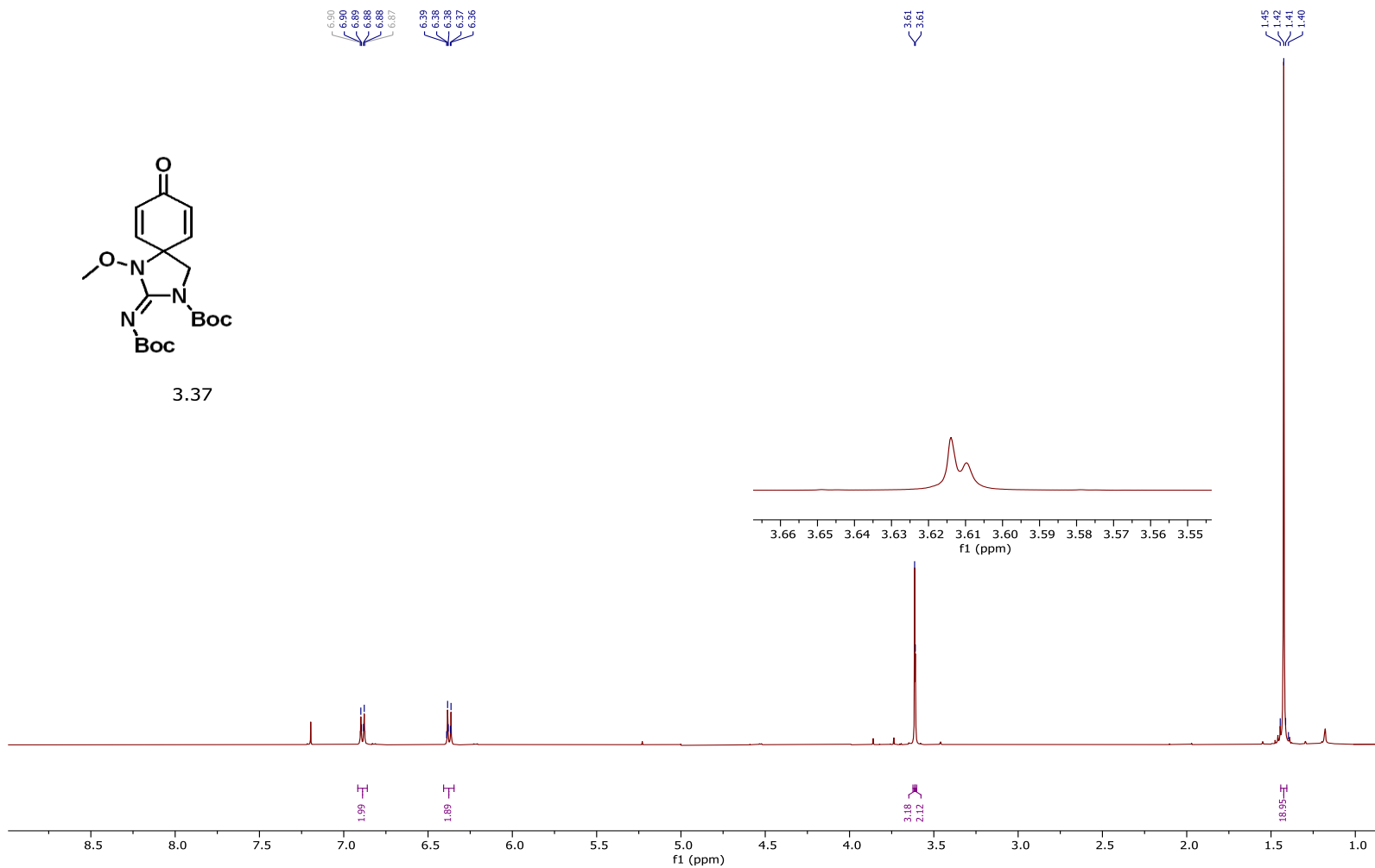


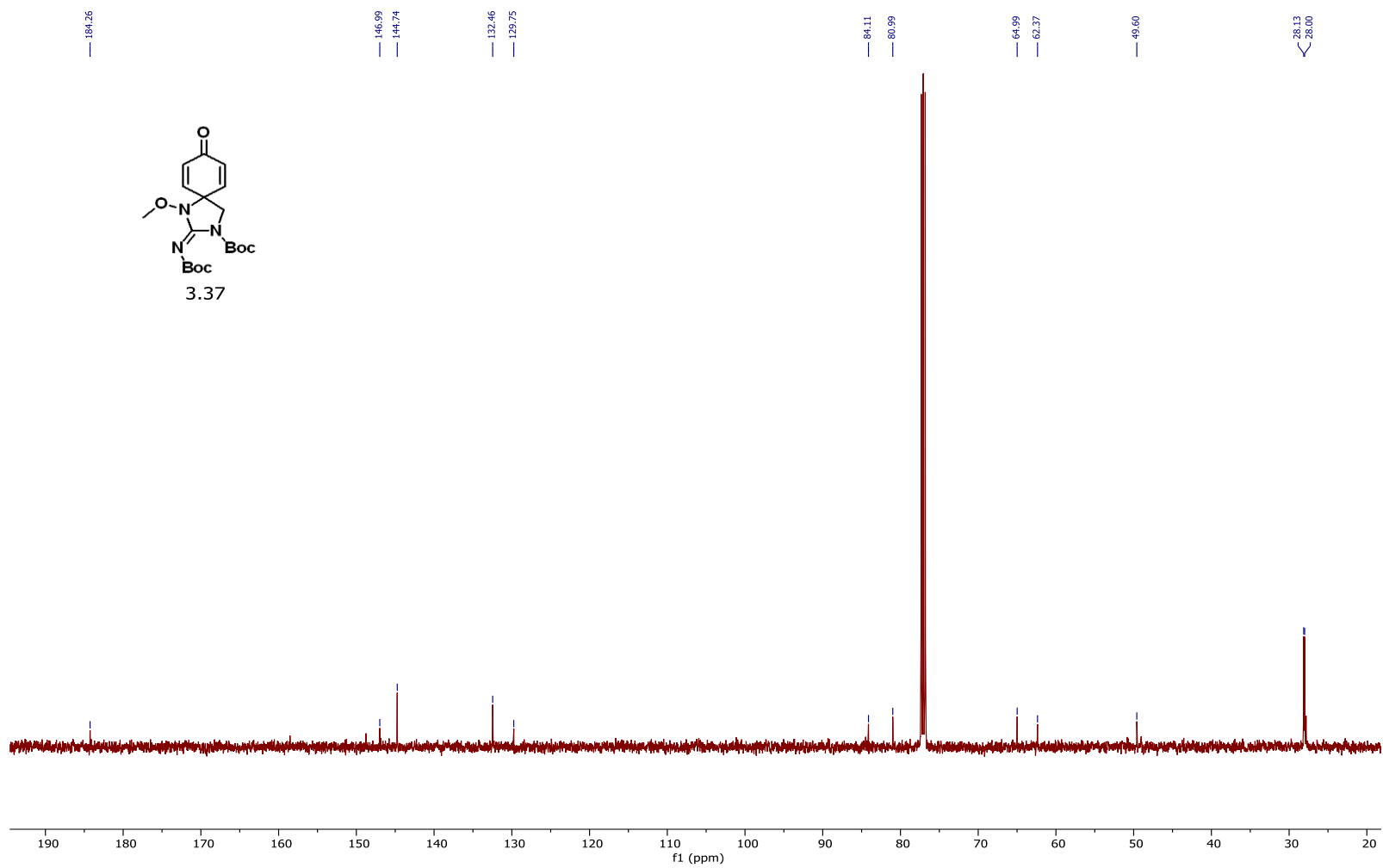


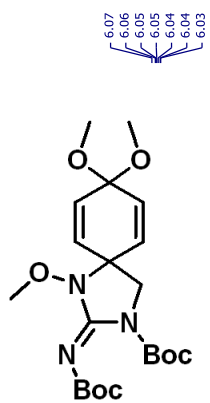




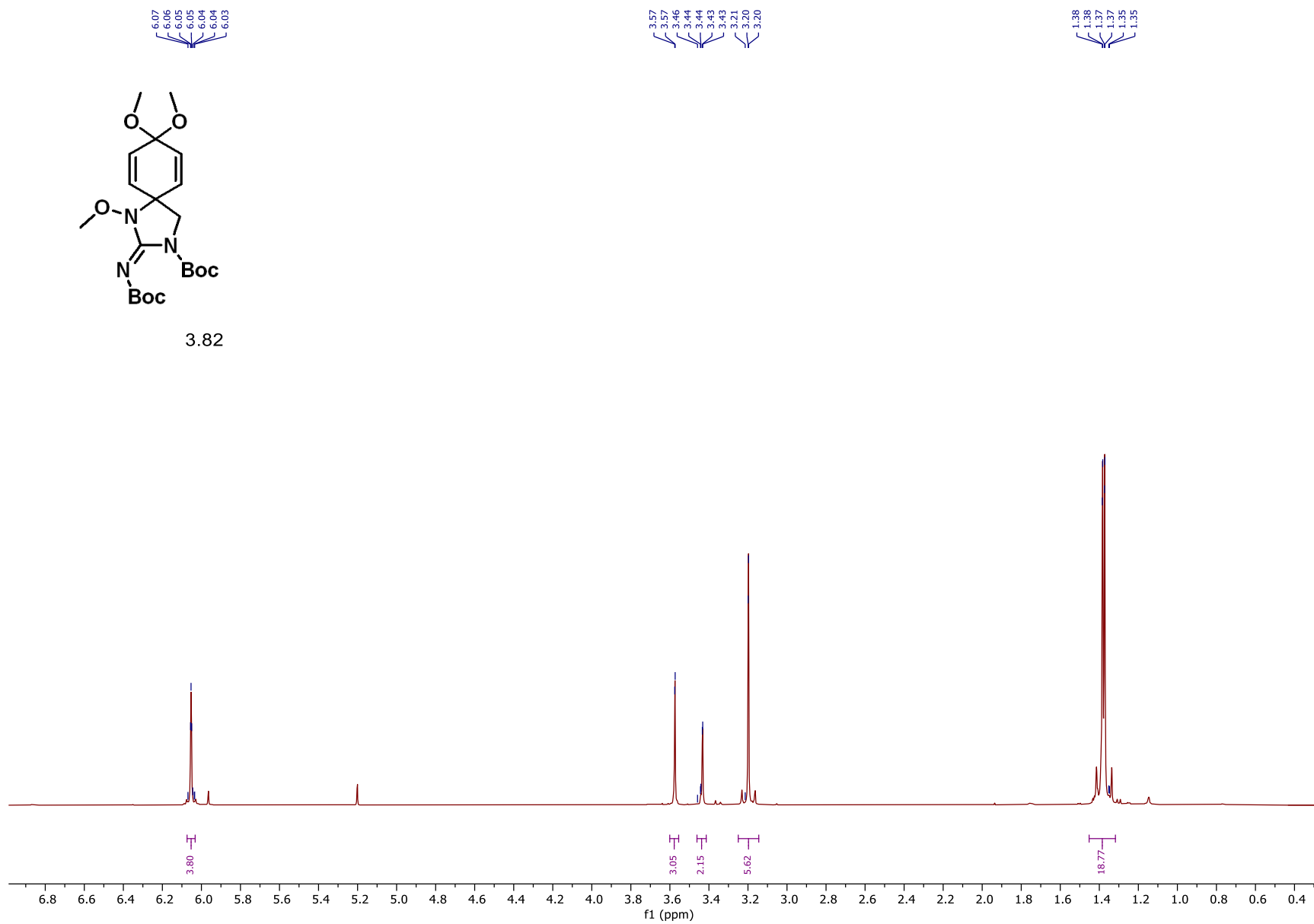
3.37



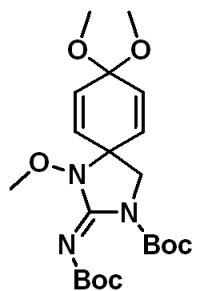




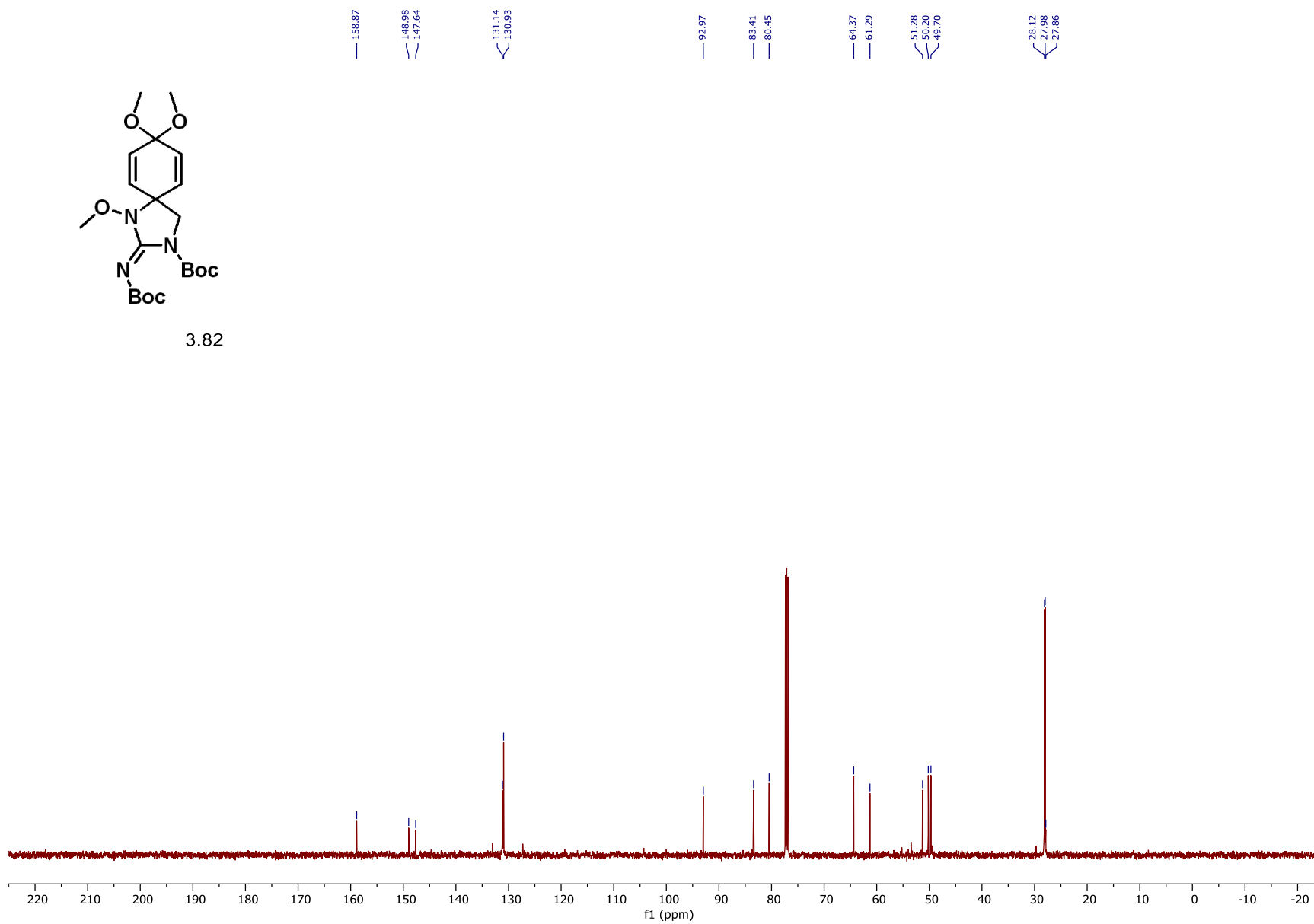
3.82

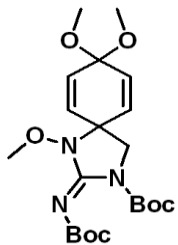






3.82





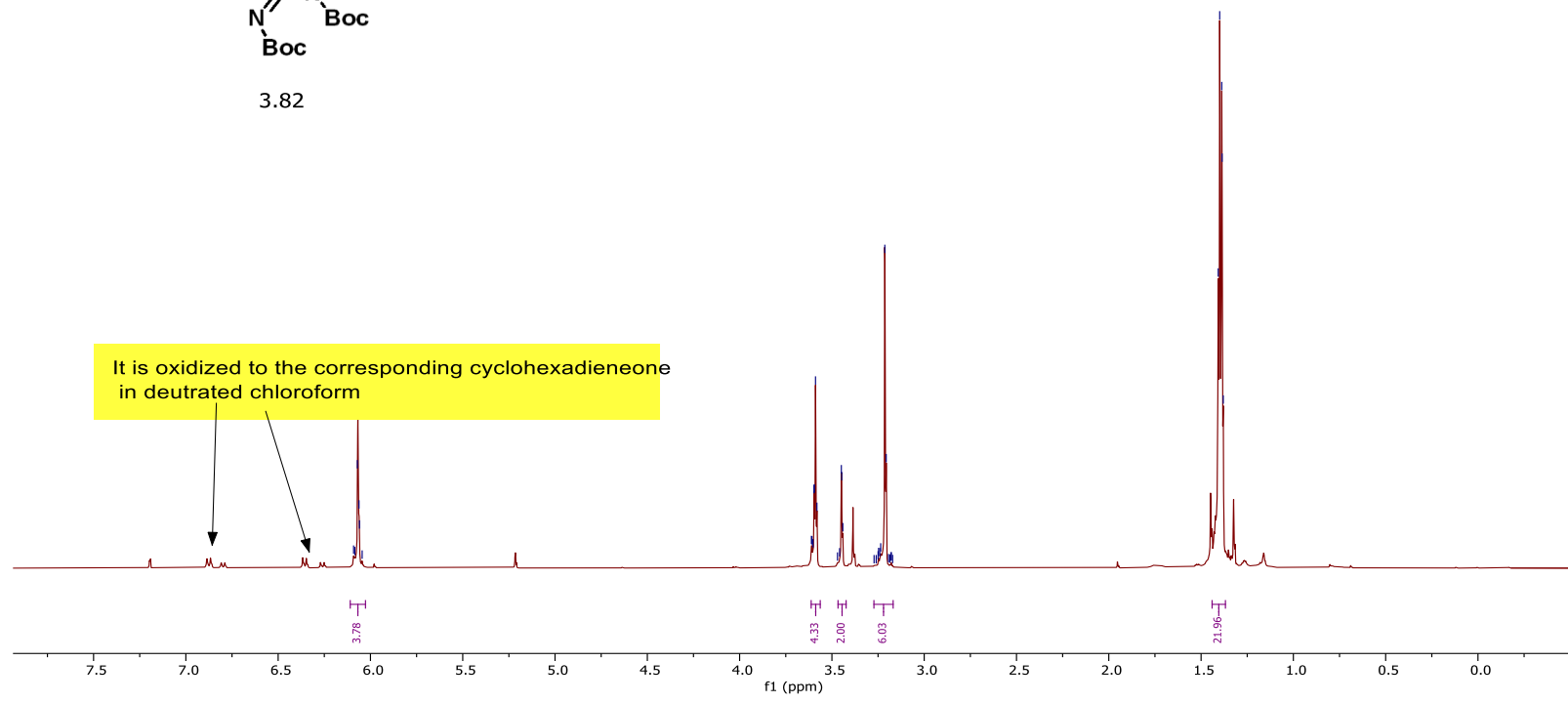
3.82

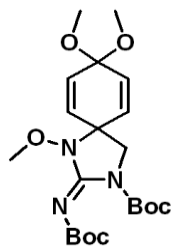
6.09  
6.08  
6.07  
6.06  
6.06  
6.04

3.61  
3.61  
3.60  
3.60  
3.59  
3.58  
3.46  
3.46  
3.45  
3.44  
3.27  
3.26  
3.25  
3.25  
3.24  
3.24  
3.21  
3.21  
3.19  
3.18  
3.18  
3.17

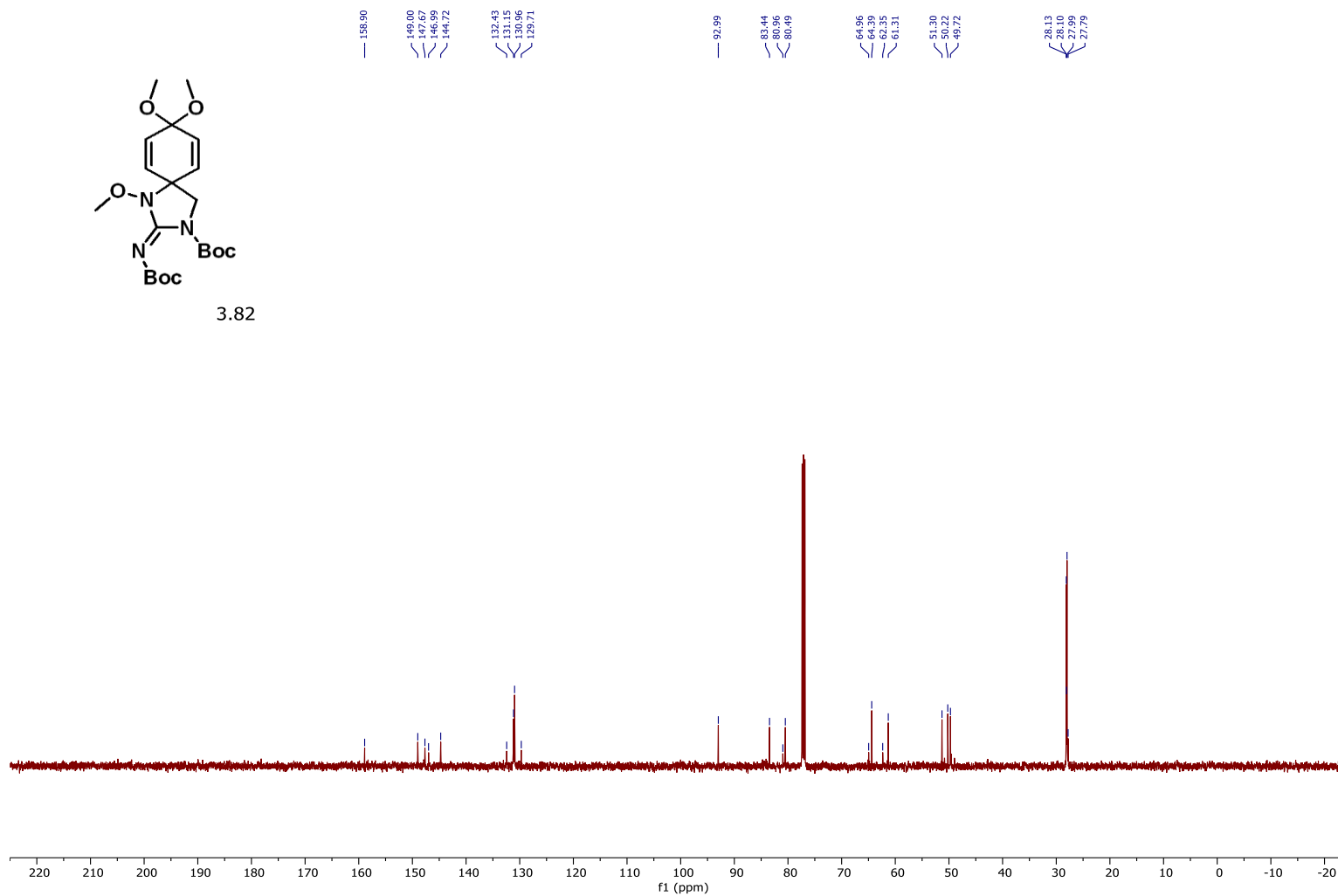
1.41  
1.40  
1.39  
1.38  
1.38

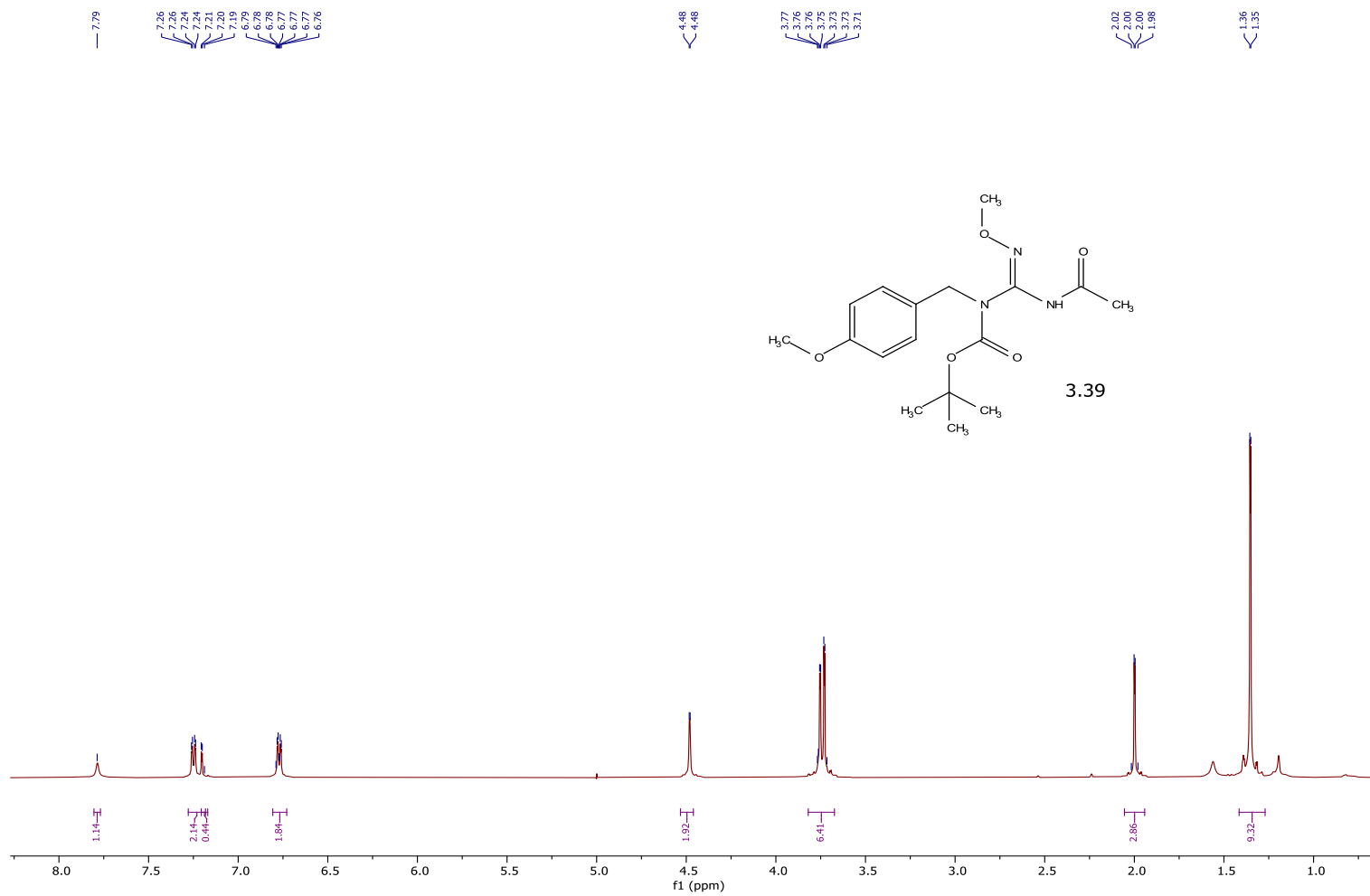
It is oxidized to the corresponding cyclohexadieneone in deuterated chloroform



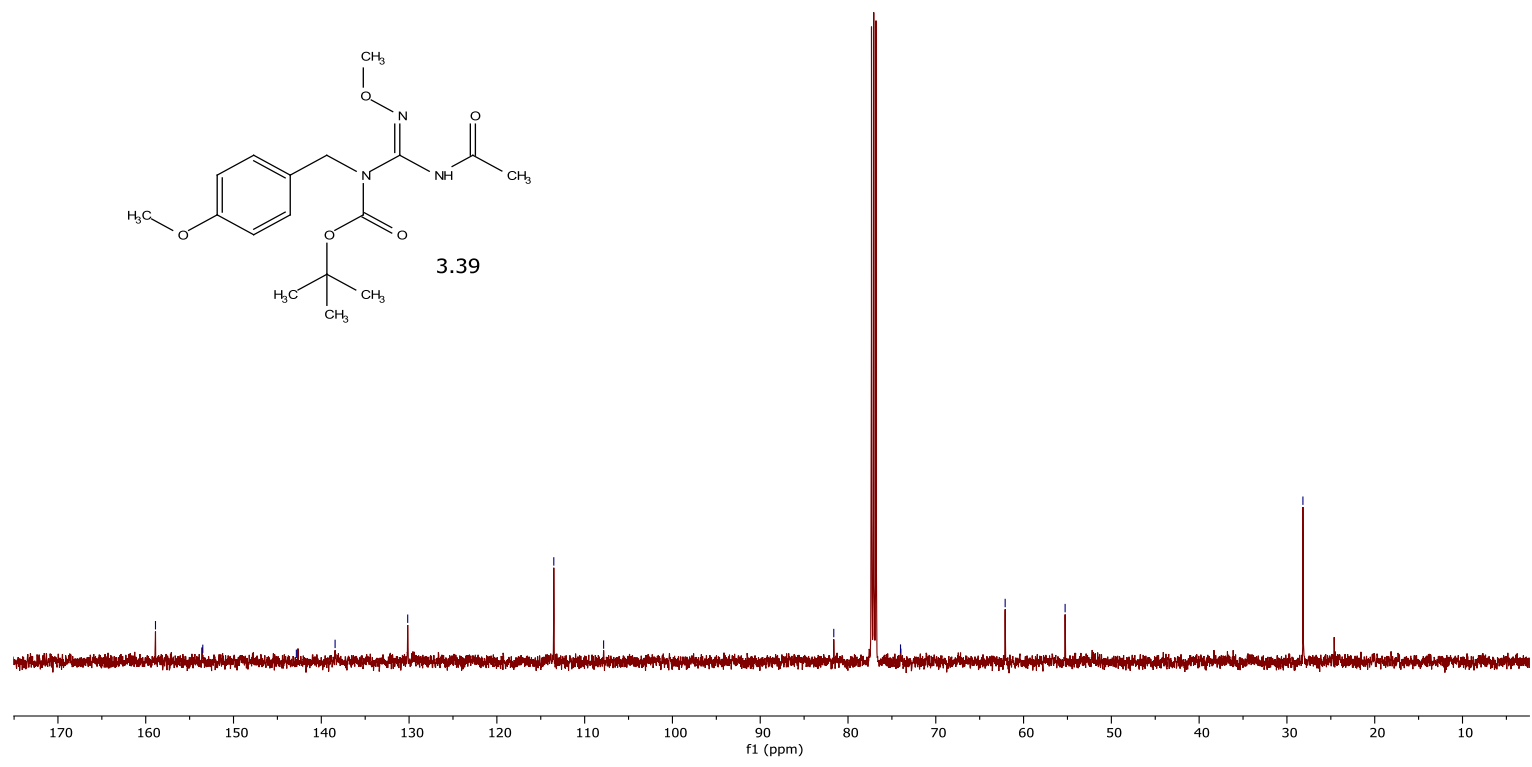
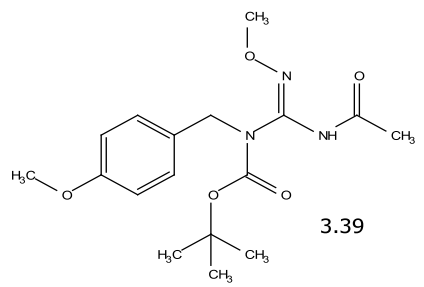


3.82





158.89  
153.50  
142.84  
138.43  
130.16  
113.52  
107.84  
81.62  
74.02  
62.10  
55.27  
28.18

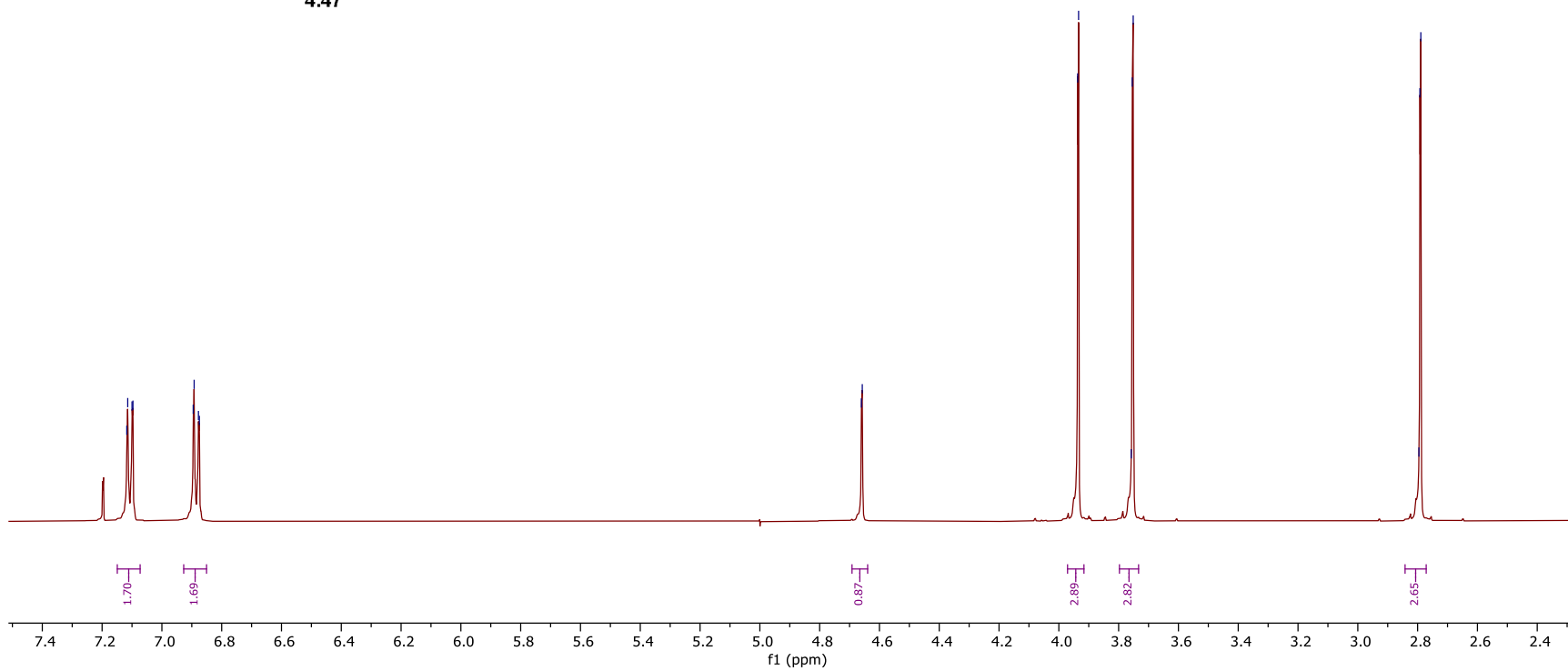
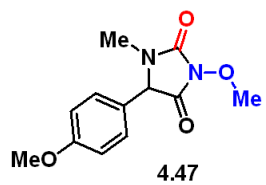


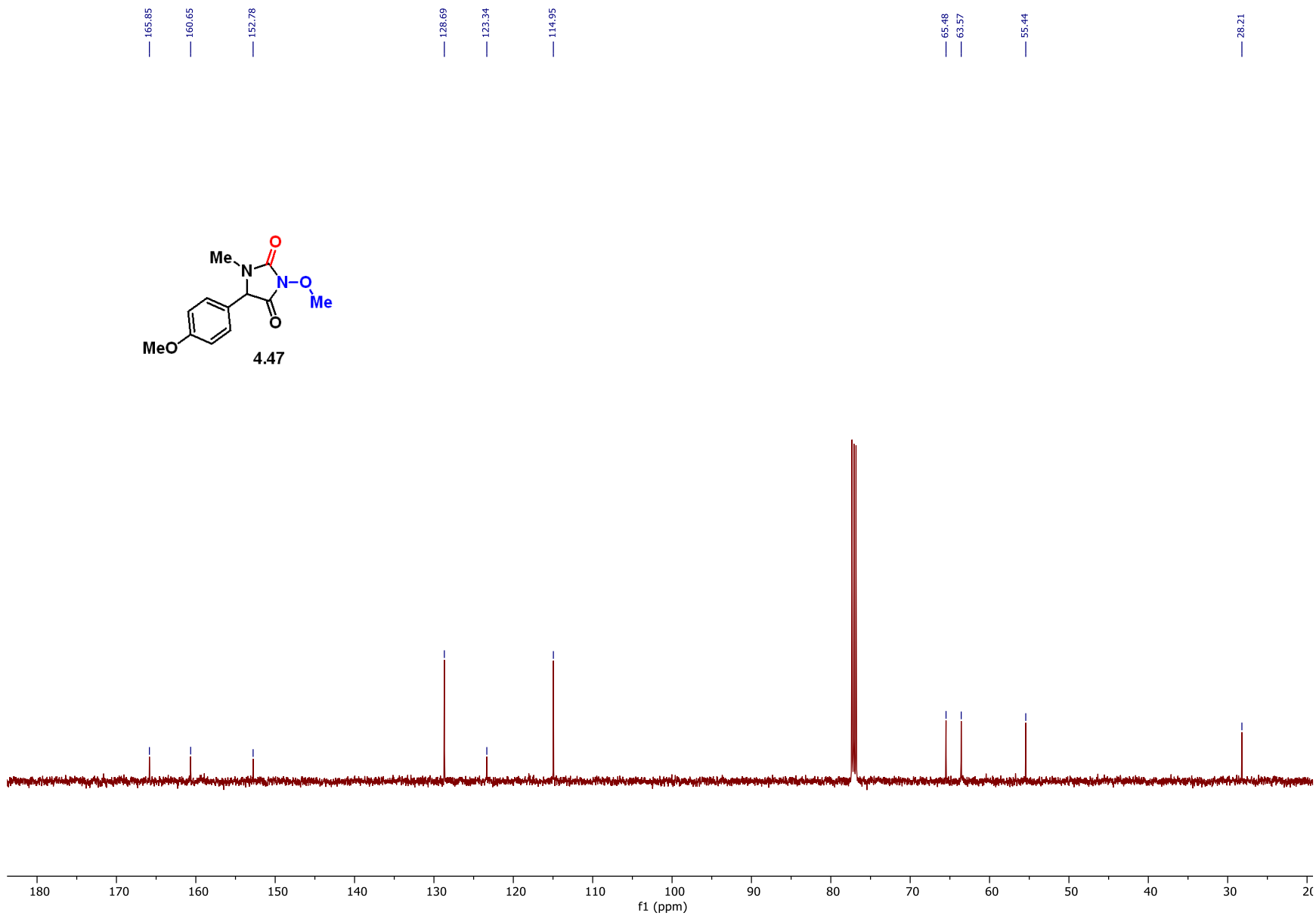
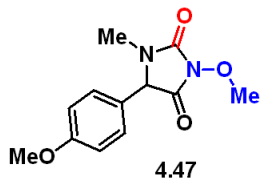
7.12  
7.11  
7.10  
7.10  
6.90  
6.89  
6.88  
6.87

4.66  
4.66

3.94  
3.93  
3.76  
3.75  
3.75

2.80  
2.79  
2.79



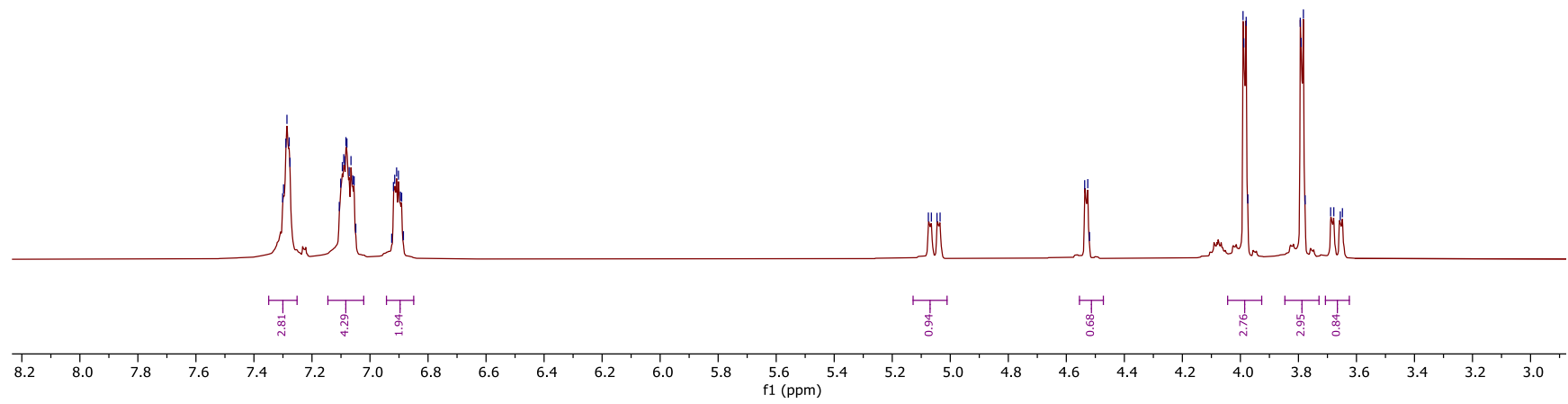
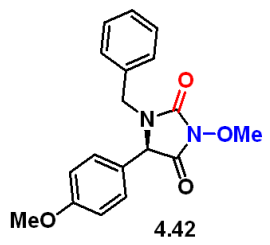


7.30  
7.30  
7.29  
7.29  
7.28  
7.28  
7.11  
7.11  
7.10  
7.10  
7.09  
7.09  
7.08  
7.08  
7.07  
7.06  
7.05  
6.93  
6.92  
6.91  
6.90  
6.90  
6.89  
6.88

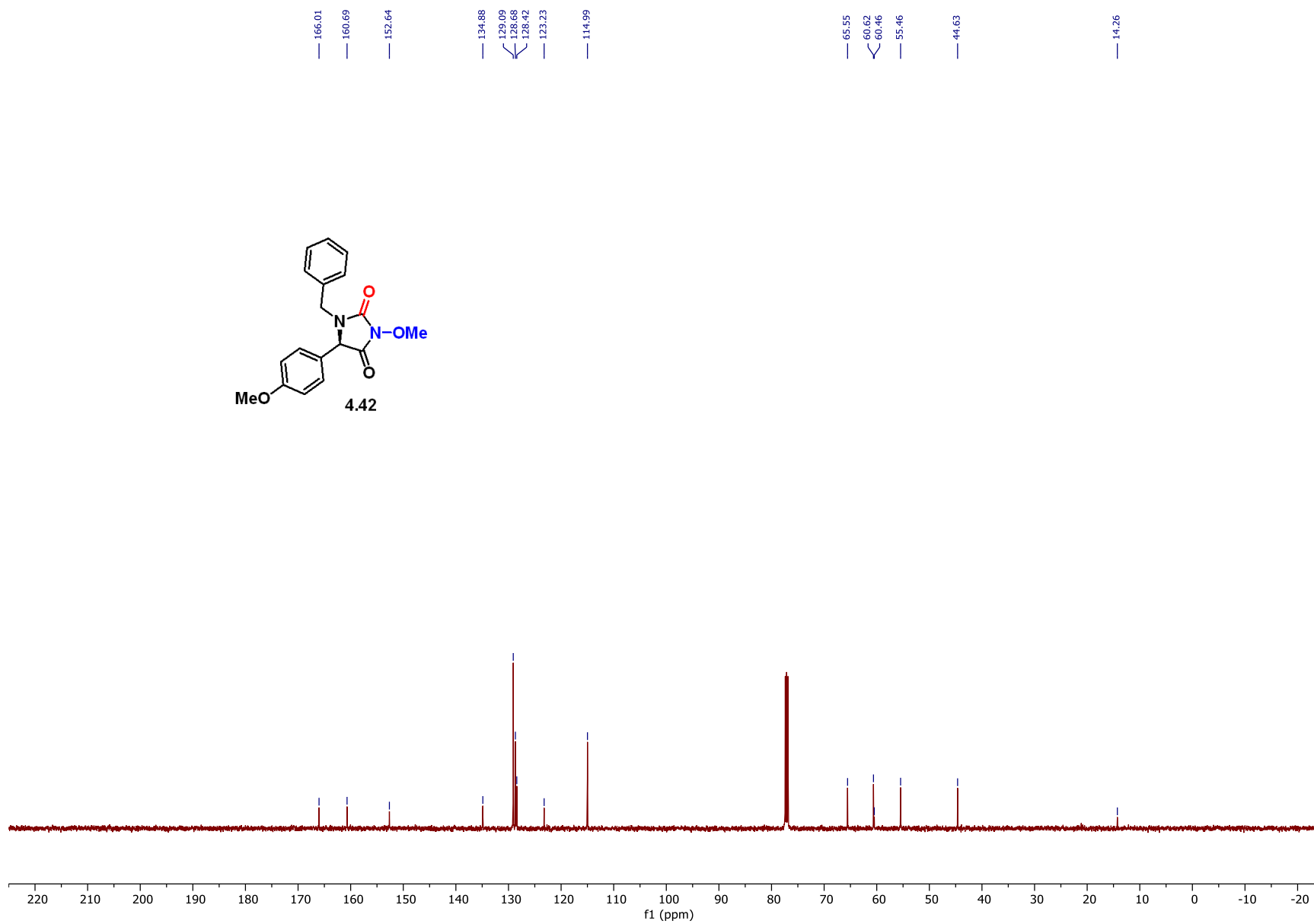
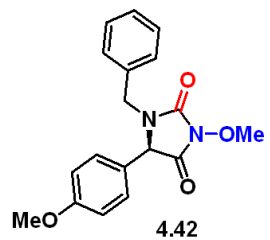
5.08  
5.07  
5.05  
5.04

4.54  
4.53  
4.52

3.99  
3.99  
3.98  
3.97  
3.78  
3.78  
3.78  
3.69  
3.68  
3.66  
3.65





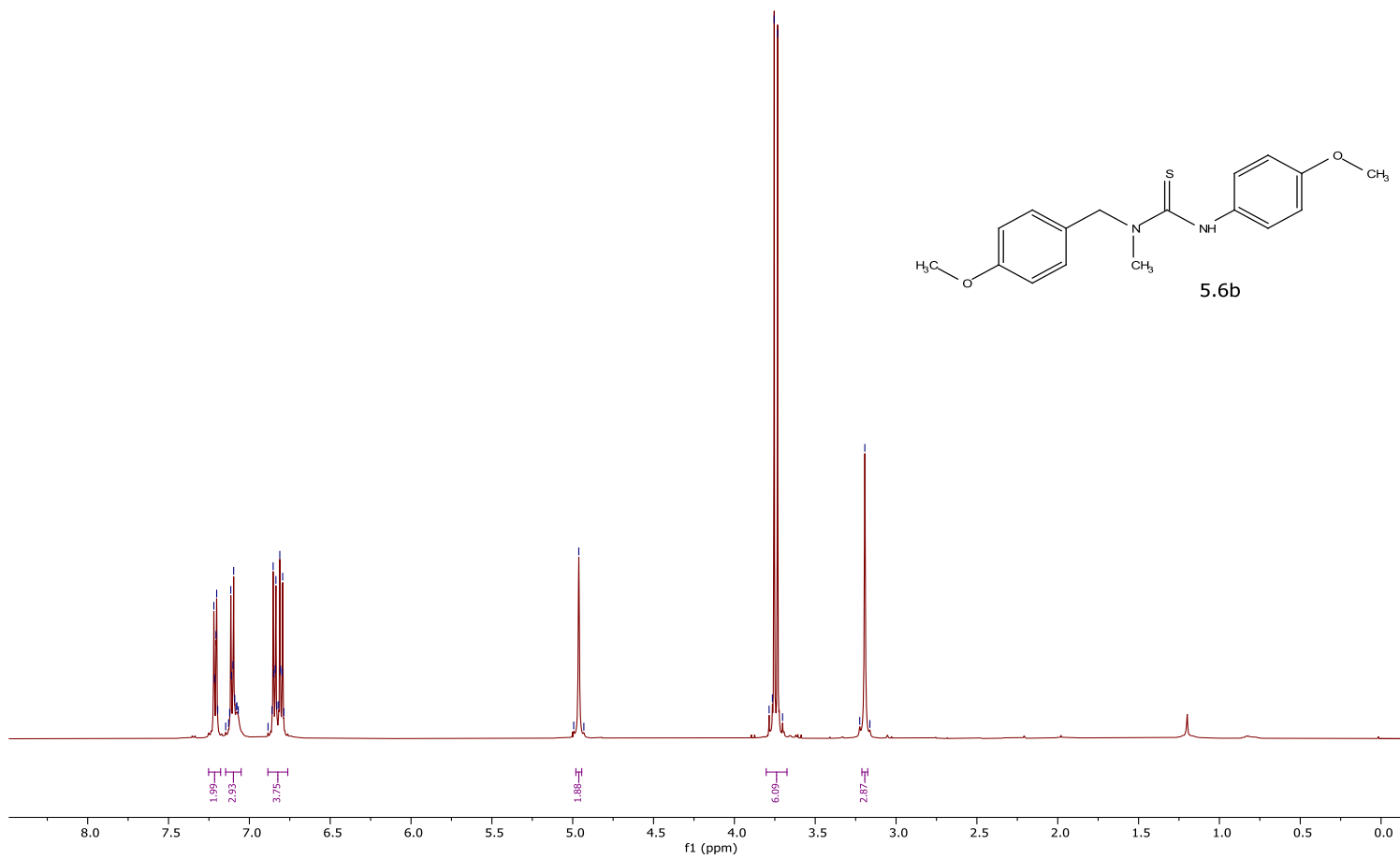
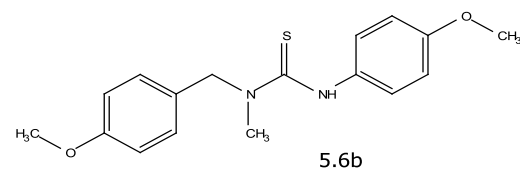


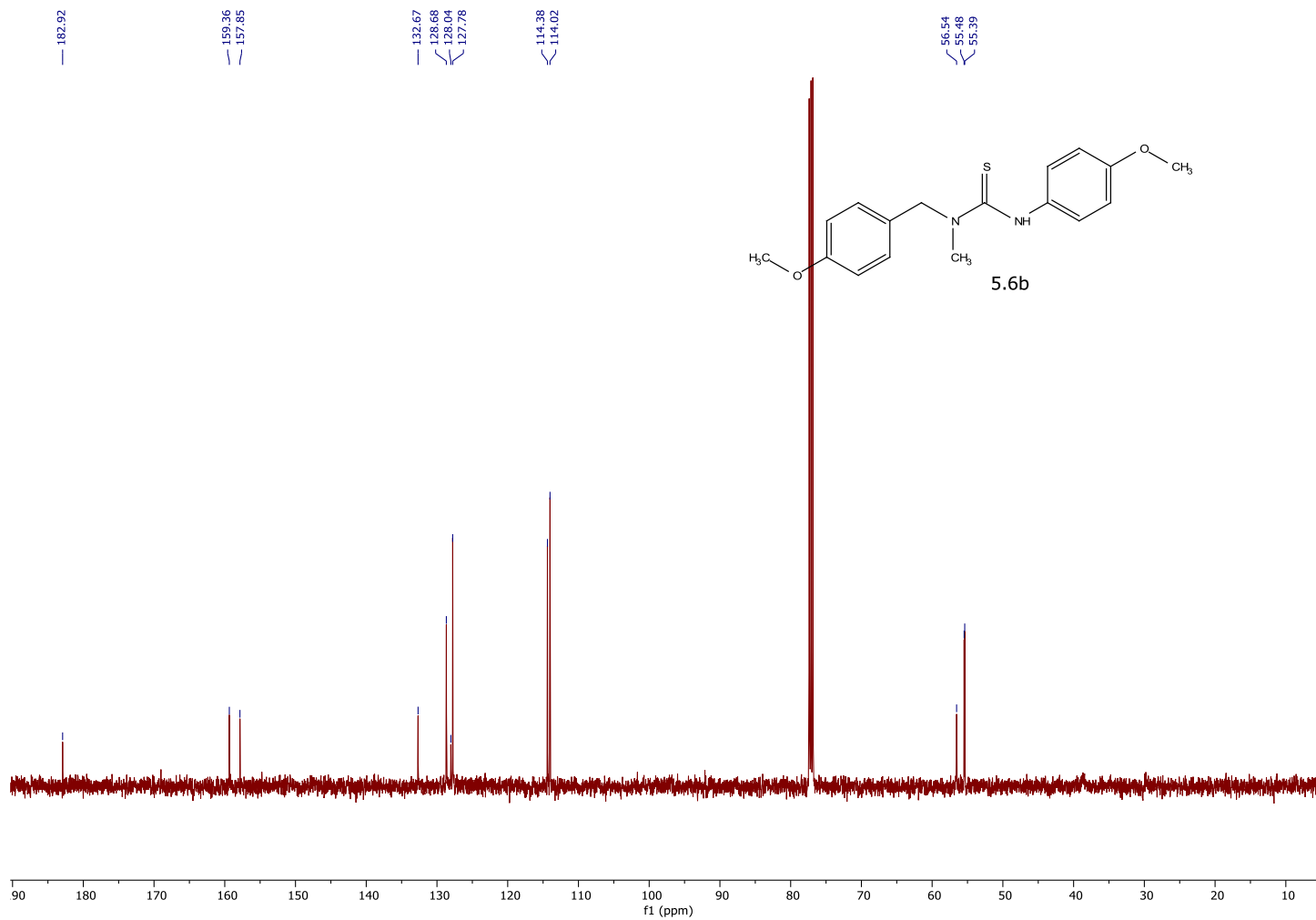
7.22  
7.22  
7.21  
7.20  
7.15  
7.13  
7.12  
7.11  
7.10  
7.10  
7.09  
7.08  
7.07  
6.88  
6.86  
6.85  
6.84  
6.84  
6.83  
6.82  
6.81  
6.81  
6.80  
6.79

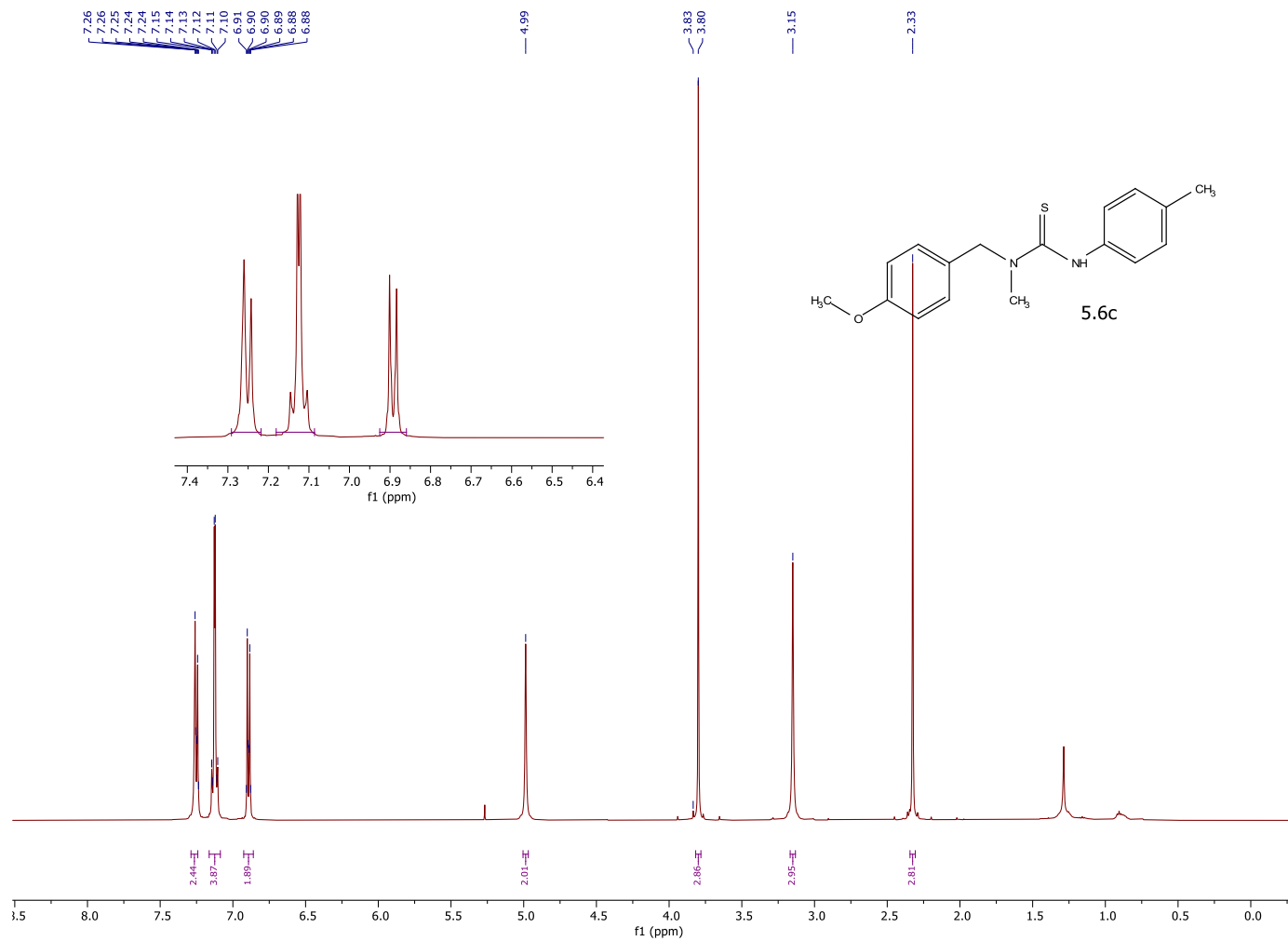
4.99  
4.96  
4.93

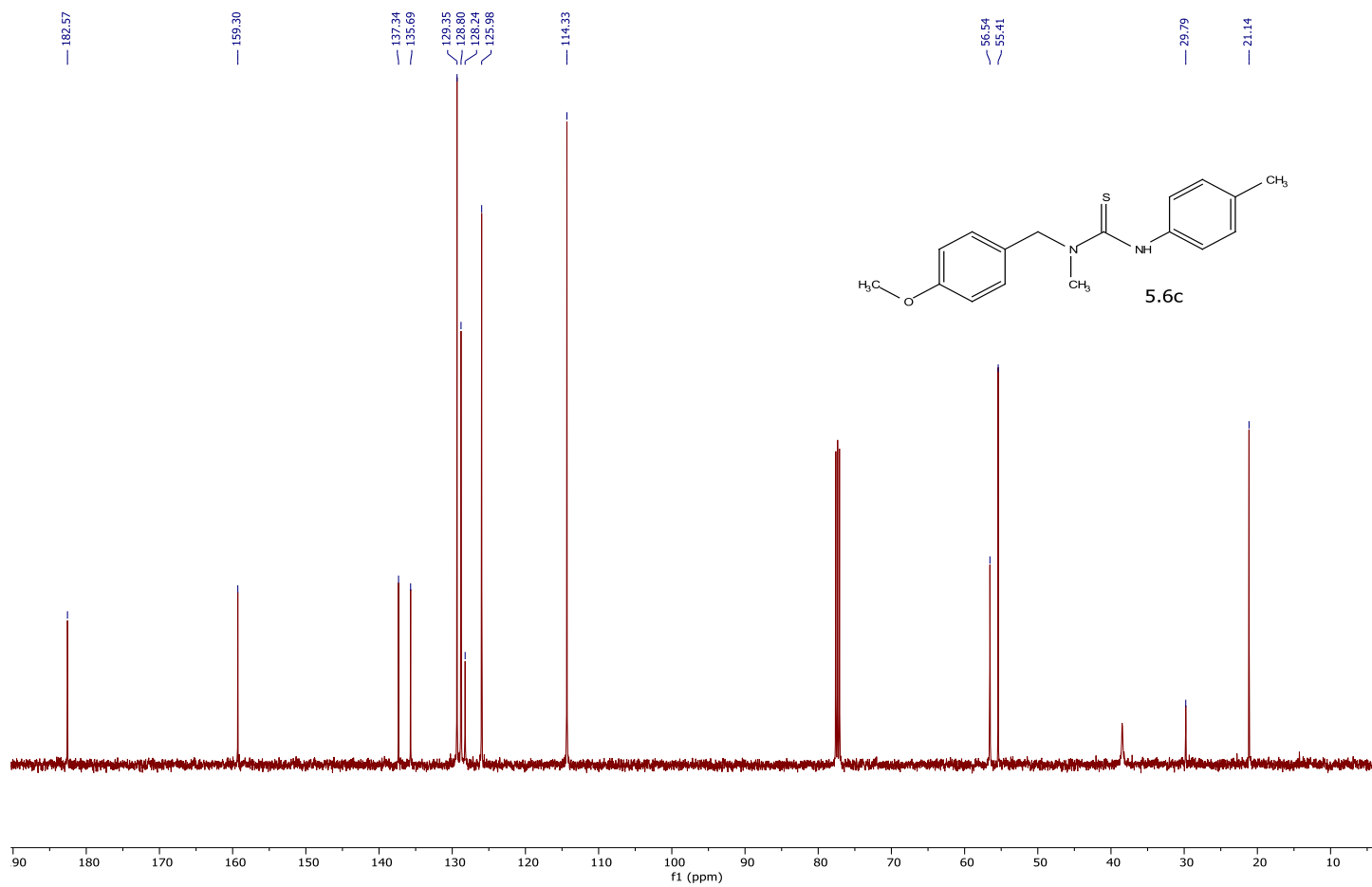
3.79  
3.76  
3.75  
3.73  
3.70

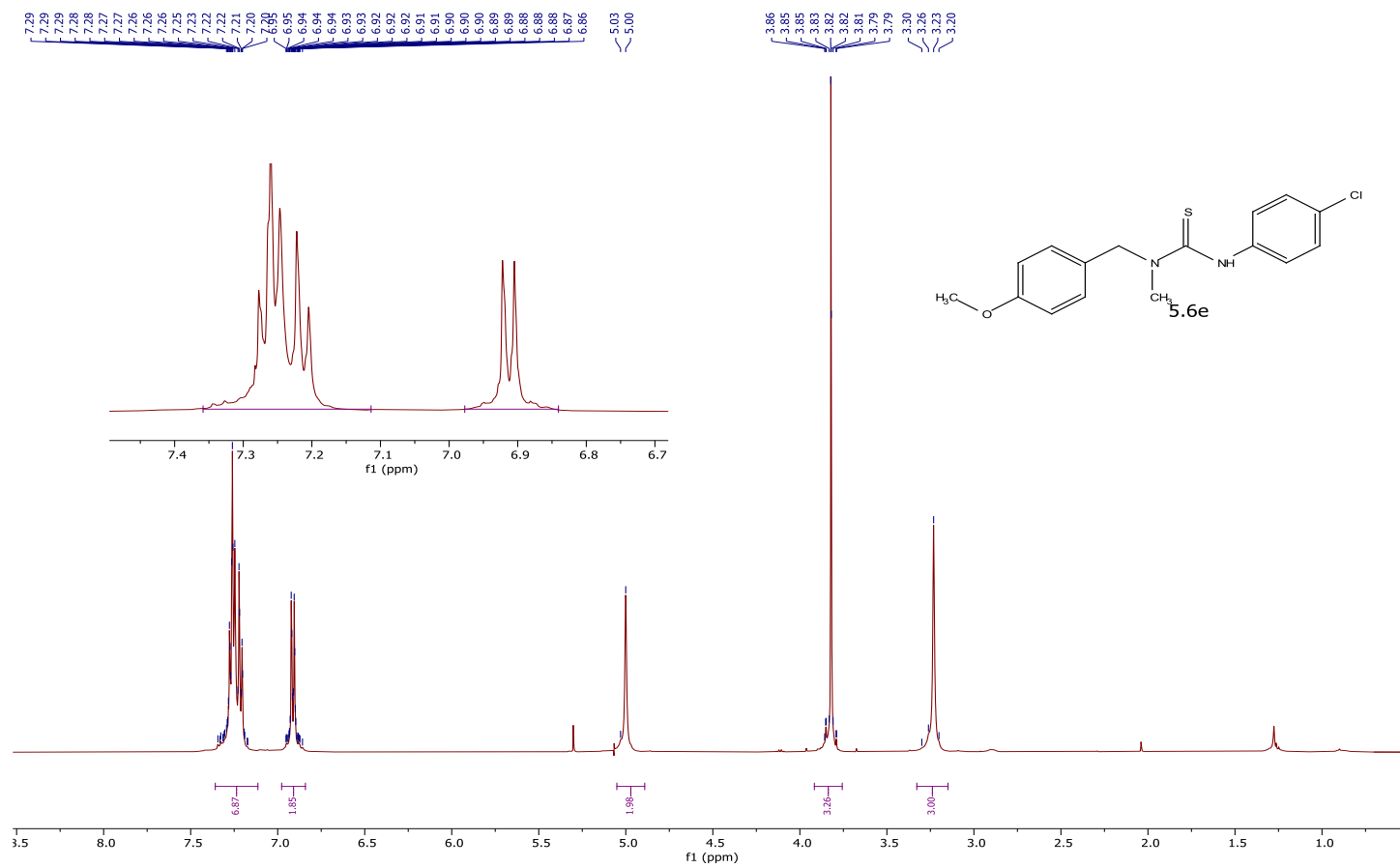
3.22  
3.19  
3.16

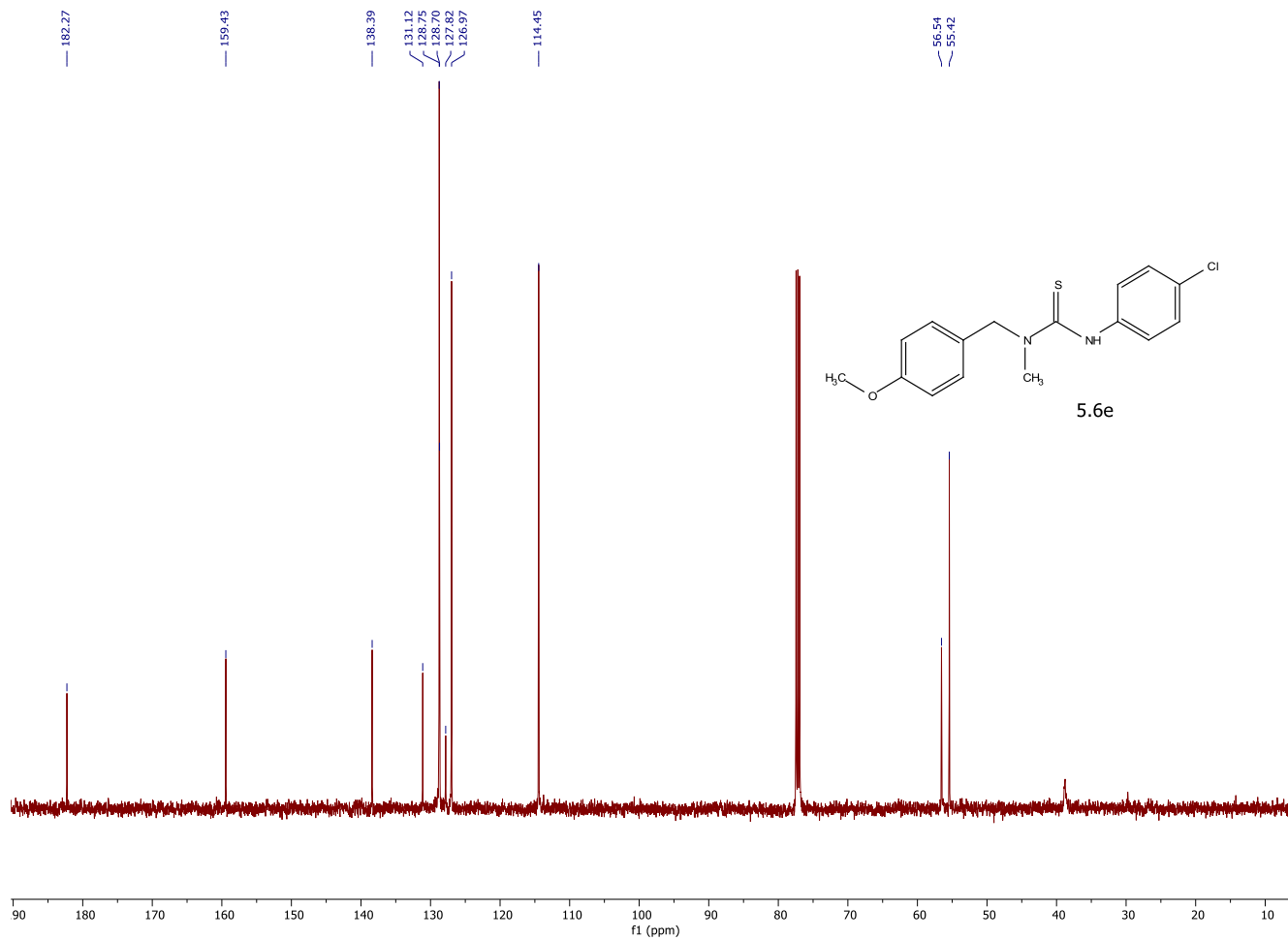












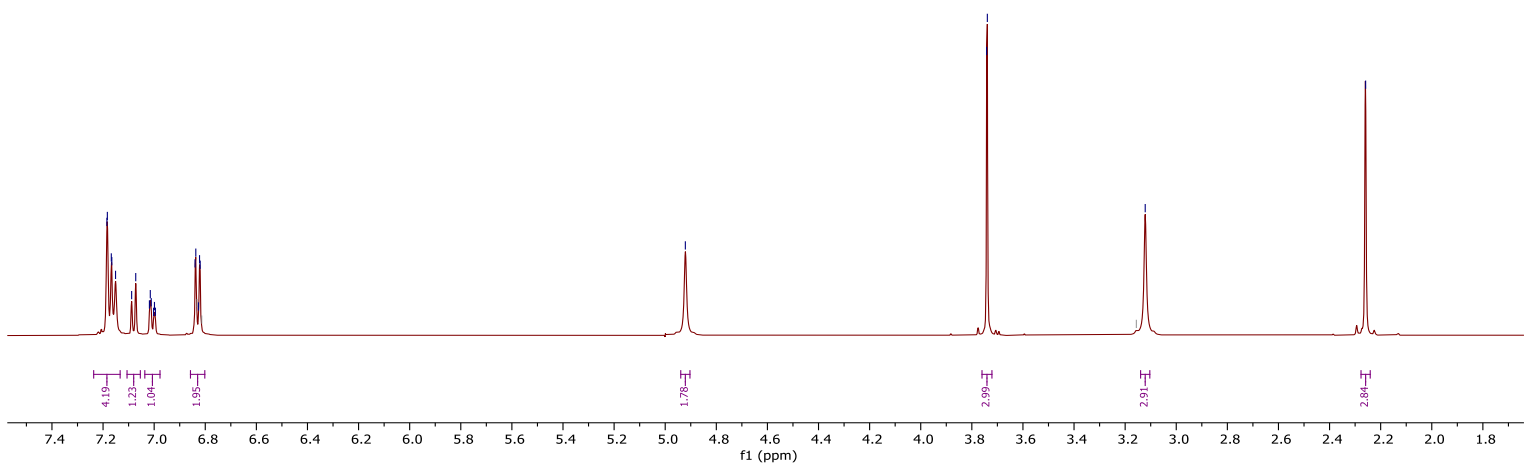
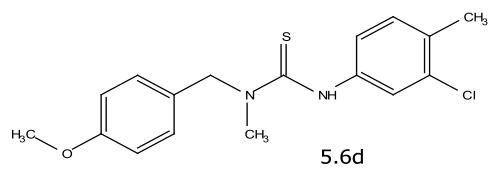
7.18  
7.17  
7.17  
7.17  
7.15  
7.09  
7.07  
7.06  
7.02  
7.01  
7.00  
6.99  
6.84  
6.83  
6.82  
6.81  
6.81

4.92

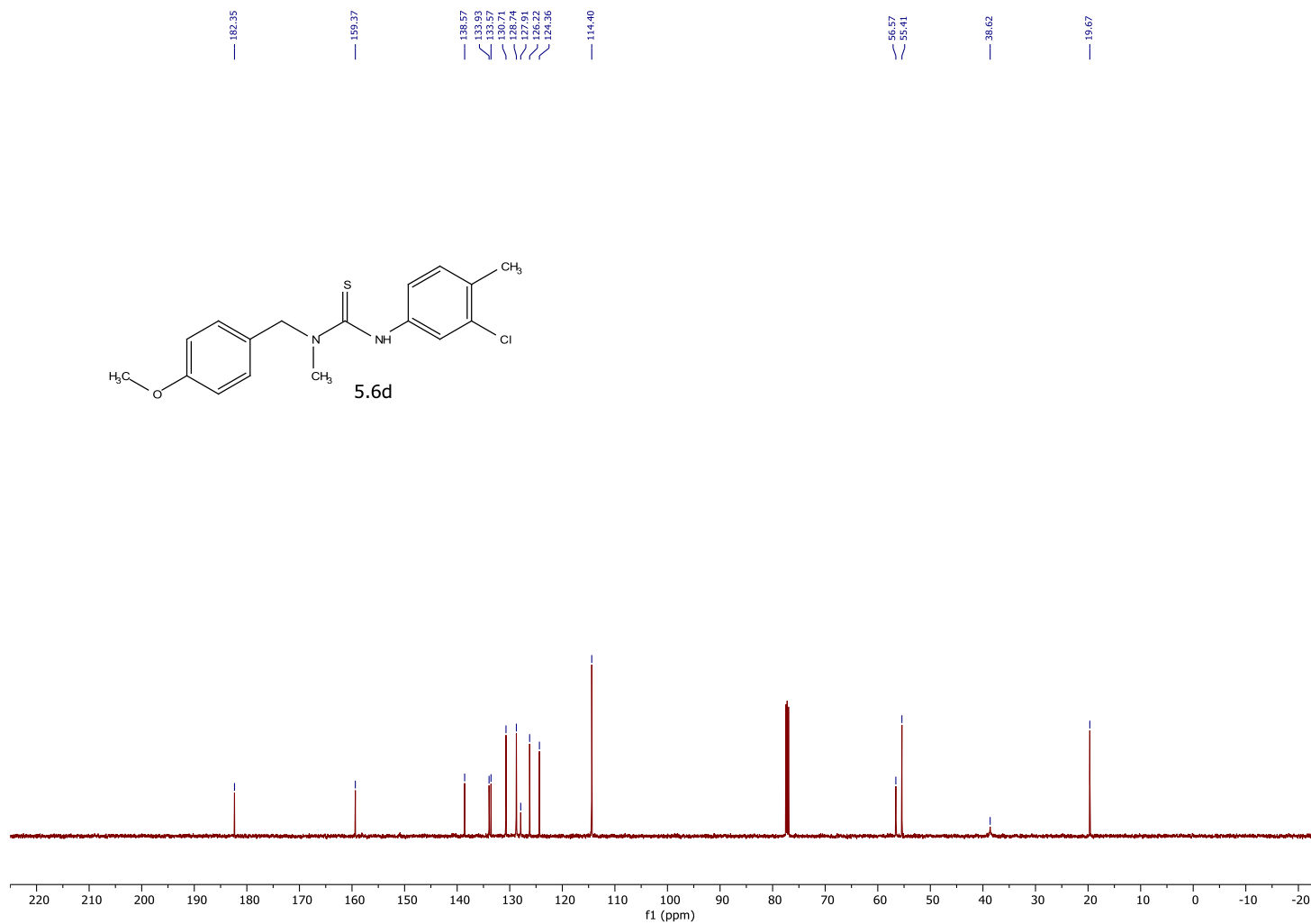
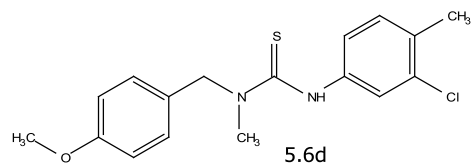
3.74  
3.74

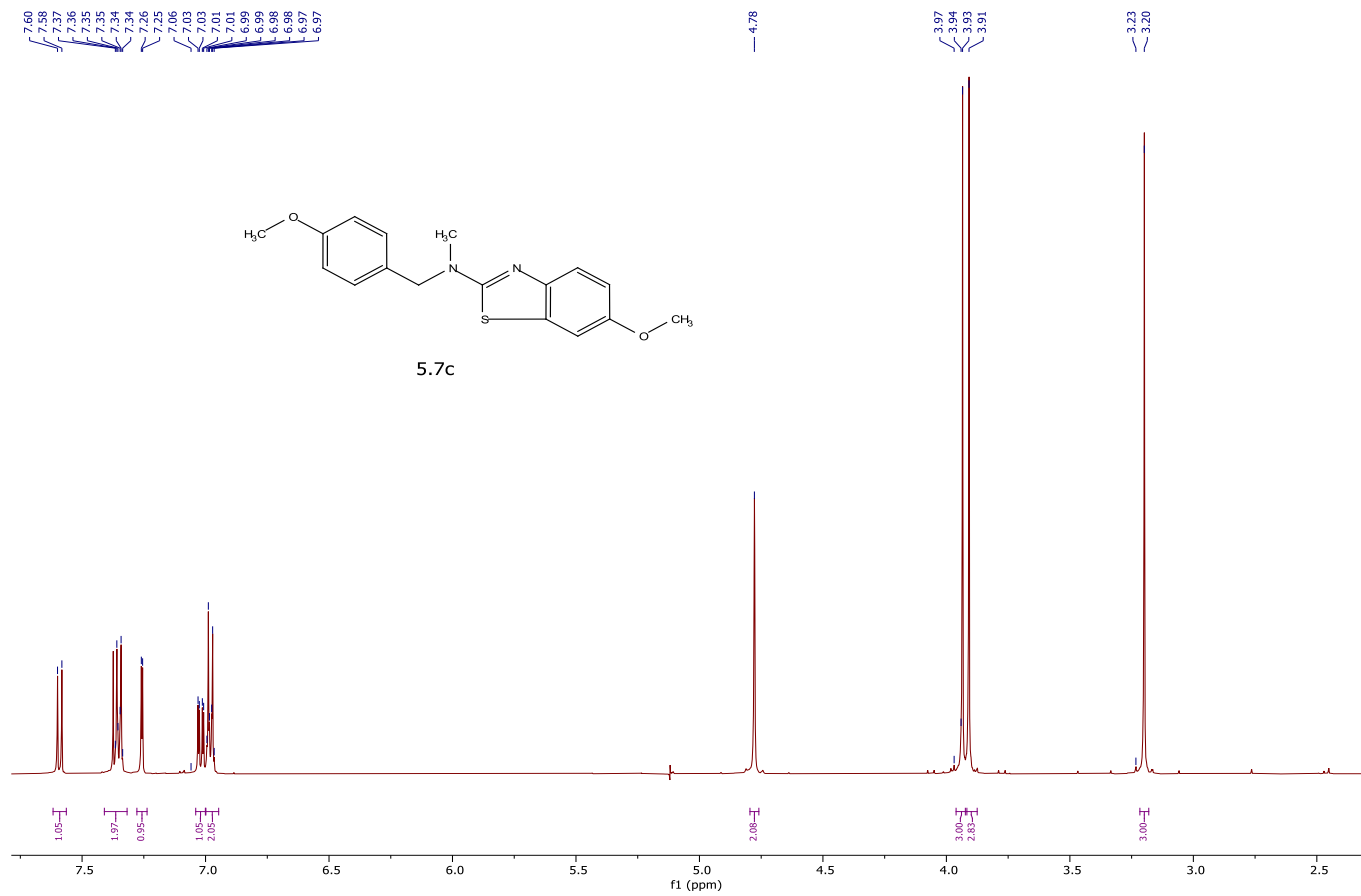
3.16  
3.12

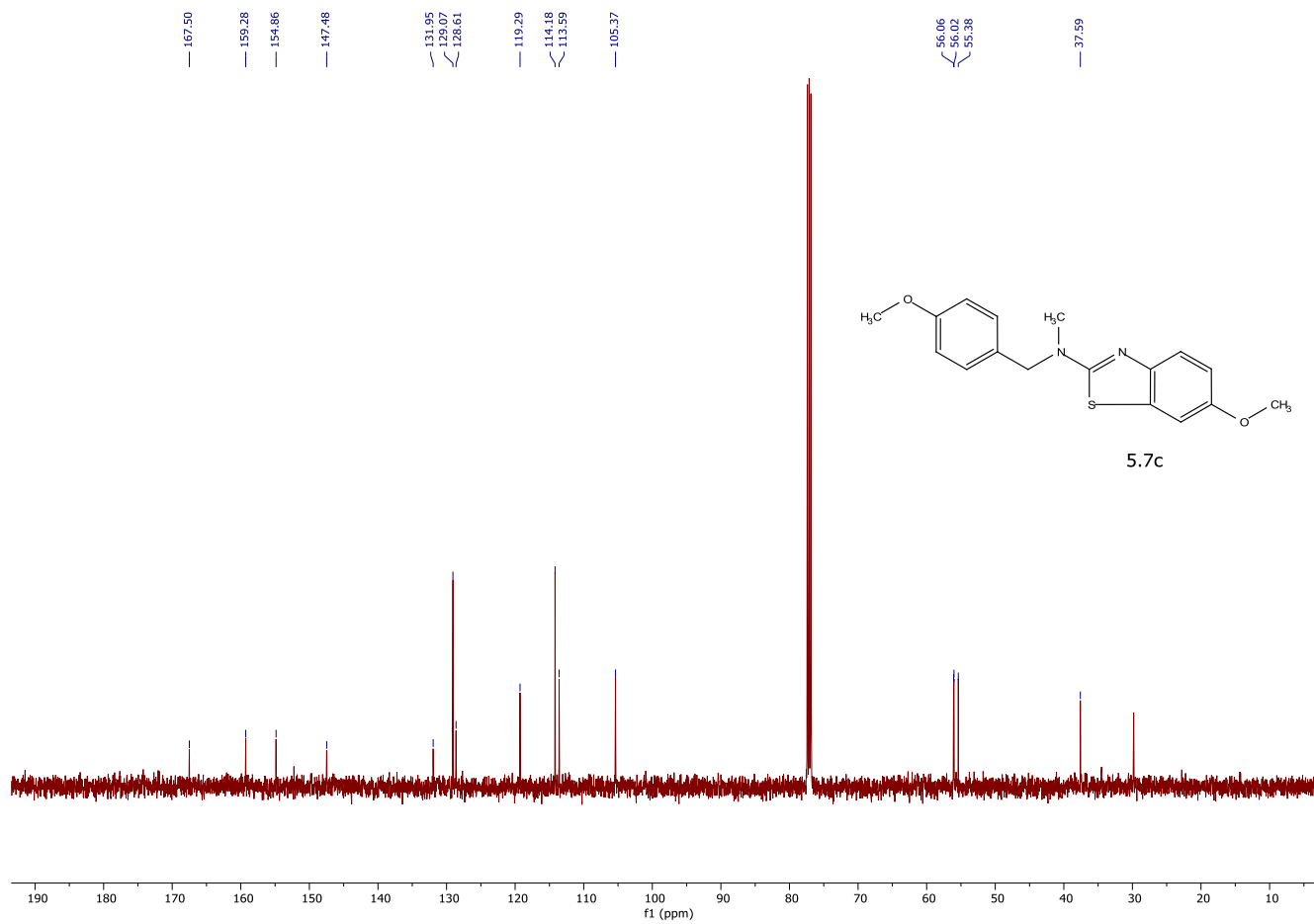
2.26

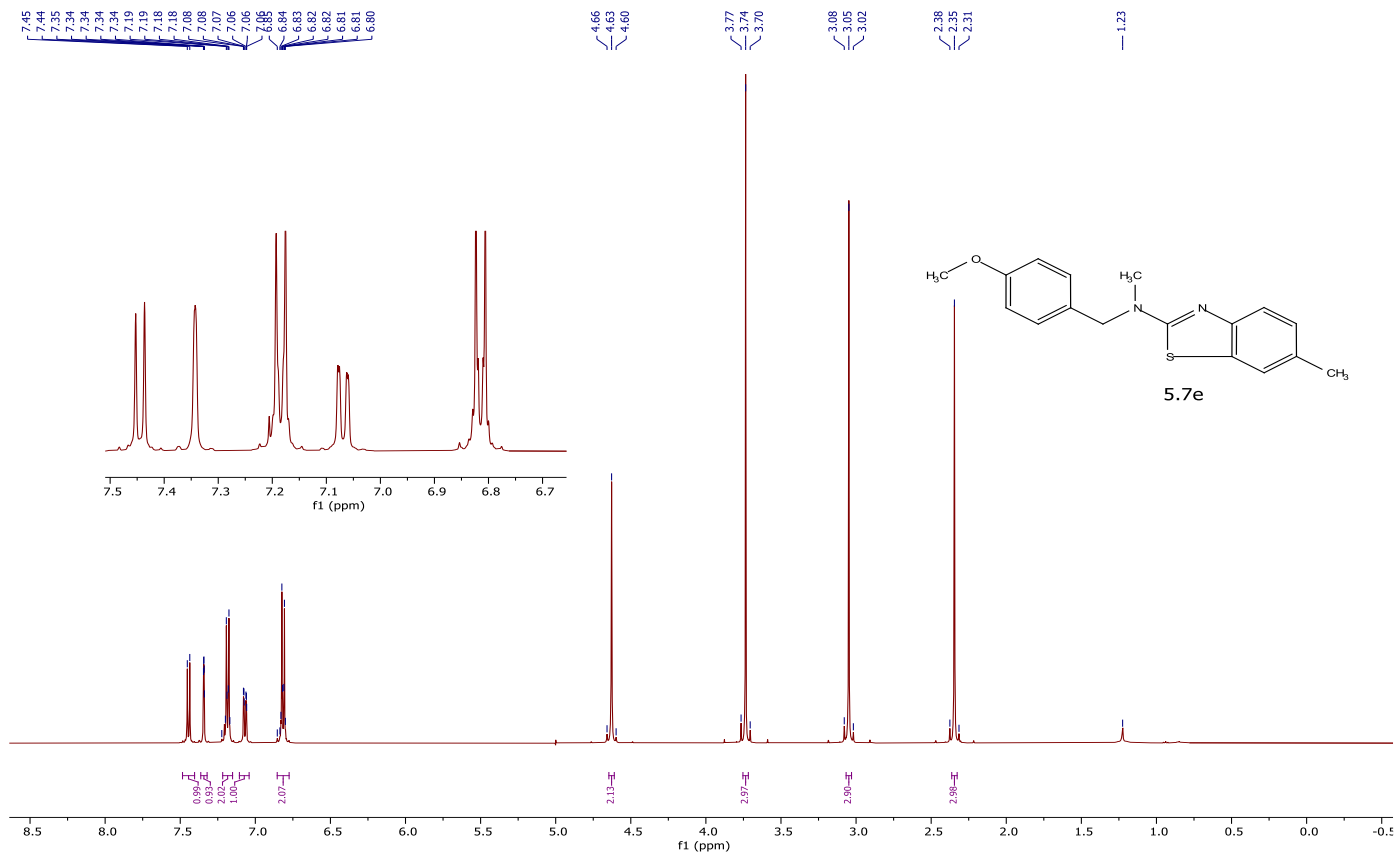


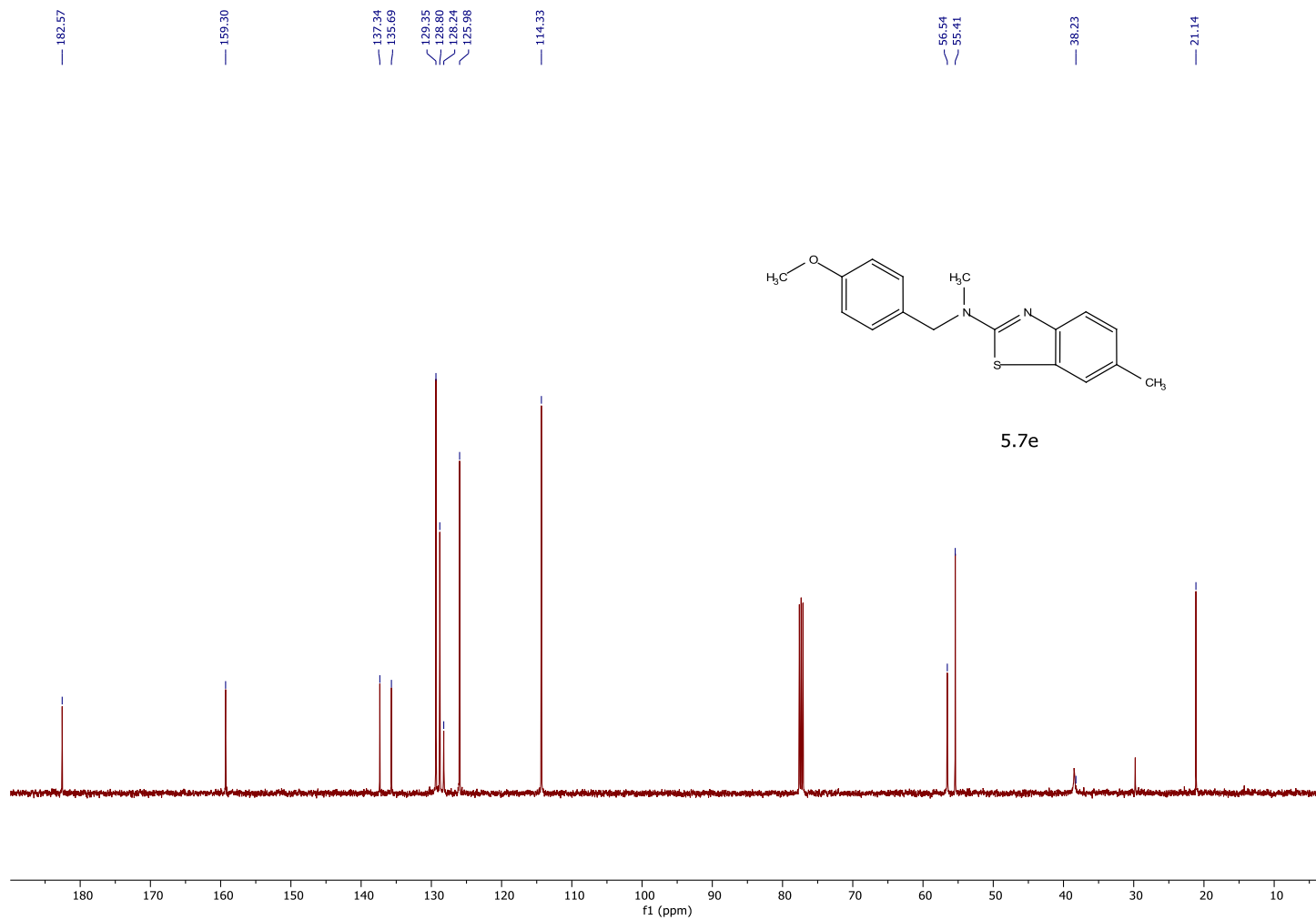


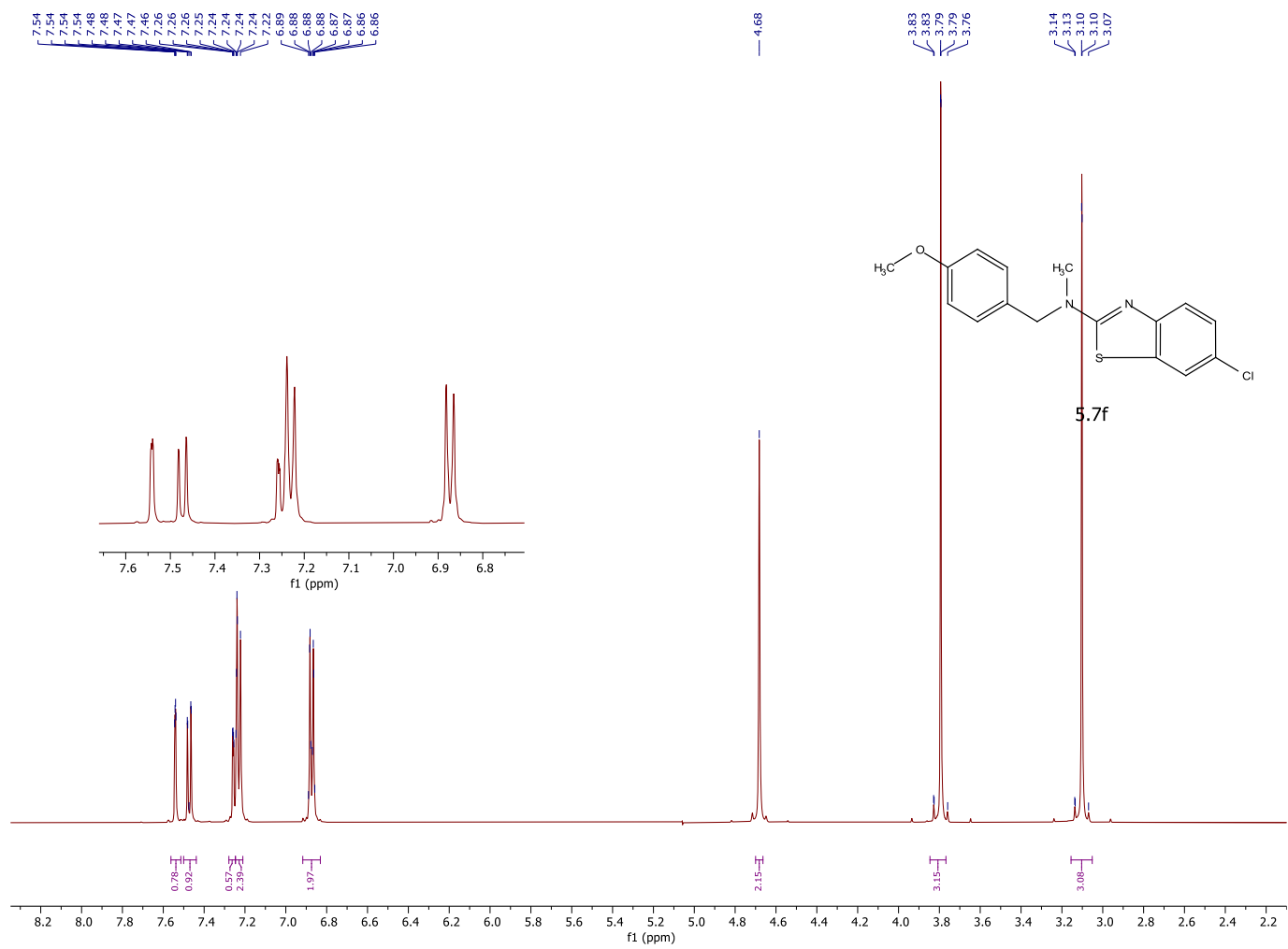








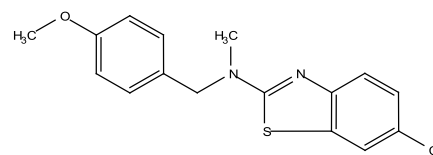




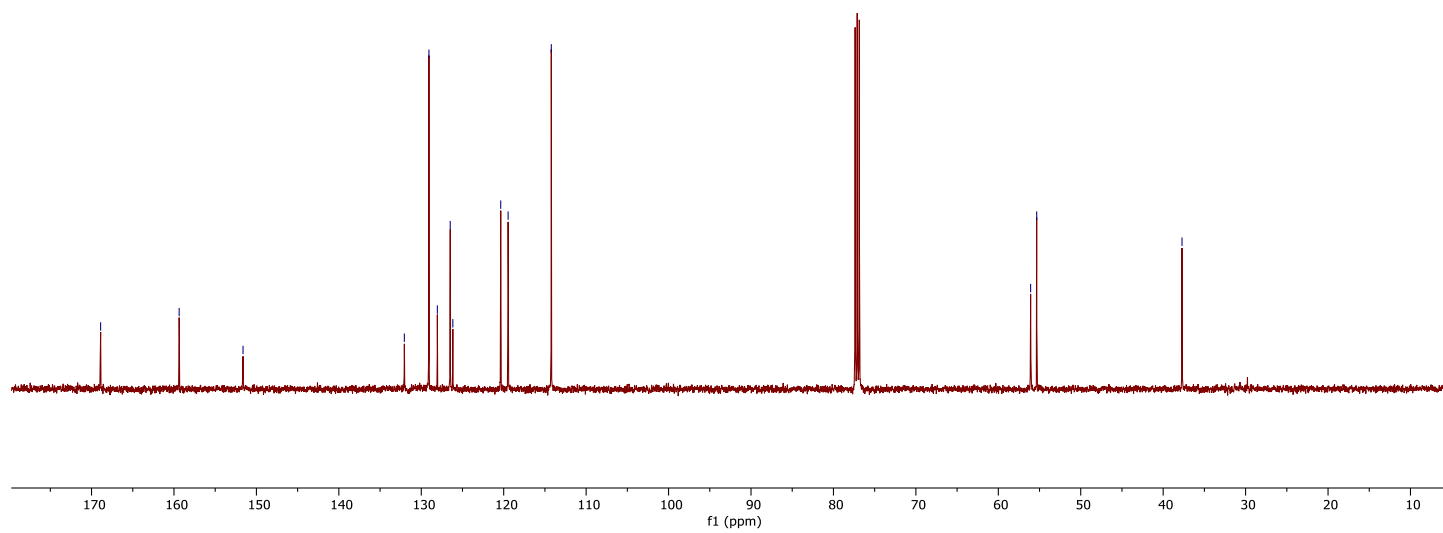
168.90  
159.37  
151.62  
132.05  
128.07  
126.99  
126.17  
120.36  
119.46  
114.23

56.08  
55.34

37.72



5.7f



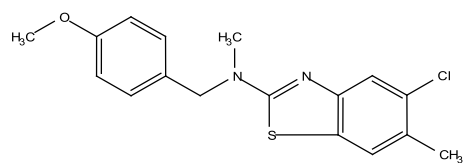
7.52  
7.35  
7.35  
7.18  
7.18  
7.17  
7.17  
6.82  
6.82  
6.81  
6.81  
6.80  
6.80

4.64  
4.63

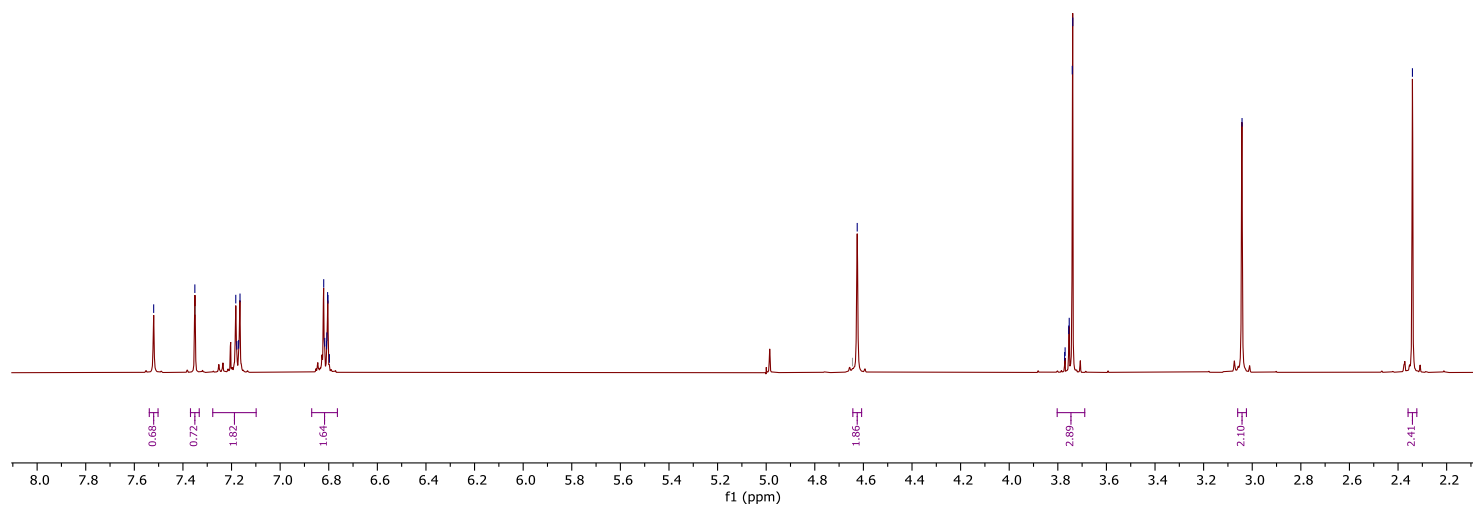
3.77  
3.77  
3.76  
3.75  
3.74  
3.74

3.04

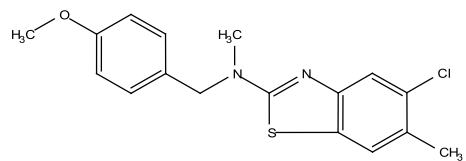
2.34



5.7g







5.7g

169.18

159.34

132.29

130.70

129.68

128.64

128.14

121.90

118.96

114.20

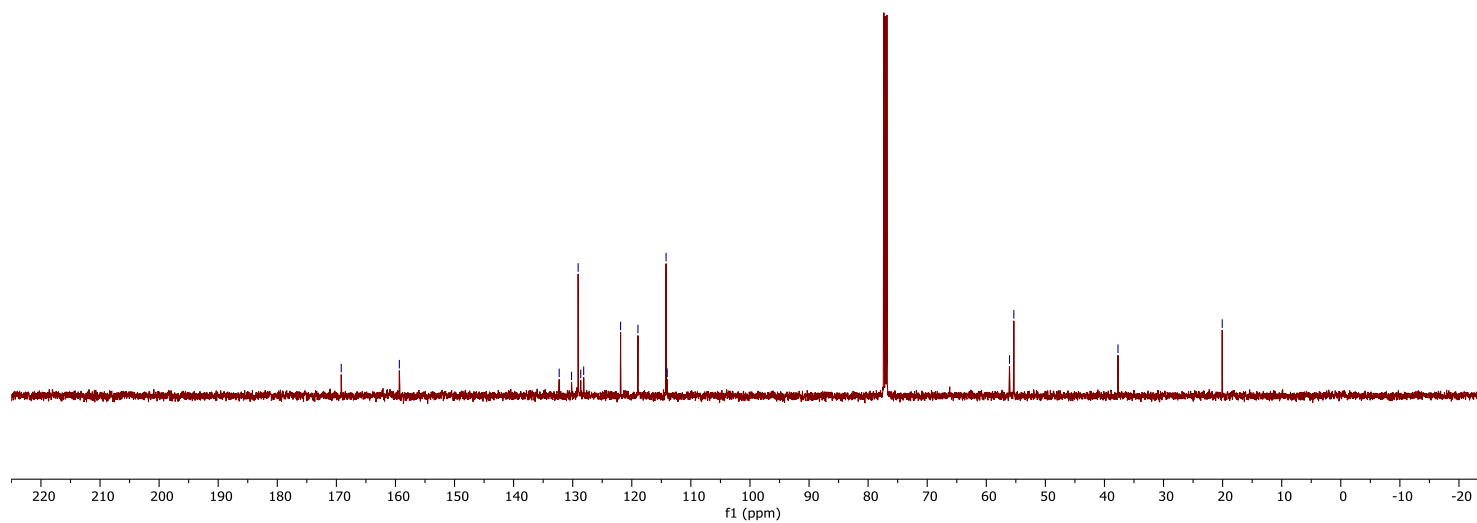
114.00

56.07

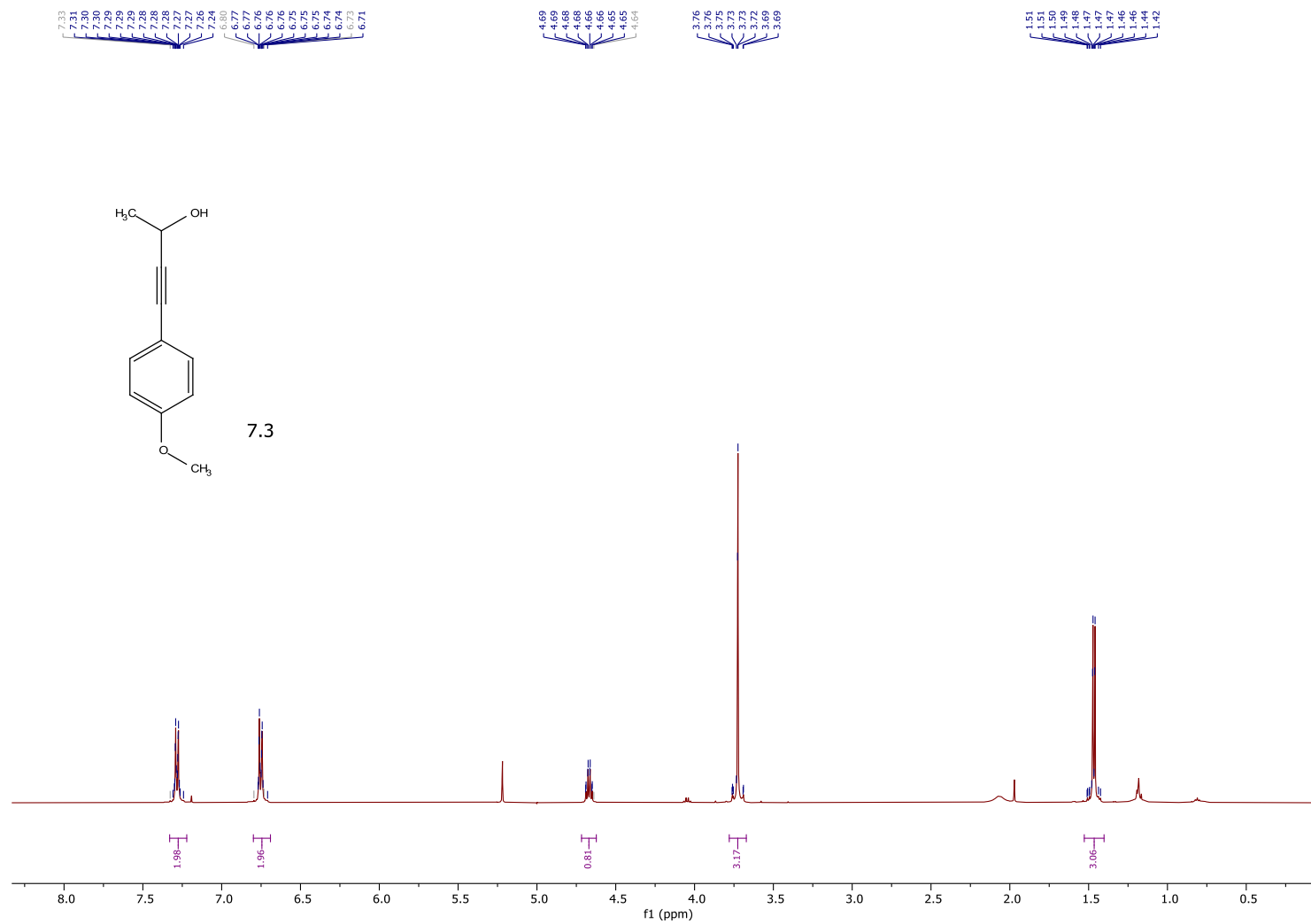
55.34

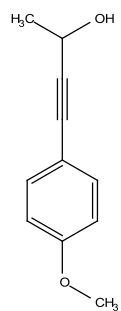
37.71

20.07

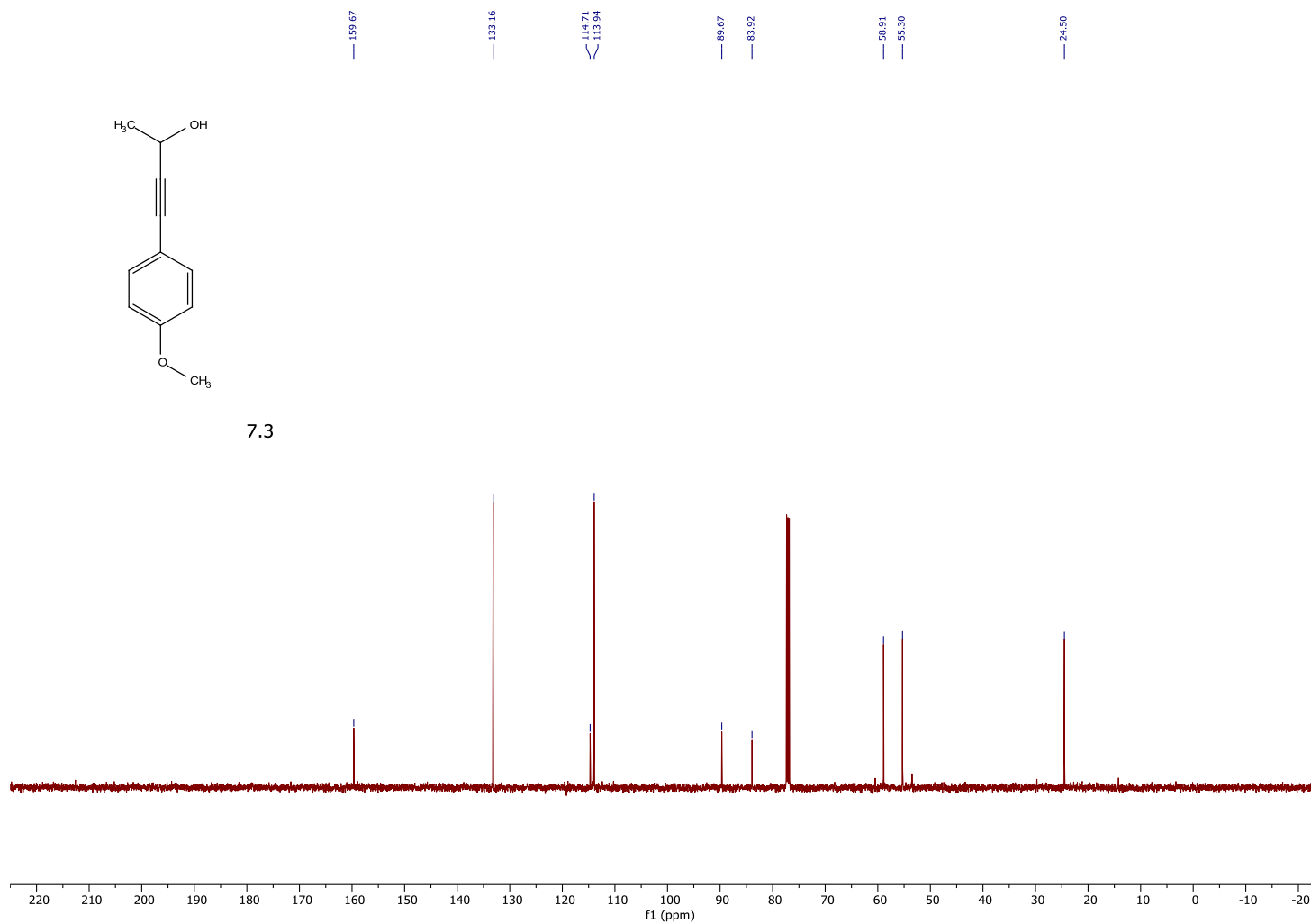


## Chapter Seven and Eight (Thiazolidines)

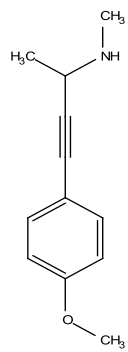




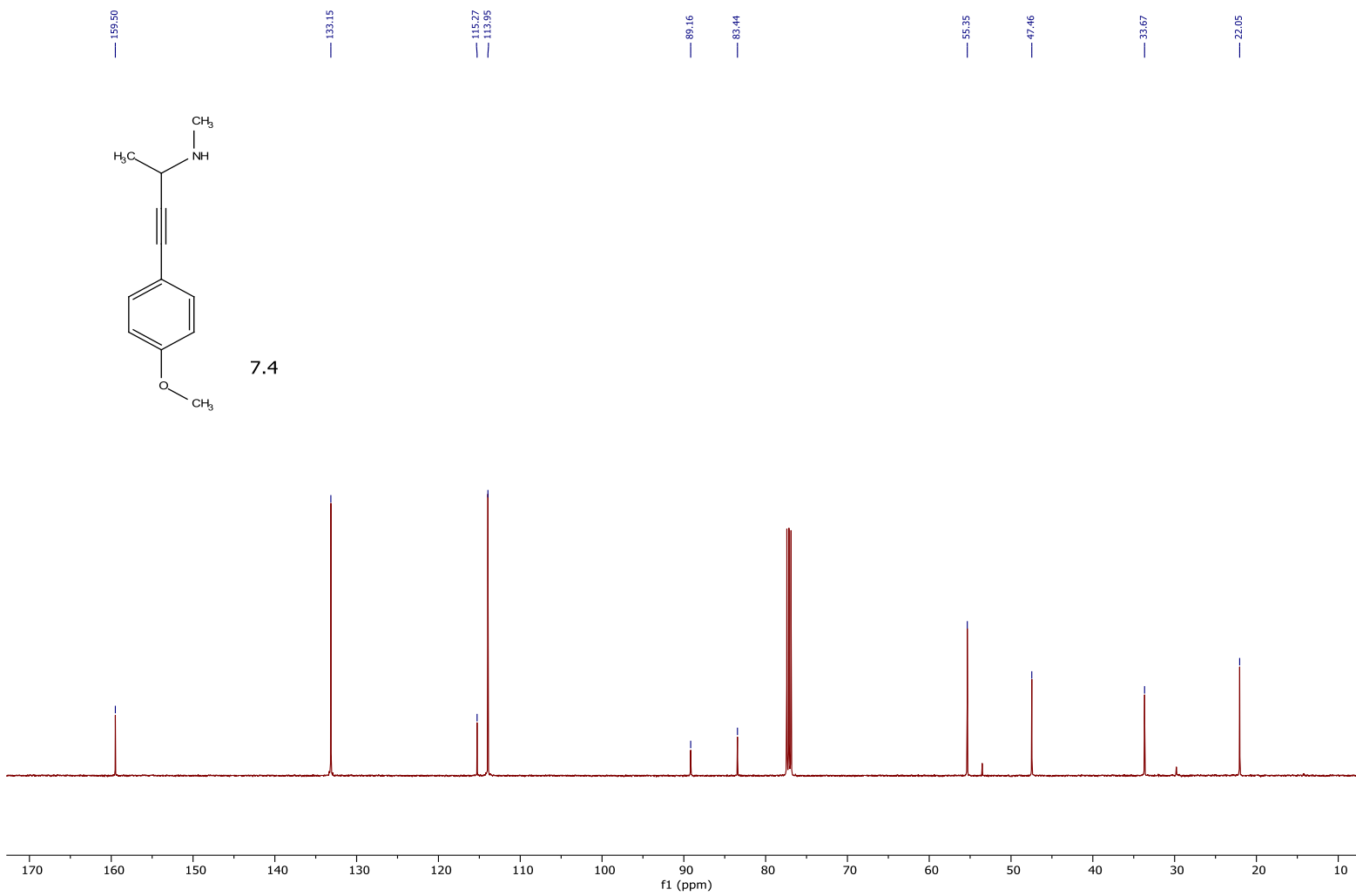
7.3







7.4



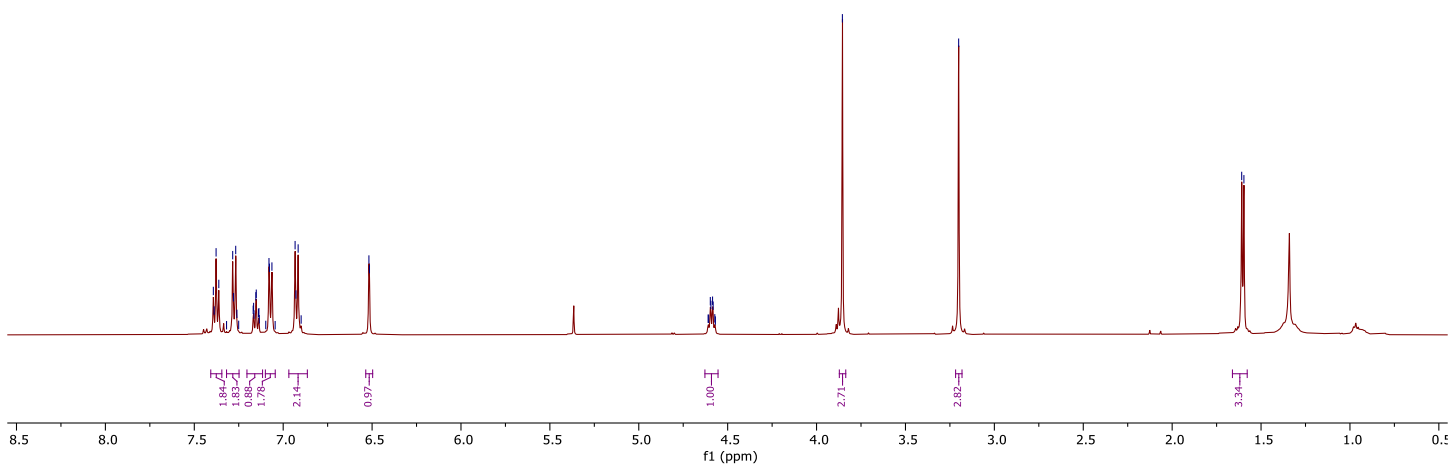
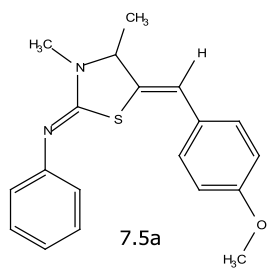
7.39  
7.39  
7.38  
7.32  
7.28  
7.27  
7.25  
7.17  
7.16  
7.15  
7.14  
7.13  
7.08  
7.06  
7.05  
6.93  
6.90  
6.52  
6.51

4.61  
4.60  
4.59  
4.58  
4.59  
4.57

3.85

3.20

1.61  
1.60



158.60  
155.85  
151.30

133.18  
132.52  
129.02  
128.66

123.28  
119.62

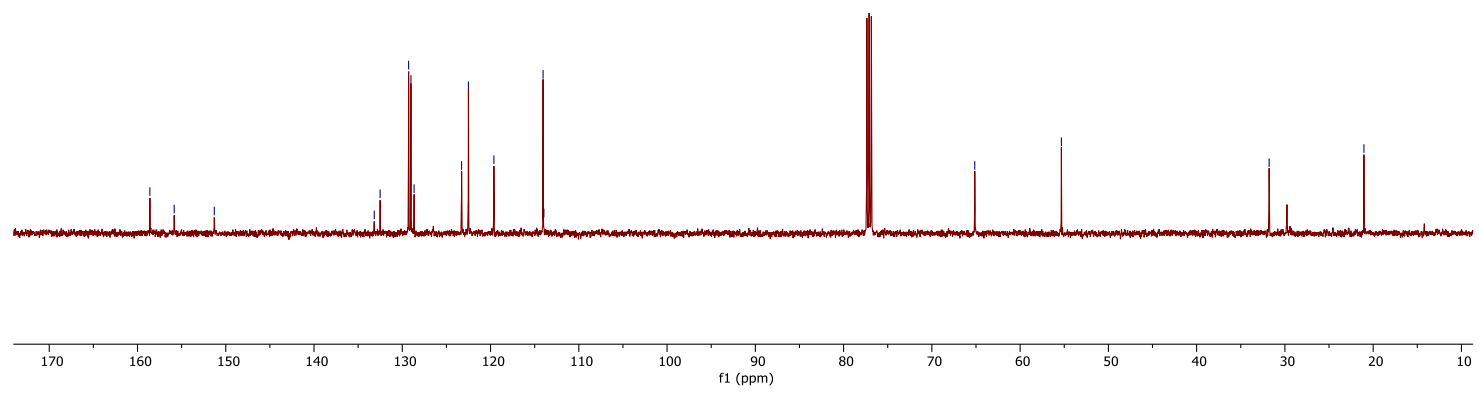
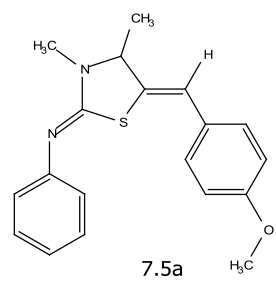
114.05  
113.96

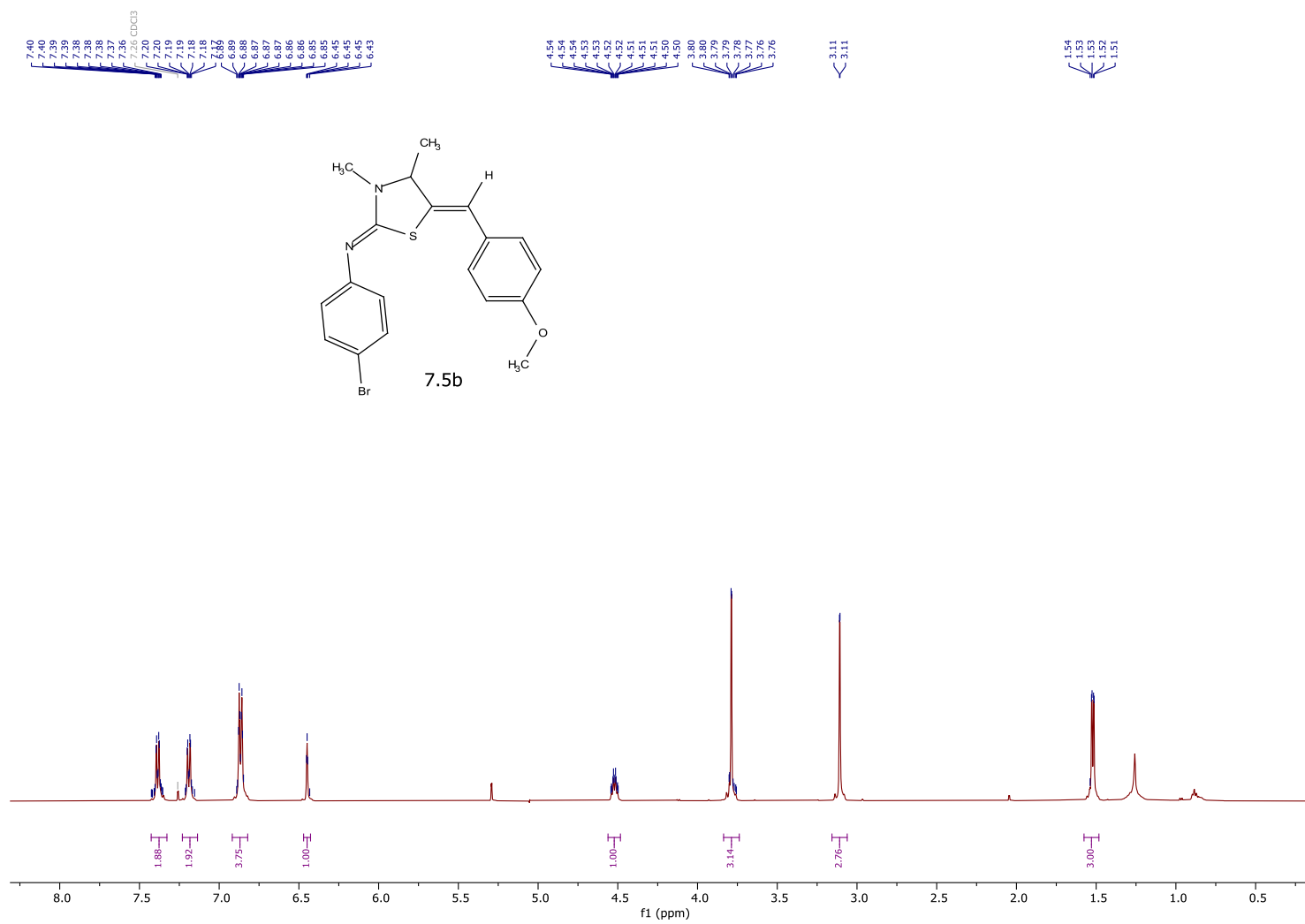
65.14

56.32

31.79

21.05







158.71

131.99

131.93

128.77

128.69

124.35

119.97

116.20

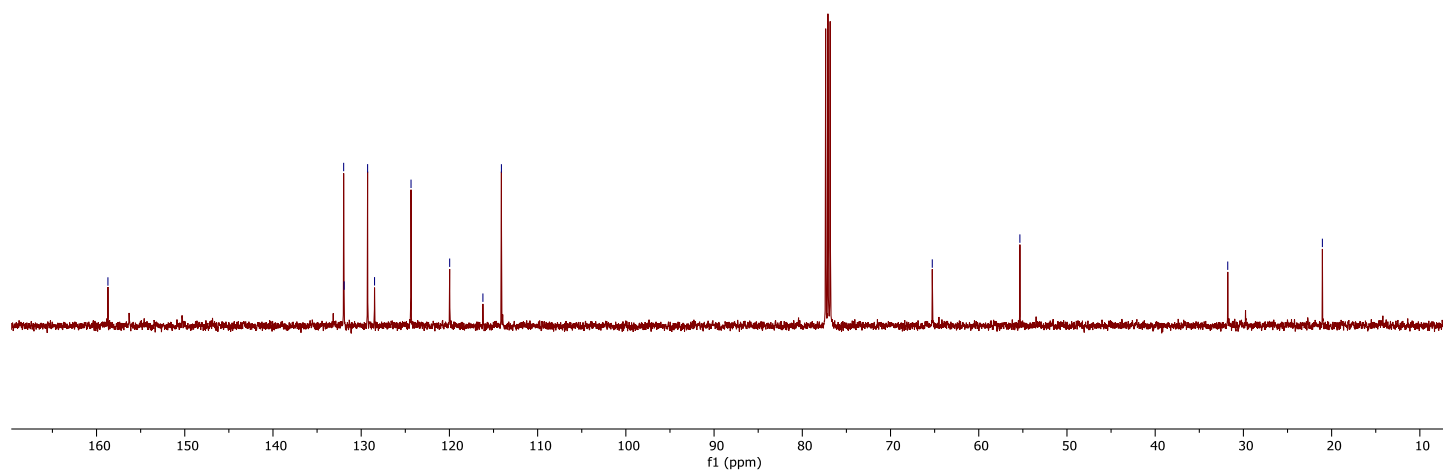
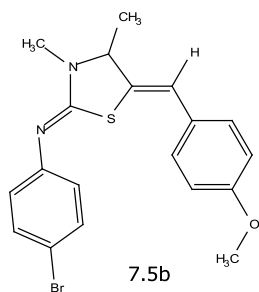
114.11

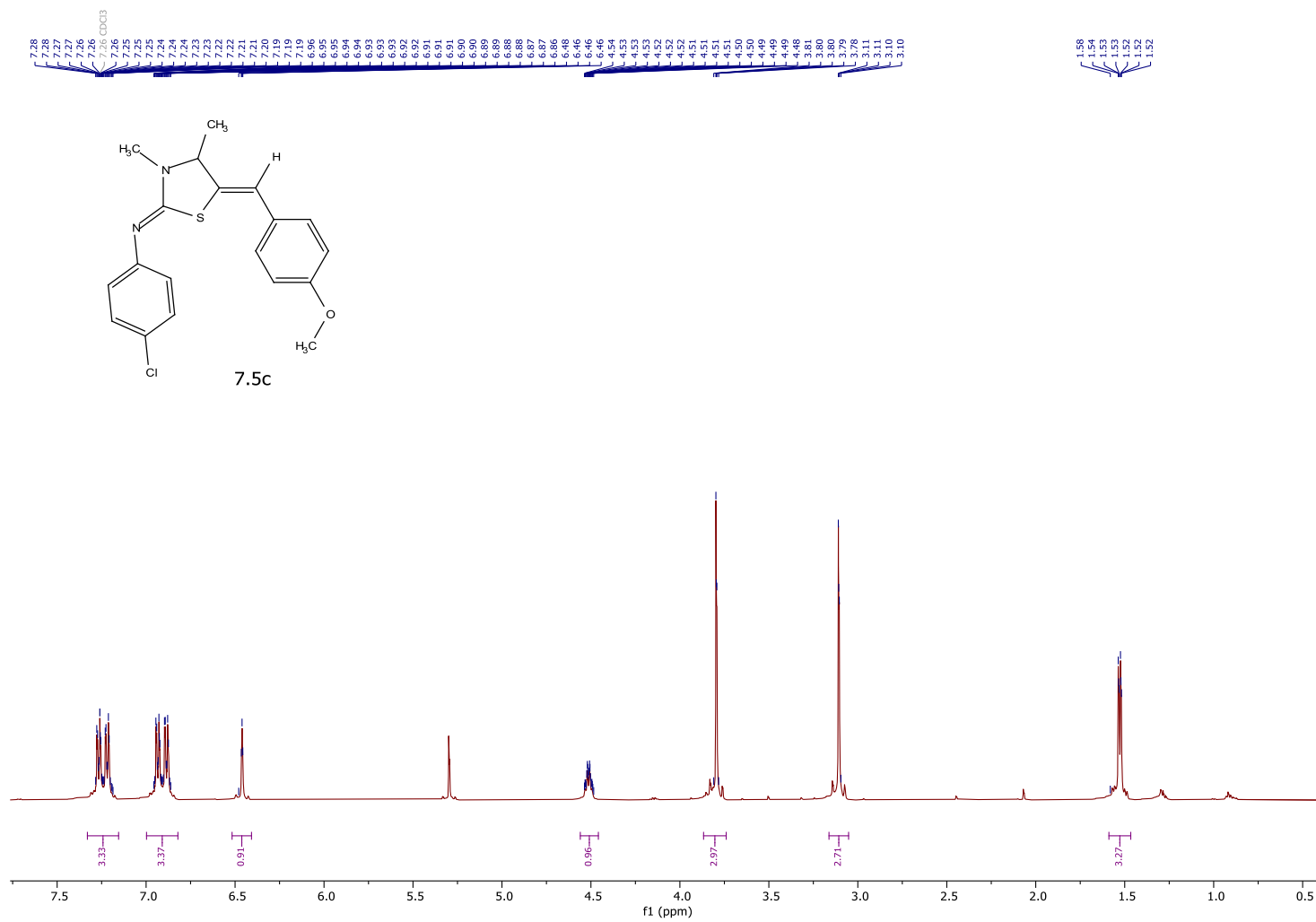
65.27

55.34

31.78

21.05





158.72  
156.10  
150.29

129.16  
129.33  
129.07  
128.61  
128.30

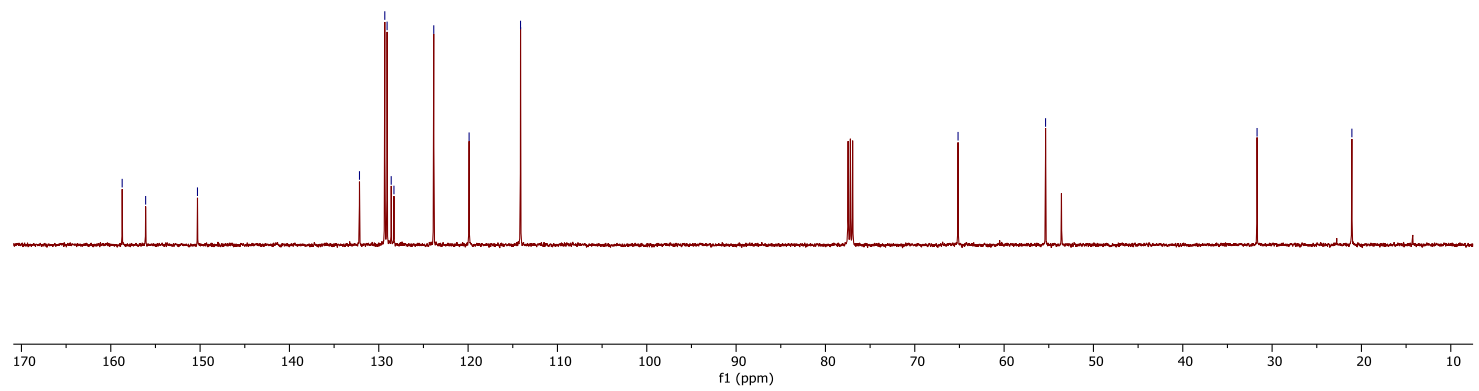
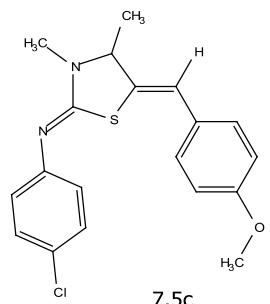
123.85  
119.89  
114.13

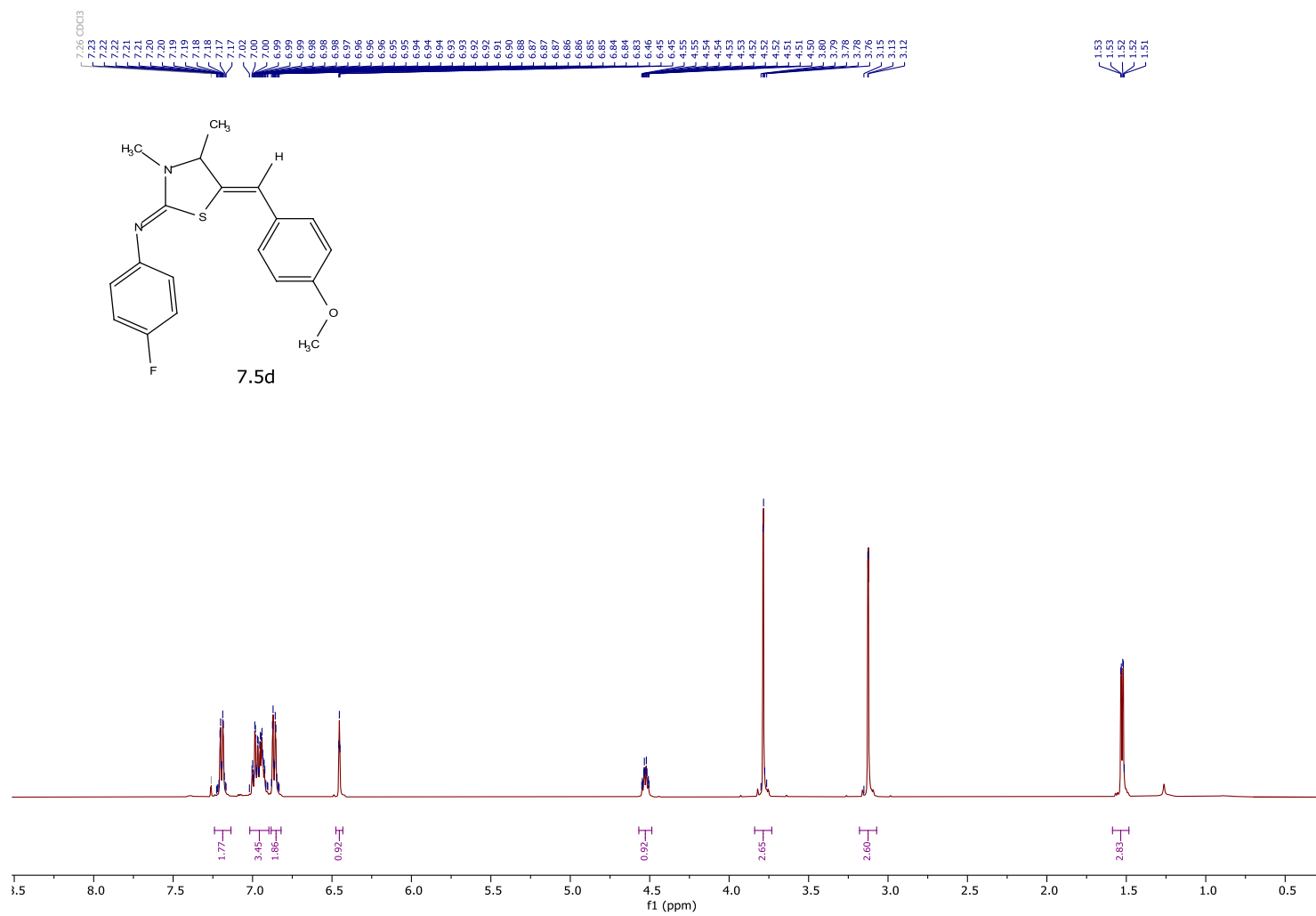
65.16

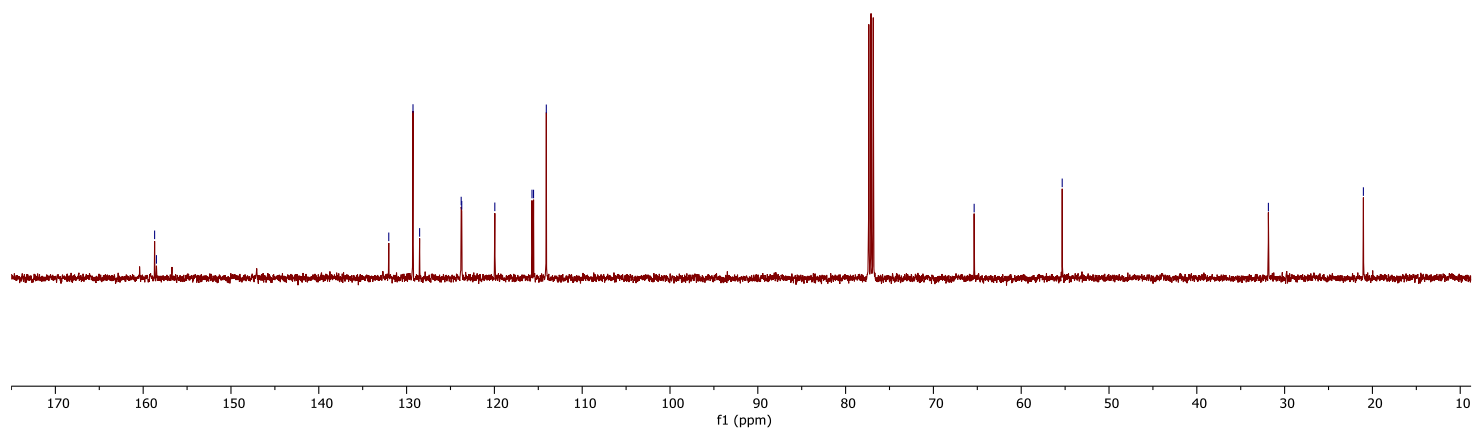
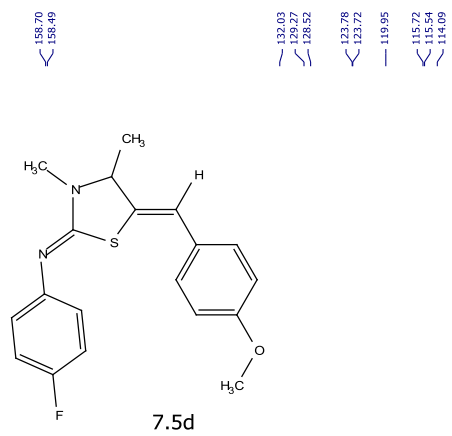
55.36

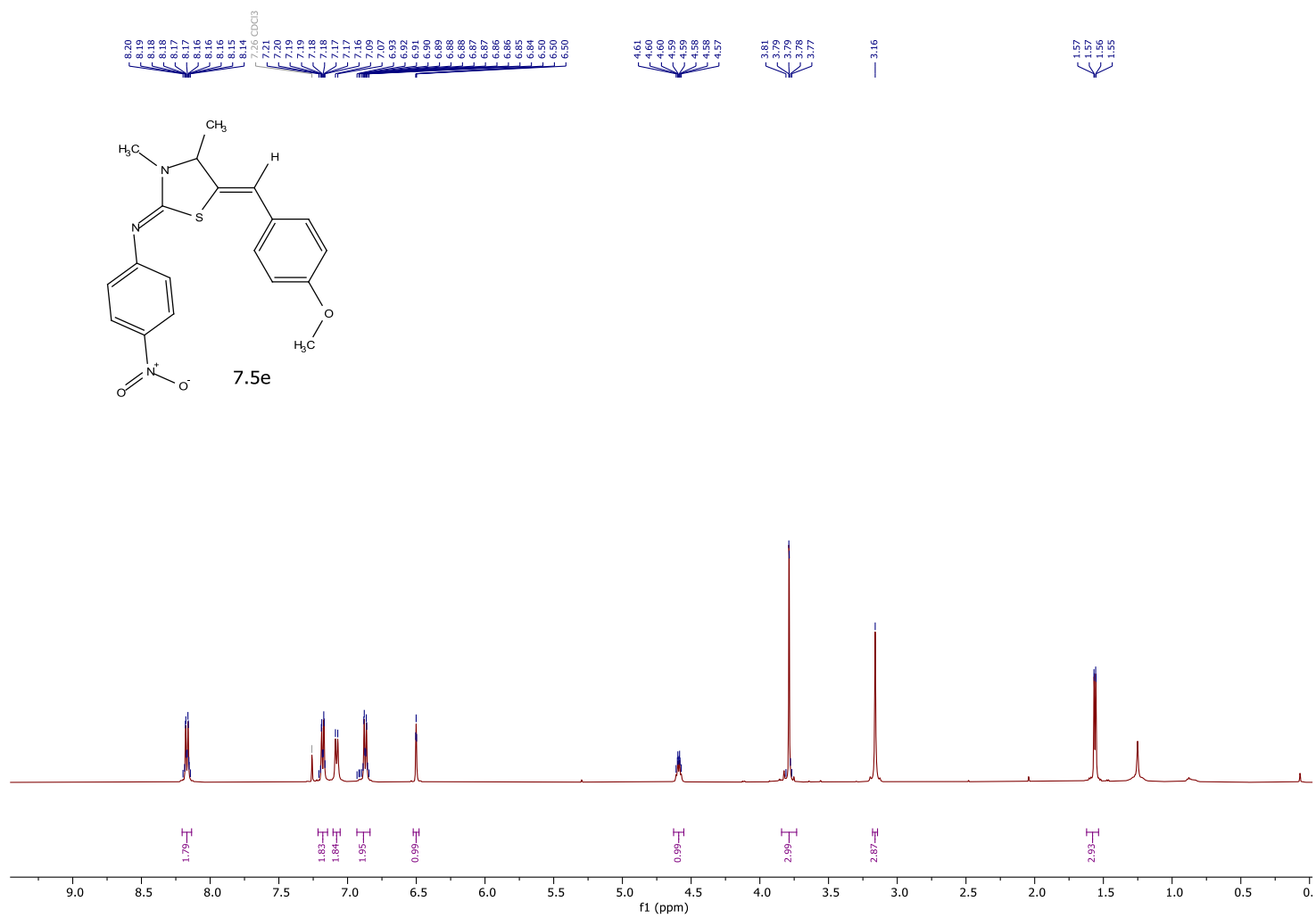
31.68

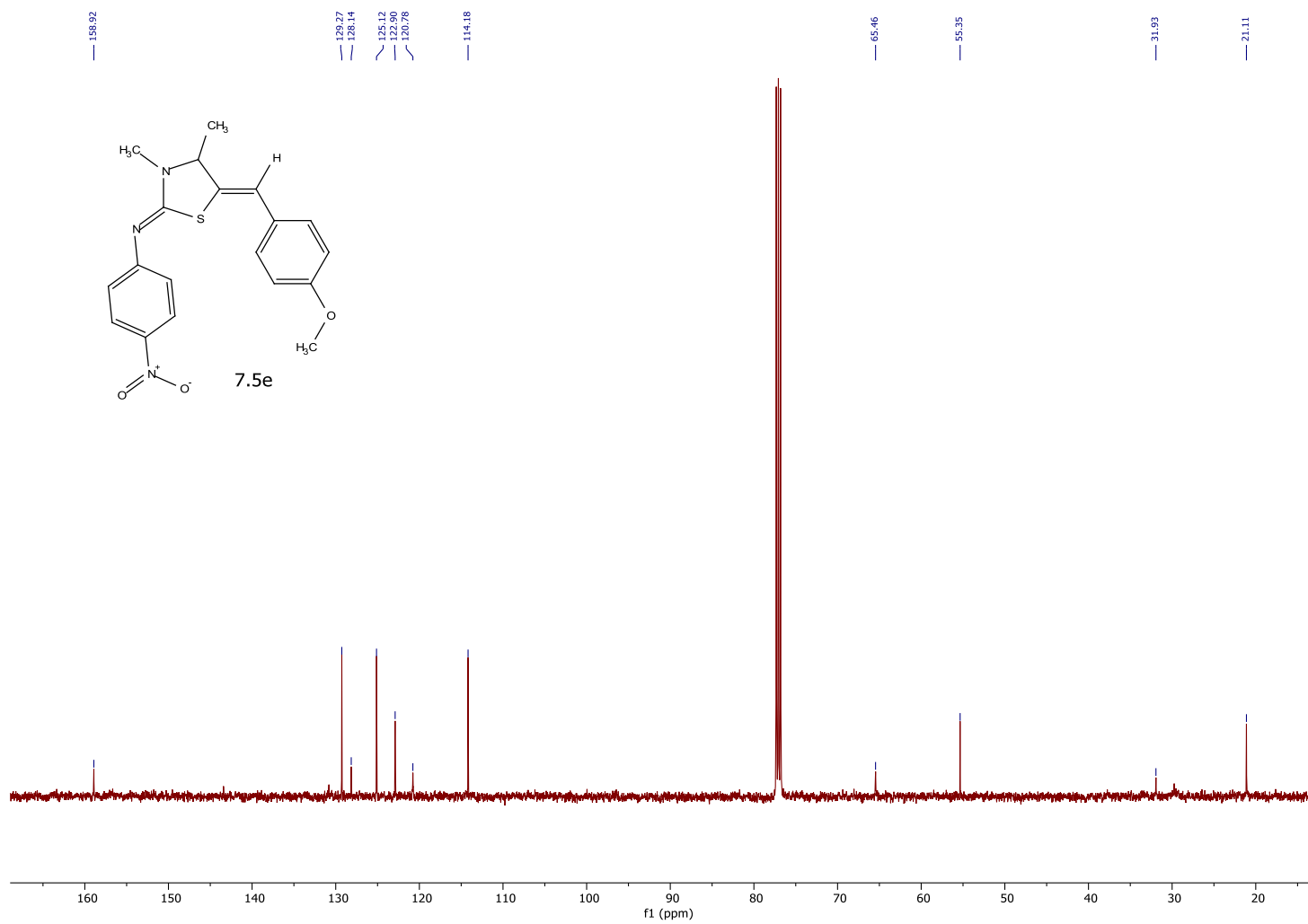
21.07

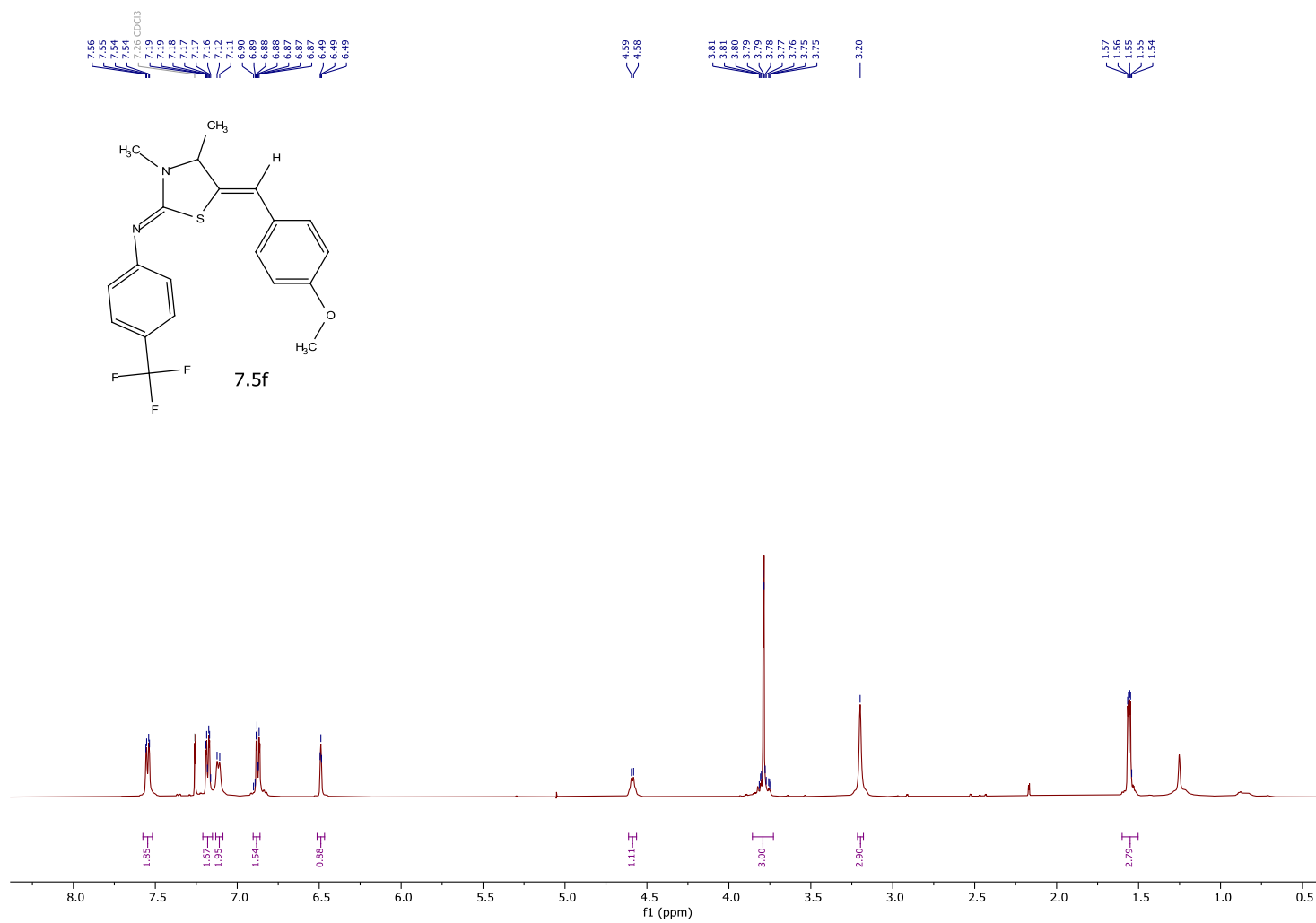














159.78  
159.44  
159.17

131.77  
129.30  
128.46  
128.28  
126.28  
126.25  
126.22  
125.10  
122.64  
120.15

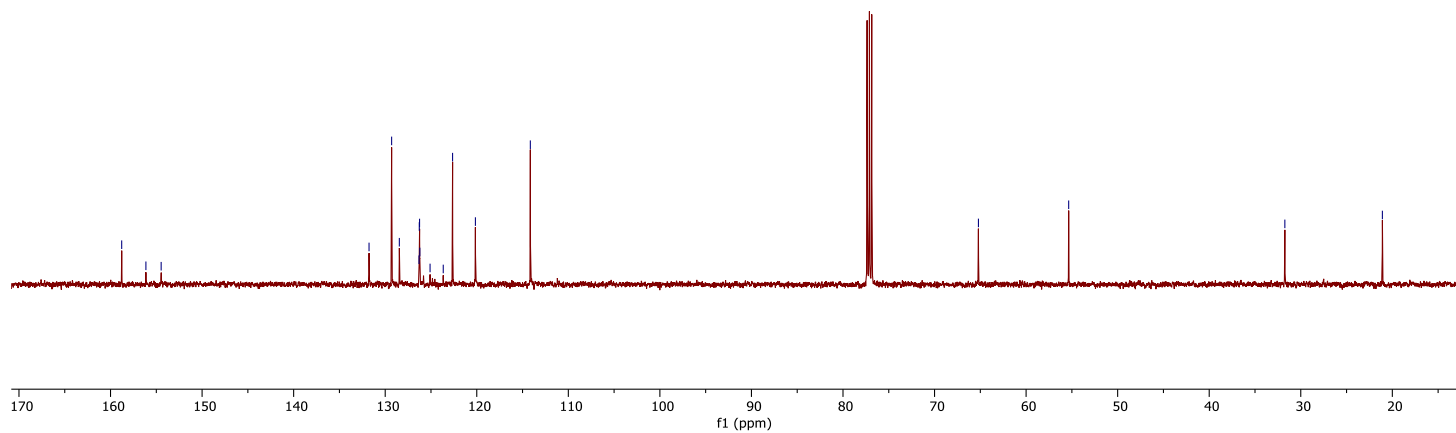
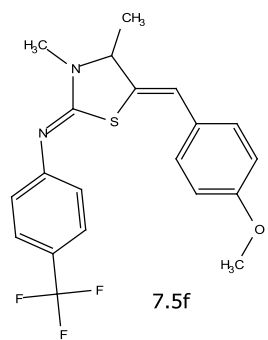
114.15

65.21

55.35

31.74

21.09





158.71  
156.23  
150.51

134.32  
132.26  
131.20  
130.41  
129.26  
128.64

123.04  
120.83  
119.87

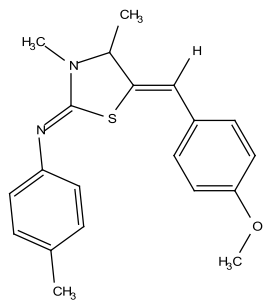
114.14

65.20

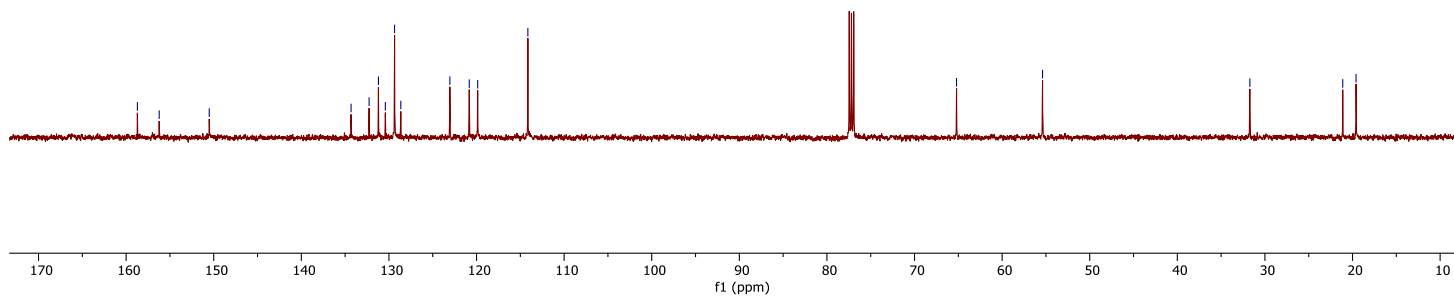
55.39

31.72

21.12  
19.60



7.5g



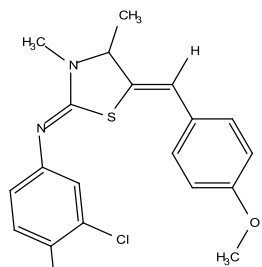
7.26 CDCl<sub>3</sub>  
 7.25  
 7.24  
 7.23  
 7.22  
 7.20  
 7.19  
 7.18  
 7.17  
 7.16  
 7.15  
 7.14  
 7.13  
 7.12  
 7.11  
 7.10  
 7.09  
 7.08  
 7.07  
 7.06  
 7.05  
 7.04  
 6.96  
 6.95  
 6.94  
 6.94  
 6.93  
 6.93  
 6.92  
 6.91  
 6.91  
 6.90  
 6.90  
 6.89  
 6.88  
 6.88  
 6.87  
 6.86  
 6.85  
 6.85  
 6.84  
 6.84  
 6.83  
 6.83  
 6.82  
 6.82  
 6.81  
 6.81  
 6.80  
 6.80  
 6.79  
 6.79

4.58  
 4.57  
 4.57  
 4.56  
 4.56  
 4.55  
 4.55  
 4.54  
 4.53  
 4.53  
 4.53  
 3.88  
 3.87  
 3.86  
 3.86  
 3.84  
 3.84  
 3.81  
 3.81

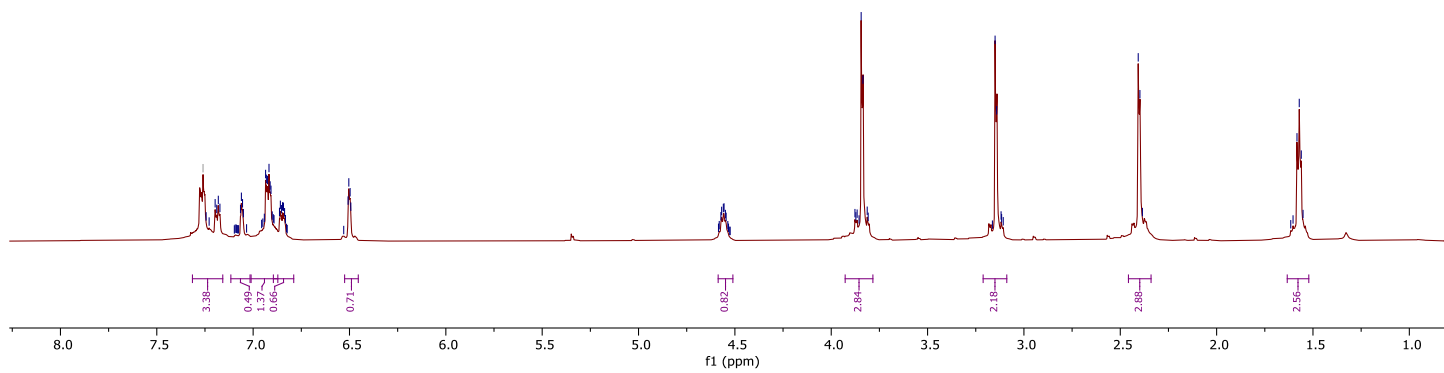
3.16  
 3.15  
 3.14  
 3.12  
 3.11

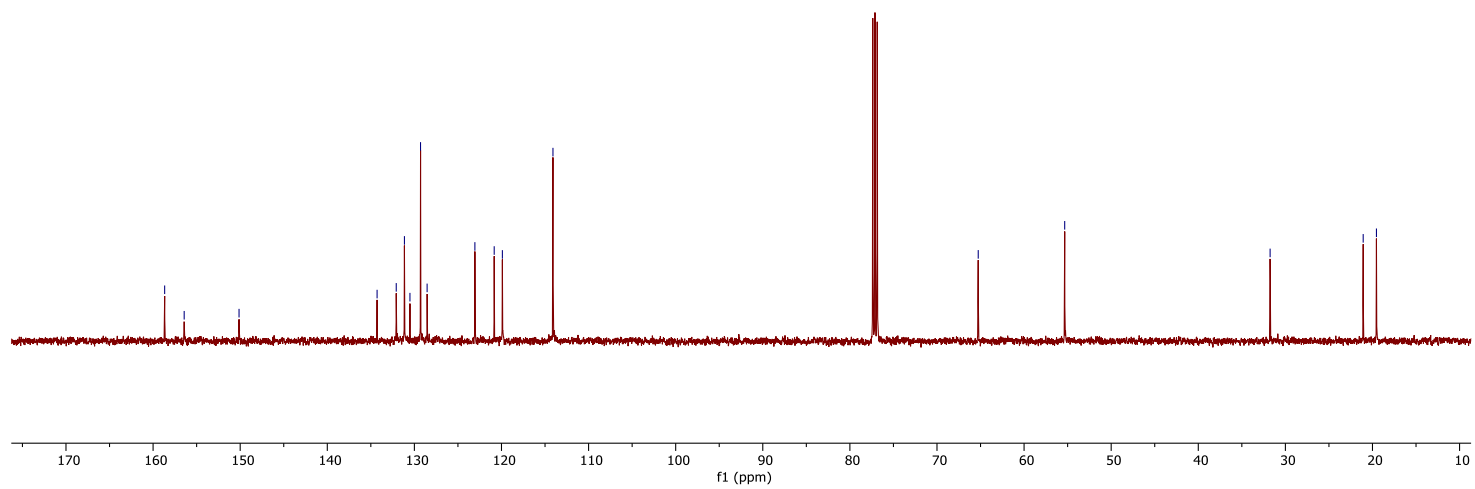
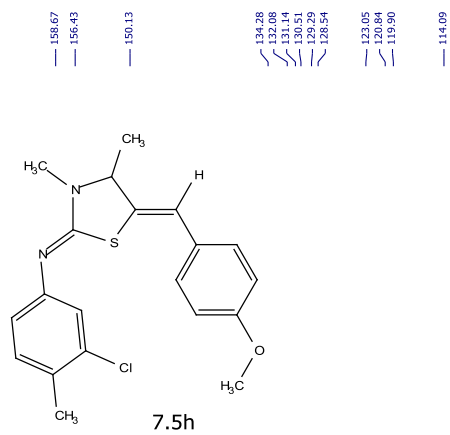
2.41  
 2.40  
 2.39

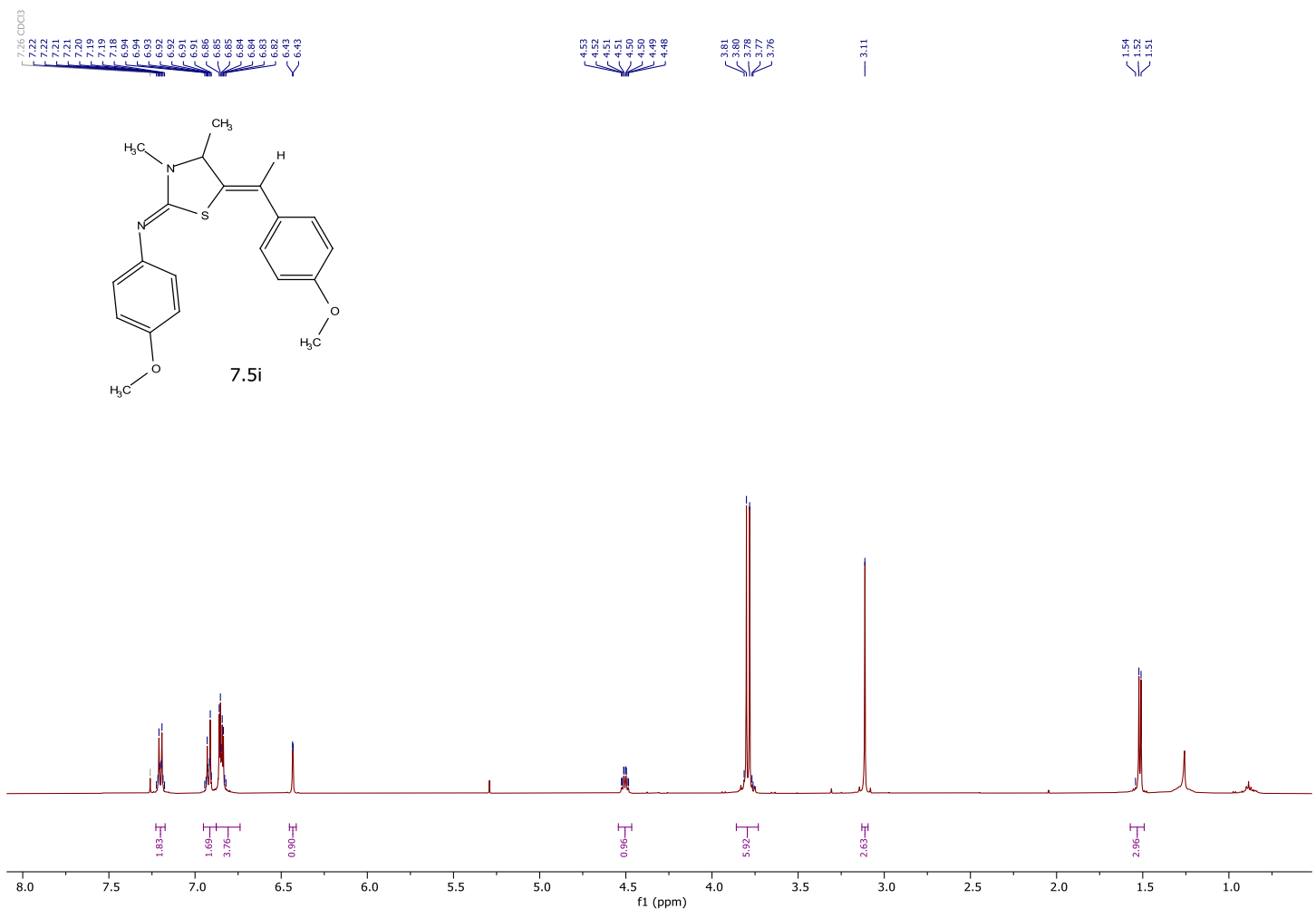
1.62  
 1.60  
 1.59  
 1.57  
 1.56  
 1.55



7.5h







158.58  
156.32  
155.88

132.60  
129.28  
128.69

123.33  
119.56

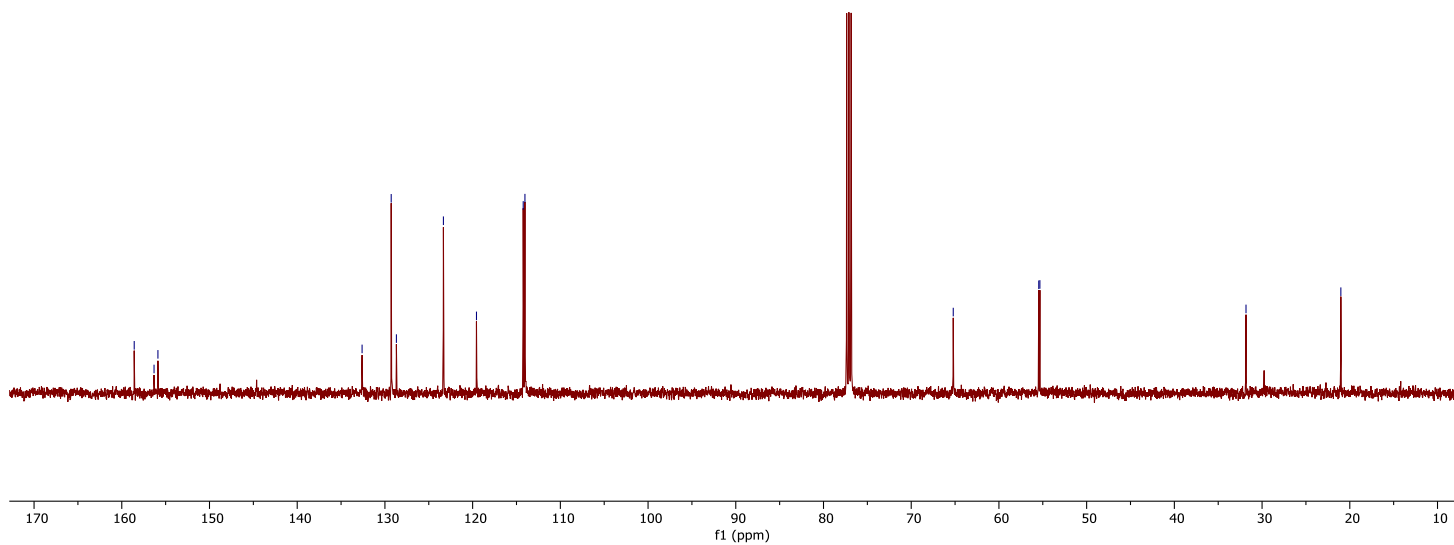
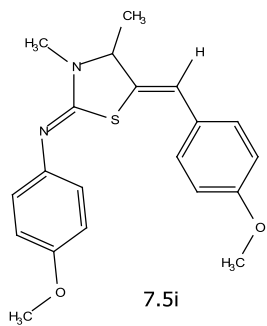
114.23  
114.04

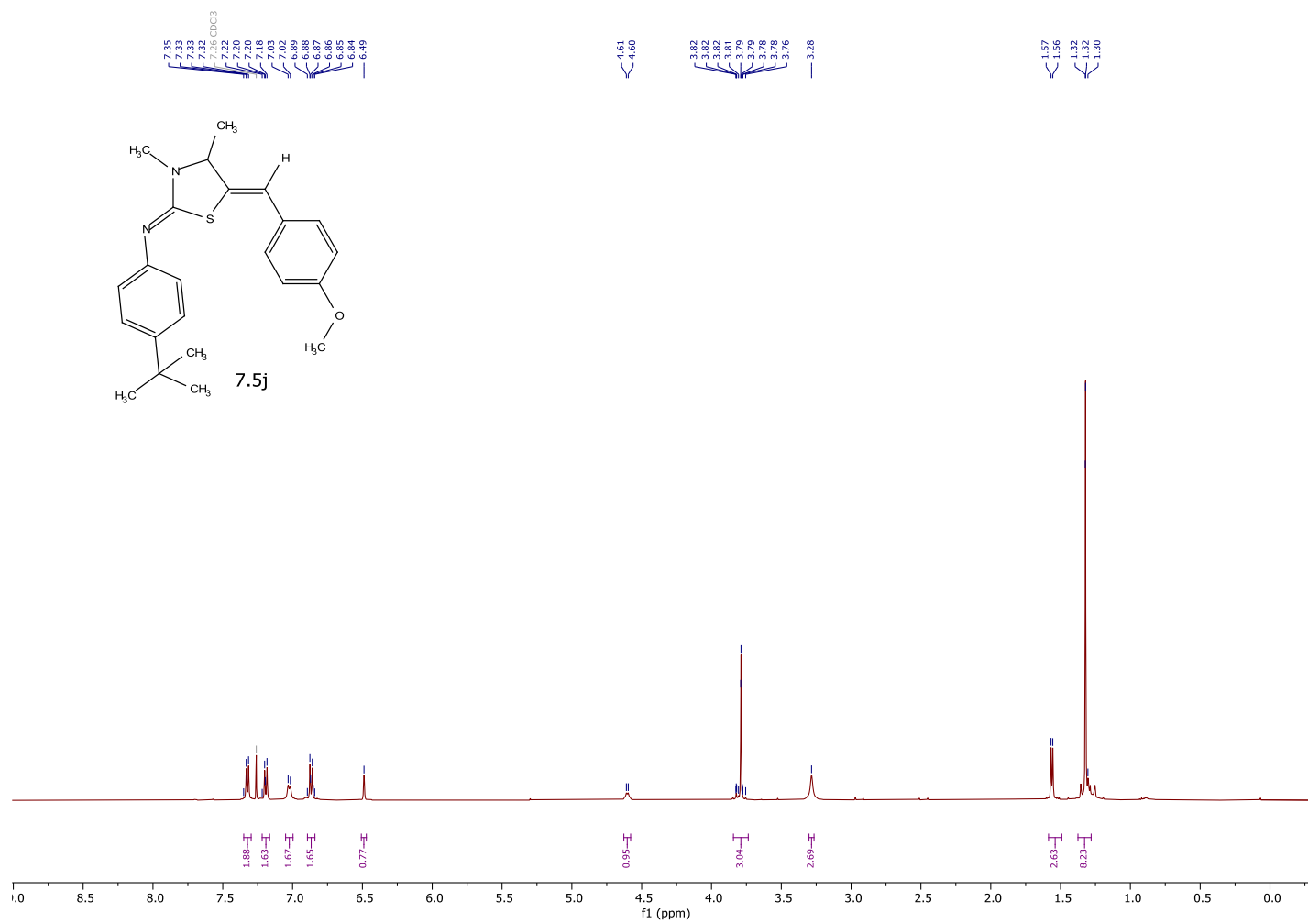
65.21

55.45  
55.33

31.83

21.02







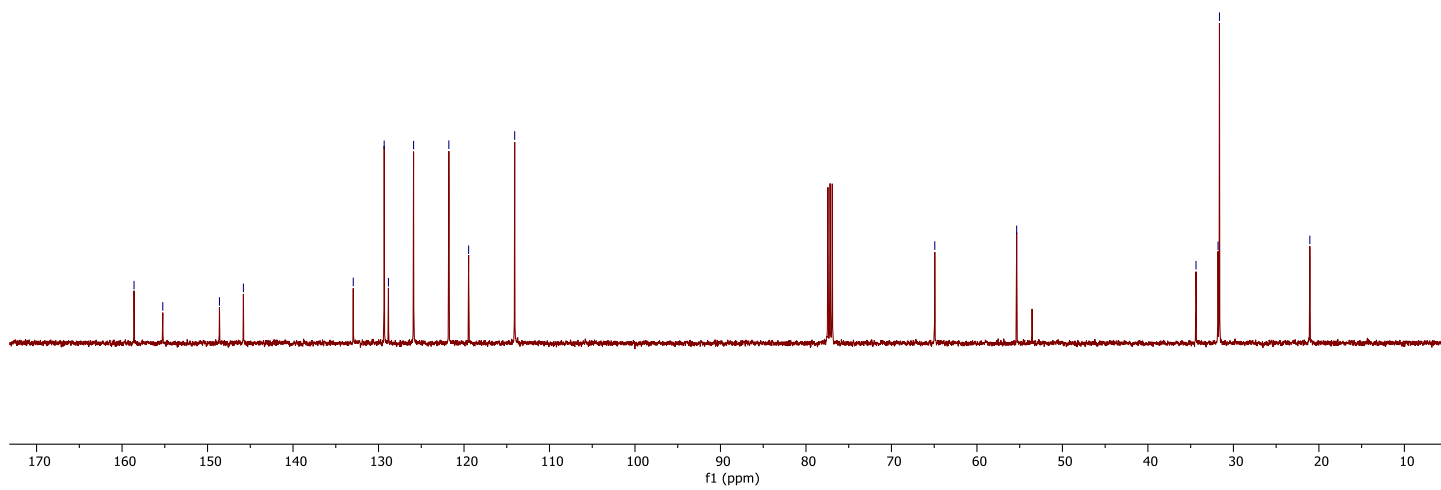
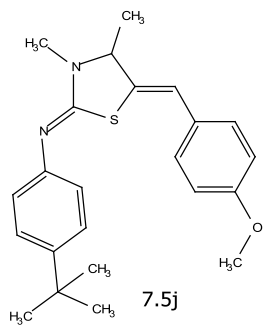
158.60  
155.24  
146.61  
145.81  
132.95  
129.34  
128.84  
125.90  
121.78  
119.46  
114.07

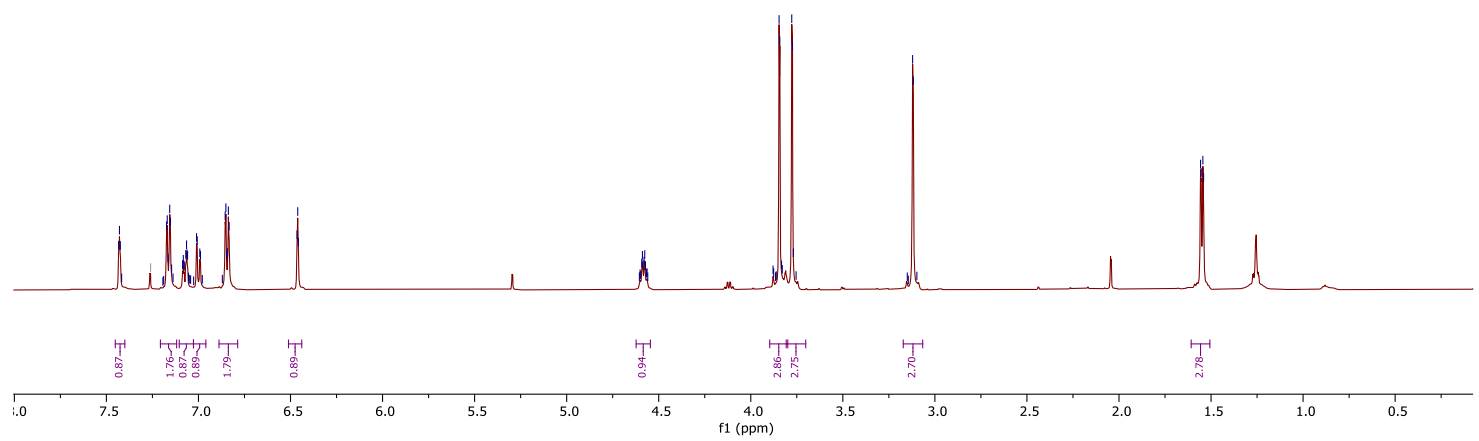
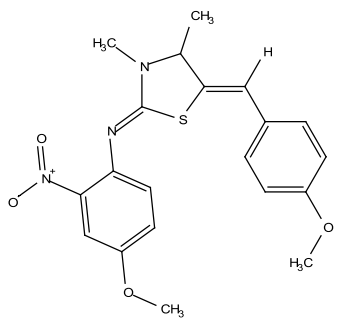
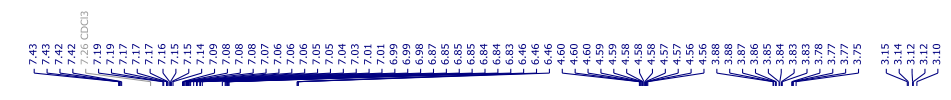
64.93

55.36

34.37  
31.80  
31.63

21.06





158.72  
155.26

131.63  
129.25  
128.45  
126.28

121.00  
120.16

114.06

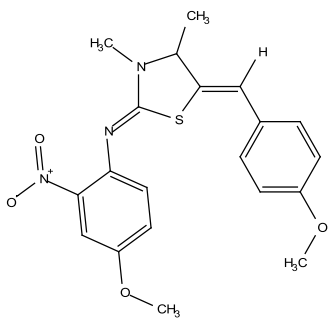
108.79

65.83

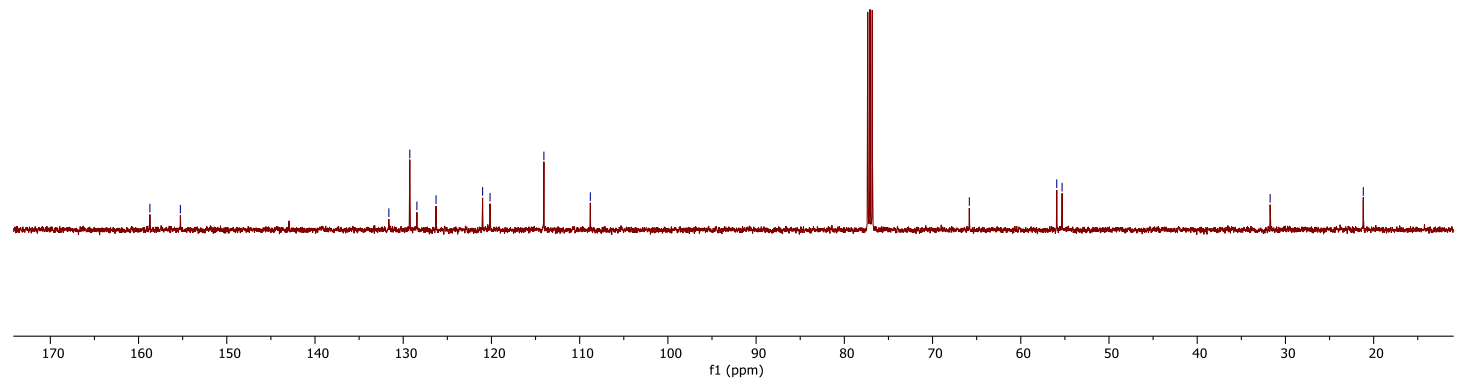
55.92  
55.32

31.73

21.17



7.5k



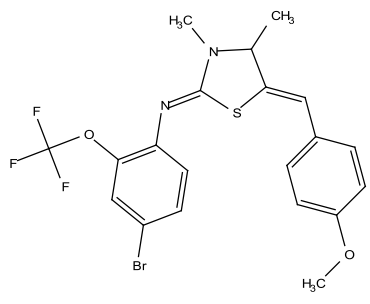
7.39  
7.39  
7.39  
7.38  
7.38  
7.35  
7.35  
7.34  
7.34  
7.33  
7.33  
7.33  
7.32  
7.32  
7.30  
7.19  
7.18  
7.18  
6.96  
6.94  
6.94  
6.88  
6.88  
6.87  
6.87  
6.86  
6.86

4.57  
4.56  
4.56  
4.55  
4.55  
4.55  
4.54

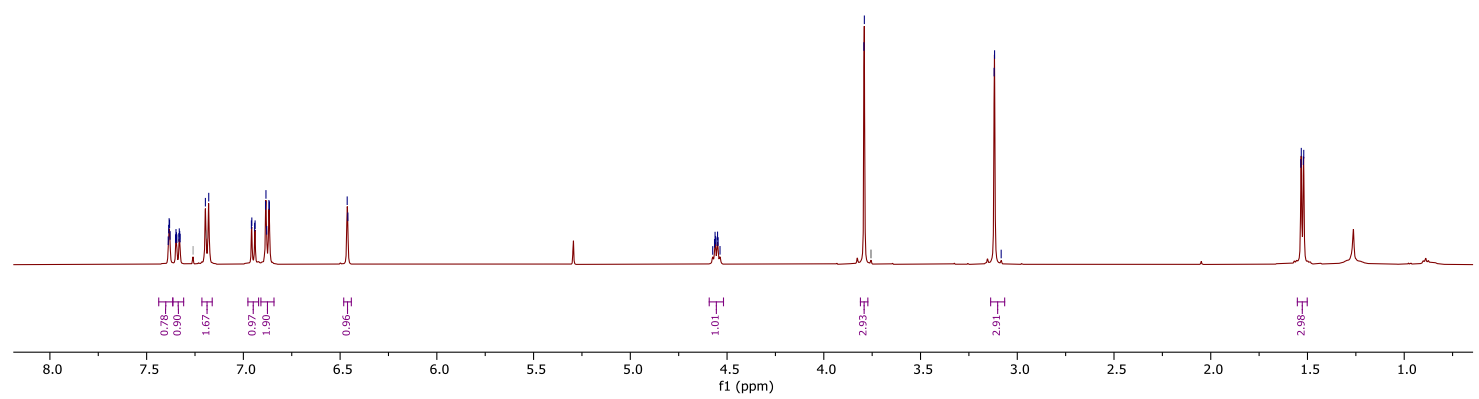
3.79  
3.79  
3.76  
3.75

3.12  
3.12  
3.08

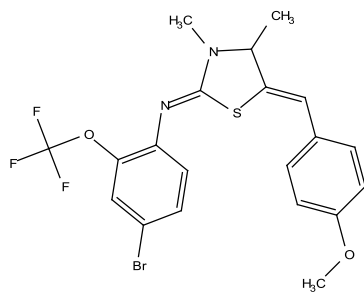
1.53  
1.52  
1.52



7.5I

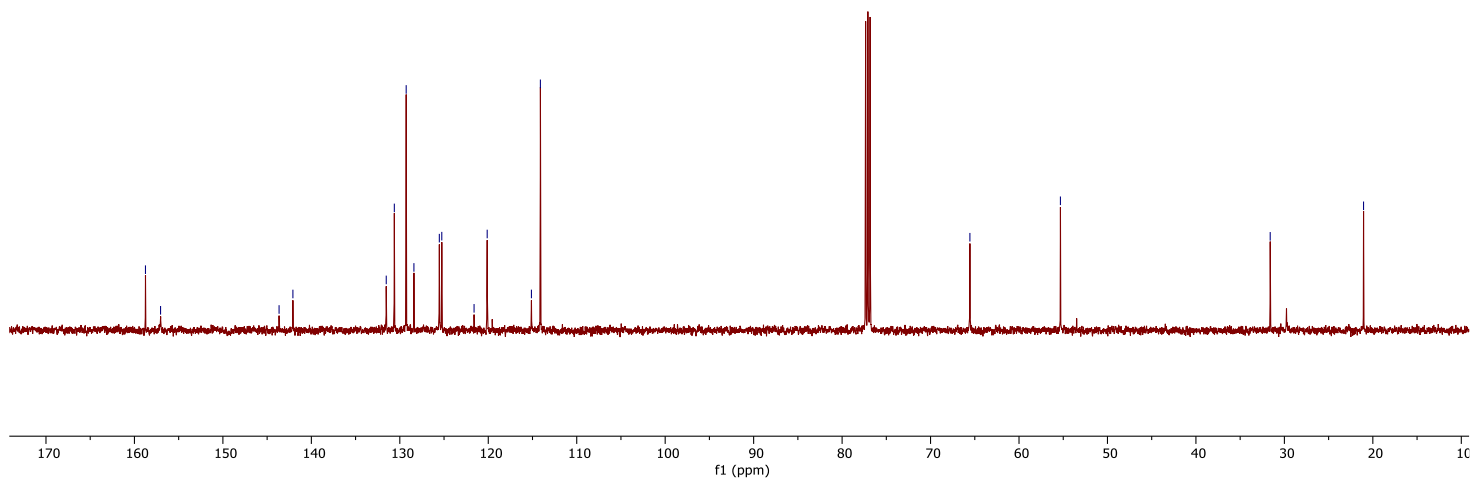


158.75  
157.05  
143.65  
142.09  
131.93  
129.28  
128.40  
125.53  
125.25  
120.12  
115.12  
114.11



7.5I

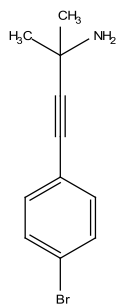
65.55  
55.32  
31.60  
21.05



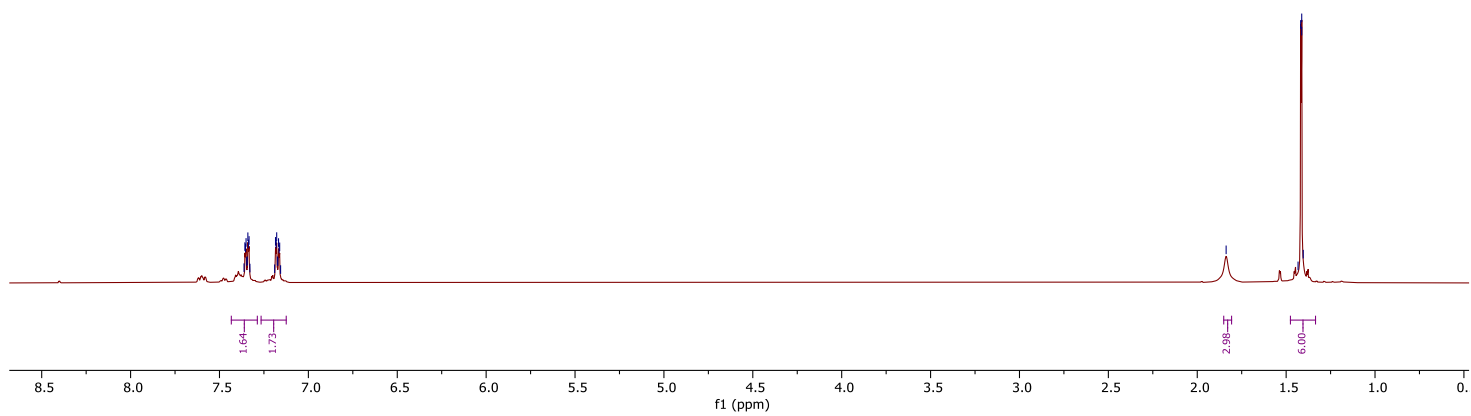
Chapter eight:

7.36  
7.36  
7.35  
7.35  
7.34  
7.34  
7.34  
7.33  
7.33  
7.19  
7.19  
7.18  
7.18  
7.17  
7.17  
7.16  
7.16  
7.16

1.84  
1.43  
1.42  
1.41  
1.40



8.8



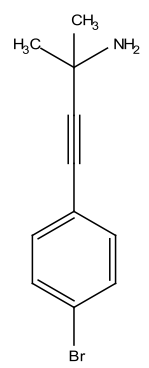
133.02  
131.49  
128.61  
128.52  
122.37  
122.02

98.08

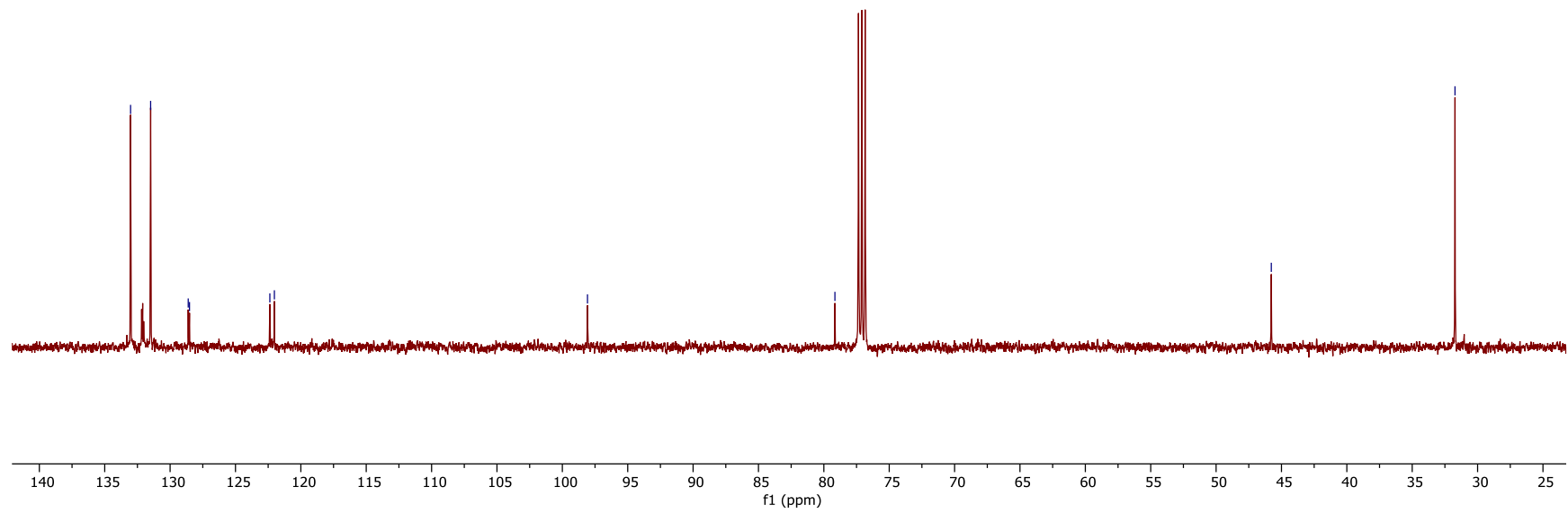
79.15

45.78

31.73



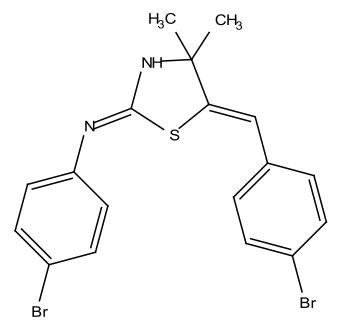
8.8



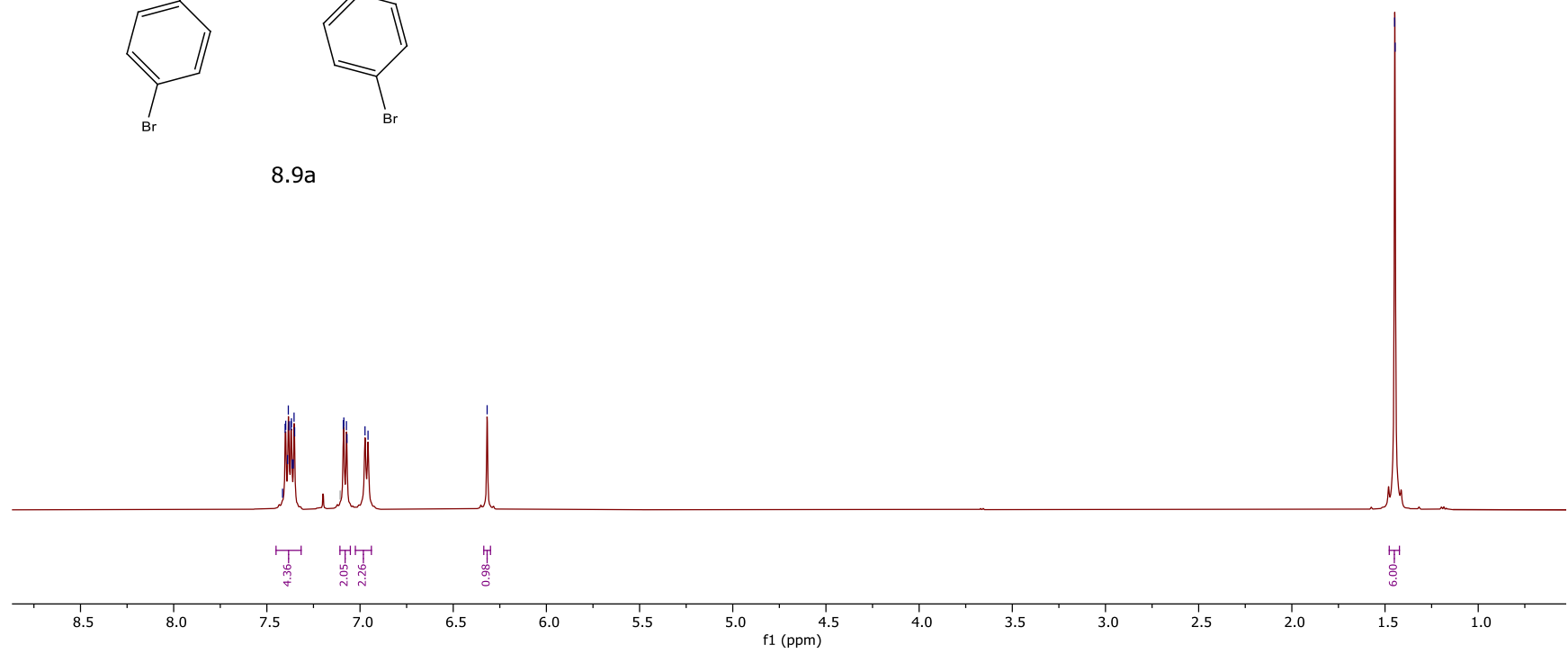
7.42  
7.40  
7.38  
7.38  
7.37  
7.36  
7.36  
7.35  
7.35  
7.11  
7.09  
7.07  
7.07  
6.97  
6.96

6.32

1.45  
1.45

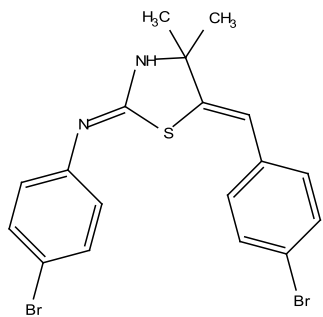


8.9a

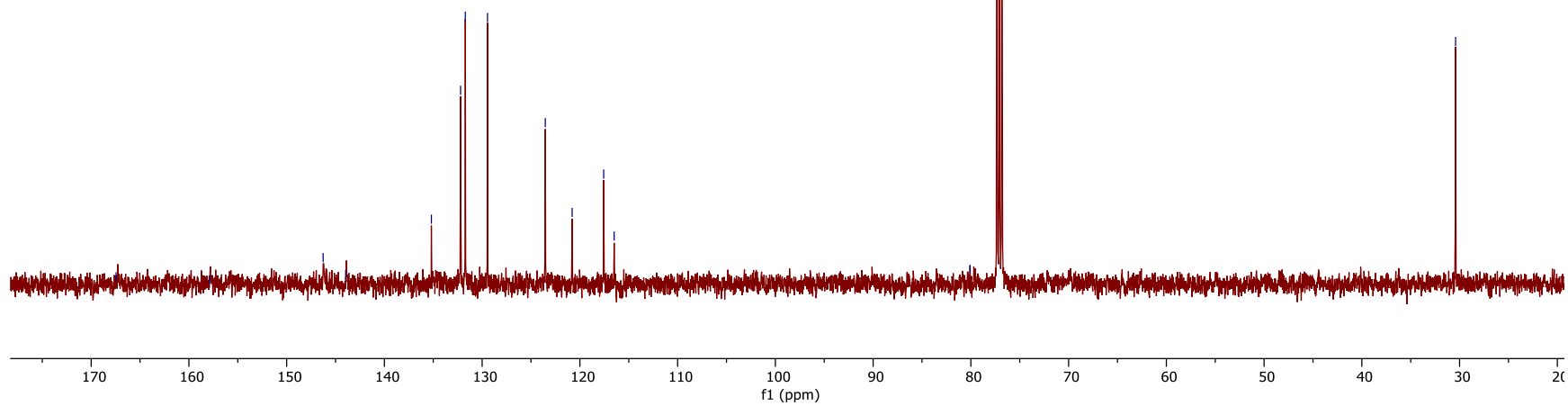


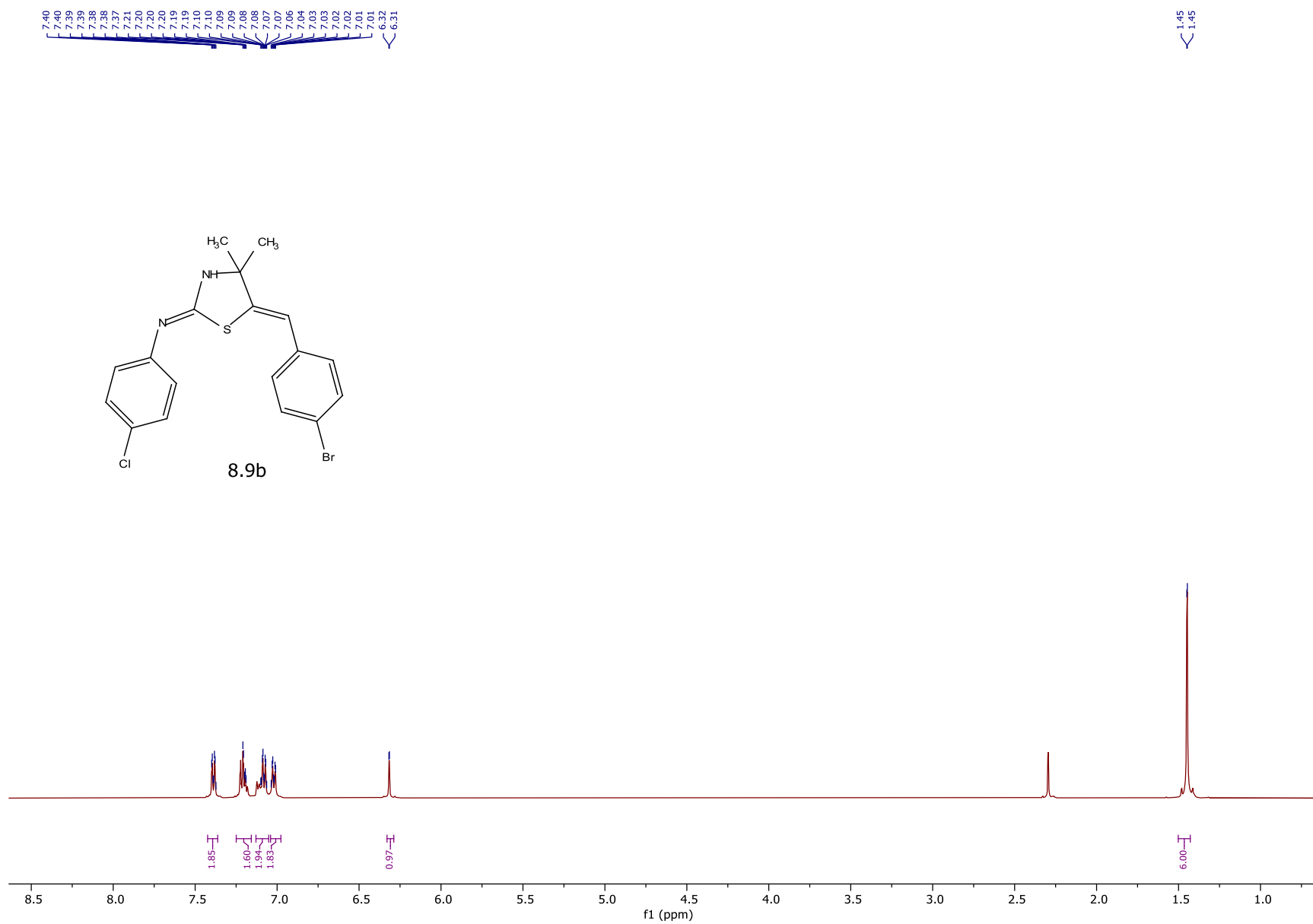


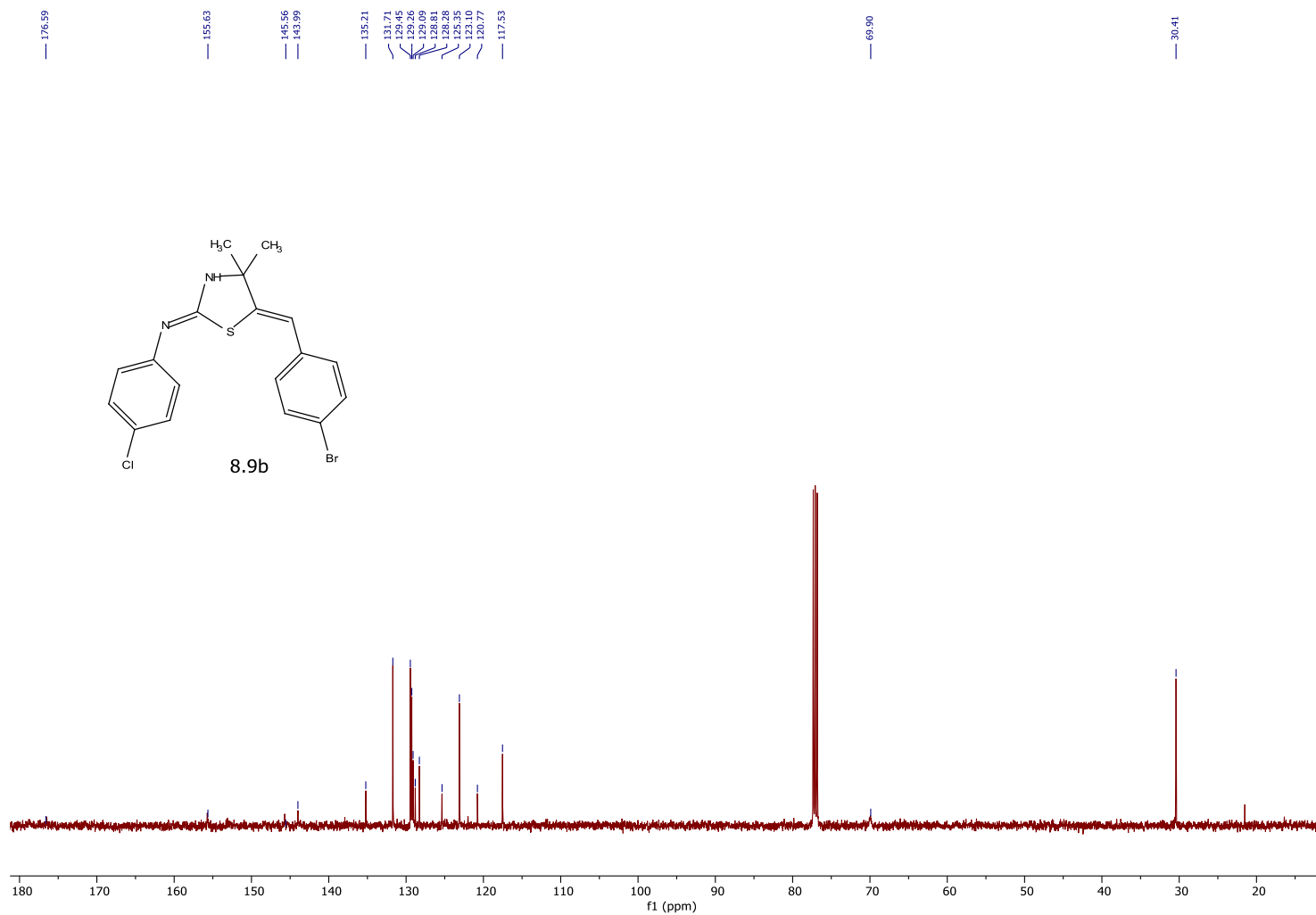
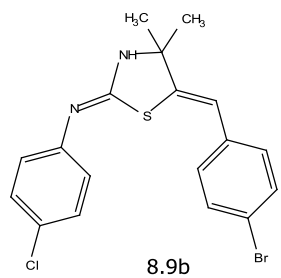
167.45  
157.91  
146.27  
143.96  
135.19  
132.21  
131.72  
129.45  
123.54  
120.79  
117.57  
116.49  
80.09  
30.41



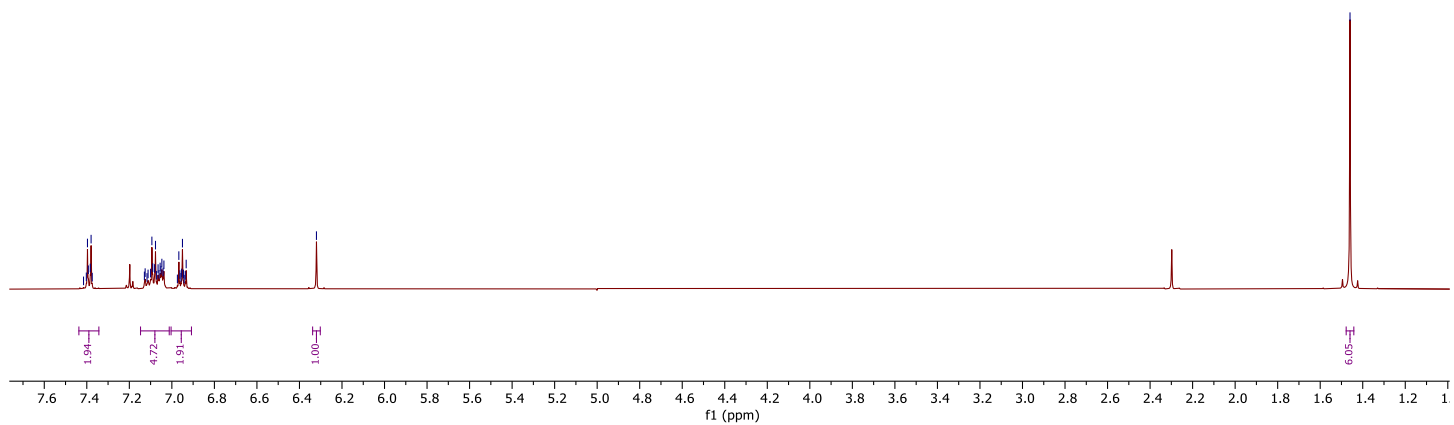
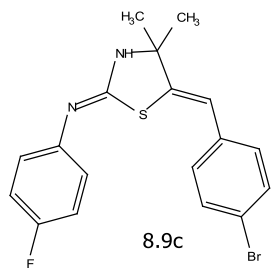
8.9a







7.42  
7.40  
7.38  
7.37  
7.36  
7.35  
7.34  
7.33  
7.32  
7.31  
7.30  
7.29  
7.28  
7.27  
7.26  
7.25  
7.24  
7.23  
7.22  
7.21  
7.20  
7.19  
7.18  
7.17  
7.16  
7.15  
7.14  
7.13  
7.12  
7.11  
7.10  
7.09  
7.08  
7.07  
7.06  
7.05  
7.04  
7.03  
7.02  
7.01  
7.00  
6.99  
6.98  
6.97  
6.96  
6.95  
6.94  
6.93  
6.92  
6.91  
6.90  
6.89  
6.88  
6.87  
6.86  
6.85  
6.84  
6.83



1.46

156.43

135.31

131.69

129.44

129.09

128.28

125.95

123.30

123.23

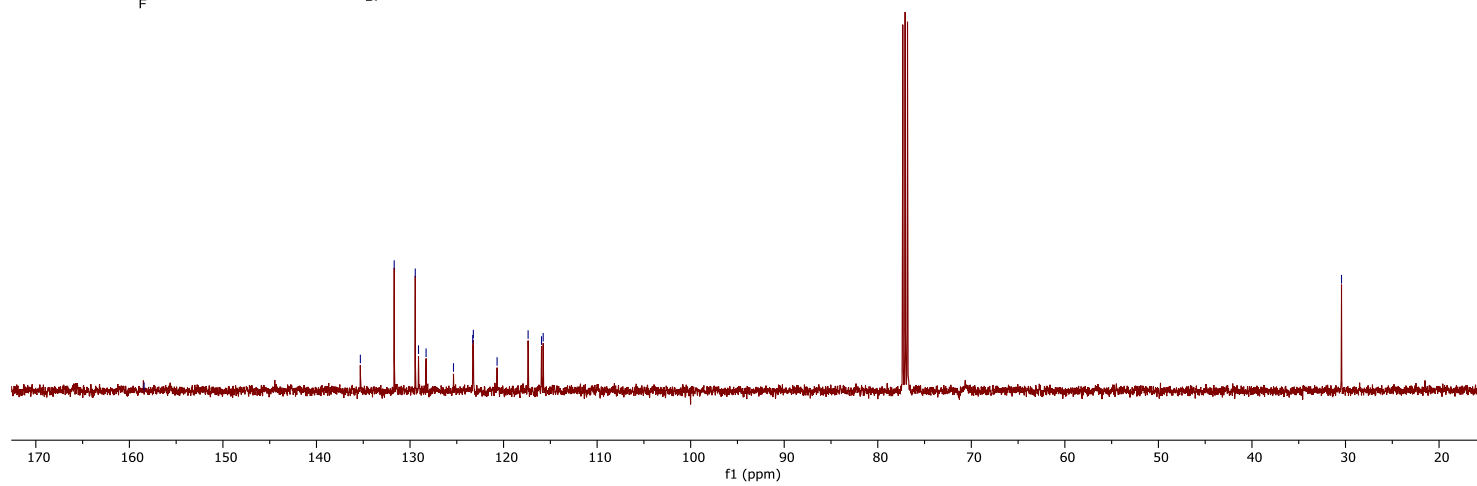
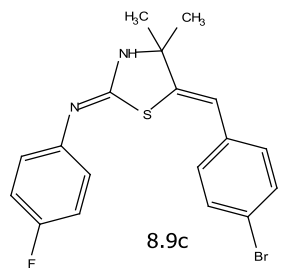
120.69

117.38

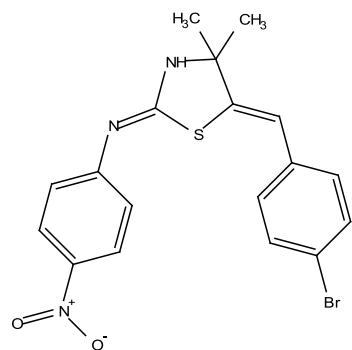
115.94

115.77

30.43

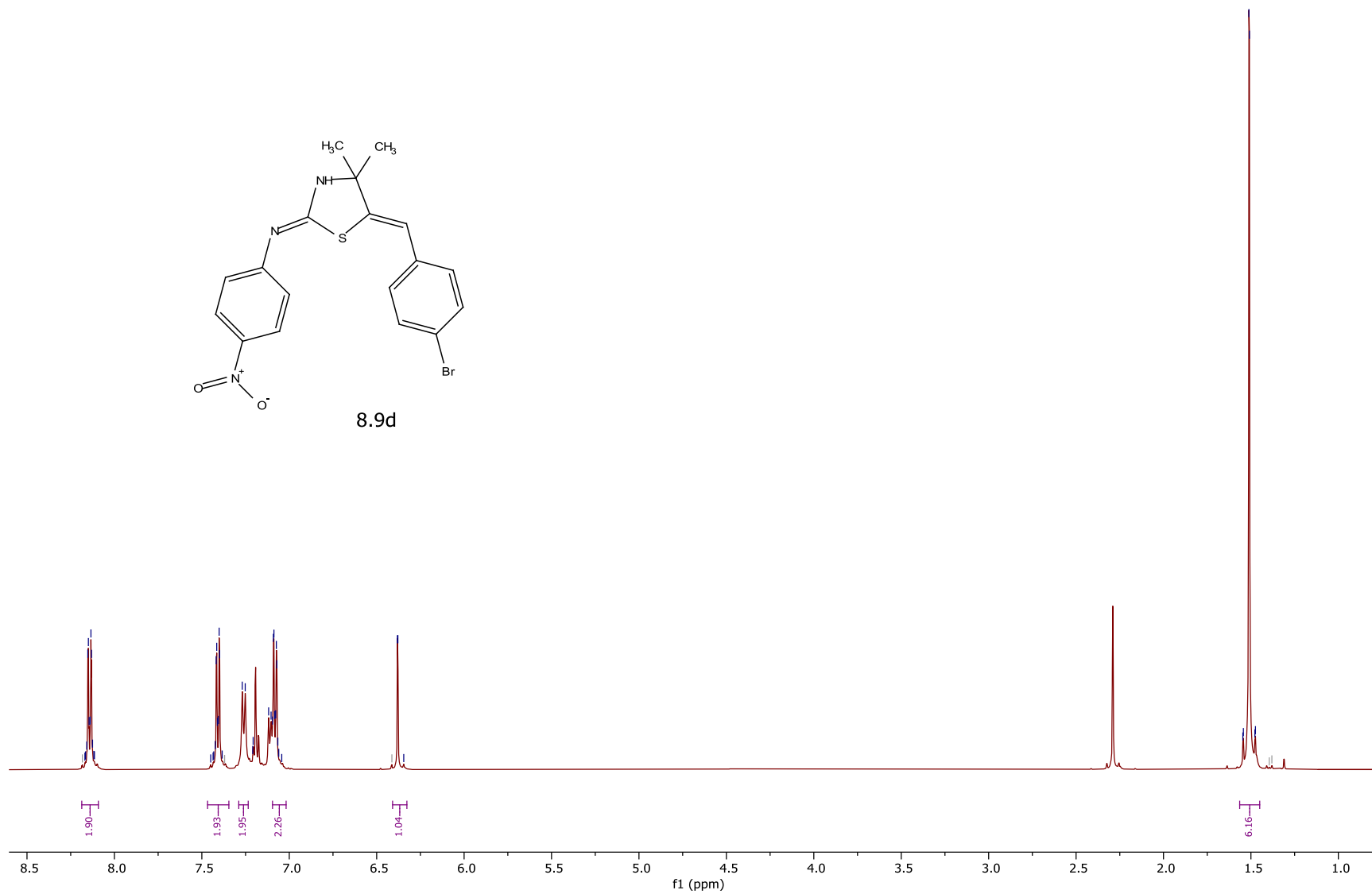


8.17  
8.16  
8.15  
8.15  
8.14  
8.14  
8.13  
8.13  
8.12  
8.12  
9.15  
7.44  
7.43  
7.42  
7.42  
7.41  
7.41  
7.41  
7.40  
7.40  
7.38  
7.37  
7.27  
7.25  
7.21  
7.11  
7.12  
7.10  
7.10  
7.09  
7.08  
7.08  
7.07  
7.07  
7.07  
7.06  
7.04  
6.41  
6.38  
6.38  
6.35

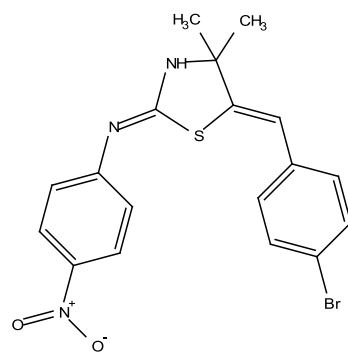


8.9d

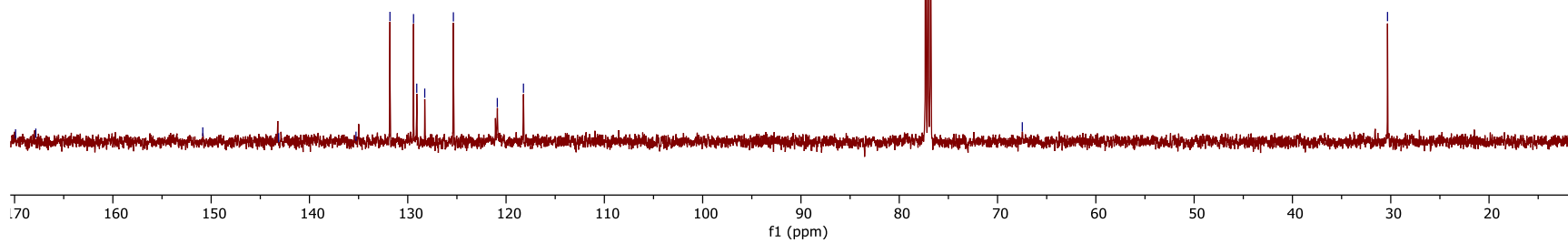
1.55  
1.54  
1.51  
1.51  
1.48  
1.47  
1.40  
1.38



169.90  
167.84  
150.85  
143.13  
135.27  
131.81  
129.41  
129.08  
128.27  
125.36  
120.89  
118.23  
67.48  
30.33

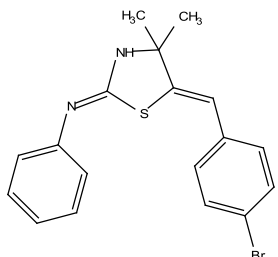


8.9d

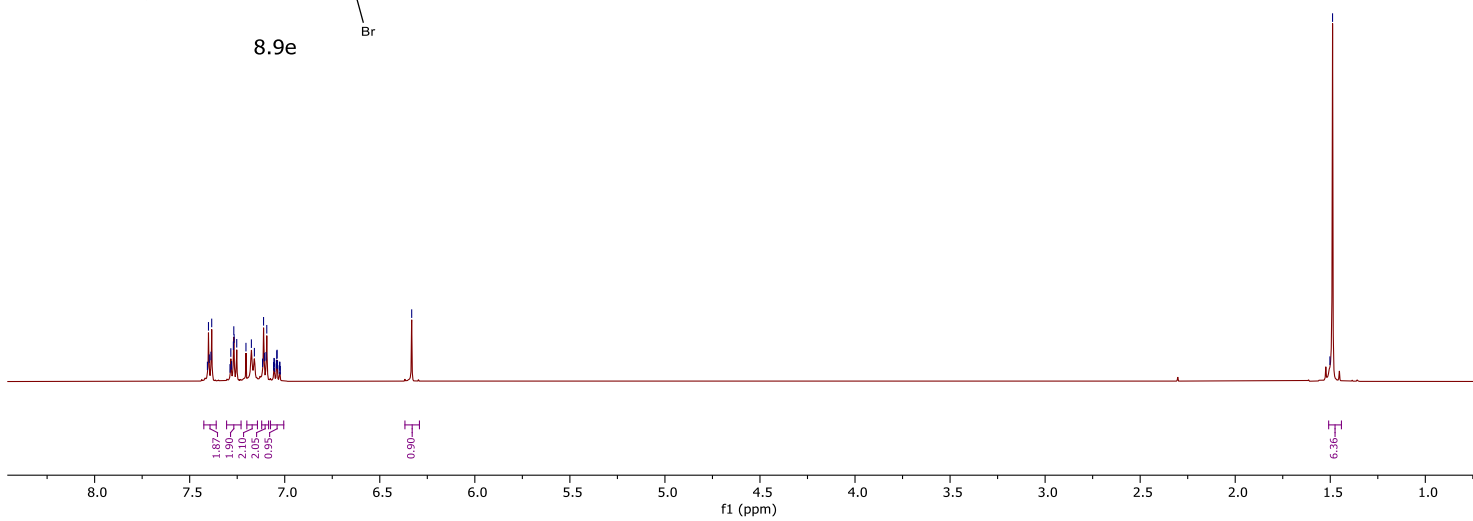


7.41  
7.40  
7.39  
7.38  
7.29  
7.28  
7.27  
7.27  
7.25  
7.25  
7.18  
7.16  
7.12  
7.11  
7.11  
7.10  
7.09  
7.06  
7.06  
7.05  
7.05  
7.04  
7.04  
7.04  
7.03  
7.03

1.50  
1.49



8.9e





153.87  
152.99  
150.73

135.51

131.66  
129.93  
129.82

123.66  
122.82  
120.53

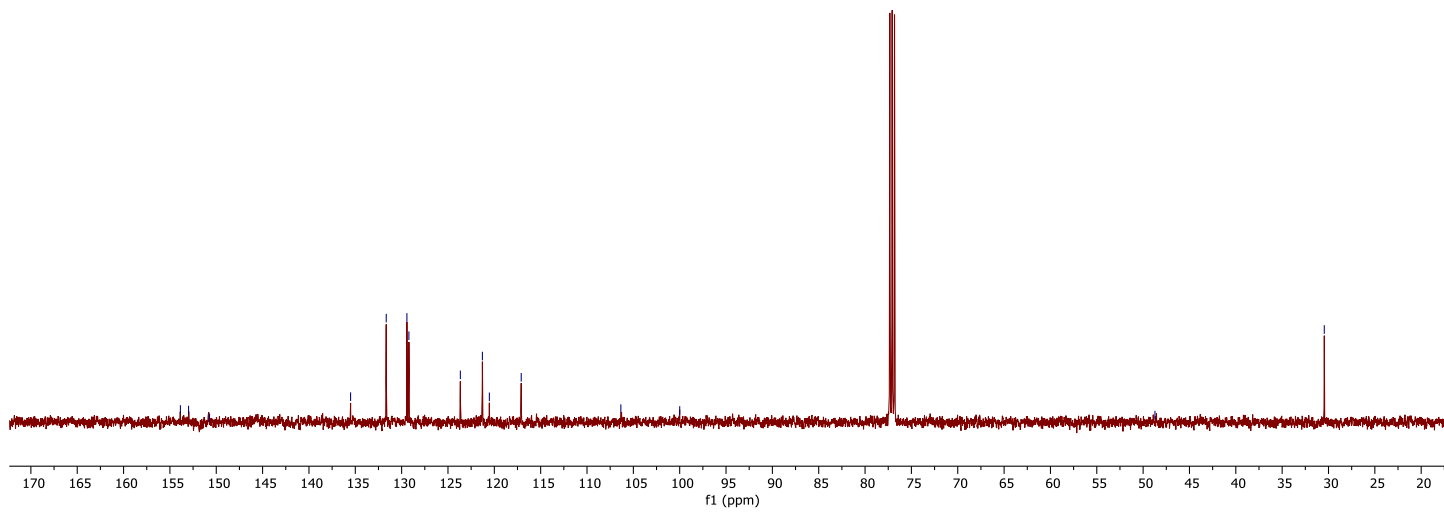
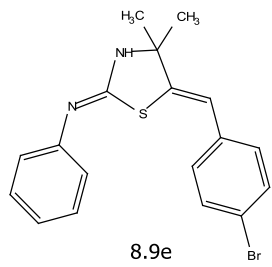
117.10

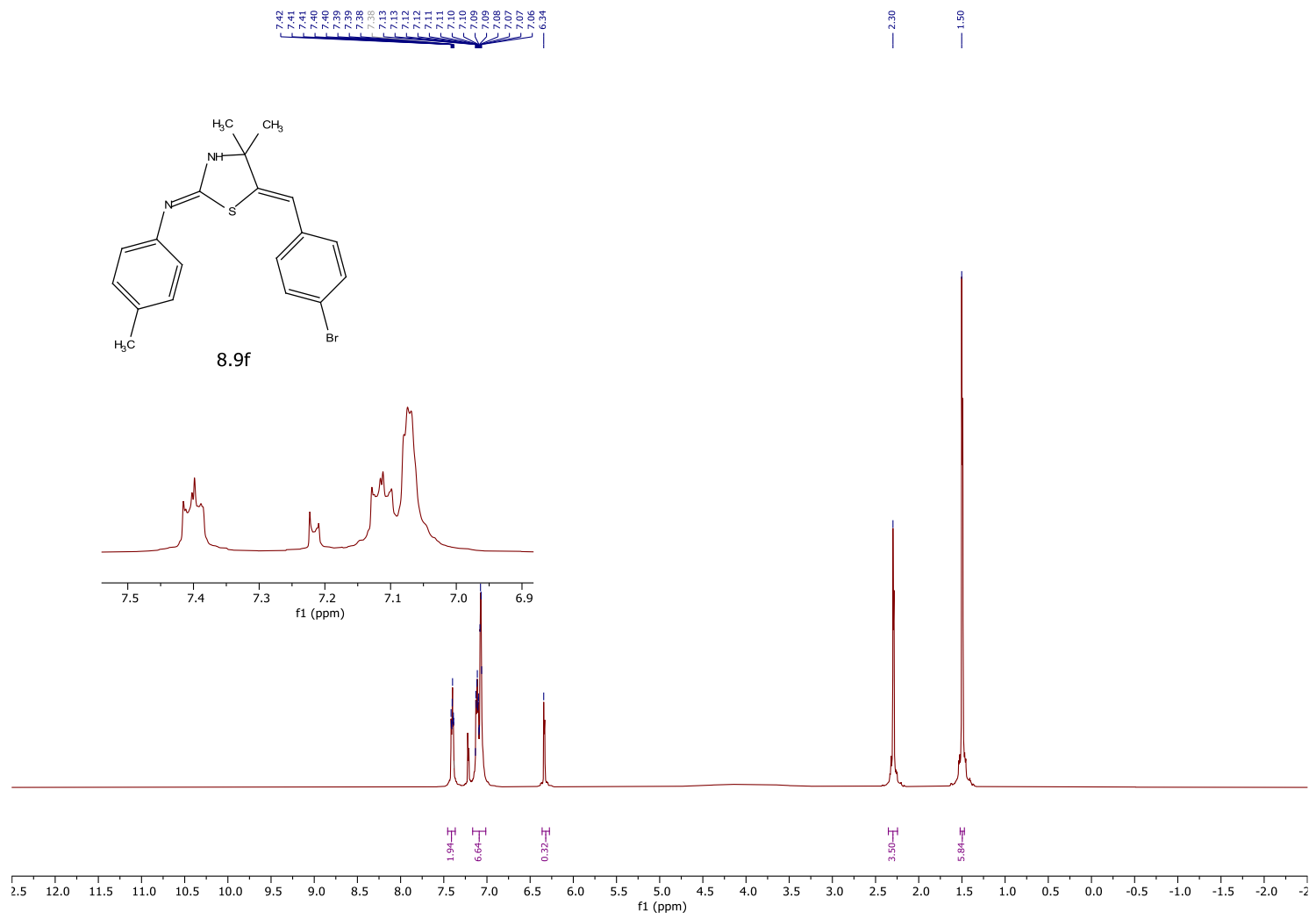
106.35

100.00

48.72

30.45





171.15

142.10

136.69

133.80

131.65

129.78

129.44

127.33

121.54

120.46

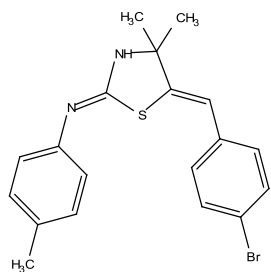
117.00

110.78

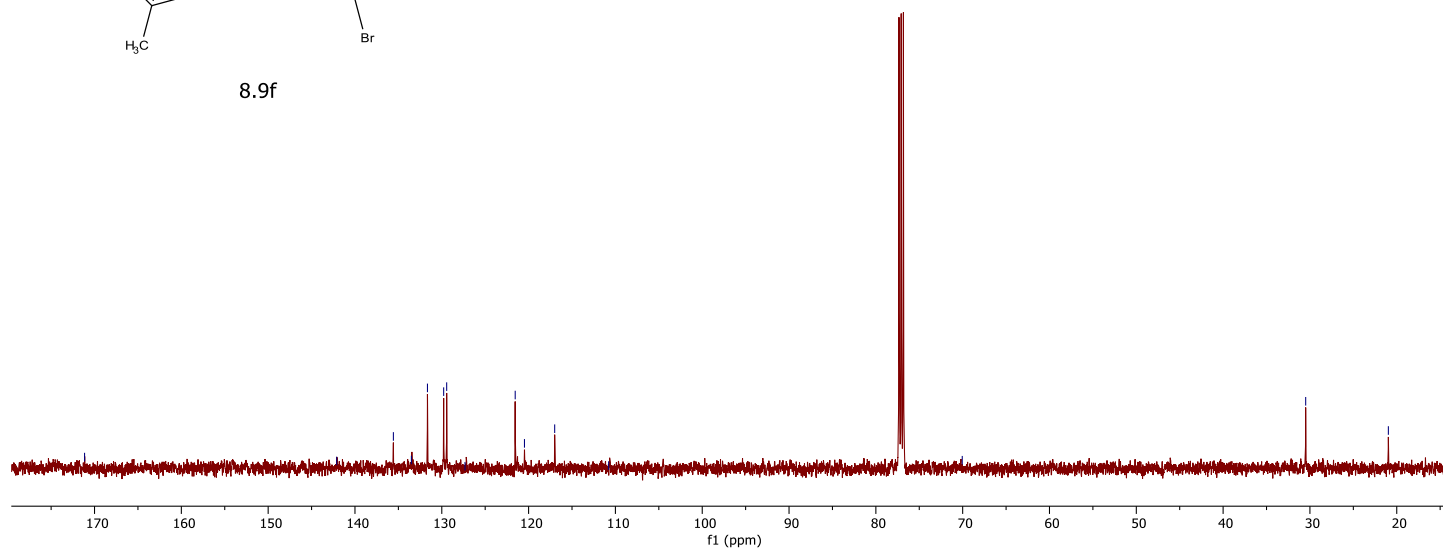
70.05

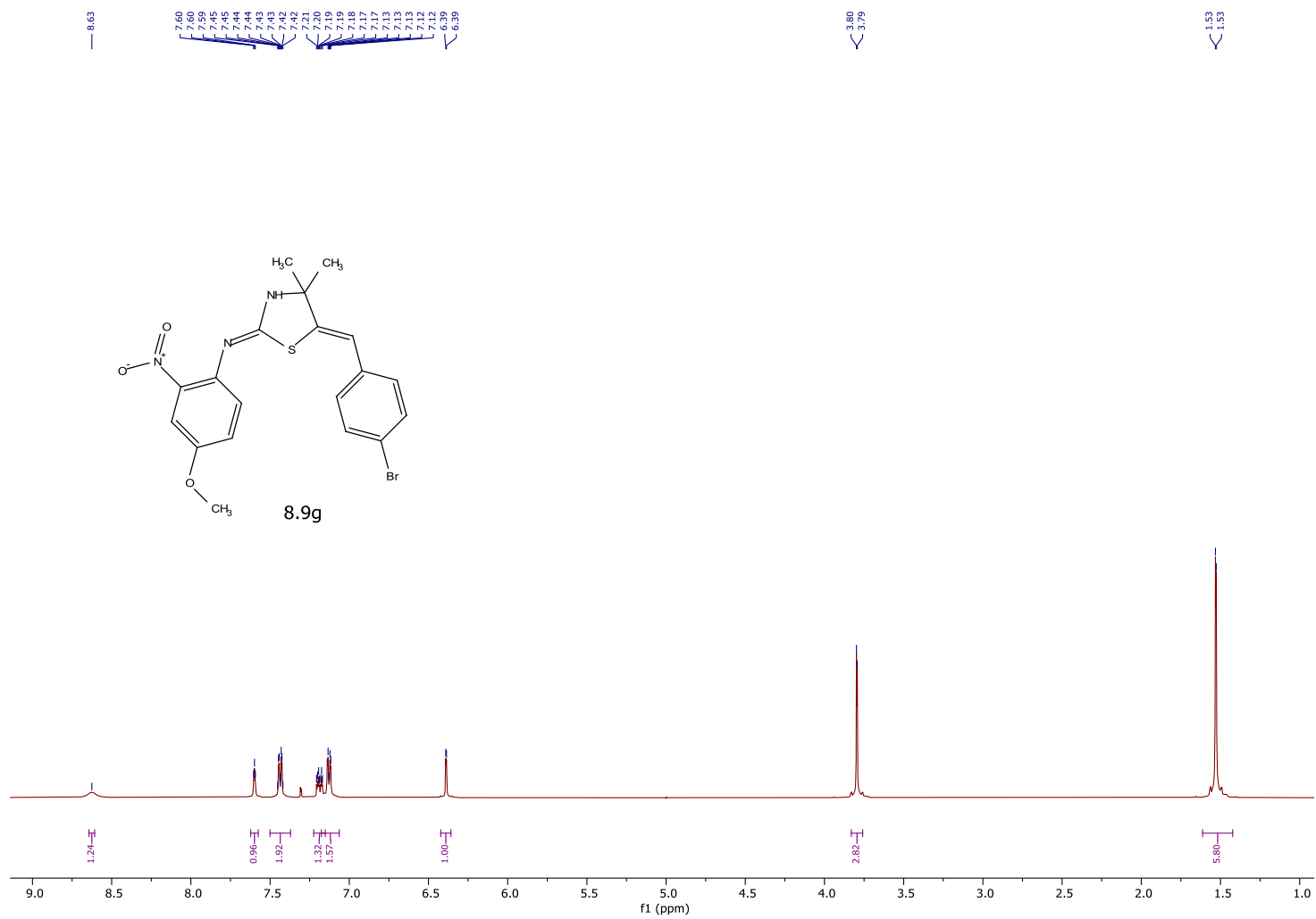
30.49

20.97



8.9f



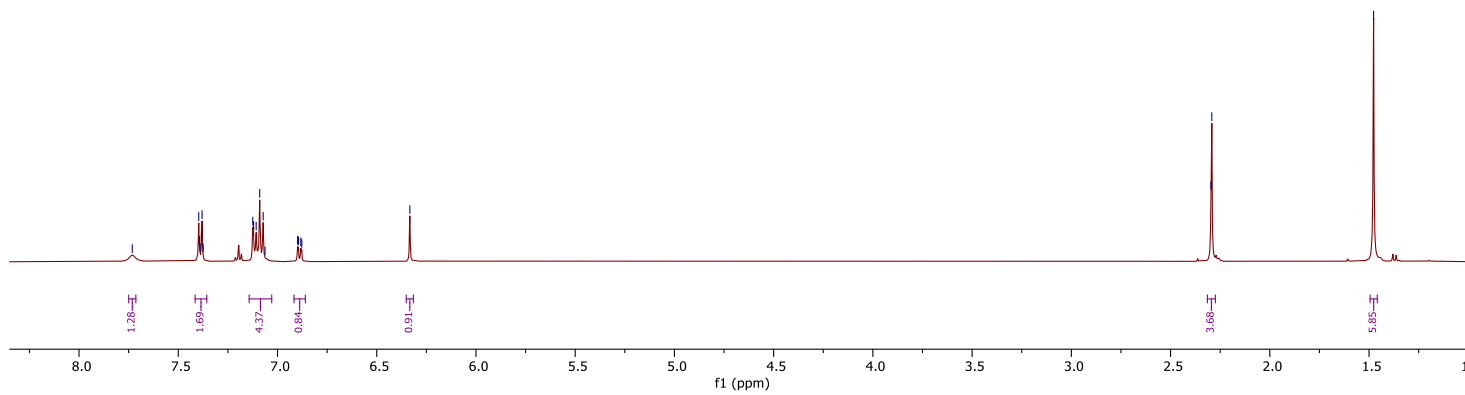
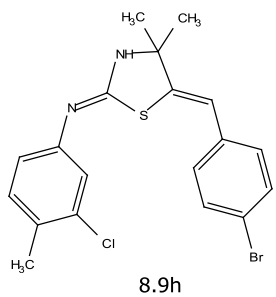




7.73  
7.50  
7.39  
7.38  
7.37  
7.12  
7.11  
7.09  
7.07  
6.90  
6.89  
6.88  
6.33

2.30  
2.29

1.48



156.76

144.55  
143.51

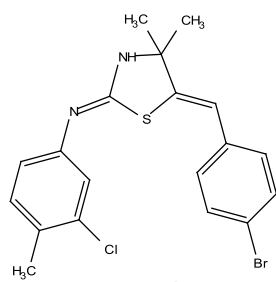
135.10  
134.60  
131.75  
131.58  
131.35  
129.46  
128.28

125.35  
122.59  
120.88  
117.77  
117.84

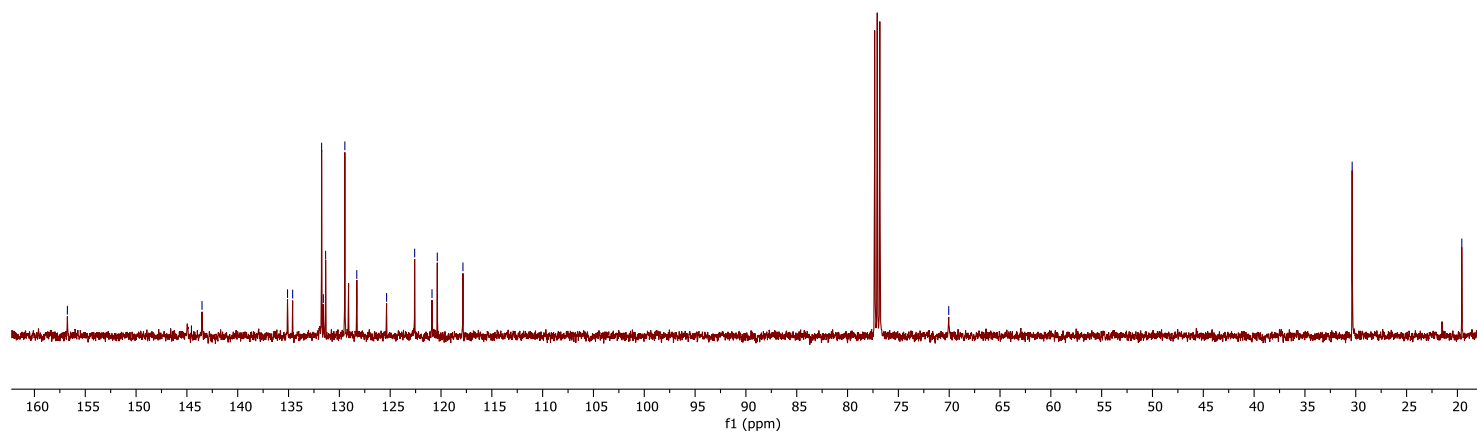
70.05

30.35

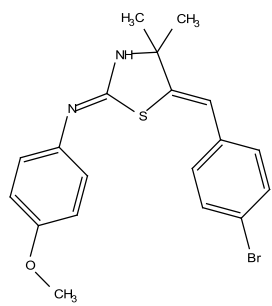
19.57



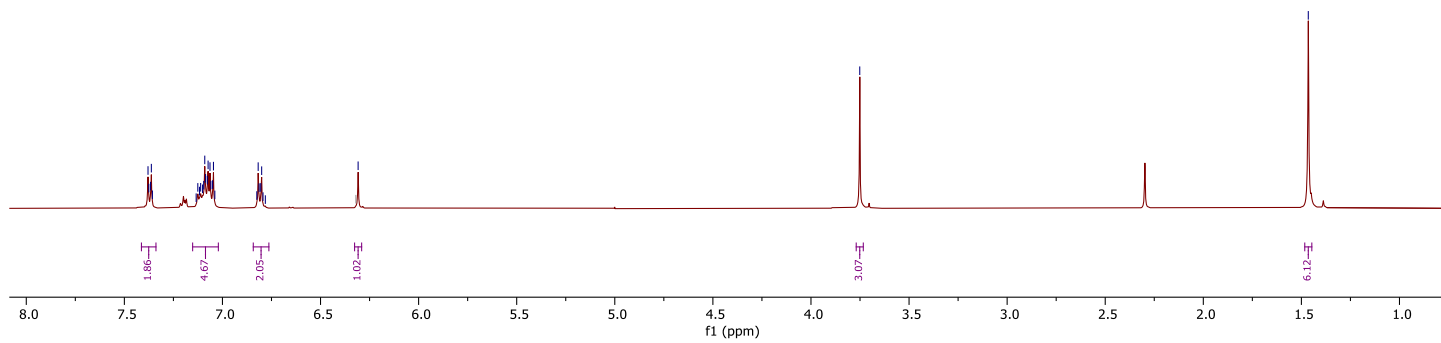
8.9h



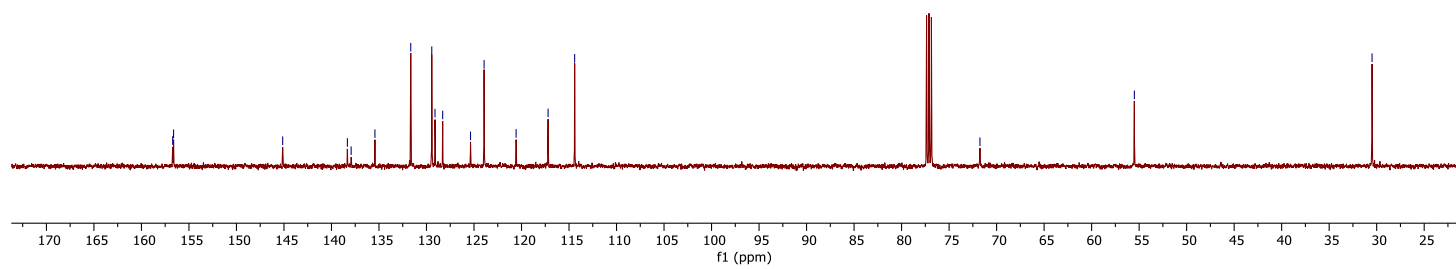
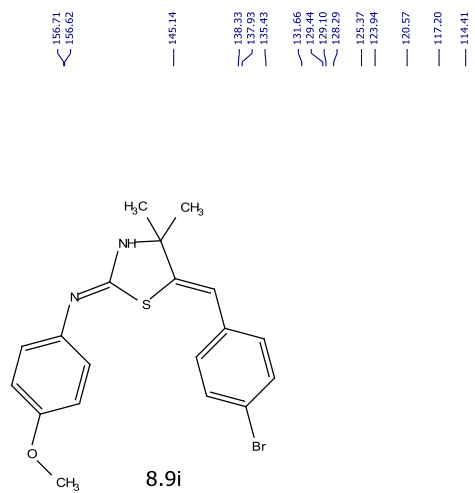
7.38  
7.38  
7.37  
7.36  
7.36  
7.13  
7.13  
7.12  
7.12  
7.10  
7.10  
7.09  
7.09  
7.07  
7.06  
7.06  
7.05  
7.04  
6.82  
6.82  
6.80  
6.80  
6.79  
6.78  
6.31  
6.31



8.9i







## BIOGRAPHICAL INFORMATION

Marian Awadalla (Marian N Aziz) is a native of Egypt and was born and grew up in a small village in Giza city called El-Qubabat. She graduated from the college of Science, Helwan University in 2011 with a bachelor's degree in Chemistry. Marian was one of the top twenty in the college of science, so she was nominated to work in one of the governmental sectors. She joined the National Research Center in 2012 to pursue her graduate studies and worked on medicinal chemistry projects serving the national needs. She received her master's degree in Organic Chemistry in 2016 from Helwan University and the National Research Center, Egypt. Then, she moved to the United States to pursue her PhD degree in 2017. She joined the Lovely group at the University of Texas at Arlington as a visitor scholar for 9 months, then she started her PhD program in August 2018. She joined the University of Texas MD Anderson Cancer Research Center as an intern during the summer of 2021. She received the prestigious award of GWIS in August 2022. Marian received her PhD degree in synthetic organic chemistry from the University of Texas at Arlington in August 2022.